

**Republic of Iraq
Ministry of Higher Education
and Scientific Research
University of Babylon
College of Engineering
Civil Engineering Department**



***NONLINEAR STATIC AND DYNAMIC
ANALYSIS OF HORIZONTALLY CURVED
BEAMS***

A Thesis

**Submitted to the College of Engineering of the University
of Babylon in Partial Fulfillment of the Requirements
for the Degree of Doctor of Philosophy
in Structural Engineering**

By

***Hayder Mohammed Kadhim Kthair
Al-Mutairee***

(B.Sc.1997, M.Sc.2000)

March, 2008



بِسْمِ اللَّهِ الرَّحْمَنِ الرَّحِيمِ

رَبِّ قَدْ آتَيْتَنِي مِنَ الْمُلْكِ وَعَلَّمْتَنِي مِنْ
تَأْوِيلِ الْأَحَادِيثِ فَاطِرَ السَّمَوَاتِ وَالْأَرْضِ
أَنْتَ وَالْإِلَهِيُّ فِيهِ الْحَيَاةُ وَالْمَوْتُ وَأَنْتَ
مُسْلِمًا
وَالْقَنِيبِيُّ بِالْمَسَالِينِ

صَدَقَ اللَّهُ الْمَلِكُ الْمَغْطَبِيُّ



Certification

We certify that the preparation of this thesis titled “*Nonlinear Static and Dynamic Analysis of Horizontally Curved Beams*” presented by “*Hayder Mohammed Kadhim Kthair Al-Mutairee*” was made under our supervision at the Department of Civil Engineering / College of Engineering / University of Babylon, as a partial fulfillment of the requirements for the degree of Doctor of Philosophy in Civil Engineering (Structural Engineering).

Signature:

Name: **Ass.Prof. Dr. M. B. Dawood**

Date: / / 2008

Signature:

Name: **Prof. Dr. S. Z. Al-Sarraf**

Date: / / 2008

CERTIFICATE OF THE EXAMINING COMMITTEE

We certify as an Examining Committee that we have read this thesis titled “*Nonlinear Static and Dynamic Analysis of Horizontally Curved Beams*” and examined the student “*Hayder Mohammed Kadhim Kthair Al-Mutairee*,” in its content and what related to it, and found it meets the standard of thesis for the degree of Doctor of Philosophy in Civil Engineering (Structural Engineering).

Signature:
Name: **Ass.Prof. Dr. Mustafa B. Dawood**
(Supervisor)
Date: / / 2008

Signature:
Name: **Prof. Dr. Sabeeh Z. Al-Sarraf**
(Supervisor)
Date: / / 2008

Signature:
Name: **Ass.Prof. Dr. Hayder T. Ninnim**
(Member)
Date: / / 2008

Signature:
Name: **Ass.Prof. Dr. Ammar Y. Ali**
(Member)
Date: / / 2008

Signature:
Name: **Ass.Prof. Dr. Ihsan A. Al-Shaarbaf**
(Member)
Date: / / 2008

Signature:
Name: **Prof. Dr. Nameer A. Alwash**
(Member)
Date: / / 2008

Signature:
Name: **Prof. Dr. Husain M. Husain**
(Chairman)
Date: / / 2008

Approved by The Head of the Civil Engineering Department

Signature:
Name: **Ass.Prof. Dr. Ammar Y. Ali**
(The Head of the Civil Engineering Department)
Date: / / 2008

Approved by The Dean of the College of Engineering

Signature:
Name: **Ass.Prof. Dr. Salah Tawfeek Al-Bazzaz**
(The Dean of the College of Engineering)
Date: / / 2008

مِنْهُ وَإِلَيْهِ مُوَلَّى

Acknowledgments

In the name of Allah, the most gracious, the most merciful

At first, thank to **Allah** my **God** who helped and enabled me to complete this research, and say "from you and to you my lord".

*I wish to express my thanks to my supervisors **Dr. Sabeeh Z. Al-Sarraf** and **Dr. Mustafa B. Dawood** for their advice, guidance and encouragement throughout this work*

*I would like to express my respect and thank to **Dr. Ihsan Al-Shaarbaf** for his assistance and explanations which are concerned with the static analysis.*

*I do not know how can I reach my big respect and thank to **Dr. Chen W.F.**, **Dr. Owen D.R.J.**, **Dr. Hinton E.**, **Dr. William W.J.** and **Dr. Paul R.J.** about their useful and beautiful books.*

Deepest thanks are also expressed to the Head of the Civil Engineering Department in the College of Engineering, University of Babylon for providing facilities throughout the duration of study.

A special thank and gratitude to my mother and my wife for their care, patience and encouragement throughout the research period.

Also I wish to thank my sisters for their encouragement during the research period.

*Finally, I would like to thank my friends **Haider Waffy**, **Raad Kamel**, **Ahmed Abbas** and **Ali Ganeem** for their help and assistance.*

Hayder Mohammed Kadhim Kthair

Al-Mutairee 24-10-2007

Abstract

The present work is devoted to study the three dimensional nonlinear finite element analysis of horizontally curved beams of (steel, reinforced concrete and composite) section subjected to static and dynamic loads. Two finite element computer programs are presented for this purpose, the first deals with the static analysis and the second with the dynamic analysis utilizing the previous models.

The 20-node isoparametric brick element has been used to represent the concrete and steel elements while reinforcing bars are idealized as axial members embedded within the concrete elements without any relative displacement between them. Also perfect bond was assumed between the concrete deck slab and the steel stem for the composite horizontally curved beams.

For steel, the Von-Mises yield criterion was used to compute the stress level at the onset of plastic deformation while for the uniaxial stress-strain relationship under tension and compression an elastic-linear hardening model was considered for static analysis and elastic-perfect plastic for dynamic analysis. The tension behavior of concrete was simulated by a smeared crack model with fixed orthogonal cracks and the strain softening has been taken into account. For concrete under compressive stresses, an elasto-plastic work hardening model followed by a linear degradation in the compressive stress f'_c begin until terminated at the onset of crushing has been adopted under static load, and an elasto – viscoplastic model was used in the dynamic analysis.

Several horizontally curved beams with different material properties and boundary conditions have been analyzed under static and dynamic loads and the analytical results of load-deflection response and the stresses are compared with the experimental and other analytical data. The static analysis revealed good agreement between the results of the present static model and the experimental data. Also the dynamic analysis revealed good agreement between the results of the present dynamic model and the results obtained from the program ANSYS, (the program was adopted due to no available experimental data).

Parametric studies have been carried out to investigate the effect of tapering ratios, curvature and many others parameters on the behavior of static and dynamic response of horizontally curved beams.

For static analysis, the investigation showed that when the effect of crushing was ignored the difference between the analytically predicted ultimate loads and the experimental data increased from 0% to 40%. While in the dynamic analysis for composite curved beams when considering the effects of cracks and crushes the amplitude of mid-span deflection increased about 23.4% and the period time required for one cycle increased also about 14.9%.

The static parametric studies proved that the increment in the ultimate load due to non-prismatic effect (for the same volume of steel) increased with the angle of curvature, and the increment reached to 25% for a simply supported curved beam and to about 101.85% for a fixed end curved beam. Also it was found that when increasing the depth of reinforced concrete curved beam at ends and decreasing at mid-span (for the same volume of concrete) the ultimate strength of the produced non-prismatic curved beam increased by about 16.0%, 59.6%, 91.3% for angles of curvature equal to 23°, 43°, 63° respectively.

The non-prismatic dynamic parametric studies appeared decrements in the amplitude of deflection reaching to 19.8% and 63.7% for a simply supported steel curved beam and reinforced concrete curved beam respectively.

The static and dynamic analysis proved that the benefit from non-prismatic effects depends largely on the degree of restrained at ends and on the angle of curvature of the curved beams, which is increased when these two parameters are increased and vice versa.

The dynamic analyses revealed softening in the strength of the composite curved beam when the tapering ratio was greater than one and showed strengthening when the tapering ratio was less or equal to one. While the dynamic analyses of steel and reinforced concrete curved beams under dynamic (or static) loads showed that the beams gained strengthening when the tapering ratio was greater than one.

Contents

Acknowledgments	I
Abstract	II
Contents	IV
Notation	VIII

Chapter 1: Introduction

1-1: General	1
1-2: Objectives of the Thesis	5
1-3: Layout of the Thesis	6

Chapter 2: Review of Literature

2-1: Introduction	8
2-2: Nonlinear Finite Element Analysis	8
2-3: Static Analysis of Horizontally Curved Beam	13
2-4: Dynamic Analysis of Horizontally Curved Beam	21

Chapter 3: Basic Concepts and Finite Element Idealizations

3-1: Introduction	28
3-2: Finite Element Formulation	29
3-2-1: Static Formulation	29
3-2-2: Dynamic Formulation	31
3-2-2-1: Dynamic Equations Formulation	31
3-2-2-2: Mass Matrix Formulation	35
3-2-2-3: Damping Matrix Formulation	36
3-3: Finite Element Idealization	36
3-3-1: Steel and Concrete Idealization	36
3-3-1-1: Shape Functions of the 20-Node Brick Element	37
3-3-1-2: Strain-Nodal Displacement Representation	38
3-3-1-3: Stiffness Matrix for 20-Node Brick Element	39
3-3-2: Reinforcement Representation	39
3-3-2-1 Displacement Representations	41
3-3-2-2 Strain-Nodal Displacement Representations	42

3-3-2-3 Stiffness Matrix Calculation	42
3-4: Numerical Integration	43

Chapter 4: Behavior and Modeling of Materials under Static Loads

4-1: Introduction	44
4-2: Modeling of the Concrete under Static Load	45
4-2-1: Observed Behavior of the Concrete under Static Load	45
4-2-1-1: Behavior under Uniaxial Compression	45
4-2-1-2: Behavior under Uniaxial Tension	46
4-2-1-3: Multiaxial Behavior of Concrete	47
4-2-2: Concrete Model Adopted in the Static Analysis	48
4-2-2-1: Stress-Strain Model	49
4-2-2-1-1: The Plasticity Model for Concrete in Compression..	49
4-2-2-1-2: The Smeared Crack Model for Concrete in Tension	56
4-2-2-1-3: A Post-Cracking Stress-Strain Relationship.....	61
4-2-2-1-4: Modeling the Reduction in Compressive Strength Due to Orthogonal Cracking	63
4-3: Modeling of the Steel under Static Load	64
4-3-1: Observed Behavior of the Steel under Static Load	64
4-3-2: Modeling of the Steel Adopted in the Analysis	66
4-4: Modeling of Reinforcing Bars under Static Load	70

Chapter 5: Behavior and Modeling of Materials under Dynamic Loads

5-1: Introduction	71
5-2: Modeling of the Concrete under Dynamic Load	72
5-2-1: Observed Behavior of the Concrete under Dynamic Load	72
5-2-2: Concrete Model Adopted in the Dynamic Analysis	74
5-2-2-1: Traditional Elasto / Viscoplastic Model	74
5-2-2-2: Strain Rate Sensitive Elasto / Viscoplastic Model for Concrete	75
5-2-2-2-1: Yield and Strength Limit Surfaces	75
5-2-2-2-2: Viscoplastic Strain Rate	78
5-2-2-2-3: Determination of Model Parameters	78
5-2-2-2-4: Smeared Crack Model for Concrete in Tension	79
5-2-2-2-5: Post-Cracking Stress-Strain Relationship	80

5-3: Modeling of the Steel under Dynamic Load	83
5-3-1: Observed Behavior of the Steel under Dynamic Load	83
5-3-2: Modeling of Steel Adopted in the Analysis	83
5-4: Modeling of Reinforcing Bars under Dynamic Load	84

Chapter 6: Nonlinear Solutions Techniques

6-1: Introduction	85
6-2: Static Analysis	85
6-2-1: Linear Incremental Method	86
6-2-2: Iterative Methods	86
6-2-3: Incremental-Iterative Methods	86
6-3: Dynamic Analysis	88
6-3-1: Direct Integration Methods	88
6-3-2: Predictor-Corrector Form of Newmark's Method	90
6-3-3: Computational Algorithm for the Implicit Form of Newmark Method	91
6-3-4: Selection of the Time Step Size	92
6-4: Convergence Criteria	94

Chapter Seven

Static Model Discussion and Testing

7-1: Introduction	95
7-2: Properties and Abilities of the Static Model	96
7-3: Structure of the Program	97
7-4: Numerical Examples	99
7-4-1: Horizontally Curved Steel Beams	99
7-4-2: Horizontally Curved Reinforced Concrete Beams	107

Chapter Eight

Dynamic Model Discussion and Testing

8-1: Introduction	126
8-2: Properties and Abilities of the Dynamic Model	127
8-3: Structure of the Program	128
8-4: Numerical Examples	130
8-4-1: Example No.1: Horizontally Curved Steel Beam	130
8-4-2: Example No.2: Horizontally Curved Reinforced Concrete Beam	137
8-4-3: Example No.3: Horizontally Curved Composite Beam	145

Chapter Nine

Parametric Studies

9-1: Introduction.....	154
9-2: Static Parametric Studies	155
9-2-1: Horizontally Curved Steel Beam	155
9-2-1-1: Effect of Tapering Ratio on the Behavior of Horizontally Curved Steel I-Section beam	155
9-2-1-2: Effect of Curvature on the Optimal Tapering Ratio	157
9-2-1-3: Effect of Type of Loading on the Optimal Tapering Ratio	158
9-2-1-4: Effect of Position of Load on the Optimal Tapering Ratio.	159
9-2-1-5: Effect of Ends Restraints on the Optimal Tapering Ratio ..	160
9-2-2: Horizontally Curved Reinforced Concrete Beam	162
9-2-2-1: Effect of Non-prismatic Sections Due to Un-equalled Depths	162
9-2-2-2: Effect of Curvature on the Tapering Ratio.....	165
9-2-2-3: Effect of the Type of Loading on the Optimal Tapering Ratio	166
9-3: Dynamic Parametric Studies	166
9-3-1: Effect of Curvature and Tapering Ratio on the Dynamic Response of Horizontally Curved Steel I-Section Beam	167
9-3-2: Effect of Curvature and Tapering Ratio on the Dynamic Response of Horizontally Curved Reinforced Concrete beam	171
9-3-3: Effect of Curvature and Tapering Ratio on the Dynamic Response of Horizontally Curved Composite beam.....	176

Chapter Ten

Conclusions and Recommendations

10-1: Conclusions	181
10-1-1: Analytical and Representations of Parameters	181
10-1-2: Horizontally Curved Steel Beam	182
10-1-3: Horizontally Curved Reinforced Concrete Beam	184
10-1-4: Horizontally Curved Composite Beam	185
10-2: Recommendations	186
References	187
Appendices	196

Notation

General Symbols

$[A]^T, \{a\}^T$	Transpose of matrix [A] and vector {a}.
$[A]^{-1}$	Inverse of matrix [A].
d, ∂	Differential symbols.
$ \quad , \det.$	Determinant of a Matrix or absolute value.
$\{ \quad \}$	Vector.
$[\quad]$	Matrix.

Scalar

A_s	Area of tension reinforcing steel.
a_0, a_1	Fluidity and damping parameters.
c	Damping parameter.
C_p	Plasticity coefficient.
$d\lambda$	Plastic multiplier.
E	Modulus of elasticity.
E_c	Modulus of elasticity of concrete.
E_s	Modulus of elasticity of steel.
f'_c	Uniaxial compressive strength of concrete (cylinder test).
f_u	Ultimate strength of steel.
F_o	Yield Surface.
F_f	Strength limit surface.
f_y	Yield strength of steel.
f_t	Uniaxial tensile strength of concrete.
f_r	Modulus of rupture of concrete.
G_f	Fracture energy.
G_o	Shear modulus of uncracked concrete.
G_c	Reduced shear modulus of cracked concrete.
H'	Hardening parameter.

H_s	Hardening parameter of steel.
I_1	First stress invariant.
J	Jacobian.
J_2	Second deviator stress invariant.
l_c	Characteristic length of crack.
V	Volume.
W	Weight of a sampling point.
w	Fictitious crack width.
W_p	Viscoplastic energy density.
W_p^f	Viscoplastic energy density at the strength limit
u, v, w	Displacement component, in x, y and z -Cartesian coordinates.
r, s, t	Natural (local) coordinates.
x, y, z	Cartesian coordinates.
α_1	Limit of elastic behavior of concrete.
α_1, α_2	Tension-stiffening parameters.
α_c	Yield surface function.
α	Softening parameter.
β	Shear retention factor.
β, δ	Parameters of Newmark method.
β_o, β_1	Failure surface parameters.
γ	Shear strength.
$\gamma_1, \gamma_2, \gamma_3$	Shear retention parameters.
$\varepsilon, \varepsilon_o$	Strain, and strain at f_c' respectively.
ε_{ref}	Maximum tensile strain reached across the crack.
ε_{su}	Strain in steel at stress f_u .
ε_e^{eff}	Uniaxial elastic strain.
$\dot{\varepsilon}_e^{eff}$	Uniaxial elastic strain rate.
ε_{cr}	Cracking strain.
ε_{vp}	Viscoplastic strain.
$\dot{\varepsilon}_{vp}$	Viscoplastic strain rate.
ν	Poisson's ratio.
$\dot{\pi}_s$	Rate of energy dissipation in the crack.

$\dot{\pi}_v$	Rate of energy dissipation in the volume.
ρ_s, ρ_c	Mass density for steel and concrete respectively.
$\sigma, \sigma_o, \sigma_f$	Stress, yield stress and failure stress respectively.

Matrix

[A]	Displacement gradient matrix.
[B]	Strain- nodal displacement matrix.
[Bs]	Strain- nodal displacement matrix of steel.
[C]	Damping elasticity matrix.
[D]	Constitutive matrix.
[J]	Jacobian matrix.
[K]	Stiffness matrix.
[M]	Mass matrix.
[N]	Shape function matrix.
[T]	Transformation matrix.

Vector

{a}	Nodal displacement or flow vector.
{ \dot{a} }, { \ddot{a} }	Vectors of nodal velocities and acceleration respectively.
{f}	External load vector.
{P}	Internal load.
{r}	Residual load vector.
{u}	Displacement vector.
{ ϵ }	Strain vector.
{ σ }, { $\dot{\sigma}$ }	Stress vector, and stress rate vector respectively.
{ ψ }	Vector of residual forces in dynamic analysis.
{ ψ_t^i }	Vector of residual forces for i-th iteration of time step.

Note: Any other symbol is explained where it appears in the text.

Chapter One

Introduction

1-1: General

Horizontally curved beams are frequently used in building construction and also in heavier engineering structures especially in bridges, Fig.(1-1). Due to the need to augment traffic capacity in urban highways and the constraints of existing land use, there has been a steady increase in the use of curved bridges particularly during the past 25 years. In many cases these bridges are located in on- and off-ramps with various radii of curvature and are characterized by complex vertical and horizontal geometries. Since 1843, when the first treatment of the analysis of curved beams was presented by *Barre' de Saint Venant* [1], thousands of articles on the subject have appeared in literature. Although there has been extensive research devoted to the behavior of horizontally curved beams, a full understanding of their response, especially with regard to non-prismatic members under static or dynamic loading, is still incomplete.

Non-prismatic members are increasingly being used in many structural applications in an effort to achieve a better distribution of strength, weight and sometimes to satisfy architectural requirements. Although the many studies devoted for horizontally curved beams but a very few researches studied the effect of non-prismatic (variable section depth) members on their static behavior, or the dynamic response.

Steel girders curved in plan are frequently employed in structures such as highway bridges. Despite the advantages of non-prismatic construction, engineers

are reluctant to use non-prismatic curved girders in construction because of mathematical complexities associated with geometry and material. Under gravity loading, beams curved in plan are subjected to twisting moments in addition to flexural moments, the interaction between flexural and torsional stresses along the span length is rather complex. Using conventional analytical methods to analyze a structure with material nonlinearities might be too difficult, if not impossible. However, the availability of high-speed digital computers makes it somewhat possible to study the complex nonlinear behavior of such structural elements.

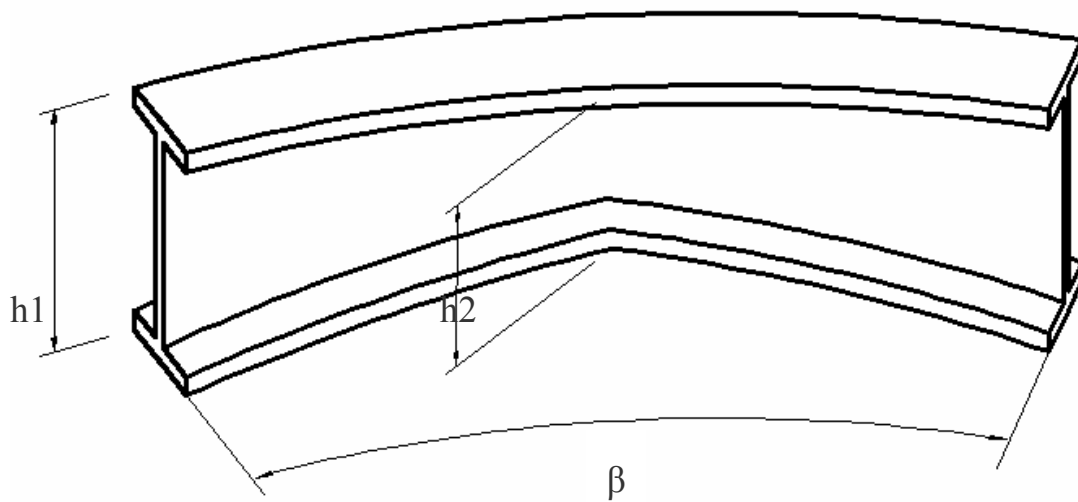


Fig.(1-1): Horizontally Curved Girder Bridges.

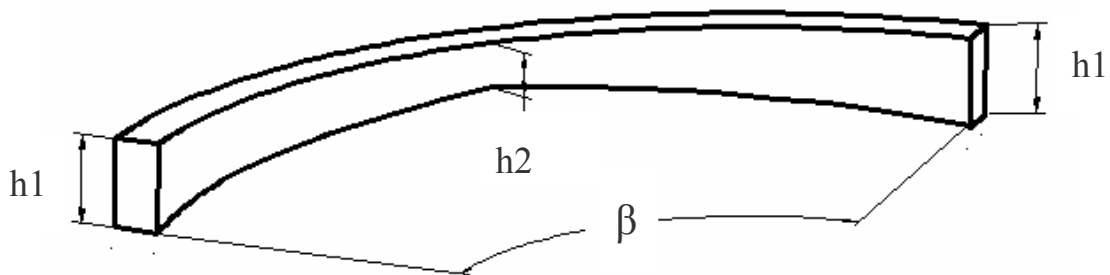
A curved beam becomes a non-prismatic member when the strength of section is not constant along the span. The non-prismatic technique incorporates redistributing of the volume of the material in a way that gives an optimal strength, to improve the behavior of the beam.

The current work is devoted to study of the effect of non-prismatic geometry on the behavior of steel, reinforced concrete and composite curved beams under static and dynamic loads, as well as to find the optimal values of tapering ratio.

The non-prismatic horizontally curved steel beam is considered in the present study including changing the depth of the beam along the span as shown in Fig.(1-2-a), because it represents the most practical case for straight beams, also the non-prismatic geometry of horizontally curved reinforced concrete beam is modeled by changing the depth of the curved beam along the span as shown in Fig.(1-2-b).



a- Non-prismatic Horizontally Curved Steel Beam.



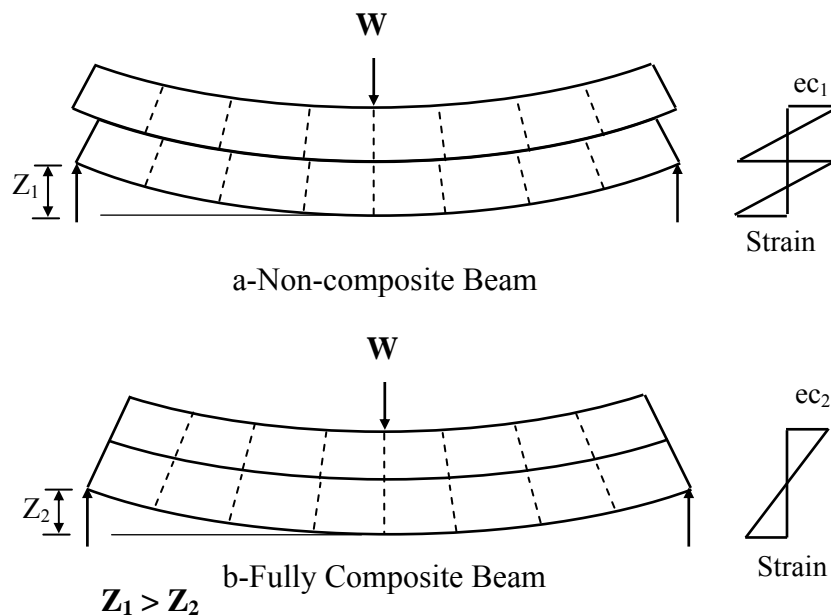
b- Non-prismatic Horizontally Curved Reinforced Concrete Beam.

Fig.(1-2): Non-Prismatic Horizontally Curved Beams.

A structure can be considered composite if the various components are connected to act as a single unit. The structural performance depends on the extent to which the composite action can be achieved. This is illustrated in Fig.(1-3),

which shows the reduction in deflection and strain due to composite action. The presence of interface slip (shown as displacement of the vertical dashed line) can also be observed from the figure. It follows that rigid connections at the interface tend to eliminate slip and hence ensure full composite action in practice; such connections are provided by shear connectors embedded in both components.

In the present study a perfect bond between the materials is assumed without considering the interface element.



Each beam consists of two identical components marked at equal intervals

Fig.(1-3): Behavior of Non-composite and Fully Composite Beams under Equal Load.

Most practical horizontally curved beams are too complex to analyze by classical methods and hence numerical methods are adopted. Among these methods, the finite element method emerged as a powerful analytical tool for analysis of such structures (because of its effectiveness and versatility). This has opened a spacious world for engineers to model rationally many aspects of the phenomenological behavior encountered in steel and reinforced concrete curved beams. These aspects include the nonlinear multi-axial material properties for steel and concrete, modeling of cracking, crushing of concrete, and yielding in steel material. Also the finite element method offers solutions for non-prismatic members of irregular or regular cross-sections under general type of loading.

1-2: Objectives of the Thesis

The main objective of this research is to present two computer programs the first for static analysis and the second for dynamic analysis to study the three dimensional nonlinear analysis of horizontally curved beam (reinforced concrete, steel and composite).

The author programmed a new static model utilizing the model of *Al-Shaarbaf* [2]. In the static model, different aspects of behavior in previously works [2,3,4] that were ignored or treated in an approximate method are taken into account and considered more rationally. Such as, the nonlinear behavior of stresses in the direction perpendicular to the crack after the crack is closed, behavior of beam after crushing at some Gauss points, degradation in the compressive strength at Gauss points when the compressive strain is greater than that one corresponding to the peak uniaxial compressive stress, the division of incremental strains into two or three or four sub-increments when one or two or three cracks are closed (or re-closed) respectively to handle each sub-increment individually, and the tensile strength in a Gauss points may be reached to zero [5]. The static model is coded in this study as, *NFHCBSL* (Nonlinear Finite element analysis of **H**orizontally **C**urved **B**eam under **S**tatic **L**oad).

The dynamic model is coded in this study as, *NFHCBDL* (Nonlinear Finite element analysis of **H**orizontally **C**urved **B**eam under **D**ynamic **L**oad), and programmed by the author utilizes the open software program named *DARC3* [6]. The differences between the two models will be mentioned in the introduction of chapter eight. The present model can deal with the reinforced concrete, steel and composite beams. Also the *NFHCBDL* can be used for solving the accelerated time history problem.

Several examples subjected to static or dynamic loads, have been analyzed. A comparison between the analytical results and the experimental (or/and other analytical) results has been carried out.

The developed computer programs have also been used to study:

- The effect of crushing at some Gauss points on the behavior of the reinforced concrete horizontally curved beam.
- The effects of non-prismatic geometry (due to depth) on the static behavior and ultimate strength of curved beams (reinforced concrete and steel).

- The effects of non-prismatic geometry on the dynamic response of the curved beams (reinforced concrete, steel and composite).
- The effects of the curvatures of the horizontally curved members on their static and dynamic behavior.
- The effect of end restraints on the optimal tapering ratio of non-prismatic horizontally curved beam for different types of loading.

1-3: Layout of the Thesis

In view of the objective, this study consists of ten chapters and seven appendices.

Chapter One monitors a general introduction describing the significance of horizontally curved beams and the benefit of using non-prismatic members as well as the problem and the aim of study.

In **Chapter Two** a brief review of early studies related with the curved beam in plan (reinforced concrete, steel and composite), nonlinear finite element analysis, static and dynamic analysis of horizontally curved beams with an interpretation of results as possible

Chapter Three describes the basic concepts of the finite element method, incorporates the static and dynamic formulation. Also the shape functions of the 20-node isoparametric brick elements which are used to model steel and concrete and the representations of the embedded reinforcement are illustrated in this chapter. The mass matrix and the damping matrix are presented in this chapter in addition to the numerical integration rules to determine the element stiffness and mass matrices.

Chapter Four describes the observed behaviors of materials under static loads and the models used in the current static study, incorporated the representation of concrete (stress-strain model to model the behavior of concrete prior to failure, failure criteria to simulate cracking and crushing types of fracture, a method of crack, a post-cracking stress-strain relationship and the modeling of the reduction in compressive strength due to orthogonal cracking), steel representation, and the representation of bars reinforcement within the concrete brick element.

Chapter Five contains the available information regarding the dynamic response in the behavior of concrete and steel. This chapter is devoted to illustrate the behavior and the adoption of model of concrete and steel under transient dynamic loads, as well as the classical elasto/viscoplastic constitutive model which was required for representation of steel and concrete structures under dynamic loads.

Chapter Six is devoted to represent the numerical techniques which were used in solving the nonlinear simultaneous equations of the numerical nonlinear static and dynamic equilibrium equations, as well as the convergence criteria adopted in the static and dynamic models.

Chapter Seven deals with the analysis of elasto-plastic horizontally curved beams under static load. Numerical tests were carried out and compared with experimental and other analytical results. Parametric studies were performed to investigate the effects of some material and numerical parameters within the static model *NFHCBSL*. The flow chart of the computer program *NFHCBSL* is also presented in this chapter.

Chapter Eight deals with the dynamic elasto-viscoplastic response of horizontally curved beams. The presented dynamic model *NFHCBDL* is used to analyze some examples and the results are compared with other analytical results drawn from *ANSYS* [7] (analytical packaged model, version 5.4) to check the applicability of the current model. The flow chart of the computer program *NFHCBDL* is also presented in this chapter.

In **Chapter Nine** many parametric studies were carried out by using the presented static and dynamic programs *NFHCBSL* and *NFHCBDL* respectively. Such studies include the effects of non-prismatic geometry, curvature of beam and ends restraints on the behavior of curved beams.

Finally, **Chapter Ten** summarizes the most important conclusions drawn from this study and gives several recommendations and suggestions for future work in this subject.

Chapter Two

Review of Literature

2-1.Introduction

The nonlinear analysis of horizontally curved beam had taken a considerable interest and a large amount of literature. In this chapter, a brief review of the various models that are available is included. The literature which concerns the three dimensional finite element nonlinear analyses is presented at first then the static analysis of horizontally curved beam is reviewed. Finally the literature of the dynamic analysis which had the same conduct is presented.

2-2.Nonlinear Finite Element Analysis:

In 1968, Nilson [8] developed a finite element system interconnected only at discrete points and the resulting structure is analyzed as an indeterminate system. The method is used to determine the internal stresses and displacements for reinforced concrete members subjected to progressively increasing load, with recognition of the several sources of nonlinearity. The resulting model permits considering the: 1-influence of reinforcement, 2-changing topology due to progressive cracking, 3-realistic bond stress transfer between concrete and reinforcement, and 4-nonlinear material properties. The incremental loading

permits a study of member behavior through the entire range from zero loads up to ultimate. The author concluded that: the accuracy of result depends upon the validity of the model. All important effects must be accurately modeled; a finite element analysis of reinforced concrete behavior provides a valuable supplement to laboratory investigations and may lead to important changes in methods of design.

In 1977, Mondkar and Powell [9] introduced theoretical and computational procedures which have been applied in the design of a general purpose computer code for static and dynamic response of a nonlinear analysis. The formulation of the incremental equations of motion for structure undergoing large displacement finite strain deformation was presented. Also the incremental equations were linearized for computational purposes, and the linearized equations were discretized using isoparametric finite element formulation. The equations of motion were integrated using *Newmark's* generalized operator. The solution strategy defined in terms of a number of solutions parameters is implemented in a computer program therefore several solution schemes can be obtained by assigning appropriate values to the parameters. The results revealed good agreement when compared with the experimental results.

In 1979, Bathe and Ramaswamy [10] presented the formulation and numerical implementation of a three-dimensional concrete model that has been incorporated and evaluated in the computer program *ADINA* [11]. Geometric and material nonlinear formulations are obtained using the principle of virtual displacements. The model adopted employs three basic features to describe the material behavior, namely: 1-a nonlinear stress-strain relation including strain-softening to allow for the weakening of the material, 2-a failure envelope that defines cracking in tension and crushing in compression, and 3-a strategy to model the post-cracking and crushing behavior of material. The authors concluded that the proposed model can already be employed effectively for solution of various problems. Also significant further studies to evaluations and improvements of the model are needed.

In 1981, Arizumi et al. [12] introduced a nonlinear finite element analysis of composite beams with incomplete interaction. A simplified nonlinear model was assumed in this approach and it can be applied to the elastic-plastic analysis of reinforced concrete and composite beams with incomplete interaction. The elastic-plastic behavior of partial composite beams without shear connectors in the negative bending moment regions was described in this study. A simply supported reinforced concrete beams and continuous composite beams were analyzed. The numerical results are compared with test results and existing values based on other numerical methods, and found to be in a good agreement. The authors concluded that the proposed method can be applied to analyze the simply supported and continuous composite beams with both regularly and irregularly spaced shear connectors.

In 1987, Chajes and Churchill [13] dedicated their study to the basic concepts involved in the construction of load-deflection curves for geometrically nonlinear systems by finite element method. Three procedures were used in solving the nonlinear problems. These are, the linear incremental, the nonlinear incremental, and the direct method. They derived the governing equation for each method and presented the procedure used to plot the load-deflection curves. They concluded that the linear incremental method requires the use of smaller load increments than those needed when using the nonlinear incremental method, because the latter is an iterative method within each load increment. In the direct method, which is iterative also, they applied the entire load as a single step.

In 1990, AL-Shaarbaf [2] presented a nonlinear finite element model suitable to analyze the reinforced concrete structures under general three dimensional state of loading. The 20-node isoparametric brick element had been used to model the concrete and the reinforcement was treated as an axial member embedded within the concrete. The compressive behavior of the concrete was simulated by an elasto-plastic work hardening model followed by a perfectly plastic plateau which is terminated at the onset of the crushing. A smeared crack

model with fixed orthogonal cracks was adopted. The nonlinear equations of equilibrium had been solved by using an incremental-iterative technique operating under load control and standard or modified *Newton-Raphson* methods were used as algorithms solution. “The study was devoted towards the analysis of reinforced concrete members which fail in shear or torsion modes”. The researcher concluded that in the presence of a compressive strength reduction model, the tension-stiffening parameters required for reinforced concrete under torsion should be similar to those used for members in which bending dominates. The researcher assumed a linear behavior of stresses in the direction perpendicular to the closed crack and ignored the nonlinearity in that direction. The analysis stopped at the first crushing of any Gauss point.

In 1996, Davidson et al. [14] used the finite element method to create detailed models of horizontally curved steel I-girder bridges connected by cross-frames. The effects of a number of parameters on the behavior of the curved girder system were established and compared with the effect of these parameters in straight girder systems. The parameters which had the most significantly effect on the behavior of the system were the degree of curvature, span length and flange width. They presented an equation which was developed and based on a nonlinear statistical regression to provide a preliminary design limit for the cross-frame spacing interval.

In 2000, Simpson [15] presented an analytical study of the nonlinear modeling of horizontally curved steel girders and bridges. This research was accomplished by incorporating large deflection and nonlinear material behavior into three dimensional finite element models generated by using the program *ANSYS*. The choice to use *ANSYS* was based upon the availability of computing resources; they need for both geometric and material nonlinear capabilities and the desire for reliable graphical review of the input and output. The researcher demonstrated that accurate predictions of load-deformation response and ultimate strength are attainable via the finite element method by using this analytical package. The method is then extended to study the behavior of a number of

horizontally curved girders for which no experimental data exists. The influence of assumptions on the elastic stability behavior of a curved beam is also examined. From the conclusion he found that the chosen shell element, **SHELL43**, represents an efficient choice for the analysis conducted in this study. Also the finite element method is evaluated as a tool for assessing the behavior of curved bridges.

In 2001, Al-Sherrawi [16] studied the nonlinear response of composite beams by using the finite element method. In this study, the material nonlinearities as a result of nonlinear response of concrete in compression, crushing and cracking of concrete, yielding of reinforcement bar, shear-slip and dowel action between the precast concrete beams and cast-in-situ slabs were presented. A two dimensional plane stress finite element type is used to simulate the concrete, while reinforcement bar was represented by using one dimensional bar element. The shear-slip and dowel action were modeled by using shear transfer interface elements with appropriate stiffness value and linkage elements with two springs at right angles. Good agreement was found when the numerical results were compared with the available experimental results.

In 2005, Al-Thebhawi [3] developed a nonlinear finite element computer program for the analysis composite steel-concrete straight beams. The 20-node isoparametric brick element has been used to represent the concrete slab and steel stem while reinforcing bars are idealized as axial members embedded within the concrete elements. Also, a space bar element which has two end nodes with three translation degrees of freedom at each end has been used to model the shear connectors at the interface between the concrete slab and steel I-section beam. He found that if the strength of concrete increases from 20 MPa to 70 MPa the ultimate load increases by about 15% and an increase in the ratio of the thickness to width of concrete slab (t/B) from 0.1 to 0.3 leads to an increase in the ultimate load by about 30%. The part of his model which is concerned with the reinforced concrete representation was taken from *Al-Shaarbaf* model thus the model stopped at the first crushing of any Gauss point; hence the entire load-deflection curve cannot be achieved.

2-3. Static Analysis of Horizontally Curved Beam:

In 1932, Oesterblom [17] presented useful graphs for circular horizontally curved beam fixed at both ends under uniformly distributed load. The theorem of least work is adopted, and using **Castigliano** method to find the bending moment at mid-span (M_c) where shear and torsion are equal to zero. Then the equations of bending (M_{Qb}) and torsion (M_{Qt}) moments along the horizontally curved beam were solved as follows:

$$M_c = w r^2 (U - 1) \quad \dots\dots\dots (2-1)$$

$$M_{Qb} = w r^2 (U \cos\alpha - 1) \quad \dots\dots\dots (2-2)$$

$$M_{Qt} = w r^2 (U \sin\alpha - \alpha) \quad \dots\dots\dots (2-3)$$

$$U = [2(K+1)\sin\theta - 2K\theta\cos\theta] / [(K+1)\theta - (k-1)\sin\theta\cos\theta] \quad \dots\dots\dots (2-4)$$

$$K = EI / (G I_t) \quad \dots\dots\dots (2-5)$$

where;

w = uniformly distributed load on curved beam per meter length

r = radius of curved beam

E = modulus of elasticity for direct stress

G = modulus of rigidity

I = equatorial moment of inertia

I_t = torsional moment of inertia

α, θ as shown in Fig.(2-1) below

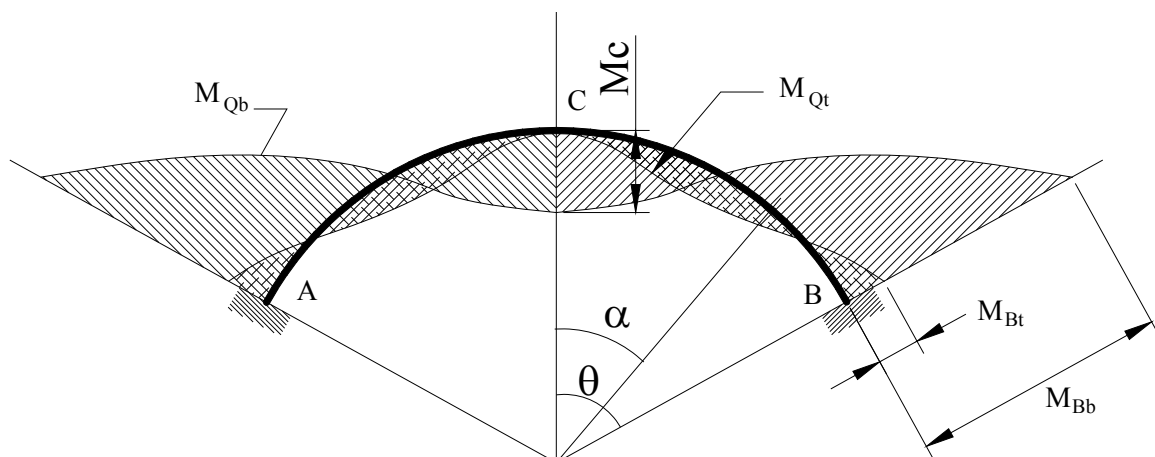


Fig.(2-1): Horizontally Curved Beam, Typical Moments Diagrams[17].

In 1963, Chu, and Thelen [18] performed a plastic analysis for a circular arc with a subtended angle not more than 180° , with a constant cross-section, fixed ends conditions, and subjected to uniformly distributed load perpendicular to the plane of arc. The yield surfaces for combined bending and torsion moments, at a section where a plastic hinge was formed, had been represented by:

$$m_o^2 + t_o^2 = 1 \quad \dots\dots\dots (2-6)$$

$$m_o = M / M_p \quad \dots\dots\dots (2-7)$$

$$t_o = T / T_p \quad \dots\dots\dots (2-8)$$

M = bending moment at the cross section (applied).

T = torsion moment at the cross section (applied).

M_p = full plastic bending capacity of the cross section.

T_p = full plastic torsional capacity of the cross section.

The method of analysis was examined, and the various mechanisms of failure were investigated. The results of the load capacity of curved members were outlined in a chart to facilitate their application.

In 1974, Jordaan et al. [19] developed plastic analysis methods for the determination of collapse loads for horizontally circularly curved beams and subtending a central angle less than 180° . The analyses were for the case of two concentrated loads placed at any point on the arc of the beam. The methods presented are an extension of existing analyses that have been developed for single concentrated loads or distributed loads. The modes of failure considered are valid for beams with constant plastic moment and torque capacities at any section of the beam. Thus, for reinforced concrete case the analyses are restricted to prismatic beams having constant reinforcement.

In the experimental part of this study, four curved and six straight reinforced concrete beams were tested. According to the amount of reinforcement, the curved beams were divided into two groups, one curved beam from each group was tested under single load while the second under two concentrated loads.

The authors concluded that, the plastic theory used could give satisfactory prediction of the mode of failure, i.e., the location and type of plastic hinge, but the

predicted values of ultimate load were conservative for some modes and were slightly higher than the experimental values for other modes.

In 1977, Badawy et al. [20] presented experimental and analytical studies to investigate the applicability of plastic methods (which include the shear effect) to predict the ultimate load and failure mode of a horizontally curved beam, as well as the effect of non-prismatic case (non-uniform distribution of shear reinforcement along the curved beam). The study contained also the effects of end restraints. Eight curved beams were tested under single load acting at the same point. Four beams were identically reinforced but tested with various end conditions. Two beams were completely fixed at both ends but had two different arrangements of reinforcement, and the remaining two beams were completely fixed at one end and torsionally restrained at the other but had two different arrangements of reinforcement. This study concluded that, the methods of plastic analysis can be applied to reinforced concrete curved beams, but it should be kept in mind that the application of these methods is conditional upon the ductility of the critical sections (where plastic hinges are formed) up to the formation of a mechanism, the flexural restraint is much more effective than the torsional restraint in increasing the ultimate load and in decreasing the deformation, and the ultimate load can be increased by increasing the strength of the cross-section in “certain regions, the location of these regions must be carefully chosen”.

The study did not show the locations that must be chosen to be heavy reinforced to improve the strength of the beam. The research did not study the non-uniform distribution in the longitudinal reinforcement. Also the effect of the curvature of the beam on the locations of the critical sections was not examined.

In 1981, Abul Mansur and Rangan [21] tested three fixed ended curved beams designed by three methods under a concentrated load at angle 30° . The methods investigated are: (1)- a collapse load method proposed by *Badawy et al. [20]*, (2)- the classical elastic method based on un-cracked sections, and (3)- a limit design method proposed by the authors. The limit design methods depended on some previous studies[22,23], which appeared that in statically indeterminate

systems, in which it is necessary to consider torsional effects, a satisfactory and economic design can be achieved by assuming an ultimate design torsional moment equal to $(0.33\sqrt{f_c'}(x^2 y/3))$ at critical sections. Another additional condition is required to obtain the solution. The location of the inflection point can be assumed. In this study the position of one of the inflection points was assumed at an angle 21° from the support closer to the load point. This position is approximately equal to the value given by the elastic analysis. The authors concluded that: 1-the redistribution of internal forces in reinforced concrete curved beams occurs at two stages: one after cracking and the second after the formulation of some of the plastic hinges, 2-the designing of a reinforced concrete curved beam for a pure flexure mode collapse “may” not economical.

In 1985, Hasebe et al. [24] investigated the effects of curvature and the effects of cross section dimensions on the effective width of horizontally simply supported curved beams of box and channel cross section under uniformly distributed loads. The theory used in this analysis was the refined beam theory by Kano et al.[25]. The effective width for curved girder bridges, inside λ_1 and outside λ_2 , are defined for the center of curvature as:

$$\int_{R-b}^{R-b+\lambda_1} \bar{\sigma} \, dr = \int_{R-b}^R \sigma \theta \, dr \quad \dots\dots\dots(2-9)$$

$$\int_{R+b-\lambda_2}^{R+b} \bar{\sigma} \, dr = \int_R^{R+b} \sigma \theta \, dr \quad \dots\dots\dots(2-10)$$

in which,

R = radius of the curved girder, $2b$ = width of the flange

$\sigma\theta$ = flange stress derived from present theory

$\bar{\sigma}$ = straight line between two maximum stresses $\sigma\theta_1, \sigma\theta_2$

The authors concluded that, in the case of a concentrated loading, the values of the effective width ratio are minimum at the center of the span length and increase rapidly towards the supports while in the case of uniformly distributed loading the values are maximum at the mid-span and decrease towards the supports. Also the

effects of curvature on the effective width was so little that to be neglected with only a few exceptions for cases with small R/L ratios and under concentrated load. Finally the effective width ratio is independent on the cross sectional dimensions of the curved beam under uniform loading but it is dependent for concentrated loading.

In 1990, Hsu et al. [26] developed an exact horizontally curved beam finite element in which the true warping degree of freedom conforms to the bimoment (warping). The variation method was used to formulate the stiffness matrix and the results of solution were compared with other studies using closed form solution. The authors demonstrated the capability of the stiffness matrix of a horizontally curved beam element. The stiffness matrix which contains the warping restraint had been given in an explicit form and can be easily implemented on a computer program. Also the results obtained from this study show good agreement when compared with the theoretical results. An important note is that, this stiffness matrix for the horizontally curved beam element is valid for both open and closed sections as long as the curved member is modeled as a curved beam structure. It is important to know that this stiffness matrix can be used for homogeneous materials only.

In 1995, Shanmugham et al. [27] tested ten steel curved beams. The results obtained from experiments on two sets of I-beams (seven comprising rolled sections and three built-up sections) are presented. The objectivity of this paper is to determine the ultimate load carrying capacity of steel I-beams with intermediate lateral restraint and to examine the effect of curvature on the behavior of these beams under bending loads. Test results for deformations and ultimate strength are found to be in good agreement with the corresponding values predicted by using the elasto-plastic finite element analysis. The effects of radius of curvature to span-length ratio (R/L) on the ultimate strength are considered. Each curved beam was subjected to a concentrated load applied at an intermediate point when the beam was laterally restrained. The ratios (R/L) which were studied were (1.562-30.0). The experimental results proved that the load carrying capacity decreases with the

decrease in the (R/L) ratio. The authors concluded that the comparison of the experimental and theoretical ultimate load results shows that the *ABAQUS* [28] finite element analysis is capable of predicting the ultimate load with reasonable accuracy. The theoretical predictions in most cases were conservative by about 8%

In 1998, Sennah and Kennedy [29] summarized the result from an extensive parametric study, using the finite element method in which 120 simply supported curved bridge prototypes were analyzed to evaluate the shear distribution in the web due to truck loading as well as dead load. The experimental study involved the construction, instrumentation and testing of four (1/12) linear scale three cell bridge model. The parameters considered in the study are: cross bracing system, aspect ratio, number of lanes, number of cells and degree of curvature. The result appeared that: 1-curvature is the most critical parameter that influences the shear distribution in multi-cell bridges (increase in the degree of curvature increase the upward shear force in web close to the outer side of curvature as well as the downward shear force in webs close to the inner side of curvature), 2-for the same number of lanes, the shear distribution factor decreases with increase in the number of cells, 3-an increase in the bridge aspect ratio increases the shear distribution factor for both the outer and inner webs, 4-the presence of intermediate cross bracing affects the shear distribution factor and it is recommended that at least three equally spaced cross bracing per span be used to produce a relatively constant shear distribution factor.

In 1999, Thevendran et al. [30] devoted their study to the behavior of structural steel-concrete composite beams curved in plan. The finite element package *ABAQUS* has been used to study the nonlinear behavior and ultimate load-carrying capacity of the horizontally curved composite beams. A three dimensional model has been adopted. Shell elements have been used for simulating the behavior of concrete slab and steel girder, and rigid beam elements to simulate the behavior of shear studs. Five large scale composite beams with span length to radius of curvature (L/R) ratios ranging from (0-0.5) were tested to failure under a

concentrated load applied at mid-span. The study concluded that the predicted initial yield loads by the analyses are somewhat larger than the values obtained from the experimental results and the maximum deviation was about 10%. While the deviation of initial crack load was between (-29% to 23%). Therefore the *ABAQUS* program can predict the yield load well but cannot predict crack loads accurately. Also the results show that the maximum deviation in the prediction of ultimate strength has been found to be 14% and the results established the validity of the proposed finite element model.

In 1999, Sennah and Kennedy [31] summarized the result from an extensive parametric study, using the finite element method in which simply supported curved composite multi-cell bridge prototypes were analyzed to evaluate the moment and deflection distributions between girders, as well as the axial forces expected in the bracing system, due to truck loading and the dead load. Results from tests on four (1/12) linear scale, simply supported curved composite concrete deck-steel multi-cell bridge model were used to substantiate and verify the analytical modeling. The authors outlined that: 1-the curvature is the most critical parameter that influences the design of girders and bracing members in multi-cell bridges, 2-increase in the degree of curvature increases the moment and deflection as well as the maximum force in a bracing member, 3-increasing the bridge span increases the moment distribution factors for the outer and inner girders and decreases them for the intermediate girders, as well as increases in the deflection distribution factors and maximum axial forces in bracing members, and 4-the presence of intermediate cross bracing had affects on the moment and deflection distribution factors as well as the maximum axial force in a bracing.

In 2000, Zureick et al. [32] presented an analytical and experimental efforts dedicated to establish the size of the full-scale components that will be tested as a part of an entire three-girder bridge system, as shown in Fig.(2-2). By the finite element method utilizing *ABAQUS* package, the system was analyzed under six concentrated loads (two-point loads on each girder).

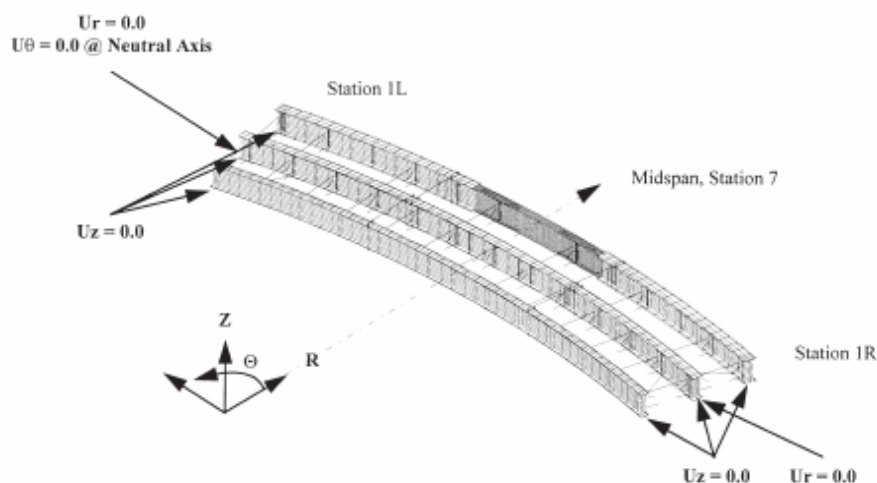


Fig.(2-2): Finite Element Model of Three-Girder Bridge System.

The results showed that the exterior girder takes most of the load, and that the interior girder contributes relatively little to the strength of the system for this loading condition only. This is true even though a substantial number of stiff cross-frames exist in the interior spaces between two girders. Also, the strength of exterior girder drops gradually by less than 10% as the buckling begins.

In 2001, Young-Lin and Bradford [33] investigated the nonlinear elastic-plastic behavior of steel I-section beams curved in plan under vertical loading and proposed a straight forward formula for their design against combined bending and torsion actions. The material and geometric nonlinearity are included in this study. Three types of simply supported I-section steel curved beam (continuously braced, centrally braced, and unbraced) under mid-span concentrated load were investigated analytically. Three lower-bound design interaction equations were proposed for steel I-section beams curved in plan based on finite element study, one for continuously braced against in-plane bending and free torsion, the second for centrally braced against in-plane bending and free torsion, and third for unbraced against in-plane bending and destabilizing torsion. Comparisons with rational finite element results and existing experimental results show that the proposed interaction equations give a good lower bound for the design of horizontally curved beams (steel I-section).

2-4. Dynamic Analysis of Horizontally Curved Beam:

In 1968, Tan, and Shore [34] introduced a method of analysis for investigating the dynamic response of an identical bridge under the passage of a forcing system consisting of masses that simulate a vehicle. The classical beam theory is adopted, neglecting the effects of shearing deformation, flexural rotatory inertia and axial forces. For the bridge-vehicle system, it is further assumed that the centrifugal force resulting from the load moving on a curved path is counteracted by the centripetal force resulting from super-elevating the horizontally curved bridge. The authors concluded that, the shape of the response curves, i.e., the dynamic increments with respect to horizontal curvature and rigidity ratio, is the same for either a moving mass or a constant force. The magnitudes of the dynamic increments in general are greater for the moving mass. Also for frequency ratio and weight ratio of the order of 0.3 or less, the response of the bridge can (for all practical purposes) is considered to be equal to that given by the constant moving force solution.

In 1969, Culver and Oestel [35] presented a method of analysis for determining the natural frequencies of multi-span horizontally curved girder. The use of the method is illustrated by developing the frequency equation for a two-span curved girder by using the *Rayleigh-Ritz* method together with the Lagrange multiplier concept. The terminal supports of the beams are assumed to be simple supports, at which the normal stresses resulting from bending and torsion are equal to zero. The bending moment and bimoment were expressed in terms of the second derivatives of the deflection v and twist ϕ and they are therefore equal to zero at the ends. Both deflection and twist are assumed to be prevented at all intermediate supports. The cross sectional shape is assumed to be constant along the entire length of the member and it is doubly symmetric. Both prismatic and thin-walled open sections were considered. The numerical results proved good agreement with the existing solutions.

In 1977, Chaudhuri and Shore[36] presented a method and a result of the dynamic analysis of simply supported horizontally curved I-girder bridges subjected to simulated highway loadings including the centrifugal forces. The effects of vehicle inertia are included in the study and found to be important. The fundamental aim of this study was to develop and suggest preliminary impact factors to be used in designing the horizontally curved I-girder bridges. The curved beam is considered to have a constant radius of curvature and with constant super-elevation, the material of the deck is assumed to be homogeneous, cylindrically orthotropic and linearly elastic so that *Hooke's* law applies, the material of the I-girders is assumed to be homogeneous, isotropic, and obey *Hooke's* law, the effect of damping is neglected. Many conclusions were outlined such as: 1-the impact factors increase as the speed of the vehicle increases. 2-the in-plane deflections are small compared to the out-of-plane deflections. 3-the impact factors for the support reactions are comparatively higher than that for straight bridge of equal span.

In 1987, Al-Marouf [37] introduced a finite element computer program to study the dynamic linear behavior of curved members under free and forced vibration. Different curved elements were used in the program to determine their effectiveness in analyzing the dynamic linear behavior of curved members. Many charts are presented that can be used to compute the natural frequencies of arches for different boundary conditions and different cross sections. A wide range of dynamic analysis was performed, including the earthquake effects, blast pressure, and impact loads. He concluded that: 1-the finite element method is an efficient method in predicting the dynamic linear behavior of curved members. 2-he found that the *Newmark- β* and *Wilson- Θ* methods more stable than the *Houbolt* method. 3-the new circular curved thin-walled bar element is an exact one considering the effects of initial curvature and warping restraint on non-deformable open and closed sections.

As shown the model cannot be used to analyze the reinforced concrete or composite members, the nonlinearity of materials and damping effects were ignored.

In 1988, Laura et al. [38] introduced a paper to deal with the determination of the fundamental frequency of vibration of circumferential arches with varying thickness by following the optimized-Ritz procedure developed in Ref.[39]. Three types of boundary conditions, hinged, clamped, and clamped-free with the effect of concentrated mass were considered and only the bending affects have been taken into account in the investigation. The fundamental mode shape is approximated by means of a polynomial co-ordinate function in the angular co-ordinate which includes an exponential optimization parameter. The results of an independent finite element solution are also presented and, in general, good agreement with the analytical solution was obtained.

In 1988, Cervera, et al. [6], presented a three dimensional nonlinear finite element computer program coded (*DARC3*) to deal with the transient dynamic analysis. Two types of materials can be considered: reinforced concrete and steel. Eight and twenty-node, hexahedral, isoparametric finite elements were used for the spatial discretization. The steel reinforcement was incorporated in the concrete brick element by assuming perfect bond and the classical elasto/viscoplastic constitutive model was adopted. A related model is adopted for concrete structures with allowance made for rate dependency and damage accumulation in the concrete. Tensile cracking is considered using the smeared crack approach and the constant fracture energy release concept. Six and fifteen Gauss integration points can be used. The lumped mass matrix was adopted and the *Newmark- β* method was used to solve the dynamic equations. The damping effect was considered by using *Rayleigh* damping method. Several examples are presented to illustrate the applications of the computer model in civil engineering.

In 1989, Rossi et al. [40], dedicated their study to the determination of the fundamental frequency coefficient of non-circular arches of non-uniform cross section, rigidly clamped at one end and carrying a concentrated mass at the other. Three methodologies are employed: approximating the fundamental mode by means of polynomial co-ordinate function, following Ritz method to generate the frequency equation and a finite element method. The vibration of the arch structural system was studied in one of its normal modes. The types of geometric

parameters that were considered are: parabola, catenaries, spiral, circle, and cycloid. A general conclusion drawn from the study that one can affirm is that **Rayleigh's** optimization approach with a single term solution yields very good engineering accuracy for the fundamental frequency coefficient of the arch-type structures considered. Good agreement was obtained by following the different methodologies for all the situations considered.

In 1992, Ahmed and Jaafar[41] considered the out of plane small vibration of a horizontally circular curved element on **Winkler-Pasternak** foundation with the effects of damping and warping are neglected. The **Timoshenko** theory [42,43] was adopted in this study. The authors concluded that: 1-the natural frequencies decrease as the central angle of the arc increases, and this effect becomes significant for lower mode, 2-the natural frequencies increase as the coefficient of subgrade reaction increases and becomes significant for the lower modes and for the larger values of the central angle, 3- the natural frequencies increase as the width of the contact area between the beam and the foundation increases (this effect becomes more significant for the lower modes and the larger value of central angle).

In 1993, Richardson and Douglas [44] introduced the results of a unique field test on a curved highway overpass. In the test, large horizontal loads were applied to the superstructure of the bridge and quickly released; causing the bridge to vibrate, resulting large-amplitude vibrations which were intended to be similar to the vibrations caused by earthquakes (horizontal accelerations of up to 25 percent of gravity were measured on the bridge deck). Well-defined lateral, longitudinal, vertical and torsional vibration modes were identified from the test data. The vibration modes were used to verify an analytical model of the bridge's dynamic response. For this paper, the model was verified by using only the fundamental vibration mode, which was primarily a horizontal vibration mode. Using a system identification procedure, the dynamic response model was adjusted until its frequency and mode shape matched the measured frequency and mode shape. Parameters in the verified model were compared with the same parameters calculated from information in the structural drawings. Because the fundamental

mode represents a horizontal mode, the bridge parameters identified in this paper were parameters that strongly influence the horizontal response of the bridge.

In 1997, Sengupta and Dasgupta[45] presented a five-node thirteen degree of freedom horizontally curved beam element with or without an elastic base. One set of fourth-degree *Lagrangian* polynomials in natural co-ordinates is used for interpolation of the beam geometry and vertical displacement while the angles of transverse rotation and twist are interpolated by another set of third-degree polynomials. For elastic subgrade, the reactive forces offered at any point are assumed to be proportional to the corresponding displacements at that point. The effect of shear deformation is accounted for in the stiffness matrix. In mass matrix evaluation, for dynamic problems, translational as well as rotary inertias have been considered and studied separately. For numerical integration of the stiffness matrix, the four-point Gaussian scheme has been found to be adequate. Numerical results for a number of sample problems and their comparison with analytical solutions have been presented for circular as well as for non-circular curved beams. The performance of the element has been found to be excellent in both static and dynamic conditions.

In 2001, Dongzhou [46] analyzed seven three-span continuous single curved box girder bridges, with overall span lengths ranging from 76.2 to 213.36 m, due to vehicles moving. The box girder is divided into a number of thin-walled beam elements; both warping torsion and distortion were considered in the study. The analytical vehicle is the HS20-44 truck included in the *AASHTO* specifications [47] and simulated as a nonlinear vehicle model with 11 degrees of freedom. Truck parameters included the body, suspensions, and tires. The author concluded that: 1-the natural frequencies of curved box girder bridges increase with the increase of radius. 2-the impact factors of bridges vary with load positions. 3-completely neglecting the effect of damping will significantly overestimate the dynamic loading of continuous single box girder bridges. 4-the impact factors of torque, distortional torque, and bimoment rapidly increase with vehicle speed, while the vertical shear and bending moment do not have such a tendency.

In 2003, Maneetes and Linzell [48] examined the response of an experimental, single-span, non-composite, curved I-girder bridge superstructure during free vibration. Finite element models for the experimental bridge system, which was tested for the FHWA Curved Steel Bridge Research Project (CSBRP), were constructed and calibrated against experimental data from dynamic investigations of the bridge by the Virginia Transportation Research Center (VTRC). Parametric studies of the experimental curved bridge system were conducted using these finite element models to investigate the effects of cross-frame and lateral bracing parameters on the structure's free vibration response. The authors concluded that the natural frequencies, stresses and displacements for this structure (X-type cross-frames) were higher than those for K-type frames. The behavior of the two systems could be considered nearly identical, also the lateral bracing orientation in plane had a negligible effect on vertical bending stress, in this structure, caused by self-weight.

In 2006, Al-Dahash [49] presented a nonlinear analysis study of three dimensional reinforced concrete arches subjected to dynamic loading by using the open software program named *DARC3* [6]. The later model takes into account the material nonlinearities such as cracking of concrete, strain softening after cracking, the nonlinear response of concrete in compression, crushing of concrete and the yielding of the reinforcement. Eight and twenty-node hexahedral isoparametric elements were used for the spatial discretization of concrete, while the steel reinforcement is assumed to have uniaxial properties in the direction of the bars and it is incorporated in the concrete brick element by assuming a perfect bond. Concrete is considered as a linear elastic-strain softening material in tension and as an elasto-viscoplastic material in compression. A classical elasto-viscoplastic model is used in the present study to model the reinforcement. One of the conclusions was the deflection and shear stresses of the arch without damping are greater than deflection and shear stresses with damping by maximum difference about (60%) and (79.6%), respectively.

In 2006, Tilley et al. [50] developed a model of the FHWA (Federal Highway Administration) curved girder bridge using both beam and shell elements and the response information was compared with experimental data and with

analytical data from other finite element codes. The experimental data were obtained during dynamic testing of the full scale bridge in the Turner-Fairbanks Structures Laboratory and analytical response information was provided from finite element models of the bridge using *ANSYS* [7] and *ABAQUS* [28]. The primary focus of the study was the prediction of frequencies and mode shapes of the full-scale curved girder both with and without a deck as shown in Fig.(2-3). *SAP2000* [51] models were found to be more adequate for predicting the lower modes and frequencies of the bridge. The results of this study gave an idea of how effective *ANSYS* and *SAP2000* can be used for the dynamic analysis.

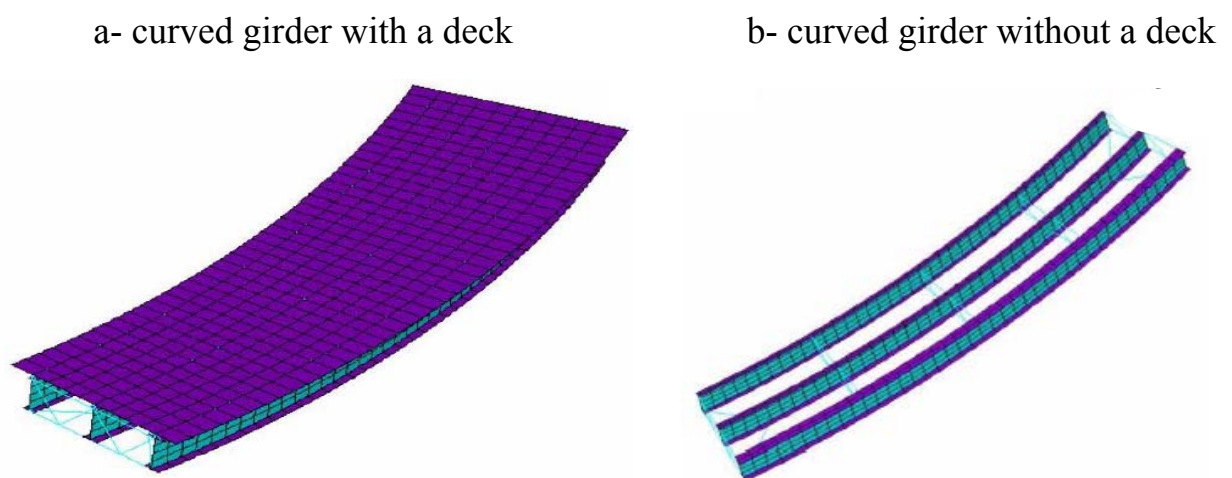


Fig.(2-3): ANSYS Finite Element Model of Curved Beam.

As shown, little research (according to the available review) towards the study of the effects of non-prismatic geometry on the static behavior and dynamic response of horizontally curved beam (steel, concrete and composite) except the research of **Badawy** [20](his research included an investigations of the effect of non-prismatic due to non-uniform distribution of a shear reinforcement on the behavior of horizontally curved reinforced concrete beam). Also many researchers were dealing with the three dimensional finite element methods but no research was found showing the effects of curvature on the amplitude of deformation, dynamic response and stresses distribution of horizontally curved beam especially for composite beams. Thus this research is concentrated on revealing these effects as well as others as will be shown lately.

Chapter Three

Basic Concepts and Finite Element Idealizations

3-1: Introduction

The finite element method received much attention during the last four decades because of its effectiveness and versatility. In this method, the structure is divided into small finite elements; each one is analyzed by considering the deformations that occur in that region of the structure. A displacement variation across the element is assumed, hence, the displacement at any point within the element can be related to the nodal displacements which are treated as unknowns. Then by integrating over the domain, the strain and kinetic energies of the element are determined in terms of the nodal variables. Consequently the strain and kinetic energies of the whole structure are obtained by summation of the energy contributions from each element. The primary advantage of the finite element method is its generality. It can be used to study the behavior of the concrete, steel, and composite members. Also, the finite element method represents a unifying approach, which offers the solution of diverse engineering problems [52].

The nonlinear finite element approach can be used to predict the behavior of concrete, steel, and composite structures for all stages (elastic, plastic, cracking load, post-cracking, crushing, post-crushing and ultimate load). The efficiency and accuracy of this method depend mainly on suitable modeling of materials phenomena. Although this approach is widely used to analyze reinforced

concrete members and steel members but very little work has been devoted to study the behavior of horizontally curved composite members.

This chapter describes the finite element model used in the present study. Section 3-2 summarizes the finite element formulation. Finite element idealization is presented in section 3-3. Section 3-4 describes the numerical integration.

3-2 : Finite Element Formulation

3-2-1: Static Formulation[2]

When considering a general three-dimensional body, subjected to a set of external forces, which consists of surface tractions and body forces, the individual element stiffness matrix can be determined easily by using the principle of virtual displacements [2,53]. The displacement vector at any point within the element $\{u\}_e$, can be interpolated as:

$$\{u\}_e = [N] \cdot \{a\}_e \quad \dots\dots\dots (3-1)$$

where $[N]$ is a matrix containing the interpolation functions which relates the displacement, $\{u\}_e$, to the nodal displacements, $\{a\}_e$, where, $\{u\}_e$, is given by .

$$\{u\}_e = [u \ v \ w]^T_e \quad \dots\dots\dots (3-2)$$

By taking suitable derivatives of Eq.(3-1), the strain-displacement relationships can be written as .

$$\{\varepsilon\}_e = [A] \cdot \{u\}_e \quad \dots\dots\dots (3-3)$$

where $[A]$ is a matrix that contains the differential operators. Substitution of Eq. (3-1) into Eq.(3-3) yields

$$\{\varepsilon\}_e = [B] \cdot \{a\}_e \quad \dots\dots\dots (3-4)$$

where $[B]$ is the strain-nodal displacement matrix given by

$$[B] = [A] \cdot [N] \quad \dots\dots\dots (3-5)$$

The vectors of stresses and strains are related through the constitutive matrix $[D]$ as:

$$\{\sigma\}_e = [D] \cdot \{\varepsilon\}_e \quad \dots\dots\dots (3-6)$$

where the corresponding vector of stresses is given by

$$\{\sigma\}_e^T = \{\sigma_x \ \sigma_y \ \sigma_z \ \tau_{xy} \ \tau_{yz} \ \tau_{zx}\} \quad \dots\dots\dots (3-7)$$

and the vector of strains, $\{\epsilon\}_e$ is given by

$$\{\epsilon\} = \begin{Bmatrix} \epsilon_x \\ \epsilon_y \\ \epsilon_z \\ \gamma_{xy} \\ \gamma_{yz} \\ \gamma_{zx} \end{Bmatrix} = \begin{Bmatrix} \partial u / \partial x \\ \partial v / \partial y \\ \partial w / \partial z \\ \partial u / \partial y + \partial v / \partial x \\ \partial v / \partial z + \partial w / \partial y \\ \partial w / \partial x + \partial u / \partial z \end{Bmatrix} \quad \dots\dots\dots (3-8)$$

Substitution of Eq.(3-4) into Eq.(3-6) gives the stress-nodal displacement relationship,

$$\{\sigma\}_e = [D] \cdot [B] \cdot \{a\}_e \quad \dots\dots\dots (3-9)$$

The principle of virtual displacements of a deformable body is used to establish the governing equations of static equilibrium. It states that “If a general structure in equilibrium is subjected to a system of small virtual displacements with a compatible state of deformation, the virtual work due to the external action, δW_{ext} , is equal to virtual strain energy due to the internal stress, δW_{int} ” [2,54] thus:

$$\delta W_{int} - \delta W_{ext} = 0 \quad \dots\dots\dots (3-10)$$

By considering a system of volume v and surface area s subjected to body forces b_i and surface tractions t_i , the external work done in moving these forces through the virtual displacement $\partial\{u\}$ can be expressed as:

$$\delta W_{ext} = \int_v \partial\{u\}^T \cdot \{b\} \cdot dv + \int_s \partial\{u\}^T \cdot \{t\} \cdot ds \quad \dots\dots\dots (3-11)$$

The internal virtual work is given by

$$\delta W_{int} = \int_v \partial\{\epsilon\}^T \cdot \{\sigma\} \cdot dv \quad \dots\dots\dots (3-12)$$

Substitution of Eq.(3-6) into Eq.(3-12) yields:

$$\delta W_{int} = \int_v \partial\{\epsilon\}^T \cdot [D] \cdot \{\epsilon\} \cdot dv \quad \dots\dots\dots (3-13)$$

When using Eq.s (3-11), (3-13) and Eq.(3-10) may be expressed as:

$$\int_v \partial \{\boldsymbol{\varepsilon}\}^T \cdot \{D\} \cdot \{\boldsymbol{\varepsilon}\} \cdot dv - \int_v \partial \{\mathbf{u}\}^T \cdot \{\mathbf{b}\} \cdot dv - \int_v \partial \{\mathbf{u}\}^T \cdot \{\mathbf{t}\} \cdot ds = \{0\} \quad \dots\dots\dots (3-14)$$

14)

The above expression represents the equation of static equilibrium for a general body. Therefore, by making use of Eq.s (3-1) and (3-4), the discretized form of Eq.(3-14) can be written as:

$$\partial \{\mathbf{a}\}^T \left[\sum_{n \ v_e} \int [B]^T \{D\} \cdot [B] \cdot dv_e \{\mathbf{a}\}_e - \sum_{n \ v_e} \int [N]^T \{\mathbf{b}\}_e \cdot dv_e - \sum_{n \ s_e} \int [N]^T \{\mathbf{t}\}_e \cdot ds_e \right] = \{0\} \quad \dots\dots\dots (3-15)$$

where n is the total number of the elements of the discrete system.

Since the vector of the virtual nodal displacements, $\partial \{\mathbf{a}\}^T$, is arbitrary, the following set of algebraic equations may be obtained.

$$\{\mathbf{f}\} = [K] \cdot \{\mathbf{a}\} \quad \dots\dots\dots (3-16)$$

where $[K]$ is the stiffness matrix of the element assemblage and is given by

$$[K] = \sum_n [k] = \sum_{n \ v_e} \int [B]^T \cdot [D] \cdot [B] \cdot dv_e \quad \dots\dots\dots (3-17)$$

where $[k]$ is the element stiffness matrix. While, $\{\mathbf{f}\}$ is the element assemblage of external nodal forces vector given by:

$$\{\mathbf{f}\} = \sum_{n \ v_e} \int [N]^T \cdot \{\mathbf{b}\}_e \cdot dv_e + \sum_{n \ s_e} \int [N]^T \{\mathbf{t}\}_e \cdot ds_e \quad \dots\dots\dots (3-18)$$

3-2-2: Dynamic Formulation [55]

3-2-2-1: Dynamic Equations Formulation

By using the principle of virtual work, the dynamic equation of motion for any finite element can be developed. Such equations contain energy-equivalent stiffness, masses and nodal loads for a typical element.

Assuming that a three-dimensional finite element with zero damping exists in Cartesian coordinates x , y and z as presented in Fig.(3-1), the displacement vector at any point within the element $\mathbf{u}(\mathbf{t})$, can be interpolated as:

$$\mathbf{u}(t) = [N] \cdot \mathbf{a}(t) \quad \dots\dots\dots (3-19)$$

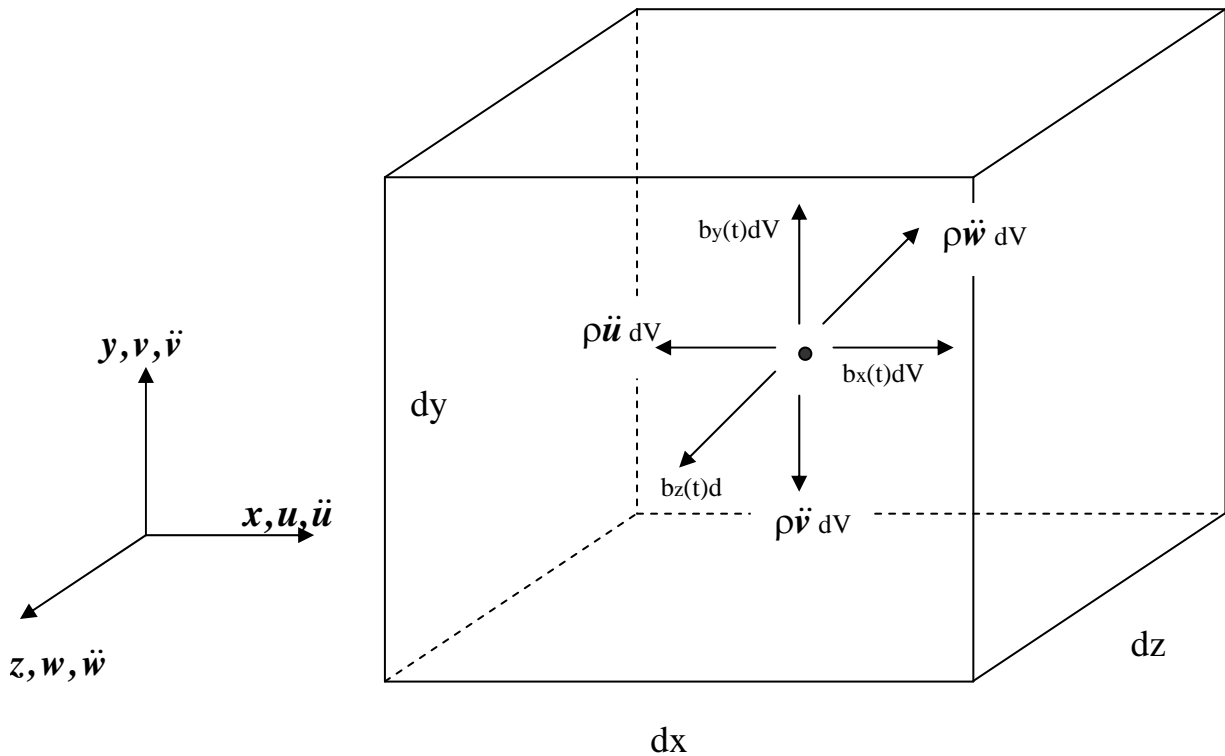


Fig.(3-1): Applied and Inertial Body Forces.

where $[N]$ is a matrix containing the interpolation functions which relates the displacement, $\mathbf{u}(t)$, to the time-varying nodal displacements $\mathbf{a}(t)$, where $\mathbf{u}(t)$, is given by:

$$\mathbf{u}(t) = [u \ v \ w]^T \quad \dots\dots\dots (3-20)$$

and, u, v and w are translations in x, y and z -directions respectively. Time-varying nodal displacements $\{\mathbf{a}(t)\}$ will be at first considered as only translations in x, y and z -directions, thus, if n_{el} = number of element nodes,

$$\mathbf{a}(t) = \{\mathbf{a}_i(t)\} \quad (i=1,2,\dots\dots\dots n_{el}) \quad \dots\dots\dots (3-21)$$

where, $\mathbf{a}_i(t) = \{ a_{xi} \ a_{yi} \ a_{zi} \} = \{ u_i \ v_i \ w_i \} \quad \dots\dots\dots (3-22)$

If the element is subjected to time-varying body forces, such forces may be placed into a vector $\mathbf{b}(t)$ as follows:

$$\mathbf{b}(t) = \{ \mathbf{b}_x \ \mathbf{b}_y \ \mathbf{b}_z \} \quad \dots\dots\dots (3-23)$$

where, \mathbf{b}_x , \mathbf{b}_y and \mathbf{b}_z represent components of force (per unit volume) acting in the reference directions at a generic point.

Similarly, time-varying nodal actions $\mathbf{p}(t)$ will temporarily be taken as only forces in the x, y and z directions at the nodes. Thus,

$$\mathbf{p}(t) = \{ \mathbf{p}_i(t) \} \quad (i=1,2,\dots\dots\dots n_{el}) \quad \dots\dots\dots (3-24)$$

$$\text{where, } \mathbf{p}_i(t) = \{ p_{xi} \ p_{yi} \ p_{zi} \} \quad \dots\dots\dots (3-25)$$

The time function p_{xi} , p_{yi} , and p_{zi} at each node may be independent and arbitrary.

By taking suitable derivatives of Eq.(3-19), the strain-displacement relationships can be written as:

$$\varepsilon(t) = [\mathbf{A}] \cdot \mathbf{u}(t) \quad \dots\dots\dots (3-26)$$

where $[\mathbf{A}]$ is a matrix that contains the differential operators. Substitution of Eq. (3-1) into Eq.(3-3) yields:

$$\varepsilon(t) = [\mathbf{B}] \cdot \mathbf{a}(t) \quad \dots\dots\dots (3-27)$$

where, $[\mathbf{B}]$ as defined previously in Eq.(3-5), matrix $[\mathbf{B}]$ gives strains at any point within the element due to unit values of nodal displacements.

The vectors of stresses and strains are related through the constitutive matrix $[\mathbf{D}]$ as:

$$\boldsymbol{\sigma}(t) = [\mathbf{D}] \cdot \varepsilon(t) \quad \dots\dots\dots (3-28)$$

Substitution of Eq.(3-27) into Eq.(3-28) gives the stress-nodal displacement relationship,

$$\boldsymbol{\sigma}(t) = [\mathbf{D}] \cdot [\mathbf{B}] \cdot \mathbf{a}(t) \quad \dots\dots\dots (3-29)$$

where, the matrix product $[\mathbf{D}].[B]$ gives stresses at a generic point due to unit values of nodal displacements.

When applying the principle of virtual work to a finite element, the equation will be (similar to Eq.(3-10)):

$$\delta U_{int} - \delta U_{ext} = 0 \quad \dots\dots\dots (3-30)$$

where, δU_{int} is the virtual strain energy of internal stresses and δU_{ext} is the virtual work of external action on the element. To develop both sides of the last equation in details, a vector $\delta \mathbf{a}(t)$ of small virtual displacement is assumed. Thus,

$$\delta \mathbf{a}(t) = \{ \delta a_i(t) \} \quad (i=1,2,\dots,n_{el}) \quad \dots\dots\dots (3-31)$$

Then the resulting virtual generic displacements become [by Eq.(3-19)]:

$$\delta \mathbf{u}(t) = [\mathbf{N}] \cdot \delta \mathbf{a}(t) \quad \dots\dots\dots (3-32)$$

Using the strain-nodal displacement relationship in Eq.(3-27), then:

$$\delta \boldsymbol{\varepsilon}(t) = [\mathbf{B}] \cdot \delta \mathbf{a}(t) \quad \dots\dots\dots (3-33)$$

Now the internal virtual strain energy can be written as:

$$\delta U_{int} = \int_v \delta \boldsymbol{\varepsilon}^T(t) \boldsymbol{\sigma}(t) dv \quad \dots\dots\dots (3-34)$$

or
$$\delta U_{int} = \int_v \delta \boldsymbol{\varepsilon}^T(t) [\mathbf{D}] \boldsymbol{\varepsilon}(t) dv \quad \dots\dots\dots (3-35)$$

where, the integration is over the volume of the element.

For external virtual work, Fig.(3-1) shows an infinitesimal element with components of applied body forces $b_x(t)dV, b_y(t)dV$ and $b_z(t)dV$. The figure also shows internal body forces $\rho \ddot{u} dV, \rho \ddot{v} dV$ and $\rho \ddot{w} dV$ due to the accelerations \ddot{u}, \ddot{v} and \ddot{w} . The symbol ρ in these expressions represents the mass density of the material, which is defined as the internal forces per unit acceleration per unit volume. Thus, when adding the external virtual work of nodal forces and distributed body forces the result will be:

$$\delta U_{ext} = \delta \mathbf{a}^T \mathbf{p}(t) + \int_v \delta \mathbf{u}^T \mathbf{b}(t) dV - \int_v \delta \mathbf{u}^T \rho \ddot{\mathbf{u}} dV \quad \dots\dots\dots (3-36)$$

Substitution of Eqs.(3-35) and (3-36) into Eq.(3-30) produce:

$$\int_v \delta \boldsymbol{\varepsilon}^T(t) [\mathbf{D}] \boldsymbol{\varepsilon}(t) dv = \delta \mathbf{a}^T \mathbf{p}(t) + \int_v \delta \mathbf{u}^T \mathbf{b}(t) dV - \int_v \delta \mathbf{u}^T \rho \ddot{\mathbf{u}} dV \quad \dots\dots\dots (3-37)$$

Now assuming that

$$\ddot{\mathbf{u}}(t) = [\mathbf{N}] \cdot \ddot{\mathbf{a}}(t) \quad \dots\dots\dots (3-38)$$

Then when substituting Eqs.(3-29) and (3-38) into Eq.(3-37) utilizing Eqs.(3-32) and (3-33) the equation will be:

$$\int_{\nu} \mathbf{B}^T [\mathbf{D}] \mathbf{B} \mathbf{a} \, dV = \mathbf{p}(t) + \int_{\nu} \mathbf{N}^T \mathbf{b}(t) \, dV - \int_{\nu} \rho \mathbf{N}^T \mathbf{N} \ddot{\mathbf{a}} \, dV \quad \dots\dots\dots (3-39)$$

Rearrangement of the resulting equations of motion gives:

$$\mathbf{M} \ddot{\mathbf{a}} + \mathbf{k} \mathbf{a} = \mathbf{p}(t) + \mathbf{p}_b(t) \quad \dots\dots\dots (3-40)$$

where matrix \mathbf{k} is the element stiffness matrix as defined previously in Eq.(3-17),

$$\text{and } \mathbf{M} = \int_{\nu} \rho \mathbf{N}^T \mathbf{N} \, dV \quad \dots\dots\dots (3-41)$$

$$\mathbf{p}_b(t) = \int_{\nu} \mathbf{N}^T \mathbf{b}(t) \, dV \quad \dots\dots\dots (3-42)$$

Eq.(3-41) gives the form of the consistent mass matrix, in which the terms are energy-equivalent actions at nodes due to unit values of nodal accelerations. The vector $\mathbf{p}_b(t)$ in Eq.(3-42) consists of equivalent nodal loads due to body forces in the vector $\mathbf{b}(t)$.

It is interesting to note that if the damping effects are considered, Eq.(3-40) becomes [6]:

$$\mathbf{M} \ddot{\mathbf{a}} + \mathbf{C} \dot{\mathbf{a}} + \mathbf{k} \mathbf{a} = \mathbf{p}(t) + \mathbf{p}_b(t) \quad \dots\dots\dots (3-43)$$

where, \mathbf{C} and $\dot{\mathbf{a}}$ represent the damping matrix and velocity vector respectively.

3-2-2-2: Mass Matrix Formulation

- Consistent mass matrix

The mass matrix is called consistent when calculated by using Eq.(3-41). In this approach, the mass coefficients are computed using the same stiffness interpolation shape functions. The major advantages of the consistent mass are the more accurate mode shapes and frequencies obtained when using this approach, but it requires a considerably more computational effort than the lumped mass.

- Lumped mass matrix

A convenient simplification is achieved by lumping the element mass to the nodes. For a simple element it is easy to devise lumping schemes based on the intuitive reasoning [56], while with higher order elements a physically obvious lumping strategy is not always available, therefore, several approaches have been proposed:

i- The nodes of an element are chosen to be the sampling points which are used in the numerical integration when computing the mass matrix. As in the standard finite element formulation, the shape function corresponding to a particular node vanishes at all other nodes locations, thus it obtains a diagonal mass matrix. However, some terms in the matrix may be negative and this can lead to the imaginary frequencies of vibration [57].

ii- In this approach a different set of shape functions (from the ones used for the stiffness matrix evaluation) is used for evaluating the mass matrix. Choosing piecewise constant functions, equal to unity in the vicinity of a node and zero elsewhere, leads to a diagonal matrix [58].

iii- The diagonal terms of the consistent mass matrix is scaled so that the total mass of the element is preserved [59]. This technique has been successfully used by many investigators [6,60,61,62]. Thus this approach is adopted in the current study.

3-2-2-3: Damping Matrix Formulation

The damping matrix C in Eq.(3-43) is not usually known, therefore different procedures have to be used to construct the damping matrix. When the total damping in the structure is assumed to be a sum of the damping of the individual modes present in the system response, a reasonable damping matrix can be obtained as follows [63]. If two modes are considered then so-called *Rayleigh* damping is a linear combination of the mass and stiffness matrices so that :

$$C = a_0 M + a_1 K \quad \dots\dots\dots (3-44)$$

where; a_0 and a_1 are constants. The principal advantage of *Rayleigh* damping leads to a banded damping matrix with the same structure as the stiffness matrix. Thus, consideration of damping does not increase the computational effort.

3-3 : Finite Element Idealization

In the present study, steel and concrete are simulated by hexahedral brick elements and reinforcement bars are modeled as one dimensional embedded elements built into the concrete brick elements.

3-3-1 Steel and Concrete Idealization

For describing the steel and concrete elements, the three dimensional modeling is adopted in the present study. The 20-node quadratic brick element has been adopted. This element has been successfully used in many three dimensional nonlinear studies [2,3,4,6,16,...etc]. The element has its own local coordinate system, r, s, t as shown in Fig.(3-2), with the origin at the center of the element such that each local coordinate ranges from (-1) to (+1).

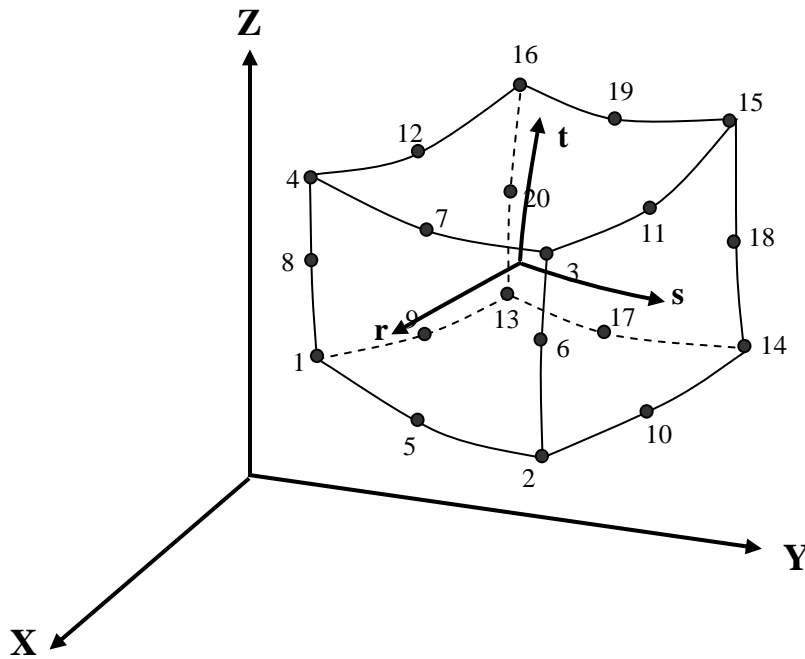


Fig.(3-2): The 20-Node Brick Element in Cartesian Coordinates.

3-3-1-1: Shape Functions of the 20-Node Brick Element

The displacement components at a particular point $p(r, s, t)$ within the element are defined using the nodal values at each of the twenty nodes and the quadratic shape functions such that:

$$u(r, s, t) = \sum_{i=1}^{20} N_i(r, s, t) \cdot u_i$$

$$v(r, s, t) = \sum_{i=1}^{20} N_i(r, s, t) \cdot v_i \quad \dots\dots\dots (3-45)$$

$$w(r, s, t) = \sum_{i=1}^{20} N_i(r, s, t) \cdot w_i$$

where $N_i(r, s, t)$ is the shape function at node i at which the nodal displacements are u_i , v_i and w_i in x, y and z-directions. The shape functions for the 20-nodes have the following forms:

$$N_i = \frac{1}{8}(1 + rr_i)(1 + ss_i)(1 + tt_i)(rr_i + ss_i + tt_i - 2) \quad i=1-4, 13-16$$

$$N_i = \frac{1}{4}(1 - r^2)(1 + ss_i)(1 + tt_i) \quad i = 6, 8, 18, 20$$

$$N_i = \frac{1}{4}(1 + rr_i)(1 - s^2)(1 + tt_i) \quad i = 5, 17, 19, 7 \dots \dots \dots (3-46)$$

$$N_i = \frac{1}{4}(1 + rr_i)(1 + ss_i)(1 - t^2) \quad i = 9, 10, 11, 12$$

For isoparametric elements, the interpolation shape functions are also used to define the geometry of the element. Hence, the Cartesian coordinate values of any point $p(r, s, t)$ within the element may be defined as:

$$x(r, s, t) = \sum_{i=1}^{20} N_i(r, s, t) \cdot x_i$$

$$y(r, s, t) = \sum_{i=1}^{20} N_i(r, s, t) \cdot y_i \quad \dots \dots \dots (3-47)$$

$$z(r, s, t) = \sum_{i=1}^{20} N_i(r, s, t) \cdot z_i$$

where x_i , y_i and z_i are the Cartesian coordinates of node i .

Since u , v , w and x , y , z are defined by the same shape functions, the element is isoparametric.

3-3-1-2: Strain-Nodal Displacement Representation

For three-dimensional finite element analysis, Cartesian components of strains are related to nodal displacements by Eq.(3-4), therefore the strains components can be evaluated as:

$$\begin{Bmatrix} \epsilon_x \\ \epsilon_y \\ \epsilon_z \\ \gamma_{xy} \\ \gamma_{yz} \\ \gamma_{zx} \end{Bmatrix} = \sum_{i=1}^{20} \begin{bmatrix} \partial N_i / \partial x & 0 & 0 \\ 0 & \partial N_i / \partial y & 0 \\ 0 & 0 & \partial N_i / \partial z \\ \partial N_i / \partial y & \partial N_i / \partial x & 0 \\ 0 & \partial N_i / \partial z & \partial N_i / \partial y \\ \partial N_i / \partial z & 0 & \partial N_i / \partial x \end{bmatrix} \begin{Bmatrix} u_i \\ v_i \\ w_i \end{Bmatrix} \dots\dots\dots (3-48)$$

The shape function N_i is a function of both local and Cartesian coordinates. The derivative of the shape function can be given by the usual chain rule as:

$$\begin{Bmatrix} \partial N_i / \partial r \\ \partial N_i / \partial s \\ \partial N_i / \partial t \end{Bmatrix} = \begin{bmatrix} \partial x / \partial r & \partial y / \partial r & \partial z / \partial r \\ \partial x / \partial s & \partial y / \partial s & \partial z / \partial s \\ \partial x / \partial t & \partial y / \partial t & \partial z / \partial t \end{bmatrix} \begin{Bmatrix} \partial N_i / \partial x \\ \partial N_i / \partial y \\ \partial N_i / \partial z \end{Bmatrix} = [J] \begin{Bmatrix} \partial N_i / \partial x \\ \partial N_i / \partial y \\ \partial N_i / \partial z \end{Bmatrix} \dots\dots\dots (3-49)$$

where [J] is known as the **Jacobian** matrix.

Then the shape function derivatives with respect to x , y and z axes can be obtained as:

$$\begin{Bmatrix} \partial N_i / \partial x \\ \partial N_i / \partial y \\ \partial N_i / \partial z \end{Bmatrix} = [J]^{-1} \begin{Bmatrix} \partial N_i / \partial r \\ \partial N_i / \partial s \\ \partial N_i / \partial t \end{Bmatrix} \dots\dots\dots (3-50)$$

3-3-1-3: Stiffness Matrix for 20-Node Brick Element

For an element of volume V , the stiffness matrix presented in Eq.(3-17) may be expressed as:

$$[k]_e = \int_{ve} [B]^T \cdot [D] \cdot [B] \cdot dv_e \dots\dots\dots (3-51)$$

In three dimensional elements, the differential volume, dv_e , may be written as:

$$dv_e = dx \cdot dy \cdot dz \dots\dots\dots (3-52)$$

Eq.(3-52) can be transformed into natural coordinates as [55]:

$$dv_e = / J / dr \cdot ds \cdot dt \dots\dots\dots (3-53)$$

where $|J|$ is the determinant of the **Jacobian** matrix. The limits of integration in the natural coordinates become -1 to +1 and the element stiffness matrix can be therefore expressed as:

$$[k]_e = \int_{-1}^{+1} \int_{-1}^{+1} \int_{-1}^{+1} [B]^T \cdot [D] \cdot [B] \cdot |J| \, dr \, ds \, dt \quad \dots\dots\dots (3-54)$$

3-3-2 Reinforcement Representation

The analysis of reinforced concrete members by the finite element method requires simple and accurate representation to simulate the reinforcing bars in a finite element model [64]. In the finite element method there are three alternative representations which have been usually used to simulate the reinforcement:

- a- discrete representation
- b- distributed representation
- c- embedded representation

A discrete modeling by using one dimensional element to idealize the reinforcement has been widely used. The major advantages of this model are its simplicity and its capability to take the bond-slip and dowel action phenomena into account [65,66], but hence the locations of the longitudinal bars and stirrups are close to each other and concrete cover is relatively small compared with the dimensions of the member which they enforce the mesh choice and the size of the brick elements. Therefore a large number of brick elements would be required to simulate the member. Hence the cost of such analyses would be very expensive in term of the computation time.

In a distributed representation, the reinforcing bars are assumed to be distributed over the concrete element in any specified direction as a layer. Perfect bond between the concrete and the reinforcement bars is assumed, and then a composite concrete-reinforcement constitutive relation must be derived. When using this technique the reinforcement bar cannot be represented at the accurate position, and each layer had one property. This technique was adopted in the present dynamic analysis.

The embedded representation shown in Fig.(3-3) is almost used with the higher order isoparametric concrete elements [56,67]. The reinforcing bar is considered to be as an axial member built into the isoparametric concrete element such that its displacements are consistent with those of the element. In this technique perfect bond between concrete and reinforcing bars is assumed. The major advantage of this approach is that the reinforcement bars can be placed in their correct positions without imposing any restrictions on mesh choice, therefore the finite element analysis can be carried out with a smaller number of brick elements when compared with the discrete approach. Also many types of reinforcement bars located at the same level can be represented. The embedded representation is adopted in the static analysis presented in this thesis.

3-3-2-1 Displacement Representations

A bar element is considered to be embedded inside the brick element parallel to r axis and has a position $s = s_i$ and $t = t_i$, as shown below. The same shape functions of the brick element can be used to represent the displacement of the bar. Hence, the Cartesian coordinates of any point along this bar are obtained by substituting the constant values s_i and t_i into Eq.(3-47) such that:

$$x(\mathbf{r}) = \sum_{i=1}^{20} N_i(\mathbf{r}) \cdot x_i$$

$$y(\mathbf{r}) = \sum_{i=1}^{20} N_i(\mathbf{r}) \cdot y_i \quad \dots\dots\dots (3-55)$$

$$z(\mathbf{r}) = \sum_{i=1}^{20} N_i(\mathbf{r}) \cdot z_i$$

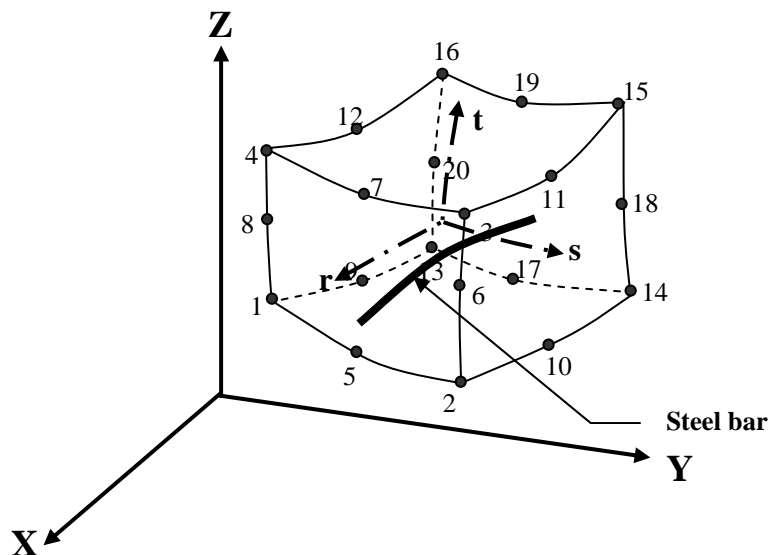


Fig.(3-3): Representation of Embedded Reinforcement.

Because full compatibility between the bar and the basic brick element is assumed, displacements of the bar are obtained from the basic element displacement field as:

$$\begin{aligned} \mathbf{u}(\mathbf{r}) &= \sum_{i=1}^{20} \mathbf{N}_i(\mathbf{r}) \cdot \mathbf{u}_i \\ \mathbf{v}(\mathbf{r}) &= \sum_{i=1}^{20} \mathbf{N}_i(\mathbf{r}) \cdot \mathbf{v}_i \\ \mathbf{w}(\mathbf{r}) &= \sum_{i=1}^{20} \mathbf{N}_i(\mathbf{r}) \cdot \mathbf{w}_i \end{aligned} \quad \dots\dots\dots (3-56)$$

3-3-2-2 Strain-nodal displacement representations

Since, the bar is capable of transmitting axial forces only; one component of strain contributes to the strain energy. As shown in *Appendix (A)* The strain-displacement relationship is given by [2,68,69]:

$$\{\varepsilon'\} = \sum_{i=1}^n \left[\frac{1}{h^2} \begin{bmatrix} c_1 & c_2 & c_3 \\ c_2 & c_4 & c_5 \\ c_3 & c_5 & c_6 \end{bmatrix} \cdot \begin{bmatrix} \partial \mathbf{N}_i / \partial x \\ \partial \mathbf{N}_i / \partial y \\ \partial \mathbf{N}_i / \partial z \end{bmatrix} \right] \begin{Bmatrix} \mathbf{u}_i \\ \mathbf{v}_i \\ \mathbf{w}_i \end{Bmatrix} \quad \dots\dots\dots (3-57)$$

where, $C_1 = (\partial x / \partial r)^2$

$$C_2 = (\partial x / \partial r) / (\partial y / \partial r)$$

$$C_3 = (\partial x / \partial r) / (\partial z / \partial r) \quad \dots\dots\dots (3-58)$$

$$C_4 = (\partial y / \partial r)^2$$

$$C_5 = (\partial y / \partial r) / (\partial z / \partial r)$$

$$C_6 = (\partial z / \partial r)^2$$

$$h = \sqrt{C_1^2 + C_4^2 + C_6^2} \quad \dots\dots\dots (3-59)$$

Finally, Eq. (3-57) may be rewritten in form:

$$\{\varepsilon'\} = [B'] \{\delta\}^e \quad \dots\dots\dots (3-60)$$

where $[B']$ is the strain-nodal displacement matrix of the reinforcement bar element.

3-3-2-3 Stiffness Matrix Calculation

The stiffness matrix of an axially loaded bar element given in Eq.(3-17) may be expressed as:

$$[K'_e] = \int_{ve} [B']^T [D'] [B'] dVe \quad \dots\dots\dots (3-61)$$

where the matrix $[D']$ represents the modulus of elasticity of steel bars and;

$$dVe = A_s . dx' = A_s . h . dr \quad \dots\dots\dots (3-62)$$

where A_s is the cross-section area of the bar. By substituting Eq.(3-62) into (3-61), the stiffness matrix of the embedded bar can be expressed as:

$$[K'_e] = A_s \int_{-1}^1 [B']^T [D'] [B'] . h dr \quad \dots\dots\dots (3-63)$$

where A_s is the cross-sectional area of the bar and $[D']$ is the constitutive matrix that represents the modulus of elasticity of the steel bar. A similar derivation can be made for bars parallel to s and t axes.

3-4: Numerical Integration

In general the evaluation of the stiffness (or mass) matrices and the equivalent nodal loads involves multiplied functions. Explicit integration for these functions may be very difficult or even impossible. Therefore, a resort to an alternative scheme of numerical integration is usually used. In the finite element work, the *Gaussian-Legendre* quadratic numerical integration technique has been found to be useful, accurate and convenient [70]. In this technique the element stiffness matrix for the brick element may be written as:

$$[k_e] = \int_{-1}^{+1} \int_{-1}^{+1} \int_{-1}^{+1} f(r, s, t) dr \cdot ds \cdot dt \cong \sum_{i=1}^p \sum_{j=1}^p \sum_{k=1}^p W_i \cdot W_j \cdot W_k \cdot f(r_i, s_j, t_k) \dots \dots \dots (3-64)$$

where p are the number of Gaussian points in r , s and t -directions. The function $f(r, s, t)$ represents the matrix multiplication $([B]^T \cdot [D] \cdot [B] \cdot \det / J /)$.

In a similar manner the steel bar element stiffness matrix can be written as:

$$[k_e] = \int_{-1}^1 f(r) \cdot dr \cong \sum_{i=1}^{P_1} W_i \cdot f(r_i) \dots \dots \dots (3-65)$$

For brick elements representing concrete or steel, the 27 ($3 \times 3 \times 3$) Gauss quadratic integration rule has been used in this study. The relative positions and the corresponding weights of the sampling points for this rule over the volume of the brick element are illustrated in *Appendix (B)*.

Chapter Four

Behavior and Modeling of Materials under Static Loads

4-1: Introduction

In any three dimensional finite element analysis the performance of any structural member under load depends on the behavior of the type of material used to construct the member. In concrete members which are made of different materials, concrete and reinforcing bars are brought together to behave as a composite system. The steel can be considered as a homogeneous material that exhibits a similar stress-strain relationship in tension and compression. While, the behavior of concrete is monitored to have grossly heterogeneous internal structure because it is very much dependent on the properties of each of its components; namely, cement mortar, aggregates and air voids.

The nonlinear finite element approach can be used to predict the behavior of concrete and steel structures at elastic stage, plastic stage, cracking load, post-cracking stage and ultimate load. The efficiency and accuracy of the computer model depend mainly on suitable modeling of material properties. Although this approach is widely used to analyze reinforced concrete members and steel members but very little work has been conducted to study the behavior of the non-prismatic horizontally curved beams (concrete, steel and composite).

This chapter describes the finite element model used in the current static study. Section 4-2 describes the modeling of concrete. Steel representation, which is used is presented in section 4-3, while section 4-4 summarizes the representation of reinforcement.

The observed behavior under different load conditions and the nonlinear models used for concrete and steel in tension and compression which are adopted to simulate the actual behavior of materials properties are illustrated.

4-2: Modeling of the Concrete under Static Load

4-2-1: Observed Behavior of the Concrete under Static Load

A lot of experimental tests show that the concrete could behave as either a linear or nonlinear material depending on the level and the nature of the stresses to which it is subjected. Under low levels of stress, concrete seemed to be behave as a linearly elastic material. For a higher value of stresses and for sustained loading; it exhibits nonlinear properties, which have a considerable effect on the behavior of curved members.

4-2-1-1: Behavior under Uniaxial Compression

A typical uniaxial compressive stress-strain curve is shown in Fig.(4-1). It can be noted that the concrete behaves as a linear elastic material when the stress level is less than about 30% of the uniaxial compressive strength f_c' . This stress level is called the point of onset of localized cracking [71]. At stress levels ranging between $0.3 f_c'$ and $0.5 f_c'$ the stress-strain curve exhibits a slight nonlinearity due to the extension of stress concentrations at crack tips, thereafter when the stress level increases from $0.5 f_c'$ to $0.75 f_c'$ mortar cracks and other cracks continue and grow slowly with a gradual increase in curvature of the curve. Beyond this level of stress, the rate of crack propagation increases rapidly and the stress-strain curve bends sharply until the peak stress level is reached. Beyond the peak stress level, concrete shows a softening response, which is presented by the descending portion of the stress-strain curve [72].

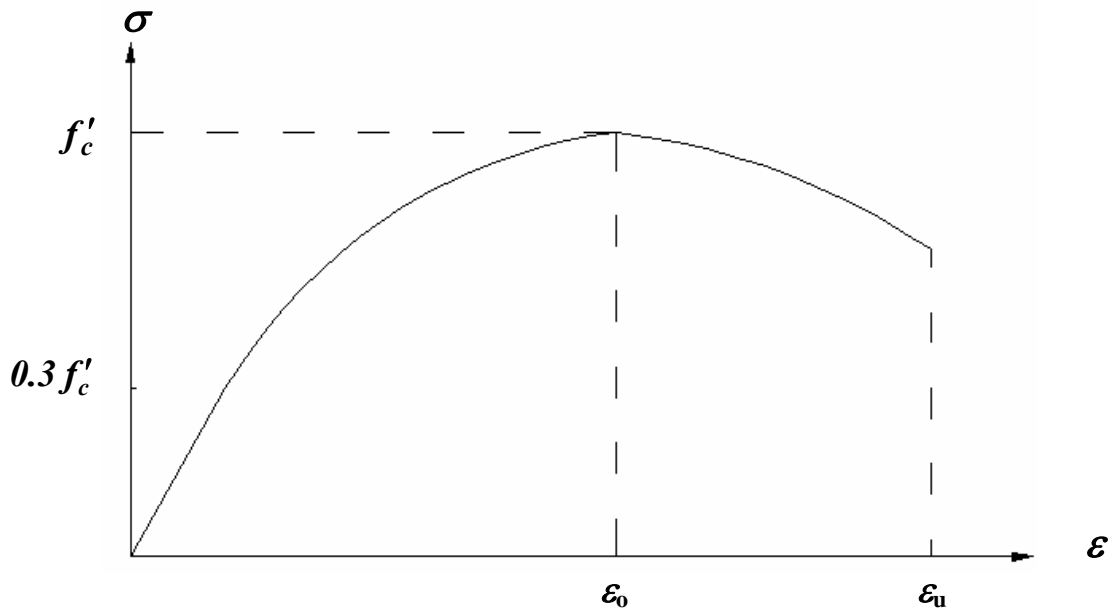


Fig.(4-1): Typical Uniaxial Stress-Strain Curve for Concrete in Compression.

The modulus of elasticity of concrete E_c , may be estimated from the ACI / Building Code 318 M-02 [73] as:

$$E_c = W_c^{1.5} (0.043) f'_c{}^{0.5} \quad (\text{MPa}) \quad \dots\dots(4-1)$$

where W_c is the unit weight of concrete in kg/m^3 and f'_c in MPa. For normal concrete, Eq.(4-1) can be reduced to

$$E_c = 4700 \sqrt{f'_c} \quad (\text{MPa}) \quad \dots\dots(4-2)$$

Poisson's ratio of concrete has been observed to remain approximately 0.2 but it ranges from 0.15 to 0.22 up to level 80% of f'_c . Beyond this level, *Poisson's* ratio increases rapidly and values in excess of 1.0 have been recorded [74].

4-2-1-2: Behavior under Uniaxial Tension

The strength of concrete in tension (f_t), is approximately a tenth of the compressive strength [75]. A typical tensile stress- strain response of concrete is linear up to a stress level of about 60 % of cracking stress (f_t) as shown in Fig.(4-2)[76]. Beyond this level bond micro-cracks start to grow and nonlinearity of the curve starts to increase as the stress level increases until peak stress is reached. The modulus of elasticity in uni-axial tension is slightly greater than that in uniaxial compression, while *Poisson's* ratio in tension is somewhat smaller than that in compression [77]. As a result of the difficulties in implementing the direct testing of concrete in pure axial tension, indirect tests are alternatively used to compute

the concrete cracking strength. These tests are the modulus of rupture f_r , which is determined from bending test, and the splitting strength f_{sp} , which is determined by splitting a concrete cylinder with a line load. The splitting tensile strength and modulus of rupture of concrete are determined using the following equations respectively [76]:

$$f_{sp} = 0.65 \sqrt{f'_c} \quad (\text{MPa}) \quad \dots\dots\dots(4-3-a)$$

$$f_r = 0.70 \sqrt{f'_c} \quad (\text{MPa}) \quad \dots\dots\dots(4-3-b)$$

In 1986, **Domigo** [78] concluded that (f_t) may be assumed between 3.5 and $4.5 \sqrt{f'_c}$ in psi or $(0.29 \text{ to } 0.37 \sqrt{f'_c})$ in MPa depending on the degree of flexural cracking. The adopted value of (f_t) in the current study is equal to:

$$f_t = 0.29 \sqrt{f'_c} \quad (\text{MPa}) \quad \dots\dots\dots(4-4)$$

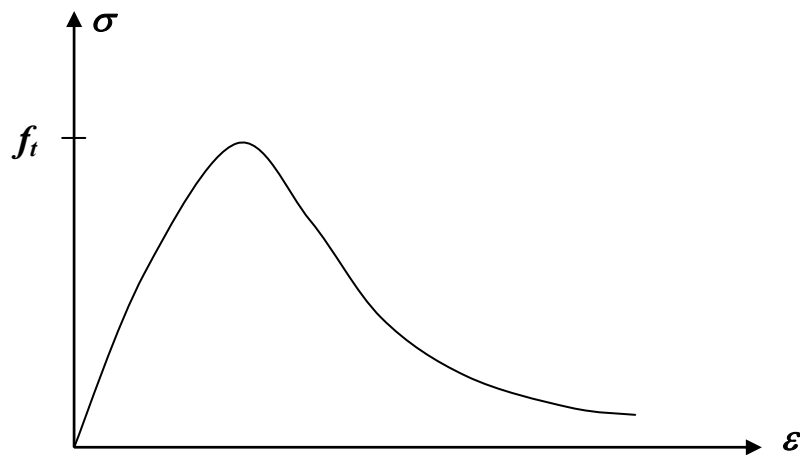


Fig.(4-2): Typical Uniaxial Stress-Strain Curve for Concrete in Tension.

4-2-1-3: Multiaxial Behavior of Concrete

Usually the failure of concrete curved members occurs under combined loading conditions, and the state of stress at failure is generally complex. Under biaxial and tri-axial states of stress, concrete exhibits strength, stiffness and stress-strain behavior somewhat different from that of uniaxial state. Extensive experimental tests on concrete under biaxial stress state have been performed by many investigators amongst them *Kupfer et al.* [79]. A typical biaxial strength envelope of concrete is shown in Fig.(4-3). When subjected to biaxial compression concrete has an increased compressive strength up to about $1.25 f'_c$ for principal

stress ratio of 0.5 and about $1.16 f'_c$ for principal stress ratio of 1.0 . When compression-tension state occurs, the tensile strength decreases almost linearly as the applied compressive stress is increases. Under biaxial tension state, concrete exhibits nearly a constant tensile strength [77,79].

When concrete is subjected to a triaxial state of compressive stress, its strength is increased as a result of the confinement pressure. Experimental studies indicate that the three-dimensional failure surface can be expressed in terms of three stress invariants, Fig.(4-4). These invariants are the first invariant of the stress tensor, I_1 , and the second and the third invariants of the deviatoric stress tensor J_2 and J_3 [76].

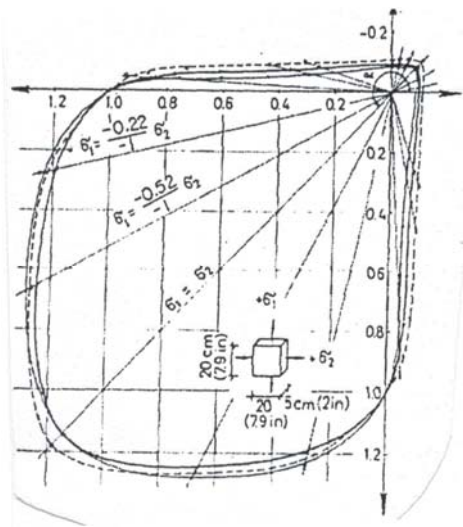


Fig.(4-3): Biaxial Strength Envelope of Concrete[76].

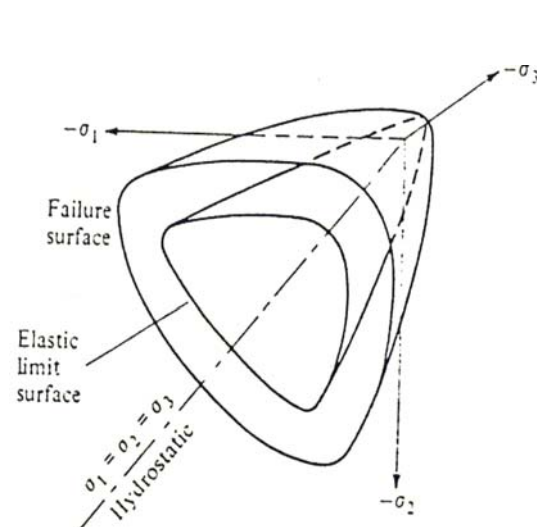


Fig.(4-4): Triaxial Strength Envelope of Concrete[76].

4-2-2: Concrete Model Adopted in the Static Analysis

Any numerical model of concrete to be used in a nonlinear finite element program must include the following constituents [2]:

- 1- A stress-strain model to represent the behavior of concrete prior to failure.
- 2- Failure criteria to simulate cracking and crushing types of fracture.
- 3- A method of crack representation.
- 4- A post-cracking stress-strain relationship.
- 5- Reduction in the compressive strength due to the orthogonal cracks.

4-2-2-1: Stress-Strain Model

The numerical material models that may be adopted in the study must be able to trace the overall behavior of the member within a sufficient degree of accuracy. In the present work, the stress-strain curve is simulated by an elasto-plastic work hardening response followed by linear deficiency response, which is terminated at the onset of crushing.

4-2-2-1-1: The Plasticity Model for Concrete in Compression

The plasticity-based model adopted in this study which was used by many researchers [2,3,4,5,16,...etc.]; assumes that if the concrete is under compressive stress, the nonlinear deformations occur when it is stressed beyond the limit of elasticity ($C_p f'_c$, where $C_p=0.3$). These deformations are separated into recoverable and irrecoverable components. The recoverable part is treated within the framework of elasticity, while the irrecoverable part is treated within the theory of plasticity. In the incremental theory of plasticity, the total strain vector $d\{\boldsymbol{\varepsilon}\}$ is the sum of the elastic and plastic components, so that

$$d\{\boldsymbol{\varepsilon}\} = d\{\boldsymbol{\varepsilon}_e\} + d\{\boldsymbol{\varepsilon}_p\} \quad \dots\dots\dots(4-5)$$

In addition to the strain decomposition, three other fundamental assumptions are required to formulate the constitutive relations for a work-hardening plastic material; they are:

- 1-The shape of an initial yield surface and subsequent loading surfaces.
- 2-The formulation of the suitable hardening rule that describes the evolution of subsequent loading surfaces.
- 3-The formulation of an appropriate flow rule that specifies the stress-strain relation in the plastic range.

- ***The yield criterion used for concrete***

Under a triaxial state of stress, the yield criterion for concrete is generally assumed to be dependent on three stress invariants, however, many studies [2,5,6,72,76] showed that a yield criterion can be adequately expressed in terms of two-stress invariants (I_1 and J_2) as:

$$f(\boldsymbol{\sigma}) = CI_1 + \sqrt{(CI_1)^2 + 3\beta J_2} = \sigma_o \quad \dots\dots\dots(4-6)$$

where C , and β are material parameters, and I_1 is the first stress invariant given by:

$$I_1 = \sigma_x + \sigma_y + \sigma_z \quad \dots\dots\dots(4-7)$$

J_2 is the second deviatoric stress invariant defined as:

$$J_2 = \frac{1}{3} \left[(\sigma_x^2 + \sigma_y^2 + \sigma_z^2) - (\sigma_x \sigma_y + \sigma_y \sigma_z + \sigma_z \sigma_x) \right] + \tau_{xy}^2 + \tau_{yz}^2 + \tau_{zx}^2 \quad \dots\dots\dots(4-8)$$

and $\sigma_o > 0$ is the equivalent effective stress at the onset of plastic deformation which can be determined from uniaxial compression test as

$$\sigma_o = C_p f'_c \quad \dots\dots\dots(4-9)$$

where C_p is a plasticity coefficient which is used to mark the initiation of plastic deformation $0 < C_p < 1.0$. According to the results obtained by *Kupfer et al.*[79] for a (uni-axial compression and the biaxial tests) failure envelope of plain concrete, the material constants can be found to be $C=0.17734$ and $\beta=1.35468$. The resulting yield criterion Eq.(4-6) is compared in Fig.(4-5) with the experimental results of *Kupfer et al.*[79] in the biaxial stress space for $\sigma_o = f'_c$.

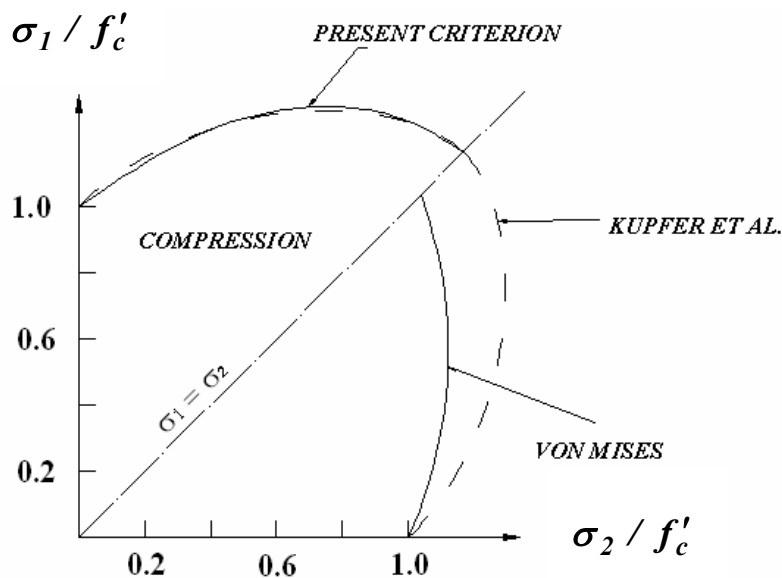


Fig.(4-5): Comparison of Present Yield Surface with Experimental Results[5].

- **The hardening rule**

Whenever a work hardening material is stressed beyond its initial yielding surface a hardening rule is required to describe the growth of subsequent loading

surfaces during plastic deformation. In the present study an isotropic hardening rule is adopted (this rule implies a uniform expansion of the initial yield surface as the plastic deformation increases). Therefore, from Eq.(4-6), the subsequent loading surfaces may be expressed as:

$$f(\sigma) = C.I_1 + \sqrt{(C.I_1)^2 + 3\beta J_2} = \sigma' \quad \dots\dots\dots(4-10)$$

where σ' represents the stress level at which further plastic deformation will occur. It can be expressed in terms of equivalent uniaxial stress or effective stress. In order to define the expansion of the current loading surface, the incremental theory of plasticity implies a relationship between the effective stress and the effective plastic strain to extrapolate the result of a uniaxial state of stress to the multi-axial states [2]. The effective, accumulated, plastic strain, ε_p , can be computed by integrating the effective plastic strain increment, $d\varepsilon_p$, along the strain path as:

$$\varepsilon_p = \int d\varepsilon_p \quad \dots\dots\dots(4-11)$$

where, the effective plastic strain increment can be calculated by using the work hardening hypothesis as:

$$d\varepsilon_p = \frac{dW_p}{\sigma'} = \frac{\sigma d\varepsilon_p}{\sigma'} \quad \dots\dots\dots(4-12)$$

In the present model, a linear relationship between stress and strain is used up to limit of elasticity $C_p f'_c$, beyond $C_p f'_c$, a parabolic uniaxial stress-strain curve is assumed, when the peak compressive stress f'_c is reached, a linear deficiency in the compressive stress f'_c begins, until termination occurs at the onset of crushing, as shown in the Fig.(4-6). This deficiency in the compressive stress f'_c which is adopted by many investigators [30,80], gives more accurate representation hence more closer to the behavior of concrete.

$$\text{i- } \sigma' = E \cdot \varepsilon_c \quad \text{for } 0 < \sigma' < C_p \cdot f'_c \quad \dots\dots\dots(4-13)$$

$$\text{ii- } \sigma' = C_p f'_c + E \left[\varepsilon_c - \frac{C_p f'_c}{E} \right] - \frac{E}{2\varepsilon'_0} \left[\varepsilon_c - \frac{C_p f'_c}{E} \right]^2 \quad \text{for } C_p \cdot f'_c < \sigma' < f'_c \quad \dots\dots\dots(4-14)$$

$$\text{iii- } \sigma' = f'_c - dF_c \quad \text{for } \varepsilon_c \geq (2 - C_p) f'_c / E \quad \dots\dots\dots(4-15)$$

where ϵ'_o is total strain corresponding to the parabolic part of the curve given by:

$$\epsilon'_o = 2(1 - C_p)f'_c / E \quad \dots\dots\dots(4-16)$$

and the deficiency in the compressive stress dF_c is:

$$dF_c = (\epsilon_c - \epsilon_o) \times (0.15 f'_c) / (\epsilon_u - \epsilon_o) \quad \dots\dots\dots(4-17)$$

where, E is the modulus of elasticity of concrete and ϵ_u is the ultimate compressive strain at which crushing occurs. **Chen [76]** found $\epsilon_u = 0.0035$ during his tests. In the present study, a value of **0.3** is assumed for plastic coefficient C_p for normal strength concrete. The plastic yielding begins at a stress level of $C_p f'_c$ as shown below.

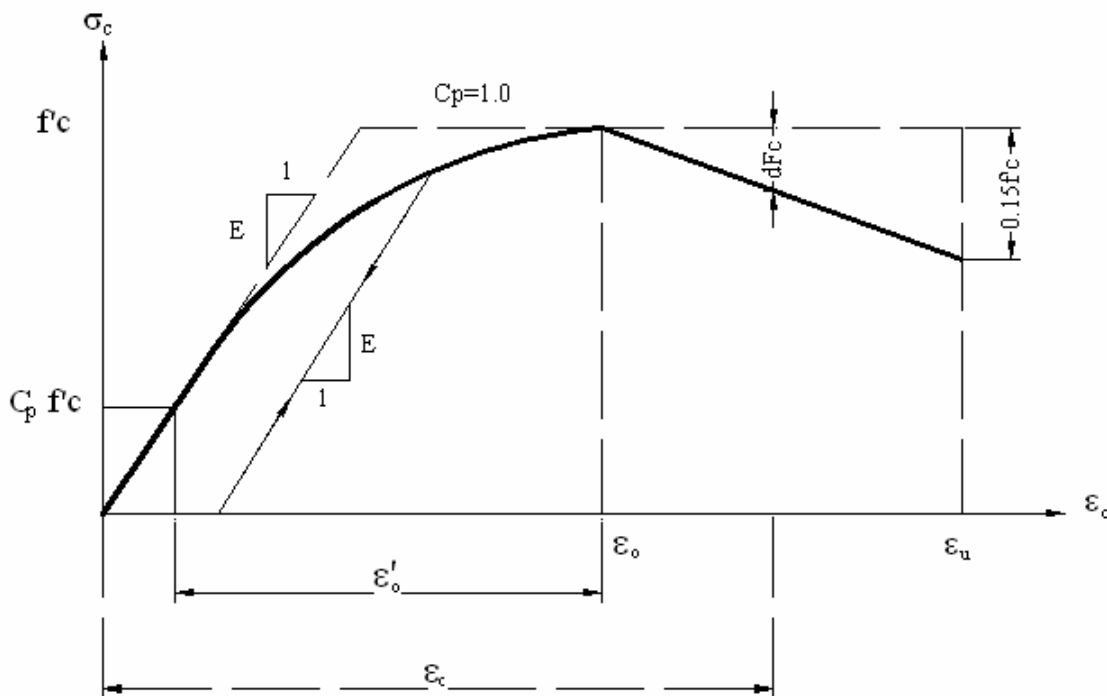


Fig.(4-6): Uniaxial Stress-Strain Curve of Concrete in Compression.

In order to derive the relationship between the effective stress and the effective plastic strain, the total strain ϵ_c is decomposed into its elastic and plastic components as:

$$\epsilon_c = \epsilon_e + \epsilon_p \quad \dots\dots\dots(4-18)$$

where ϵ_e is the elastic strain component given by;

$$\epsilon_e = \sigma' / E_c \quad \dots\dots\dots(4-19)$$

When substituting Eq.(4-18) and Eq.(4-19) into Eq.(4-14), the effective stress-plastic strain relationship can be expressed as:

$$\sigma' = C_p \cdot f_c' - E \cdot \varepsilon_p + \sqrt{2E^2 \cdot \varepsilon_o' \varepsilon_p} \quad \dots\dots\dots(4-20)$$

The slope of the effective stress-plastic strain curve, the hardening coefficient, is used in the formulation of the elasto-plastic incremental stress-strain relationship. Therefore, by differentiating Eq.(4-20) with respect to effective plastic strain, the hardening coefficient, H_c' can be expressed as [2,5]:

$$H_c' = \frac{d\sigma'}{d\varepsilon_p} = E \left(\sqrt{\frac{\varepsilon_o'}{2\varepsilon_p}} - 1.0 \right) \quad \dots\dots\dots(4-21)$$

- **The flow rule**

In order to establish the stress-strain relation in the plastic range, the concept of a plastic potential function $g(\sigma)$ is introduced [2,76]. The plastic strain increment vector is assumed to be proportional to the stress gradients of the plastic potential function, so that:

$$d\varepsilon_p = d\lambda \frac{\partial g(\sigma)}{\partial \sigma} \quad \dots\dots\dots(4-22)$$

where $d\lambda$ is a positive scalar of proportionality, Eq(4-22) is called the **flow rule** since it governs the plastic flow after yielding. The gradient of the potential surface $[\partial g(\sigma)/\partial \sigma]$ defines the direction of the plastic strain increment vector and the length is computed by the factor $d\lambda$. However when the current loading surface and the plastic potential function coincide, $\partial f(\sigma) \equiv \partial g(\sigma)$, Eq.(4-22) becomes:

$$d\varepsilon_p = d\lambda \frac{\partial f(\sigma)}{\partial \sigma} \quad \dots\dots\dots(4-23)$$

The last equation is known as the associated flow rule, because it is connected with the loading surface, also it is termed the normality condition since $[\partial f(\sigma)/\partial \sigma]$ represents a vector directed normal to the current loading surface at the stress point under consideration. The yield function is Eq.(4-6) and the derivatives with respect to the stress components define the flow vector $\{a\}$ as:

$$\{a\} = \left\{ \frac{\partial f}{\partial \sigma_x}, \frac{\partial f}{\partial \sigma_y}, \frac{\partial f}{\partial \sigma_z}, \frac{\partial f}{\partial \tau_{xy}}, \frac{\partial f}{\partial \tau_{yz}}, \frac{\partial f}{\partial \tau_{zx}} \right\}^T \quad \dots\dots\dots(4-24)$$

• **Incremental stress-strain relationship**

The derivation of the incremental stress-strain relation for an elastic-work hardening plastic material based on the associated flow rule Eq.(4-23) is presented here. During the plastic loading, both the initial yield and the subsequent stress states must satisfy the yield condition, $F(\sigma, k) = 0$. The yield function first defined in Eq.(4-6) can be rewritten as:

$$F(\sigma, k) = f(\sigma) + K(k) = 0 \quad \dots\dots\dots(4-25)$$

where, k is the hardening parameter which governs the expansion of the yield surface. When differentiating Eq.(4-25) the result will be:

$$dF = \frac{\partial F}{\partial \sigma} d\sigma + \frac{\partial F}{\partial k} dk = 0 \quad \dots\dots\dots(4-26)$$

or, $\{a\}^T d\sigma - A d\lambda = 0 \quad \dots\dots\dots(4-27)$

where, $A = \frac{1}{d\lambda} \frac{\partial F}{\partial k} dk \quad \dots\dots\dots(4-28)$

For the yield function adopted in the analysis, the scalar term A in Eq.(4-28) can be proved to be equal to the slope of the effective stress-plastic strain curve, H'_c , by using *Euler's* theorem for homogeneous functions and the work hardening rule [5,76,81]. The total incremental strain vector given by Eq.(4-5) can be rewritten by substitution of Eq.(4-23) gives:

$$d\{\varepsilon\} = d\{\varepsilon_e\} + d\lambda \frac{\partial f}{\partial \sigma} \quad \dots\dots\dots(4-29)$$

The elastic strain increment $d\{\varepsilon_e\}$ is related to the stress increment by the elastic constitutive relation which is given by:

$$d\{\sigma\} = [D] d\{\varepsilon_e\} \quad \dots\dots\dots(4-30)$$

where $[D]$, is the elastic constitutive matrix given by:

$$D = \frac{E}{(1-2\nu)(1+\nu)} \begin{bmatrix} 1-\nu & \nu & \nu & 0 & 0 & 0 \\ \nu & 1-\nu & \nu & 0 & 0 & 0 \\ \nu & \nu & 1-\nu & 0 & 0 & 0 \\ 0 & 0 & 0 & 0.5-\nu & 0 & 0 \\ 0 & 0 & 0 & 0 & 0.5-\nu & 0 \\ 0 & 0 & 0 & 0 & 0 & 0.5-\nu \end{bmatrix} \quad \dots\dots\dots(4-31)$$

Substituting of Eq.(4-30) into Eq.(4-29) yields:

$$d\{\varepsilon\} = [D]^{-1} d\{\sigma\} + d\lambda \{a\} \quad \dots\dots\dots(4-32)$$

Pre-multiplying both sides of Eq.(4-32) by, $\{a\}^T \cdot [D]$ and eliminating $\{a\}^T \cdot d\{\sigma\}$, utilizing Eq.(4.27), the following expression for the plastic multiplier, $d\lambda$, is obtained;

$$d\lambda = \left[\frac{\{a\}^T \cdot [D]}{H'_c + \{a\}^T \cdot [D] \cdot \{a\}} \right] \cdot d\{\varepsilon\} \quad \dots\dots\dots(4-33)$$

Substituting Eq.(4-33) into Eq.(4-29) and pre-multiplying both sides by $[D]$, the complete elasto-plastic incremental stress-strain relationship is obtained as:

$$d\{\sigma\} = \left[[D] - \frac{[D] \cdot \{a\} \{a\}^T \cdot [D]}{H'_c + \{a\}^T \cdot [D] \cdot \{a\}} \right] d\{\varepsilon\} \quad \dots\dots\dots(4-34)$$

As shown in Eq.(4-34) the second term in the bracket represents the stiffness degradation due to the plastic deformation. If the stress point departs from the loading surface, it is scaled back to the loading surface by relaxing the excess stress in several stages using the technique described by **Chen [76]** and by **Owen and Hinton [81]**.

- **The crushing condition**

In present models, the hardening-plastic model described above governs the increase of the inelastic deformation in concrete under compressive stress. Inelastic deformation continues in the concrete until crushing occurs. The crushing type of fracture is a strain-controlled phenomenon. The failure surface in the strain space must be defined so that this type of fracture can be taken into account. A simple way to do that, despite the lack of experimental data on concrete ultimate deformation capacity under muliaxial loading [5], is to assume a crushing surface

in the strain space whose size is related to a maximum equivalent strain extrapolated from uniaxial tests. Therefore the following failure surface can be used [5,6]:

$$\sqrt{3} J'_2 = \varepsilon_{cu} \quad \dots\dots\dots(4-35-a)$$

where J'_2 is the second deviatoric strain invariant and ε_{cu} is the ultimate crushing strain of concrete. Also when crushing occurs the stress state must be compressive and the following conditions must be satisfied[76]:

$$\sqrt{J'_2} \leq -\frac{I_1}{\sqrt{3}} \quad \text{and} \quad I_1 \leq 0 \quad \dots\dots\dots(4-35-b)$$

However, when the sampling Gauss point is crushed its stresses drop abruptly to zero (as specify in the program).

4-2-2-1-2: The Smeared Crack Model for Concrete in Tension

A smeared crack model with fixed orthogonal cracks is adopted to represent the fractured concrete in the current model. The adopted model is described in terms of; a cracking criterion, a post-cracking formulation and a shear retention model. The cracking criterion of concrete is expressed in terms of principal tensile stresses or strains. Here, the maximum tensile stress criterion is adopted. The behavior of concrete in tension is modeled as linear elastic prior to cracking. The onset of cracking is governed by a maximum principal stress criterion.

- **The cracking criterion**

The initiation of cracking is controlled by a maximum tensile stress criterion. For previously uncracked sampling Gauss point, the principal stresses and their directions are calculated (as illustrated in *Appendix (C)*). At the sampling point under consideration, if the major principal stress σ_1 exceeds the limiting tensile strength a crack is assumed to form. The limiting tensile stress required to define the onset of cracking can be calculated for the state of triaxial tensile stress and for combinations of tensile and compressive principal stresses as follows [2]:

a) For the tri-axial tension zone: $(\sigma_1 \geq \sigma_2 \geq \sigma_3 > 0)$

$$\sigma_i = \sigma_{cr} = f_t \quad i = 1, 2, 3 \quad \dots\dots\dots(4-36)$$

b) For the case of the tension-tension-compression zone: $(\sigma_1 \geq \sigma_2 > 0, \sigma_3 \leq 0)$

$$\sigma_i = \sigma_{cr} = f_t \left[1.0 + \frac{0.75\sigma_3}{f'_c} \right] \quad i = 1, 2 \quad \dots\dots\dots(4-37)$$

c) For the case of tension-compression- compression zone. ($\sigma_1 > 0, \sigma_2 \leq \sigma_3 \leq 0$)

$$\sigma_1 = \sigma_{cr} = f_t \left[1.0 + \frac{0.75\sigma_2}{f'_c} \right] \cdot \left[1.0 + \frac{0.75\sigma_3}{f'_c} \right] \dots\dots\dots(4-38)$$

where, σ_{cr} , f_t and f'_c are the cracking stress, the tensile and compressive concrete strength (positive values) respectively. Eqs.(4-37) and (4-38) incorporates the fact that compression in one direction favors cracking in the other directions and thus reduces the tensile strength of the material. Fig.(4-7) shows the tensile failure envelope resulting from Eq.(4-36) to Eq.(4-38) in principal stress space. It is important to note that in the current study the compressive strength is not constant, but reduced to $\lambda f'$ due to orthogonal crack, and the tensile strength may be equal zero.

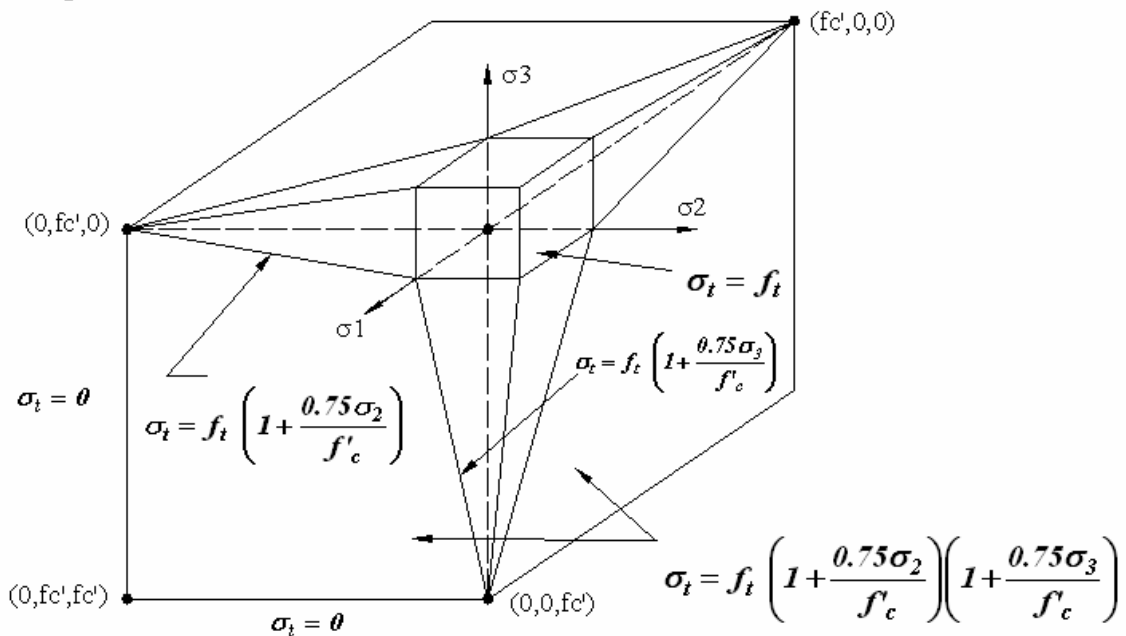


Fig.(4-7):Three Dimensional Tensile Failure Envelope of Concrete Model.

When the principal stress σ_1 , violates the cracking criterion, the elastic modulus in the direction of maximum tensile stress σ_1 , is reduced to E_1 , and, the shear modulus across the failure plane is reduced to $\beta_1 G$, also planes of failure develop perpendicular to its direction as shown in Fig.(4-8-a). The concrete behavior becomes orthotropic with the direction of σ_1 , while the behavior of the material between two adjacent failure planes remains isotropic. Because of the lack of interaction between orthogonal planes caused by cracking, *Poisson's* ratio is set to zero. The incremental stress-strain relationship in the local material axes may be expressed as:

$$\begin{Bmatrix} \Delta\sigma_1 \\ \Delta\sigma_2 \\ \Delta\sigma_3 \\ \Delta\tau_{12} \\ \Delta\tau_{23} \\ \Delta\tau_{31} \end{Bmatrix} = \begin{bmatrix} E_1 & 0 & 0 & 0 & 0 & 0 \\ 0 & E/(1-\nu^2) & \nu E/(1-\nu^2) & 0 & 0 & 0 \\ 0 & \nu E/(1-\nu^2) & E/(1-\nu^2) & 0 & 0 & 0 \\ 0 & 0 & 0 & \beta_1 G & 0 & 0 \\ 0 & 0 & 0 & 0 & G & 0 \\ 0 & 0 & 0 & 0 & 0 & \beta_1 G \end{bmatrix} \begin{Bmatrix} \Delta\varepsilon_1 \\ \Delta\varepsilon_2 \\ \Delta\varepsilon_3 \\ \Delta\gamma_{12} \\ \Delta\gamma_{23} \\ \Delta\gamma_{31} \end{Bmatrix} \dots\dots(4-39)$$

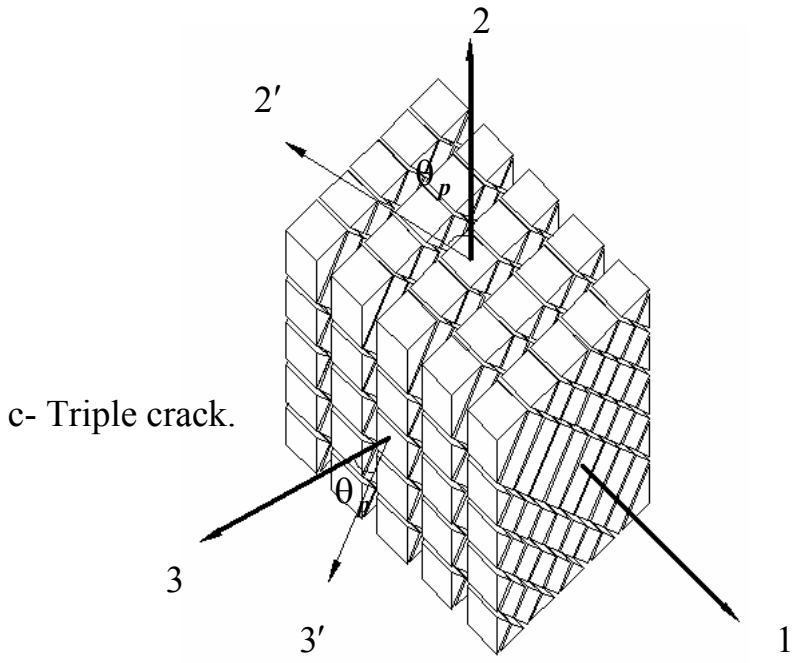
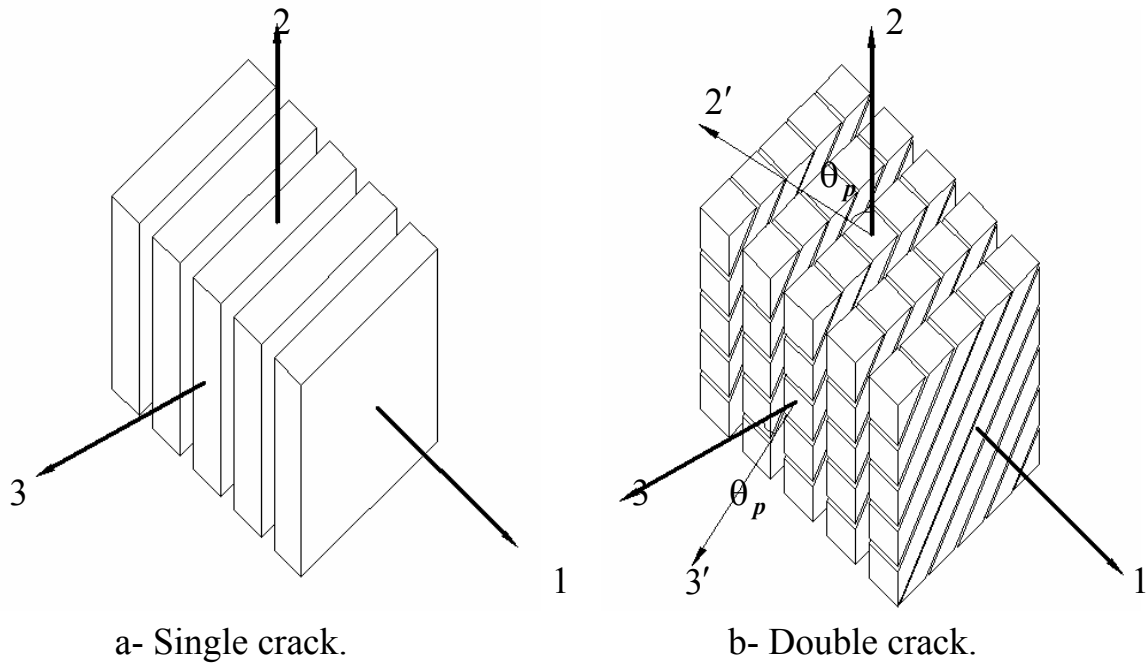


Fig.(4-8): Crack Patterns in Local Material Axes.

Eq.(4-39) may be written in the form:

$$\{\Delta\sigma\} = [D_{cr}].\{\Delta\varepsilon\} \quad \dots\dots\dots(4-40)$$

Then, the stress increment in the global axes (x, y, z) may be obtained by using the coordinate transformation matrix such that

$$\{\Delta\sigma\} = [T]^T . [D_{cr}] [T].\{\Delta\varepsilon\} \quad \dots\dots\dots(4-41)$$

where $[T]$, is the strain transformation matrix expressed in terms of direction cosines as [55,56,82]:

$$[T] = \begin{bmatrix} l_1^2 & m_1^2 & n_1^2 & l_1m_1 & m_1n_1 & n_1l_1 \\ l_2^2 & m_2^2 & n_2^2 & l_2m_2 & m_2n_2 & n_2l_2 \\ l_3^2 & m_3^2 & n_3^2 & l_3m_3 & m_3n_3 & n_3l_3 \\ 2l_1l_2 & 2m_1m_2 & 2n_1n_2 & (l_1m_2 + l_2m_1) & (m_1n_2 + m_2n_1) & (n_1l_2 + n_2l_1) \\ 2l_2l_3 & 2m_2m_3 & 2n_2n_3 & (l_2m_3 + l_3m_2) & (m_2n_3 + m_3n_2) & (n_2l_3 + n_3l_2) \\ 2l_3l_1 & 2m_3m_1 & 2n_3n_1 & (l_3m_1 + l_1m_3) & (m_3n_1 + m_1n_3) & (n_3l_1 + n_1l_3) \end{bmatrix} \quad \dots\dots\dots(4-42)$$

where l_i, m_i and n_i ($i = 1,2,3$) represent the direction cosines of the principal directions 1,2 and 3 with respect to x, y and z -directions, respectively.

When the tension-tension-compression or the triaxial tension states of stresses exist, the cracking criterion may be violated by the major principal stress σ_1 and the second principal stress σ_2 simultaneously. As a result, there exists a possibility of developing two sets of orthogonal failure planes. These planes are perpendicular to the principal axes 1 and 2, respectively. In this case, *Poisson's* ratio is set to zero in all directions and the constitutive matrix in the local material axis is reduced to the following form:

$$D_{cr} = \begin{bmatrix} E_1 & 0 & 0 & 0 & 0 & 0 \\ & E_2 & 0 & 0 & 0 & 0 \\ & & E & 0 & 0 & 0 \\ & & & \beta_1 G & 0 & 0 \\ sym. & & & & \beta_2 G & 0 \\ & & & & & \beta_1 G \end{bmatrix} \quad \dots\dots\dots(4-43)$$

In the fixed crack model, the rotation of the principal stresses is cancelled after the formation of the first crack, but, if the second crack is initiated at a subsequent stage of loading, rotation of the principal stresses within the planes

perpendicular to the direction of σ_1 may be considered. The magnitudes and directions of the second set of the principal stresses, σ'_2 and σ'_3 , as illustrated in Fig.(4-8-b), can be calculated from the original principal stresses σ_2 and σ_3 , and the shear stress τ_{23} accumulated during loading stages beyond the formulation of the first crack. Thus;

$$\sigma'_i = \frac{\sigma_2 + \sigma_3}{2} \pm \left[\frac{(\sigma_2 - \sigma_3)^2}{2} + \tau_{23}^2 \right]^{0.5} \quad i = 1, 2 \quad \dots\dots\dots(4-44)$$

The failure planes corresponding to the second crack are assumed to be perpendicular to the direction of the second principal stress σ'_2 , as shown in Fig.(4-8-b). The angle between the original (first principal or first local) directions and the new in-plane (second principal or second local) principal directions, θ_p , can be computed as [55,56,82]:

$$\theta_p = \frac{1}{2} \tan^{-1} \frac{2\tau_{23}}{\sigma_2 - \sigma_3} \quad \dots\dots\dots(4-45)$$

The local in-plane constitutive matrix with respect to the new principal directions (2',3') is expressed as:

$$D_{cr} = \begin{bmatrix} E_2 & 0 & 0 \\ 0 & E & 0 \\ 0 & 0 & \beta_2 G \end{bmatrix} \quad \dots\dots\dots(4-46)$$

The last matrix can be transformed to the original principal directions (first local) (2,3) by using the in-plane coordinates transformation matrix, which is defined as:

$$T_p = \begin{bmatrix} C^2 & S^2 & CS \\ S^2 & C^2 & -CS \\ -2CS & 2CS & C^2 - S^2 \end{bmatrix} \quad \dots\dots\dots(4-47)$$

where, $C = \cos \theta_p$, and $S = \sin \theta_p$. In the present static model, a maximum of three sets of cracks are allowed to be formed at each sampling point, as shown in Fig.(4-8-c), the third crack may occur when the principal stress (σ_3 or σ'_3) exceeds the uniaxial tensile strength f_t .

4-2-2-1-3: A Post-Cracking Stress-Strain Relationship.

- *Tension stiffening model*

The experimental data show that the tensile stresses normal to a cracked plane are gradually released as the crack width increases. This response is usually modeled in the finite element analysis using either the tension-stiffening or the strain-softening concepts. The former concept is suitable for analyzing reinforced concrete structures where the behavior is characterized by the formulation of a lot of closely spaced cracks. While the strain-softening concept is useful for analyzing plain concrete structures where the behavior is governed by the formation of a single macro-crack or a few dominant cracks [2], therefore the first concept is adopted in this study, which has been adopted by many researchers [2,5,80,83,...etc.]. Two approaches have been suggested to consider tension-stiffening effects [83]; the first is characterized by increasing the stiffness of reinforcing steel bars, while the second is characterized by a gradual decrease of the tensile stress in the cracked concrete over a specified strain range. In the current study, the second approach is adopted to represent the tension-stiffening effect. Fig.(4-9) shows the formulation of this approach as:

$$\sigma_n = \alpha_2 \sigma_{cr} \frac{(\alpha_1 - \varepsilon_n / \varepsilon_{cr})}{(\alpha_1 - 1.0)} \quad \text{when } \varepsilon_{cr} \leq \varepsilon_n < \alpha_1 \varepsilon_{cr} \quad \dots\dots\dots(4-48)$$

$$\sigma_n = 0.0 \quad \text{when } \varepsilon_n \geq \alpha_1 \varepsilon_{cr} \quad \dots\dots\dots(4-49)$$

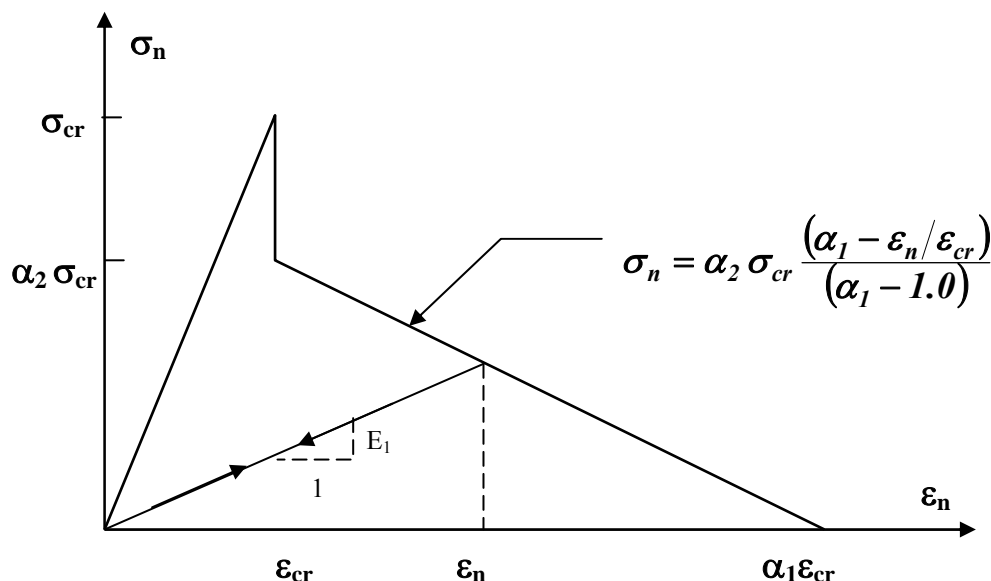


Fig.(4-9): Post-Cracking Model for Concrete in Tension [2].

where; σ_n and ε_n are the stress and strain normal to the crack plane, ε_{cr} is the cracking strain associated with the cracking stress σ_{cr} , α_1 is the rate of post-cracking stress decay as the strain increases, α_2 is the sudden loss in stress at instant of cracking. In nonlinear finite element analyses, *Cope* [84] used $\alpha_1 = 15$ which gave good predictions to the results of *Clark* and *Speirs* [85]. The values of α_1 and α_2 in the ranges of 5-25 and 0.2-1.0 respectively have been used by many investigators [2].

- **Shear retention model**

When the sampling point is cracked, its shear stiffness becomes progressively smaller as the crack widens. So the shear modulus of elasticity is reduced to, βG . Before cracking the factor β is equal to 1.0. When the cracks has occurred a sudden loss in the shear factor β is assumed. Thereafter when the cracks propagate a linearly decreasing function of the strain normal to the cracked plane is assumed. Finally when the crack width reaches $\gamma_1 \varepsilon_{cr}$ a constant value is assigned to β account for dowel action. The adopted shear retention model is shown in Fig.(4-10) [2,83].

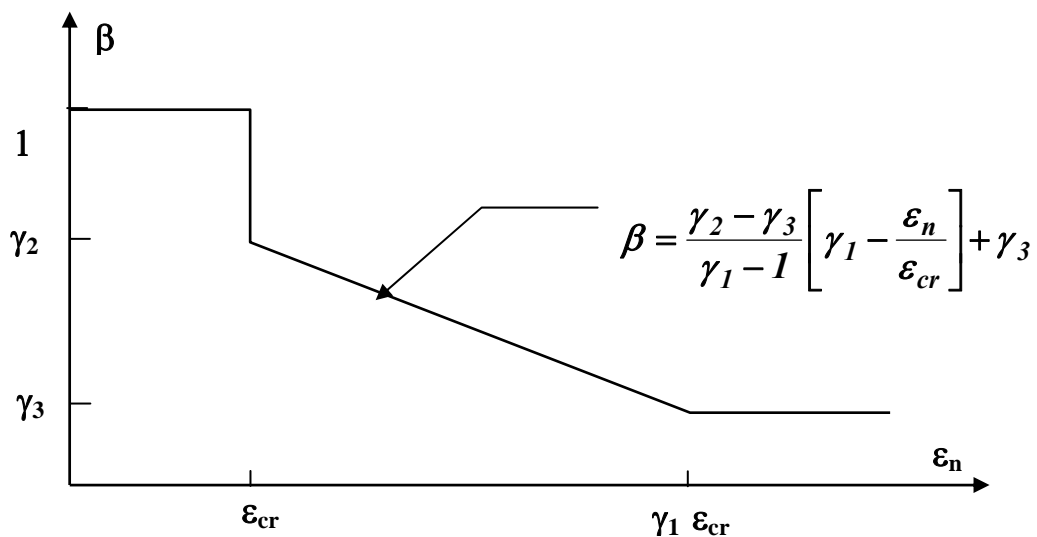


Fig.(4-10): Shear Retention Model for Concrete[2].

where γ_1, γ_2 and γ_3 are the shear retention parameters. γ_1 represents the rate of decay of shear modulus as the crack widens. γ_2 represents the sudden loss in the shear modulus at the onset of cracking. γ_3 represents the residual shear modulus due to the dowel action.

- **Closing and re-opening of cracks**

The redistribution of internal stresses (especially when crushing occurs) enforces the neighboring points to be under unloading state. The unloading of a cracked sampling Gauss point is assumed to follow a secant path, see Fig.(4-9). The secant modulus, E_1 , can be evaluated from the previously stored accumulative strain developed normal to the cracked plane. This secant modulus can be used to determine the retained stress as:

$$\sigma_n = E_1 \varepsilon_n \quad \dots\dots\dots(4-50)$$

The external loads applied as increments, whenever the increment of loads causes any direction of previously cracked Gauss point to be closed the load increment must be divided into another sub-increments for that Gauss point as individual form. For illustration of this important situation, it is assumed that the Gauss point previously cracked in one direction as shown in Fig.(4-8-a), and the other two directions (planes) represent a two-dimensional state, when this crack is closed during the current increment of load, the increment must be divided into two sub-increments. The first is applied to the previous state of Gauss point, while the second sub-increment is applied to the current state of Gauss point (i.e., three-dimensional isotropic state). Also when two directions are closed at any Gauss point during the same increment, this increment must be divided into three sub-increments. The author presented a static model *NFHCBSL* to dealing with one, two, or even three closed crack directions (for any Gauss point) during the same increment.

When the crack is completely closed, the effects of any residual strains are neglected and the Gauss point is assumed to be healed [76]. It is important to illustrate that when the Gauss point is re-cracked the previously stored secant modulus is taken in the computation of this point in that re-cracked direction.

4-2-2-1-4: Modeling the Reduction in Compressive Strength Due to Orthogonal Cracking.

A lot of investigations [86,87,88] showed that in a reinforced concrete members, a significant degradation in compressive strength can result due to

presence of transverse tensile strain after cracking. *Cervenka's* [88] model, which is adopted in the current study (this technique was used also by *Al-Shaarbaf* in 1990 and gave good result), proposed the use of a reduction factor to reduce both the peak stress and the corresponding strain. Therefore from Eq.(4-13) to Eq.(4-16), the modified stress-strain relationships may be expressed as:

$$\text{i- } \sigma' = \lambda E \cdot \varepsilon_c \quad \text{for } 0 < \sigma' < \lambda C_p \cdot f'_c \quad \dots\dots(4-51)$$

$$\text{ii- } \sigma' = \lambda C_p f'_c + E \left[\varepsilon_c - \frac{\lambda C_p f'_c}{E} \right] - \frac{E}{2\varepsilon'_o} \left[\varepsilon_c - \frac{\lambda C_p f'_c}{E} \right] \text{ for } \lambda C_p f'_c < \sigma' < \lambda f'_c \dots\dots(4-52)$$

$$\text{iii- } \sigma' = \lambda (f'_c - dF_c) \quad \text{for } \varepsilon_c \geq (2 - C_p) \lambda f'_c / E \dots\dots(4-53)$$

$$\text{where, } \varepsilon'_o = 2(1 - C_p) \lambda f'_c / E \quad \dots\dots(4-54)$$

Thus, the effective stress-plastic strain relation Eq.(4-20) will be modified as:

$$\sigma' = \lambda C_p \cdot f'_c - E \cdot \varepsilon_p + \sqrt{2E^2 \lambda \varepsilon'_o \varepsilon_p} \quad \dots\dots(4-55)$$

Consequently, the hardening parameter can be expressed as:

$$H'_c = \frac{d\sigma'}{d\varepsilon_p} = E \left(\sqrt{\frac{\lambda \varepsilon'_o}{2\varepsilon_p}} - 1.0 \right) \quad \dots\dots(4-56)$$

For a singly cracked sampling point, the compressive reduction factor is given by:

$$\lambda = 1.0 - k_1 \frac{\varepsilon_1}{0.005} \leq 1.0 - k_1 \quad \dots\dots(4-57)$$

where, ε_1 is the transverse tensile strain in principal direction 1 (the strain normal to the cracked plane). For a doubly cracked sampling point the reduction factor is expressed as:

$$\lambda = 1.0 - k_1 \frac{(\varepsilon_1^2 + \varepsilon_2^2)^{0.5}}{0.005} \leq 1.0 - k_1 \quad \dots\dots(4-58)$$

where, ε_2 is the tensile strain normal to the second plane crack.

4-3: Modeling of the Steel under Static Load

4-3-1: Observed Behavior of the Steel under Static Load

Typical stress-strain curves for different types of steel are shown in Fig.(4-11). Grade 40 bar, having a specified yield strength of 275 MPa, represents a hot-

rolled steel with a characteristic yield point (f_y , ϵ_{sy}), yield plateau (f_y , ϵ_{st}), and a portion of strain hardening before peak stress point (f_u , ϵ_{su}) which leads to failure at point (f_f , ϵ_{sf}). The stress-strain curves for grade 40, 50, or 60 steel are characterized normally by the following general features [76]:

- 1- An initial linear elastic region up to the point (f_y , ϵ_{sy}) is observed. The mean modulus of elasticity is $E_s = 200000$ MPa with a coefficient of variation of 3.3 percent and the mean yield stress is $f_y = 336$ and 490 MPa for grades 40 and 60, respectively, with coefficients of variation of 10.7 and 9.3 percent.
- 2- A yield plateau from ϵ_{sy} to the strain-hardening strain ϵ_{st} is recorded. A typical value for the strain-hardening modulus H_s is 4800 MPa and a typical ratio of ($\beta = \epsilon_{st}/\epsilon_{sy}$) is 12. When the elastic limit is reached, elongation ranging from 8 to 15 times the elastic-limit strain can take place without any decrease in stress. Afterwards some increase in strength is exhibited as the material strain hardens.
- 3- A strain-hardening region starting from ϵ_{st} to the ultimate strain ϵ_{su} is recorded. An ultimate strength of approximately 1.55 times the yield strength has generally been observed.

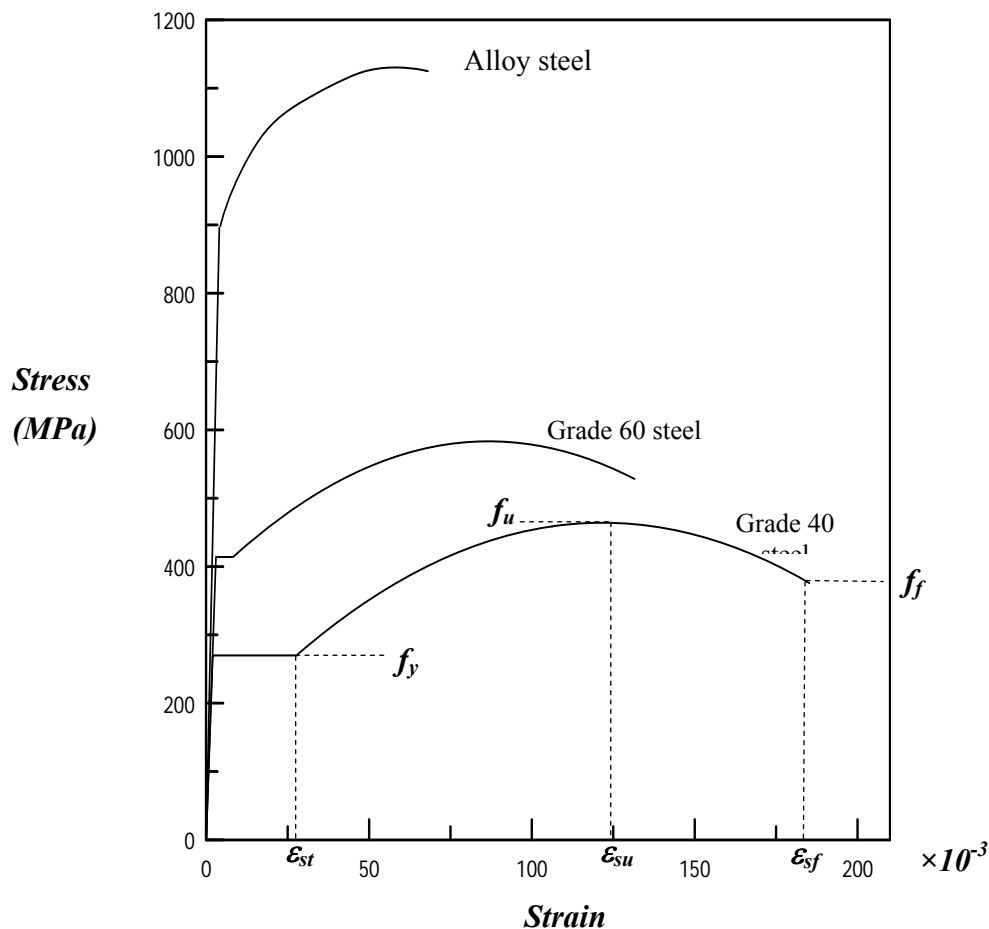


Fig.(4-11): Typical Stress-Strain Curves for Steel [76].

The stress-strain curves for steel are assumed to be identical in tension and compression. The essential properties of steel are given as follows [76]:

- ***Yield strength (f_y)***

This parameter could be considered as the limit (or end) of elastic range. It is quite distinguished in low strength steels having a definite yield plateau while it is not so in high strength steel, which lacks such a plateau. It is usually assumed for the latter case, that yield strength is the stress corresponding to a strain of 0.01 or the stress causing a residual strain of 0.02 after unloading. However this parameter is usually given by conventional tests.

- ***Elastic modulus (E_s)***

This parameter is the most important property of steel members since steel is elastic at working load range of steel members. It has a value ranging between 186000-207000 MPa.

- ***Hardening modulus (H_s)***

This parameter is used to introduce the effect for strain-hardening region. It was usually estimated on an arbitrary way in most studies by adopting a bilinear steel model. It has a value as a percentage of the elastic modulus (E_s) ranging between (0.3-2.5%).

- ***Ultimate steel strain (ϵ_{su})***

It is a function of the steel grade. Actually, it has higher values for low strength steel. It has a value ranging between (0.12-0.2).

4-3-2: Modeling of the Steel Adopted in the Analysis

In the finite element programs, numerical material models are usually kept as simple as possible so that they can be easily used. However, such models should accurately trace the overall behavior of steel in the steel and composite steel-concrete members within an engineering degree of accuracy. The present steel model is suitable for the nonlinear static analysis of three-dimensional steel and composite (steel-concrete) structures.

- **Yield criterion used for steel**

A yield criterion for isotropic materials must be independent of choice of the coordinates system in which the stress state is defined. Hence, it should be a function of the stress invariants only [76,81]. In the present work, the *Von-Mises* yield criterion has been used to monitor the stress level at the onset plastic deformation for steel material. It can be expressed as

$$f(\sigma) = \sqrt{3J_2} = \sigma_o \quad \dots\dots\dots(4-59)$$

where J_2 is the second deviatoric stress invariant, and it is given by:

$$J_2 = \frac{1}{3} [(\sigma_1^2 + \sigma_2^2 + \sigma_3^2) - (\sigma_1 \cdot \sigma_2 + \sigma_2 \cdot \sigma_3 + \sigma_3 \cdot \sigma_1)] \quad \dots\dots\dots(4-60)$$

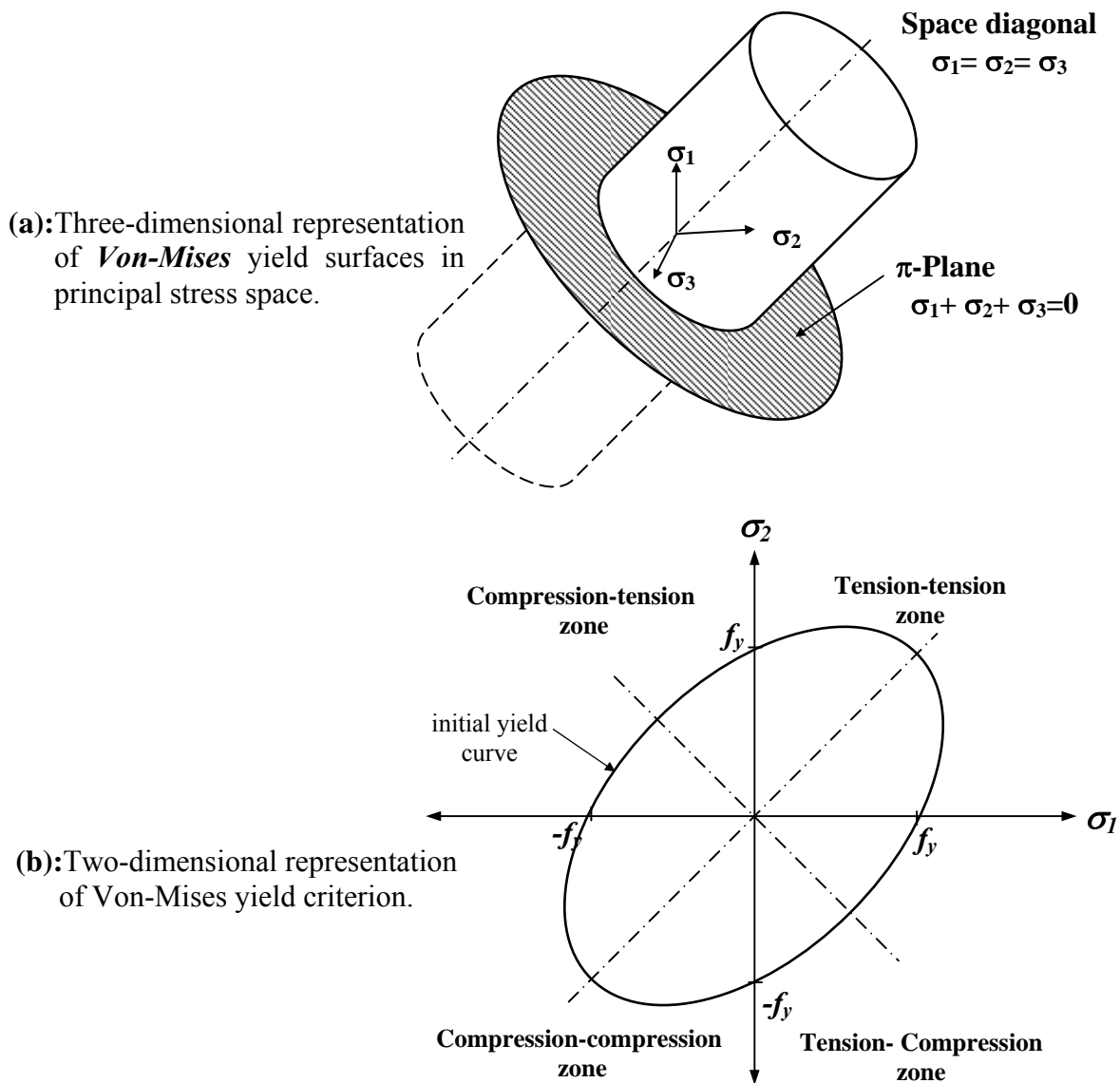


Fig.(4-12): The Yield Criterion Adopted in Current Steel Model [81].

and σ_o is the equivalent effective stress at the onset of plastic deformation which can be determined from the uniaxial stress test as:

$$\sigma_o = f_y \quad \dots\dots\dots(4-61)$$

where f_y is the yield stress which is used to mark the initiation of the plastic deformation.

In the three-dimensional principal stress space, the resulting *Von-Mises* yield criterion Eq.(4-59) is a circular cylinder with axis in the line $\sigma_1 = \sigma_2 = \sigma_3$. Therefore, the intersection of the *Von-Mises* circular cylinder with the coordinate $\sigma_3=0$ is an ellipse, as shown in Fig.(4-12).

- ***Elasto-plastic stress-strain relation for steel***

When the material is stressed beyond its initial yielding surface, a hardening rule is required to describe the growth of subsequent loading surfaces during plastic deformation. This rule implies a uniform expansion of the initial yield surface as the plastic deformation increases. Therefore, from Eq.(4-59) the subsequent loading function may be expressed as:

$$f(\sigma) = \sqrt{3J_2} = \sigma' \quad \dots\dots\dots(4-62)$$

where, σ' represents the stress level at which further plastic deformation will occur.

A tri-linear model is adopted in this study for the equivalent uni-axial stress-strain relationship for steel. The first line represents the elastic stage of behavior and sloped by the elastic modulus (E_s). A yield plateau flow continues from (ϵ_{sy}) until reaching the strain-hardening stage (ϵ_{st}) which is represented by the second line. Beyond that a third line represents the work-hardening stage of behavior and sloped by the hardening modulus (H_s) which is a small percentage of the elastic modulus (E_s). Fig.(4-13-a) shows the equivalent uniaxial stress-strain model for steel in various stages of behavior. These are given by:

$$\text{i- } \sigma' = E_s \cdot \epsilon_s \quad \text{for } 0 \leq \epsilon_s \leq \epsilon_{sy} \quad \dots\dots\dots(4-63)$$

$$\text{ii- } \sigma' = f_y \quad \text{for } \epsilon_{sy} \leq \epsilon_s \leq \epsilon_{st} \quad \dots\dots\dots(4-64)$$

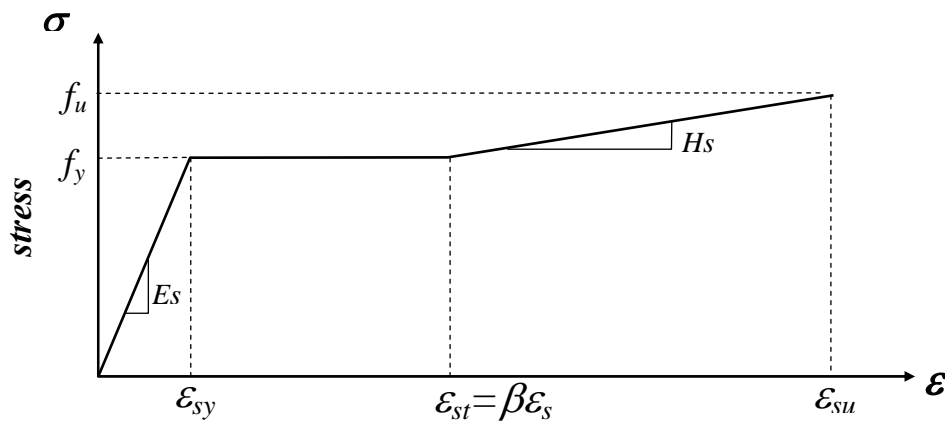
$$\text{iii- } \sigma' = f_y + (\epsilon_s - \epsilon_{st}) H_s \quad \text{for } \epsilon_s \geq \epsilon_{st} \quad \dots\dots\dots(4-65)$$

The complete elasto-plastic incremental stress-strain relationship for steel can be expressed as [2,5]:

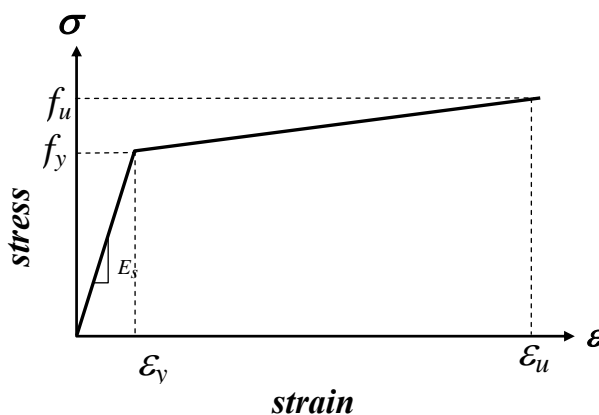
$$d\{\sigma\} = [D_{e-p}]_s d\{\varepsilon\} \quad \dots\dots(4-66)$$

where, $[D_{e-p}]_s = \left[[D] - \frac{[D]\{a\}\{a\}^T \cdot [D]}{H_s + \{a\}^T \cdot [D] \cdot \{a\}} \right] \quad \dots\dots(4-67)$

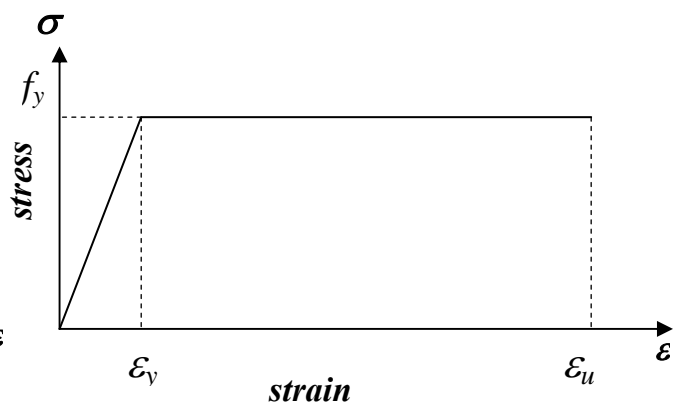
the second term in the brackets represents the stiffness degradation due to the plastic deformation. Definitions of elastic constitutive matrix $[D]$ and flow vector $\{a\}$ are given previously. When β is equal to zero the equivalent uniaxial stress-strain relationship becomes as in Fig.(4-13-b), while if H_s is equal to zero it becomes as shown in Fig.(4-13-c).



(a)



(b)



(c)

Fig.(4-13): Idealization of Stress-Strain Curve for Steel.

4-4: Modeling of Reinforcing Bars under Static Load

In reinforced concrete members (straight or curved) the reinforcing bars are normally long and relatively slender, therefore, they can be generally assumed capable of transmitting axial force only. Modeling of reinforcing bars in the finite element analysis is much simpler when compared to modeling of concrete.

A typical uniaxial stress-strain curve for a reinforcing steel bar specimen loaded monotonically in tension is shown in Fig.(4-11). In the present model, the uniaxial stress-strain behavior of reinforcing bars has been simulated by a tri-linear model which is similar to the model which is used to simulate the stress-strain behavior of steel beam as shown in Fig.(4-13a).

Chapter Five

Behavior and Modeling of Materials under Dynamic Loads

5-1: Introduction

This chapter is devoted to illustrate the behavior and the adopted modeling of concrete and steel under transient dynamic loads. A classical elasto/viscoplastic constitutive model is adopted for steel and concrete structures. This model is used for concrete structures but allowance is made for rate dependency and damage accumulation in the concrete. Furthermore, tensile cracking is considered using the smeared crack approach and the constant fracture energy release concept, where the strain softening effect is related to the element size to make the response prediction mesh – size dependent. The amount of shear stresses which can be transferred across the rough surfaces of cracked concrete is represented. Material nonlinearities of reinforced concrete in compression are described as inelastic response by elastic– viscoplastic relationships. Steel reinforcement is incorporated in the concrete brick element by assuming perfect bond.

This chapter describes the finite element model used in the current dynamic study. Section 5-2 describes the modeling of concrete. Steel representation, which is used, is presented in section 5-3. Finally section 5-4 summarizes the representation of the reinforcement bars.

5-2: Modeling of the Concrete under Dynamic Load

5-2-1: Observed Behavior of the Concrete under Dynamic Load

Many of experimental studies have been carried out on concrete under monotonic quasi-static loading (strain rate about 10^{-6} sec $^{-1}$ or less)[6], while a little investigation is devoted for dynamic loads. Some researchers [89-94] studied the influence of loading rate for specimens with uniaxial compressive loads.

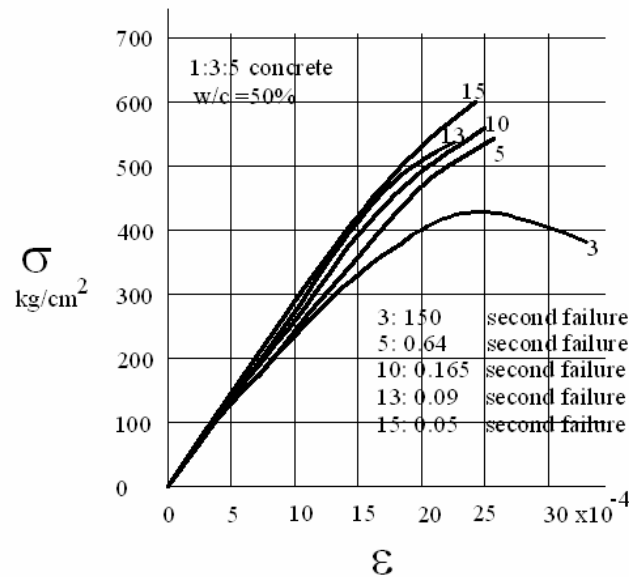


Fig.(5-1): Typical Experimental Results from Direct Compressive Dynamic Uniaxial Tests [90,91].

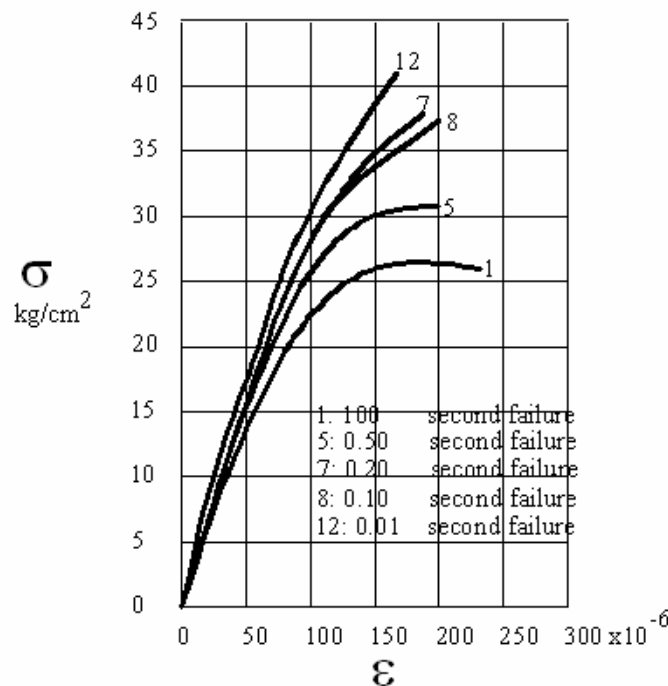


Fig.(5-2): Typical Experimental Results from Direct Tensile Dynamic Uniaxial Tests [95].

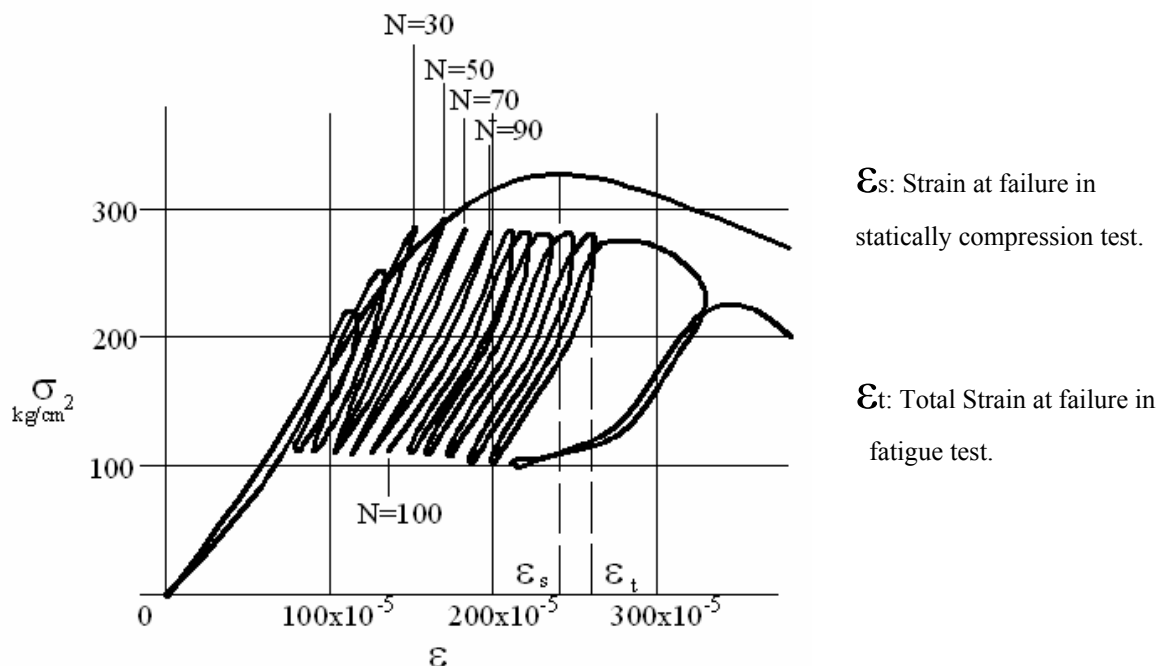


Fig.(5-3): Typical Experimental Stress-Strain Relations in Compression and Low Cycle Fatigue Tests [96,97].

Some valuable direct tensile tests on cylinders under impulsive load were conducted by *Hantano* [95], he also investigated the fatigue failure under periodic compressive loads [96,97]. Also biaxial tests under different rates of straining were performed by *Nelissen* [98]. A typical experimental results from dynamic uniaxial tests are plotted in Figs.(5-1) to (5-3), for (1:3:5) concrete. Form these experimental results, the principal features of the behavior of plain concrete under dynamic loading conditions are now listed [6,99,100]:

- a - The strength of plain concrete depends on the straining rate.
- b - The initial elastic modulus depends on the straining rate.
- c - The failure strain remains almost constant for any rate of straining for a particular concrete.
- d - Cyclic compressive loading produces a pronounced hysteresis effect in the stress-strain curve.
- e – For the stress-strain curves under compressive load histories there is a bounding curve which may be considered identical to the stress – strain curve under the constant strain-rate test.

It is important to note that these results are drawn from uniaxial tests and they will not necessarily hold in multiaxial states. However, these concluded features are the

requirements that the numerical material model should meet until more experimental data are available.

5-2-2: Concrete Model Adopted in the Dynamic Analysis

It is obvious from the previous section that any numerical model presented for concrete subjected to transient analysis should be rate and history dependent [6]. Elasto/plastic and elasto/viscoplastic models in the traditional basic formulation do not meet these requirements, but they can be modified to include the important features mentioned above.

5-2-2-1: Traditional Elasto / Viscoplastic Model

Usually in the theory of elasto/viscoplasticity, the total strain ε and strain rate $\dot{\varepsilon}$ are decomposed into elastic and viscoplastic parts as:

$$\varepsilon = \varepsilon_e + \varepsilon_{vp} \quad \dots\dots\dots (5-1)$$

$$\dot{\varepsilon} = \dot{\varepsilon}_e + \dot{\varepsilon}_{vp} \quad \dots\dots\dots (5-2)$$

The stress rate $\{\dot{\sigma}\}$ is related to the elastic strain rate $\{\dot{\varepsilon}_e\}$ by the elasticity matrix [D] as:

$$\{\dot{\sigma}\} = [D]\{\dot{\varepsilon}_e\} \quad \dots\dots\dots (5-3)$$

where, “ $\dot{\quad}$ ”, represents differentiation with respect to time. Viscoplastic flow occurs for positive values of a scalar yield function F_o :

$$F_o(\sigma) = f(\sigma) - \sigma_o(k) \quad \dots\dots\dots (5-4)$$

where σ_o is a value defining the position of the yield surface, and k is a hardening or softening parameter. According to the associated elasto/ viscoplasticity, the viscoplastic flow rule introduced by *Perzyna* [101] has been widely used. The viscoplastic strain rate is given as:

$$\dot{\varepsilon}_{vp} = \gamma \langle \phi(F_o) \rangle \partial f / \partial \sigma \quad \dots\dots\dots (5-5)$$

where γ is the fluidity parameter. The expression $\langle \phi(F_o) \rangle$ is equal to $\phi(F_o)$ for positive value of F_o and zero otherwise, and the term $\partial f / \partial \sigma$ is a vector normal to the potential surface and it defines the direction of the viscoplastic flow [6]. In this work, the flow function is defined to be:

$$\phi(F) = F_o / \sigma_o = (f(\sigma) - \sigma_o) / \sigma_o \quad \dots\dots\dots (5-6)$$

5-2-2-2: Strain Rate Sensitive Elasto / Viscoplastic Model for Concrete

Bićanić [99] introduced a strain-rate sensitive elasto/viscoplastic model with progressive degradation of the strength as a modification of *Perzyan's* elasto /viscoplastic model [101]. In 1983, the original model of *Bićanić* was extended to include tensile cracking [102]. However, similar concepts had been adopted by *Cervera* [6]. The model had two main differences when compared with the traditional elasto/viscoplastic model:

- a – The fluidity parameter is not constant, and it is assumed to be dependent on the elastic strain rate (or stress rate).
- b –A variable strength limit surface is introduced to monitor the damage caused by viscoplastic flow. If the stress point reaches the strength limit surface, then the degradation of the yield surface is initiated.

This model is adopted in the present work.

5-2-2-2-1: Yield and Strength Limit Surfaces

The yield surface F_o , defining the onset of viscoplastic behavior, and the strength limit surface F_f , defining the initiation of material degradation will be described in terms of the first and second invariants only. They can be expressed as (similar to the yield criterion used in previous chapter, Eq.(4-6)):

$$F_o(\sigma, \sigma_o) = CI_1 + \sqrt{(CI_1)^2 + 3\beta J_2} - \sigma_o = 0 \quad \dots\dots\dots(5-7)$$

$$F_f(\sigma, \sigma_f) = CI_1 + \sqrt{(CI_1)^2 + 3\beta J_2} - \sigma_f = 0 \quad \dots\dots\dots(5-8)$$

where; I_1 , J_2 , C , and β as defined previously(see section 4-2-2-1-1). During inelastic straining both surfaces F_o and F_f change depending on the viscoplastic energy density W_p [6]:

$$F_o(\sigma, \sigma_o(W_p, k)) = 0 \quad \dots\dots\dots(5-9)$$

$$F_f(\sigma, \sigma_f(W_p)) = 0 \quad \dots\dots\dots(5-10)$$

where; $\sigma_o(W_p, k)$ defines the change of the yield stress level in uniaxial compression σ_o , $\sigma_f(W_p)$ define the change of the failure stress level in uniaxial compression σ_f and W_p is the viscoplastic energy density defined as :

$$W_p = \int_0^t \sigma^T \dot{\epsilon}_{vp} dt \quad \dots\dots(5-11)$$

and, k is the viscoplastic work density in the softening range . It is defined as :

$$k = W_p - W_p^f = \int_{t_f}^t \sigma^T \dot{\epsilon}_{vp} dt \quad \dots\dots(5-12)$$

and t_f and W_p^f are the time and viscoplastic energy density when the strength limit is reached.

As illustrated in Fig.(5-4-a), when the stress path remains inside the yield surface the behavior of concrete is linearly elastic (i.e. ,no viscoplastic straining is developed), hence the yield and failure surfaces remain stationary. When the stress path is outside the yield surface, inelastic straining occurs, and the values of σ_f vary as shown in Fig.(5-4-b). It is important to know that if the hardening is considered σ_0 increases with the viscoplastic work and the yield surface expands.

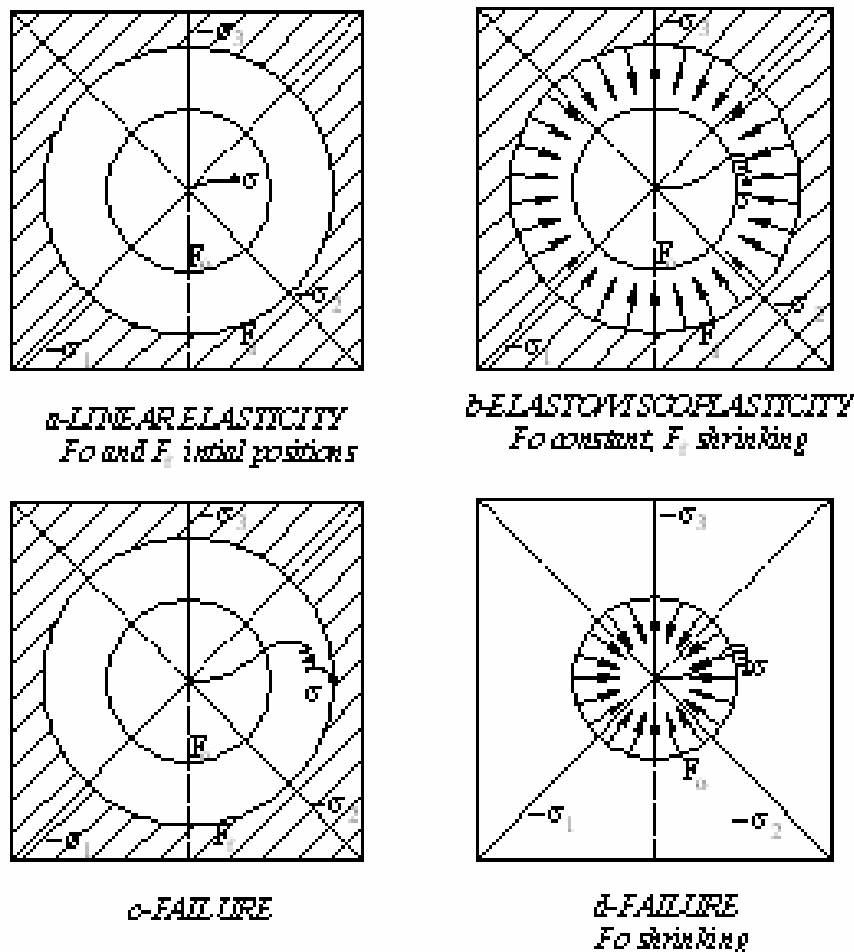


Fig.(5-4):Evolution of the Yield and Failure Surfaces[6].

However, σ_f decreases with the increase of damage, and the strength limit surface shrinks. The strength limit surface is only a monitoring device to define where and when the failure occurs. When the stress path reaches the strength limit surface, degradation of the material is initiated as shown in Fig.(5-4-c). After that, the strength limit surface is no longer considered and the yield surface begins to shrink according to the post - failure dissipated energy density k , see Fig.(5-4-d).

In the current dynamic model, no hardening will be considered for concrete and an exponential function will be used to simulate the post – failure behavior. Therefore, the function $\sigma_o(W_p, k)$ is defined by the expression (see Fig.(5-5)) :

$$\sigma_o(W_p, k) = \alpha_1 f'_c \quad \text{for } W_p \leq W_p^f \quad \dots\dots(5-13)$$

$$\sigma_o(W_p, k) = \alpha_1 f'_c \exp(-\alpha_c k) \quad \text{for } W_p > W_p^f \quad \dots\dots(5-14)$$

where, α_1 defines the limit for elastic behavior (typically [2,6] = 0.3 - 0.4) and α_c simulates the degradation after failure. The parameter f'_c is the static compressive strength of concrete. The failure stresses will be assumed to be a linear function of the viscoplastic energy density, and the function $\sigma_f(W_p)$ can be defined by the expression [6]:

$$\sigma_f(W_p) = \beta_o f'_c (1 - \beta_1 W_p) \quad \dots\dots(5-14)$$

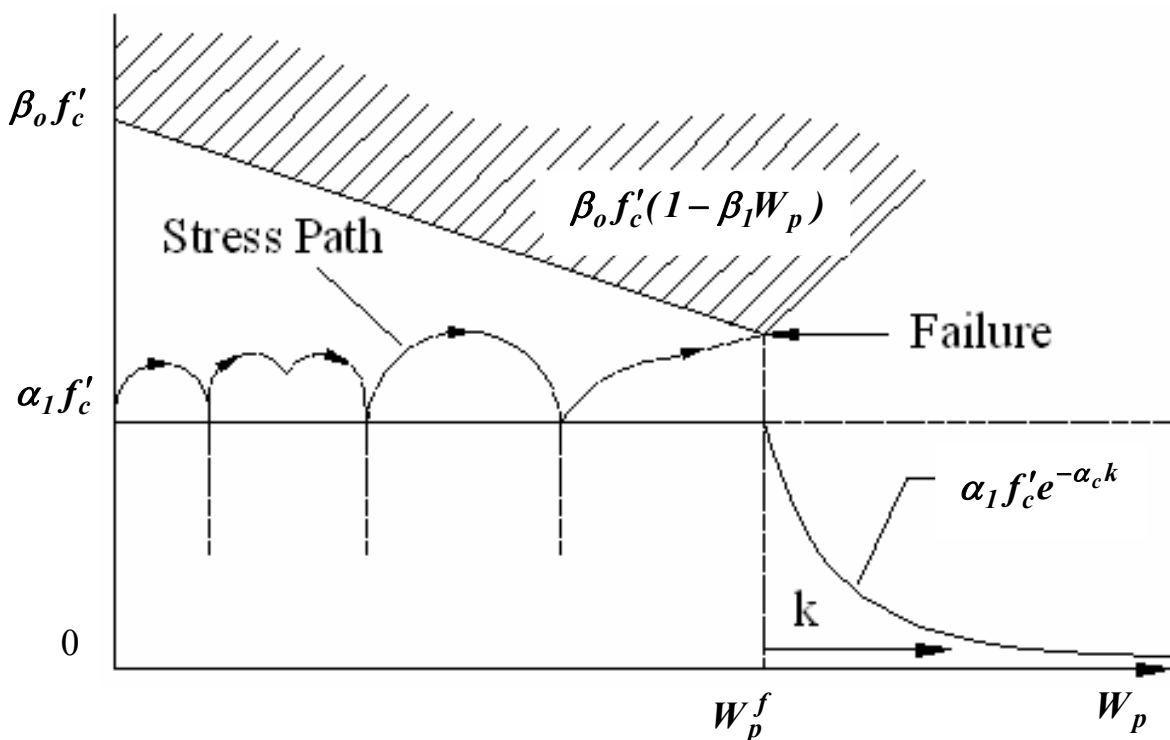


Fig.(5-5): Variation of the Yield and Failure with the Dissipated Energy Density [6].

The parameters β_0 and β_1 are determined from experiments and $\beta_0 f'_c$ is the compressive strength obtained with infinite load rates and no inelastic strains. Fig.(5-5) shows the yield and failure stresses varying with the dissipated energy. **Bićanić** [99] assumed linear relationship between the failure stress and the dissipated energy density in Eq.(5.14) ; but this is a crude approximation for all ranges of straining. When only moderate and fast strain rates are considered, the assumed linear dependency appears to be satisfactory [6].

5-2-2-2-2: Viscoplastic Strain Rate

The rate of viscoplastic straining in Eq.(5-5) is modified and rewritten to depend on the rate of elastic strain (or loading) and on the position of the yield surface as :

$$n = \partial f / \partial \sigma \quad \dots\dots\dots (5-16)$$

and $\phi(F_o) = F_o / \alpha_1 f'_c \quad \dots\dots\dots (5-17)$

The fluidity parameters are related to the elastic strain rate through an exponential function of an effective elastic strain rate:

$$\gamma(\dot{\epsilon}_e) = a_0 (\dot{\epsilon}_e^{eff})^{a_1} \quad \dots\dots\dots (5-18)$$

where a_0 and a_1 are parameters computed experimentally and the effective elastic strain is defined as [6]:

$$\epsilon_e^{eff} = (3J'_{2e} / (1 + \nu)^2)^{0.5} \quad \dots\dots\dots (5-19)$$

because deviatoric strains cause most damage to concrete and ϵ_e^{eff} is equal to the uniaxial elastic strain for a uniaxial stress state .

5-2-2-2-3: Determination of Model Parameters

Parameters f'_c , α_1 , and α_c can be determined from uniaxial static tests. Whereas, parameters β_0 , β_1 , a_0 and a_1 defining σ_f and γ as a function of the viscoplastic energy density and the elastic strain rate respectively can be computed from dynamic monotonic direct compression tests. **Bićanić** [99,100] illustrated how these dynamic parameters can be determined from experimental data. **Hatano** considered three different equalities of concrete mixes (1:2:4), (1:3:5) and (1:4:7) under several loading conditions. The model parameters identified from **Hatano's** tests are shown in Table (5-1).

		0.405	0.831	1.967	0.792
1 : 3 : 5	444.0	0.306	0.760	1.836	1.088
1 : 4 : 7	275.0	0.413	0.747	2.291	2.365

With the material parameters given in Table(5-1), the prediction stress-strain curve from the model are presented in the Fig.(5-6) below.

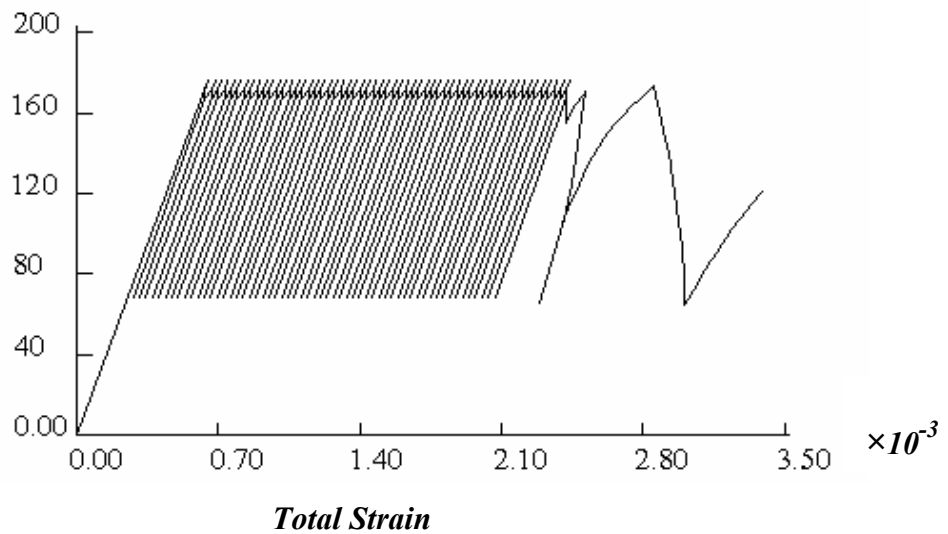


Fig.(5-6): Predicted Stress-Strain Curve under Cyclic Loading for 1:4:7 Concrete Mix[6].

Also, the same crushing condition used in section 4-2-2-1-1(Eq.(4-35)), is adopted here.

5-2-2-2-4: Smeared Crack Model for Concrete in Tension

The same smeared crack model with fixed orthogonal cracks and the cracking criterion (maximum tensile stress criterion) which is used in the static model is adopted here to represent the fractured concrete in the current dynamic model.

Utilizing the static results, the probability of forming cracks in three directions at the same Gauss point was found very little, therefore two sets of cracks are allowed to form at each sampling point. Also, the effect of compressive stress which exists in some directions on the tensile strength of concrete in other

direction is neglected. Finally the reduction in the compressive strength due to orthogonal crack is ignored here. These three assumptions have been adopted also by many researchers [6].

5-2-2-2-5: Post-Cracking Stress-Strain Relationship.

In the dynamic analysis it is widely accepted to make the constitutive model objective with regard to the size of the finite elements used in the mesh [6,103]. Hence the softening curve must be related to the fracture energy of the concrete.

• *Strain-softening model*

Assuming that the stress, σ , across an opening crack is a function of the crack width, w , the fracture energy is defined as:

$$G_f = \int_0^{\infty} \sigma(w) dw \quad \dots\dots\dots (5-20)$$

where G_f represents the energy needed to separate the two crack surfaces . Typical values of the fracture energy for normal concrete are in the range of 50 to 200 N/m according to Ref.[6] , and 40 to 120 N/m according to Ref.[28].

As known the smeared crack approach does not represent individual cracks, so the crack width, w , must be smeared into an equivalent crack strain, ε_c , related to the physical crack opening by a characteristic length l_c . *Nilsson* and *Oldenburg* [103] presented this relation considering a control volume, V , containing a crack with an area S (see Fig.(5-7)). By assuming that when the crack is formed, all inelastic deformations inside the control volume takes place in the crack, the rest of the volume remaining elastic and the rate of energy dissipation in the crack is:

$$\dot{\pi}_s = \int \sigma \dot{w} ds \quad \dots\dots\dots (5-21)$$

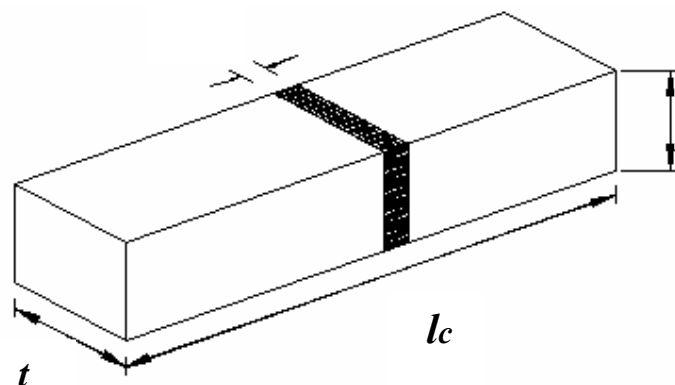


Fig.(5-7): Illustration of Characteristic Length for a Prismatic Control Volume [6].

By assuming that the control volume is subjected to the same state of stresses as the crack, but strained by the equivalent strain ε_c , the rate of energy dissipation in the volume is:

$$\dot{\pi}_v = \int_v \sigma \dot{\varepsilon}_c dv \quad \dots\dots\dots (5-22)$$

When assuming the stress, strain and crack width to be constant inside the considered volume, then equating the rate of energy dissipation in the crack Eq.(5-21) to that in the control volume Eq.(5-22) gives the relationship between the crack width and the fictitious crack strain as :

$$w = (V / S) \varepsilon_c = l_c \varepsilon_c \quad \dots\dots\dots (5-23)$$

As appeared this relation defines the characteristic length as the ratio between the control volume and the crack surface.

In the current study, an exponential function is used to simulate the strain - softening effect as:

$$\sigma = E_o \varepsilon_o \exp(-(\varepsilon - \varepsilon_o) / \alpha) \quad \dots\dots\dots (5-24)$$

where, E_o : is the elastic *Young's* modulus,

ε_o : is the strain at cracking,

ε : is the nominal tensile strain in the crack zone, and

α : is the softening parameter .

The adopted curve is shown in Fig.(5-8).

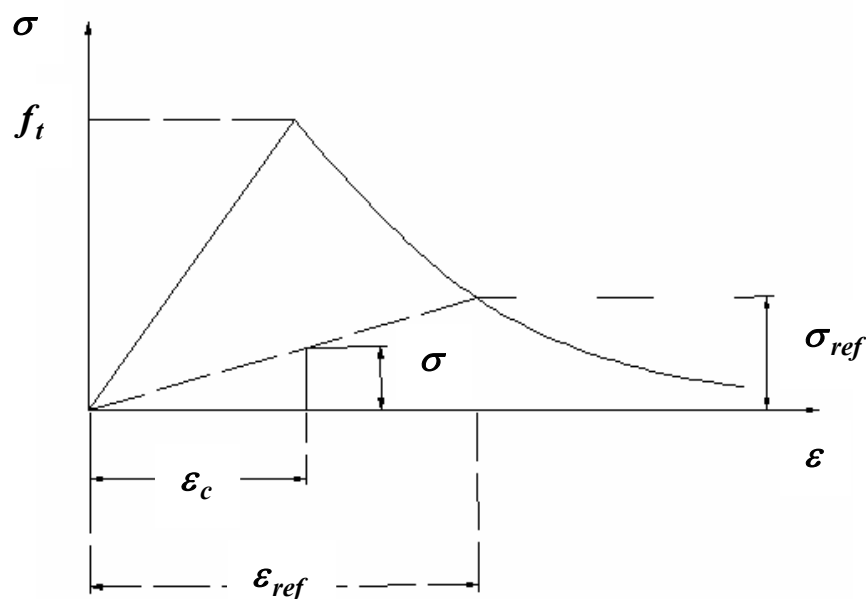


Fig.(5-8): Strain-Softening Curve with Secant Unloading and Re-Loading [6].

The softening parameter, α , is determined by the evaluation of the integral in Eq.(5-20), and by the introducing of the relation of Eq.(5-23). These yields:

$$\alpha = (G_f - \frac{E_o \varepsilon_o^2 l_c}{2}) / (E_o \varepsilon_o l_c) > 0 \quad \dots\dots\dots (5-25)$$

According to the finite element computations, the control volume for crack monitoring is the volume associated with a sampling point in a given element. In the present model, the characteristic length is computed for each sampling point as:

$$l_c = (dv)^{1/3} \quad \dots\dots\dots (5-26)$$

where dv is the volume of concrete represented by the sampling point . It is important to point that this approach for computing the strain-softening is only directly applicable to plain concrete. The classical ‘tension-stiffening’ effect due to the presence of reinforcement has not been accounted for. The effect of the reinforcement can be included by assuming higher fracture energy for reinforced concrete than for plain concrete [6].

The redistribution of stresses due to cracking or crushing in other neighboring sampling points, or due to further loading may enforce some of the previously-opened cracks to be closed partially or fully . This behavior is allowed in the present model. If the current strain ε is smaller than the strain ε_{ref} recorded as the maximum tensile strain reached across the crack under consideration, the stress normal to the crack, σ , is computed from;

$$\sigma = \sigma_{ref} \times \varepsilon / \varepsilon_{ref} \quad \dots\dots\dots (5-27)$$

where σ_{ref} is the interpolated stress corresponding to the strain ε_{ref} , as shown in Fig.(5-8). The re-opening of the crack follows the same path until ε_{ref} is exceeded, thereafter Eq.(5-24) will be used.

- **Shear retention model**

A simplified approach is adopted here to simulate the effect of shear transfer across the crack. The process consists of assigning to the shear modulus corresponding to the crack plane a reduced value, G_c , as defined:

$$G_c = \beta G_o \quad \dots\dots\dots (5-28)$$

in which G_o is the shear modulus of uncracked concrete and β is a reducing factor running between zero to one. In the present model, the following expression is used [104]:

$$\beta = 1 - (\varepsilon_t / 0.005)^{k_1} \quad \dots\dots\dots (5-29)$$

where ε_f is the fictitious tensile strain normal to the crack plane, and k_1 is a parameter in the range of (0.3 to 1.0) [104].

5-3: Modeling of the Steel under Dynamic Load

5-3-1: Observed Behavior of the Steel under Dynamic Load

The mechanical properties of steel are well known, in contrast to concrete. From dynamic uniaxial tests [105], as shown in Fig.(5-9), some major conclusions can be drawn:

- a–The yield stress and the ultimate stress of the steel increase with the straining rate.
- b–The initial elastic modulus is relatively unaffected by the straining rate.
- c– Ductility is observed to decrease with increasing straining rate.
- d– The rate effects are approximately equal in tension and compression.

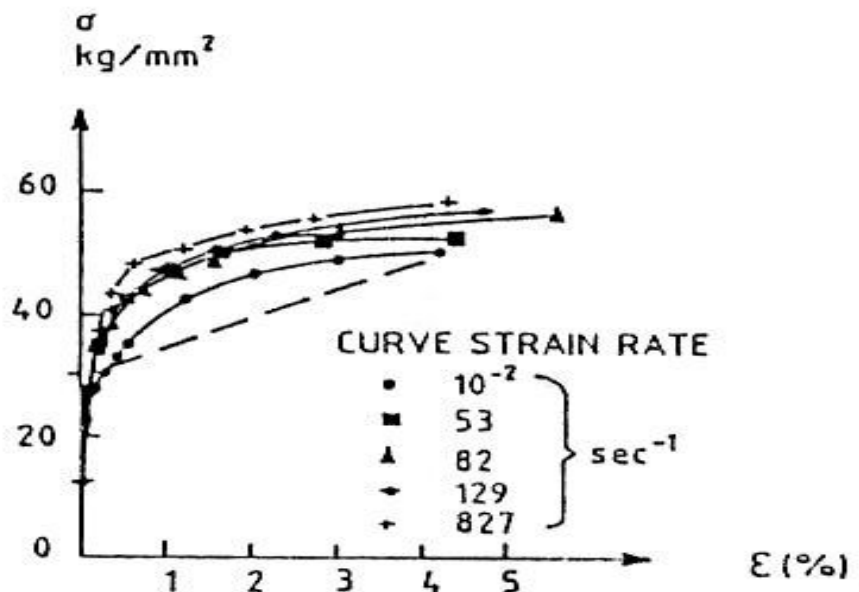


Fig.(5-9):Dynamic Stress-Strain Diagram for Steel[105].

5-3-2: Modeling of Steel Adopted in the Analysis

The elasto/viscoplastic model described previously for concrete is used here for steel with some modifications in the material parameters as follows [6]:

- a- If the constants $C = 0$, and $\beta = 1$ are used in the definition of the yield surface Eq.(5-7) and Eq.(5-8) then the criterion reduces to the classical *Von-Mises* cylinder.
- b- A large value for the cracking strain and the crushing strain will ensure that steel does not crack or crush during the analysis.
- c- The expression for the fluidity parameter is;

$$\gamma(\dot{\epsilon}_e) = a_o (\dot{\epsilon}_e)^{a_1} \quad \dots\dots\dots (5-30)$$

if a_1 is set to zero in Eq.(5-30), then the model is strain rate independent and a_o is then the usual fluidity parameter.

- d- A large value for β_o and a small one (or zero) for β_1 will ensure that the steel suffers no softening.

Thus, the strain-rate sensitivity and damage accumulation can be retained in the steel model if the appropriate parameters are chosen.

5-4: Modeling of Reinforcing Bars under Dynamic Load

Concrete and reinforcement are represented as a single element and perfect bond is assumed between them. The stiffness and internal forces associated with the reinforcement are integrated and added to those of the concrete to get the total stiffness and internal forces of the element. Each set of reinforcing bars are simulated as a smeared two-dimensional membrane (layer) of equivalent thickness. The layer is placed inside the solid element to coincide with the surface corresponding to (r, s, constant), (r, constant, t) and (constant, s, t) as appropriate. The proposed restriction has the advantage of an easy definition of the sampling points used to perform the necessary surface integration over the steel reinforcement membrane. Stresses and the local stiffness matrix for each bar, are first evaluated in the local system, and then transformed into the global system [6]. Reinforcing steel is assumed to have uniaxial properties in the direction of the bars. A classical elasto – viscoplastic model is used in the dynamic model with:

$$\dot{\epsilon}_{vps} = \pm \gamma (\dot{\epsilon}_s) (|\sigma_s| - f_y) / f_y \quad \dots\dots\dots (5-31)$$

where; σ_s is the current stress level in the steel and f_y is the yield stress of the material which is assumed to be constant, although strain rate sensitivity may be readily incorporated.

Chapter Six

Nonlinear Solutions Techniques

6-1: Introduction

This chapter presents a description of the numerical techniques which are used in solving nonlinear simultaneous equations. As known all structures have the material nonlinearity, while the geometric nonlinearity is related to the large deformations. In the horizontally curved reinforced concrete or composite beams, the geometric nonlinearities are neglected as a result of the early onset of material nonlinearities, where, the major sources of material nonlinearity are yielding of steel, cracking of concrete, plastic deformation of steel and concrete and crushing of concrete. The first part of this chapter deals with the static analysis, while the second part deals with the dynamic analysis, finally the adopted convergence criteria will be described.

6-2: Static Analysis

The solution of nonlinear problems by the finite element method is usually attempted by one of three basic techniques [70].

- 1- Linear incremental method.
- 2- Iterative methods.
- 3- Incremental-Iterative methods.

6-2-1: Linear Incremental Method

In this method the load is applied to the structure as a series of equal or unequal increments and for each of these load increments the changes in deformation is determined by using a linear analysis, thus the nonlinear problems is treated as a series of linear problems, and the stiffness matrix takes different values during differential load increments. However, the displacement increments are accumulated to give the total displacement at any stage of loading, and the incremental process is repeated until the total load has been reached.

6-2-2: Iterative Methods

In these methods, the structure is fully loaded, and then attempts are made to correct the solution by successive iterations. There are many types of iterative methods according to the updating of the tangent stiffness matrix (T.S.M.) such as:

- 1- Conventional *Newton-Raphson* (N-R) method: In this method the T.S.M. is updated at each iteration.
- 2- Modified N-R method: This method differs from the conventional N-R method only in that the computation of the T.S.M. isn't updated at each iteration.
- 3- Combined conventional and modified N-R method: Here, the T.S.M. is held constant for several iterations and it is updated when the rate of convergence begins to deteriorate.
- 4- Direct method: In this method the deformation corresponding to any load along the load-deformation curve is obtained by applying the load in a single step. Thus this method deals with total deformation and total loads.

6-2-3: Incremental-Iterative Methods

In a three dimensional analysis with a considerable material nonlinearity, if the total load is applied in a single step the iterative method may lose convergence and thus fail. Also if the linear incremental method is used, the solution may drift further and further from the true response curve at each load increment. Therefore, for these two reasons, the incremental-iterative methods are widely adopted in the nonlinear analysis.

In these methods, the load is applied as a series of increments and at each increment, iterative solution is carried out to find the true response. The iterations continue until the specified tolerance is achieved, as shown in Fig.(6-1). In the current study the incremental-iterative technique has been adopted.

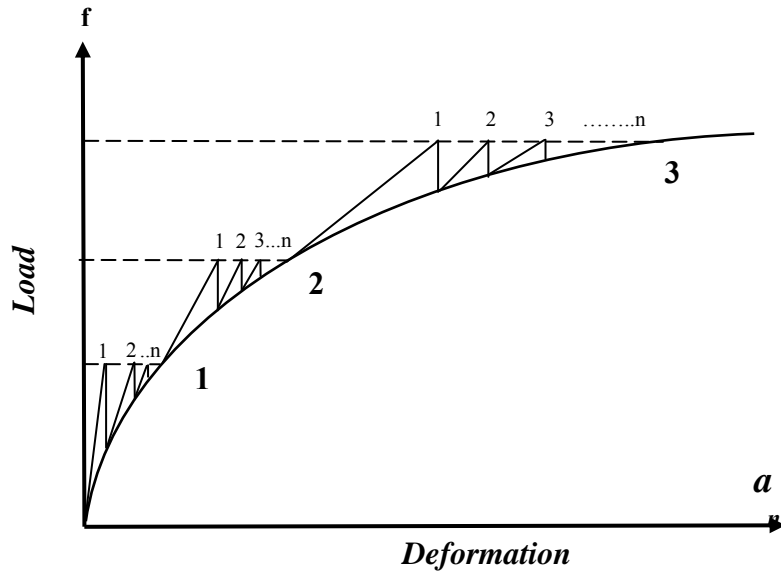


Fig.(6-1): Incremental- Iterative Techniques

The solution of Eq.(3-16) depends on obtaining a balance between the external and internal forces, whence controlling such a balance is done by choosing a suitable convergence tolerance. Therefore, referring to the vectors of external loads $\{f\}$ and internal forces $\{p(a)\}$ the out of balance, i.e. residual force vector $\{r(a)\}$ can be determined form:

$$\{r(a)\} = \{p(a)\} - \{f\} \quad \dots\dots\dots (6-1)$$

where $\{a\}$ represents the vector of nodal displacements. The internal nodal load vector is given by:

$$\{p(a)\} = \int_v [B]^T \cdot \{\sigma\} dv \quad \dots\dots\dots (6-2)$$

The computer program *NFACBSL* incorporates also a modified incremental-iterative N-R method, in which the stiffness matrix is updated at the 1st, 11th, 21st, or 2nd, 12th, 22nd, ... , iterations (as specified in the input data) of each increment of loading.

6-3: Dynamic Analysis

In the nonlinear dynamic analysis systems, the applicable method for solving the second order differential equation of motion is the direct time-integration method, where in this approach is to write the equation of motion in a matrix form, at specific instance of time as [106]:

$$[M]_n \{\ddot{a}\}_n + [C]_n \{\dot{a}\}_n + [K]_n \{a\}_n = \{p(t)\}_n \quad \dots\dots\dots (6-3)$$

It is noted that the body forces $\{p_b(t)\}$ here is equal to zero, also Eq.(6-3) represents Eq.(3-43) but in a matrix form and all terms are defined previously.

6-3-1: Direct Integration Methods

The direct numerical integration is based on two ideas. First, the dynamic equilibrium equation, Eq.(6-3), is satisfied at discrete time intervals (Δt) apart. The second idea a variation of displacements, velocities and accelerations within each time interval (Δt) is assumed. Different forms of these assumed variations give rise to different direct integration schemes each of which has different accuracy, stability and cost [107]. The direct integration methods are generally, subdivided into explicit and implicit methods.

Explicit methods have the form [106]:

$$\{a\}_{n+1} = f(\{a\}_n, \{\dot{a}\}_n, \{\ddot{a}\}_n, \{a\}_{n-1}, \dots\dots\dots) \quad \dots\dots\dots (6-4)$$

As appeared the displacements $\{a\}_{n+1}$ permit to be determined in terms of completely historical information. These methods require little computer storage and are inexpensive per time step, but these algorithms are conditionally stable and need strict limits to evaluate the time step size.

Implicit methods have the form [106]:

$$\{a\}_{n+1} = f(\{\dot{a}\}_{n+1}, \{\ddot{a}\}_{n+1}, \{a\}_n, \dots\dots\dots) \quad \dots\dots\dots (6-5)$$

Hence, computation $\{a\}_{n+1}$ requires knowledge of the time derivatives of $\{a\}_{n+1}$ which are unknown. These methods are usually unconditionally stable, permitting larger time step. However, the storage required and the cost per step is high

because it is necessary to factorize the stiffness matrix at each time step. Some of these methods are *Newmark-β*, *Wilson-Θ*, *Hilber-α* and *Houbolt* methods [106].

6-3-1-1: Newmark-β Method

The most widely used family of implicit methods of direct time integration for solving the dynamic equation of motion is the *Newmark-β* family of methods [108]. *Newmark*, in 1959, presented equations for approximating the velocity and the displacement system at time t_{n+1} as follows:

$$\{a\}_{n+1} = \{a\}_n + \Delta t \{\dot{a}\}_n + \frac{\Delta t^2}{2} \left[(1 - 2\beta)\{\ddot{a}\}_n + 2\beta \{\ddot{a}\}_{n+1} \right] \quad \dots\dots\dots(6-6)$$

$$\{\dot{a}\}_{n+1} = \{\dot{a}\}_n + \Delta t \left[(1 - \gamma)\{\ddot{a}\}_n + \gamma \{\ddot{a}\}_{n+1} \right] \quad \dots\dots\dots(6-7)$$

where, $\{a\}_n$, $\{\dot{a}\}_n$, and $\{\ddot{a}\}_n$ are values of displacements, velocities and accelerations known at time (t). Parameters β and γ control the stability and accuracy of the method. When γ is equal to (1/2) and β equal to (1/4) the average acceleration method is obtained (assuming constant acceleration during the time step), which is unconditionally stable. A linear acceleration method is obtained when β is equal to (1/6) and γ equal to (1/2) which assumes that the acceleration varies linearly during the time step, here *Newmark's* method is treated as a conditionally stable scheme [109].

6-3-1-2: Wilson-Θ Method

This method is essentially an extension of the linear acceleration method where the acceleration is assumed to vary linearly from time t to time $(t + \theta\Delta t)$ with $\theta \geq 1.0$, for $\theta = 1.0$, the method is reduced to the *Newmark's* linear acceleration method. The method is unconditionally stable for $\theta \geq 1.37$ [55]. The basic equations used to find the displacement and the velocities at time $t + \theta\Delta t$, according to the *Wilson-Θ* method are [107]:

$$\dot{a}_{t+\theta\Delta t} = \dot{a}_t + \frac{\theta\Delta t}{2} [\ddot{a}_{t+\theta\Delta t} + \ddot{a}_t] \quad \dots\dots\dots (6-8)$$

$$\text{and, } a_{t+\theta\Delta t} = a_t + \theta\Delta t \dot{a}_t + \frac{(\theta\Delta t)^2}{6} [\ddot{a}_{t+\theta\Delta t} + 2\ddot{a}_t] \quad \dots\dots\dots (6-9)$$

6-3-1-3: Harmonic Acceleration Method

In this method a harmonic relationship for the acceleration-time is assumed. The basic equation for the assumed harmonic acceleration at any time, τ , where $t < \tau < t + \Delta t$, is [110]:

$$\ddot{a}_\tau = A \sin[\omega(\tau - t) + B] \quad \dots\dots\dots (6-10)$$

where A and B are constants, and ω is the frequency of the system. The coefficients, A and B , can be found by applying the boundary conditions:

$$1- \text{ At } \tau = t \quad , \quad \ddot{a}_\tau = \ddot{a}_t \quad \dots\dots\dots (6-11)$$

$$2- \text{ At } \tau = t + \Delta t \quad , \quad \ddot{a}_\tau = \ddot{a}_t + \Delta\ddot{a}_t \quad \dots\dots\dots (6-12)$$

Many other methods exist in the literature such as *Beta-m*, modified *Wilson- Θ* , *Hilber- α* , and *Houbolt* methods. In the present study the *Newmark's* average acceleration method is adopted, due to its stability, accuracy and efficiency.

6-3-2: Predictor-Corrector Form of *Newmark's* Method

Hughes [111,112] developed a predictor-corrector form of the *Newmark's* method which is most suitable for nonlinear transient analysis. The *Newmark's* equations (6-6) and (6-7) can be expressed in another form as:

$$\{a\}_{n+1} = \{a^P\}_{n+1} + \Delta t^2 \beta \{\ddot{a}\}_{n+1} \quad \dots\dots\dots (6-13)$$

$$\{\dot{a}\}_{n+1} = \{\dot{a}^P\}_{n+1} + \Delta t \gamma \{\ddot{a}\}_{n+1} \quad \dots\dots\dots (6-14)$$

with predictor values given as:

$$\{a^P\}_{n+1} = \{a\}_n + \Delta t \{\dot{a}\}_n + \frac{\Delta t^2}{2} (1 - 2\beta) \{\ddot{a}\}_n \quad \dots\dots\dots (6-15)$$

$$\{\dot{a}^P\}_{n+1} = \{\dot{a}\}_n + \Delta t (1 - \gamma) \{\ddot{a}\}_n \quad \dots\dots\dots (6-16)$$

The terms $\{a\}_{n+1}$ and $\{\dot{a}\}_{n+1}$ are corrector values and $\{a^P\}_{n+1}, \{\dot{a}^P\}_{n+1}$ are the predictor values. The corrector values for the acceleration values can be obtained from Eq.(6-13) as:

$$\{\ddot{a}\}_{n+1} = (\{a\}_n - \{a^P\}_{n+1}) / (\beta \Delta t^2) \quad \dots\dots\dots (6-17)$$

Substituting Eqs.(6-13) to (6-17) into Eq.(6-3) an “effective static problem” is formed in terms of the unknown Δa [81] as:

$$K^* \Delta a = \Psi \quad \dots\dots\dots (6-18)$$

where the “effective stiffness matrix” is

$$K^* = [M] / (\beta \Delta t^2) - \gamma [C]_T / (\beta \Delta t) + [K]_T \quad \dots\dots\dots (6-19)$$

and the residual forces are

$$\Psi = \{ p(t) \}_{n+1} - [M] \{ \ddot{a}^P \}_{n+1} - [C]^T \{ \dot{a}^P \}_{n+1} - f(\{ a^P \}_{n+1}) \quad \dots\dots\dots (6-20)$$

Note: to start the step-by-step procedure the values for initial displacements a_o and initial velocities \dot{a}_o must be given. Initial accelerations \ddot{a}_o can be obtained by solving Eq.(6-3) for time $t=0$.

6-3-3: Computational Algorithm for the Implicit Form of Newmark Method

The computations needed in a typical time step of the implicit form of the *Newmark* method can be described in the following steps (for single degree of freedom):

- a- Set iteration counter $i=0$.
- b- Enter the predictor phase.

$$\begin{aligned} a_{n+1}^i &= a_{n+1}^P \\ \dot{a}_{n+1}^i &= \dot{a}_{n+1}^P \\ \ddot{a}_{n+1}^i &= 0 \end{aligned} \quad \dots\dots\dots (6-21)$$

- c- Solve the incremental “effective static problem”

$$K^* \Delta a^i = \Psi^i \quad \dots\dots\dots (6-22)$$

$$\text{where, } K^* = [M] / (\beta \Delta t^2) - \gamma [C]_T / (\beta \Delta t) + [K]_T \quad \dots\dots\dots (6-23)$$

$$\text{and, } \Psi^i = \{ p(t) \}_{n+1} - [M] \{ \ddot{a}^i \}_{n+1} - [C]_T \{ \dot{a}^i \}_{n+1} - f(\{ a^i \}_{n+1}) \quad \dots\dots\dots (6-24)$$

are the effective stiffness matrix, and the residual forces vector, respectively, and

$$[K]_T = \partial f / \partial a \quad \dots\dots\dots (6-25)$$

being the tangential stiffness matrix.

d- Perform the corrector phase.

$$\begin{aligned} a_{n+1}^{i+1} &= a_{n+1}^i + \Delta a^i \\ \ddot{a}_{n+1}^{i+1} &= (a_{n+1}^{i+1} - a_{n+1}^P) / (\beta \Delta t^2) \quad \dots\dots\dots (6-26) \\ \dot{a}_{n+1}^{i+1} &= \dot{a}_{n+1}^P + \Delta t \gamma \ddot{a}_{n+1}^{i+1} \end{aligned}$$

e- If the convergence criterion selected is not satisfied, then set $i=i+1$ and go to step (c).

f- Set the solution at time t

$$\begin{aligned} a_{n+1} &= a_{n+1}^{i+1} \\ \dot{a}_{n+1} &= \dot{a}_{n+1}^{i+1} \quad \dots\dots\dots (6-27) \\ \ddot{a}_{n+1} &= \ddot{a}_{n+1}^{i+1} \end{aligned}$$

for use in the next time step. Also set $n=n+1$ and go to step (a).

It is interesting to note that when the mesh involves only implicit elements and large time steps are adopted with $\gamma = 1/2$, a set of alternative predictor values is recommended in Ref.[81]:

$$\begin{aligned} a_{n+1}^o &= a_n \\ \dot{a}_{n+1}^o &= \dot{a}_n \quad \dots\dots\dots (6-28) \\ \ddot{a}_{n+1}^o &= (a_{n+1}^o - a_{n+1}^P) / (\beta \Delta t^2) \end{aligned}$$

where a_{n+1}^P is given by Eq.(6-15)

6-3-4: Selection of the Time Step Size [6]

As mentioned previously, the viscoplastic flow rule is valid for all time (t) as:

$$\dot{\epsilon}_{vp} = \gamma (\dot{\epsilon}_e) < \phi(F_o) > n \quad \dots\dots\dots (6-29)$$

In a step-by-step numerical procedure this relationship will only be satisfied for discrete time stations (Δt) apart. The viscoplastic strain is given by:

$$\epsilon_{vp} = \int \dot{\epsilon}_{vp} dt \quad \dots\dots\dots (6-30)$$

which can be approximated numerically as :

$$\epsilon_{vp)t+\Delta t} = \epsilon_{vp)t} + [(1 - \beta) \dot{\epsilon}_{vp)t} + \beta \dot{\epsilon}_{vp)t+\Delta t}] \Delta t \quad \dots\dots\dots (6-31)$$

Therefore the change of the viscoplastic straining within the interval is defined in terms of the viscoplastic flow rule at both ends of the interval. If $\beta=0$, the explicit Euler integration scheme is obtained, where only the flow rule at the beginning of the interval is relevant.

$$\varepsilon_{vp}(t+\Delta t) = \varepsilon_{vp}(t) + \dot{\varepsilon}_{vp}(t)\Delta t \quad \dots\dots\dots (6-32)$$

Euler integration has been found computationally efficient for quasi-static problems, despite the stability limitations on the length of the time step. The stability limit for Eq.(6.32) depends on the specific form of the viscoplastic potential used in the flow rule. *Cormeau* [113] derived theoretical stability limits for some yield criteria with linear flow function, namely *Von-Mises*, *Tresca*, *Drucker-Prager* and *Mohr-Coulomb*.

However, an estimation of the allowable time step can be obtained by substituting some representative values from *Hatano*'s tests into one of the criteria given in Ref.[63]. For *Von-Mises* yield criterion (a particular case for the compressive yield criterion, obtained using $C=0$ in Eq.(5-7)) the stability limit is given by [6]:

$$\Delta t \leq 4(1+\nu)\sigma_o / (3 \gamma E) \quad \dots\dots\dots (6-33)$$

when taking $\sigma_o = 0.3 f'_c$ and elastic strain rates varying from 10^{-6} sec^{-1} to 10^{-1} sec^{-1} (the range in which the present material model is assumed to be valid) the critical time steps obtained are shown in Table(6-1).

Table(6-1): The Critical Time Steps for Some Concrete Mixes (assuming Von-Mises yield criterion)(as Cited in [6])

Concrete mix	$\Delta t_{cr} (\dot{\varepsilon}_e = 10^{-6} \text{ sec}^{-1})$	$\Delta t_{cr} (\dot{\varepsilon}_e = 10^{-1} \text{ sec}^{-1})$
1 : 2 : 4	33.57	2.345 -02
1 : 3 : 5	122.33	1.936 -02
1 : 4 : 7	93.84	9.711 -03

In dynamic analysis, these stability limits will rarely be decisive [6]. If an explicit integration scheme is used then the stability limit for step-by-step integration of the equation of motion will normally govern the choice of the time step length.

Implicit schemes are usually unconditionally stable, but the time step size is limited by accuracy considerations. In particular, when cracking is involved, the time step must be selected so that cracks spread progressively throughout the structure. When a large number of cracks are formed in the same interval, considerable difficulties in convergence may occur. From experience, it appears that the time step size with implicit algorithms should be chosen to limit the speed at which the cracks spread.

It should be noted that these stability limits were obtained for quasi-static elasto/viscoplasticity, with the flow rule being a function of stress only. When the flow rule (adopted in this study) involves both stresses and stress rates, the limits derived in Ref.[63] are not strictly applicable.

6-4: Convergence Criteria

A termination criterion for any iterative process should be used to stop iteration. At certain iteration within the increment of loading, if the difference between the external and the internal forces becomes negligibly small, the convergence is assumed to have occurred. The convergence criteria for nonlinear structural problems can usually be classified as:

- 1- Displacements convergence criterion.
- 2- Force convergence criterion.

The force convergence criterion which is considered in the numerical models *NFHCBSL* and *NFHCBDL* can be expressed in the form:

$$\frac{\sqrt{\{\mathbf{r}(a)\}^T \cdot \{\mathbf{r}(a)\}}}{\sqrt{\{\mathbf{f}\}^T \cdot \{\mathbf{f}\}}} \leq \text{Specified Tolerance} \quad \dots\dots\dots (6-34)$$

While the displacements convergence criterion which is considered in the numerical models *NFHCBSL* can be expressed in the form:

$$\left[\frac{\sum_{i=1}^n (\Delta a)_i^2}{\sum_{i=1}^n (a)_i^2} \right]^{0.5} \leq \text{Specified Tolerance} \quad \dots\dots\dots (6-35)$$

Chapter Seven

Static Model Discussion and Testing

7-1: Introduction

To illustrate the theoretical developments introduced in the previous chapters, a finite element analytical static model *NFHCBSL* has been programmed utilizing the previous work *AL-Shaarbaf* [2]. Furthermore, in order to verify the reliability of this model, several examples will be checked with other available experimental and theoretical results as possible. In this static model, different aspects of behavior by several previously researchers [2,3,4] ignored or treated in an approximate way which are considered more rationally in this work such as:

- 1- The nonlinear behavior of the stress in the direction perpendicular to the plane of the crack after being closed.
- 2- Behavior of the beam beyond crushing at some Gauss points.
- 3- The crack direction combination with the other two directions (after the crack is completely closed) i.e. is not being treated individually, and the Gauss point being healed. Also, if two crack directions are perfectly closed, the model combined with the third direction automatically, i.e. is not handled individually.
- 4- Degradation in the compressive strength at Gauss point is considered when the compressive strain is greater than that corresponding to the peak uniaxial compressive stress.

- 5- Division of the increment strains (or loads) into two or three or even four sub-increments whenever one or two or three cracks are closed (or re-closed) respectively to handle each sub-increment individually.
- 6- Other model is adopted in simulating the crushing conditions.
- 7- The tensile strength in Gauss point may be reach to zero.

7-2: Properties and Abilities of the Static Model

The computer program *NFHCBSL* is introduced to achieve some requirements of the present study. The main objective of this program is to analyze horizontally curved (steel, concrete and the composite) members under general three-dimensional states of monotonic loads. The program is coded in FORTRAN-77 language. The numerical analyses were carried out on 1700 MHz Pentium IX processor (PSI) computer that is provided with a 512 MB RAM. The main properties of the program are summarized as below:

- 1-Type of Curved member;** The computer model asks the user about the value of the indicator which specifies the type of member (CSC) 1 or 2 or 3 for concrete ,steel and composite respectively, .
- 2-Steel and Concrete Representation;** The 20-node isoparametric brick element has been incorporated in the program to model the steel and concrete. In order to distinguish the types of elements materials, numbers (1,6) and (2,7) are used to name the concrete and steel elements respectively.
- 3-Reinforcing bar representation;** Reinforcing bars are simulated as axial members embedded in the concrete brick elements. Numbers (3,4,5) are used to name the reinforcement bars.
- 4-Integration rule used;** To evaluate the stiffness matrices of steel and concrete brick elements, the 27 (3x3x3) Gauss-quadrature rule had been implemented in the computer program.
- 5-Material nonlinearities;** Many material nonlinearities are considered in the static model such as: yielding of steel element or reinforcement bars, plastic

deformation of steel element or reinforcement bar, nonlinear response of concrete in compression, crushing and cracking of concrete and strain stiffening after cracking.

6-Nonlinear solution algorithms; The following incremental iterative solution algorithms are incorporated in the program.

- a- The initial stiffness method.
- b- The modified *Newton-Raphson* method in which the stiffness matrix is updated at the first iteration of each increment of loading.
- c- The modified *Newton-Raphson* method in which the stiffness matrix is updated at the 2nd, 12th, 22nd, ... iterations of each increment of loading.

The solution of the banded set of algebraic equilibrium equations is carried out by using the *Cholesky* factorization technique.

7-Loading schemes; The computer program employs a load increments as specified by the user. In finite element analyses, the external concentrated loads are simulated by a set of equivalent nodal forces.

8-Convergence criteria; The force and displacement convergence criteria are available in the program.

9-Termination of the analysis; The analysis is terminated automatically always, as observed, when:

- a- Steel beam or reinforcing bars have been fractured.
- b- Crushing at successive Gauss points within the load increment prior to failure.

7-3: Structure of the Program

The *NFHCBSL* computer program consists of a main master model and many subroutines, each subroutine has been designed to deal with a part of the analysis and that part may be repeated more than once. The sequence of the operations in the main routine is summarized in the flow-chart shown in Fig.(7-1).

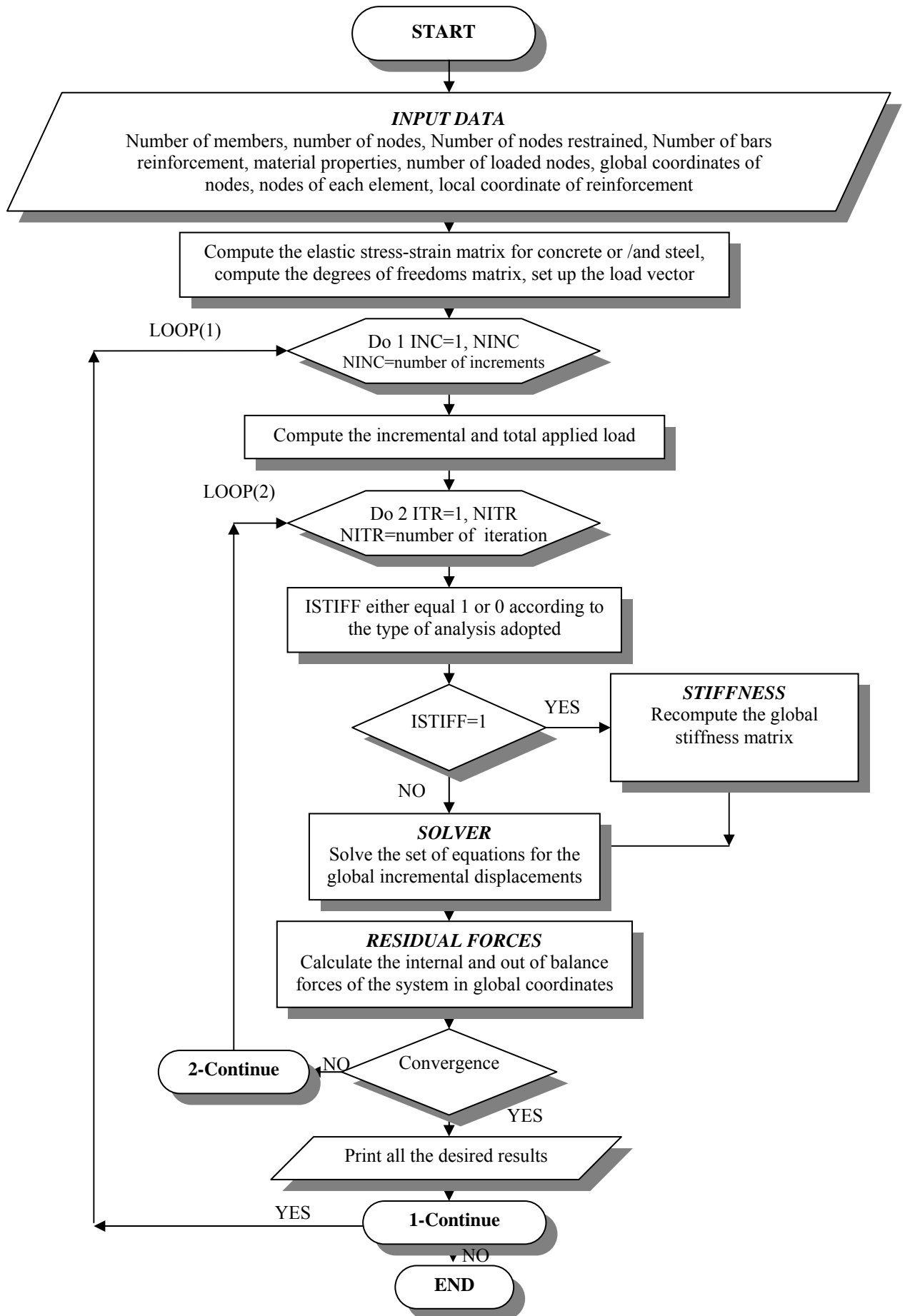


Fig.(7-1):Flowchart of the Static Model Computer Program *NFHCBSL*.

7-4: Numerical Examples

In order to verify the reliability of the computer static model *NFHCSL*, some examples are considered here and divided into two main types, steel and reinforced concrete curved beams.

7-4-1: Horizontally Curved Steel Beams

Example No.1: Shanmugam et al. Curved Beam (CB5)

The first example to be solved is the **Shanmugam et al.** curved beam (CB5, $\theta = L/R = 1.90986^\circ$), which was tested and analyzed in 1995 [27]. The finite element analysis package **ABAQUS** [28] was used in that analytical study, the typical mesh was chosen from a convergence study carried out earlier (**Tan et al.** 1992)[114]. However, the full length of the beam is analyzed here since the applied loading and support conditions are not symmetrical. Due to being cold bent, initial stresses are deduced and considered here by a special subroutine. Fig.(7-2) shows the geometry, properties, and loading conditions of the curved beam. It is important to note that the location of the origin of the Cartesian coordinates at the left end of the beam.

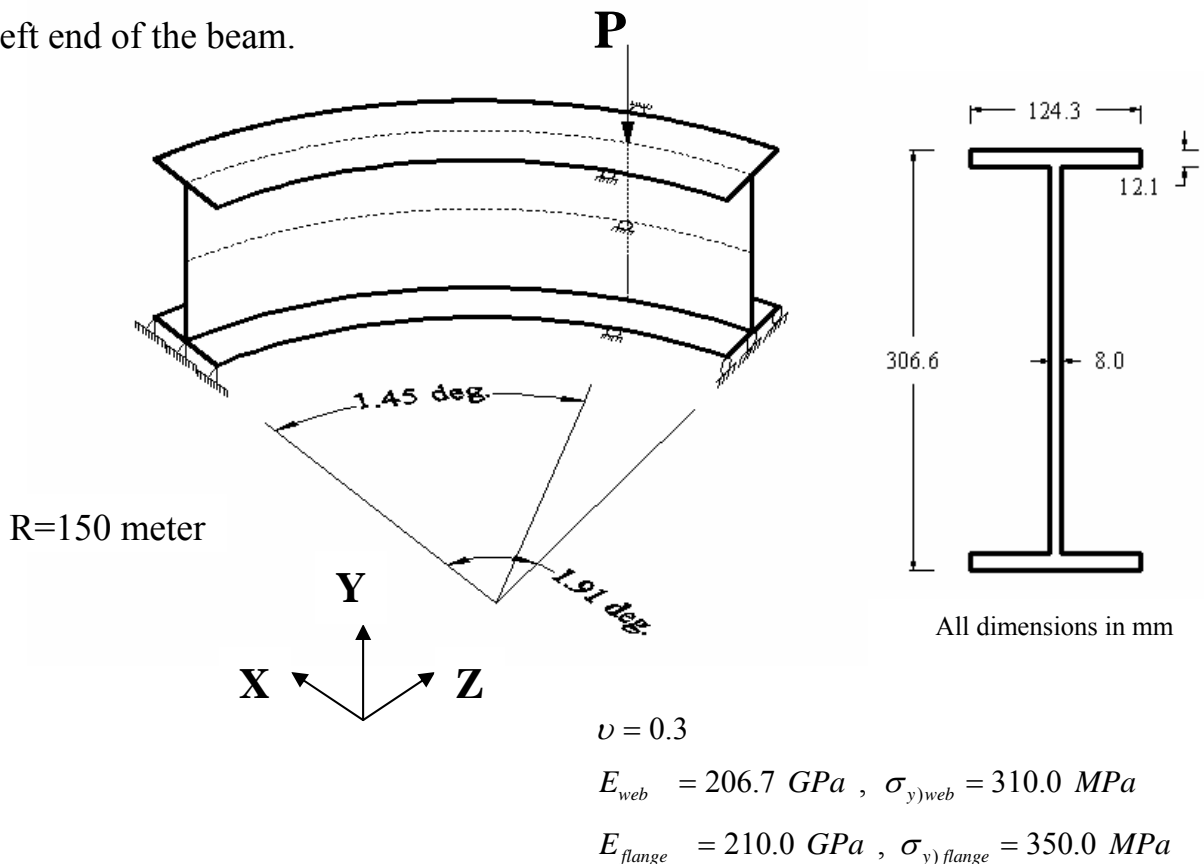


Fig.(7-2): Geometry, Properties and Loading Conditions of the Shanmugam et al . Curved Beam (CB5).

The boundary conditions is assumed such that nodes 1-3 on the bottom flange at support(A), as illustrated in Fig.(7-3), are constrained in X, Y and Z-directions and nodes 15-17 at support(B) are allowed to move only in Z-direction. While the nodes 4-8, 9-14 and 18-22, are assumed to be restrained only in the X-direction.

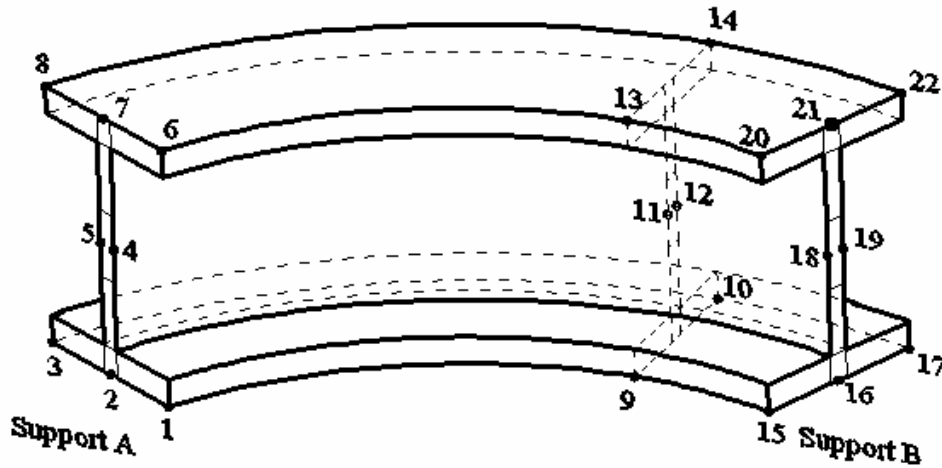


Fig.(7-3): Boundary Conditions in Finite Element Modeling.

The residual stresses are considered here, as adopted in *Shanmugam et al.* analytical study, and illustrated in Fig.(7-4).

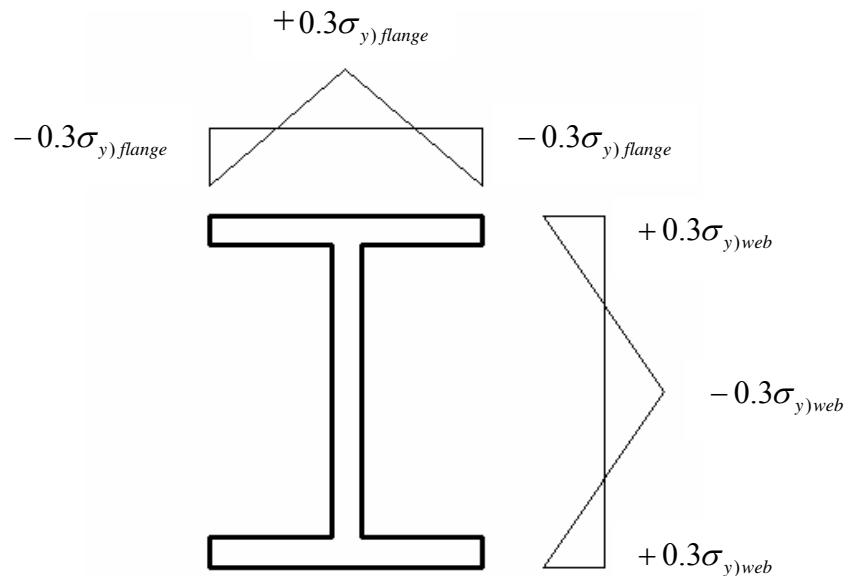


Fig.(7-4): Residual Stresses Pattern.

A convergence study of the horizontally curved steel beam CB5, is conducted including five different meshes involving a total of 27, 45, 90, 135, 180 elements, and the obtained results are compared. The results of comparison are illustrated in

Fig.(7-5). As shown the difference between the ultimate strength corresponding to 90 elements and 135 elements is about 5.4%, and that between the corresponding to 135 elements and 180 elements is about 1.6%. The two curves corresponding to the modeling with 135 elements and 180 elements are much closed; hence the finite element analysis based on 135 brick elements has been adopted, and the corresponding mesh as shown in Fig.(7-6).

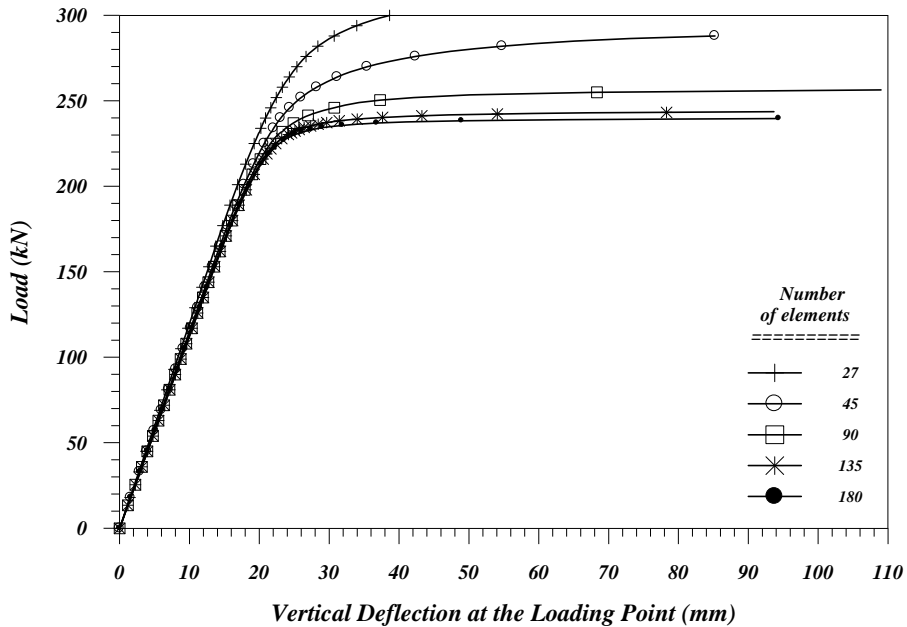


Fig.(7-5): Convergence Study of Load-Vertical Displacement Curves of CB5.

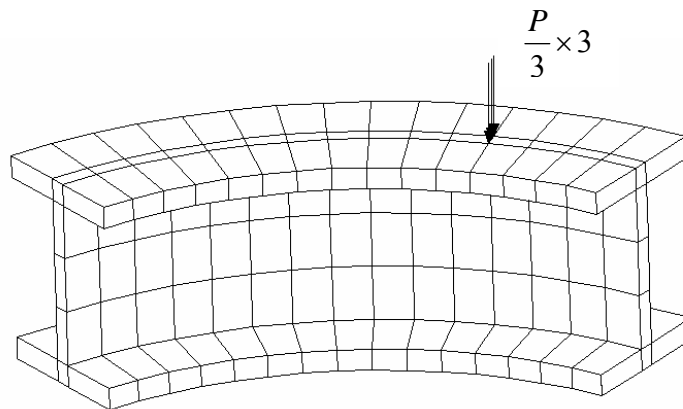


Fig.(7-6): Finite Element Mesh of 135 Brick Elements of CB5.

Comparison was made between the analytical results, obtained by the present nonlinear finite element static model *NFHCBSL*, and the experimental results. Also the analytical results of the nonlinear finite element analysis package *ABAQUS*, presented by *Shanmugam et al.* is drawn in Fig.(7-7).

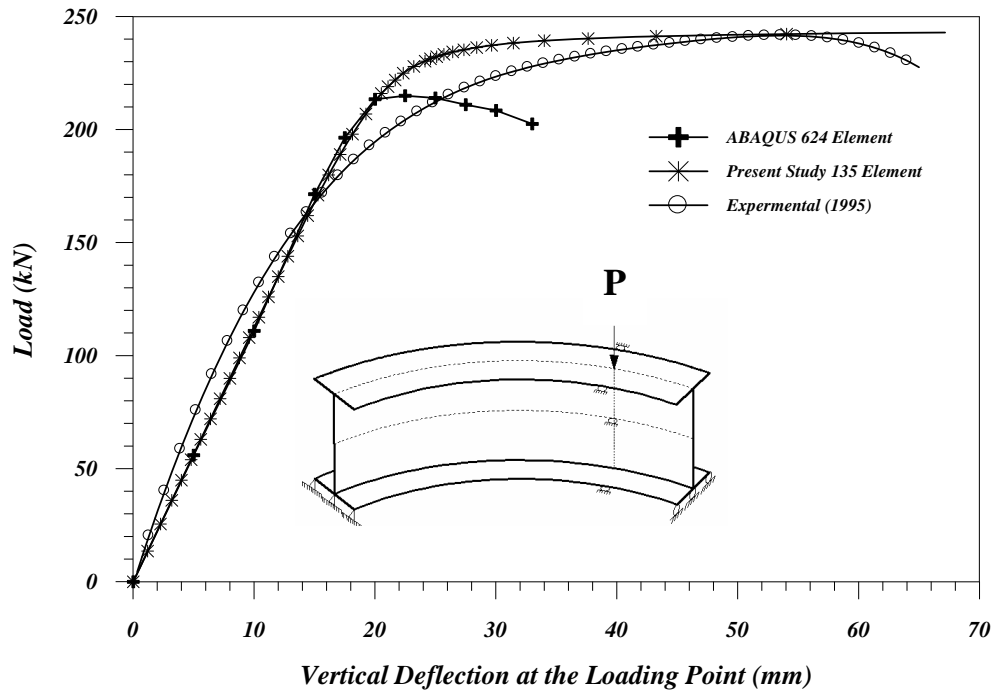


Fig.(7-7): Load-Deflection Curves for Shanmugam et al. Curved Beam CB5.

The figure showed a good agreement between the present and the experimental results. Table(7-1) contains a comparison of the analytical ultimate loads, obtained from *ABAQUS* and *NFHCBSL* with the experimental ultimate load. As shown, the current model gives results more accurate than the results of *ABAQUS* model, this of course is due to the more accurate representation of the brick elements than the shell elements. The displacements convergence criterion is used with tolerance 0.1%, also when the tolerance was changed to 0.5%, 1%, 2% or even 3% the results were not affected.

Table(7-1): Comparison of Ultimate Loads Predicted by *ABAQUS*, *NFHCBSL* Analytical Models with the Experiment.

Type of Results	Experimental	<i>ABAQUS</i> 624 Shell Element	<i>NFHCBSL</i> 135 Brick Element
P ultimate (kN)	242.00	215.00	243.66
P _{ult.} / P _{experimental}	1.000	0.8884	1.007

Non-uniform increments were applied as detailed in Table(7-2). The increments close to the ultimate load must be appreciably small else the solution may not converge. However, the beam is failed analytically at the increment 125.

The modified *Newton-Raphson* method (where the stiffness matrix is updated at the first iteration only) was adopted in the analysis.

Table(7-2): The Incremental Analytical Scheme of Applying the Load.

Number of Increments	≤ 4	≥ 5	≥ 9	≥ 70	≥ 84
The Applied Load $\Delta P(\text{kN})$	4.50	3.75	3.00	1.00	0.33

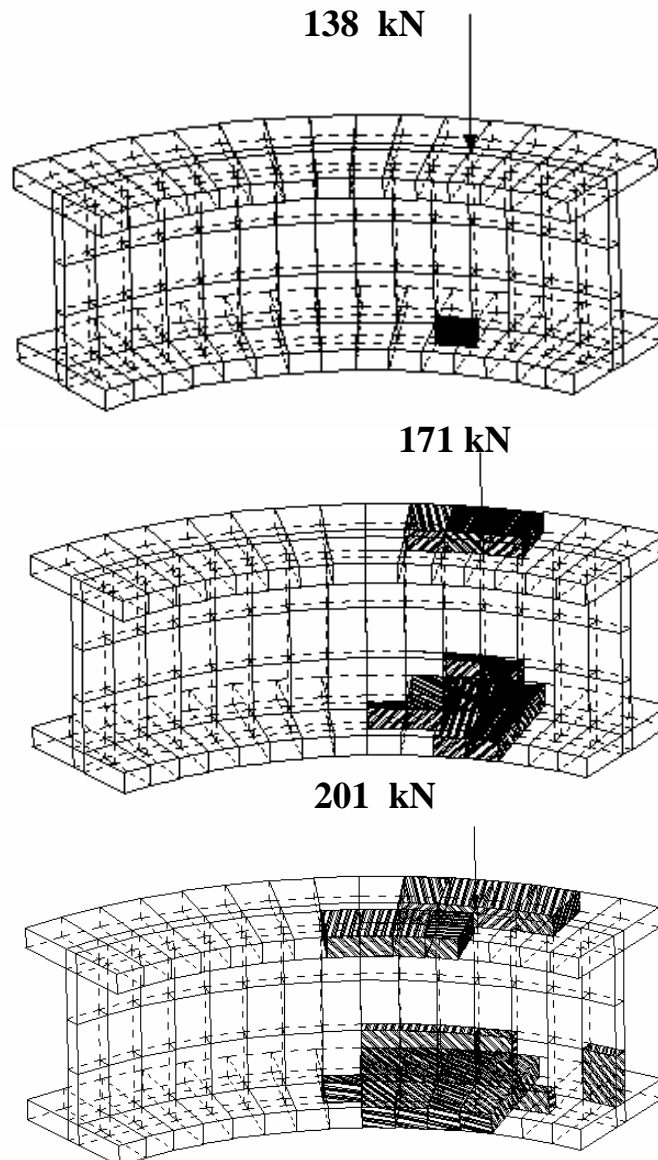


Fig.(7-8): Sequence of proposal Plastic Zones.

As shown in Fig.(7-8), the plastic zone initiated under the load at extreme web edge, then the plastic zone extended and appeared in the upper flange step by step

as load increased. The shaded elements mean that there is at least one Gauss point reached the plastic stage within the element.

Example No.2: Shanmugam et al. Curved Beam (CB1)

The second horizontally curved steel beam example examined here was also solved by *Shanmugam et al.*, named CB1, ($\theta = L/R = 14.325^\circ$), which was tested and analyzed by the same procedure discussed in example one previously. Also the initial stresses and the boundary conditions are similar to those mentioned there. Fig.(7-9) shows the geometry, properties and loading conditions of this beam.

$$\nu = 0.3$$

$$E_{web} = 222.2 \text{ GPa}$$

$$\sigma_{y,web} = 395.0 \text{ MPa}$$

$$E_{flange} = 205.1 \text{ GPa}$$

$$\sigma_{y,flange} = 337.0 \text{ MPa}$$

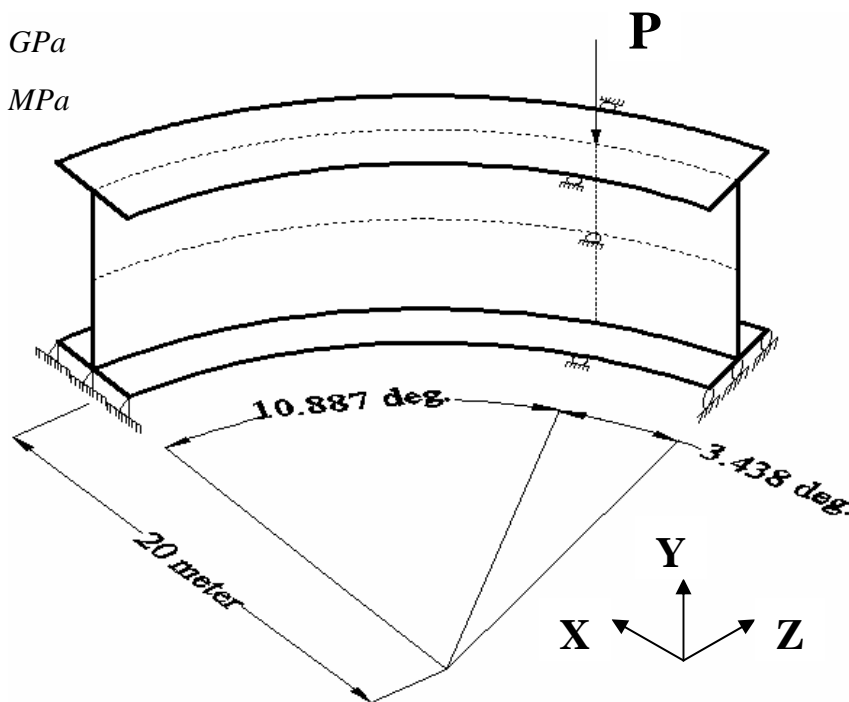


Fig.(7-9): Geometry, Properties, and Loading Conditions of the Shanmugam Curved Beam(CB1).

The convergence study of the horizontally curved steel beam CB1, is conducted including five different meshes involving a total of 90, 180, 270, 360, 450 elements. The results of comparison are illustrated in Fig.(7-10). As shown the difference between the results of the 270 elements mesh and the results of the 360 elements mesh is about 2.9% and that between the corresponding to 360 elements and 450 elements is about 0.6%. The last two curves corresponding to the modeling with 360 elements and 450 elements are much close; hence the finite

element analysis based on 360 brick elements has been adopted, and the corresponding mesh is as shown in Fig.(7-11). Due to the high curvature of the current curved beam the analysis required a dense mesh; therefore the study state was not achieved until the number of elements reached 450. Also in this convergence study, some turbulence in the results was observed, whence the results of 180 elements mesh were more accurate than the 270 elements mesh at the beginning and medium stages of loading. Therefore, the researcher must continue increasing the number of elements until it achieves the correct study state (where the difference between the last two meshes can be ignored).

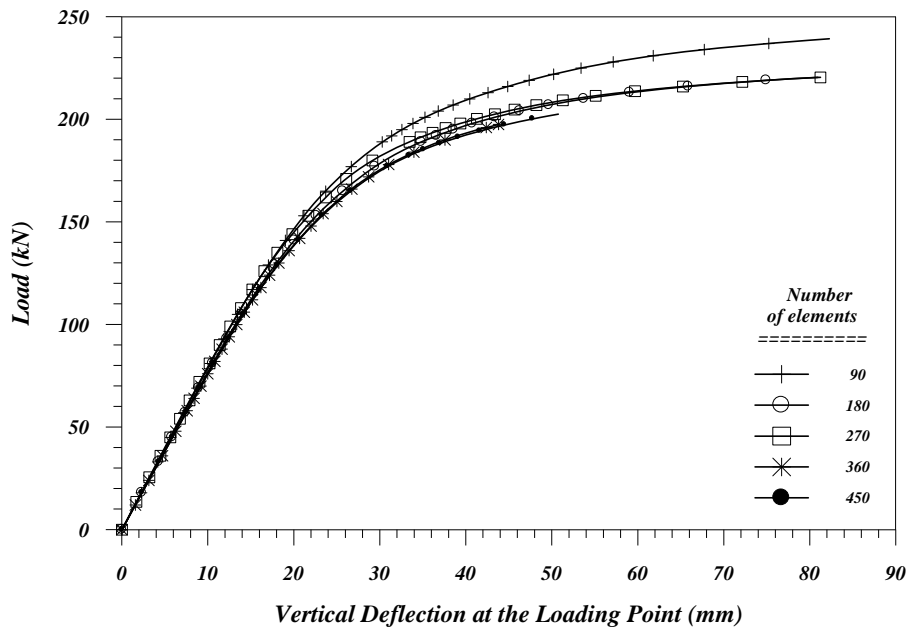


Fig.(7-10): Convergence Study of Load-Vertical Displacement Curves of CB1.

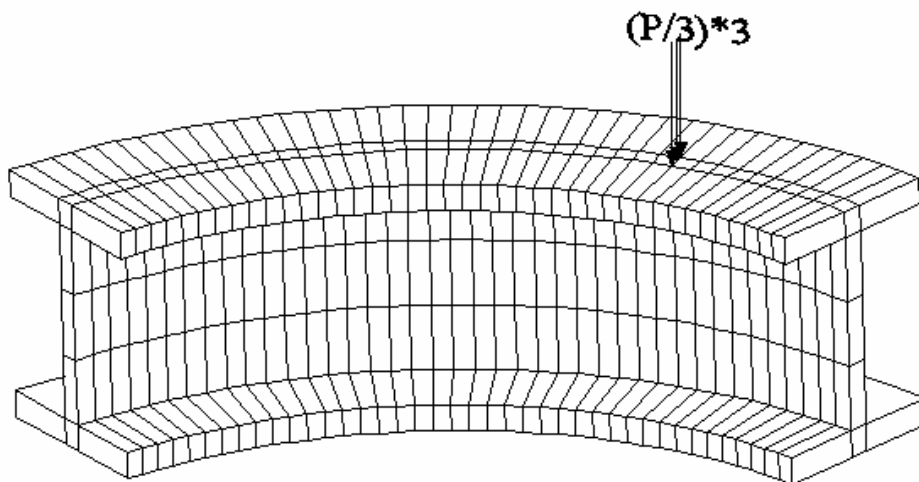


Fig.(7-11): Finite Element Mesh of 360 Brick Elements of CB1.

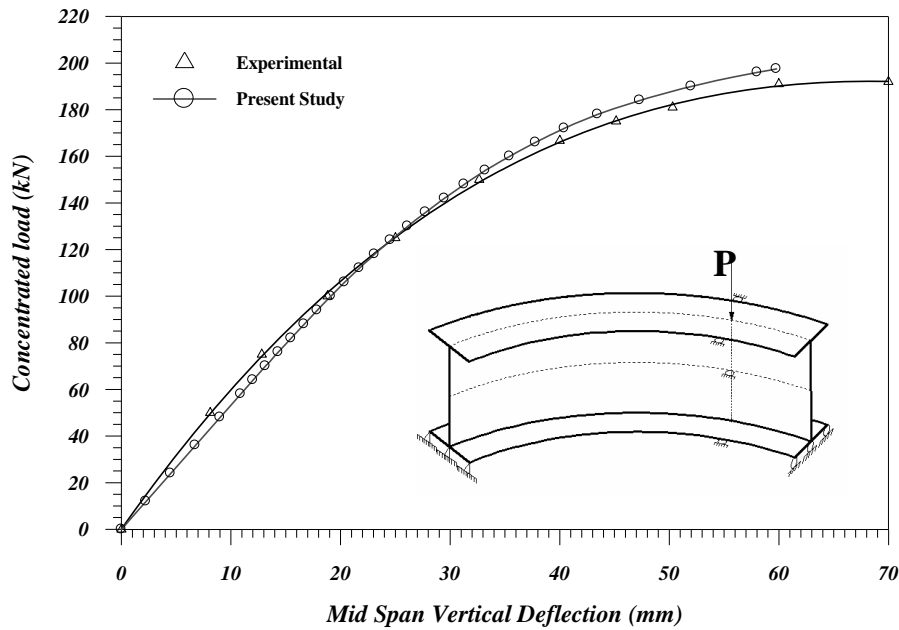


Fig.(7-12): Load-Deflection Curves for Shanmugam et al. Curved Beam CB1.

Fig(7-12) reveals good agreement between the experimental and the predicted load-deflection curves throughout the entire range of behavior of the tested specimen. The computed ultimate load (197.27 kN) was slightly higher than the experimental one (192 kN), hence, the difference between them is 2.7%. The deflected profile in the vertical direction obtained from *ABAQUS* and *NFHCBSL* numerical results and the experimental results are graphed in Fig.(7-13).

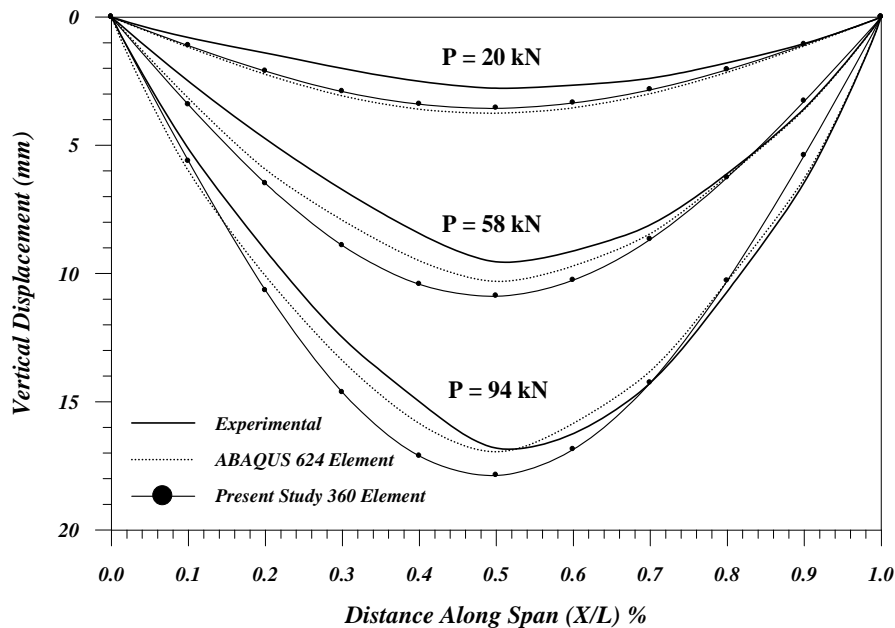


Fig.(7-13): Experimental and Numerical Vertical Displacement Profile for CB1.

The scheme of applying the concentrated load is detailed in Table(7-3). However, the beam failed numerically at the increment 88, for 360-element mesh. The modified *Newton-Raphson* method (where the stiffness matrix was updated at the first iteration only) was used in the analysis of this example. The displacements convergence criterion was used with tolerance 0.1%.

It is important to know that when the force convergence criterion is used the tolerance must be larger than 1%, because the solution does not converge neighboring the limit point. For the current example, 5% tolerance must be used to achieve the entire load-deflection curve if the force criterion is adopted.

Table(7-3): The Incremental Analytical Scheme of Applying the Load.

Number of Increments	≤ 14	≥ 15	≥ 85	≥ 87
The Applied Load ΔP(kN)	4.00	2.00	0.50	0.25

7-4-2: Horizontally Curved Reinforced Concrete Beams

Example No.3: Badawy et al. Fixed-Ended Curved Beam (C1)

This example is considered to check the reliability of the static model *NFHCBSL* to tracing the load-deflection curve of the horizontally reinforced concrete beams as well as to predict the ultimate loads for such members. *Badawy et al.* tested this fixed-ended curved beam, in 1977 [20]. The angle of curvature ($\theta = L/R$) is 75° . The properties of materials and the parameters adopted in the analysis are as detailed in Table(7-4).

Table(7-4): Properties of Materials and Parameters Adopted in the Analysis.

<i>Materials Properties</i>		<i>Parameters</i>
The compressive strength of concrete	$f'_c = 30.04$ MPa	$\alpha_1 = 40$
The yield strength for longitudinal reinforcements	$f_{yl} = 475.0$ MPa	$\alpha_2 = 0.4$
The yield strength for stirrups reinforcements	$f_{ys} = 300.3$ MPa	$\gamma_1 = 10$
The modulus of elasticity (Eq.(4-2))	$E_c = 25,760$ MPa	$\gamma_2 = 0.5$
The tensile strength of concrete(Eq.(4-4),page47)	$f_t = 1.606$ MPa	$\gamma_3 = 0.1$
Concrete: $\nu = 0.2$, $\varepsilon_u = 0.0035$. Reinforcement: $\nu = 0.0$, $\varepsilon_u = 0.20$		$C_p = 0.3$

The modulus of elasticity of steel	$E_s = 200 \text{ GPa}$	Tole.= 0.15%
------------------------------------	-------------------------	--------------

Fig.(7-14) shows the geometry and loading conditions. The full length of the beam was analyzed, and the nodes located at the perimeter of the ends were considered fixed. Also the location of the origin of the Cartesian coordinates at the left end of the beam.

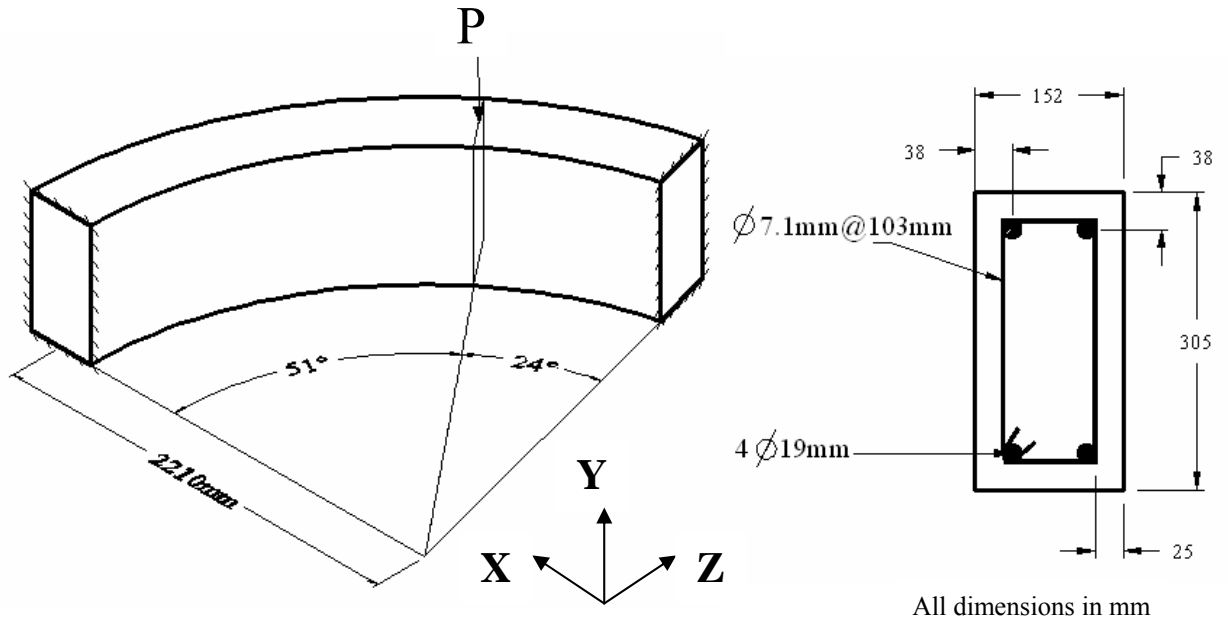


Fig.(7-14): Geometry and Loading Conditions of Badawy et al. Curved beam(C1).

The steady state of discretization is achieved in this example at 256 element, where the difference between the 256 element and the 228 element meshes is equal

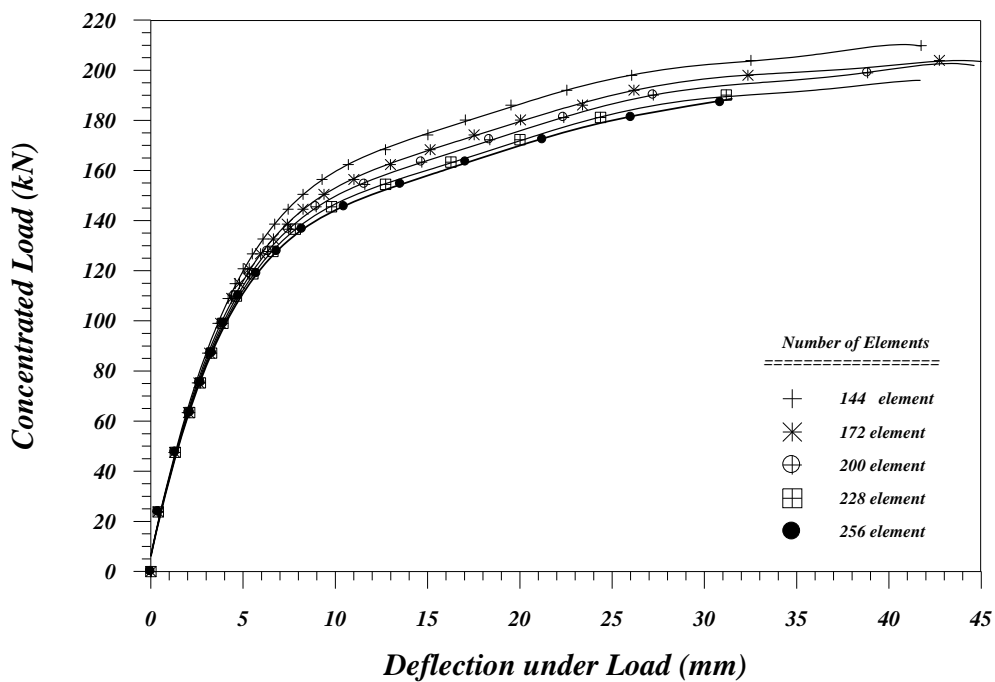


Fig.(7-15): Convergence Study Load-Vertical Displacement Curves of C1. 8

to 0.66% while the difference between 228 element and 200 element meshes is equal to 2% as shown in Fig.(7-15). Therefore the mesh of 256, Fig.(7-16), is adopted in the following analyses.

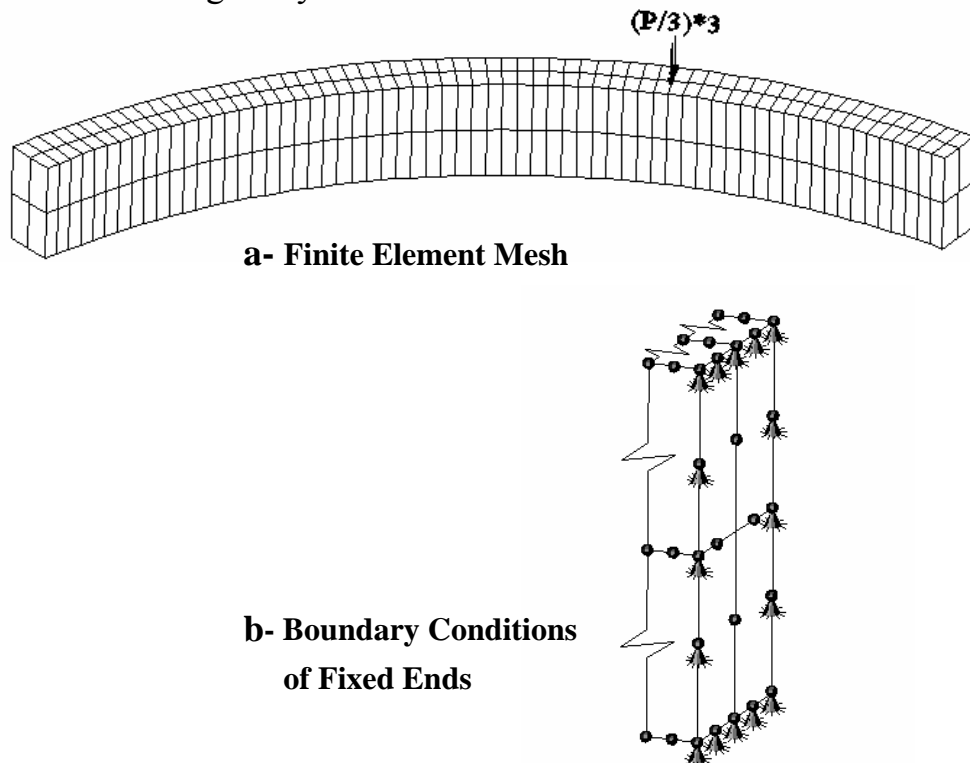


Fig.(7-16): Finite Element Mesh and Boundary Conditions of 256 Brick Elements of Badawy et al. (C1).

The loads applied as a non-uniform increments are detailed in Table(7-5). The beam failure occurred analytically at the increment 50. The modified *Newton-Raphson* method (where the stiffness matrix is updated at 1st, 6th, 11th, 16thetc iteration) and the displacement convergence criterion are adopted in the analyses of all reinforced concrete examples.

Table(7-5): The Incremental Analytical Scheme of Applying the Load.

Number of Increments	≤ 7	≥ 8	≥ 21	≥ 46
The Applied Load ΔP (kN)	8.00	4.00	3.00	2.00

Good agreement is obtained between the experimental and the predicted load-deflection curves as shown in Fig(7-17). The computed ultimate load (189.1 kN) was slightly higher than the experimental one (184.5 kN), hence, the difference

between them is equal to 2.5%. If crushing is ignored the predicted ultimate load is equal to 212. kN and the difference becomes 15.4%. This figure shows obviously the importance of considering the crushing phenomenon.

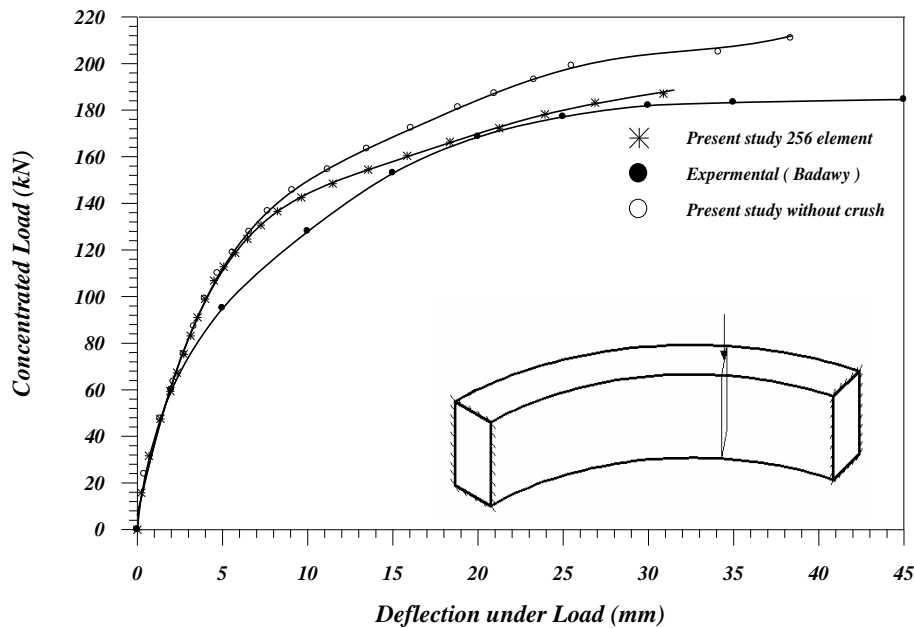


Fig.(7-17): Load-Deflection Curves for Badawy et al. Curved Beam (C1).

The effects of parameters on the predicted load-deflection curves are presented here, as illustrated in Figs.(7-18) to (7-25). Fig.(7-18) shows the significant effect of the tolerance values. As shown when the tolerance is larger than 0.15% the results will have effective accumulative errors. This occurred because the solution converged from the first (or second or third) iteration without correcting the errors. Fig.(7-19) proved that the best performance in tracing the load-deflection curve can be achieved when the deficiency in the compressive strength of concrete is equal to 15% at the ultimate strain (crushing strain). Fig.(7-20) shows that the better performance can be obtained when the rate of stress is released as the crack widens $\alpha_1=50$. Fig.(7-21) shows that the significant effect of the sudden loss of stress is at the instant of cracking (parameter α_2), and it shows the optimal value of $\alpha_2=0.4$. Figs.(7-22) and (7-23) show the minor effects of the rate of decay of shear stiffness γ_1 , and the sudden loss in shear stiffness γ_2 , while Fig.(7-24) reveals the major effect of the residual shear stiffness due to the dowel action γ_3 , as appeared with the optimal value of $\gamma_3=0.1$. In Fig.(7-25) the effects of the ultimate strain is drawn, as expected when the ultimate strain limit of crushing increase the strength of reinforced concrete beam increases, but this increase was something small.

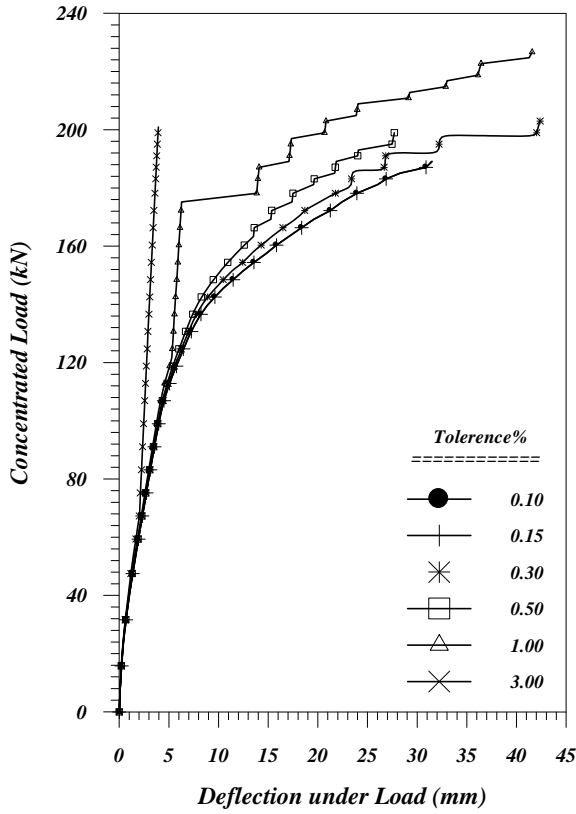


Fig.(7-18): Effect of Tolerance.

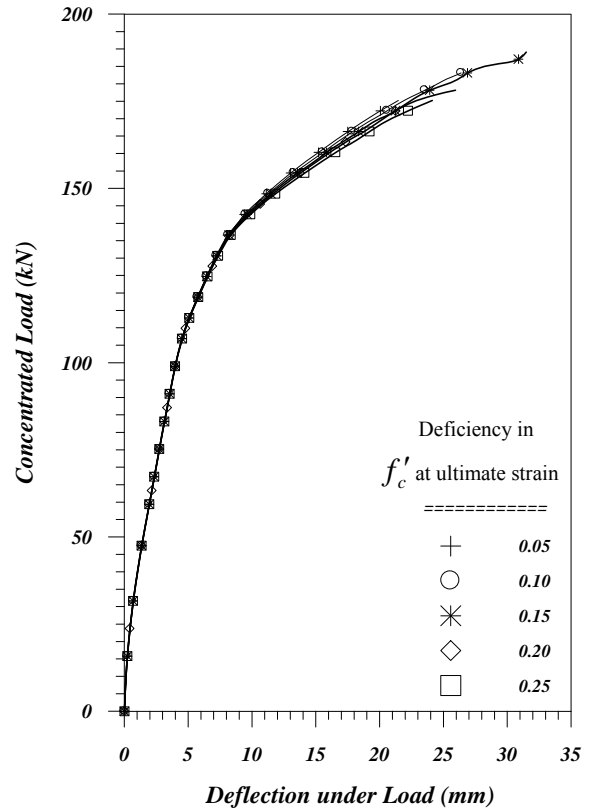


Fig.(7-19): Effect of Deficiency in f'_c .

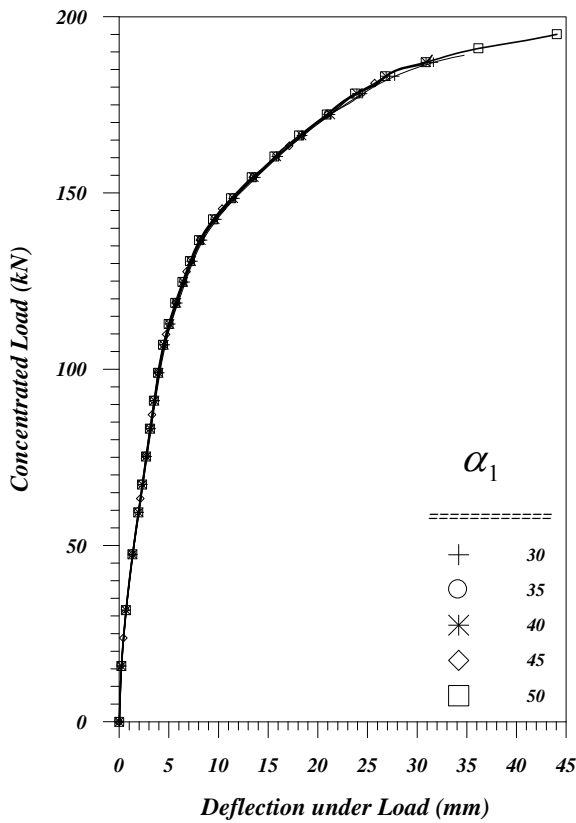


Fig.(7-20): Effect of α_1 .

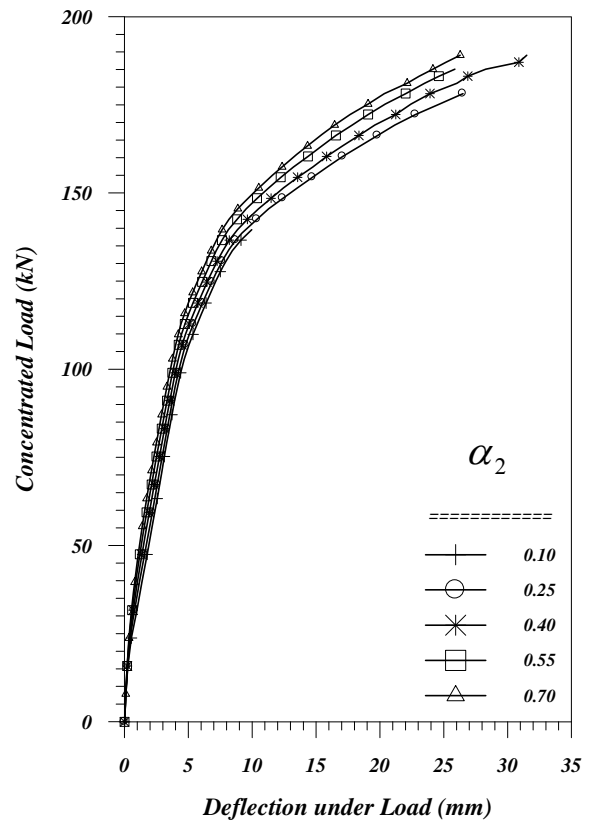


Fig.(7-21): Effect of α_2 .

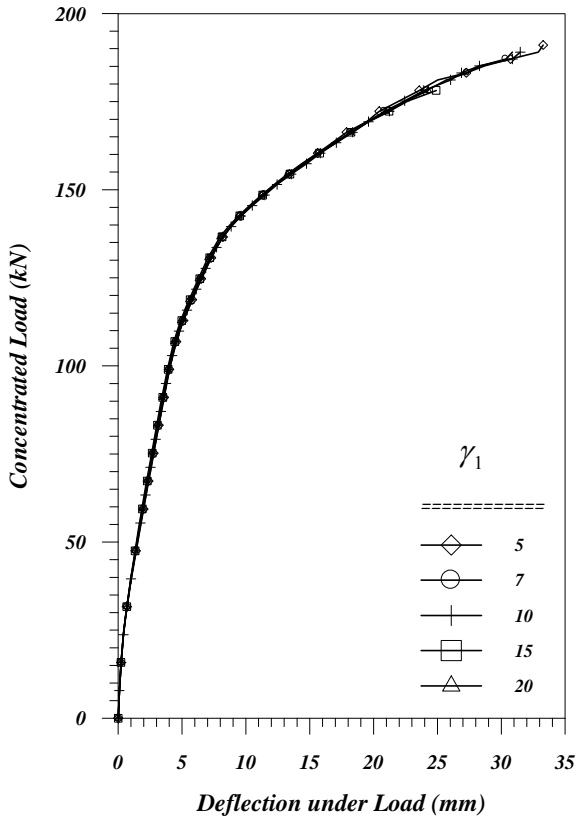


Fig.(7-22): Effect of γ_1 .

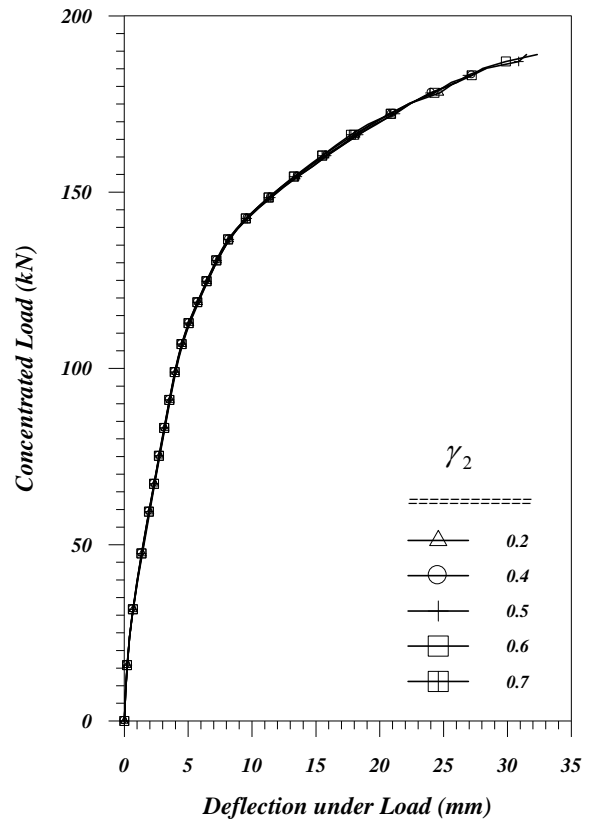


Fig.(7-23): Effect of γ_2 .

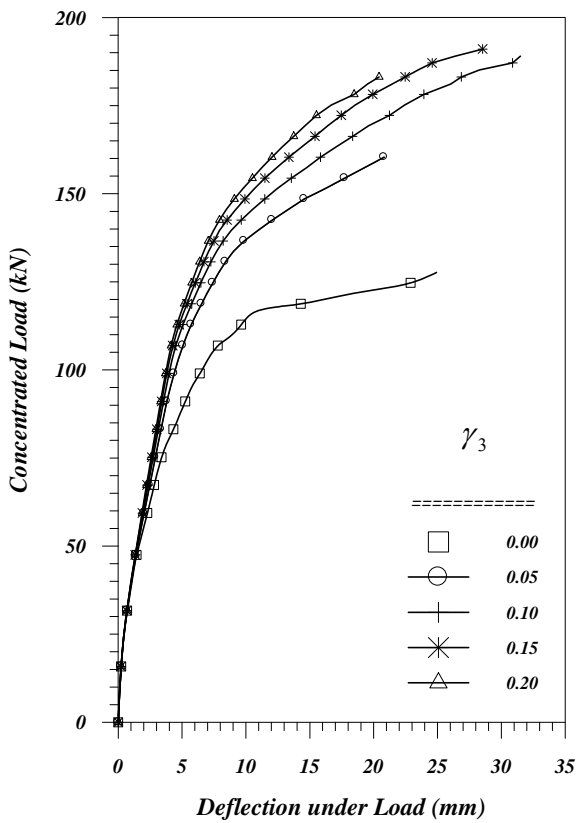


Fig.(7-24): Effect of γ_3 .

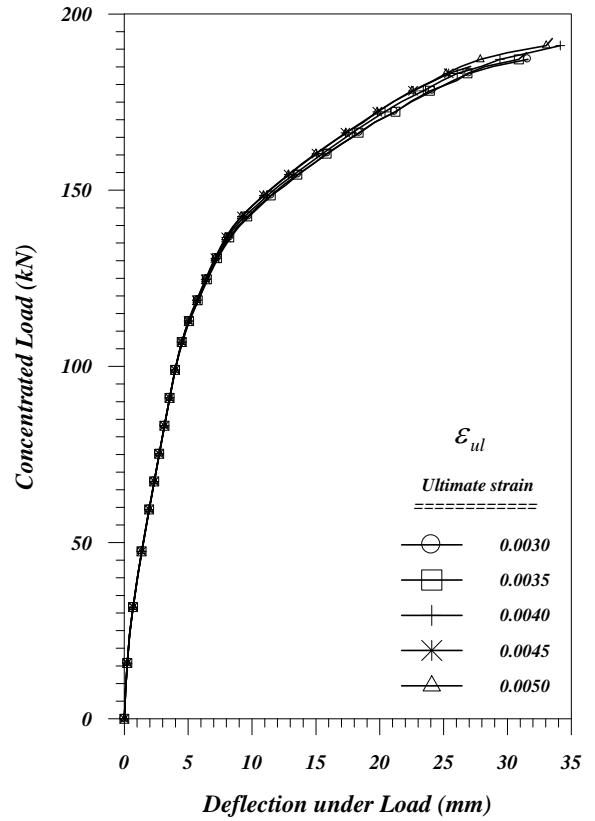
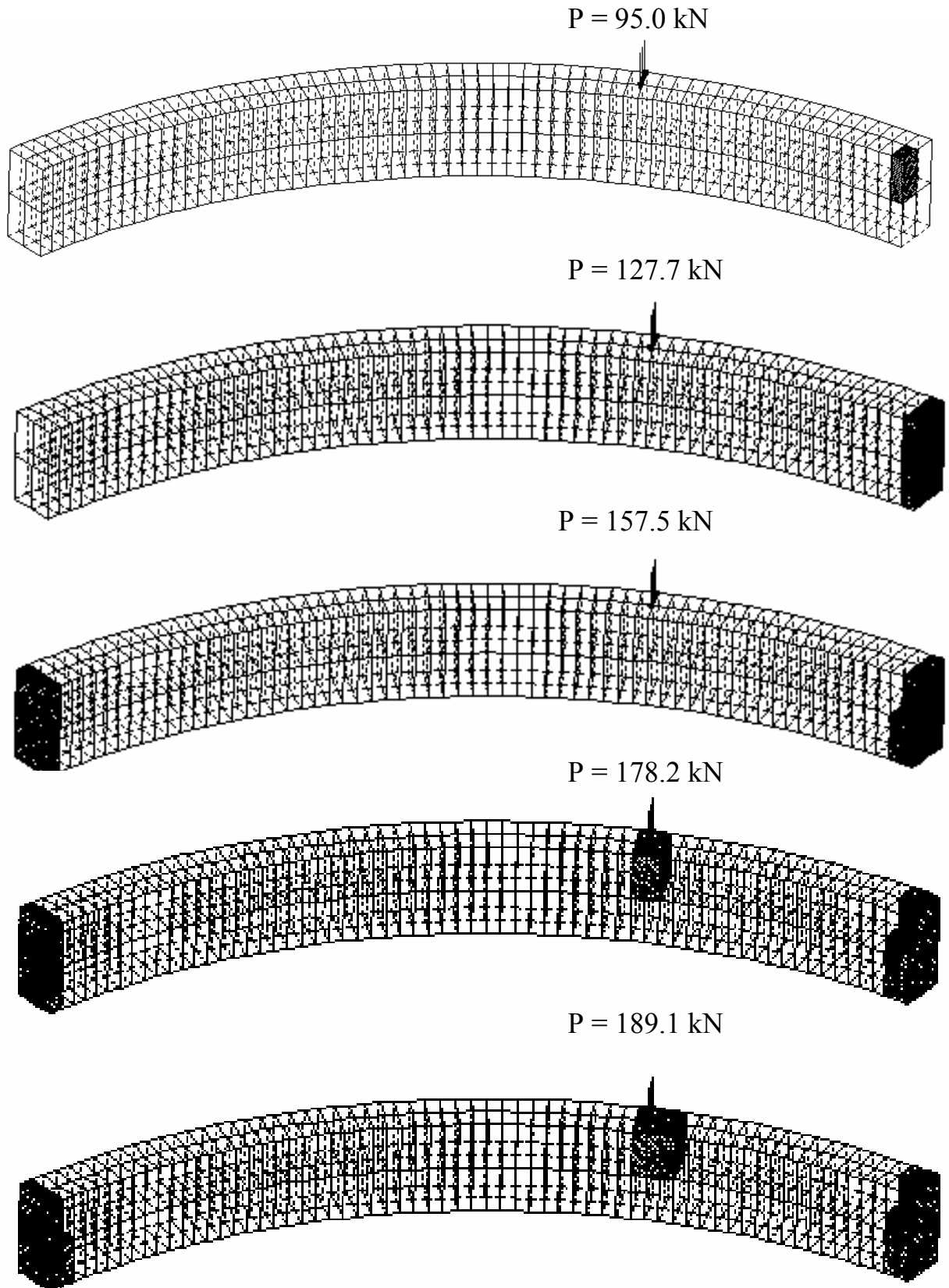


Fig.(7-25): Effect of ϵ_{ul} .



Note: When element is indicated this means at least having one Gauss point

Fig.(7-26): Sequence of the Crushing for Badawy et al. 256 Mesh Element.

As illustrated in Fig.(7-26) the critical sections are located at the fixed ends and under the load. It is important to note that the first crush occurred at the upper and inner element of right support as a plain crushed Gauss point (i.e., cracked Gauss point in one direction). Also the initial plastic load is equal to 39.6 kN.

Example No.4: Jordaan et al. Fixed-Ended Curved Beam (C3)

Jordaan et al. tested and analyzed this fixed-ended curved beam, in 1974 [19]. The angle of curvature ($\theta = L/R$) is 86° . Owing to the geometric and loading symmetry, the analysis was carried out for half of the beam. Properties of materials and the parameters adopted in the analysis are as detailed in Table(7-6).

Table(7-6): Properties of Materials and Parameters Adopted in the Analysis.

<i>Materials Properties</i>		<i>Parameters</i>
The compressive strength of concrete	$f'_c = 41.40$ MPa	$\alpha_1 = 40$
The yield strength for longitudinal reinforcements	$f_{yl} = 384.0$ MPa	$\alpha_2 = 0.4$
The yield strength for stirrups reinforcements	$f_{ys} = 240.0$ MPa	$\gamma_1 = 10$
The modulus of elasticity (Eq.(4-2),page 46)	$E_c = 30,241$ MPa	$\gamma_2 = 0.5$
The tensile strength of concrete (Eq.(4-4),page47)	$f_t = 1.885$ MPa	$\gamma_3 = 0.1$
Concrete: $\nu = 0.2, \epsilon_u = 0.0035$. Reinforcement: $\nu = 0.0, \epsilon_u = 0.20$		Cp=0.3
The modulus of elasticity of steel	$E_s = 200$ GPa	Tole.= 0.15%

Fig.(7-27) shows the geometry and loading conditions. The nodes located at the perimeter of the ends were considered fixed, while the nodes located at mid-span were restrained in the tangential direction only.

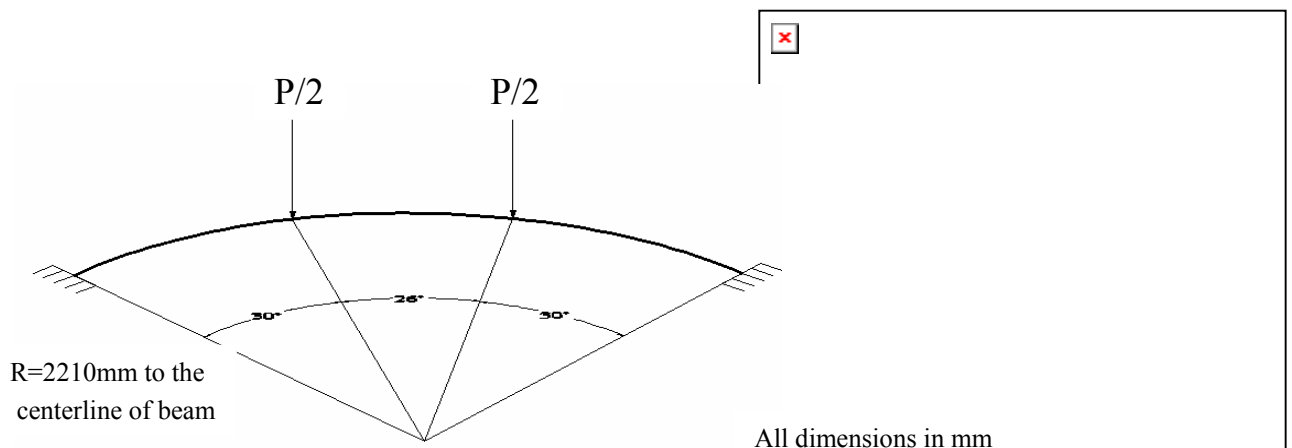


Fig.(7-27): Geometry and Loading Conditions of Jordaan et al. Curved beam(C3).

A convergence study of *Jordaan et al.* horizontally reinforced concrete curved beam (C3), was conducted including seven different meshes involving a total of 68, 84, 100, 116, 132, 148 and 160 elements. The results of comparison are illustrated in Fig.(7-28). As shown the difference between any successive meshes decreased until it reached 1% between the 148 element and 160 element meshes. Therefore the mesh of 148, Fig.(7-29), is adopted in the analyses.

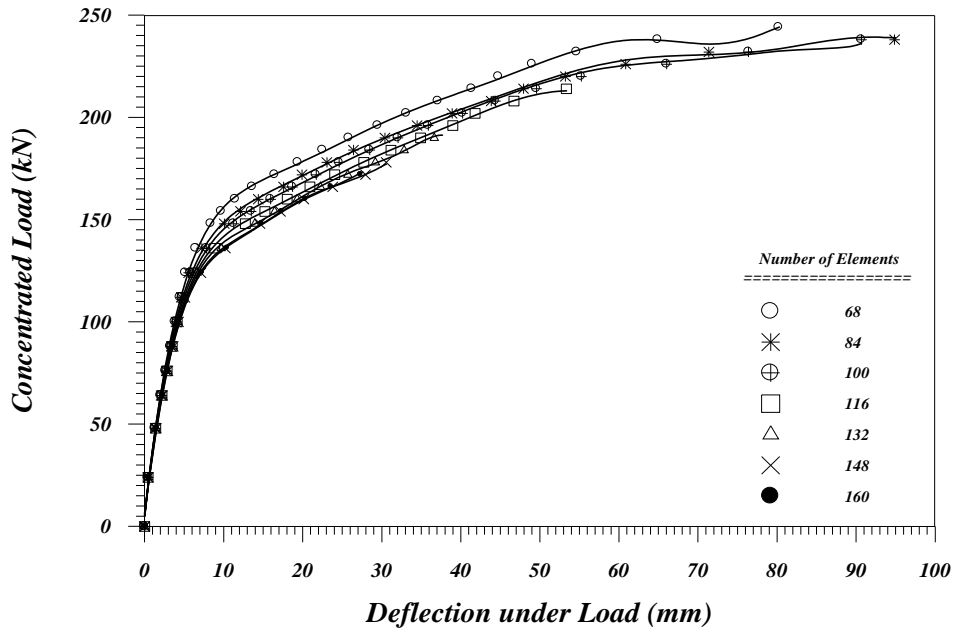


Fig.(7-28): Convergence Study of Load-Vertical Displacement Curves of (C3).

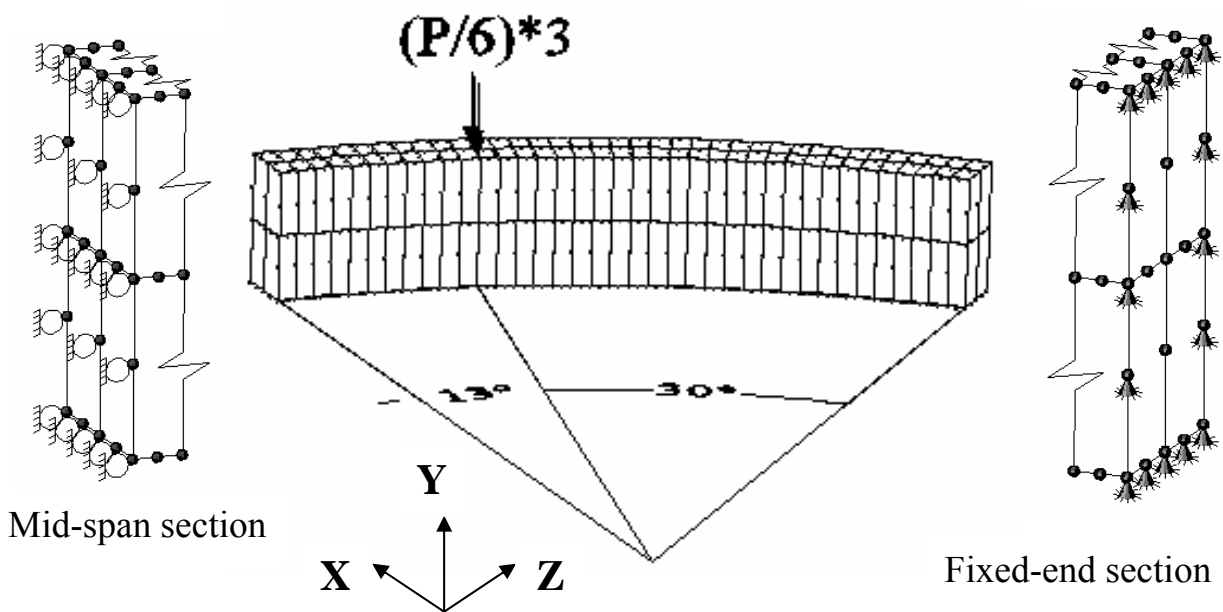


Fig.(7-29): Finite Element Mesh and Boundary Conditions of 148 Brick Elements of Jordaan et al. (C3).

Load increments are applied as detailed in Table(7-7). The beam failed analytically at the increment 46. The Cartesian coordinates at mid-span section.

Table(7-7): The Incremental Analytical Scheme of Applying the Load.

Number of Increments	≤ 7	≥ 8	≥ 31
The Applied Load ΔP (kN)	4.00	2.00	1.00

Good agreement is obtained between the experimental and the predicted load-deflection curves as shown in Fig(7-30). The predicted ultimate load coincided with the experimental value and it is equal to (178 kN), while the predicted ultimate load by *Jordaan et al.* was 188 kN. Also when crushing is ignored the obtained ultimate load was equal to 250 kN, thus the difference between the predicted load and the experimental value is 40%. Also the results showed that rupture occurred in reinforcement bars near the fixed ends at the last increment of loading (increment 46) consequently the collapse mechanism happened.

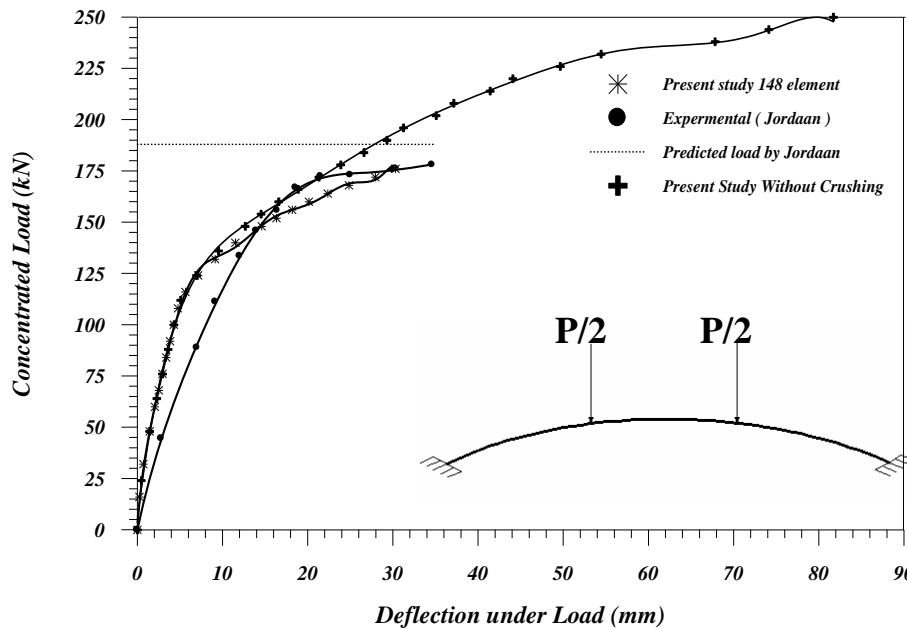


Fig.(7-30): Load – Deflection Curves for Jordaan et al. Curved Beam (C3).

From Figs.(7-31) to (7-38), one can conclude the optimal values of parameters which must be used in the analytical static model *NFHCBSL*. These values coincide approximately with the optimal parameters of the previous example, summarized in Table(7-8). These values give results more closely to the experimental results than others. Also the values of the tolerance, α_2 and γ_3 have more sensitive effects than the other parameters hence they must be chosen deliberately for other cases.

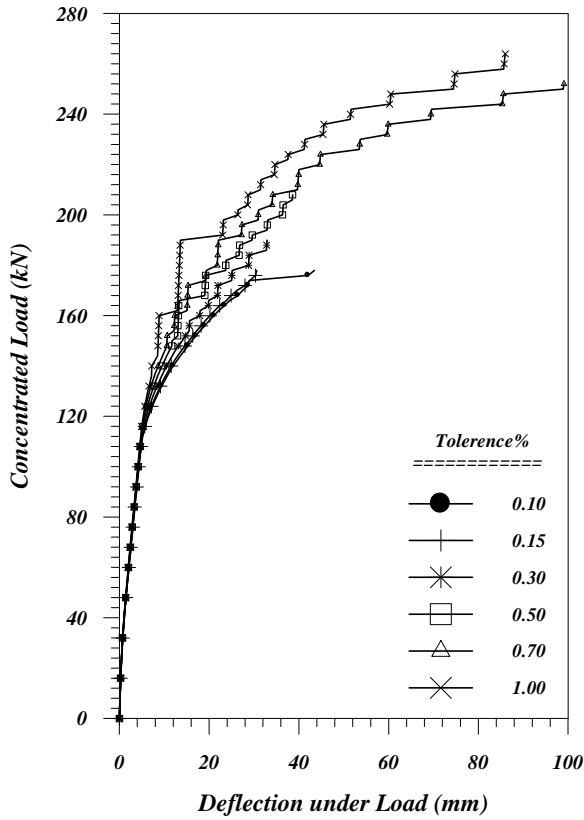


Fig.(7-31): Effect of Tolerance.

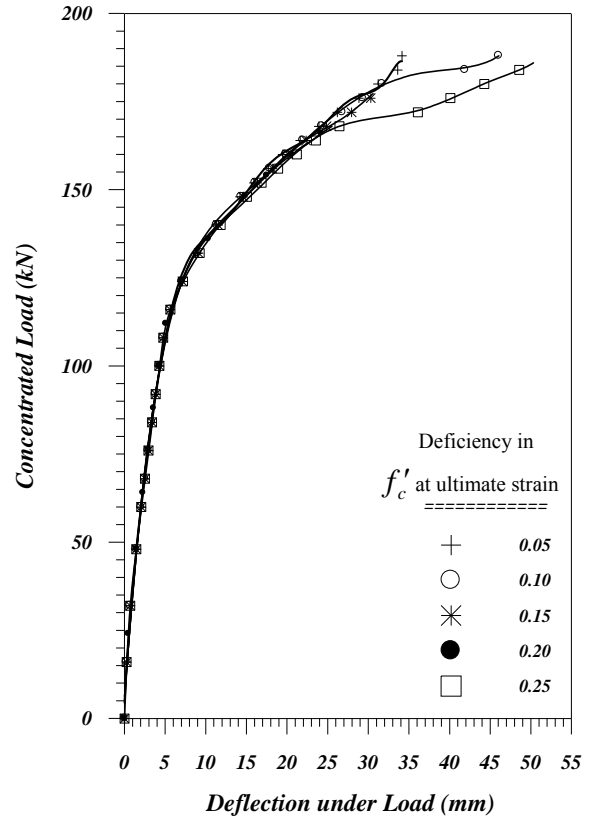


Fig.(7-32): Effect of Deficiency in f'_c .

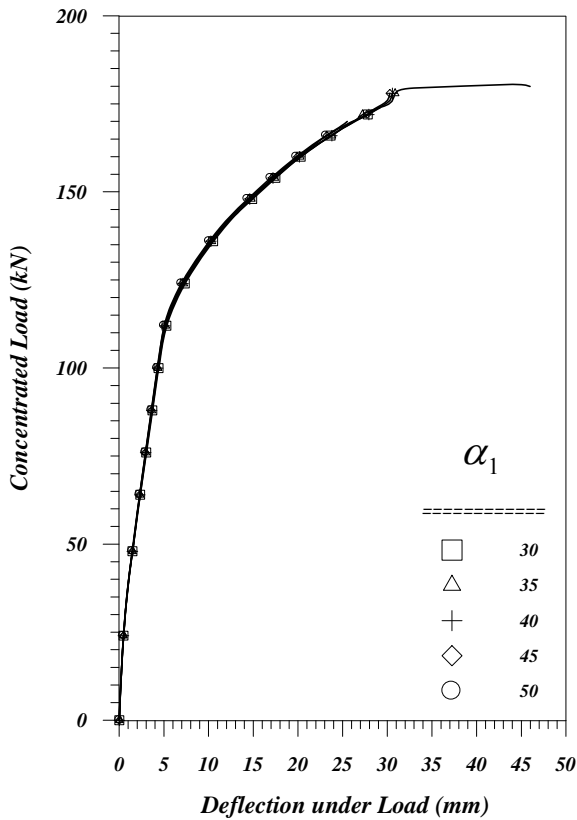


Fig.(7-33): Effect of α_1 .

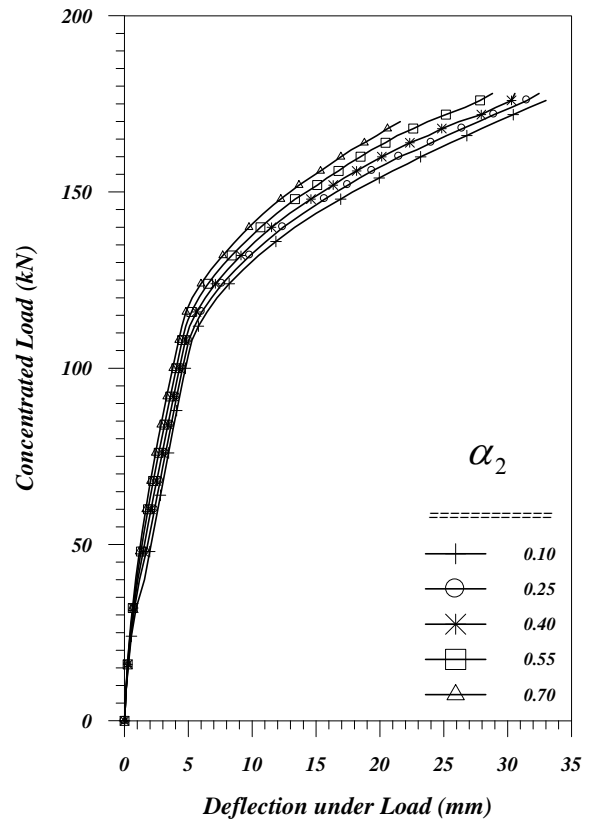


Fig.(7-34): Effect of α_2 .

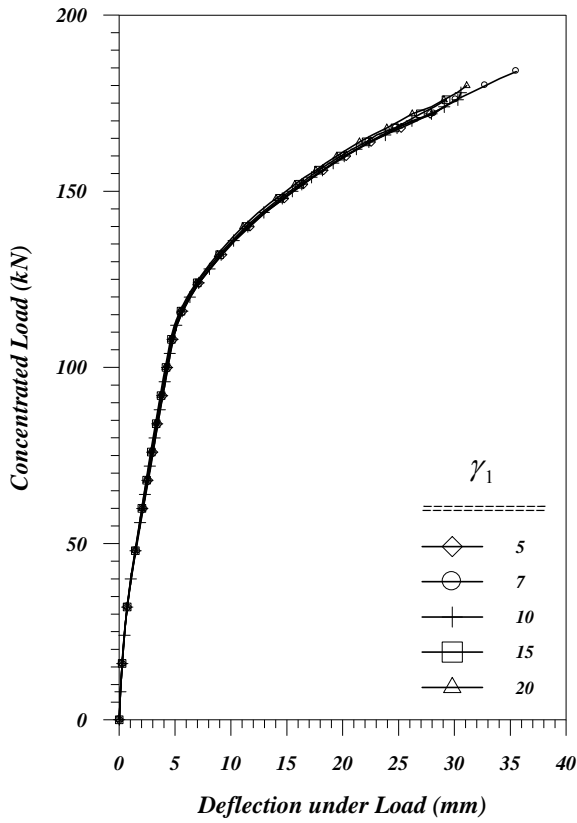


Fig.(7-35): Effect of γ_1 .

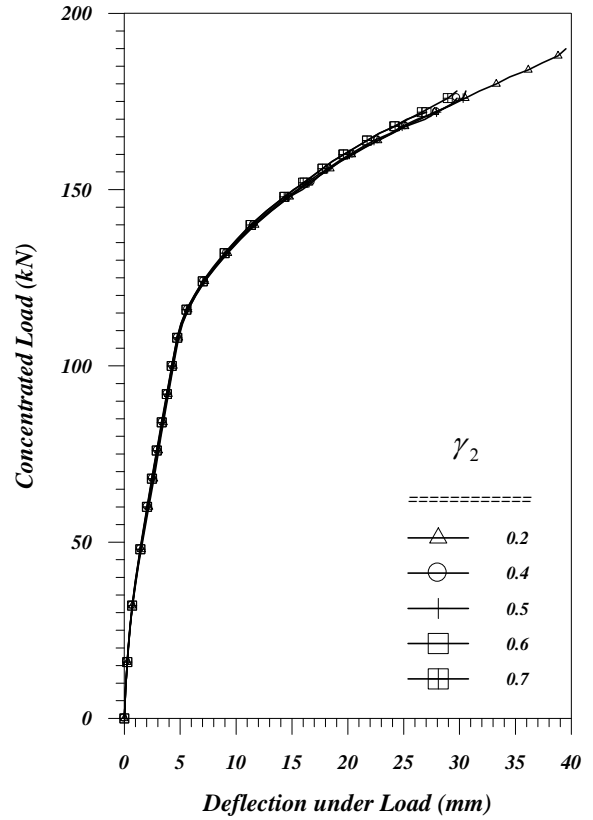


Fig.(7-36): Effect of γ_2 .

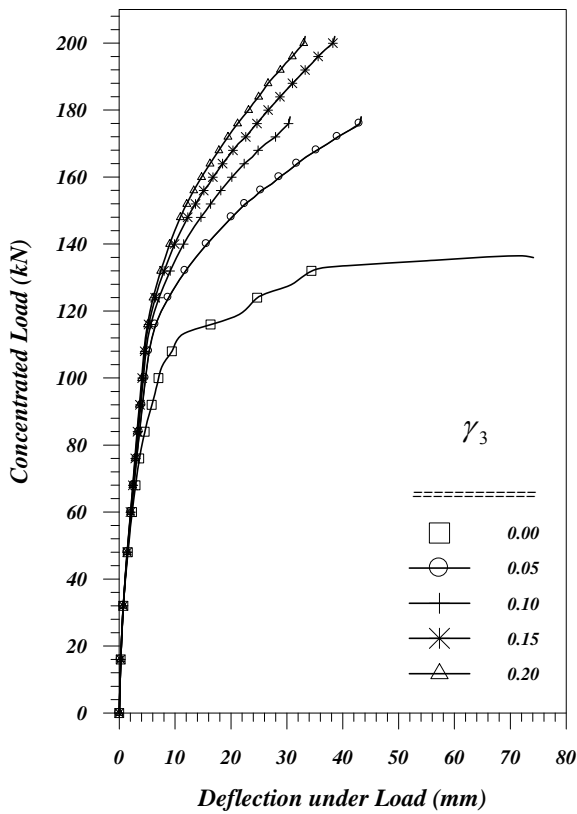


Fig.(7-37): Effect of γ_3 .

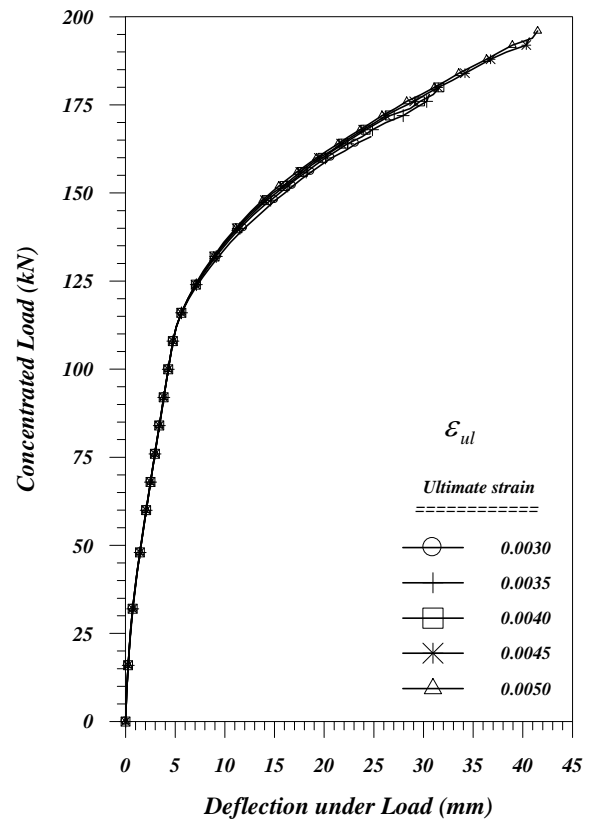
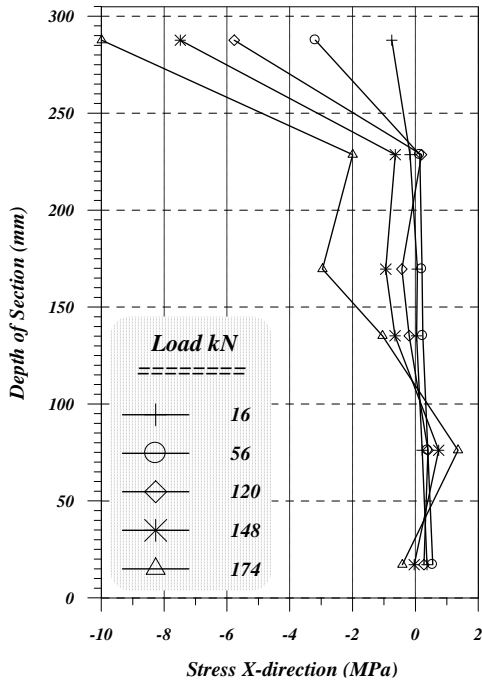


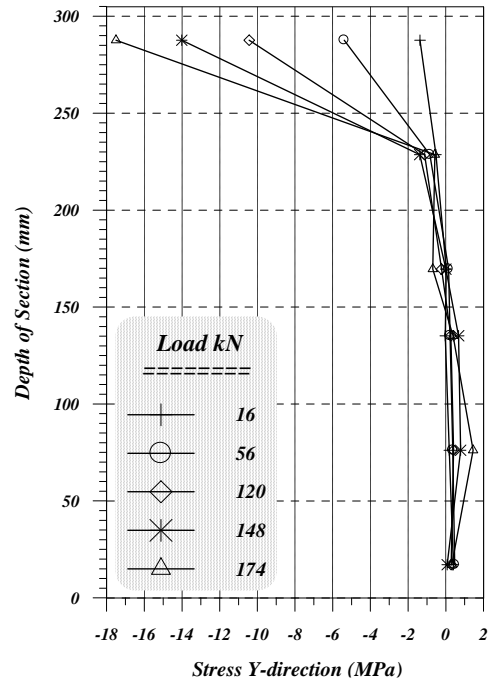
Fig.(7-38): Effect of ϵ_{ul} .

Table(7-8): The optimal Values of Parameters for *Jordaan et al. (C3)*.

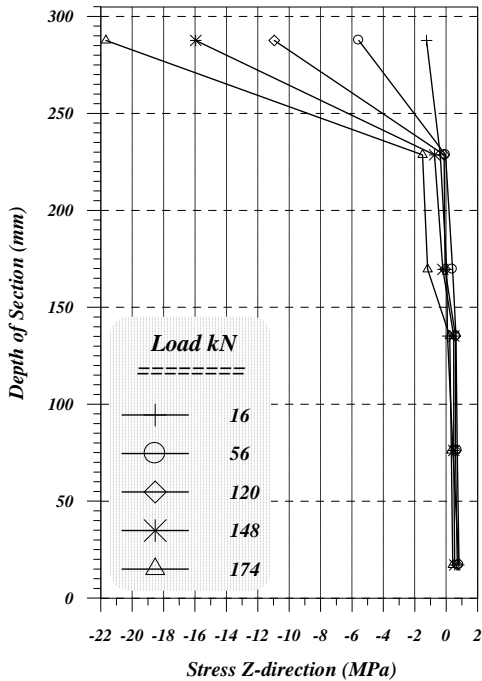
Parameters	Tolerance %	Deficient in f'_c %	α_1	α_2	γ_1	γ_2	γ_3	Ultimate strain ϵ_{ul}
Optimal Values	≤ 0.15	15	40 - 50	0.2 - 0.4	$\cong 10$	$\cong 0.5$	0.1-0.12	0.0035



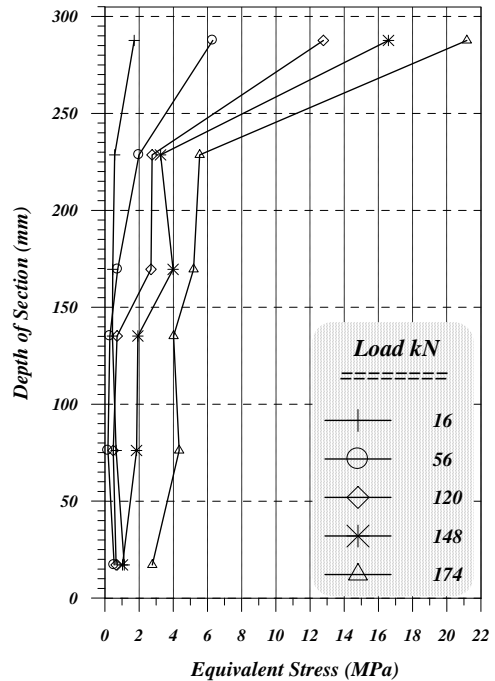
a- Stress in X- Direction



b- Stress in Y- Direction



c- Stress in Z- Direction



b- Equivalent Stress

Fig.(7-39): Stresses Distributions (About) under the Load at Centerline.

Fig.(7-39) reflects the stresses in x, y and z-directions as well as the equivalent stress at the section approximately under the load. As shown the normal stress σ_z is larger than σ_y and the last is larger than σ_x for any load, also the results in this figure proved that maximum compressive stresses take place at extreme fibers. It is important to note that due to the degradation in the compressive strength of concrete the maximum strength limit is smaller than f'_c .

Example No.5 Badawy et al. Non-prismatic Curved Beam (C6)

This example is considered as an assessment for the reliability of the static model *NFHCBSL* to tracing the load-deflection curve of the non-prismatic horizontally reinforced concrete beams and to predict the ultimate loads for such members. This fixed-ended curved beam was tested by *Badawy et al.*[20]. The angle of curvature ($\theta = L/R$) is 83.6° and the radius is 2210mm to the centerline of the beam. The properties of materials and the parameters adopted in the analysis are detailed in Table(7-9).

Table(7-9): Properties of Materials and Parameters Adopted in the Analysis.

<i>Materials Properties</i>		<i>Parameters</i>
The compressive strength of concrete	$f'_c = 30.04$ MPa	$\alpha_1 = 40$
The yield strength for longitudinal reinforcements f_{yl}	$= 475.0$ MPa	$\alpha_2 = 0.4$
The yield strength for stirrups ϕ 7.1mm	$f_{ys} = 300.3$ MPa	$\gamma_1 = 10$
The yield strength for stirrups ϕ 9.5mm	$f_{ys} = 366.8$ MPa	$\gamma_2 = 0.5$
The modulus of elasticity (Eq.(4-2), page 46)	$E_c = 25,760$ MPa	$\gamma_3 = 0.1$
The tensile strength of concrete (Eq.(4-4), page 47)	$f_t = 1.606$ MPa	$C_p = 0.3$
Concrete: $\nu = 0.2$, $\varepsilon_u = 0.0035$. Reinforcement: $\nu = 0.0$, $\varepsilon_u = 0.20$		Tolerance 0.15 %
The modulus of elasticity of steel	$E_s = 200$ GPa	

Fig.(7-40) shows the geometry and loading conditions. The full length of the beam was analyzed, and the nodes located at the ends were considered fixed.

The nonlinear finite element solution reached to the steady state in this example at 200 element mesh. The difference between 200 element and 172

element meshes was less than 0.5% and the two curves are approximately identical as shown in Fig.(7-41), therefore the 172 element mesh is adopted here Fig.(7-42).

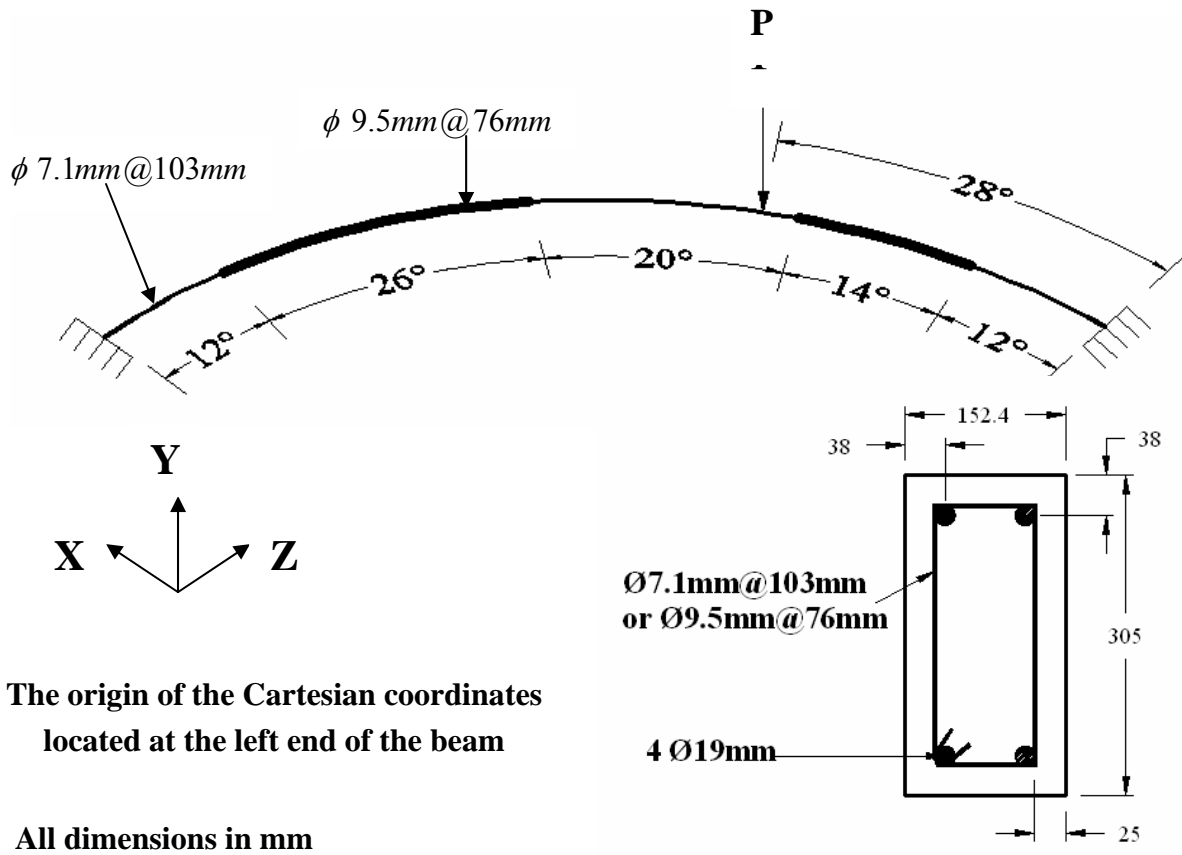


Fig.(7-40):Geometry and Loading Condition of the Non-prismatic Badawy Curved beam(C6).

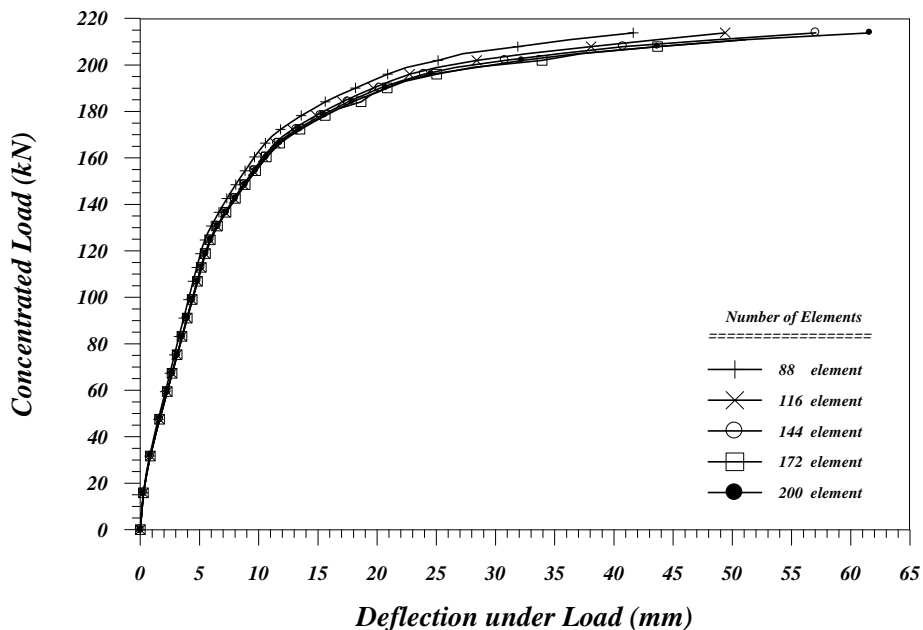


Fig.(7-41): Convergence Study of Load-Vertical Displacement Curves of C6.

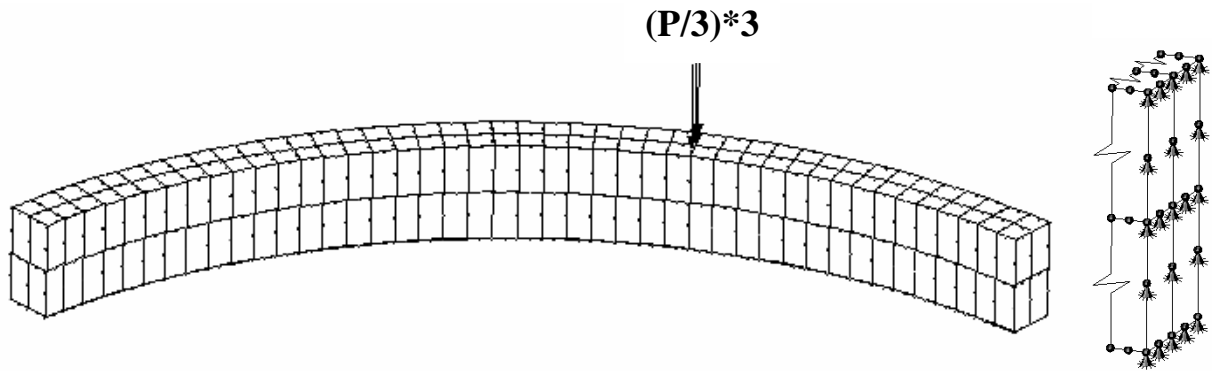


Fig.(7-42): Finite Element Mesh and Boundary Conditions of 172 Brick Elements of the Non-prismatic Badawy et al. Curved Beam(C6).

The loads was applied in non-uniform increments as detailed in Table(7-5). The beam is failed analytically at the increment 56.

Table(7-10): The Incremental Analytical Scheme of Applying the Load.

Number of Increments	≤ 7	≥ 8	≥ 21	≥ 46
The Applied Load ΔP (kN)	8.00	4.00	3.00	2.00

Good agreement is obtained between the experimental and the predicted load-deflection curves as shown in Fig(7-43). The predicted ultimate load (211 kN) was slightly higher than the experimental value (204.5 kN), hence, the difference between them is equal to 3.2%.

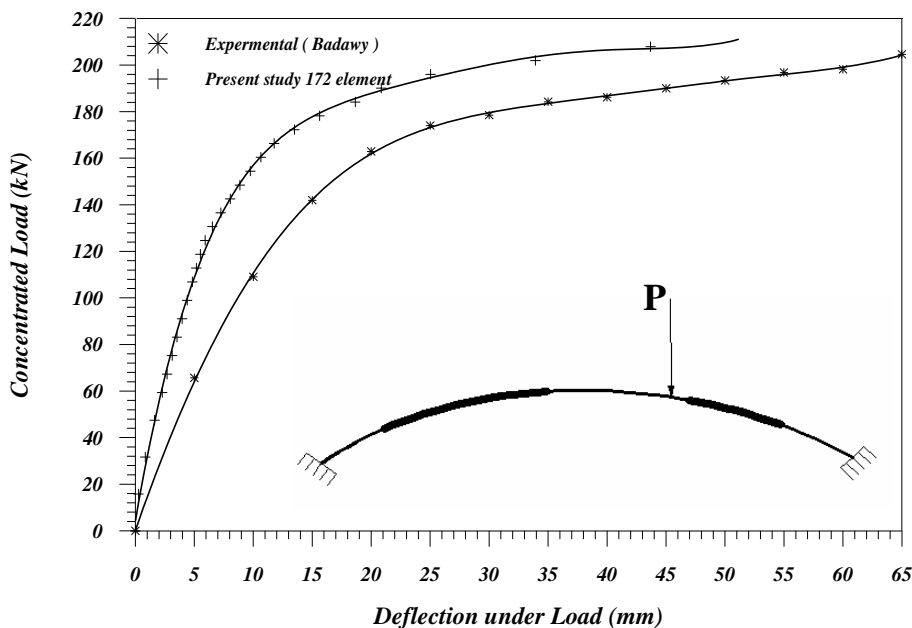


Fig.(7-43): Load – Deflection Curves for Badawy et al. Curved Beam C6.

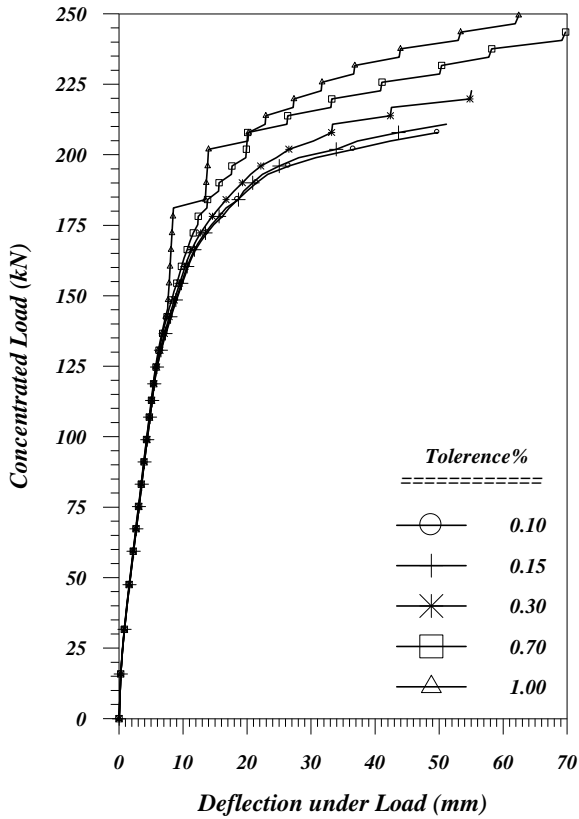


Fig.(7-44): Effect of Tolerance.

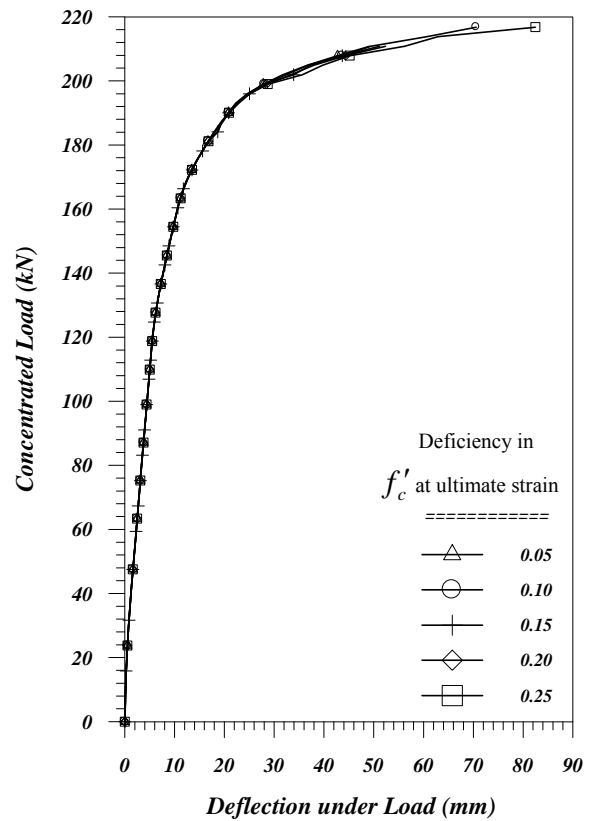


Fig.(7-45): Effect of Deficiency in f'_c .

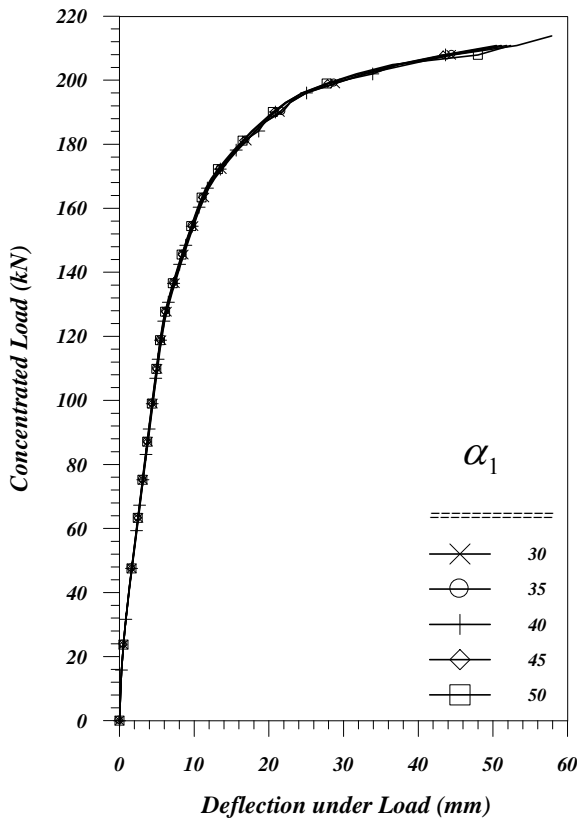


Fig.(7-46): Effect of α_1 .

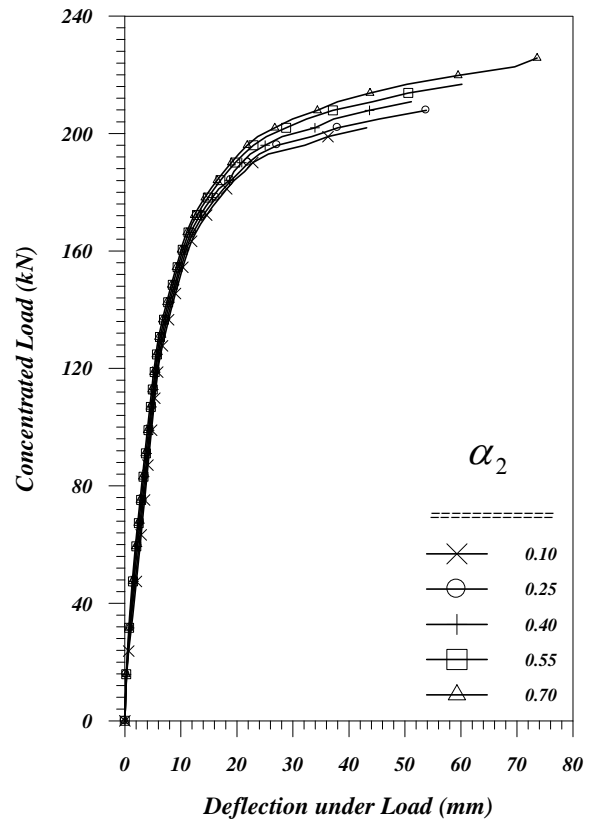


Fig.(7-47): Effect of α_2 .

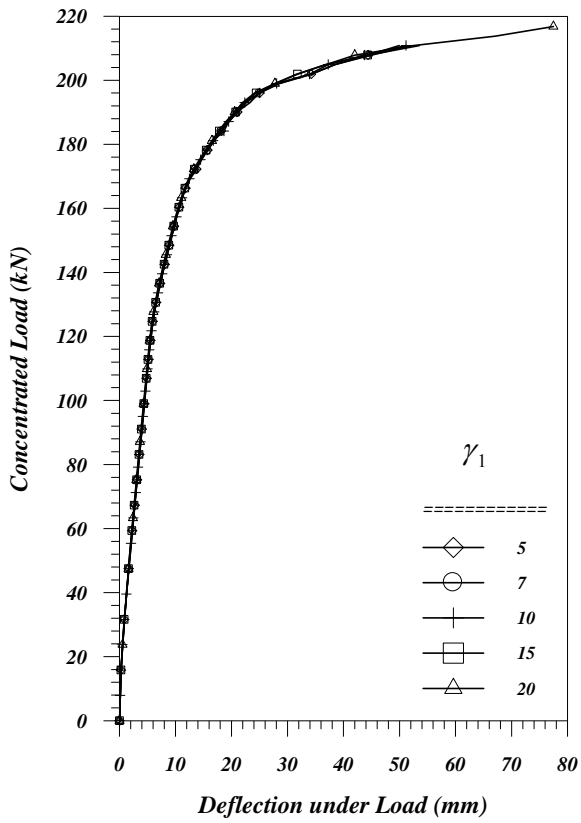


Fig.(7-48): Effect of γ_1 .

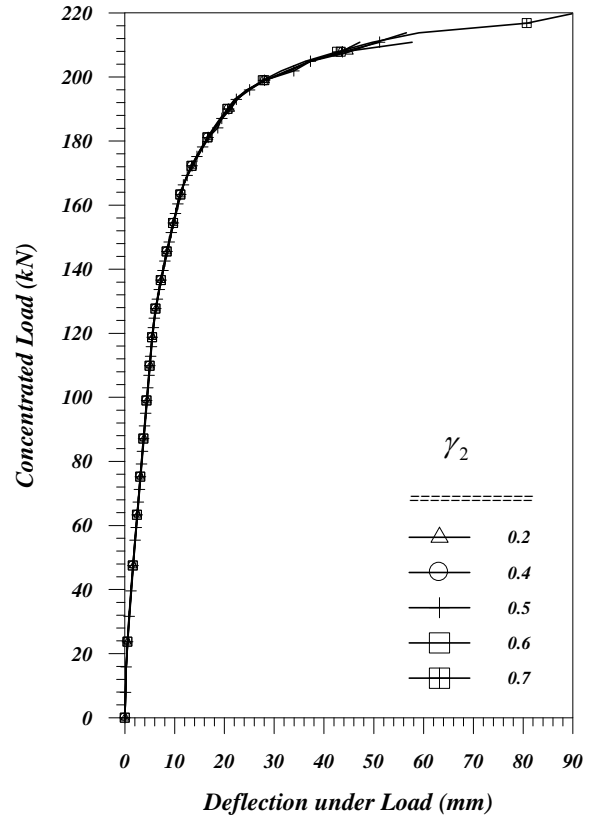


Fig.(7-49): Effect of γ_2 .

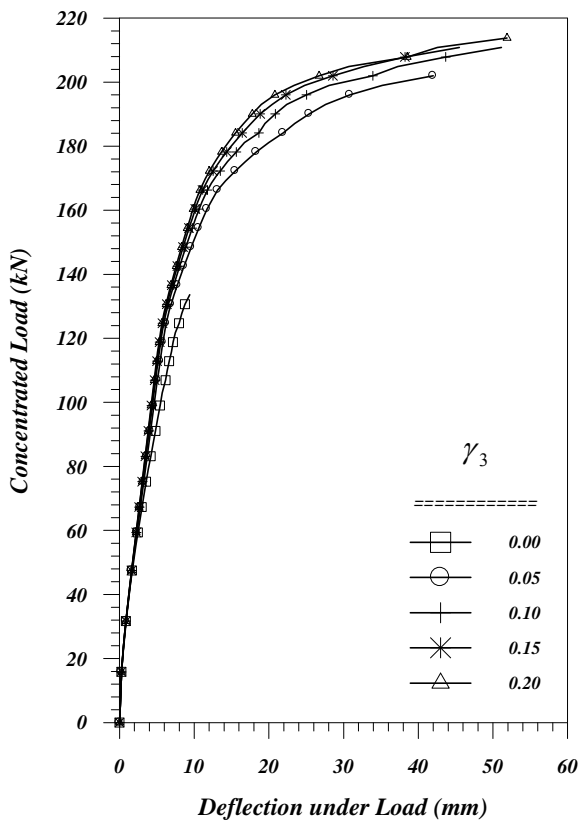


Fig.(7-50): Effect of γ_3 .

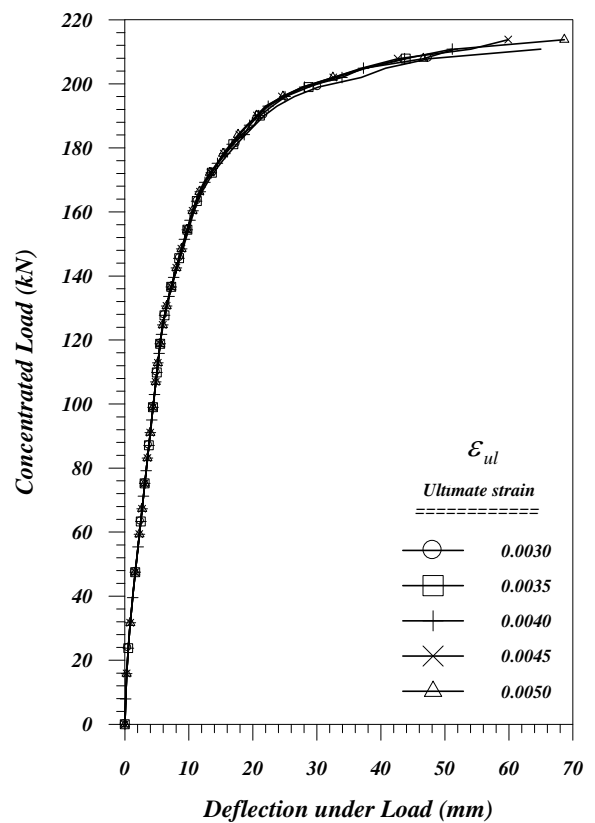


Fig.(7-51): Effect of ϵ_{ul} . 24

The result in Figs(7-44) to (4-51) insisted that the optimal and preferable values of the studied parameters are as indicated in Table(7-8).

All predicted ultimate loads for reinforced concrete examples were higher than the experimental ultimate loads. This is due to the complex stresses which occurred in the horizontally curved reinforced concrete beam which may have enforced the axes of the principal stresses to rotate after crack formulation, while in the current model *NFHCBSL* (fixed crack model adopted) the principal directions remain in the same directions after crack formulation at the Gauss points. This situation leads to a stiffer response and an overestimate of failure loads as *Cope* [115] and *Gupta* [116] had mentioned.

Chapter Eight

Dynamic Model Discussion and Testing

8-1: Introduction

This chapter is devoted to illustrate the theoretical developments introduced in the previous chapters related to the dynamic analysis. A finite element computer dynamic model *NFHCBDL* has been developed based on the previous work *Hinton et al.*[6]. No experimental data are available concerned with the curved beam under dynamic loads (where the position of load is constant and the value of load is variable or constant with time), and in order to verify the reliability of the present dynamic model, several examples will be checked with *ANSYS* [7] theoretical program results, as many researchers did [15,50].

The major differences between the present dynamic model *NFHCBDL* and *DARC3* [6], can be concluded as follows:

- 1-The ability of *NFHCBDL* to analyze the composite beams (as well as the steel and concrete beams), while *DARC3* can analyze either steel or concrete only and individually.
- 2-The definition of nodes in *NFHCBDL* model is according to the left hand clockwise screw which is more easy in handling than the right hand counter clockwise screw adopted by *DARC3*.

- 3-Each element is represented by **27** Gauss points in the present model, while **14** Gauss point is used within each element in *DARC3*. Thus the results of the current model will be more accurate than *DARC3* but the computation effort will be increased.
- 4-*DARC3* adopts a combination of tolerances technique, consisting of a small tolerance (represented in the input data) for nonlinear state Gauss points and a large tolerance (default in the program) for linear state Gauss points. This technique is ignored in the current *NFHCBDL* model.
- 5-The local coordinates in *DARC3* do not have similarity with the global coordinates, thus the representation of input data will be more complex than that in *NFHCBDL* where the local and global coordinates are similar.
- 6-*DARC3* adopts two types of brick elements (20 and 8) nodes isoparametric solid brick element, while *NFHCBDL* contains only the 20-nodes solid brick element.
- 7-Also the input data in the current model *NFHCBDL* is not restricted by format statements as in the *DARC3* model.

8-2: Properties and Abilities of the Dynamic Model

The computer program *NFHCBDL* is introduced to achieve the requirements of the present study. The main objective of the program was to analyze the nonlinear horizontally curved (steel, concrete and composite) members under general three-dimensional states of dynamic loads. The program is coded in FORTRAN-77 language. The numerical analyses were carried out on 1.70 GHz Pentium IX processor (PSI) computer that is provided with 512 MB RAM. The main properties of the program are summarized as below:

- 1-Type of Curved beam;** Definition of the type of curved beam is specified through the number of materials which make the beam. The computer model can handle many types of materials such as steel and concrete depending on the input data term (NMATS).
- 2-Steel and Concrete Representation;** The 20-noded isoparametric brick element has been incorporated in the program to model the steel and concrete.

3-Reinforcing bar representation; Reinforcing bars are simulated as an axial distributed area (layer) along the width of beam embedded in the concrete brick elements.

4-Integration rule used; To evaluate the stiffness and mass matrices of steel and concrete brick elements, the 27 (3x3x3)-Gauss quadrature rule had been implemented in the computer program.

5-Material nonlinearities; Many material nonlinearities are considered in the dynamic model such as: yielding of steel element or reinforcement bars, plastic deformation of steel element or reinforcement bar, nonlinear response of concrete in compression, crushing and cracking of concrete and the strain stiffening after cracking.

6-Nonlinear solution algorithms; The following iterative solution algorithms are incorporated in the program.

a-The initial stiffness method.

b-The modified *Newton-Raphson* method in which the stiffness matrix is updated after N time step.

7-Dynamic Loads; Many types of load functions can be represented in this model such as: Heaviside load (step load), harmonic excitation, linear-constant, linear-harmonic and acceleration time history.

8-Convergence criteria; The force and displacement convergence criteria are available in the program.

9-Termination of the analysis; The analysis is terminated automatically when the specified time of dynamic analysis finish, or whenever the solution diverges.

8-3: Structure of the Program

The *NFHCBDL* computer program consists of a main master model and many subroutines; each subroutine has been designed to deal with a part of the analysis which may be repeated more than once. The sequence of the operations in the main routine are summarized in the flow-chart shown in Fig.(8-1).

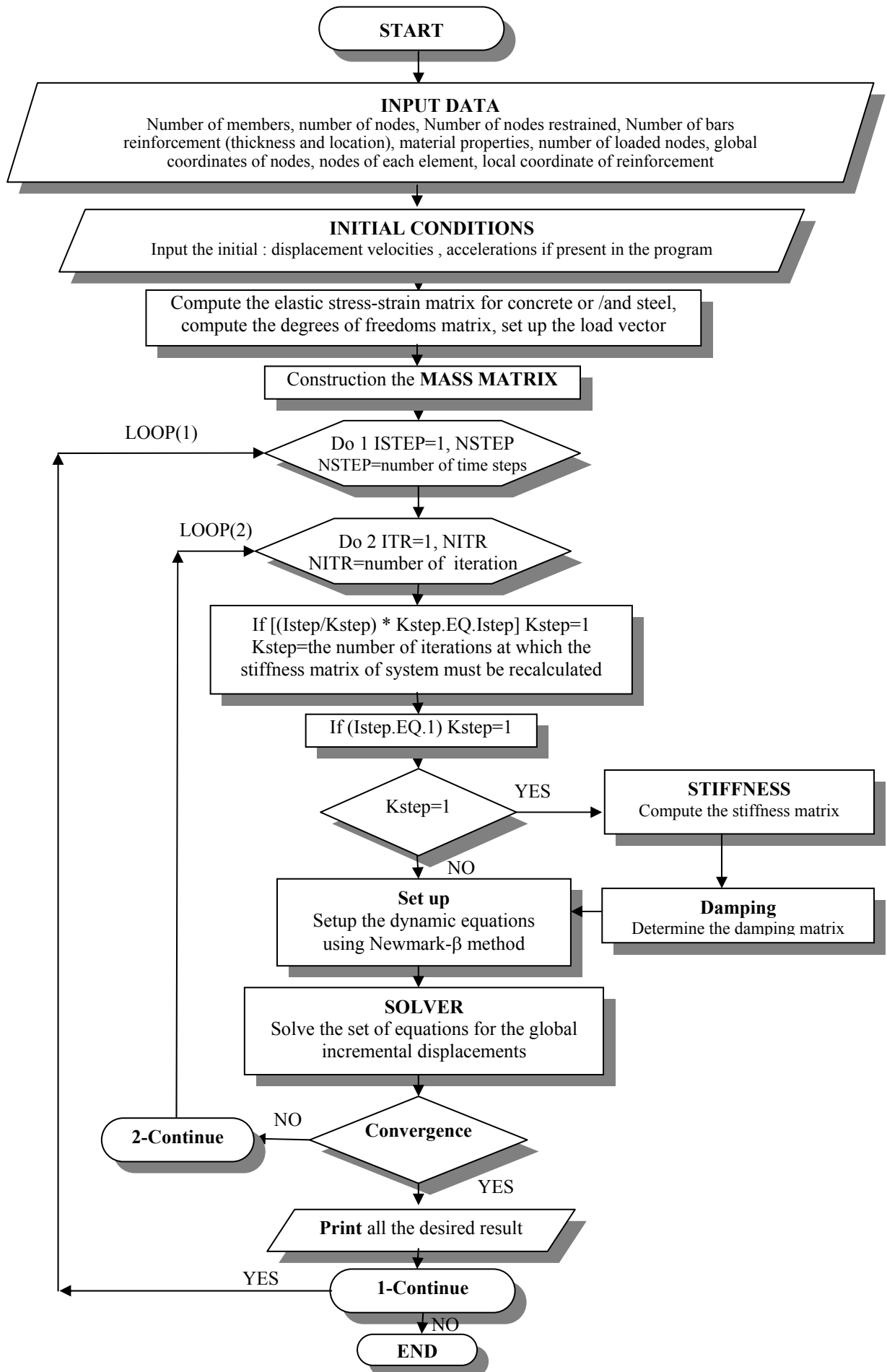


Fig.(8-1) : Flowchart of the Dynamic Model Computer Program NFHCBDL.

8-4: Numerical Examples

In order to verify the reliability of the computer dynamic model *NFHCBDL*, some examples are considered here and divided into three main types, steel, reinforced concrete, and composite curved beams. It is important to note that a convergence study was not done here because no experimental results are available to be referenced as well as the same finite element meshes will be used in *NFHCBDL* and *ANSYS*, therefore if the adopted meshes have any error the results of two models will be affected equally. Also the *Newmark- β* method which is unconditionally stable ($\gamma = 0.5$ and $\beta = 0.25$, average acceleration method) and the force convergence criterion are adopted in all dynamic analysis models.

8-4-1: Horizontally Curved Steel Beam

The first example selected, here, to be analyzed is the simply supported steel curved beam ($\theta = L/R = 45^\circ$, and $R = 7500$ mm). The geometry, material properties, boundary conditions and the applied dynamic load are shown in Fig.(8-2), the origin of the Cartesian coordinates located at the left end of the beam. The full length of the beam is analyzed here since the supports conditions are assumed not symmetrical. The stress-strain curve adopted here was elastic perfect-plastic.

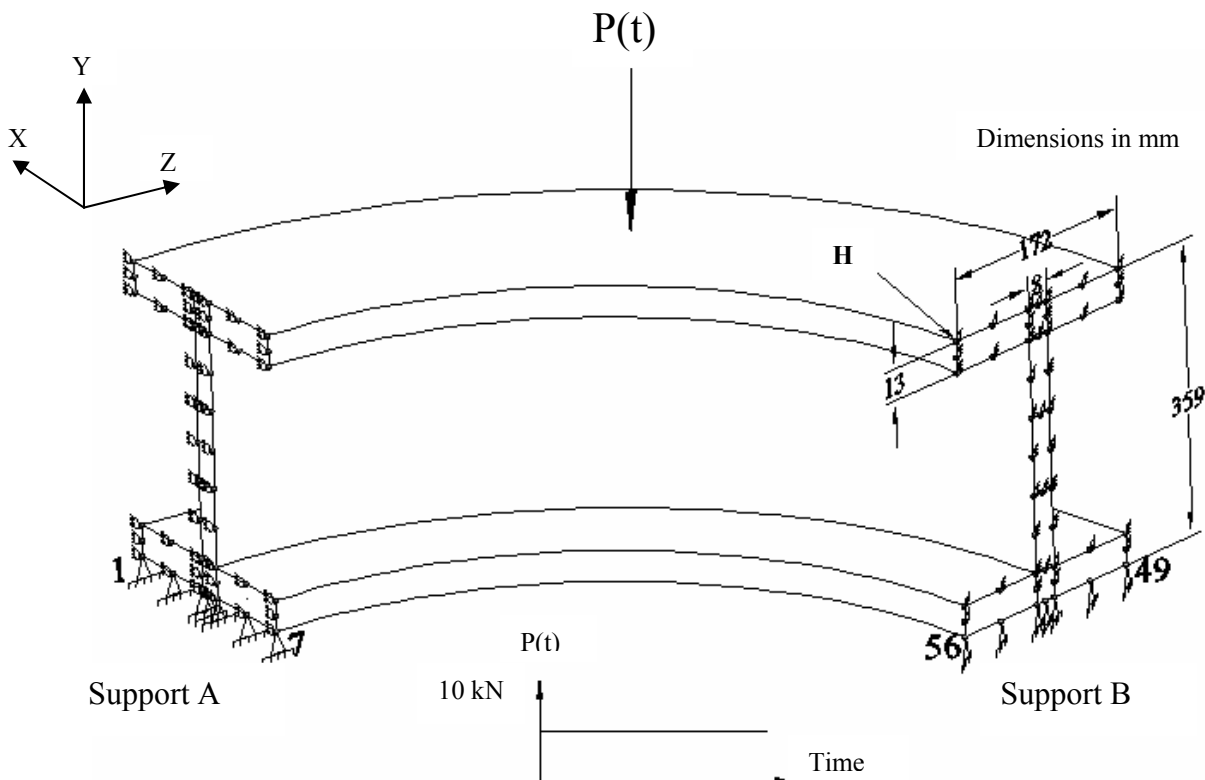


Fig.(8-2) : The Geometry, Dimensions, Boundary Conditions and the Dynamic Step Load of Steel Curved Beam.

As shown in Fig.(8-2), all nodes at supports are restrained in X- direction as well as the nodes (1 to 7) at support **A** are prevented from movement in the other two directions (Y and tangential), while the nodes (49 to 56) at support **B** are restrained in Y- direction. The load is located at mid-span. The material properties used are: $f_y = 391\text{MPa}$, $E_s = 218\text{GPa}$, $\nu = 0.3$, and $\text{density} = 7850\text{kg} / \text{m}^3$. The beam is divided into 405 element and the adopted mesh is as shown in Fig.(8-3). The initial tangent stiffness matrix, tolerance 5%, force convergence criterion and maximum number of iteration equal to 50 are used in the analysis. While the adopted fluidity parameters a_0 and a_1 are equal to 1.539 and 0.971(from the experimental results [6]) respectively. The load is divided into three parts along the width of web on the top flange, and the adopted $\Delta t = 0.0005$ second.



Fig.(8-3): The Finite Element Mesh of the Steel Curved Beam (405 Element).

The response curves for vertical deflection at mid-span is presented in Fig.(8-4). The result revealed good agreement between the results of *NFHCBDL* and *ANSYS*, the maximum difference in the mid-span deflection was 5.1% at time 0.06 second while the cycle time coincided. To show the difference between the results of *NFHCBDL* and *DARC3*, the beam was analyzed by *DARC3* model and results were plotted also in Fig.(8-4). As shown obviously, the large difference is between the results of *DARC3* and *NFHCBDL* or *ANSYS*. The analytical investigation proved that the major effect causing this defect was the combination of tolerance technique.

Also the dynamic response curves for stresses in X- direction at critical Gauss point (the nearest Gauss point to node **H**, see Fig.(8-2)) is presented in Fig.(8-5). The results showed good agreement between the two analytical models. The maximum difference between the two curves was 8.9% at time 0.06 second.

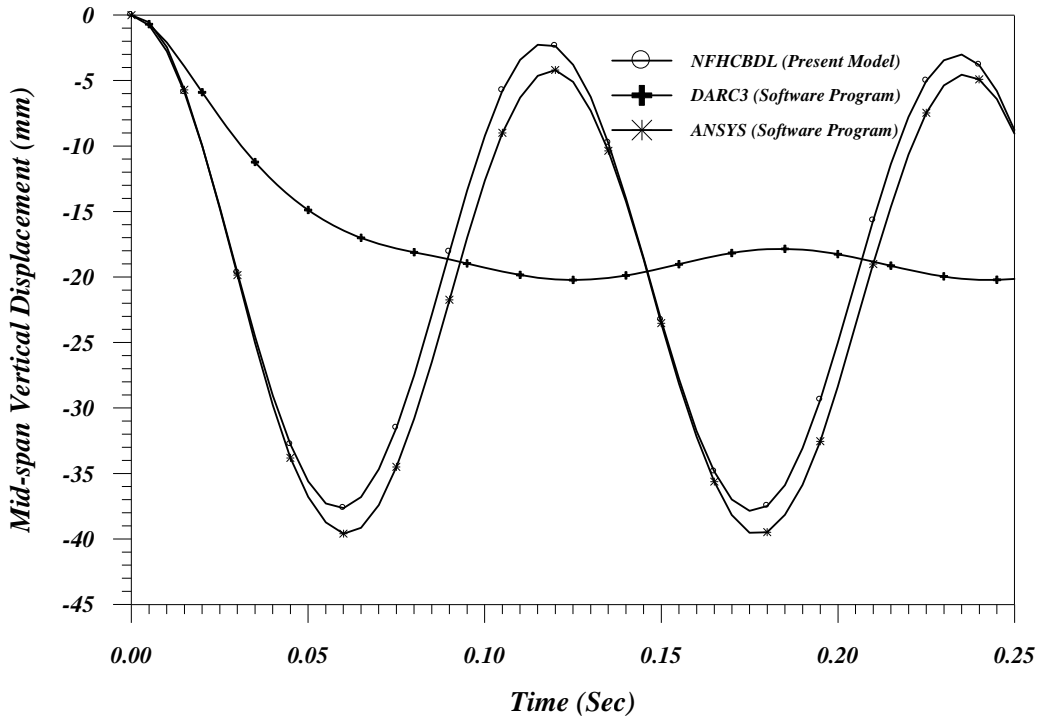


Fig.(8-4): Dynamic Response Curves of the Vertical Deflection at Mid-span.

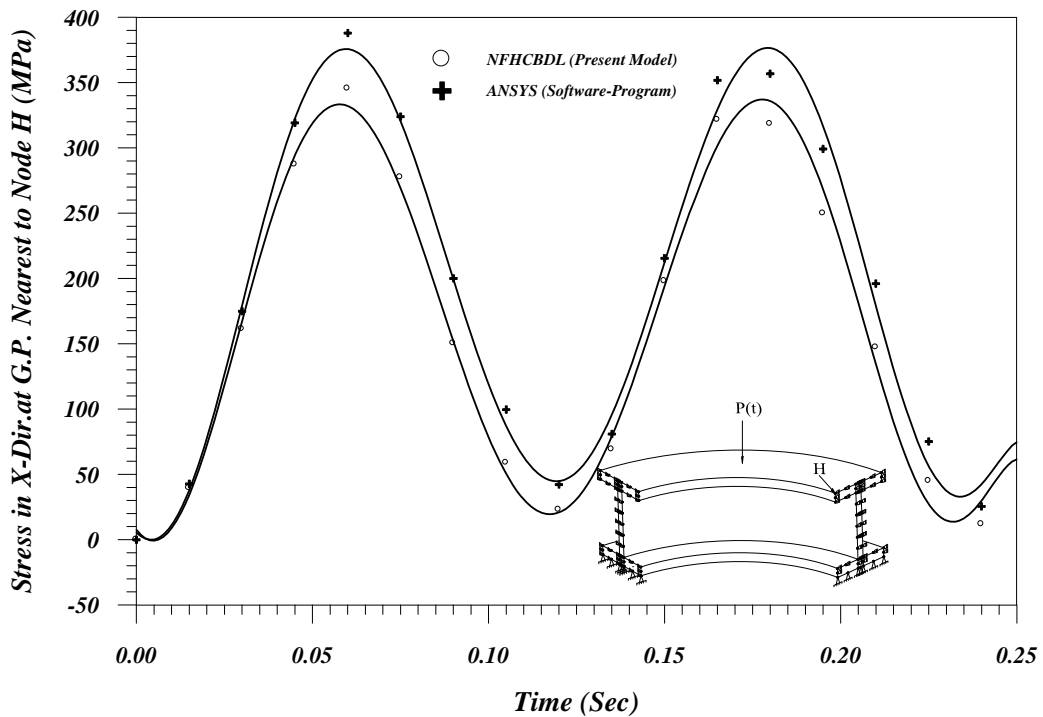


Fig.(8-5): Dynamic Response Curves of the Stress in X-Direction at the Nearest Gauss Point to Node H .

A picture of the distribution of the stresses along the span of the steel curved beam during the time is shown in Figs.(8-6) and (8-7) which present the stresses in X and Z-directions respectively at mid-top flange (extreme level of Gauss points

which is closer to the surface of flange) for five selected time steps. As shown, the critical sections of stresses are located at $0.25L$ from support **A** and at $0.22L$ from support **B** according to the stresses in X-direction, and at $0.28L$ from support **B** according to the stresses in Z-direction. The figures reveal also that the mid-span section suffers low level of stresses during the response and relatively to higher level of stresses at and near the support **B**. The figures also show how one can utilize the redistribution of the volume of steel to achieve the best non-prismatic curved beam.

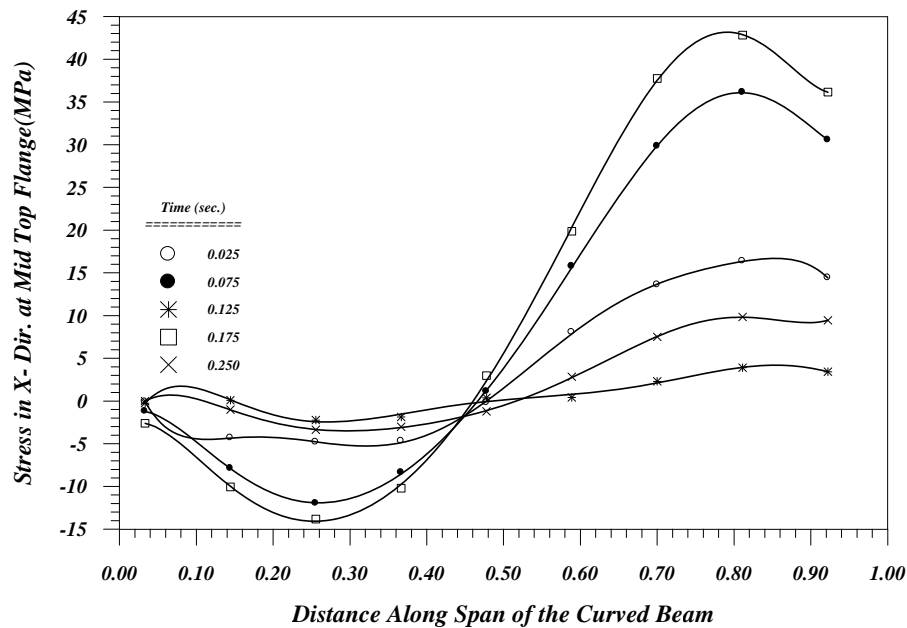


Fig.(8-6): Distribution of Stress in X-Direction Along the Curved Beam.

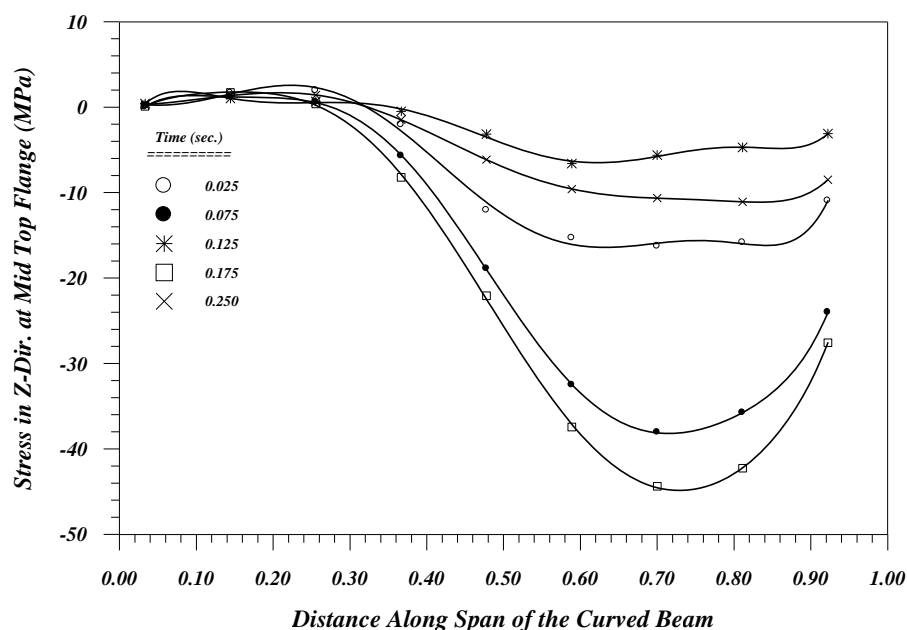


Fig.(8-7): Distribution of Stress in Z-Direction Along the Curved Beam

To show the stress tensor components Fig.(8-8) is presented to show the stresses at a Gauss point representing the nearest to the mid-span bottom flange (mid-flange). As shown, the major component is the normal stresses (tangential stresses, equal 32 MPa), which represents $(32/391=8.1\%)$ from the ultimate strength (if the other components are ignored), while the maximum component at support **B** is the stress in X-direction which is 388 MPa representing $(388/391=99.2\%)$ from the ultimate strength (if the other components are ignored). It is important to note that X,Y and Z-coordinates in Figs.(8-8) and (8-9) represent the global coordinates and not local ones.

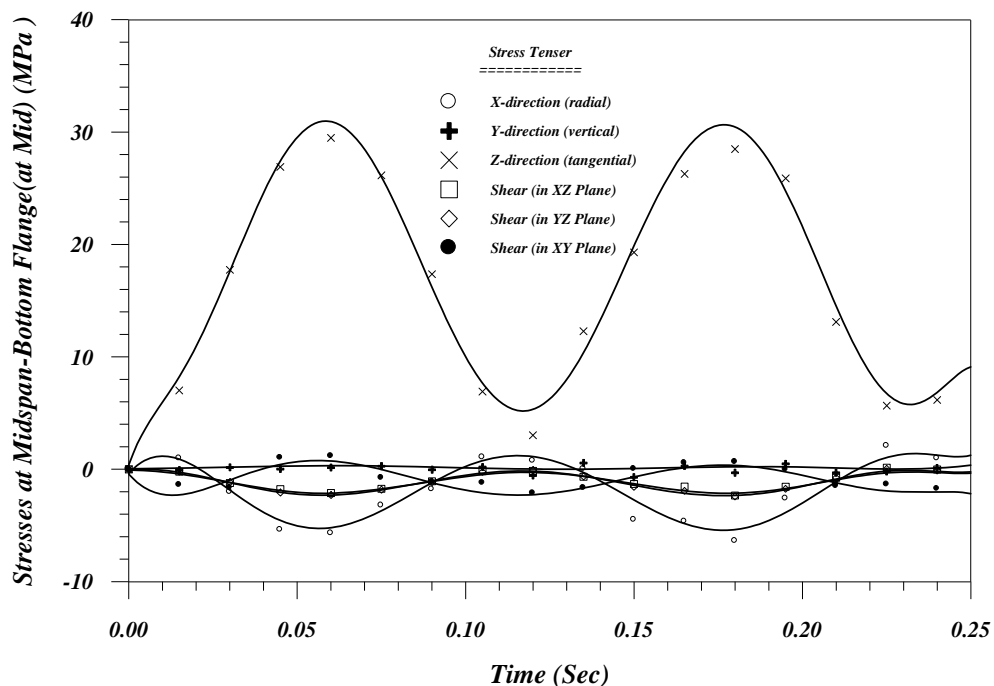


Fig.(8-8): Response Curves of Stress Tensor for the Nearest Gauss Point to the Mid-span Bottom Mid-flange .

Utilizing the plotting ability of *ANSYS* the contours in figures are presented in Fig.(8-9). These figures were selected at time step 120, i.e. at time 0.06second, when the maximum deflection and stresses occurred. The first three figures show that the maximum stresses occurred near the support **B**, the negative values means opposite to the global positive direction. Also the maximum deformation happen about mid-span and the lateral deformations outwards (positive) causing (almost) tensile stresses at ends especially at nodes having more than one degree of freedom restrained.

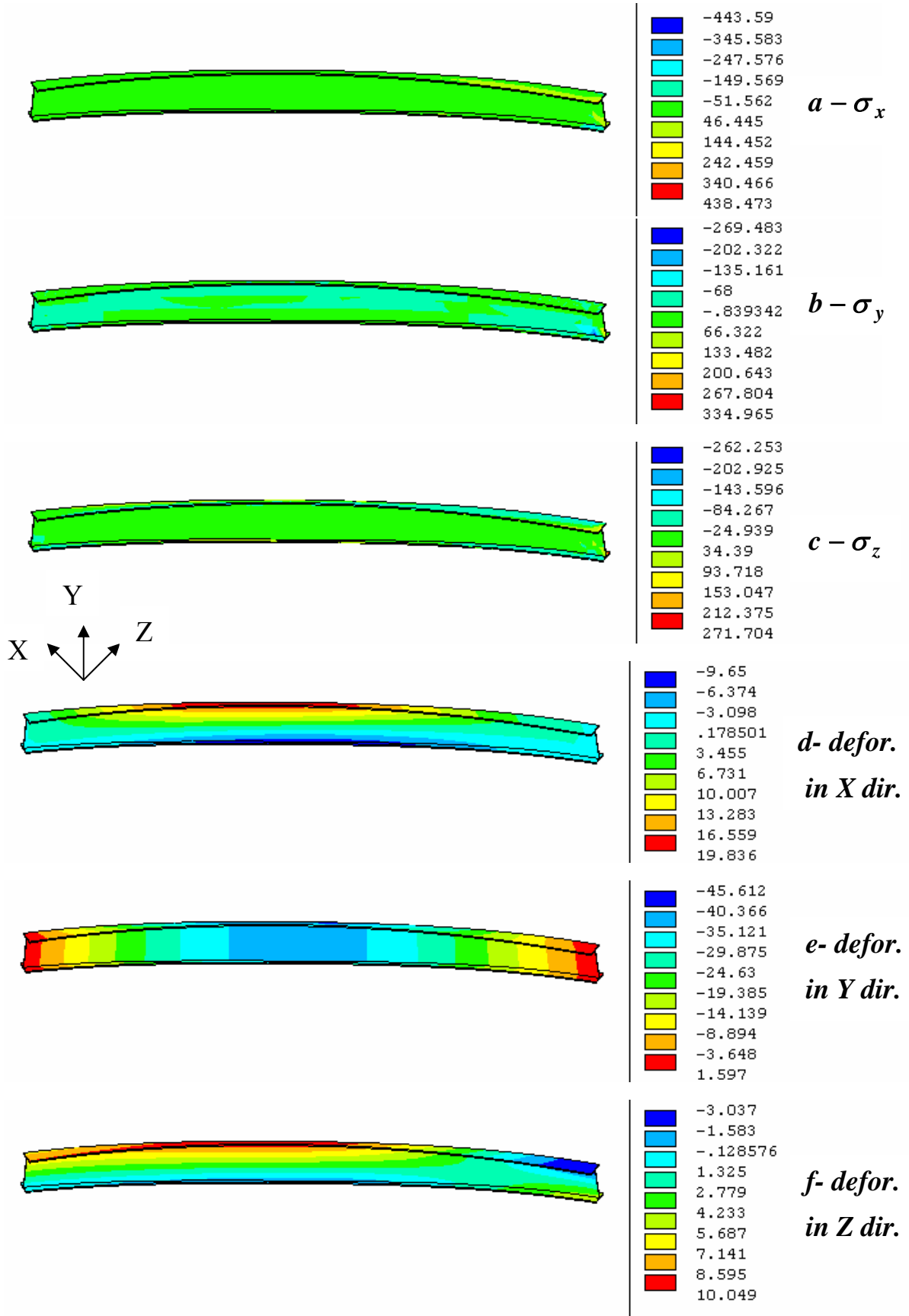


Fig.(8-9): Contours of Stresses (MPa) and Deformations (mm) for Steel Curved Beam under Dynamic Step Load (at Time 0.06 Second).

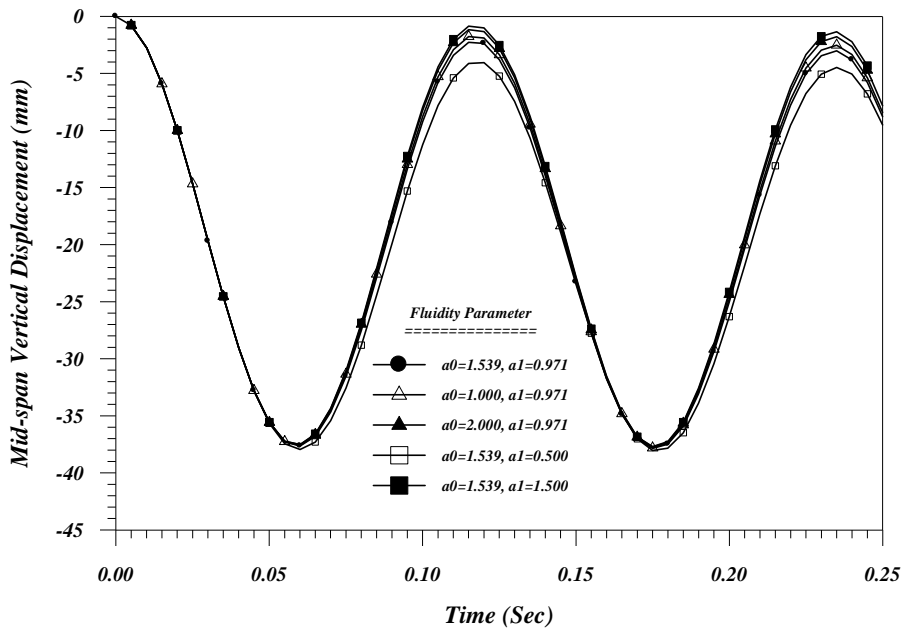


Fig.(8-10): Effects of the Fluidity Parameters (a_0 , and a_1).

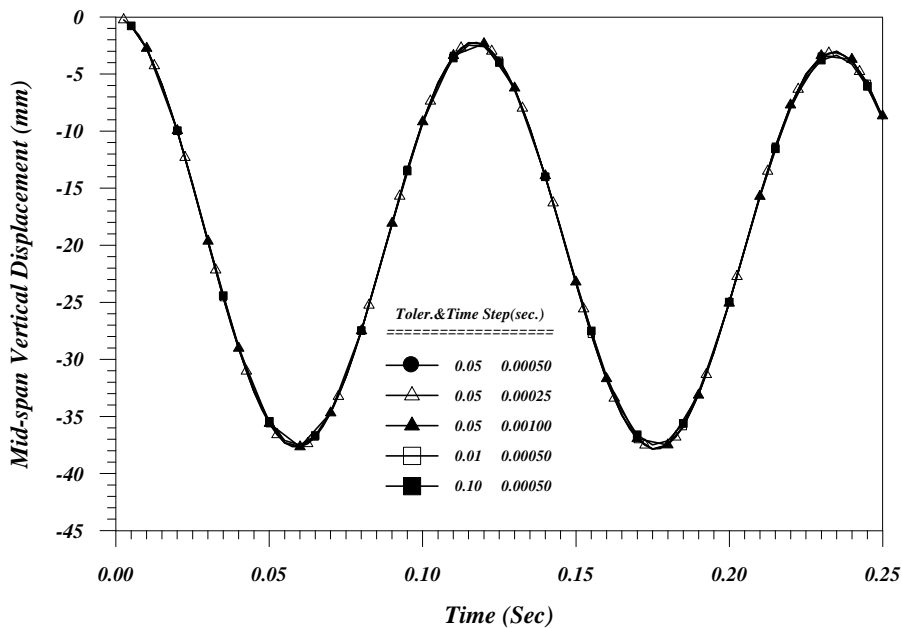


Fig.(8-11): Effects of Tolerance and Time Step.

The effects of fluidity parameters (a_0 and a_1) are presented in Fig.(8-10). The results show that all these parameters were not effected on the amplitude value of deformation and the time period of the cycle, but when the value of a_0 decreased to 1 or increased to 2 the remainder of deformation decreased, while when a_1 is increased the remainder of deformation decreased and vice versa as shown in Fig.(8-10). Fig.(8-11) revealed the small effects of tolerance and time step on the dynamic response of steel curved beam.

8-4-2: Example No. 2: Horizontally Curved Reinforced Concrete Beam

A fixed-ended reinforced concrete horizontally curved beam is presented here to check the reliability of the current dynamic model to analyze this type of beams and comparing with the analytical results of *ANSYS*. The geometry, dimensions and the dynamic linear-constant applied loads are illustrated in Fig.(8-12). The angle of curvature is ($\theta = L/R = 60^\circ$) and the radius is ($R=5730$ mm). Utilizing the geometric and loading symmetry, the analysis was carried out for half of the beam, thus all nodes located at mid-span were prevented from movement in the tangential direction, while the nodes located at the fixed ends were restrained in all directions during the analysis of the half beam. The properties of materials and the values of parameters adopted in the analysis are detailed in Table(8-1). The finite element mesh adopted in this example consisting from 240 element to represent half of the beam is shown in Fig.(8-13).

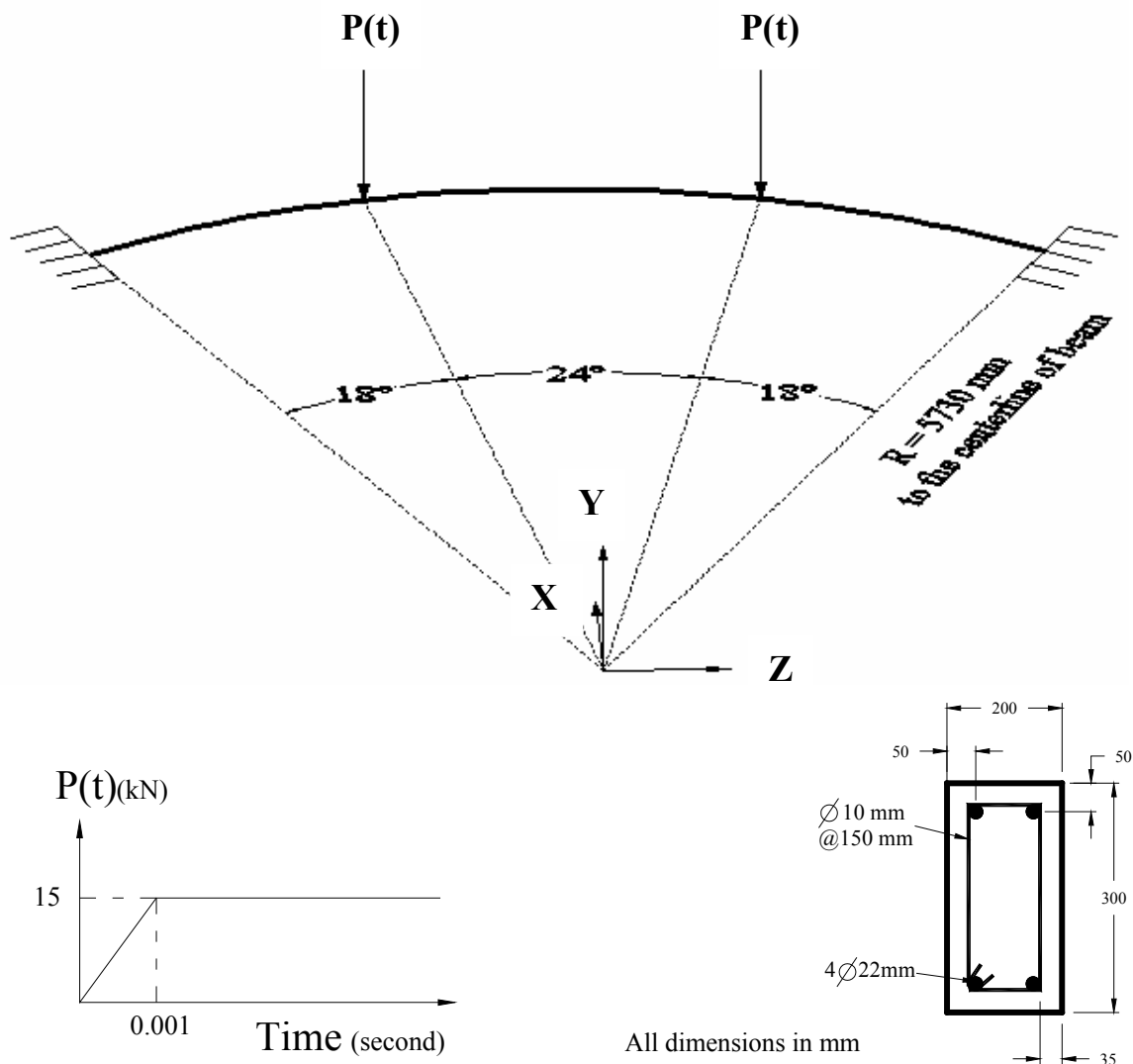


Fig.(8-12) : The Geometry, Dimensions, and the Dynamic Linear Constant Loads of Reinforced Concrete Curved Beam (Ex2).

Table(8-1): Properties of Materials and Parameters Adopted in the Analysis.

<i>Materials Properties</i>		<i>Parameters</i>
The compressive strength of concrete	$f'_c = 25$ MPa	$\alpha_1 = 1.0$
The yield strength for longitudinal reinforcement	$f_{yl} = 350$ MPa	$\alpha_c = 10$
The yield strength for stirrups reinforcements	$f_{ys} = 400$ MPa	$\beta_o = 1.967^*$
The modulus of elasticity of concrete(Eq.(4-2))	$E_c = 23500$ MPa	$\beta_1 = 0.792^*$
The modulus of elasticity of reinforcement	$E_s = 200000$ MPa	$a_o = 0.405^*$
The tensile strength of concrete (Eq.(4-4), page 47)	$f_t = 1.48$ MPa	$a_1 = 0.831^*$
Density of concrete = 2400 kg/m^3 , Density of steel = 7850 kg/m^3		Toleran.= 5%
Concrete: $\nu = 0.15, \epsilon_u = 0.0035, G_f = 0.1, k_1 = 0.0$. Reinf.: $\nu = 0.0$		$\Delta t = 1E-5$ sec.

*For concrete mix 1:2:4, Table(5-1), page 79.

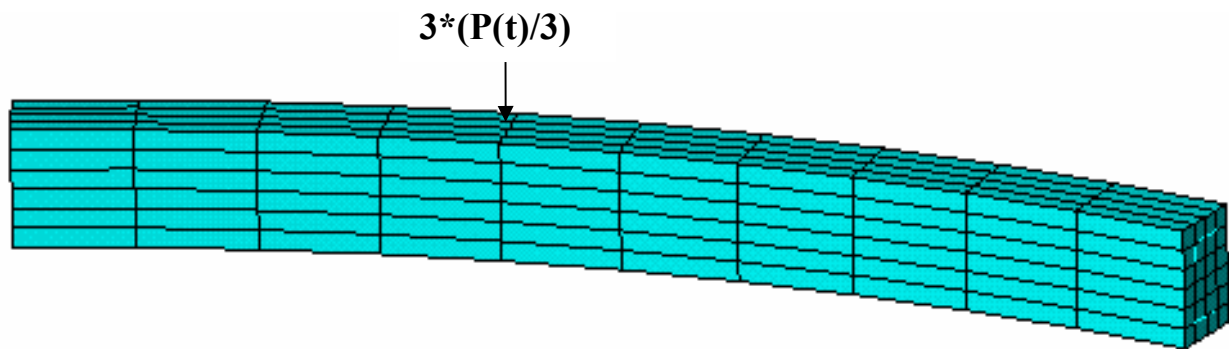


Fig.(8-13): The Finite Element Mesh of the Reinforced Concrete Curved Beam (Ex2) of 240 Element.

The stress-strain curve adopted here for concrete and reinforcement is elastic perfect plastic and the initial tangent stiffness matrix used in the dynamic analysis has maximum number of iteration equal to 25.

The dynamic response curves for vertical deflection at mid-span and under the load is presented in Fig.(8-14). The result revealed good agreement between the results of *NFHCBDL* and *ANSYS*. The maximum difference in the amplitude of mid-span deflection was 0.35mm ($0.35/10.03=3.5\%$), while the difference in the cycle time was 1.5% ($1-0.033/0.0335$). Under the concentrated load the difference in the amplitude of vertical deflection was 0.28 mm, and the difference in the cycle

time was also 1.5%. The results reflected divergence in the results of the remainder of deformation. This may be due to the difference in the yield criterion adopted in each model. The yield criterion adopted by the analytical closed package *ANSYS* is called (Concrete CONCR).

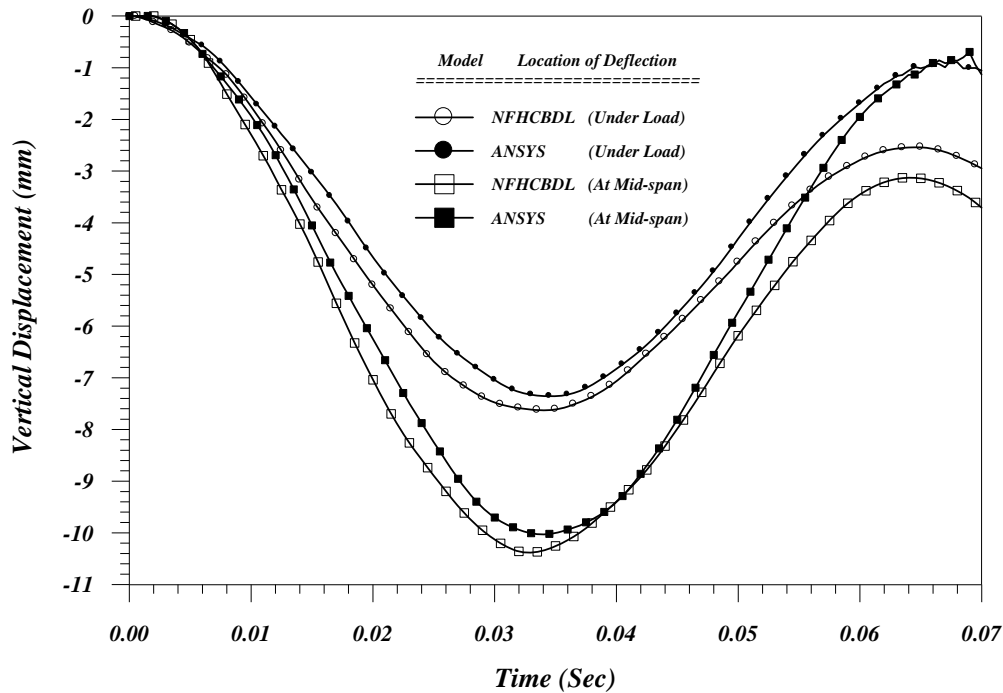


Fig.(8-14): Dynamic Response Curves of the Vertical Deflection.

Also the dynamic response curves for stresses in Z- direction at mid-span top level Gauss point (the nearest Gauss point to centerline) are presented in Fig.(8-15). The results showed good agreement between the two analytical models. The maximum stresses obtained from results of *NFHCBDL* and *ANSYS* were 6.85 MPa at time 0.0325 and 5.63 MPa at time 0.031 respectively. Thus the difference between the two maximum stresses was 18% at the amplitude of deformation of the first cycle. However, it is important to note here that the solid brick element adopted in the analysis of *ANSYS* was (*Solid 65*) which represented the unique solid element available that could consider the effects of crash and crack phenomena. This element consists of eight nodes not twenty, thus the edges of elements will be linear not curved. Also all brick elements existing in the library of *ANSYS* are represented by 14 Gauss points not 27 as in the present model. These reasons lead to increase the differences between the results of *NFHCBDL* and

ANSYS. However the results of the current model are more conservative, as shown in Figs.(8-14) and (8-15).

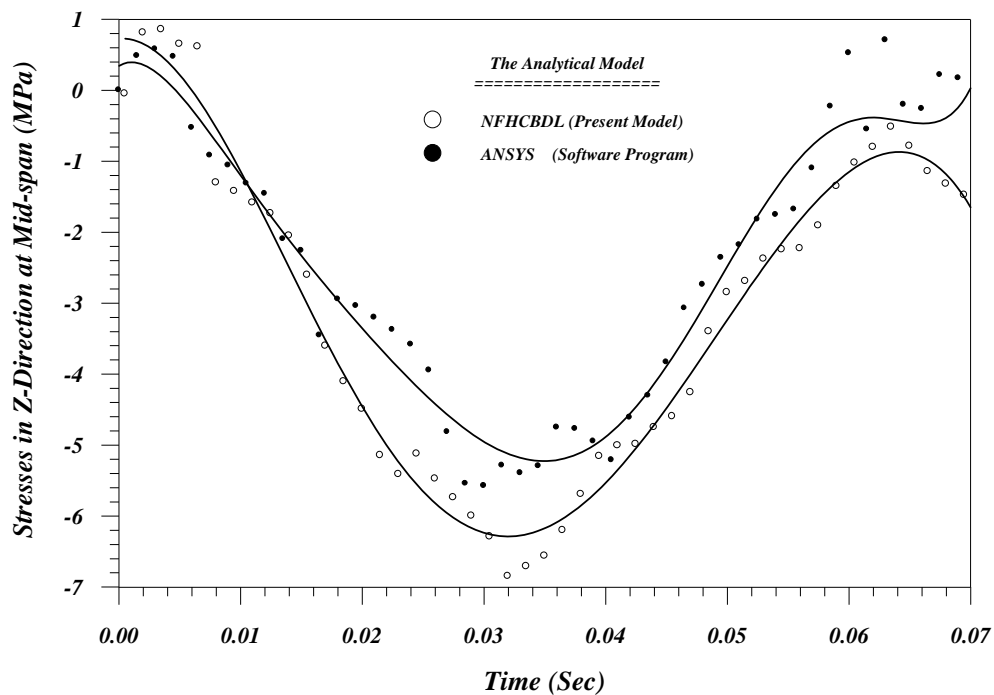


Fig.(8-15): Dynamic Response Curves of the Stress in Z-Direction at the Nearest Gauss Point to the Mid-span Top Level .

Figs.(8-16) and (8-17) are devoted to reveal the distribution of the stresses (in X,Y and Z-directions) along the span of the reinforced concrete curved beam during the time at mid-bottom and top levels respectively(extreme levels of Gauss points which are closer to the bottom and top surface of the beam) for two selected time steps (0.02, and 0.035 second).

As shown the stresses in Z-direction represent the critical stress and it is tension at the bottom level and compression at the top level at sections from mid-span to about 0.6 from the length of the half beam (this point represents the inflection point of bending moment). Thereafter the stresses are reversed and become compression at bottom level and tension at top level (negative moment).

The figures also illustrate the low level of stresses in X and Y-directions during the response and the increase in stresses in Y-direction near the support.

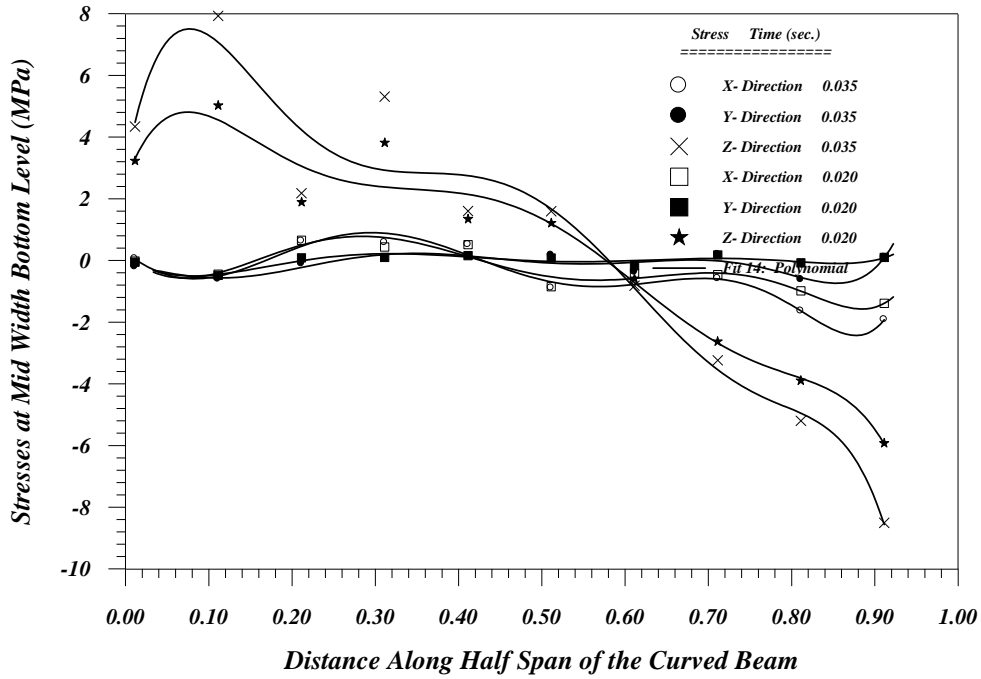


Fig.(8-16): Curves of the Normal Stresses Distribution Along Half of Span (at Bottom Level).

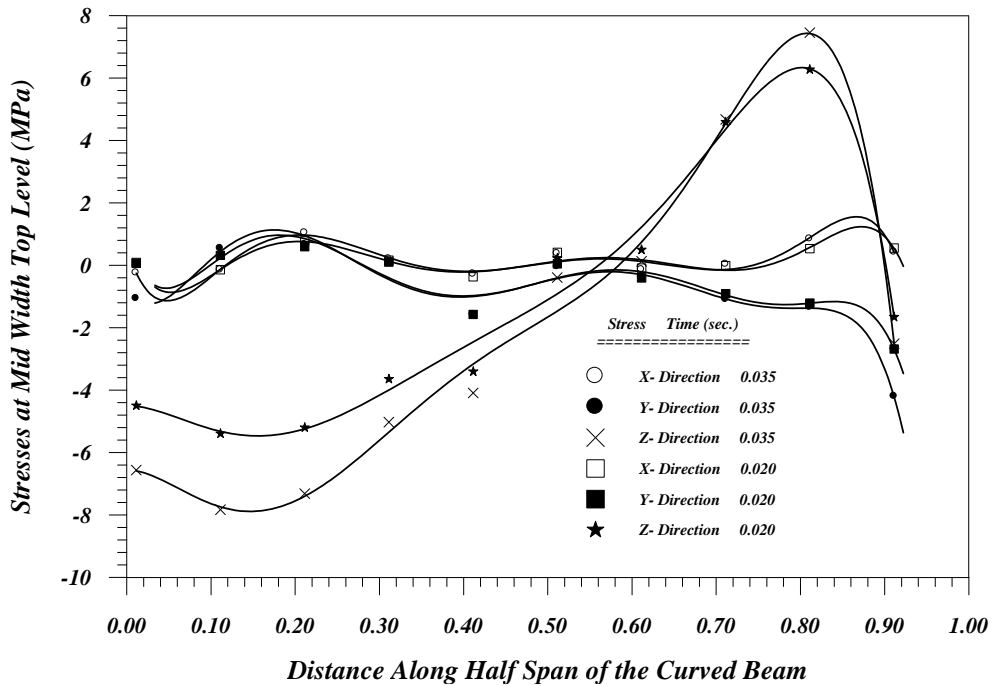


Fig.(8-17): Curves of the Normal Stresses Distribution Along Half of Span (at Top Level).

The effects of fluidity parameters (a_0, a_1), tolerance and time step are presented in Figs.(8-18) and (8-19) respectively. The results proved that these parameters show sensitive effect on the dynamic response of the reinforced

concrete curved beam more than that of the steel curved beam (This is of course due to the non-homogeneous material of concrete). The amplitude value of deformation and the time period of the cycle increased when the values of (a_0 and a_1) changed as recommended by Ref.[6], but when the values of (a_0 and a_1) decrease the remainder of deformation increases and vice versa as shown in Fig.(8-18).

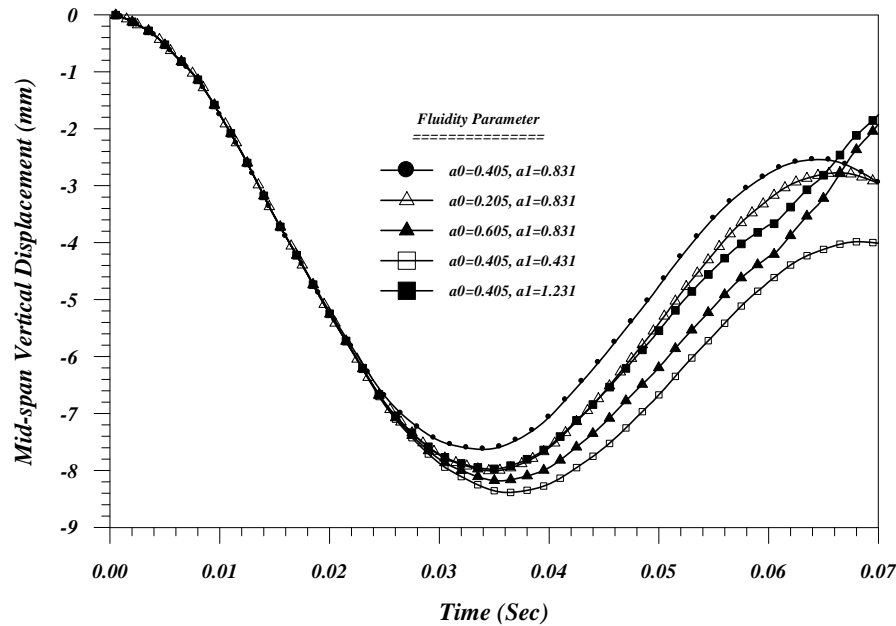


Fig.(8-18): Effects of the Fluidity Parameters (a_0 , and a_1).

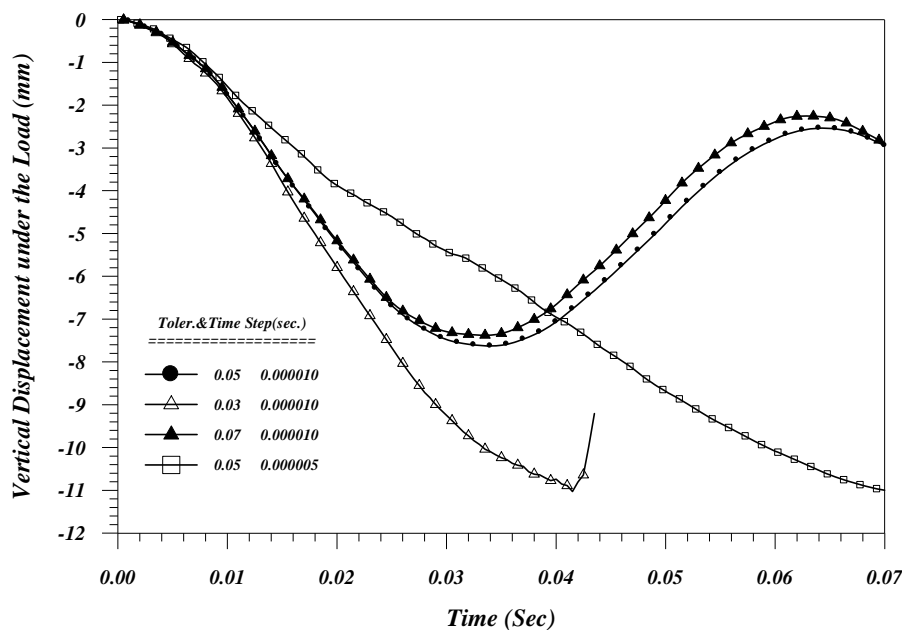


Fig.(8-19): Effects of Tolerance and Time Step.

When the tolerance value decreased to 3% the amplitude of deflection increased, but after 0.04 second the result was not acceptable, while when it increased to 7% the amplitude of deflection decreased, this is of course due to the accumulative error which increased and decreased with the tolerance. However the analytical investigation proved that the maximum number of iterations must be suitable with the chosen tolerance, and must be chosen carefully to prevent the program from passing any time step without occurring of convergence. This point can be observed in the current model but it cannot be pointed in the package model. Yet the problem is not finished at this limit because both tolerance and maximum number of iterations are related also with the time step. During the time step interval the maximum number of iterations can be applied, while tolerance decides when the program analysis passes to another time step. The problem of estimating the suitable values of these parameters is very complex especially with the high nonlinearity of materials and combination of many types of stresses existing in the situation of the horizontally reinforced concrete curved beam.

When the time step decreased to 0.000005 sec. the amplitude of deflection and the period of one cycle increased although the deflection decreased firstly, also when the time step increased to 0.00002 sec. the deformation will not be rationally calculated whence oscillating between +52 mm at time 0.001 sec. and -3525 mm at time 0.07 sec. (This cannot be graphed in Fig.(8-19)). Thus it is interesting to note that the values of time step given in Eq.(6-33) and recommended by Ref.[112] cannot be depended here because (as mentioned) these stability limits were obtained for Guasi-static elasto/viscoplasticity, with the flow rule being a function of stress only. Thus the problem required experimental results to investigate each parameter individually and then finally the optimal values.

Nevertheless in the present example the maximum number of iterations was 25, tolerance 5% and time step 0.00001 second for two models. Thus any error occurring implicitly will be effective equally on the results of the two models

Fig.(8-20) shows the locations of the cracked and crushed Gauss points along half of the beam, utilizing the plotting ability of *ANSYS*. This figure was selected at the critical time 0.07 second. As shown, the cracks (red lines represent the first crack, green lines represent the second crack and the blue lines represent the third crack at Gauss points) distributed at mid-span under the centerline of the

beam then transformed gradually to the top surface of the beam near the support. Also the cracks appeared at the inner edge of beam. The crushed Gauss points (black points) are concentrated under and near the load as well as at mid-span section.

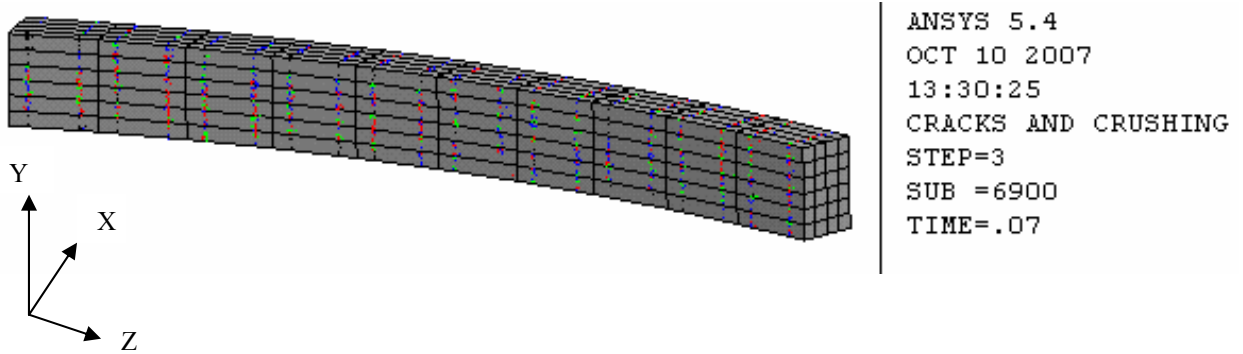


Fig.(8-20): Locations of the Cracked and Crushed Gauss Points.

Fig.(8-21) shows the contours of shear stresses at time 0.035 second, which represent the critical time when the maximum deflection has occurred. As shown low level of shear stresses occurred at this time, also the figure reveals that τ_{xz} represent relatively the critical shear stress especially near the support.

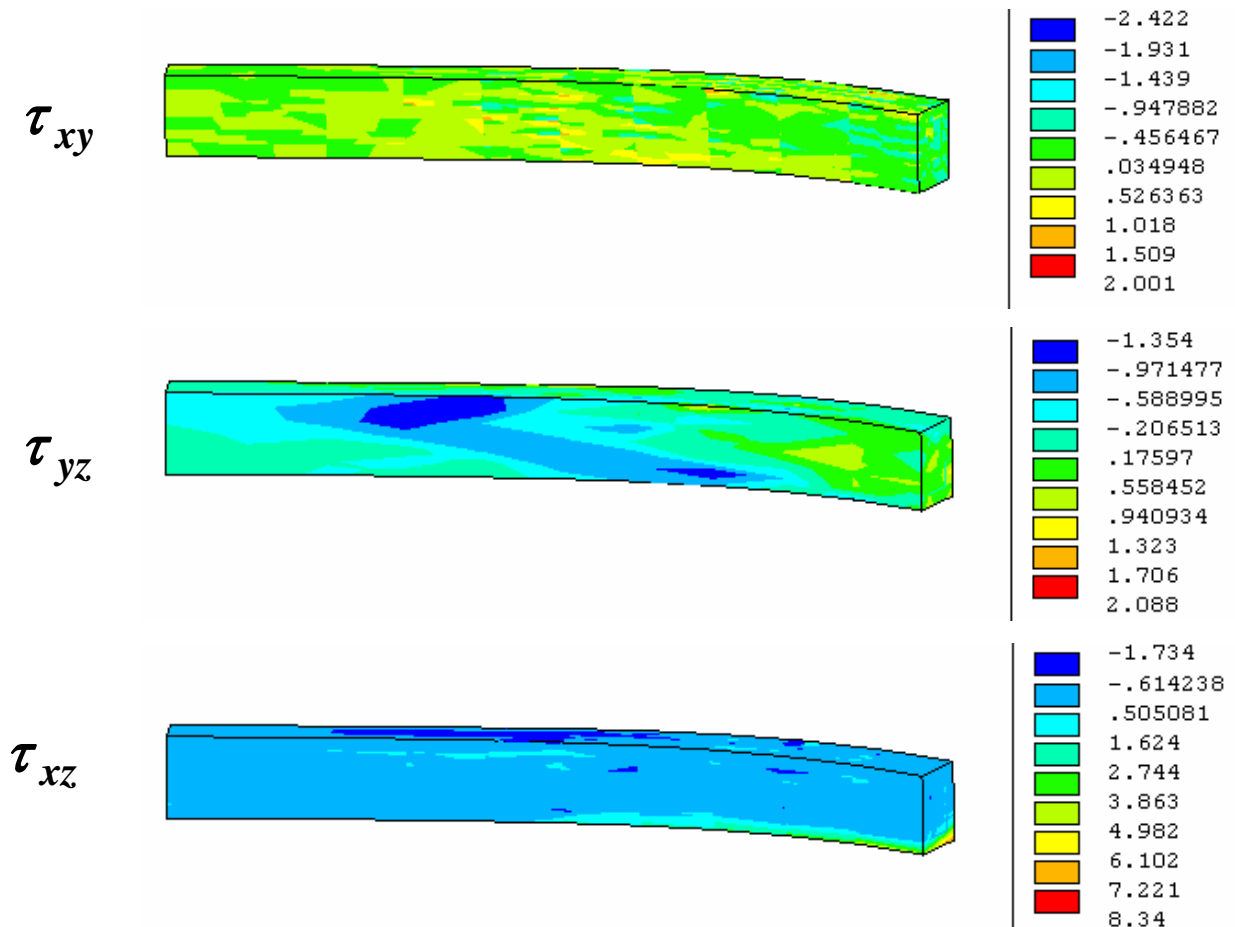


Fig.(8-21): Contours of Shear Stresses(MPa) (at Time 0.035 Second).

8-4-3: Example No.3: Horizontally Curved Composite Beam

A composite simply supported horizontally curved beam is presented here to inspect the ability of the present dynamic model *NFHCBDL* to analyze these types of structures (of course full connection between concrete deck and steel I-beam is assumed). The geometry, dimensions and the dynamic load step applied at mid-span are illustrated in Fig.(8-22). The angle of curvature ($\beta = L/R = 12.892^\circ$) and the radius ($R=10\text{m}$). The nodes (1 to 7) located at support A were prevented from movement in the all directions, while the nodes (8-14) located at support B were restrained in X and Y-directions. The properties of materials and the values of parameters adopted in the analysis are as detailed in Table(8-2). The finite element mesh adopted in this example consists of 345 elements, as shown in Fig.(8-23).

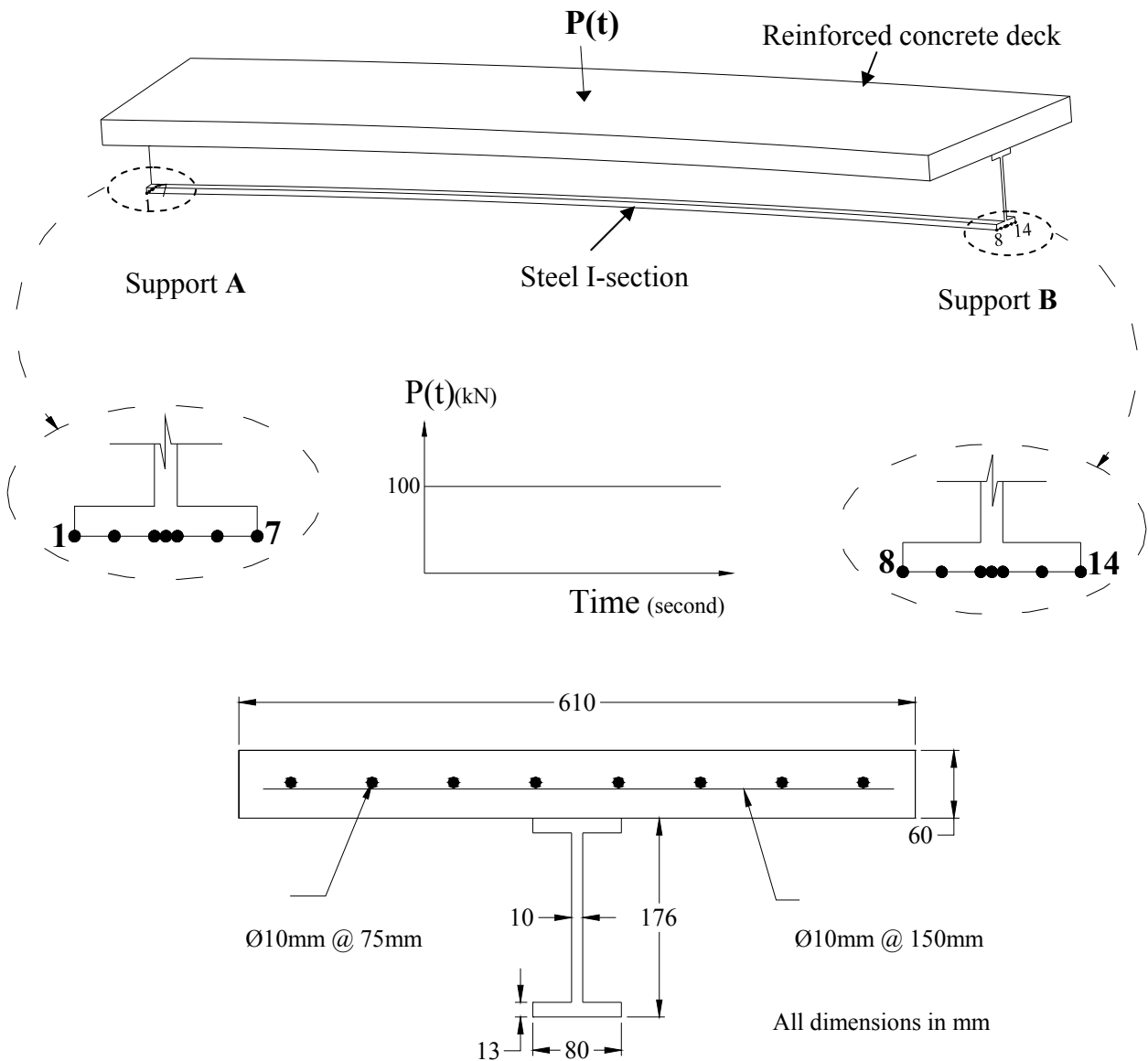


Fig.(8-22) : Geometry, Dimensions and the Dynamic Step Load of Composite Horizontally Curved Beam (Ex3).

Table(8-2): Properties of Materials and Parameters Adopted in the Analysis.

<i>Materials Properties</i>		<i>Parameters</i>
Compressive strength of concrete	$f'_c = 48$ MPa	$\alpha_1 = 1.0$
Yield strength for all reinforcement	$f_y = 310$ MPa	$\alpha_c = 10$
Yield strength for steel I-section	$f_{ys} = 285$ MPa	$\beta_o = 1.967^*$
Modulus of elasticity of concrete(Eq.(4-2),page46)	$E_c = 32562$ MPa	$\beta_1 = 0.792^*$
Modulus of elasticity of reinf. and steel	$E_s = 200000$ MPa	$a_o = 0.405^{*+}$
Tensile strength of concrete (Eq.(4-4),page 47)	$f_t = 2.03$ MPa	$a_1 = 0.831^{*+}$
Density of concrete = 2400 kg/m^3 , Density of steel = 7850 kg/m^3		$k_1 = 0.0$
Concrete: $\nu = 0.15$. Reinforcement: $\nu = 0.0$. Steel: $\nu = 0.3$		Toleran. = 5%
Crushing strain $\epsilon_u = 0.004$. Fracture energy $G_f = 0.1$.		$\Delta t = 1\text{E-}6$ sec.

*For concrete mix 1:2:4, Table(5-1).

+ For steel $a_o = 1.539$, $a_1 = 0.971$ from experimental results [6].

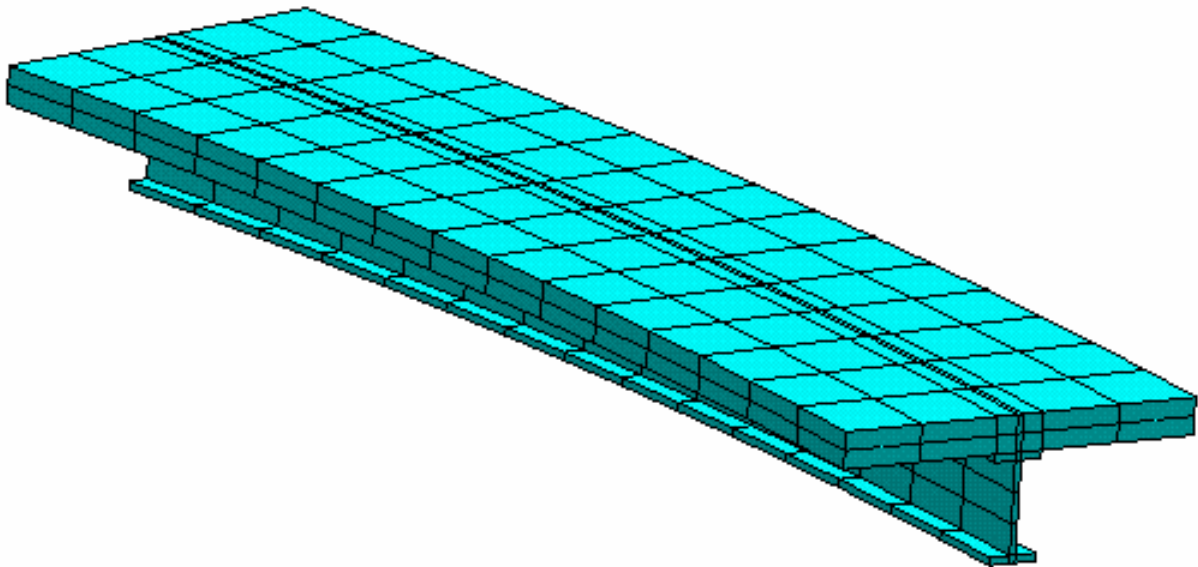


Fig.(8-23): The Finite Element Mesh of the Composite Curved Beam (Ex3) of 345 Elements.

The stress-strain curve adopted here for concrete and reinforcement was elastic-perfect plastic and the initial tangent stiffness matrix was used in the dynamic analysis with maximum number of iteration equal to 25.

During the analysis of this example an important representative problem appeared, that the current model *NFHCBDL* that deals only with brick elements of 20 nodes. Thus each concrete element over the top steel flange was connected by 8 nodes with the steel element under its location. While in the dynamic model *ANSYS* the available solid element which can represent the crack and crush phenomena consists of 8 nodes only, consequently the concrete and steel elements will be connected by only 4 nodes. Therefore the analysis here is branched into two types. The first includes a representation of elements of concrete in the *ANSYS* by 8 nodes using solid element called (*Solid 65*), thus the concrete and steel elements will be connected by only 4 nodes. This analysis gives good agreement until time 0.0032 sec., thereafter the solution diverges as shown in Fig.(8-24). The second type of analysis (by using the *ANSYS* model) consists of representation of concrete as the steel elements by solid brick element called (*Solid 95*) but this type does not take into account the effect of cracks and the crush which occurs at the Gauss points, therefore a second type of analysis of this example had to be done by the current model *NFHCBDL* ignoring the effects of cracks and crush at Gauss points, as shown in Fig.(8-24). However the second type of analysis is adopted in the comparison between the two analytical models.

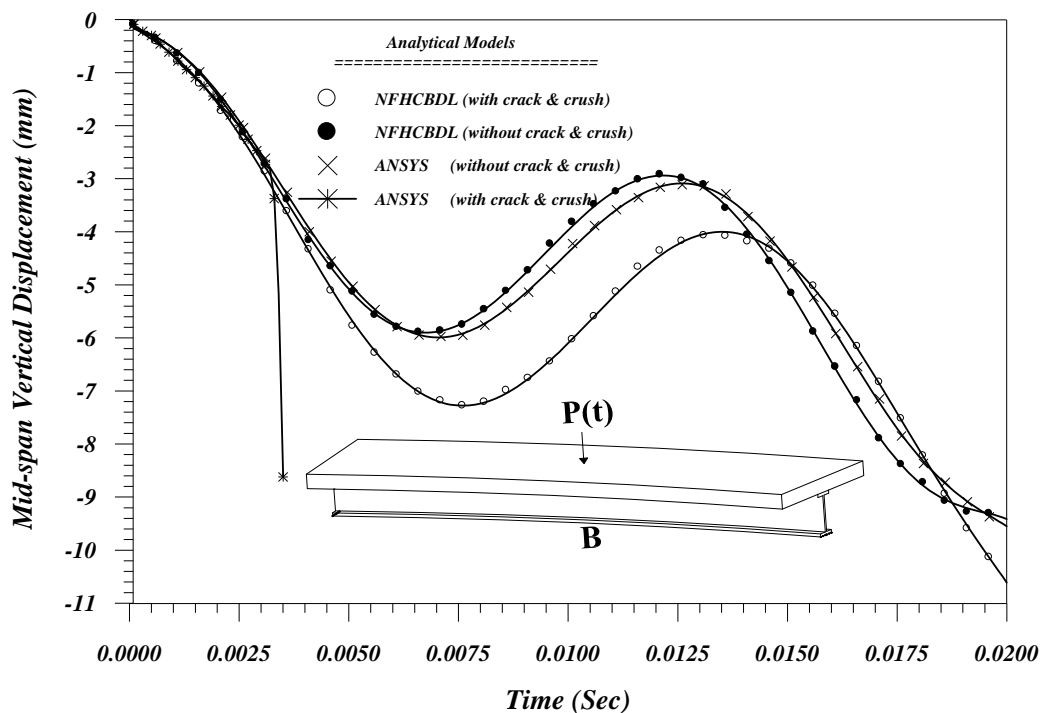


Fig.(8-24): Dynamic Response Curves of the Vertical Deflection.

The dynamic response curves for vertical deflection at mid-span (under the load) are presented in Fig.(8-24). The results showed good agreement between the results of *NFHCBDL* and *ANSYS*. The maximum difference in the amplitude of mid-span deflection was 0.175mm ($0.175/9.475=1.85\%$) at time 0.02 sec., while the difference in the period of one cycle was 4% ($1-0.0120/0.0125$). It is important to note that when the crack and crush were considered the amplitude of deflection increased to 7.28 mm at time 0.0077 sec. instead of 5.90 mm at time 0.0067 sec., i.e., the maximum deflection for the first cycle increased by 23.4% ($1.38/5.90$) and the period of one cycle increased also about 14.9% ($0.001/0.0067$).

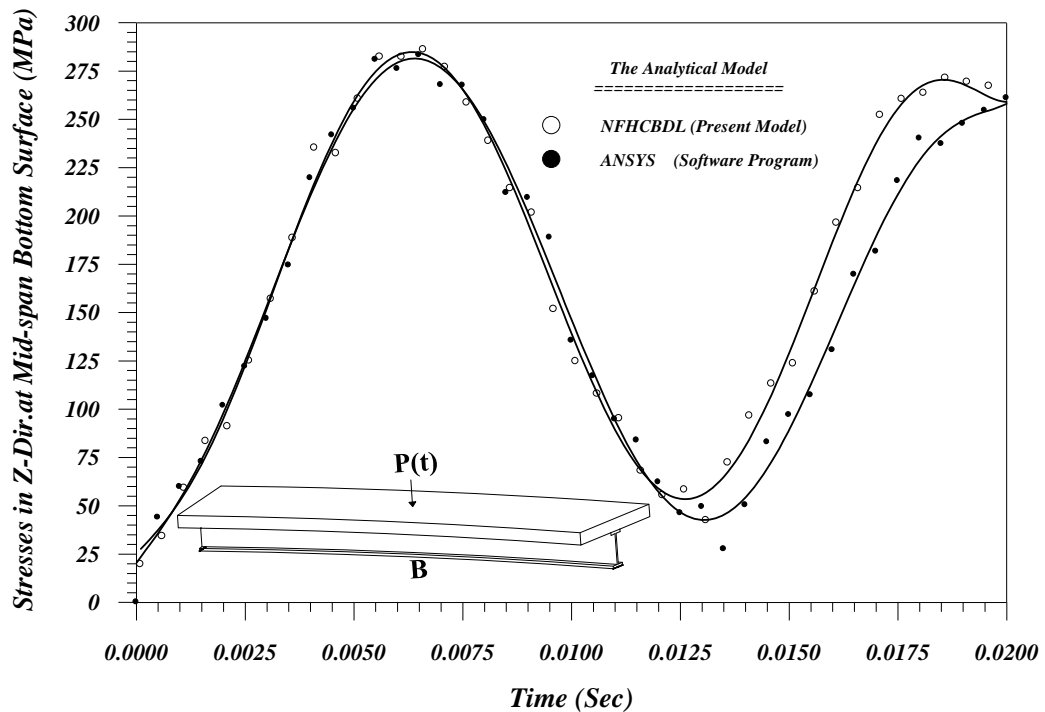


Fig.(8-25): Dynamic Response Curves of the Stress in Z-Direction at B (Nearest Gauss Point) .

The dynamic response curves for stresses in Z-direction at mid-span point **B** (the nearest Gauss point to centerline) are presented in Fig.(8-25). The results reflected good agreement between the two analytical models. The maximum stresses obtained from results of *NFHCBDL* and *ANSYS* were 293.0 MPa at time 0.0063 and 282.5 MPa at time 0.0059 respectively. Thus the difference between the two maximum stresses was 3.7% ($293.0/282.5-1$) at the amplitude of deformation of the first cycle.

Fig.(8-26) is drawn to illustrate the dynamic response curves for stresses in Z-direction under the load (the nearest Gauss point to centerline). The results showed good agreement between the two analytical models. The maximum stresses obtained from results of *NFHCBDL* and *ANSYS* were -35.20 MPa at time 0.0057 and -38.03 MPa at time 0.0065 respectively. Thus the difference between the two maximum stresses was 7.4% (2.83/38.03) during the first cycle.

Also one can note that the maximum stresses (Figs.(8-25) and (8-26)) do not increase during the second cycle although the vertical displacement increases as shown in Fig.(8-24). This absolutely is due to the accumulative plastic strains.

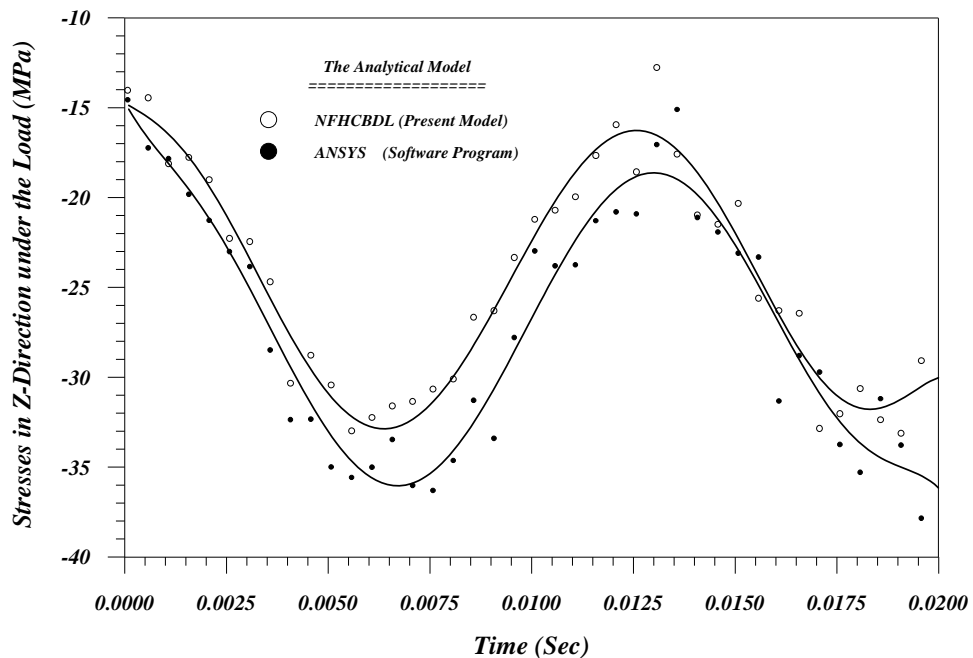


Fig.(8-26): Dynamic Response Curves of the Stress in Z-Direction under the Load (Nearest Gauss Point) .

Fig.(8-27) incorporates the stresses in Z-direction across the depth of the cross-section of the composite curved beam at many locations along the span. As shown the stresses for Gauss points located at, about, $(Y/YI) \geq 0.7$ suffer from compressive stresses while other Gauss points (near the centerline) are under tensile stresses. This means that all the concrete Gauss points are located near the centerline of the beam under compressive stress in Z-direction. Also the stress increased when the section is near to the mid-span, thereafter the stresses decreased. Approximately the stresses have the same shape as obviously plotted in the figure, but the scales are variable along the span.

The maximum stress in Z-direction was at distance along the span equal to 0.41 (from support A) and was 233.5 MPa. This does not mean that the state of these Gauss points located at ($Y/YI=0.047$) were elastic because 233.5MPa is smaller than the yield strength of steel which is equal to 285 MPa, hence firstly the yield strength f_y specified for equivalent stress represents a result of combination of six stresses (stress tensor), secondly this Gauss point does not represent the extreme Gauss point located at ($Y/YI=0.008$), thirdly the time is not the critical 0.0067second.

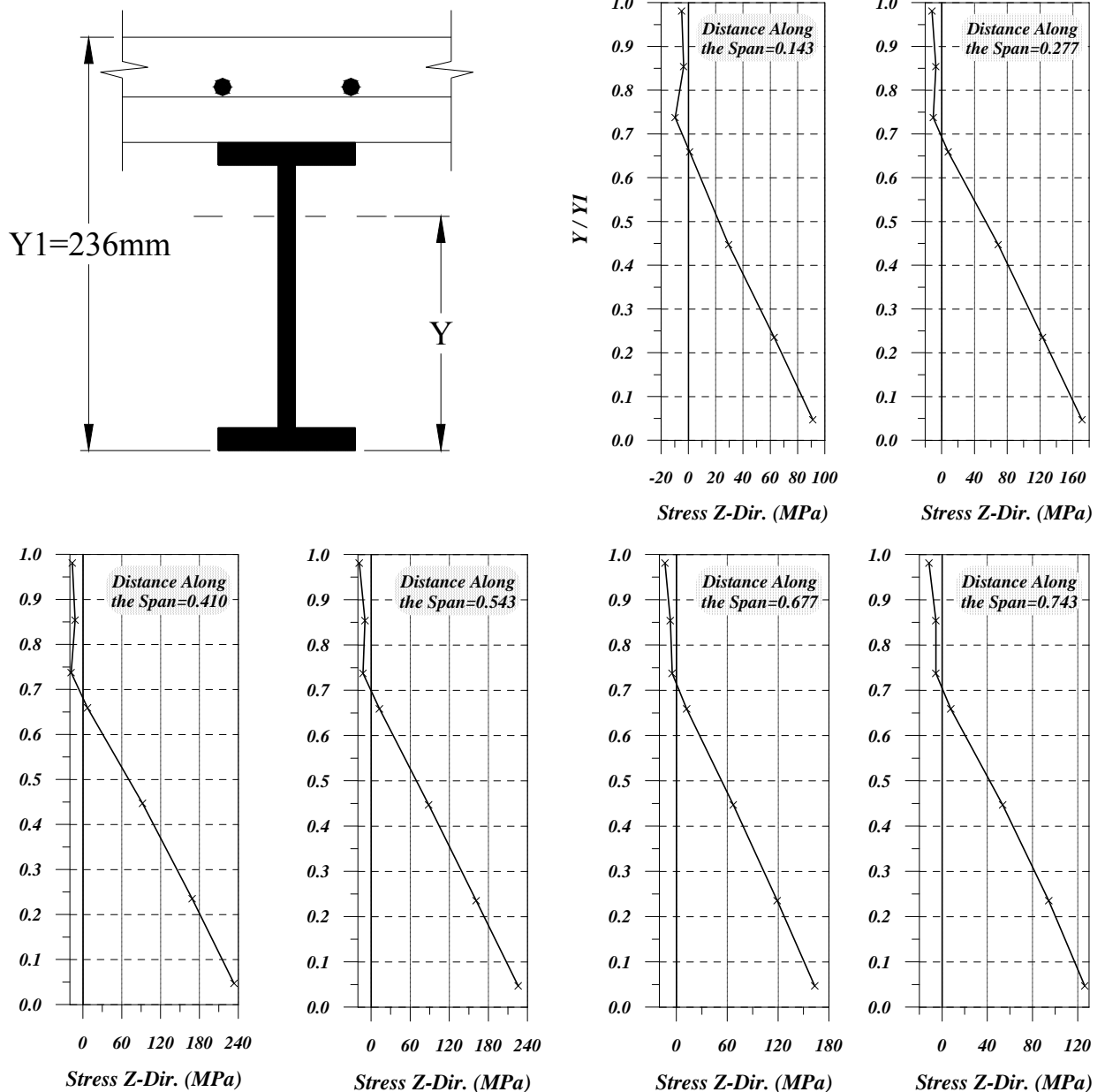


Fig.(8-27): Distribution Curves for Stresses in Z-Direction-Entire Depths of Curved Composite Beam at Many Positions Along the Span and at Time 0.0077 Second.

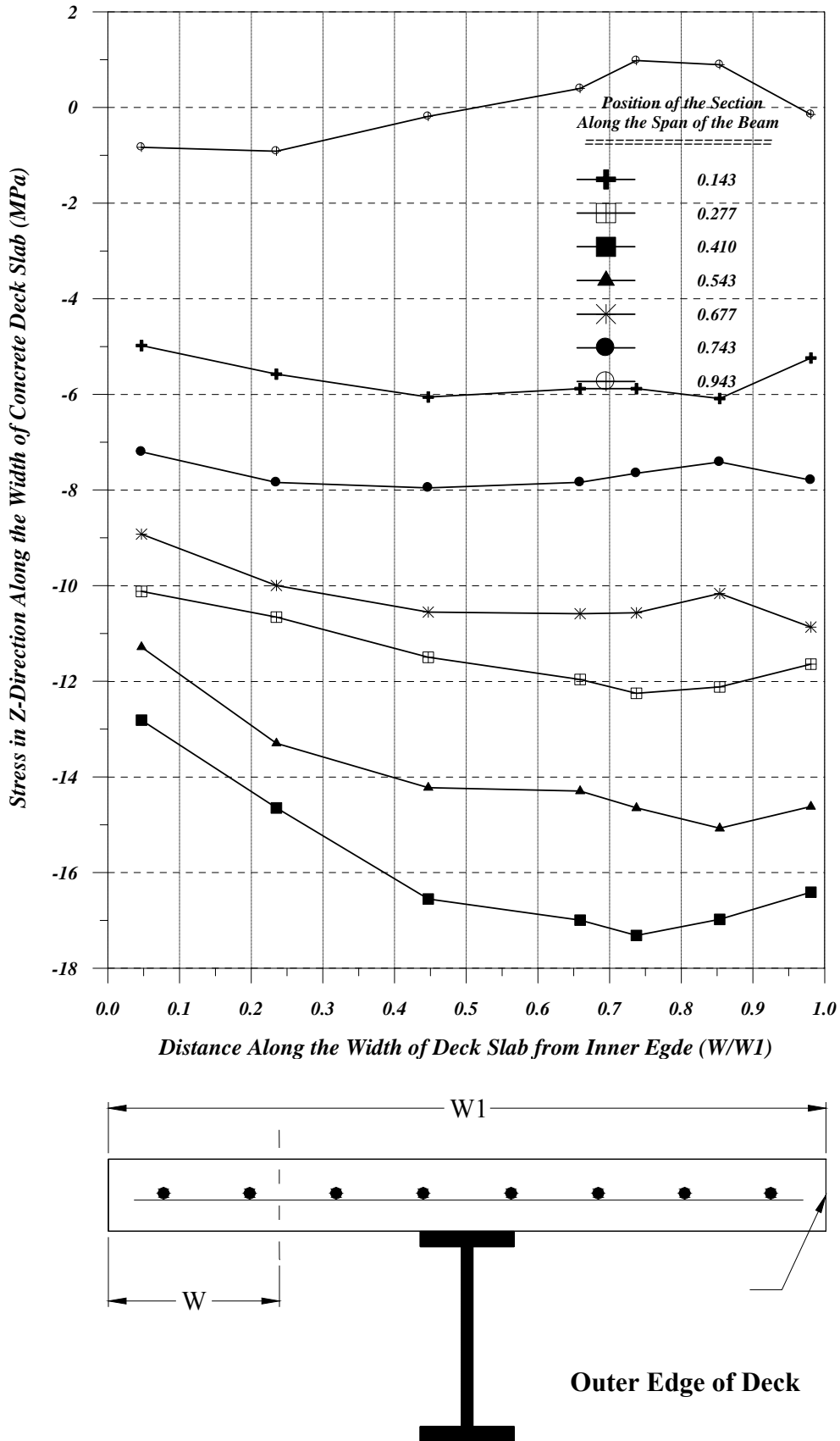


Fig.(8-28): Distribution Curves for Stresses in Z-Direction-Entire Width of Concrete Deck at Many Positions Along the Span of Curved Composite Beam and at Time 0.0077 Second.

The distribution of stresses across the width of the slab presented in Fig.(8-28) at many locations along the span. The analysis revealed that the stresses at the outer edges were larger than the stresses at the inner edges for all sections except at section (W/WI) is equal to 0.143. Also the critical sections located near the mid-span (due to existing of the maximum bending moment). The stresses in Z-direction adopted here because represent the critical stress among the other stresses.

Other investigations were carried out to show the effects of tolerance and time step on the dynamic response of the horizontally curved composite beam. The results showed when the time step is small enough the effect of tolerance decreased. Also the analysis appeared the convergence occurred within the first two iterations at each time step. While when time step is larger than 0.000001second the results diverges within the first ten time steps even when Δt is equal to 0.000012 second. However, when $\Delta t = 0.0000008$ second the results are not affected. These investigations proved that the error comes from the assumption of constant acceleration during the time step decrease when Δt decreased until it reached to the steady state as shown in Fig.(8-29). But the difficulty is appeared, whence the analysis must contain a large number of time steps to achieve at least one cycle. Here when $\Delta t = 0.000001$ second the number of time steps required to achieve one cycle was 12500 time step, consequently a large time of run required (reached here to about 3 hours by *NFHCBDL* and to about 7 hours by *ANSYS* for duration time 0.02 second).

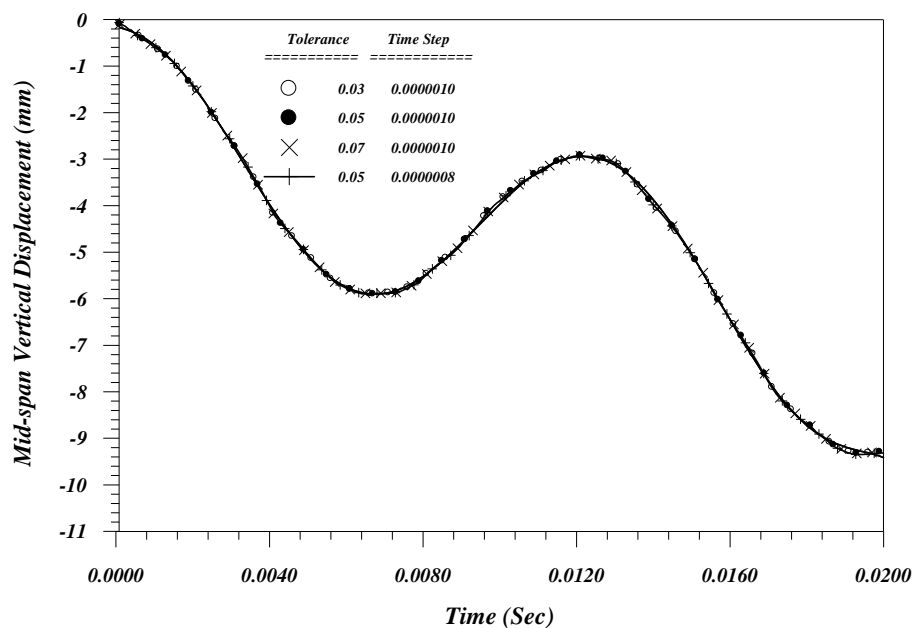


Fig.(8-29): Effects of Tolerance and Time Step.

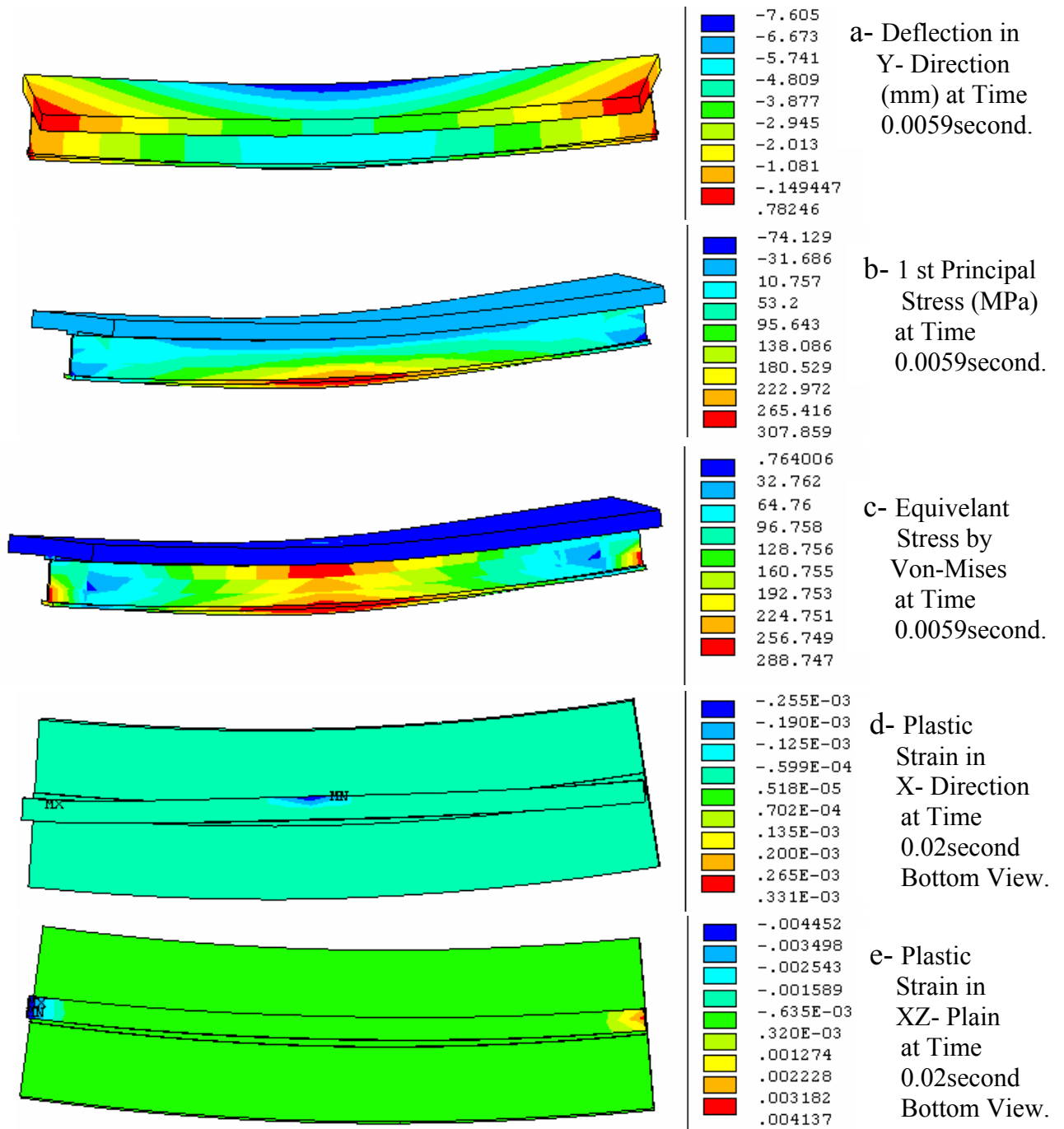


Fig.(8-30): Contours of Deformation, Stresses and Plastic Strain for Horizontally Composite Curved Beam (Ex3).

Fig.(8-30-a) shows the deformation of the beam in Y-direction, while Fig.(8-30-b) shows the contours of the 1st principal stress. In Fig.(8-30-c) the equivalent stress by Von-Mises plotted, as appeared the stress exceed the yield strength at four locations. Fig.(8-30-d) represents the bottom view of the beam contain the plastic strain in X-direction along the beam, as illustrated almost the elements hading plastic strain. Finally Fig.(8-30-e) monitored bottom view of the beam also incorporating the shear plastic strain in the XZ-plane.

Parametric Studies

9-1: Introduction

Many parametric studies were performed in this chapter to assess the influence of several parameters especially those which are concerned with the effects of tapering ratio on the behavior and strengthening of horizontally (steel, reinforced concrete and composite) curved beams. These parametric studies are divided into two categories, the first deals with the static analysis while the second with the dynamic analysis. Among these parametric studies are listed as follows:

- 1- The effects of tapering ratio on the behavior of steel I-section and reinforced concrete curved beam under static loads.
- 2- The effects of curvature, type of loading, position of load and type of restrained ends on the optimal tapering ratio.
- 3- The effects of tapering ratio on the dynamic response of horizontally curved steel I-section, reinforced concrete and composite beams.
- 4- The effects of curvature on the dynamic response of horizontally curved steel I-section, reinforced concrete and composite beams.
- 5- The effects of tapering ratio on the distribution of stresses across the depth and along the span of horizontally curved beams.

9-2: Static Parametric Studies

Two case studies are presented here to reveal the important effects of non-prismatic section on the behavior of horizontally curved beams, the first is for steel curved beam while the second is for reinforced concrete curved beam.

9-2-1: Horizontally Curved Steel Beam

The *Shanmugam et al.(CB1)* simply supported curved beam of 360 brick element mesh is considered. Example two in chapter seven is selected here to be the first case study with the same geometry, properties and loading conditions as shown in Fig.(7-9) page 104, also the same boundary conditions illustrated in Fig.(7-3) are used here except the intermediate lateral restraints which are ignored here to show the effect of lateral brace by the way.

9-2-1-1: Effect of Tapering Ratio on the Behavior of Horizontally Curved Steel I-Section beam.

To investigate the influence of tapering ratio ($u = h1/h2$), the beam in Fig.(9-1) is considered, on the behavior of steel I-section curved beam. Many ratios are presented in the analysis of this case study. It is important to mention that the tapering ratio will not affect the volume of steel. Also the width of flange is still constant while the depth of beam at ends and mid-span changes. The modified *Newton-Raphson* method (where the stiffness matrix is updated at the first iteration only) is adopted in the analysis.

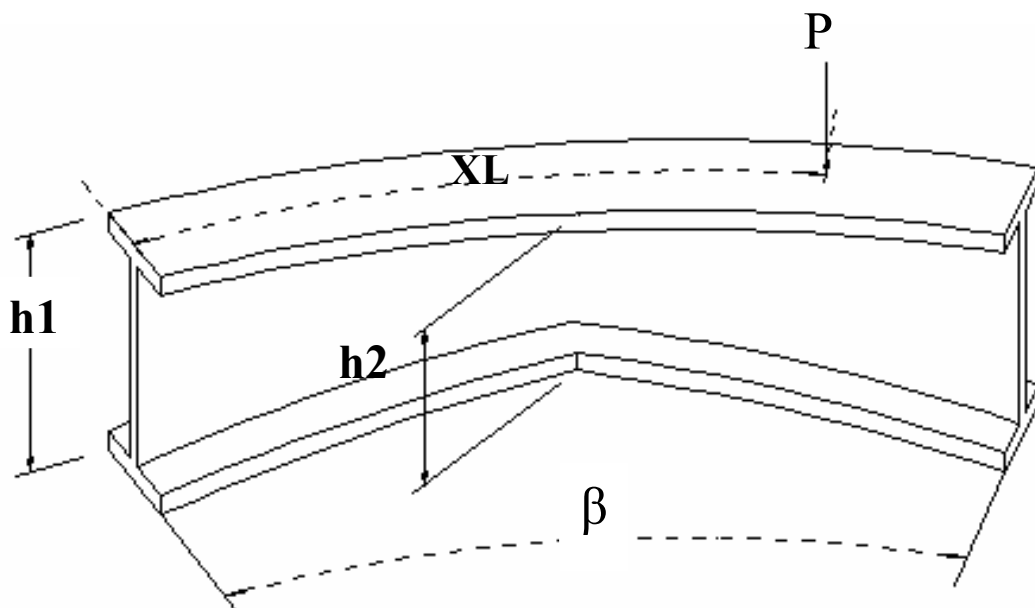


Fig.(9-1): Non-prismatic Horizontally Steel Curved Beam.

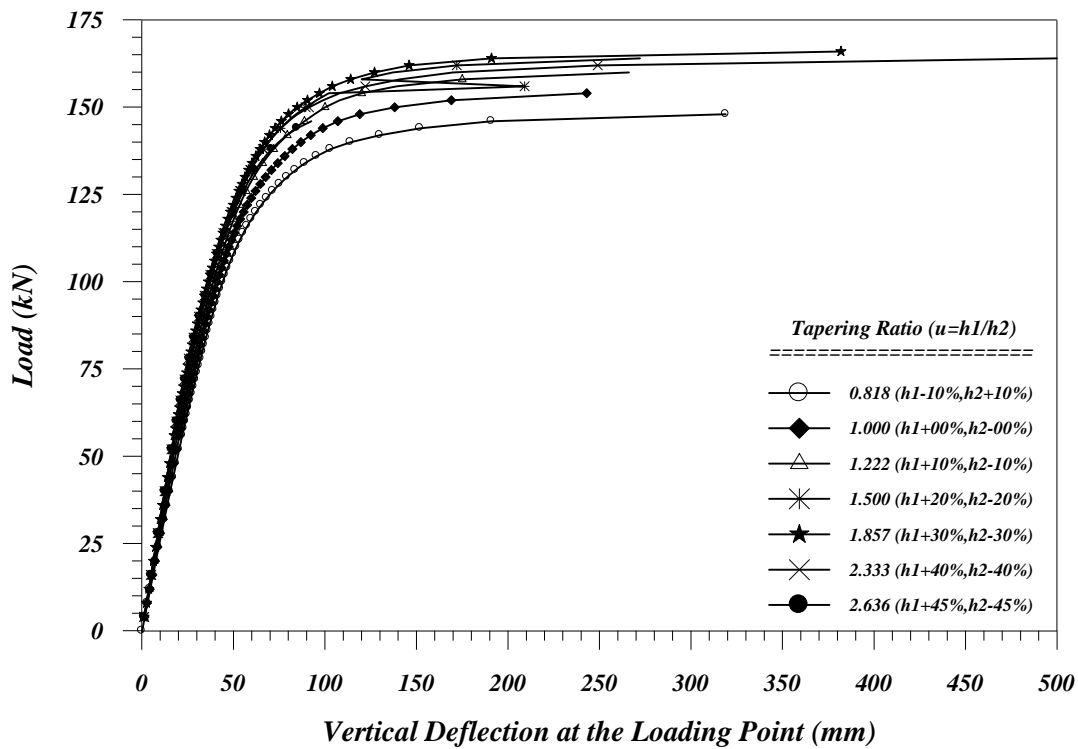


Fig.(9-2): Load-Displacement Curves for Shanmugam et al. (CB1) Curved Beam [Showing the Effect of Tapering Ratio].

Fig(9-2) reveals that the strength of curved beam decreases when increases the depth at mid-span and decreases at ends, while when the tapering ratio u increases (i.e., $h1$ increase and $h2$ decrease) the strength of beam increases until $u = 2.333$, thereafter the strength of beam also decreases when u increases. The optimal value of (u) achieved a maximum strengthening equal to 1.667, at this tapering ratio the ultimate load of beam equal to 166 kN, and hence the ultimate load when ($u=1$) equal to 154 kN, the increment in the ultimate load was 7.79%. Fig.(9-2) not only appears the effects of tapering ratios but also discovers the important effect of the intermediate restrained. Whence the ultimate load of this beam decreases from 197.27 to 154 kN when the intermediate restrained was ignored, due to the increment in the length of the span in the horizontal plane (i.e., the increment in the span of the bending moments produces from torsional warping).

The optimal value of tapering ratio affected by many parameters such as the angle of curvature(β), type of loading, location of the concentrated load(XL) and the effect of the ends restraints, to investigated these affects the following parametric studies are presented, during these studies the length of beam remain constant ($L=5$ meter).

9-2-1-2: Effect of Curvature on the Optimal Tapering Ratio

Previously the value of ($\beta=14.325^\circ$), now will be changed (increase and decrease) to investigate the optimal values of the tapering ratio u for each (β). As shown in Fig.(9-3), the optimal value of u increases when (β) increases, also the economical benefit from non-prismatic section increases and reach to 25% for ($\beta=37.242^\circ$) at u equal to (3.5). The optimal values of u , the corresponding increments in the ultimate loads as well as the ultimate loads for each (β) were written in Table (9-1).

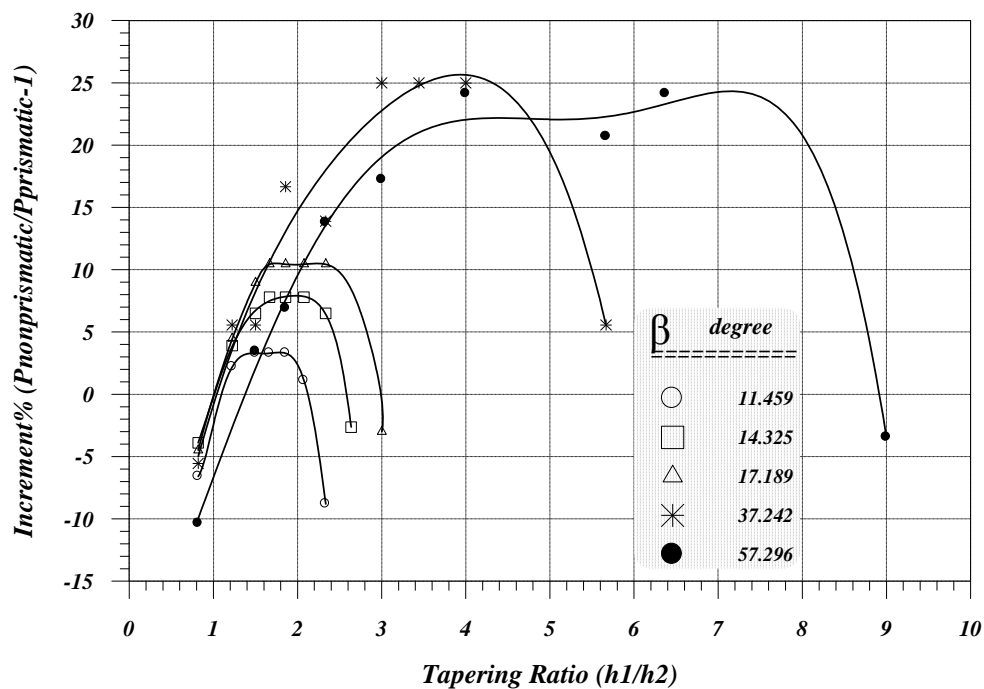


Fig.(9-3): Effect of Angle of Curvature (β) on the Optimal Tapering Ratio for Non-prismatic Steel Curved Beams under Concentrated Load.

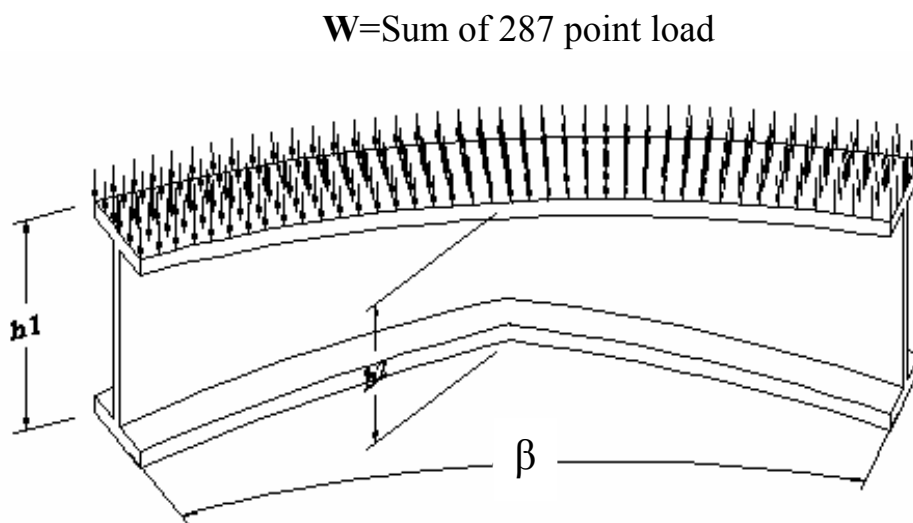
Table(9-1): Effects of the angle of Curvature (β) on the Optimal Value of Tapering Ratio and Ultimate Loads for Nonprismatic Steel Curved Beams.

β degree	11.459	14.325	17.189	37.242	57.286
Optimal $u=h1/h2$	1.500	1.667	1.857	3.500	6.370
Ultimate $P_{prism.}$, kN	182	154	134	72	58
Ultim. $P_{nonprism.}$, kN	188	166	148	90	72
Maxi. Increment %	3.30	7.79	10.45	25.00	24.14

Table (9-1) appears also the degradation in the strength of curved beam with increases of (β).

9-2-1-3: Effect of Type of Loading on the Optimal Tapering Ratio

For the same case study when the type of loading was changed from concentrated load to a uniformly distributed load, see Fig.(9-4) The effect of tapering ratio u presents here to three values of (β). The results in Fig.(9-5) show, approximately, the same effects for concentrated load.



(9-4): Non-prismatic Steel Curved Beam under Uniformly Distributed Load.

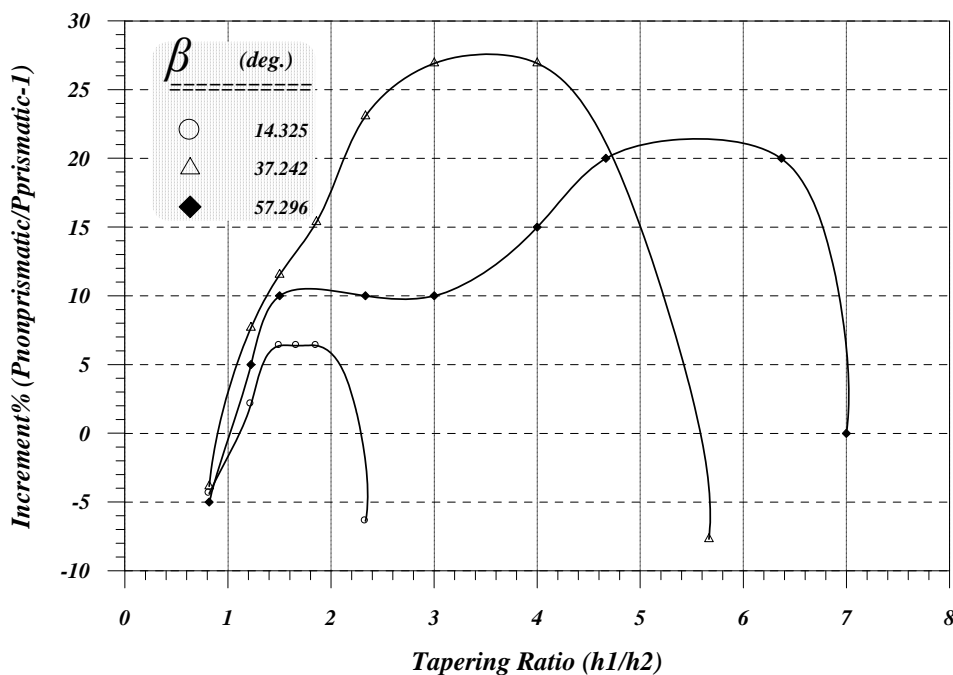


Fig.(9-5): Effect of Angle of Curvature (β) on the Tapering Ratio for Non-prismatic Steel Curved Beam under Uniform Distributed Load.

The applied load is subdivided into 287 point load. Summation of these loads gives the total applied load which equal to, at the ultimate stage for prismatic beam, to 180, 78 and 60 kN for ($\beta=14.325^\circ$, 37.242° and 57.296°) respectively and the optimal values of u equal to 1.667, 3.5, 5.667 respectively too. The maximum increment in the strength of beam was 26.92% for $u=3.5$ and $\beta=37.242^\circ$, because the ultimate load was equal to 99 kN. It is important to know that the tapering ratio increases the lateral deflection (at the original position, i.e., $XL=0.76L$, see Fig.(9-1)) whenever it is smaller than 2.333 although the ultimate load (total load) increases. But when u is grater than 2.333 the lateral deflection decreases even when the ultimate capacity decreases at $u = 5.667$ as shown in Fig.(9-6).

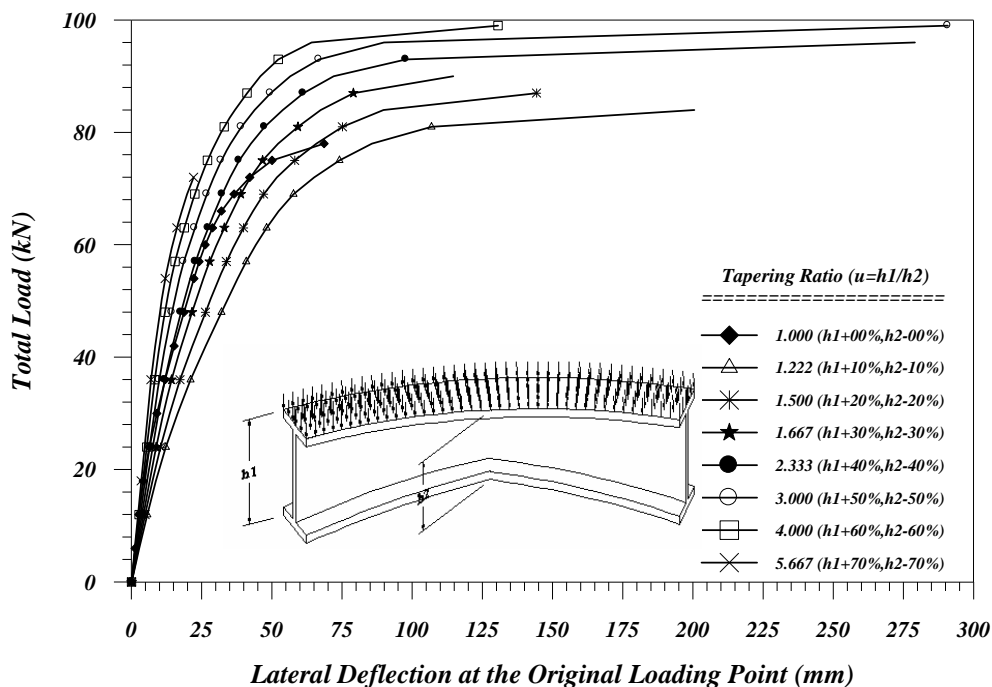


Fig.(9-6): Effect of the Tapering Ratio on the Lateral Deflection for Shanmugam (CB1) Curved Beam under Uniform Load.

9-2-1-4: Effect of Position of Load on the Optimal Tapering Ratio

Here the position of the concentrated load ($XL=0.76L=3.8$ meter, see Fig.(9-1)page 155) is changed, to examine this effect on the optimal tapering ratio. For $\beta=14.325^\circ$, the optimal u for *Shanmugam* simply supported curved beam was 1.667, which gives increment in the ultimate load equal to 7.79%, see Table(9-1). The results showed when the concentrated load at the mid-span($X=0.5$) the optimal

u decreases to 1.35, and the economical benefit decreases too from 7.79% to 1.79%, but when ($X=0.88$), the optimal value of u is equal to 2.077 and the corresponding increment equal 11.59%, as shown in Fig.(9-7). It is of interest to note that when (X) decreased 26% (from 0.76 to 0.50) the optimal increment decreases 6% thus the rate of decreasing is equal to 23% (6%/26%), while when (X) increased 12% (from 0.76 to 0.88) the optimal increment increases to 3.8% thus the rate of increasing is equal to 31.67% (3.8%/12%). These results reveal the importance of tapering ratio when the concentrated load is located near the supports as well as the sensitive effect of the restraints.

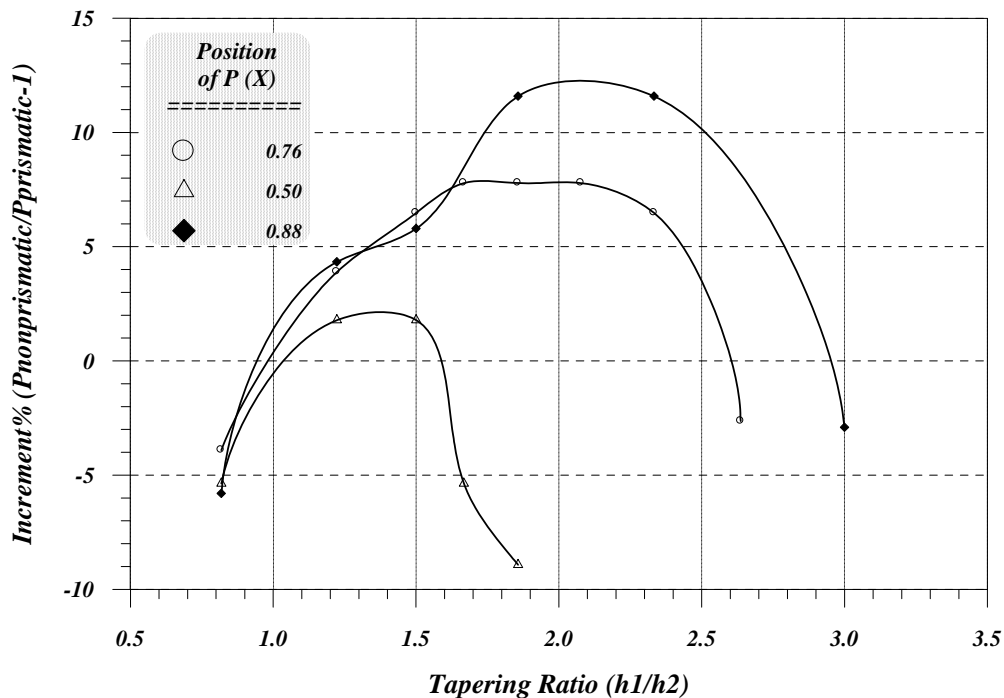


Fig.(9-7): Effect of Location of Concentrated Load on the Optimal Tapering Ratio for Non-prismatic Steel Curved Beam .

9-2-1-5: Effect of Ends Restraints on the Optimal Tapering Ratio

To illustrate the effect of ends restraints on the optimal tapering ratio the fixed-ends beam of *Shanmugam et al. (CB1)* is proposed here (u , v and w equal zero at all nodes located at the ends) in place of the previously adopted boundary conditions (see, Fig.(7-3), page 100). Three values of curvature are studied here ($\beta=14.325^\circ$, 37.242° , 57.296°), and the location of the concentrated load is still at the same position ($X=0.76$). The results of analysis revealed the important effect of

tapering ratio on the strength of the fixed-ended curved beam under concentrated load, whence the increment reached to 102% in some cases. Also the new behavior appearing here is different from the previous analysis, the strength of the beam still increases with the increasing of tapering ratio ($u=h1/h2$) for β grater than and equal to 37.242° until the top flange touch the bottom flange at ($u=24$), as shown in Fig.(9-8). The ultimate loads (for prismatic and non-prismatic) of curved beam, the optimal u and the maximum increment achieved for each β are tabulated in Table(9-2).

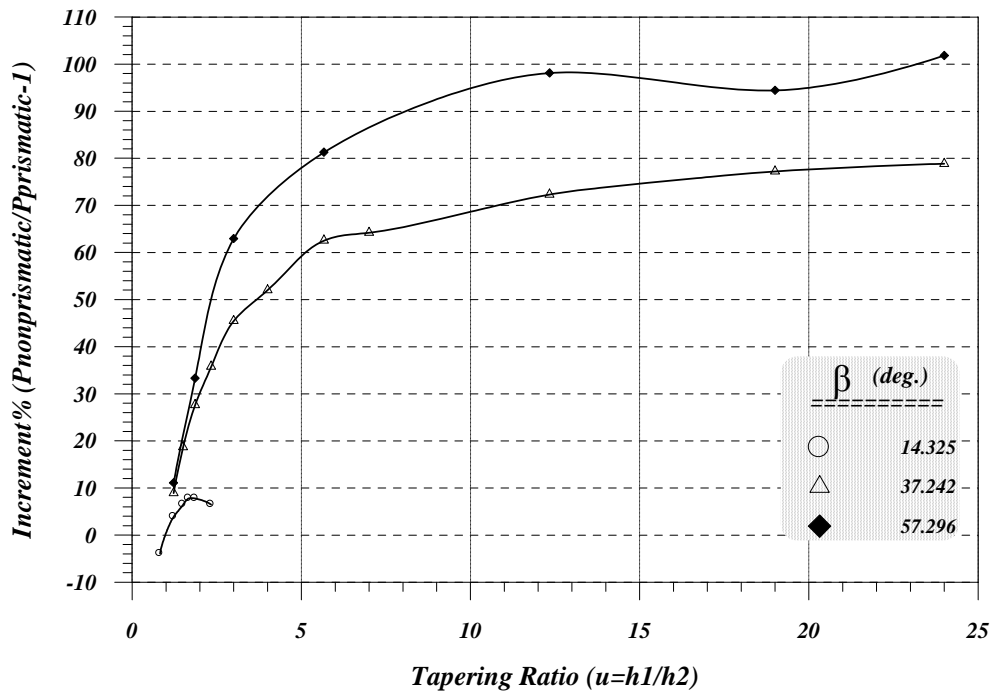


Fig.(9-8): Effect of Angle of Curvature on the Optimal Tapering Ratio for Non-prismatic Steel Curved Beam .

Table(9-2) gives also a picture of the sensitive effect of ends restrained. When comparing the results of this table with that one of Table(9-1), one can conclude that the strength of the prismatic curved beam ($\beta=14.325^\circ$) increases to 199.4%(form 154 to 455 kN) when the ends transform from simply supported to fixed ends and when ($\beta=37.242^\circ$) the increment will be 327.1% (from 72 to 307.5 kN) and when β is 57.286° the increment will be 365.5% (from 58 to 270 kN). As shown, the sensitivity effect of restrained ends increases with (β), as well as the economical benefit is due to non-prismatic sections.

It is very important to know that each point on each curves of Figures (9-3), (9-5), (9-7) and (9-8) represents run of the static model *NFHCBSL* which in turn

requires (19468) input data for each run of this case study (which consisting from mesh of 360 brick element).

Table (9-2): Effects of the Angle of Curvature (β) on the Optimal Tapering Ratio (u) and Ultimate Loads for Fixed Ends ShanmugamCB1.

β degree	14.325	37.242	57.286
Optimal $u=h1/h2$	1.667	19.00	24.00
Ultimate $P_{prism.}$, kN	455	307.5	270
Ultim. $P_{nonprism.}$, kN	495	545	545
Maxi. Increment %	8.79	77.24	101.85

9-2-2: Horizontally Curved Reinforced Concrete Beam

The *Jordaan (C3)* fixed ended reinforced concrete curved beam of 148 brick elements mesh, example four in chapter seven, is considered here to be the second case study with the same geometry, properties and loading conditions as shown in Fig.(7-27) and Table(7-6) page 114, also the same boundary conditions are illustrated in Fig.(7-29) page 115 used here.

9-2-2-1: Effect of Non-prismatic Sections Due to Unequal Depths

The effect of tapering ratio ($u = h1/h2$) on the behavior of reinforced concrete horizontally curved beam for many ratios is presented here. The study incorporated increasing or decreasing the depths of concrete at ends and decreasing or increasing at mid-span respectively. Thus the volume of concrete is still constant. The variation of depth is chosen here rather than the width of beam because the major effect of depth on the strength of curved beam as well as the capability to performance in the practical site represent less difficulty than the variation in width of beam, thus the width of beam is still constant during the analyses. It is interesting to note that the covers of longitudinal and transverse reinforcement is still constant 38mm and 24mm respectively, see Fig(7-27) page 114, along the span of the beam. This leads to adjust the local coordinates in the s direction which is parallel to global Y - direction, while the other local coordinates are still having the same values of the prismatic beam.

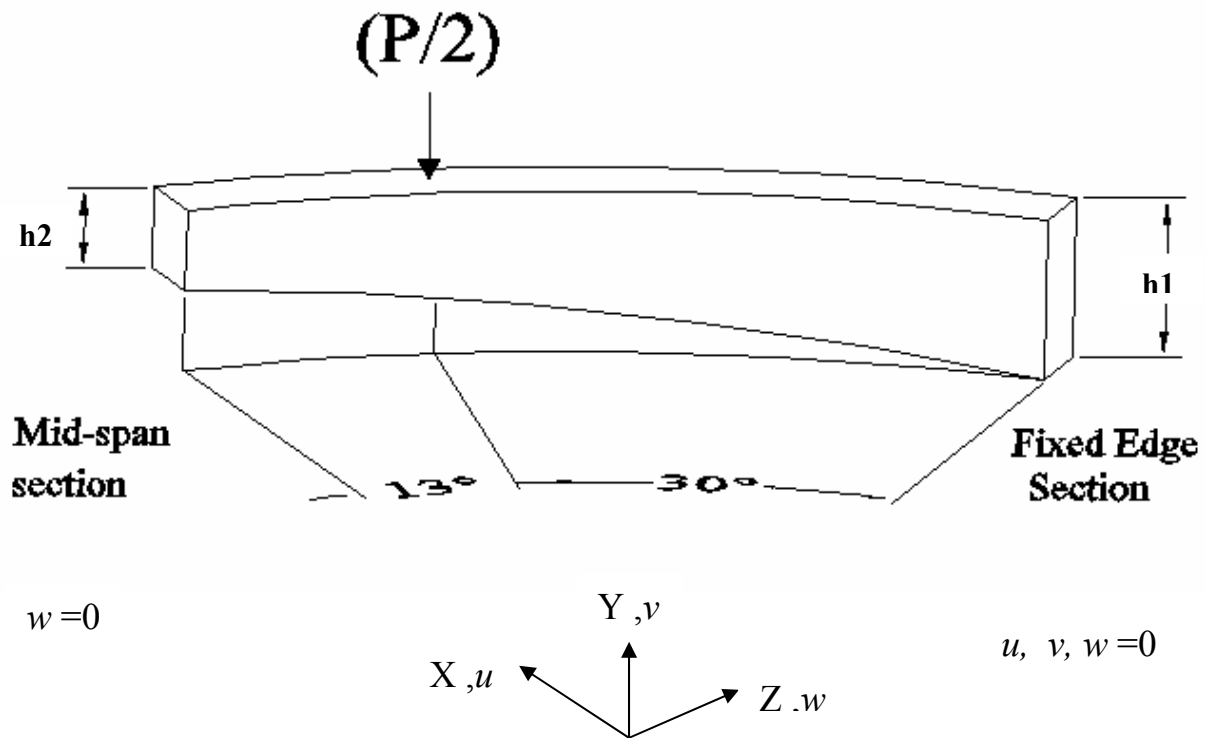


Fig.(9-9): Non-prismatic Horizontally Reinforced Concrete Curved Beam.

The analytical investigation revealed that when increasing the mid-span depth and decreasing the edge depth ($u = 0.818$, for example) the strength of fixed ended beam decreased. This behavior is similar to that one of *Shanmugam* simply supported curved beam mentioned previously, Fig.(9-2) page 156. While when the depths at ends increased and the depth at mid-span decreased the strength of beam increased as shown in Fig.(9-10). This is due to the important effect of the membrane action which responsible on the behavior and strength of beam which increased when the depths at ends increased and vice versa. Also the shear forces and bending moments are more critical at ends, hence when strengthening the sections at ends the strength of beam increase. However, the maximum increment in the ultimate capacity of beam is achieved for ($u = 4$), where the ultimate load is equal to 284 kN, the increment in the ultimate load is equal to 59.6% ($(284/178-1)$). The investigation stopped at ($u = 4$) due to practical reasons, where $h_2 = 122\text{mm}$ for $u = 4$. Thus the spacing between the longitudinal top and bottom reinforcement equal to 46mm at mid-span. The results of Fig.(9-10) proved that the strength of fixed ended horizontally reinforced concrete curved beam increases with increases the tapering ratio (u). This conclusion compatible with the previously results for

steel fixed ended curved beam, is as shown in Fig.(9-8), but this conclusion is not absolutely for all values of (β) as for steel curved beam, as illustrated in following paragraph.

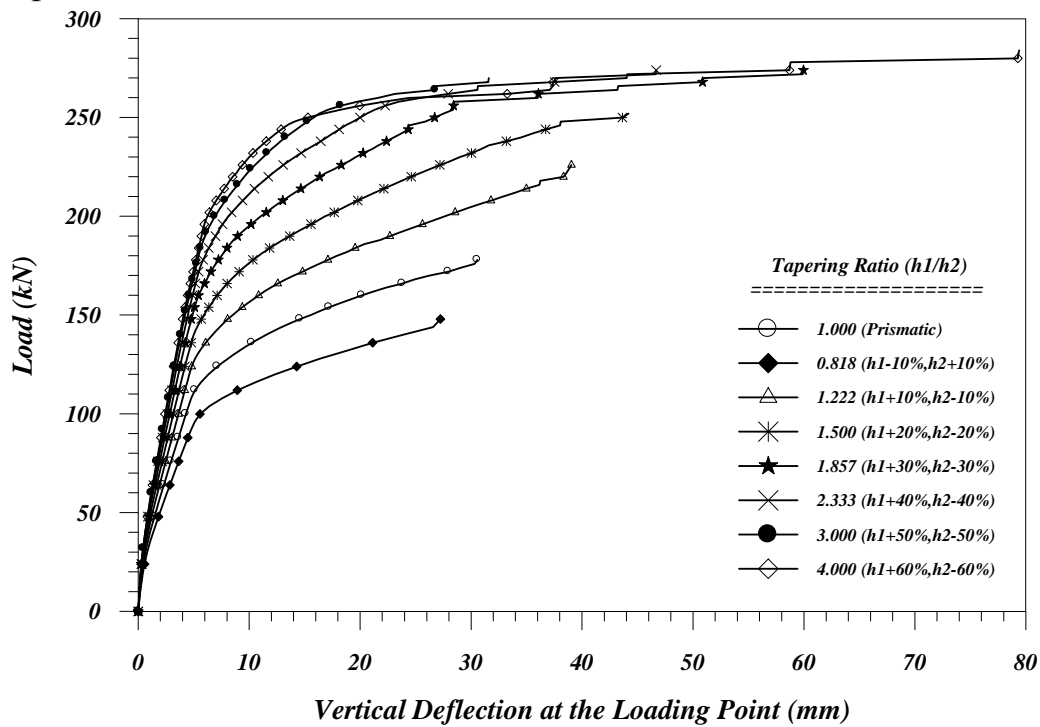


Fig.(9-10): Load-Displacement Curves for Jordaan (C3) Curved Beam [Showing the Effect of Tapering Ratio] under Concentrated Load.

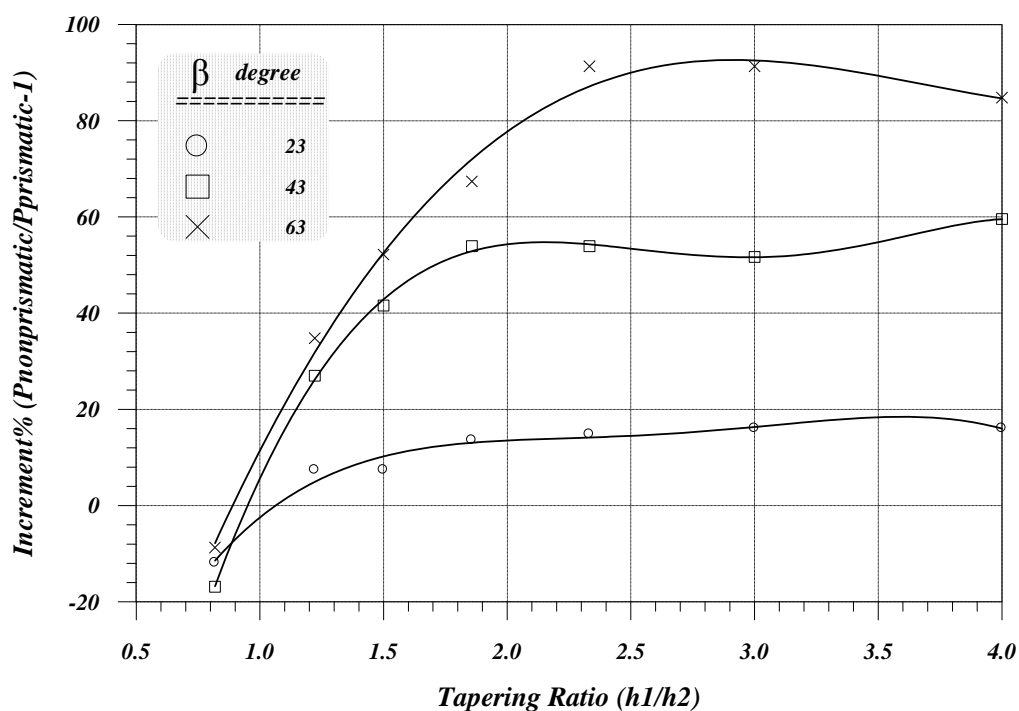


Fig.(9-11): Effect of Angle of Curvature (β) on the Tapering Ratio for Non-prismatic Reinforced Concrete Curved Beam under Concentrated Load.

9-2-2-2: Effect of Curvature on the Tapering Ratio

Here the value of ($\beta=43^\circ$) will be changed (increase to 63° and decrease to 23°) to investigate the effect of tapering ratio u for each (β). As shown in Fig.(9-11), the optimal value of u is equal to 4 when (β) is equal 23° and 43° , while the optimal value of u equal 2.5 when ($\beta=63^\circ$). As shown the economical benefit from non-prismatic section increases with (β), which reached 91.3% for ($\beta=63^\circ$) at u equal (2.5). The optimal values of u and the corresponding increments in the ultimate loads as well as the ultimate loads for each (β) are written in Table (9-4).

Table(9-4): Effects of the angle of Curvature (β) on the Optimal Value of Tapering Ratio, and Ultimate Loads for Fixed Ended Jordaan C3.

β degree	23	43	63
Optimal $u=h1/h2$	4.0	4.0	2.5
Ultimate $P_{prism.}$, kN	243	178	138
Ultim. $P_{nonprism.}$, kN	282	284	264
Maxi. Increment %	16.05	59.55	91.30

The tabulated values of ultimate loads in Table(9-4) shows also the deficiency in the ultimate strength of prismatic curved beam when the angle of curvature (β) increases.

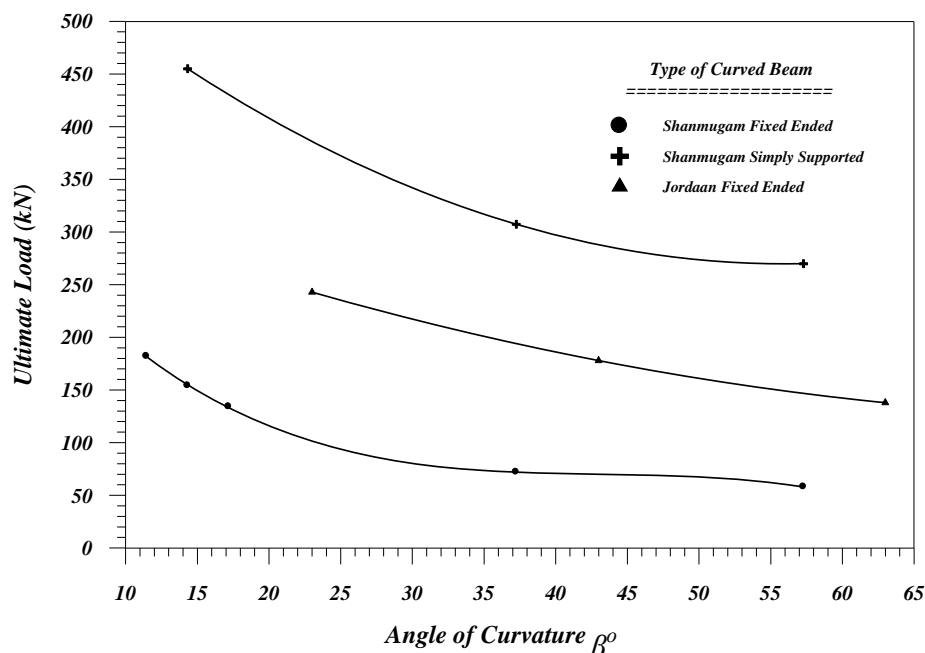


Fig.(9-12): Effect of Angle of Curvature (β) on the Ultimate Load of Shanmugam and Jordaan Curved Beams

Fig.(9-12) illustrated this deficiency graphically for *Shanmugam* steel and *Jordaan* reinforced concrete curved beams, utilizing the results of Tables(9-1), (9-2) and (9-4) respectively.

9-2-2-3: Effect of the Type of Load on the Optimal Tapering Ratio

For the same case study when the type of loading changed from concentrated load to a uniformly distributed load, the effect of tapering ratio u is presented here for ($\beta=43^\circ$). The results in Fig.(9-13) shows, approximately, the same effects for concentrated load. The maximum economical benefit equal 54.41% achieved at ($u=3$).

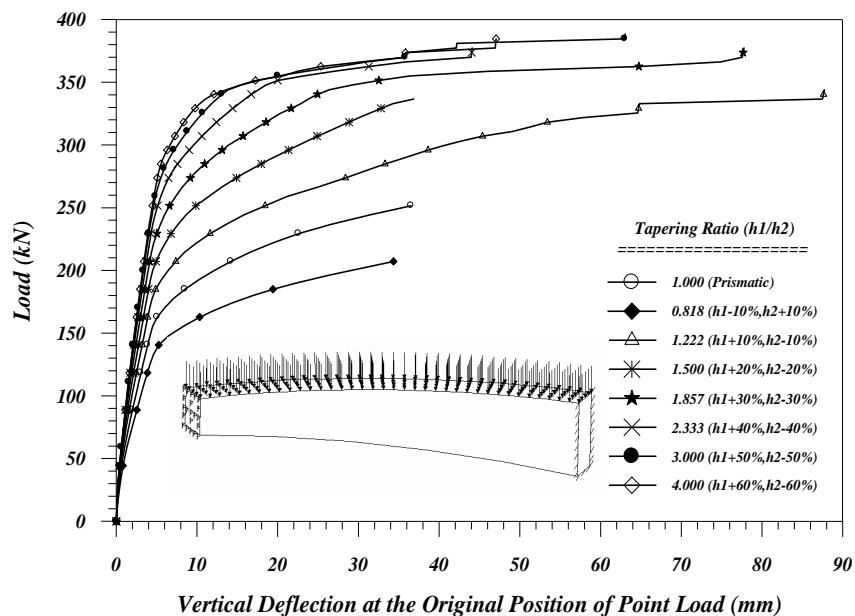


Fig.(9-13): Load-Displacement Curves for Jordaan (C3) Curved Beam [Showing the Effect of Tapering Ratio] under Uniformly Distributed Load.

9-3: Dynamic Parametric Studies

The dynamic parametric case studies presented here are concerned with the same three examples presented in chapter eight. The investigation devoted to reveal the effects of non-prismatic section on the behavior of horizontally curved beams. The tapering ratio represents the depth of beam at ends to the depth at mid-span as previously defined. For composite curved beam the investigation of non-prismatic is concerned with the depth of steel I-section only, i.e., the thickness of deck slab is still constant and not changed.

9-3-1: Effect of Curvature and Tapering Ratio on the Dynamic Response of Horizontally Curved Steel I-Section Beam

The investigation presented here is related with the steel curved beam in paragraph 8-4-1, Fig.(8-2) page 130. The properties, load conditions and all analytical parameters are as taken previously. The non-prismatic effect will be studied for three magnitude of curvatures ($\beta = L/R = 25^\circ, 45^\circ$ and 65°) but the length of the beam is still constant. Thus the radius of curvature will be ($R=13500, 7500$ and 5192 mm) respectively. Figures (9-14), (9-15) and (9-16) show the effects of tapering ratios on the dynamic response of these curved beams. The results of Fig.(9-14) revealed that the optimal value of tapering ratio equal 3 which decreases the amplitude deflection 19.37mm to 15.93mm, i.e., 17.8% , and the time period for one cycle was reduced by 5.3%. Fig.(9-15) appeared that the optimal value of $u = 4$, where the maximum deflection and period time of one cycle were decreased by 17.64% and 8.7 respectively. While Fig.(9-16) illustrated that the largest decrement in the maximum displacement is at $u = 4$ also, whence the amplitude deflection was reduced from 48.36mm to 38.8mm, i.e., 19.8% and the time period decreased about 11.5%.

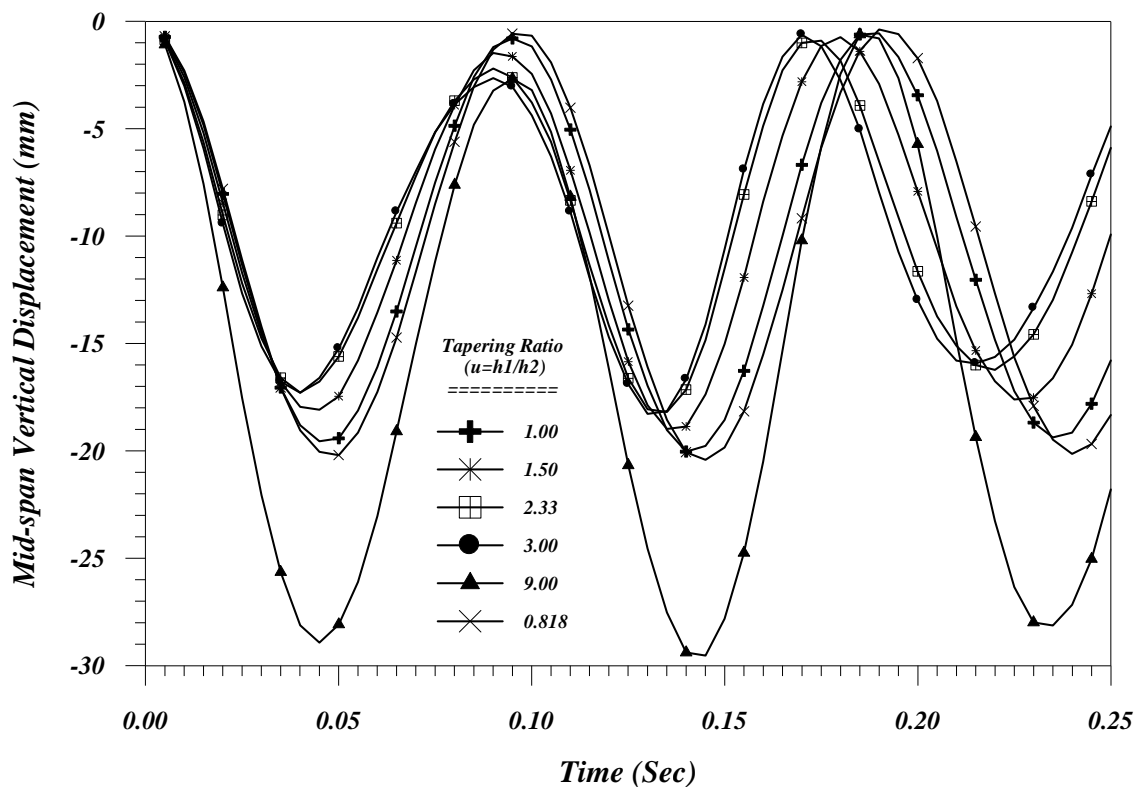


Fig.(9-14): Effect of Tapering Ratio (u) on Mid-span Deflection of Steel Curved Beam when Angle of Curvature Equal 25° .

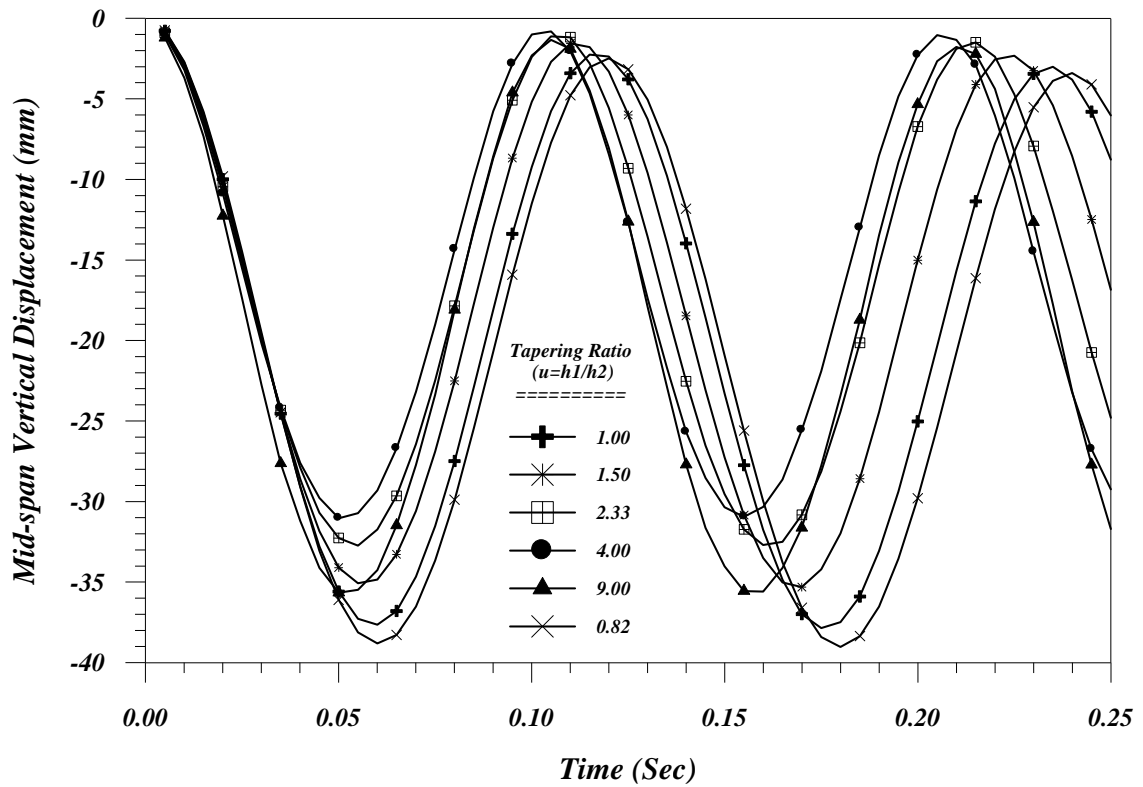


Fig.(9-15): Effect of Tapering Ratio (u) on Mid-span Deflection for Steel Curved Beam when Angle of Curvature Equal 45° .

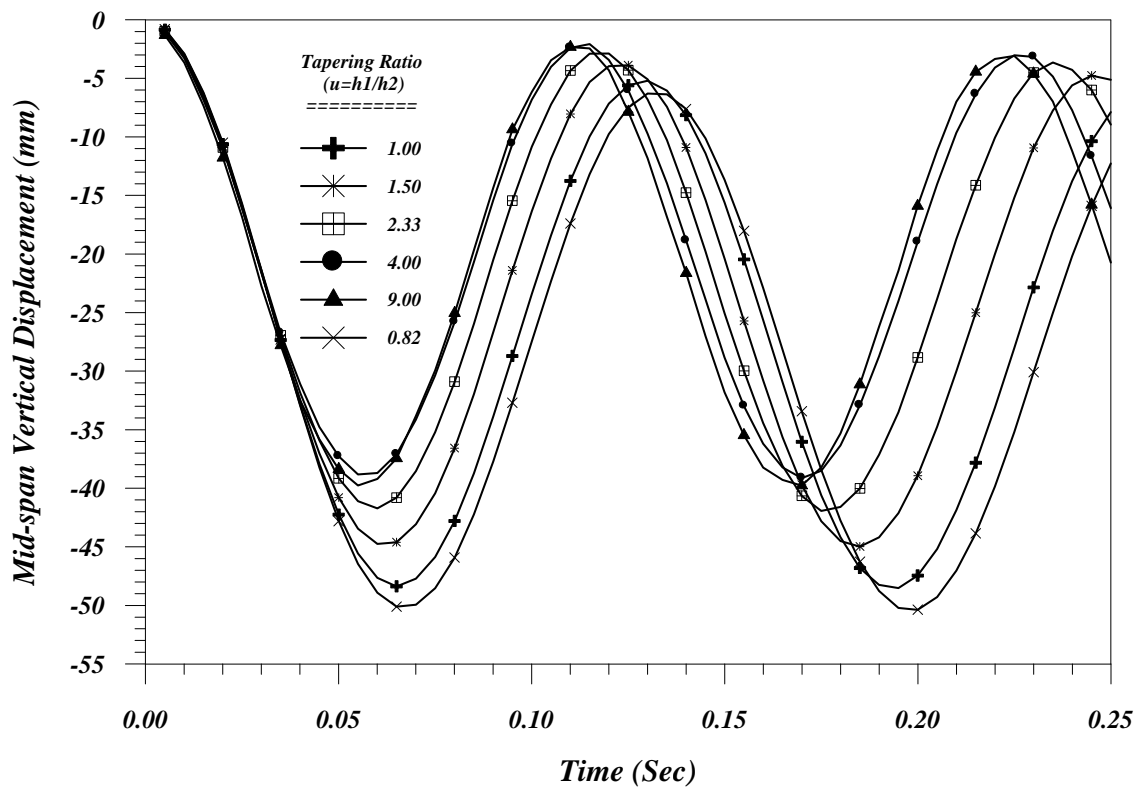


Fig.(9-16): Effect of Tapering Ratio (u) on Mid-span Deflection of Steel Curved Beam when Angle of Curvature Equal 65° .

Thus one can conclude that the optimal value of tapering ratio is not affected largely by angle of curvature as in the static analysis and its range between "3 - 4". Also it is interesting to note that when the tapering ratio is increased larger than the optimal value the deflection increased too as shown in the three previous figures for $u = 9$, and the same behavior observed previously in the static analysis when u is equal and less to one the beam appeared softening not strengthening.

The stress in Z-direction at mid-span bottom flange is investigated also for the same values of curvatures and the results plotted in Fig.s(9-17), (9-18) and (9-19). At first all these figures proved that when the depth of curved beam decreased at mid-span and increased at ends, i.e. $u > 1$, the stress in Z-direction increased although the beam appeared stiffening until u reached to the optimal values. This situation revealed the good redistribution of the volume of steel.

Also for curvatures ($\beta = L/R = 25^\circ, 45^\circ$ and 65°) the amplitude deflection and the stress in Z-direction at mid-span bottom flange for prismatic curved beams were 19.37mm, 37.6mm, 48.4mm and 30Mpa, 31.6Mpa, 36.8MPa respectively, Thus the effect of curvature is obvious and as shown in Fig.(9-14) to Fig.(9-19).

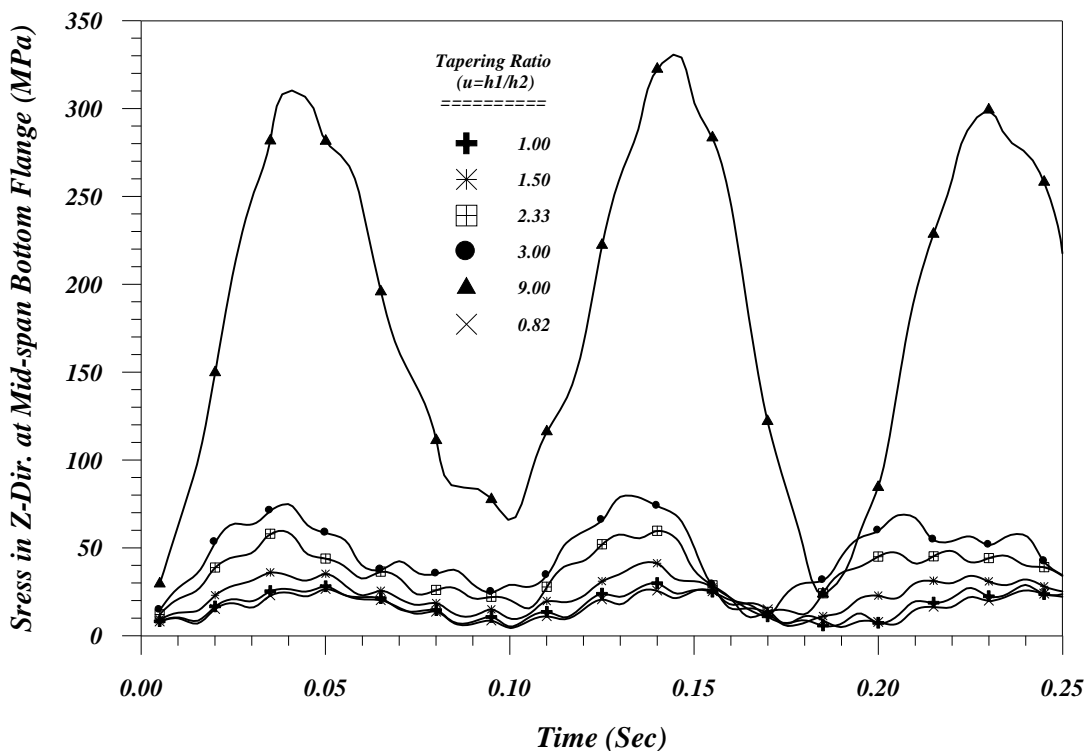


Fig.(9-17): Effect of Tapering Ratio (u) on Mid-span Deflection for Steel Curved Beam when Angle of Curvature Equal 25° .

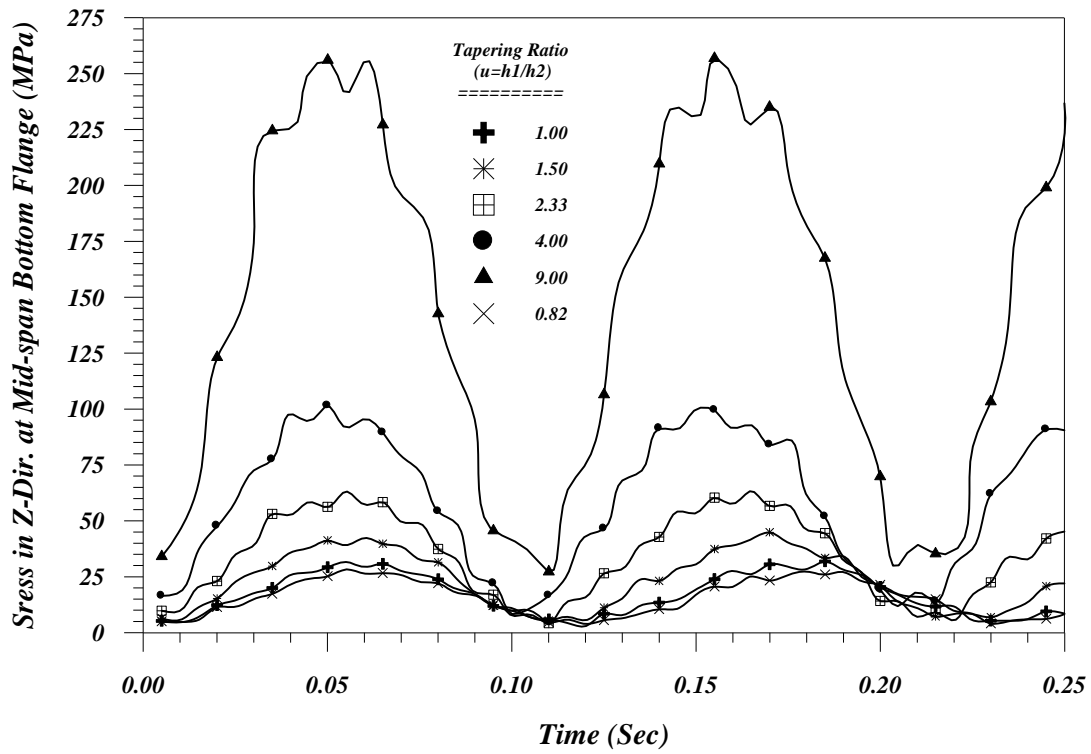


Fig.(9-18): Effect of Tapering Ratio (u) on Stress in Z-Direction for Steel Curved Beam when Angle of Curvature Equal 45°.

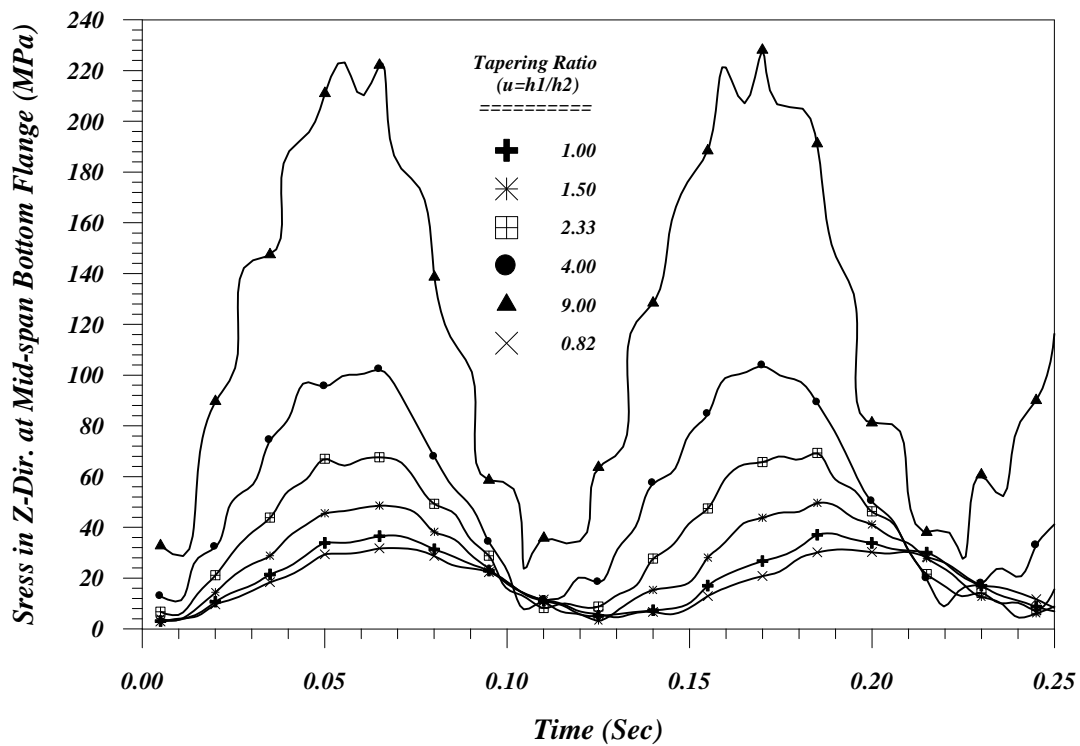


Fig.(9-19): Effect of Tapering Ratio (u) on Stress in Z-Direction for Steel Curved Beam when Angle of Curvature Equal 65°.

9-3-2: Effect of Curvature and Tapering Ratio on the Dynamic Response of Horizontally Curved Reinforced Concrete Beam

A horizontally curved fixed-ended reinforced concrete beam presented previously in chapter eight paragraph 8-4-2 page 137 will be studied here. The properties, load conditions and all analytical parameters are as taken previously. The depth of the beam will be changed along the span, but the volume of concrete is still constant. The effect of tapering ratio will be studied for three magnitudes of curvatures ($\beta = L/R = 40^\circ, 60^\circ$ and 80°) but the length of the beam is still constant, thus the radius of curvature will be ($R=8595, 5730$ and 4297.5 mm) respectively. Figures (9-20), (9-21) and (9-22) show the sensitive effect of non-prismatic geometry on the dynamic response of these curved beams and reveal that the optimal value of tapering ratio for all studied curvatures is equal to nine. This optimal tapering ratio reduces the amplitude of deflections under the loads 51.3%, 43.6%, and 63.7% for ($\beta = 40^\circ, 60^\circ$ and 80°) respectively and the time period is reduced also by 14.61% and 11.62% for $\beta = 40^\circ$ and 60° respectively. As shown, the beam still gives stiffening when the depth at mid-span (h_2) decreases and depth at ends (h_1) increases until the depth at mid-span reaches to a minimum value.

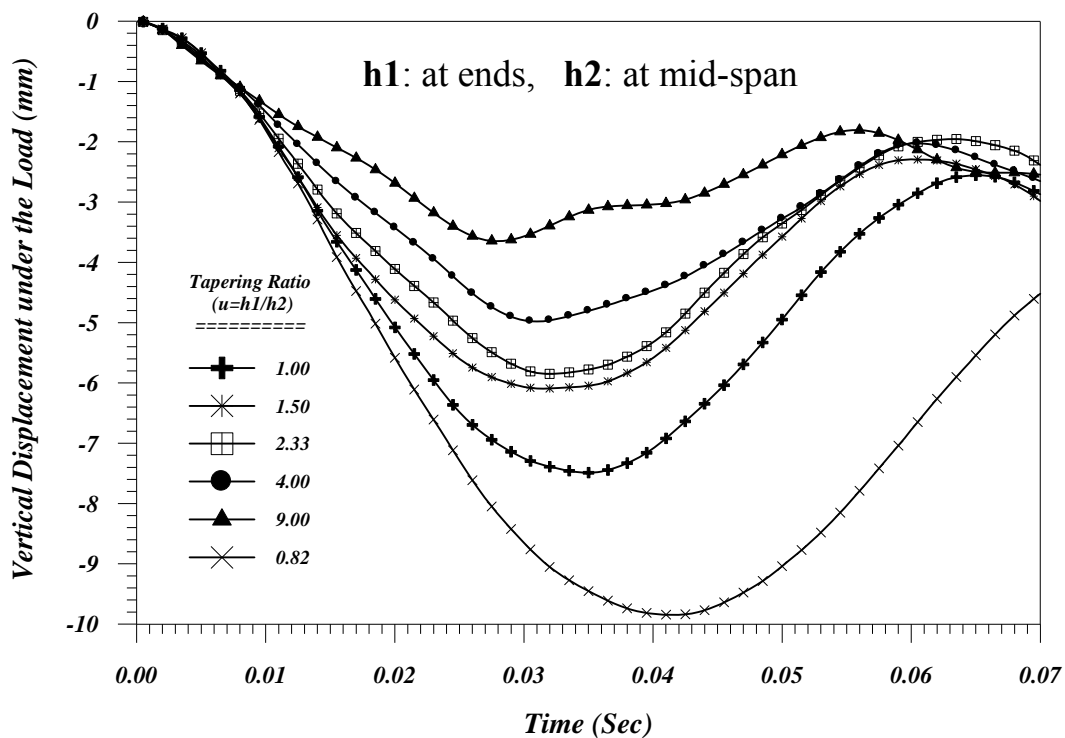


Fig.(9-20): Effect of Tapering Ratio (u) on Deflection under Load for Reinforced Concrete Curved Beam when Angle of Curvature = 40° .

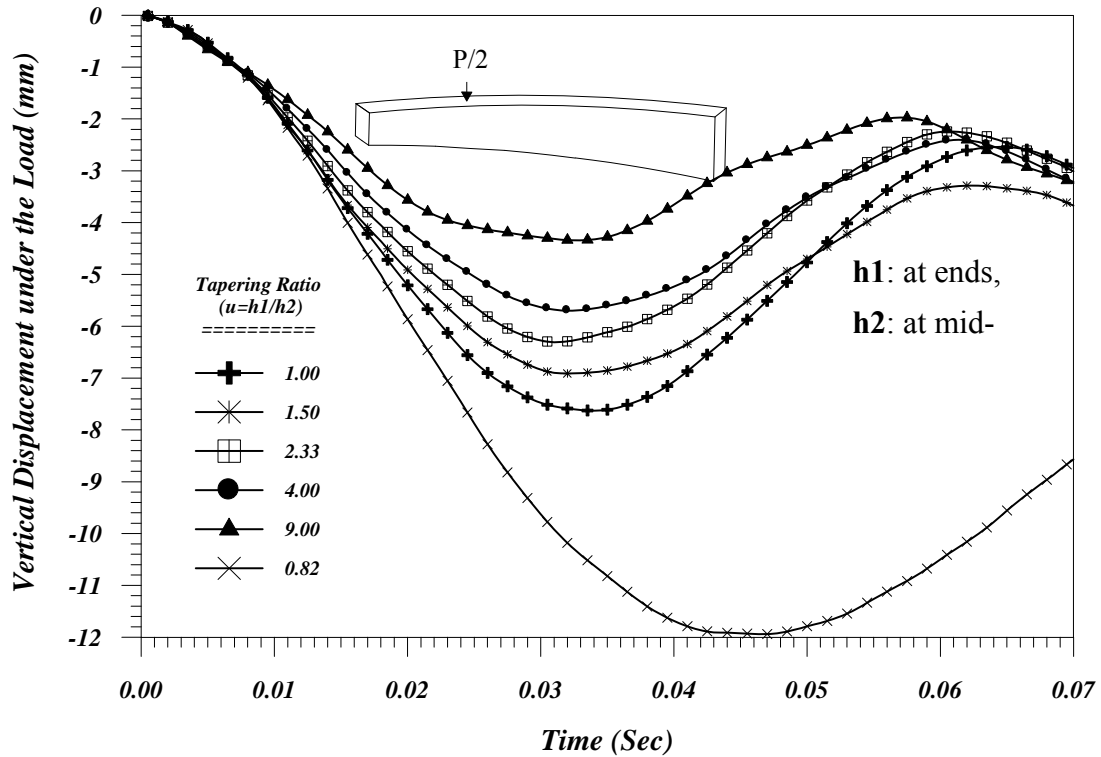


Fig.(9-21): Effect of Tapering Ratio (u) on Deflection under Load for Reinforced Concrete Curved Beam when Angle of Curvature = 60° .

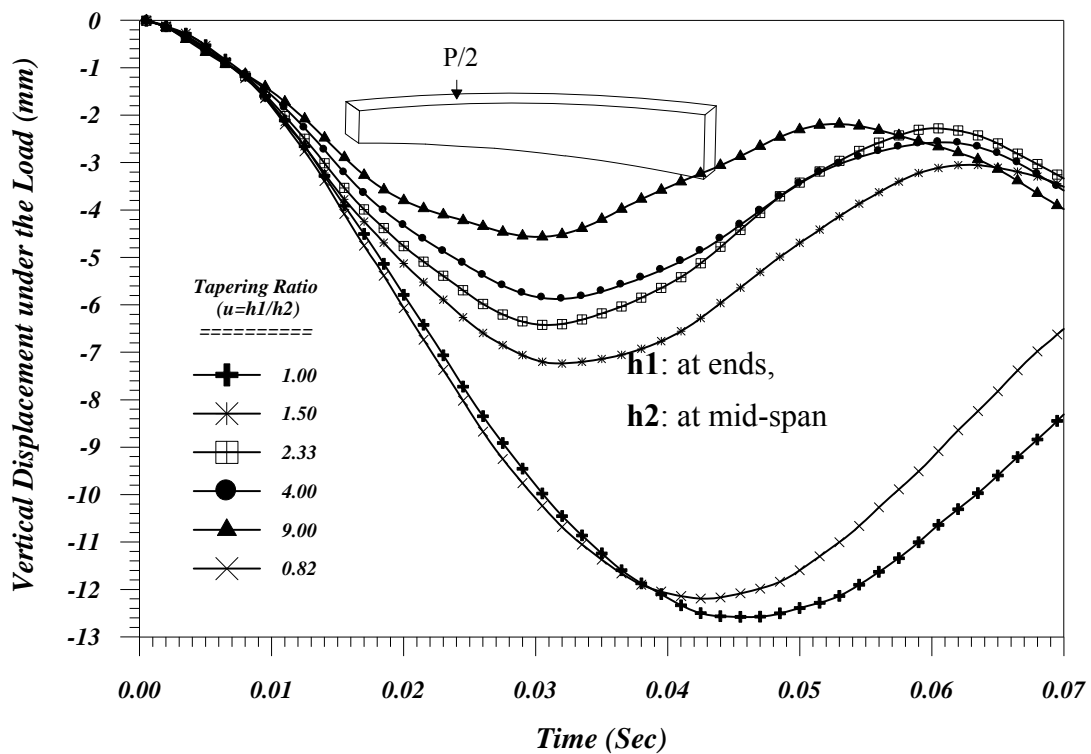


Fig.(9-22): Effect of Tapering Ratio (u) on Deflection under Load For Reinforced Concrete Curved Beam when Angle of Curvature = 80° .

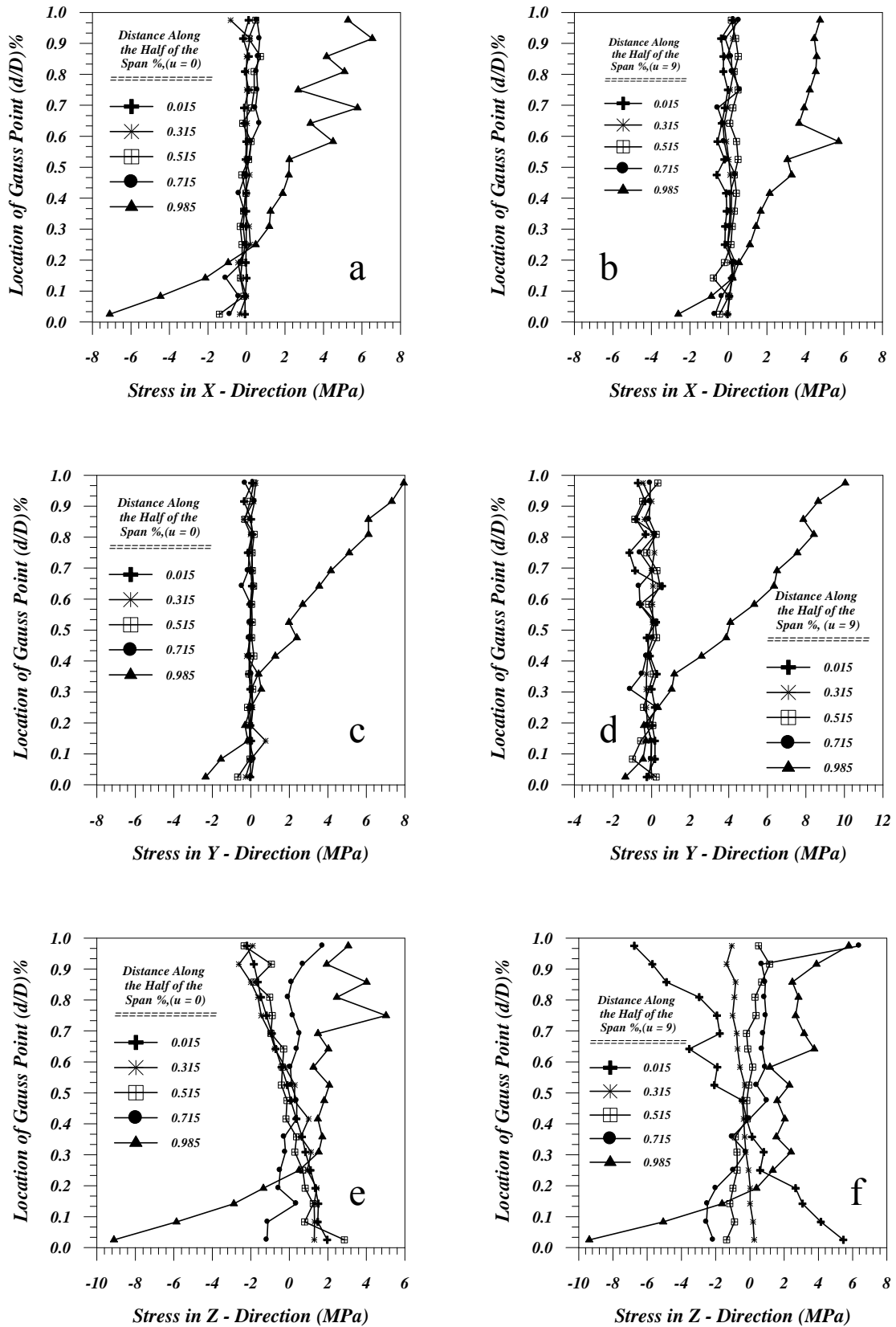


Fig.(9-23): Distributions of Stresses Near the Centerline of Fixed-Ended Reinforced Concrete Curved Beam for $u = 0$ and 9.

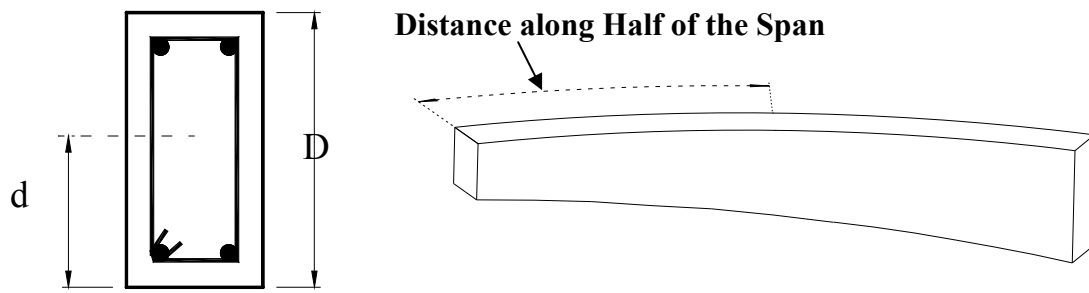


Fig.(9-24): Useful Details.

As mentioned previously due to symmetry, half of the beam had been analyzed. For this half of the span the stress distributions in X, Y, and Z- directions across the section and along the span are presented in Fig.(9-23) for prismatic ($u = 0$) and non-prismatic ($u = 9$) curved beams and for angle of curvature equal to 80° . As shown in Fig.(9-23) the values of stresses in X and Y-directions are approximately constant along the span (half of span) as well as across the depth of section except near the fixed end where the stresses in X-direction reached 6 MPa near the top surface, to -8 MPa near the bottom surface for the prismatic curved beam Fig.(9-23-a) and to about 5 MPa near the top surface and to -2.8 MPa near the bottom surface for the non-prismatic curved beam Fig.(9-23-b).

Also the investigation illustrated that the compressive stress in X-direction near the fixed end is reduced from -7.4MPa for prismatic to -2.4 for $u=9$. This is near centerline while it is reduced to -9.4MPa for prismatic and to -1MPa for $u=9$ at the same location but near the inner face Gauss points as shown in Figures **a** and **b** in Figs.(9-23) and (9-25) respectively. At mid-span the stress in Z-direction is increased in non-prismatic curved beam than in prismatic one at centerline and at inner face as shown in Figures **e** and **f** in Figs.(9-23) and (9-25) respectively.

The optimization in distribution of the volume of material can be illustrated when making a comparison between the curves of non-prismatic curve beam ($u = 9$) Fig.(9-23) b,d,f with the corresponding curves of prismatic curved beam ($u = 0$) Fig.(9-23) a,c,e. One can show the contribution of stresses along the span which is larger in non-prismatic than in prismatic beam especially for Z-direction even for Gauss points near the inner face of the curved beam Fig.(9-25).

However, all graphs in Figs.(9-23) and (9-25) for prismatic curved beam ($u = 0$) are plotted from results at 0.017 sec., while the results of non-prismatic curved beam ($u = 9$) are taken at time 0.0305 sec., because at these different times the

deflection under the loads for prismatic and non-prismatic curved beam is studied equally and having value equal to 4.5mm as shown in Fig.(9-22)

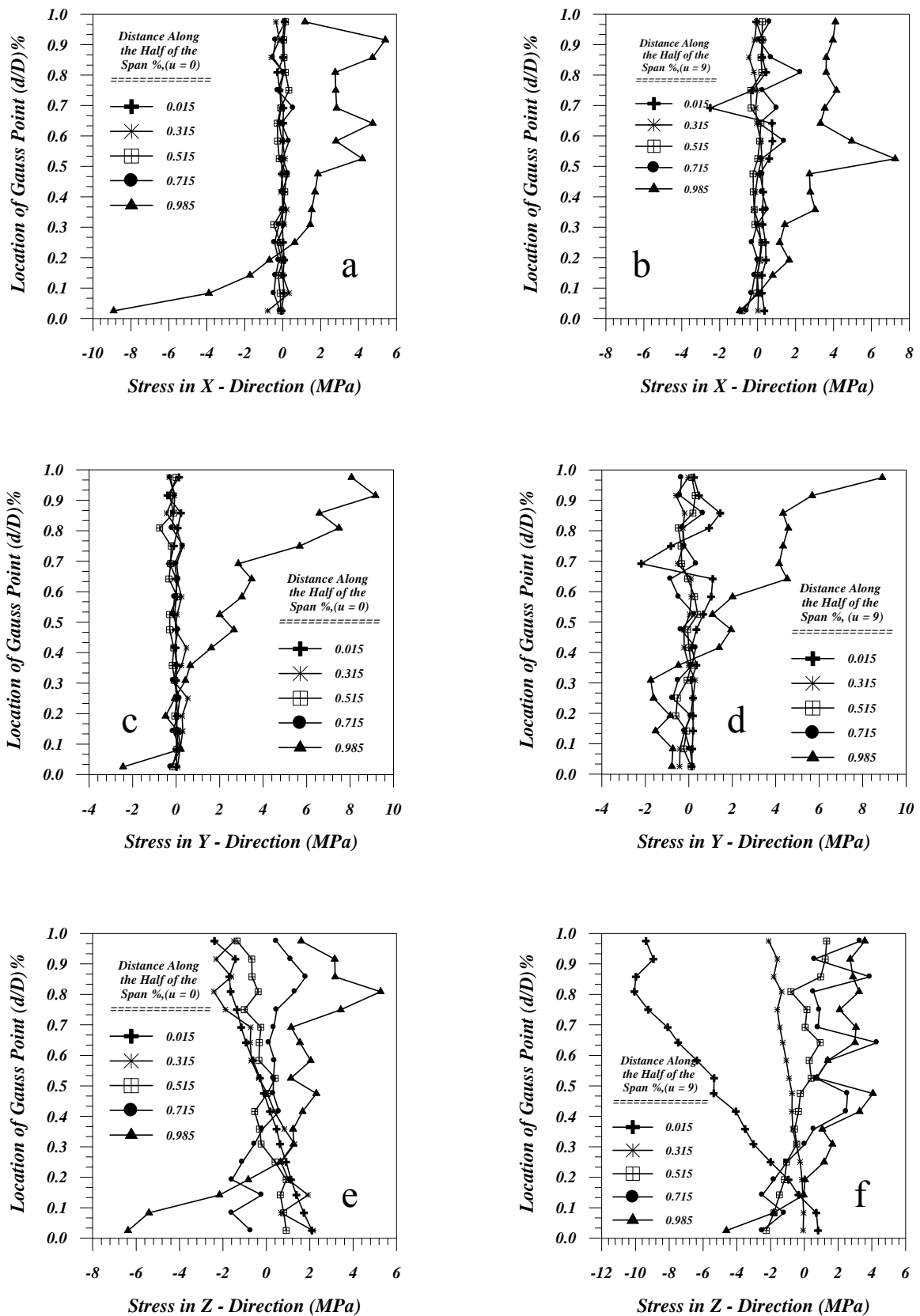


Fig.(9-25): Distributions of Stresses Near the Inner Face of Fixed-Ended Reinforced Concrete Curved Beam for $u = 0$ and 9.

9-3-3: Effect of Curvature and Tapering Ratio on the Dynamic Response of Horizontally Curved Composite Beam

A simply supported composite curved beam presented previously in chapter eight paragraph 8-4-3 page 145 will be considered here with the same properties, load conditions and all analytical parameters. The depth of the steel I-section beam will be changed along the span, but the volume of steel remains constant and the geometry of slab is not changed. The magnitude of the curvature was $\beta = L/R = 12.892^\circ$, here the parametric studies will be conducted on three values of β , 2.892° , 12.892° and 22.892° , however, the length of the beam is still constant. Thus the radius of curvature will be ($R=44.577, 10$ and 5.631 m) respectively. Fig.(9-26) repeats the previous geometry, boundary conditions and dynamic load step adopted in this case study. The nodes (1 to 7) located at support **A** were prevented from movements in all directions, while the nodes (8-14) located at support **B** were restrained in X and Y-directions only. The dynamic response curves for three values of β are presented in Fig.(9-27), for many values of tapering ratios. All these curves show softening in the strength of the curved beam when the tapering ratio is grater than one while the beams show strengthening when the tapering ratio (u) is ≤ 1 . This behavior differs from all the previous non-prismatic parametric studies for steel and reinforced concrete curved beams under static and dynamic loads which demonstrated that the beams give strengthening when (u) is ≥ 1 and vise verse.

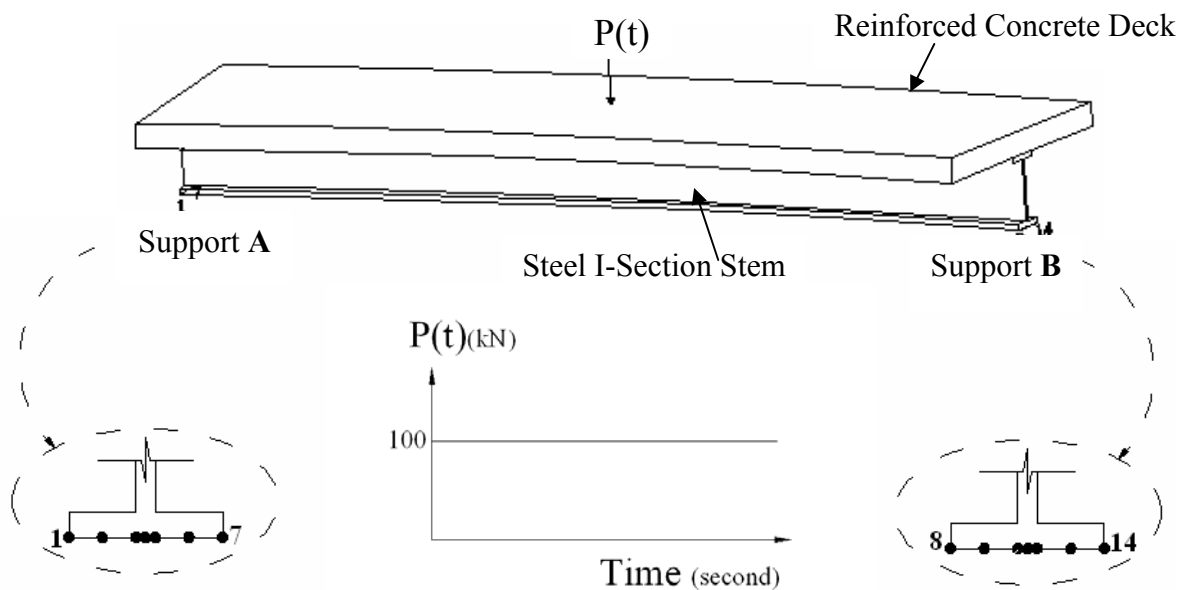
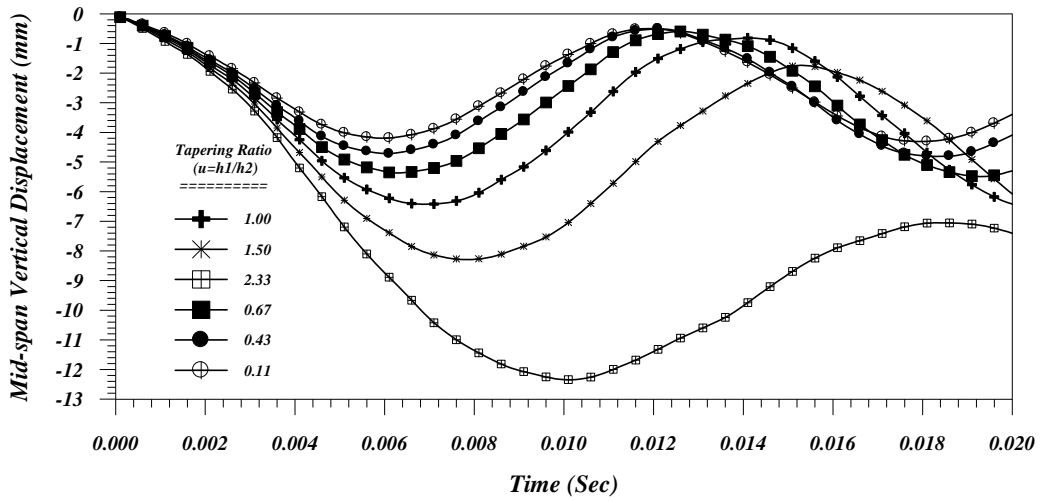
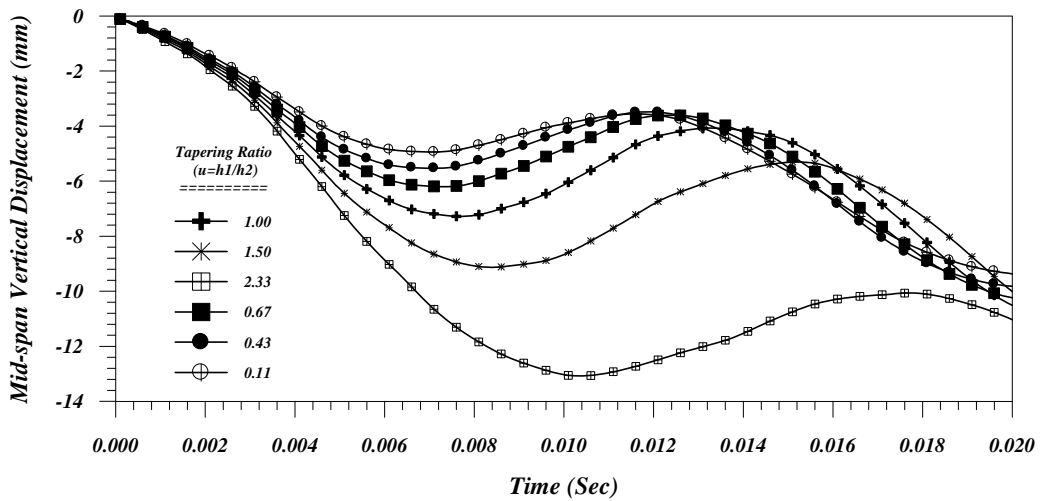


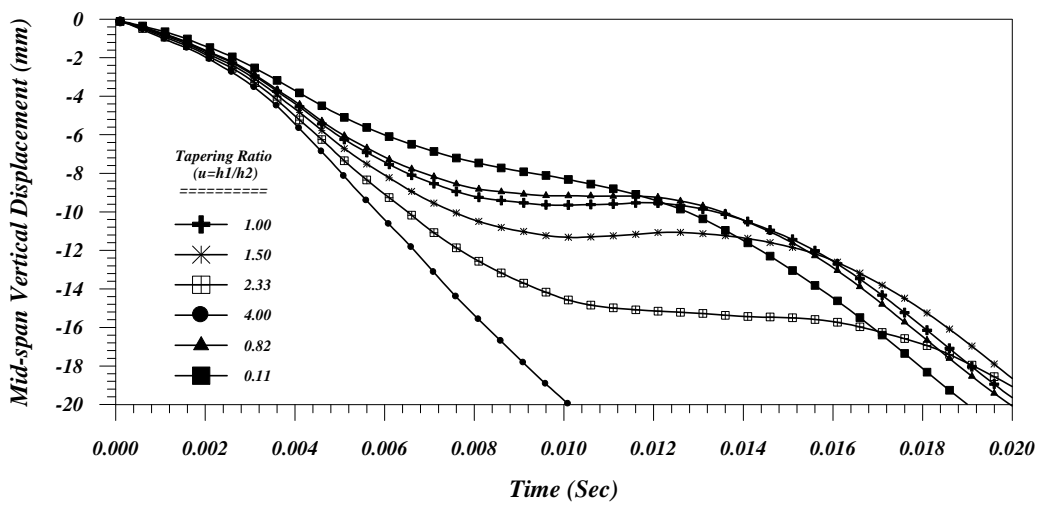
Fig.(9-26): Geometry, Boundary Conditions and Dynamic Load Step for Horizontally Curved Composite Beam.



a) $\beta=2.892^\circ$



b) $\beta=1\ 2.892^\circ$



c) $\beta=2\ 2.892^\circ$

Fig.(9-27): Effect of Tapering Ratio on the Dynamic Response of the Composite Curved Beam, with 14 Nodes Restrained Only.

Fig.(9-27-c) shows softening in the behavior of the beam even for prismatic section. This may be due to unsuitability of restrained conditions with the third angle of curvature 22.892° (small degree of stability). However, the effect of cracks and crush at Gauss points are considered here. The analyses for β equal to 2.892° and 12.892° reveal the optimal tapering ratios (u) equal to 0.11, which reduces the amplitude of deflections at mid-span to 34.6% and 32.1% respectively.

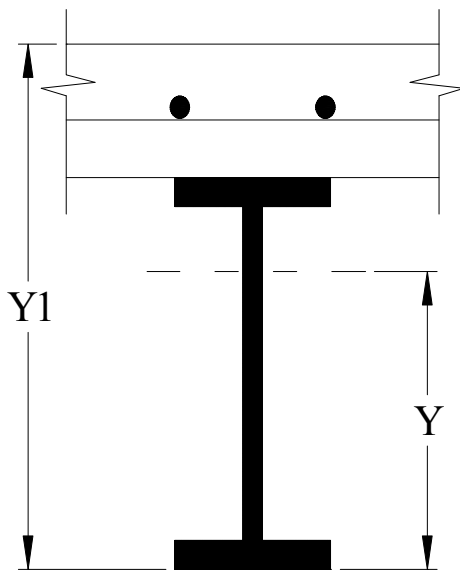


Fig.(9-28): Cross-Section of Composite Curved Beam.

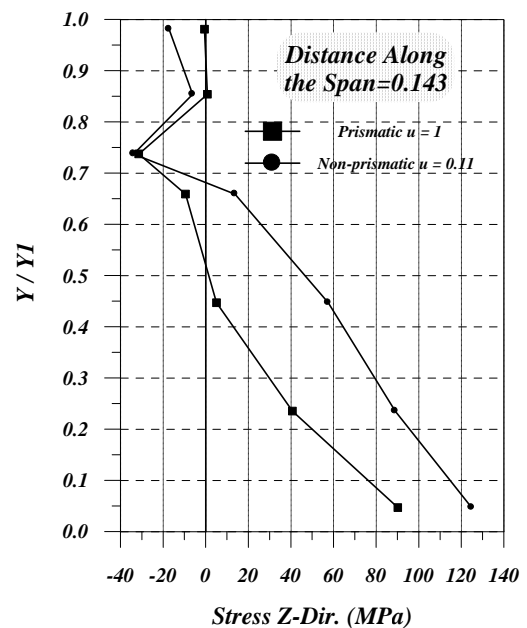


Fig.(9-29): Distribution of Stresses in Z-Direct. at 0.143 along the Span.

The stress distribution curves for stress in Z - direction across the section of the composite curved beam and along the span are presented in Figs.(9-29) to (9-35) which are for angle of curvature β equal to 2.892° for prismatic and non-prismatic beam. The curves of stresses near the supports show that the stresses for non-prismatic beam are larger than the prismatic beam as shown in Figs.(9-29) and (9-35), due to the decrease in the depths at ends. While near $L/4$ and $3L/4$, the inverse occurred. At the mid-span (where the depth of beam is increased) the stresses in non-prismatic beam were lower than the stresses for prismatic beam as shown in Fig.(9-32).

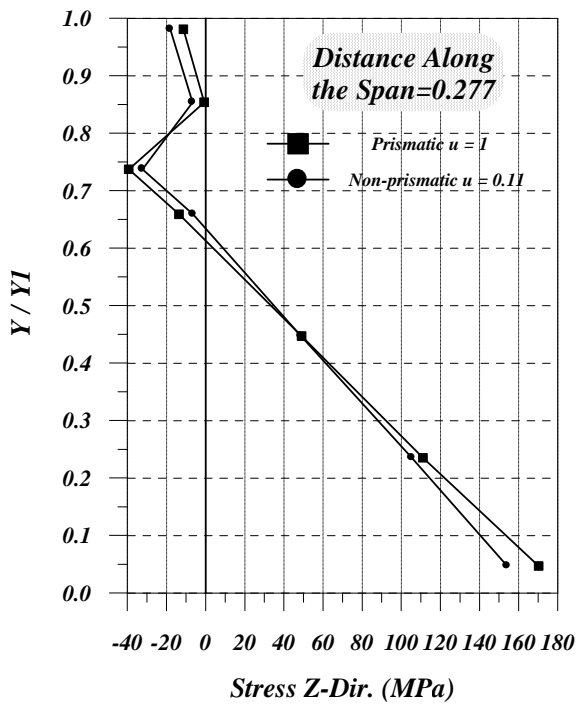


Fig.(9-30): Distribution of Stresses in Z- Dir. at 0.277 along the Span.

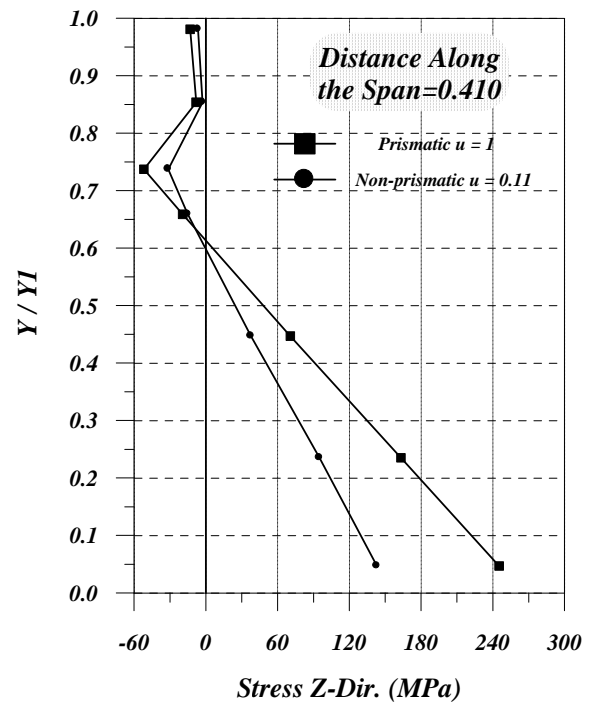


Fig.(9-31): Distribution of Stresses in Z- Dir. at 0.410 along the Span.

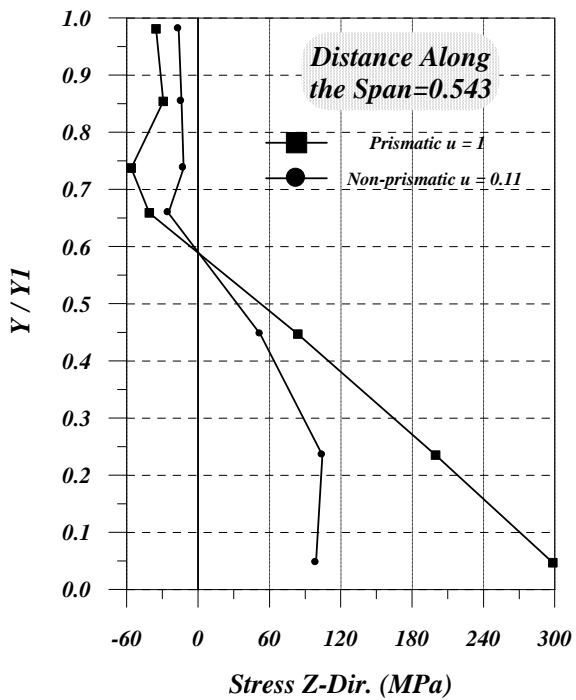


Fig.(9-32): Distribution of Stresses in Z- Dir. at 0.543 along the Span.

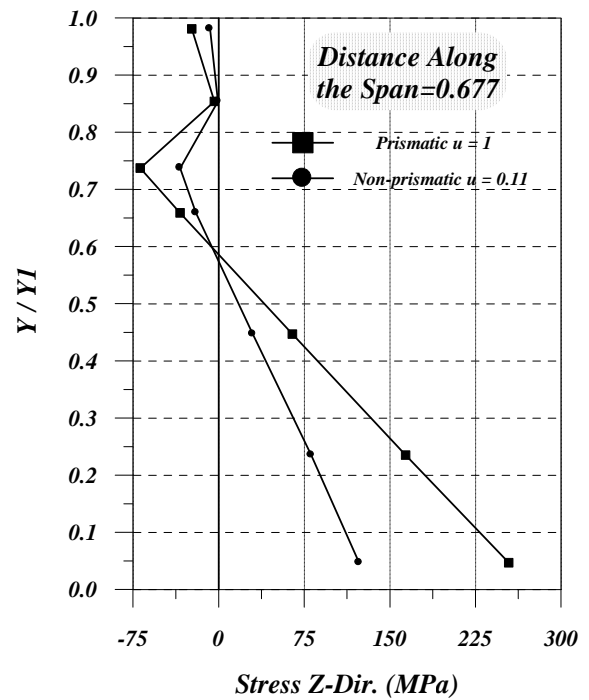


Fig.(9-33): Distribution of Stresses in Z- Dir. at 0.677 along the Span.

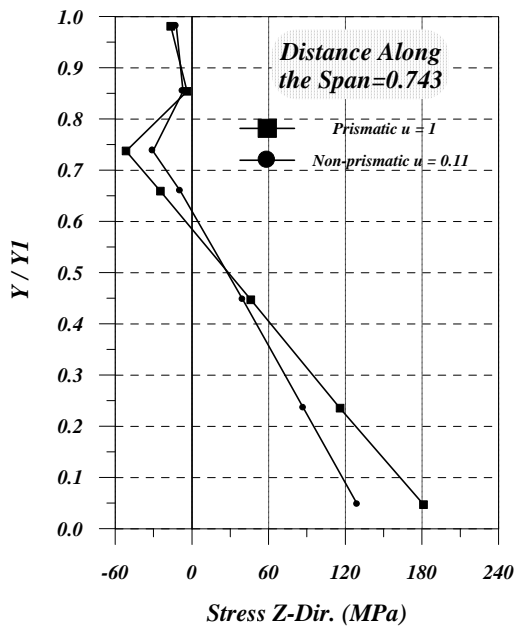


Fig.(9-34): Distribution of Stresses in Z- Dir. at 0.743 along the Span.

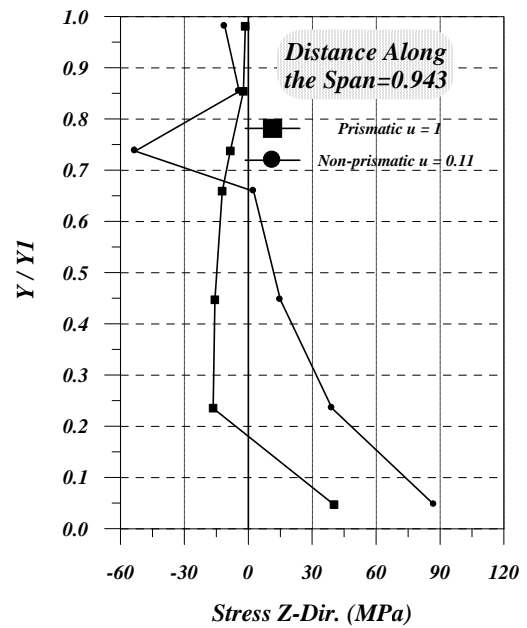


Fig.(9-35): Distribution of Stresses in Z- Dir. at 0.943 along the Span.

The dynamic parametric studies revealed softening in the strength of composite curved beam when the tapering ratio is greater than one and showed strengthening when the tapering ratio (u) is less one. This behavior differs from all the previous non-prismatic parametric studies for steel and reinforced concrete curved beams under static and dynamic loads which demonstrated that the horizontally curved beams gives strengthening when (u) is greater than one.

This behavior showed due to (as the researcher think), when the tapering ratio decreases the depth of steel-I section at ends decreases consequently the vertical distance between the location of the applied load and the restrained nodes (which is located at the bottom surface of the bottom flange) decreases, thus the ability of the adopted composite curved beam to deflect laterally decreases and the beam will be more stable. In another words, the upper flange and deck are not restrained in this case study, hence when the tapering ratio decreases the effectiveness of the membrane action increases due to the decreases in the distance between the applied load and the restraint nodes. As well, the maximum bending moment is at mid span where the section increases when tapering ratio decreases.

Conclusions and Recommendations

10-1: Conclusions

Based on the analytical results obtained in the present study, several conclusions can be drawn and summarized as follows:

10-1-1: Analytical and Representations Parameters

- 1- The convergence study must be done by increasing the number of elements, step by step, until the analysis reaches to the study state, where the difference between the results of the last two meshes is not larger than 1%. The analyses revealed the number of elements of mesh at the study state increases when the angle of curvature increases.
- 2-The suitable tolerance values which can be adopted in the analysis of steel curved beam were found between (0.1%-3%) for displacement criterion and (1%-5%) for force criterion. For static analysis of reinforced concrete curved beam the value of tolerance must be $\leq 0.15\%$ (for displacement criterion) to avoid the accumulative errors, as shown in chapter seven. In the dynamic analysis of reinforced concrete curved beam the value of tolerance must be suitable and compatible with the maximum number of iteration to achieve the convergence without going to the next time step with a big value of errors.

- 3-The modified **Newton-Raphson** method (where the stiffness matrix updated at the first iteration only) represents a good technique for solution of the nonlinear equilibrium equations of static analysis.
- 4-The dynamic results appeared that the fluidity parameters (a_0, a_1) do not effect on the amplitude value of deformation and the time period of the cycle, for horizontally steel curved beam.
- 5-In the static model the optimal value of deficiency in f'_c within the equivalent stress-strain curve was 15%, and the more suitable values of $\alpha_1, \alpha_2, \gamma_1, \gamma_2, \gamma_3$ and ϵ_{ul} were (40-50), (0.2-0.4), 10, 0.5, (0.1-0.12) and 0.0035 respectively. While in the dynamic model the optimal values of a_0, a_1 equal 1.539, 0.971 for steel, and 0.405, 0.831 for concrete as recommended by [6], also the optimal value of α_1 in the viscoplastic dynamic model was 1, i.e., elastic-perfect plastic model.
- 6-The time step recommended by [6] (Eg.(6-33), page 93) can not be applicable for horizontally curved beam (steel, concrete and composite).

10-1-2: Steel Curved Beam

- 1-The nonlinear finite element models **NFHCBSL** and **NFHCBDL** presented in this study had been successfully used to predict the elasto-plastic behavior of the steel curved beam under static or dynamic loads. With respect to static analyses the numerical results were in a good agreement with the experimental data through of the entire range of loading, and the maximum difference between the **NFHCBSL** results and the available experimental results was 2.7% (see Fig.(7-12),page 106). In the dynamic analysis the maximum difference between the results of the present model **NFHCBDL** and the results of **ANSYS** was 5.1% in the displacement and 8.9% in the stress (see Fig.(8-4) and Fig.(8-5),page 132) at the critical section. These results demonstrate obviously the validity of the present models to analysis the steel curved beams.
- 2-The results of **NFHCBSL** (containing 135 solid brick elements) were more accurate than the results of the **ABAQUS** (containing 624 shell elements). This is of course due to the assumption of uniform distribution of transverse shear strains through the thickness as well as the assumption of the plane stress adopted in the plate analysis.

- 3-The static and dynamic analyses for steel curved beams demonstrated that when tapering ratio was larger than one (i.e., depth at ends increased and at mid-span decreased) the beams give increments in strength and vice versa.
- 4-The increment in the ultimate load due to the non-prismatic sections increased with the angle of curvature, the increment was 3.3% for ($\beta=14.325^\circ$), and reached to 25% for ($\beta=37.242^\circ$). Also the optimal tapering ratio α increased with the angle of curvature (see Table(9-1), page 157).
- 5-The results of analysis revealed the important effect of tapering ratio on the strength of the fixed-ended steel curved beam. The benefit from non-prismatic section increased with angle of curvature and the increments in the ultimate strength equal to 8.79%, 77.24% ,101.85% for $\beta=14.325^\circ$, 37.242° , 57.286° respectively (see Table(9-2), page 162).
- 6-The sensitive effect of ends restrained reveal as a result of comparison between the results of the ultimate strength loads of the prismatic simply supported curved beam with results of fixed ended of the same curved. For ($\beta=14.325^\circ$, 37.242° , 57.286°) the ultimate loads for simply supported curved beam were (154, 72, 58 kN) respectively, while for the same curved steel beam when the ends restrains transformed to fixed the ultimate loads were (455, 307.5, 270 kN) respectively, i.e., the increments were (199.4%, 327.1%, 365.5%) respectively. As appeared the sensitivity of ends restrains increased with the angle of curvature (see page 161 and 162).
- 7- The dynamic results proved that the normal stresses in the Z-direction represent the critical component of stresses at the mid-span bottom flange of the steel curved beams for all angles of curvature had been studied.
- 8-The dynamic parametric studies for the studied steel curved beam appeared that the range of the optimal tapering ratio (3 to 4) which achieved decrement in the amplitude deflection reached to 19.8%.

10-1-3: Reinforced Concrete Curved Beam

- 1-According to the examples studied, the current models *NFHCBSL* and *NFHCBDL* presented in this work have been successfully used to predict the elasto-plastic behavior of the reinforced concrete curved beam under static or dynamic load. The maximum difference between the static analytical results and the experimental data at the ultimate loads was 3.2% (see Fig.(7-43),page 122). In the dynamic analysis the maximum differences between the results of the present model *NFHCBDL* and the results of *ANSYS* were 1.5% in the amplitude mid-span deflection and 18% stress (see Fig.(8-14) and Fig.(8-15), page 139 and 140 respectively). These results proved the validity of the present models to analyze the reinforced concrete curved beams.
- 2-The static and dynamic analysis for reinforced concrete curved beams demonstrated that when tapering ratio is larger than one (i.e., depth at ends increased and at mid-span decreased) the beam gives increment in strength and vice verse.
- 3-For the same volume of concrete the benefit from non-prismatic affect increased with the angle of curvature, where the increments in the ultimate strength were equaled to 16.0%, 59.6%,91,3% for angles of curvature equal to 23°,43°, 63° respectively, (as shown in Table(9-4), page 165).
- 4-When the effect of crushing ignored the difference between the analytical predicted ultimate loads and the experimental data increased from 2.5% to 15.4% for *Badawy* curved beam and from 0% to 40% for *Jordaan* curved beam (see Fig.(7-17) and Fig.(7-30), page 110 and 116 respectively). Of course the consideration of phenomena of crushing decreased the predicted ultimate load.
- 5-The dynamic stresses analysis along the span illustrated that the normal stress σ_z is larger than σ_y and the last is larger than σ_x . Also the same result achieved in the static analysis, as well as the contour dynamic results reveal that τ_{xz} represent relatively the critical shear stress especially near the supports.
- 6-Results of the dynamic parametric studies proved that the fixed-ended reinforced concrete curved beam still appeared strengthening when tapering ratio increased for any values of curvature and the decrement in the amplitude deflections under

the loads reached to 51.3%, 43.6%, 63.7% for ($\beta = 40^\circ, 60^\circ$ and 80°) respectively (as shown in Fig.s(9-20) to (9-22), pages 170 to 172) .

10-1-4: Composite Curved Beam

- 1-The analytical investigation demonstrated that the dynamic model *NFHCBDL* presented in this work has been successfully used to predict the elasto-plastic dynamic response of the composite curved beam, whence the maximum differences in the results of the present model *NFHCBDL* and the results of *ANSYS* were 1.85% in the amplitude mid-span deflection and 7.4% in the stresses of Z-direction under the load. (see Fig.(8-24) and Fig.(8-26), page 147 and 149 respectively). These results proved the validity of the present models to analysis the composite curved beams.
- 2-The dynamic parametric studies for composite curved beam demonstrated, when the tapering ratio larger than one (i.e., depth at ends increased and at mid-span decreased) the beam gives softening effect not stiffening and vice verse, inverse situation of the steel and concrete non-prismatic curved beams.
- 3-When considered the effects of cracking and crushing the amplitude mid-span deflection increased about 23.4% and the period time required for the one cycle increased also about 14.9%, as shown in Fig.(8-24), page 147.
- 4-The stresses in the Z-direction represent the critical component and this stress for gauss points near the centerline and located at level , about, $(Y/YI) \geq 0.7$ suffers from compression of stresses while other gauss points (near the centerline) are under tensile stresses, (see Fig.(8-27), page 150). Also the critical section along the span is located at 0.41 along the span (from the lift end of the beam).
- 5-The numerical investigation of stresses cross the width of deck slab revealed that the stresses at the outer edges were always larger than the stresses at the inner edges for all sections except the section having position along the span equal to 0.143. According to these stresses the critical section along the span located at 0.41 along the span (from the lift end of the beam), and the critical location of stresses along the width of slab located at $(W/WI=0.74)$.

10-2: Recommendations

The following recommendations and suggestions can be considered as an extension for present study:

- 1-The current analytical dynamic results required to be supplemented by experimental results obtained from tests on model or full scale horizontally curved beams (steel, concrete and composite).
- 2-The present study was concerned mainly with the effect of material non-linearity. A promising field for extending this work to including the geometrical non-linearity.
- 3-In order to get more accurate results of composite curved beam interface, elements can be considered such as shear connectors between the steel stem and concrete deck.
- 4-Modern researches of the horizontally curved beam toward studying the behavior of beam under moving track loads, thus one can transform the type of loading to be moving along the span of beam.
- 5-Due to the big volume of work the effect of damping on the dynamic response is not studied in this thesis although it is considered in the dynamic model, thus a future work can be done to appear this effect.
- 6-The investigation of the effective width of the continuous multi-span horizontally composite curved beam represents an important research that can be studied if the interface elements are considered in the static and dynamic model.
- 7-The time of run in some applications reached to about 15 hours, to overcome this problem the line search technique can be considered.
- 8-To give complete and obvious analytical pictures about the important effect of lateral restrains on the static behavior and dynamic response of horizontally curved beams many parametric studies must be done.

References

- 1- **De Saint-Venant B.** Me´moire sur le calcul de la r´esistance et de la flexion des pi`eces solides a` simple ou a` double courbure, en prenant simultane´ment en consideration les divers efforts auxquels elles puevent eˆtre soumise dans tous les sens. CR Acad Sci Paris 1843;XVII(942):1020–31. (Cited in Ref.[]).
- 2- **Al-Shaarbaf, I. A. S.**, “Three-Dimensional Nonlinear Finite Element Analysis of Reinforced Concrete Beams in Torsion”, Ph.D. Thesis University of Bradford, 1990.
- 3- **Al-Thebhawi, H. W. A.**, “Nonlinear Finite Element Analysis of Composite Steel -Concrete Beam”, Ph.D Thesis, University of Technology-Baghdad, September 2005.
- 4- **Haidar, A. A. H.**, “Three-Dimensional Nonlinear Finite Element Analysis of Reinforced Concrete Horizontally Curved Deep Beams”, M.Sc. Thesis University of Kufa, August, 2005.
- 5- **Cervera, M., Hinton, E., and Hassan, O.**, “Nonlinear Analysis of Reinforced Concrete Plate and Shell Structures Using 20-Noded Isoparametric Brick Elements”, Journal of Computers & Structures, Vol.25, No. 6, pp. 845-869, 1987.
- 6- **Cervera, M., Hinton, E., Bonet, J., and Bicanic, N.**, “Nonlinear Transient Dynamic Analysis of Three Dimensional Structures - A Finite Element Program For Steel and Reinforced Concrete Materials”, pp. 320-550.in Hinton E. Book’s, “Numerical Methods and Software for Dynamic Analysis of Plates and Shell”,Prinerdge Press, 550, pages, 1988, ISBN, 0-906674-48-4.
- 7- **ANSYS Standard User’s Manual Version 5.4**, CA&SI, 2004 S. Wright Street, Urbana, IL 61821, Ph (217)244-7875, Fax (217)244-7874.
- 8- **Nilson, A. H.**, “Nonlinear Analysis of Reinforced Concrete by the Finite Element”, Journal of ACI, pp. 757-766, September, 1968.
- 9- **Mondkar, D. P., and Powell, G. H.**, “Finite Element Analysis of Non-Linear Static and Dynamic Response”, International Journal for Numerical Methods in Engineering, Vol. 11, pp. 499-520, 1977.
- 10- **Bathe, K. J., and Ramaswamy, S.**, “On Three Dimensional Nonlinear Analysis of Concrete Structures”, Journal of Nuclear Engineering and Design, 52(1979), pp. 385-409.

References

- 11-**Bathe, K. J.**, Massachusetts Institute of Technology Report 82448-1 (1977).
- 12-**Arizumi, Y., Hamada, S., and Kajita T.**, “Elasti-Plastic Analysis of Composite Beams with Incomplete Interaction by Finite Element Method”, *Journal of Computers & Structures*, Vol. 14, No. 5-6, pp. 453-462, 1981.
- 13-**Chajes, A., and Charchill, J. E.**, “Non-Linear Frame Analysis by Finite Element Method”, *Journal of Structural Engineering*, ASCE, Vol. 113, No. ST6, pp. 1221-1235, June, 1987.
- 14-**Davidson, J. S., Keller, M. A., and Yoo, C. H.**, “Cross-Frame Spacing and Parametric Effects in Horizontally Curved I-Girder Bridges”, *Journal of Structural Engineering*, ASCE, Vol. 122, No. 9, September, 1996.
- 15-**Simpson M. D.**, “Analytical Investigation of Curved Steel Girder Behaviour”, Ph.D. Thesis, University of Toronto, Copyright by Michael D. Simpson, 2000. From Internet (<http://adt.caul.edu.au>).
- 16-**Al-Sherrawi, M. H. M.**, “Shear and Moment Behavior of Composite Concrete Beams”, Ph. D. Thesis, University of Baghdad, Iraq, 2001.
- 17- **Oesterblom, I.**, “Bending and Torsion in Horizontally Curved Beams”, *Journal ACI*, Vol. 29, pp.597-606, November, 1932.
- 18-**Chu, K., and Thelen, A.**, “Plastic Analysis of Circular Balcony Girders”, *Journal of Struc. Divi. ASCE*, Vol. 89, No. ST6, pp. 159-185, December, 1963.
- 19-**Jordaan, I. J., Khalifa, M. M. A., and McMullen, A. E.**, “Collapse of Curved Reinforced Concrete Beams”, *Journal of ASCE*, Vol.100, No.ST11,Nov. 1974.
- 20-**Badawy, H. E. I., McMullen, A. E., and Jordaan, I. J.**, “Experimental Investigation of the Collapse of Reinforced Concrete Curved Beams”, *Magazine of Concrete Research*, Vol. 29, No. 99, pp. 59-69, June, 1977.
- 21-**Mansur, M. A., and Rangan, B. V.**, “Study of Design Methods for Reinforced Concrete Curved Beams”, *Journal of ACI*, Vol. 78, No. 3,pp.226-231 May-June, 1981.
- 22-**Hsu, T. T. C., and Burton, K. T.**, “Design of Reinforced Concrete Spandrel Beams”, *Proceedings, ASCE*, Vol. 100, ST3, pp. 209-229, 1974.
- 23-**Mansur, M. A., and Rangan, B. V.**, “Torsion in Spandrel Beams”, *Proceedings, ASCE*, Vol. 104, ST7, pp. 1061-1075, July, 1978.
- 24-**Kaoru, H., Seizo, U., and Yasushi, H.**, “Shear Lag Analysis and Effective Width of Curved Girder Bridges”, *Journal of Engineering Mechanics*, Vol. 111, No. 1, pp. 87-92, January, 1985.
- 25-**Kano, T.,Usuki, S., and Hasebe, K.**, “Theory of Thin-Walled Curved Member with Shear Deformation”, *Ingenieiu-Archiv*, 51, 1982.

References

- 26-**Hsu, Y. T., Fu, C. C., and Schelling, D. R.**, “An Improved Horizontally Curved Beam Element”, *Journal of Computers & Structures*, Vol. 34, No. 2, pp.313-318, 1990.
- 27-**Shanmugam, N. E., Thevendran, V., Richard Liew, J. Y., and Tan, L. O.**, “Experimental Study on Steel Beams Curved in Plan”, *Journal of Structural Engineering*, *Journal of ASCE*, Vol. 121, No. 2, pp. 249-259, February, 1995.
- 28-**ABAQUS Standard User’s Manual Version 4.8**, (1985), **Hibbit, Karlsson and Sorensen Inc.**, abaqus, Pawtucket, R. I.
- 29-**Khaled, S., and John, B. K.**, “Shear Distribution in Simply-Supported Curved Composite Cellular Bridges”, *Journal of Bridge Engineering*, Vol. 3, No. 2, pp. 47-55, May, 1998.
- 30-**Thevendran, V., Chen, S., Shanmugam, N. E., and Richard Liew, J. Y.** (1999), “Nonlinear Analysis of Steel-Concrete Composite Beams Curved in Plan”, *Journal of Finite Elements in Analysis and Design*, 32(3), pp.125-139.
- 31-**Khaled, S., and John, B. K.**, “Simply Supported Curved Cellular Bridges: Simplified Design Method”, *Journal of Bridge Engineering*, Vol. 4, No. 2, pp. 85-94, May, 1999.
- 32-**Zureick, A., Linzell, D., Leon, R.T., and Burrell, J.**, “Curved steel I-girder bridges: experimental and analytical studies”, *Journal of Engineering Structures*, Vol. 22, pp. 180-190, 2000.
- 33-**Yong-Lin, P., and Bradford, M. A.**, “Strength Design of Steel I-Section Beams Curved in Plan”, *Journal of Structural Engineering*, Vol. 127, No. 6, pp. 639-646, June, 2001.
- 34-**Tan, C. P., and Sore, S.**, “Response of Horizontally Curved Bridge to Moving Load”, *Journal of the Structural Division*, Vol. 94, No. ST9, pp. 2135-2150, September, 1968.
- 35-**Culver, C. G., and Oestel, D. J.**, “Natural Frequencies of Multi-span Curved Beams”, *Journal of Sound and Vibration*, Vol. 10, No. 3, pp. 380-389, 1969.
- 36-**Chaudhuri, S. K., and Shore, S.**, “Dynamic Analysis of Horizontally Curved I-Girder Bridges”, *Journal of the Structural Division*, Vol. 103, No. ST8, pp. 1589-1604, August, 1977.
- 37-**Al-Marroof, M. A.**, “Dynamic Analysis of Curved Members Using Curved Finite Elements”, M.Sc. Thesis, University of Baghdad, September 1987.
- 38-**Laura, P. A. A., Verniere, P. L., Carnicer, R., and Bertero, R.**, “A Note on Vibration of Circumferential Arch with Thickness Varying in a Discontinuous Fashion”, *Journal of Sound and Vibration*, Vol. 120, No. 9, pp. 95-105, 1988.

References

- 39-**Laura, P. A. A., Filipich, C. P., and Cortinez, V. H.**, “In-Plane Vibrations of and Elastically Cantilevered Circular Arc with a Tip Mass”, *Journal of Sound and Vibration*, Vol. 115, pp. 437-446, 1986.
- 40-**Rossi, R. E., Laura, P. A. A., and Verniere, P. L.**, “In-Plane Vibrations of Cantilevered Non-Circular Arcs of Non-Uniform Cross-Section with a Tip Mass”, *Journal of Sound and Vibration*, Vol. 129, No. 2, pp. 201-213, 1989.
- 41-**Ahmad, A. M., and Jaafar, R.**, “Natural Frequencies of Continuous Curved Beams on Winkler-Pasternak Foundation”, *Journal of Engineering and Technology*, Vol. 11, No. 12, pp. 87-101, 1992.
- 42-**Hung, T. C.**, “The Effect of Rotary Inertia and Shear Deformation on The Frequency and Normal Mode Equations of Uniform Beams with Simple End Conditions”, *ASME, Journal of Applied Mechanics*, Vol. 28, pp.579-584, 1961.
- 43-**Issa, M. S., Wang, T. M., and Hsiao, B. T.**, “Extensional Vibration of Continuous Circular Curved Beams With Rotary Inertia and Shear Deformation, I : Free Vibration”, *Journal of Sound and Vibration*, Vol. 114, No. 2, pp. 297-308, 1987.
- 44-**Richardson, J. A., and Douglas, B. M.**, “ Results from Field Testing a Curved Box-Girder Bridge Using Simulated Earthquake Loads”, *Earthquake Engineering and Structural Dynamics*, Vol. 22, No. 10. , 1993.
- 45-**Sengupta, D., and Dasgupta, S.**, “Static and Dynamic Applications of a Five Noded Horizontally Curved Beam Element with Shear Deformation”, *International Journal for Numerical Methods in Engineering*, Vol. 40, No. 10, May, 1997.
- 46-**Dongzhou Huang, P. E.**, “Dynamic Analysis of Steel Curved Box Girder Bridges”, *Journal of Bridge Engineering*, Vol. 6, No. 6, pp. 506-513, November/December, 2001.
- 47-**Standard specifications for highway bridges**, (1996), 16th Ed., AASHTO, Washington, D.C.
- 48-**Maneetes, H., and Linzell, D.G.**, “Cross-Frame and Lateral Bracing Influence on Curved Steel Bridge Free Vibration Response”, *Journal of Constructional Steel Research* 59 (2003) 1101–1117.
- 49-**Al-Dahash, R. F. Y.**, “Nonlinear Dynamic Analysis of Reinforced Concrete Arch Structures By Finite Element Method”, M.Sc. Thesis University of Babylon, December, 2006.

- 50-**Tilley, M. R., Barton, F. W., and Gomez, J. P.**, “Dynamic Analysis and Testing of a Curved Girder Bridge”, Virginia Transportation Research Council, Virginia, May 2006, Report: VTRC 06-R32.
- 51-**SAP2000**-“Dynamics and Earthquake Engineering Finite Element Analysis and Design Software for Structures and Bridges”, www.caepIDhaka.com; www.siberkeley.com; www.computersandstructures.com Tel: 8802 9676 269 Mob: 0152 329243 E-Mail: souren@caepIDhaka.com
- 52-**Hinton, E., and Owen, D. R. J.**, “Finite Element Programming”, Academic Press Inc. Ltd., London, 1977.
- 53-**Al-Refaie, W., and Govel A.**, “Finite Element Methods for Structural Engineers: A Basic Approach”, Wiley Eastern Limited, New Delhi, 1991.
- 54-**Dawe, D.J.**, “Matrix and Finite Element Displacement Analysis of Structures”, Clarendon Press, Oxford, 1984.
- 55-**William, W. J., and Paul, R. J.**, “Structural Dynamic by Finite Elements”, Prentice-Hall, INC., Englewood Cliffs, New Jersey, 1987.
- 56-**Cook, R. D.**, “Concepts and Applications of Finite Element Analysis”, 2nd. Ed., John Wiley and Sons, New York, 1981.
- 57-**Cook, R. D.**, “Remarks about Diagonal Mass Matrix”, International Journal of Numerical Methods in Engineering, Vol. 17, 1427-1429, 1981.
- 58-**Clough, R. W.**, “Analysis of Structural Vibrations and Dynamic Response”, in Recent Advances in Mathematical Methods of Structural Analysis and Design, 441-485, R. H. Gallagher et al. (eds.), University of Alabama Press, 1971.
- 59-**Hinton, E., Rock, T., and Zeinkiewicz, O. C.**, “A Note on Mass Lumping and Related Processed in the Finite Element Method”, Earthquake Engineering and Structural Dynamic, Vol. 4, 246-249, 1976.
- 60-**Shantaram, D., Owen, D. R. J., and Zeinkiewicz, O. C.**, “Dynamic Transient Behavior of Two and Three Dimensional Structures Including Plasticity, Large Deformation Effects and Fluid Interaction”, Earthquake Engineering and Structural Dynamic, Vol. 4, 561-578, 1976.
- 61-**Rock, T., and Hinton, E.**, “Free Vibration and Transient Response of Thick and Thin plates using the Finite Element Method”. (Cited in Ref.[6]).
- 62-**Liu, C. Q.**, “Nonlinear and Transient Finite Element Analysis of General Reinforced Concrete Plates and Shells”, Ph.D. Thesis, University of Wales, Swansea, 1985.
- 63-**Wilson, E. L., and Penzien, J.**, “Evaluation of Orthogonal Damping Matrices”, International Journal of Numerical Methods in Engineering, Vol. 4, 5-10, 1972.

References

- 64-*ASCE* Committee on Concrete and Masonry Structures, "A State of The Art Report on The Finite Element Analysis of Reinforced Concrete", Task Committee on Finite Element Analysis of Reinforced Concrete Structure, ASCE, Sept. Publ., 1981.
- 65-*Khouzan, M.*, "A Finite Element Investigation of Reinforced Concrete Beams", Mechanical Engineering Thesis, McGill University, Montreal, Canada, 1977.
- 66-*Imbabi, M. S.*, "Nonlinear Analysis of Reinforced Concrete Planar Structures", Ph.D. Thesis, University of Liverpool, 1984.
- 67-*Al-Mahaidi, R. S. H.*, "Nonlinear Finite Element Analysis of Reinforced Concrete Deep Members", Report No. 79, Department of Structural Engineering, Cornell University, 1979.
- 68-*Mohamed, M. S.*, "A Finite Element and Experimental Study of Reinforced Concrete in Torsion", Ph.D. Thesis, University of Glasgow, 1986.
- 69-*Phillips, D. V.*, and *Zienkiewicz, O. C.*, "Finite Element Nonlinear Analysis of Concrete Structures", Proceedings, Institution of Civil Engineers, Vol. 61, Part 2, pp. 59-88, 1976.
- 70-*Zienkiewicz, O.C.*, "The Finite Element Method", Third Edition, Mc Graw-Hill, London, 1977.
- 71-*Propoy, S.*, "A Review of Stress-Strain Relationships of Concrete", *ACI Journal* Vol. 67, No.3, pp. 243-248, March, 1970.
- 72-*Gerstle, k.H.*, "Behavior of Concrete under Multi-axial Stress State", *Journal of The Eng., Mech. Div., ASCE.* Vol.106, No.EM6 December, 1980, pp.1383-1403.
- 73-*ACI* Committee 318, "Building Code Requirements for Structural Concrete (ACI 318M-02) and Commentary (ACI 318RM-02)", 2002.
- 74-*Maekawa, K.*, and *Okamura, H.*, "The Deformational Behavior and Constitutive Equation of Concrete Using the Elasto-Plastic and Fracture Model", *Journal of the Faculty of Engineering, University of Tokyo (B)*, Vol. XXXVII, No. 2, 1983.
- 75-*Hughes, B. P.*, and *Chapman, G. P.*, "The Deformation of Concrete and Micro Concrete in Compression and Tension with Particular Reference to Aggregate Size", *Magazine of Concrete Research, London*, Vol. 18, No. 54, pp. 19-24, March, 1966.
- 76-*Chen, W.F.*, "Plasticity in Reinforced Concrete", Third Edition, McGraw-Hill Book Company, 1982.
- 77-*Tasuji, M. E.*, *Slate, F. O.*, and *Nilson, A. H.*, "Stress-Strain Response and Fracture of Concrete in Biaxial Loading", *ACI Journal*, Vol. 75, No. 7, pp. 306-312, July, 1978.

References

- 78-**Domingo, J. C.**, and **Kuang-Han Chu.**, “Stress-Strain Relationship for Reinforced Concrete in Tension”, Journal of ACI, pp.21-28, January-February, 1986.
- 79-**Kupfer, H., Hilsdorf, H.K.**, and **Rusch, H.**, “Behavior of Concrete under Biaxial Stress”, Journal of ACI, Vol.66, No.8, pp.656-666, August 1969.
- 80-**Hyo-Gyoung, K.**, and **Filip C. F.**, “Finite Element Analysis of Reinforced Concrete Structures under Monotonic Loads”, University of California, Structural Engineering Mechanics and Materials, Report No.Ucb/sem-90/14, November, 1990.
- 81-**Owen, D.R.J.**, and **Hinton, E.**, “Finite Elements in Plasticity Theory and Applications”, Pineridge Press, Swansea, U.K, 1980.
- 82-**Arther, P. B.**, and **Richard, J. S.**, “Advanced Mechanics of Materials”, 6th. Ed., John Wiley and Sons, United State of America, 2003.
- 83-**Pognani, T., Slater, J., Aneur-Mosor, R.**, and **Boyukozurk, O.**, “ A Non-linear Three-Dimensional Analysis of Reinforced Concrete Based on Bounding Surface Model”, Computers & Structures, Vol.43, No.1, pp.1-12, 1992.
- 84-**Cope, R. J.**, “Material Modeling of Real Reinforced Concrete Slabs”, Proc. Int. Conf. on Computer Aided Analysis and Design of Concrete Structure, Eds. Damjanic et al., Vol. I, Split, Yugoslavia, pp. 85-117, September, 1984.
- 85-**Clark, L. A.**, and **Speirs, D. M.**, “Tension Stiffening in Reinforced Concrete Beams and Slabs under Short Term Loads”, Tech. Report, Cement and Concrete Associated, London, 1978.
- 86-**Robinson, J. R.**, and **Demorieux, J. M.**, “Essais de Traction-Compression sur Modèles d’âme de Poutre en Béton Armé”, Institute de Recherches Appliquées du Béton Armé (IRABA), Part 1, June 1968 and Part 2, May, 1972.
- 87-**Vecchio, F.** and **Collins, M. P.**, “The Response of Reinforced Concrete to In-Plane Shear and Normal Stresses”, Publication No. 82-03, University of Toronto, Canada, 1982.
- 88-**Cervenka, V.**, “A Constitutive Model for Reinforced Concrete”, Journal of ACI, Vol. 82, pp. 877-882, November-December, 1985.
- 89-**Watstein, D.**, “Effect of Straining Rate on the Compressive Strength and Elastic Properties of Concrete”, ACI Journal, Vol. 24, pp. 729-744, 1953. (Cited in Ref.[6]).

References

- 90-**Hatano, T.**, “Relations between Strength of Failure, Strain Ability Elastic Modulus and Failure Time of Concrete ”, Central Research Institute of Electric Power Industry, C-6001, Tokyo, 1960. (Cited in Ref.[6]).
- 91-**Hatano, T.**, and **Tsutsumi, H.**, “Dynamic Compressive Deformation and Failure of Concrete under Earthquake Load”, Proc. 2nd WCEE, Tokyo, 3, pp. 1963-1978, 1960. (Cited in Ref.[6]).
- 92-**Spooner, D. C.**, “Stress-Strain-Time Relationships for Concrete”, Magazine of Concrete Research, Vol. 23, 73-76, 1971. (Cited in Ref.[6]).
- 93-**Sparks, D. R.**, and **Menzies, J. B.**, “The Effect of Rate of Loading in Plain Concrete”, Magazine of Concrete Research, Vol. 25, 73-80, 1973.
- 94-**Mainstone, R. J.**, “Properties of Material at High Rates of Straining or Loading”, Materials and Constructions, Vol. 8, 102-116, 1975.
- 95-**Hatano, T.**, “Dynamic Behavior of Concrete under Impulsive Tensile Load”, Central Research Institute of Electric Power Industry, C-6002, Tokyo, 1960. (Cited in Ref.[6]).
- 96-**Hatano, T.**, “Dynamic Behavior of Concrete under Periodical Compressive Load”, Central Research Institute of Electric Power Industry, C-6104, Tokyo, 1962. (Cited in Ref.[6]).
- 97-**Hatano, T.**, and **Watanabe, H.**, “Fatigue Failure of Concrete under Periodic Compressive Load”, Transactions JSCE, Vol. 3, pp. 106-107, 1971. (Cited in Ref.[6]).
- 98-**Nelissen, L. J. M.**, “Biaxial Testing of Normal Concrete”, Heron, Vol. 18, No. 1, Delft, 1972. (Cited in Ref.[6]).
- 99-**Bićanić, N.**, “Nonlinear Finite Element Transient Response of Concrete Structures”, Ph.D. Thesis, University of Wales, Swansea, 1978. (Cited in Ref.[6]).
- 100-**Bićanić, N.**, and Zienkiewicz, O. C., “Constitutive Model for Concrete under Dynamic Loading”, Earthquake Engineering and Structural Dynamics, 11, 689 – 710, 1973. (Cited in Ref.[6]).
- 101- **Perzyna, P.**, “Fundamental Problems in Viscoplasticity”, Advanced Applied Mechanics, Vol. 9, pp. 243 – 377, 1966. (Cited in Ref.[6]).
- 102-**Zienkiewicz, O. C.**, **Fejzo, R.**, and **Bićanić, N.**, “Experience in Analyzing Plain Concrete Structures Using a Rate Sensitive Model with Crack Monitoring Capabilities”, Int. Conf. on Constitutive Laws for Engng. Materials, University of Arizona, 1983.

References

- 103-*Nilsson, L.*, and *Oldenburg, M.*, “Nonlinear Wave Propagation in Plastic Fracturing Materials – a Constitutive Modelling and Finite Element Analysis”, IUTAM Symp. on ‘Nonlinear Deformation Waves’, Tallin, 1982.
- 104-*Červenka, V.*, “Constitutive Model for Cracked Reinforced Concrete”, *ACI Journal*, Vol. 82, pp. 877-882, 1985.
- 105-*Hardings, J.*, “Effect of High Strain Rate on the Room-Temperature Strength and Ductility of Five Alloy Steels”, *Journal of the Iron and Steel Institute*, pp. 432-435, 1966.
- 106-*Cook, R. D.*, *Malkus, D. S.*, and *Plesha, M. E.*, “Concepts and Applications of Finite Element Analysis”, 3rd . Edition, John Wiley and Sons, New York, 1989.
- 107-*Dokaniish, M. A.*, and *Subbaraj, K.*, “A Survey of Direct Time Integration in Computational Structural Dynamics-I. Explicit Methods”, *International Journal of Computers and Structures*, Vol. 32, No. 6, pp. 1371-1386, 1989.
- 108-*Newmark, N. M.*, “A Method of Computation for Structural Dynamics”, *Journal Engineering Mechanical Division, ASCE*, Vol. 85, 1959.
- 109-*Hughes, T. J. R.*, and *Belytschko, T.*, “A Precise of Developments in Computational Methods for Transient Analysis”, *Journal of Applied Mechanics*, Vol. 45, pp. 371- 374, 1978.
- 110-*Al-Sarraf, S. Z.*, “Dynamic Analysis by Harmonic Acceleration Method”, be published 1996.
- 111-*Hughes, T. J. R.*, and *Liu, W. K.*, “Implicit-Explicit Finite Elements in Transient Analysis Implementation and Numerical Examples”, *Journal Appl. Mech. Engng.*, Vol. 45, pp.375-378, 1978.
- 112-*Hughes, T. J. R.*, *Pister, K. S.*, and *Taylor, R. L.*, “Implicit-Explicit Finite Elements in Nonlinear Transient Analysis”, *Comp. Meth. Appl. Mech. Engng.*, Vol. 17/18, pp.159-182, 1979.
- 113-*Cormeau, I. C.*, “Viscoplasticity and Plasticity in the Finite Element Method”, Ph.D. Thesis, University of Wales, Swansea, 1976.
- 114-*Tan, L. O.*, *Thevendran, V.*, *Liew, J. Y. R.*, and *Shanmugam, N. E.*, “Analysis and Design of I-Beams Curved in Plan”, *Steel Structure*, Singapore, 3(1), pp. 39-45, 1992.
- 115-*Cope, R. J.*, and *Rao, P.V.*, “Moment Redistribution in Skewed Slab Bridges”, *Proc. In Structural Civil Engineering*, Vol. 75, pp. 419-452, 1983.
- 116-*Gupta, A. K.*, and *Akber, A.*, “Cracking in Reinforced Concrete Analysis”, *Journal of Structural Division, ASCE*, Vol. 110, pp. 1735-1746, 1984.

Appendix (A)

Derivation of the Strain-Displacement Relationship for the Reinforcement Bars [2]

Since, the bar is capable of transmitting axial forces only; one component of strain contributes to the strain energy, which is defined locally as:

$$\varepsilon' = \partial u' / \partial x' \quad \dots\dots\dots(A-1)$$

where x', y', z' , are defined as local coordinates system at any point p with y', z' , being normal to the line of the bar and u', v', w' , are the corresponding displacements.

A distortion matrix S at any point p is defined as:

$$S = \begin{bmatrix} \partial u / \partial x & \partial v / \partial x & \partial w / \partial x \\ \partial u / \partial y & \partial v / \partial y & \partial w / \partial y \\ \partial u / \partial z & \partial v / \partial z & \partial w / \partial z \end{bmatrix} = \sum_{i=1}^{20} \begin{bmatrix} \partial N_i / \partial x \\ \partial N_i / \partial y \\ \partial N_i / \partial z \end{bmatrix} [u_i \quad v_i \quad w_i] \quad \dots\dots\dots(A-2)$$

Substitution of Eq.(3-24) into Eq.(A-2) yields:

$$S = \sum_{i=1}^{20} [J]^{-1} \begin{bmatrix} \partial N_i / \partial r \\ \partial N_i / \partial s \\ \partial N_i / \partial t \end{bmatrix} [u_i \quad v_i \quad w_i] \quad \dots\dots\dots(A-3)$$

As S is a second order tensor, it transforms on coordinate rotation from x, y, z , to r, s, t , according to:

$$S' = \begin{bmatrix} \partial u' / \partial x' & \partial v' / \partial x' & \partial w' / \partial x' \\ \partial u' / \partial y' & \partial v' / \partial y' & \partial w' / \partial y' \\ \partial u' / \partial z' & \partial v' / \partial z' & \partial w' / \partial z' \end{bmatrix} = R S R^T \quad \dots\dots\dots(A-4)$$

where R is the rotation matrix of direction cosines at point p defined as:

$$\mathbf{R} = \begin{bmatrix} \partial x / \partial x' & \partial y / \partial x' & \partial z / \partial x' \\ \partial x / \partial y' & \partial y / \partial y' & \partial z / \partial y' \\ \partial x / \partial z' & \partial y / \partial z' & \partial z / \partial z' \end{bmatrix} \quad \dots\dots\dots(\text{A-5})$$

As x' and r coincide and differ only in magnitude;

$$\mathbf{R} = \frac{1}{h} \begin{bmatrix} \partial x / \partial r & \partial y / \partial r & \partial z / \partial r \\ \partial x / \partial r & \partial y / \partial r & \partial z / \partial r \\ \partial x / \partial r & \partial y / \partial r & \partial z / \partial r \end{bmatrix} \quad \dots\dots\dots(\text{A-6})$$

where ,

$$\begin{aligned} C_1 &= (\partial x / \partial r)^2 \\ C_2 &= (\partial x / \partial r) / (\partial y / \partial r) \\ C_3 &= (\partial x / \partial r) / (\partial z / \partial r) \end{aligned} \quad \dots\dots\dots(\text{A-7})$$

$$\begin{aligned} C_4 &= (\partial y / \partial r)^2 \\ C_5 &= (\partial y / \partial r) / (\partial z / \partial r) \\ C_6 &= (\partial z / \partial r)^2 \\ h &= \sqrt{C_1^2 + C_4^2 + C_6^2} \end{aligned} \quad \dots\dots\dots(\text{A-8})$$

From Eq.s (A-1), (A-4) and (A-6), it is obtained that:

$$\{\varepsilon'\} = \sum_{i=1}^n \left[\frac{1}{h^2} \begin{bmatrix} c_1 & c_2 & c_3 \\ c_2 & c_4 & c_5 \\ c_3 & c_5 & c_6 \end{bmatrix} \cdot \begin{bmatrix} \partial N_i / \partial x \\ \partial N_i / \partial y \\ \partial N_i / \partial z \end{bmatrix} \right] \begin{Bmatrix} u_i \\ v_i \\ w_i \end{Bmatrix} \quad \dots\dots\dots(\text{A-9})$$

Appendix (B)

The Corresponding Weight and Locations for the Integration Rule

The 27 ($3 \times 3 \times 3$) Gauss quadratic integration rule has been used. The corresponding weight and locations are defined in Table (B-1), also the relative positions of the sampling points for this rule over the volume of the brick element are shown in Fig.(B-1) below [2,3].

Table (B-1): Weights and locations of sampling point in 27-point integration rule.

Sampling Point	Local Coordinates			Weight
	r	s	t	
1, 3, 5, 7, 19, 21, 23, 25	± 0.7746	± 0.7746	± 0.7746	0.171468
2, 6, 20, 24	0	± 0.7746	± 0.7746	0.274348
4, 8, 22, 26	± 0.7746	0	± 0.7746	0.274348
10, 12, 14, 16	± 0.7746	± 0.7746	0	0.274348
9, 27	0	0	± 0.7746	0.438957
11, 15	0	± 0.7746	0	0.438957
13, 17	± 0.7746	0	0	0.438957
18	0	0	0	0.702332

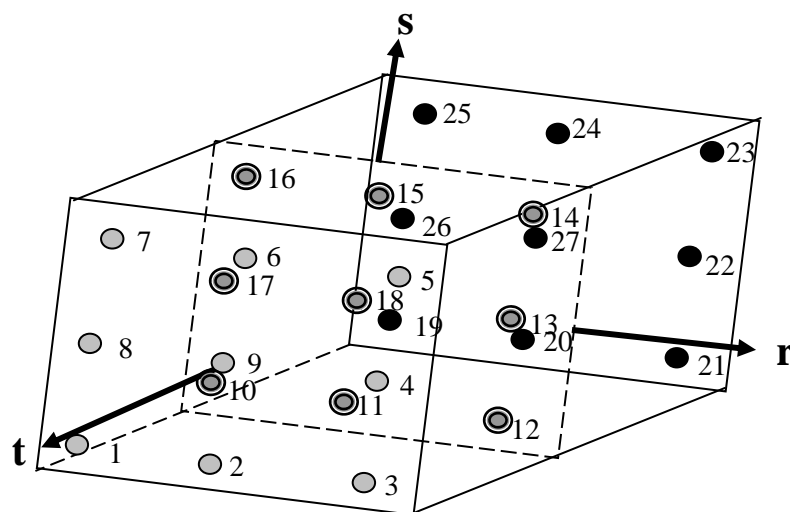


Fig.(B-1): Distribution of the Sampling Points over the Element (27-Points Integration Rule).

Appendix (C)

The Determination of the Principal Stresses for Three Dimensional States

The principal stresses and their directions for any point under three dimensional state of stress can be determined from the Cartesian stress components. The procedure for evaluating the principal stresses and their directions is described in Refs.[82], the roots of the following cubic equation represent the values of the principal stresses, σ_1 , σ_2 , and σ_3 ;

$$\sigma_i^3 - I_1\sigma_i^2 + I_2\sigma_i - I_3 = 0 \quad \dots\dots\dots(C-1)$$

where; I_1 is the first stress invariant previously defined and I_2 , I_3 are the second and the third stress invariants given by:

$$I_2 = \sigma_x\sigma_y + \sigma_y\sigma_z + \sigma_z\sigma_x - \tau_{xy}^2 - \tau_{yz}^2 - \tau_{zx}^2 \quad \dots\dots\dots(C-2)$$

$$I_3 = \sigma_x\sigma_y\sigma_z - \sigma_x\tau_{yz}^2 - \sigma_y\tau_{zx}^2 - \sigma_z\tau_{xy}^2 + 2\tau_{xy}\tau_{yz}\tau_{zx} \quad \dots\dots\dots(C-3)$$

For any given state of stress, the principal directions can be always be found to be a set of three mutually orthogonal directions. These directions can be expressed through the direction cosines as:

$$\begin{aligned} l_i &= \cos \theta_{xi} \\ m_i &= \cos \theta_{yi} \\ n_i &= \cos \theta_{zi} \end{aligned} \quad \dots\dots\dots(C-4)$$

For illustration, the direction cosines of the major principal stress, σ_1 , with respect to the x, y, and z-axes are l_1 , m_1 , and n_1 respectively. These direction cosines are as follows:

$$\begin{aligned} l_1 &= A / (A^2 + B^2 + C^2)^{0.5} \\ m_1 &= B / (A^2 + B^2 + C^2)^{0.5} \\ n_1 &= C / (A^2 + B^2 + C^2)^{0.5} \end{aligned} \quad \dots\dots\dots(C-5)$$

where;

$$\begin{aligned} A &= (\sigma_y - \sigma_1)(\sigma_z - \sigma_1) - \tau_{yz}^2 \\ B &= \tau_{yz}\tau_{zx} - \tau_{xy}(\sigma_z - \sigma_1) \\ C &= \tau_{xy}\tau_{yz} - \tau_{zx}(\sigma_y - \sigma_1) \end{aligned} \quad \dots\dots\dots(C-6)$$

The direct evaluation of the roots from Eq.(C-1) is not easy until the similarity of this equation to the trigonometric identity is observed [76]:

$$\cos^3 \theta - \frac{3}{4} \cos \theta - \frac{1}{4} \cos 3\theta = 0 \quad \dots\dots\dots(C-7)$$

For if $s = \rho \cos \theta$ is substituted into Eq.(C-1), then:

$$\cos^3 \theta - \frac{J_2}{\rho^2} \cos \theta - \frac{J_3}{\rho^3} = 0 \quad \dots\dots\dots(C-8)$$

Comparing terms with Eq.(C-7) results in;

$$\rho = \frac{2}{\sqrt{3}} \sqrt{J_2} \quad \dots\dots\dots(C-9)$$

$$\text{and } \cos 3\theta = \frac{4J_3}{\rho^3} = \frac{3\sqrt{3}}{2} \frac{J_3}{J_2^{3/2}} \quad \dots\dots\dots(C-10)$$

If θ_o denotes the first root of Eq.(C-10) for the angle 3θ in the range 0 to π , it follows that the angle θ_o must be within the range;

$$0 \leq \theta_o \leq \pi/3 \quad \dots\dots\dots(C-11)$$

Noting the cyclic nature of $\cos(3\theta_o \pm 2n\pi)$, the three and only three possible values of $\cos \theta$ giving the three principal stresses are;

$$\begin{aligned} \cos \theta_o \\ \cos(\theta_o - \frac{2}{3} \pi) \\ \cos(\theta_o + \frac{2}{3} \pi) \end{aligned} \quad \dots\dots\dots(C-12)$$


```

WRITE (NOUT,9040)
READ (NIN,*) ELTYP, TOTELS, NODEL
WRITE (NOUT,9020) ELTYP,TOTELS, NODEL
DO 1050 I=1,TOTELS
READ (NIN,*) ELNUM, (NWORK(J),J=1,NODEL), MPROP(ELNUM)
WRITE (NOUT,9090) ELNUM, (NWORK(J),J=1,NODEL), MPROP(ELNUM)
ELTOP(ELNUM,1) = ELTYP
ELTOP(ELNUM,2) = NODEL
DO 1050 J=1,NODEL
1050 ELTOP(ELNUM,J+2) = NWORK(J)
      IF(CSC.EQ.2)GOTO 1910
CCCCC          READ REINFORCEMENT BARS          CCCCC
READ(NIN,*)NBAR
WRITE(NOUT,9020)NBAR
DO 1900 I=1,NBAR
READ(NIN,*)BN,(NWORK(J),J=1,2),MPROP(BN+L7),(WORK(K),K=1,3)
WRITE(NOUT,9035)BN,(NWORK(J),J=1,2),MPROP(BN+L7),(WORK(K),K=1,3)
DO 1900 J=1,3
IF(J.LT.3)ELTOPB(BN,J)=NWORK(J)
1900 RLNTH(BN,J)=WORK(J)
CCCCC  INPUT OF MATERIAL PROP. & CONST.OF ELASTIC STRESS-STRAIN MATRIX D
WRITE (NOUT,9050)
READ(NIN,*) A1,A2,GA1,GA2,GA3
WRITE(NOUT,9170) A1,A2,GA1,GA2,GA3
1910 READ(NIN,*)NMATS
WRITE(NOUT,9020)NMATS
      DO 1060 JMAT = 1,NMATS
READ (NIN,*) IMAT,NU, E, FY , A , H ,FT, FC,SLN
POS(IMAT) = NU
EE(IMAT) = E
FYFY(IMAT) = FY
AA(IMAT) = A
HH(IMAT)=H
FTFT(IMAT)=FT
FCFC(IMAT)=FC
SSLN(IMAT)=SLN
1060 WRITE (NOUT,9170)NU, E, FY , A , H , FT ,FC,SLN
c ---- [D]co -----
IF(CSC.EQ.2)GOTO 1063
      NU=POS(1)
      E=EE(1)
      CALL DISO(Dco,6,6,E,NU,6)
      CALL MATNUL(DE,3,3)
      DE(1,1)=E/(1.0-NU*NU)
      DE(2,2)=DE(1,1)
      DE(1,2)=NU*E/(1.0-NU*NU)
      DE(2,1)=DE(1,2)
      DE(3,3)=E/(2.0+2.0*NU)
c ----- [D]st -----
1063  IF(CSC.EQ.1)GOTO 1064
      NU=POS(2)
      E=EE(2)
      CALL DISO(Dst,6,6,E,NU,6)
C  INPUT OF NUMBER OF DEGREES OF FREEDOM PER NODE, INPUT OF RESTRAINED NODE
C  DATA AND CONSTRUCTION OF NODAL FREEDOM ARRAY NF
1064 WRITE (NOUT,9070)
      READ (NIN,*) RESNOD
      WRITE (NOUT,9020) RESNOD
      DO 1070 I=1,RESNOD
      READ (NIN,*) (RESTR(I,J),J=1,4)
1070 WRITE (NOUT,9020) (RESTR(I,J),J=1,4)
CCCCC  FORM & WRITE NF(TOTNOD,3)  CCCCC
TOTDOF=0
DO 50 I=1,L4

```

```

DO 50 J=1,3
NF(I,J)=1
JJ=J+1
DO 60 II=1,RESNOD
IF(RESTR(II,1).EQ.I.AND.RESTR(II,JJ).NE.0)NF(I,J)=0
60 CONTINUE
IF(NF(I,J).NE.0)TOTDOF=TOTDOF+1
IF(NF(I,J).NE.0)NF(I,J)=TOTDOF
50 CONTINUE
DO 51 I=1,L4
51 WRITE(2,7)I,NF(I,1),NF(I,2),NF(I,3)
7 FORMAT(14,' NF',3I4)
IF(MBA.EQ.1)WRITE(*,*)'TOTDOF=',TOTDOF
CCCCC          LOADING DATA INPUT          CCCCC
WRITE (NOUT,9080)
READ (NIN,*)LODNOD
WRITE(NOUT,*)LODNOD
CALL VECNUL(ORLOAD,L1)
DO 1090 I=1,LODNOD
READ (NIN,*)NODNUM,(WORK(J),J=1,3)
WRITE (NOUT,9030)NODNUM,(WORK(J),J=1,3)
DO 1090 J=1,3
K = NF(NODNUM,J)
1090 IF (K.NE.0) ORLOAD(K)=WORK(J)
WRITE(NOUT,9020)NALGO,NINC,NITR,ICONVER,NOUTP,TOL,KI,KY
CALL VECNUL(LOADS,L1)
CALL VECNUL(INLOAD,L1)
CALL VECNUL(TDISP,L1)
CALL VECNUL(EPSTN,L5)
CALL VECNUL(EFFST,L5)
CALL VECNUL(CURY,L6)
CALL MATNUL(STRSG,6,L5)
CALL MATNUL(STRNG,6,L5)
CALL MATNUL(ABC,3,L6)
CALL MATNUL(SCR,3,L6)
CALL MATNUL(ECRK,3,L6)
CALL MATNUL(TRSTRS,6,L6)
CALL MATNUL(TRSTRN,6,L6)
CALL MATNUL(TPSTRN,3,L6)
CALL MATNUL(TPSTRS,3,L6)
CALL MATNUL(CLOS,3,L6)
DO 111 J=1,L5
DO 111 I=1,3
111 IND(I,J)=0
DO 1760 K=1,L6
DM(K)=1.0
DO 1760 I=1,6
DO 1760 J=1,6
DDC(K,I,J)=0.0
IF(I.LE.3.AND.J.LE.3)THEN
DCOSN(K,I,J)=0.0
DDN(K,I,J)=0.0
ENDIF
1760 DCOSS(K,I,J)=0.0
CALL VECNUL(ERR,L1)
CALL VECNUL(UX,L7)
CALL VECNUL(UY,L7)
CALL VECNUL(UZ,L7)
CCCCC          LOOP OVER EACH INCREMENT          CCCCC
P=0.0
CALL QUD27(WGHT,ABSS,27)
CALL QLIN2(WGHTR,2,ABSSR,2)
DO 1110 INC=1,NINC
IF(INC.LE.7 )FACTR=4.00

```

```

      IF(INC.GE.8)FACTR=2.00
      IF(INC.GE.21)FACTR=1.50
      IF(INC.GE.46)FACTR=1.0
      DO 1120 K=1,L1
      LOADS(K)=FACTR*ORLOAD(K)
      INLOAD(K)=INLOAD(K)+LOADS(K)
1120  P=P+LOADS(K)
CCCCC                                LOOP OVER EACH ITERATION                                CCCCC
      DO 1130 ITR = 1,NITR
      KRESL=2
      IF(INC.EQ.1.AND.ITR.EQ.1)KRESL=1
      IF(NALGO.EQ.2)KRESL=1
      IF(NALGO.EQ.3.AND.ITR.EQ.1)KRESL=1
      IF(NALGO.EQ.4.AND.ITR.EQ.2)KRESL=1
CCC  ITR=== 1 , 6 , 11 , .....
      IF(NALGO.EQ.5)THEN
      I=(ITR-1)/5
      K=ITR-1
      IF(K.EQ.5*I)KRESL=1
      ENDIF
CCC  ITR=== 2 , 12 , 22 , .....
      IF(NALGO.EQ.6.AND.ITR.GE.2)THEN
      I=(ITR-2)/10
      K=ITR-2
      IF(K.EQ.10*I)KRESL=1
      ENDIF
CCC  ITR=== 1 , 26 , 51 , .....
      IF(NALGO.EQ.7)THEN
      I=(ITR-1)/25
      K=ITR-1
      IF(K.EQ.25*I)KRESL=1
      ENDIF
CCCCC CHECK WETHER THE EVALUATION OF STIFNESS MATRIX IS REQUIRED CCCCC
      IF(KRESL.EQ.1)THEN
C*          ***** STIFFNESS MATRIX *****
      CALL STIFFK(BEE,CEE,CES,INC,ITR,NTEMP,MBA,DETR)
      IF(DETR.EQ.0.0)GOTO 9180
      IRES=0
      ELSE
      IRES=1
      ENDIF
C*          ***** EQUATION SOLUTION *****
      CALL SOLVE (L1,L9,L1,L9,SYSK,LOADS,IRES)
      CALL VECNUL(ERR,L1)
C*          ***** RESIDUAL FORCES *****
      REWIND(NTEMP)
      CALL RESIDU(BEE,CEE,CES,NTEMP,DE,INC,ITR,A1,A2,GA1,GA2,GA3
      *,Ecrsh,ZFC,KGC)
      DO 1450 K=1,L1
      ERR(K)=INLOAD(K)-PLOAD(K)
1450  TDISP(K)=TDISP(K)+LOADS(K)
C*          ***** CONVERGENCE CRIETERIA *****
      NCHEK=0.0
      RESID=0.0
      RETOT=0.0
      IF(ICONVER.EQ.1)THEN
      DO 1430 K = 1,L1
      RESID=RESID+ERR(K)*ERR(K)
1430  RETOT=RETOT+INLOAD(K)*INLOAD(K)
      ELSE
      DO 1435 K = 1,L1
      RESID=RESID+LOADS(K)*LOADS(K)
1435  RETOT=RETOT+TDISP(K)*TDISP(K)
      ENDIF

```

```

DO 1440 K=1,L1
1440 LOADS(K)=ERR(K)
RATIO=RATIOO*SQRT(RESID)/SQRT(RETOT)
IF(RATIO.GT.TOL)NCHEK=1
IF(RATIO.GT.PVALU)NCHEK=999
PVALU=RATIO
C* ***** OUTPUT OF THE RESULTS *****
C IF SOLUTION HAS CONVERGED STOP ITERATING AND OUTPUT RESULTS
WRITE(*,114)INC,ITR,-1*P,RATIO,TDISP(NF(KI,KY))
WRITE(2,114)INC,ITR,-1*P,RATIO,TDISP(NF(KI,KY))
114 FORMAT('INS=',I3,5X,'ITR=',I3,5X,'P=',2F8.3,5X,'DISP=',F8.3)
IF(ABS(TDISP(NF(KI,KY))).GT.100)STOP
IF(NCHEK.EQ.0)GOTO 7930
1130 CONTINUE
IF(NALGO.EQ.2)GOTO 7930
IF(ITR.GT.NITR)WRITE(NOUT,*)'ERROR ITR GT NITR LINE 403'
STOP
CCCCC OUTPUT DISPLACEMENT CCCCC
7930 CONTINUE
IF(NOUTP.EQ.1)THEN
MCON=1
DO 30 I=1,L4
DO 20 J=1,3
IF(NF(I,J).EQ.0)WORK(J)=0.0
IF(NF(I,J).NE.0)WORK(J)=TDISP(MCON)
IF(NF(I,J).NE.0)MCON=MCON+1
20 CONTINUE
IF(I.EQ.KI)WRITE(5,12)INC,-1.0*P,WORK(KY)*(-1)
12 FORMAT(5X,'INC=',5X,I3,5X,'P=',5X,F10.2,5X,'Y=',F8.2)
30 CONTINUE
ENDIF
CCCCC OUTPUT OF STRESSES CCCCC
IF(NOUTP.EQ.2)THEN
IF(INC.EQ.1)WRITE(5,9007)
DO 1686 K=1,L5
WRITE(5,13) K,STRSG(3,K)
13 FORMAT(' K=',I4,3x,'STRESS Z =',F10.2)
1686 CONTINUE
ENDIF
CCCCC OUTPUT OF STRAINS CCCCC
IF(NOUTP.EQ.3)THEN
IF(INC.EQ.1)WRITE(5,9009)
DO 1687 K=1,L5
WRITE(5,14) K,STRNG(3,K)
14 FORMAT(' K=',I4,3x,'STRAIN Z =',F10.4)
1687 CONTINUE
ENDIF
1110 CONTINUE
9007 FORMAT (1H //24H***** STRESSES *****//)
9009 FORMAT (1H //24H***** STRAINS *****//)
9010 FORMAT (1H //24H***** NODAL GEOMETRY ****//)
9020 FORMAT (8I5)
9030 FORMAT (I5,5F12.4)
9035 FORMAT (4I5,3F12.4)
9040 FORMAT (1H //26H***** ELEMENT TOPOLOGY ****//)
9050 FORMAT (1H //29H***** MATERIAL PROPERTIES ****//)
9070 FORMAT (1H //24H***** RESTRAINT DATA ****//)
9080 FORMAT (1H //22H***** LOADING DATA ****//)
9090 FORMAT (22I3)
9170 FORMAT (11F10.3)
9180 END
CCCCC THE 27 POINT INTEGRATION RULE CCCCC
SUBROUTINE QUD27(WGHT,ABSS,L3)
IMPLICIT REAL*8 (A-H,O-Z)

```

```

DIMENSION WGHT(L3),ABSS(3,L3)
A=0.774596669
CALL MATNUL(ABSS,3,27)
ABSS(1,1)=A
ABSS(1,3)=-A
ABSS(1,4)=-A
ABSS(1,5)=-A
ABSS(1,7)=A
ABSS(1,8)=A
ABSS(1,10)=A
ABSS(1,12)=-A
ABSS(1,13)=-A
ABSS(1,14)=-A
ABSS(1,16)=A
ABSS(1,17)=A
ABSS(1,19)=A
ABSS(1,21)=-A
ABSS(1,22)=-A
ABSS(1,23)=-A
ABSS(1,25)=A
ABSS(1,26)=A
ABSS(2,1)=-A
ABSS(2,2)=-A
ABSS(2,3)=-A
ABSS(2,5)=A
ABSS(2,6)=A
ABSS(2,7)=A
ABSS(2,10)=-A
ABSS(2,11)=-A
ABSS(2,12)=-A
ABSS(2,14)=A
ABSS(2,15)=A
ABSS(2,16)=A
ABSS(2,19)=-A
ABSS(2,20)=-A
ABSS(2,21)=-A
ABSS(2,23)=A
ABSS(2,24)=A
ABSS(2,25)=A
DO 162 L=1,9
162 ABSS(3,L)=-A
DO 164 L1=19,27
164 ABSS(3,L1)=A
H1=125.0/729.0
H2=200.0/729.0
H3=320.0/729.0
H4=512.0/729.0
WGHT(1)=H1
WGHT(2)=H2
WGHT(3)=H1
WGHT(4)=H2
WGHT(5)=H1
WGHT(6)=H2
WGHT(7)=H1
WGHT(8)=H2
WGHT(9)=H3
WGHT(10)=H2
WGHT(11)=H3
WGHT(12)=H2
WGHT(13)=H3
WGHT(14)=H2
WGHT(15)=H3
WGHT(16)=H2
WGHT(17)=H3

```

```

WGHT(18)=H4
WGHT(19)=H1
WGHT(20)=H2
WGHT(21)=H1
WGHT(22)=H2
WGHT(23)=H1
WGHT(24)=H2
WGHT(25)=H1
WGHT(26)=H2
WGHT(27)=H3
RETURN
END
CCCC
SUBROUTINE QLIN2(WGHTR,IWGHTR,ABSSR,IABSSR)
IMPLICIT REAL *8 (A-H,O-Z)
DIMENSION WGHTR(IWGHTR),ABSSR(IABSSR)
ABSSR(1)=-0.577340269
ABSSR(2)=0.577340269
WGHTR(1)=1.0
WGHTR(2)=1.0
RETURN
END
C *****
C ***** STIFFNESS MATRIX FORMULATION *****
C *****
SUBROUTINE STIFFK(BEE,CEE,CES,INC,ITR,NTEMP,MBA,DETR)
IMPLICIT REAL*8 (A-H,O-Z)
PARAMETER(L1=3207,L4=1101,L5=4640,L6=3888,L7=144,L8=376,L9=123)
REAL *8 JAC,JACIN,MEAN,INLOAD,LOADS,NU
INTEGER DOFEL,ELTOP,STEER,ELTOPB
DIMENSION B(6,60),BT(60,6),DB(6,60),DER(3,20),DVECT(6),JACIN(3,3)
*,ELK(60,60),FUN(20),PD(6,6),BR(60),STEER(60),BTDB(60,60),COSS(6,6)
*,T(6,6),COSST(6,6),GEOM(20,3),JAC(3,3),DC(6,6),DERIV(3,20),STRS(6)
*,AVECT(6)
COMMON SYSK(L1,L9),TDISP(L1),INLOAD(L1),COORD(L4,3),Dco(6,6),AA(7)
*,Dst(6,6),LOADS(L1),FTFT(7),FCFC(7),DDC(L6,6,6),SSLN(7),CLOS(3,L6)
*,DCOSN(L6,3,3),HH(7),ABC(3,L6),RLNTH(L8,3),STRNG(6,L5),DDN(L6,3,3)
*,FYFY(7),H1H1(L8,2),STRSG(6,L5),PLOAD(L1),EFFST(L5),WGHT(27),EE(7)
*,ECRK(3,L6),CURY(L6),EPSTN(L5),TRSTRN(6,L6),DCOSS(L6,6,6),ABSSR(2)
*,TPSTRN(3,L6),SCR(3,L6),UX(L7),UY(L7),UZ(L7),TRSTRS(6,L6),NF(L4,3)
*,TPSTRS(3,L6),IND(3,L5),ELTOP(L7,22),ABSS(3,27),DDET(L7,27),POS(7)
*,MPROP(L7+L8),WGHTR(2),ELTOPB(L8,2),DM(L6),DCOSA(L6,6,6)
REWIND(NTEMP)
CALL MATNUL(SYSK,L1,L9)
CCCCC                                LOOP OVER EACH ELEMENT                                CCCCC
KGT=0
KGC=0
DO 1140 NEL=1,L7
NODEL=ELTOP(NEL,2)
DOFEL=NODEL * 3
IMAT=MPROP(NEL)
FY=FYFY(IMAT)
H=HH(IMAT)
NU=POS(IMAT)
E=EE(IMAT)
FT=FTFT(IMAT)
FC=FCFC(IMAT)
G=E/(2.0+2.0*NU)
A=AA(IMAT)
SLN=SSLN(IMAT)
      if(eltop(NEL,1).eq.1)then
CALL ELGEOM(NEL,ELTOP,L7,22,COORD,L4,3,GEOM,20,3,3)
CALL MATNUL(ELK,60,60)
CCCCC CONCRETE OR STEEL ELEMENT STIFFNESS MATRIX CCCCC

```

```

DO 1150 IGP=1,27
  KGT=KGT+1
  IF(MPROP(NEL).EQ.1.OR.MPROP(NEL).EQ.6)KGC=KGC+1
  IF(INC.EQ.1.AND.ITR.EQ.1)THEN
    XI = ABSS(1,IGP)
    ETA = ABSS(2,IGP)
    ZETA= ABSS(3,IGP)
    CALL BRK20(FUN,20,DER,3,20,XI,ETA,ZETA)
c ---- cal. [J] -----
  CALL MATMUL(DER,3,20,GEOM,20,3,JAC,3,3,3,NODEL,3)
c ---- cal. [J] -1 -----
  CALL MATINV(JAC,3,3,JACIN,3,3,3,DET)
  DDET(NEL,IGP) = DET
  CALL MATMUL(JACIN,3,3,DER,3,20,DERIV,3,20,3,3,NODEL)
C FORMATION OF STRAIN-DISP.MATRIX B AND OUTPUT TO WORK FILE FOR LATER RECOVERY PROCESS
c ---- cal. [B] -----
  CALL B3C3(B,6,60,DERIV,3,20,NODEL)
  WRITE (NTEMP) ((B(I,J),I=1,6),J=1,DOFEL)
  ELSE
  READ (NTEMP) ((B(I,J),I=1,6),J=1,DOFEL)
  ENDIF
c----- To calculate [D][B] for concrete & Steel -----
  If(MPROP(NEL).Eq.2.OR.MPROP(NEL).Eq.7)then
C ---[D][B] FOR ----- STEEL -----
  IF(INC.NE.1.AND.EPSTN(KGT).NE.0.0)THEN
    DO 1171 I=1,6
1171 STRS(I)=STRSG(I,KGT)
    CALL INVAR3(STRS,MEAN,YIELD,THETA)
    CALL YIELDIF(AVECT,DVECT,Dst,H,STRS,YIELD,ABETA)
    DO 1181 I=1,6
    DO 1181 J=1,6
1181 PD(I,J)=Dst(I,J)-ABETA*DVECT(I)*DVECT(J)
c ---- cal. [Dp][B] -----
  CALL MATMUL(PD,6,6,B,6,60,DB,6,60,6,6,DOFEL)
  ELSE
  CALL MATMUL(Dst,6,6,B,6,60,DB,6,60,6,6,DOFEL)
  ENDIF
  elseIf(MPROP(NEL).Eq.1.OR.MPROP(NEL).Eq.6)then
c ---- [D]*[B] FOR ----- CONCRETE -----
  IF(INC.NE.1)THEN
  IF(IND(1,KGT).EQ.7.OR.IND(2,KGT).EQ.7.OR.IND(3,KGT).EQ.7)THEN
    DO 2017 I=1,6
    DO 2017 J=1,60
c----- [D]*[B] = (for CRUSH gauss point)-----
2017 DB(I,J)=0.1D-50
    ELSEIF(IND(1,KGT).EQ.2.OR.IND(2,KGT).EQ.2.OR.IND(3,KGT).EQ.2)THEN
    DO 2020 I=1,6
    DO 2020 J=1,6
    COSS(I,J)=DCOSS(KGC,I,J)
2020 DC(I,J)=DDC(KGC,I,J)
    CALL MATMUL(COSS,6,6,DC,6,6,T,6,6,6,6,6)
    CALL MATRAN(COSS,6,6,COSST,6,6,6,6)
    CALL MATMUL(T,6,6,COSST,6,6,DC,6,6,6,6,6)
c----- [D] [B] = (with cracking in tesion zone) -----
  CALL MATMUL(DC,6,6,B,6,60,DB,6,60,6,6,DOFEL)
  ELSEIF(IND(1,KGT).EQ.-4)THEN
    DO 1170 I=1,6
1170 STRS(I)=STRSG(I,KGT)
    CALL INVARc(BEE,CEE,CES,AVECT,STRS,YIELD)
    CALL FLOWPLc(AVECT,DVECT,Dco,ABETA,EPSTN,KGT,E,FC,L5)
    DO 1180 I=1,6
    DO 1180 J=1,6
c----- [Dp][B]=(with plastic in compression zone)-----
1180 PD(I,J)=Dco(I,J)-ABETA*DVECT(I)*DVECT(J)

```

```

      CALL MATMUL(PD,6,6,B,6,60,DB,6,60,6,6,DOFEL)
      ELSE
c ---- [D][B]=(with elastic concrete )
      CALL MATMUL(Dco,6,6,B,6,60,DB,6,60,6,6,DOFEL)
      ENDIF
      ELSE
      CALL MATMUL(Dco,6,6,B,6,60,DB,6,60,6,6,DOFEL)
      ENDIF
    endif
    IF(INC.EQ.1.AND.ITR.EQ.1)THEN
      CALL MATRAN(B,6,60,BT,60,6,6,DOFEL)
      WRITE(NTEMP) ((BT(I,J), I=1,DOFEL), J=1,6)
      ELSE
      READ(NTEMP) ((BT(I,J), I=1,DOFEL), J=1,6)
      ENDIF
      CALL MATMUL(BT,60,6,DB,6,60,BTDB,60,60,DOFEL,6,DOFEL)
      QUOT = ABS(DDET(NEL,IGP))*WGHT(IGP)
      DO 1190 I=1,DOFEL
      DO 1190 J=1,DOFEL
1190 BTDB(I,J) = BTDB(I,J)*QUOT
      CALL MATADD(ELK,60,60,BTDB,60,60,DOFEL,DOFEL)
1150 CONTINUE
CCCCC      REINFORCEMENT ELEMENT STIFFNESS MATRIX      CCCCC
      IF(MPROP(NEL).EQ.1.OR.MPROP(NEL).EQ.6)THEN
      DO 1910 IBAR=1,L8
      IF(ELTOPB(IBAR,1).EQ.NEL)THEN
      DO 1920 IGP=1,2
      KGT=KGT+1
      IF(INC.EQ.1.AND.ITR.EQ.1)THEN
      IF(ELTOPB(IBAR,2).EQ.1)THEN
      XI=ABSSR(IGP)
      ETA=RLNTH(IBAR,2)
      ZETA=RLNTH(IBAR,3)
      ELSEIF(ELTOPB(IBAR,2).EQ.2)THEN
      XI=RLNTH(IBAR,1)
      ETA=ABSSR(IGP)
      ZETA=RLNTH(IBAR,3)
      ELSE
      XI=RLNTH(IBAR,1)
      ETA=RLNTH(IBAR,2)
      ZETA=ABSSR(IGP)
      ENDIF
      CALL BRK20(FUN,20,DER,3,20,XI,ETA,ZETA)
      CALL MATMUL(DER,3,20,GEOM,20,3,JAC,3,3,3,NODEL,3)
      CALL MATINV(JAC,3,3,JACIN,3,3,3,DET)
      CALL MATMUL(JACIN,3,3,DER,3,20,DERIV,3,20,3,3,NODEL)
      DO 1930 I=1,3
      IF (ELTOPB(IBAR,2).EQ.I)THEN
      C1=JAC(I,1)*JAC(I,1)
      C2=JAC(I,1)*JAC(I,2)
      C3=JAC(I,1)*JAC(I,3)
      C4=JAC(I,2)*JAC(I,2)
      C5=JAC(I,2)*JAC(I,3)
      C6=JAC(I,3)*JAC(I,3)
      ENDIF
1930 CONTINUE
      H1=SQRT(C1+C4+C6)
      IF(H1.EQ.0.0)H1=0.000001
      H1H1(IBAR,IGP)=H1
      DO 1940 J=1,NODEL
      DO 1940 K=1,3
      L=3*(J-1)+K
      IF(K.EQ.1)THEN
      BR(L)=(C1*DERIV(1,J)+C2*DERIV(2,J)+C3*DERIV(3,J))/(H1*H1)

```

```

ELSEIF(K.EQ.2)THEN
BR(L)=(C2*DERIV(1,J)+C4*DERIV(2,J)+C5*DERIV(3,J))/(H1*H1)
ELSE
BR(L)=(C3*DERIV(1,J)+C5*DERIV(2,J)+C6*DERIV(3,J))/(H1*H1)
ENDIF
1940 CONTINUE
WRITE(NTEMP)(BR(J),J=1,DOFEL)
ELSE
READ(NTEMP)(BR(J),J=1,DOFEL)
ENDIF
DO 1990 I=1,DOFEL
DO 1990 J=1,DOFEL
1990 BTDB(I,J)=BR(I)*BR(J)
IMAT=MPROP(IBAR+L7)
E=EE(IMAT)
H=HH(IMAT)
A=AA(IMAT)
FMULT=1.0-E/(E+H)
IF(INC.EQ.1)FMULT=1.0
IF(IND(1,KGT).EQ.0.OR.IND(1,KGT).EQ.5)FMULT=1.0
E=E*FMULT
QUOT=A*E*WGHTR(IGP)*H1
DO 1950 I=1,DOFEL
DO 1950 J=1,DOFEL
IF(IND(1,KGT).EQ.7)BTDB(I,J)=0.1D-10
1950 BTDB(I,J)=BTDB(I,J)*QUOT
CALL MATADD(ELK,60,60,BTDB,60,60,DOFEL,DOFEL)
1920 CONTINUE
ENDIF
1910 CONTINUE
ENDIF
endif
CCCCC ASSEMBLY OF SYSTEM STIFFNESS MATRIX SYSK CCCCC
CALL DIRECT(NEL,ELTOP,L7,22,NF,L4,3,3,STEER,60)
CALL ASSYM(SYSK,L1,L9,ELK,60,60,STEER,60,DOFEL,MBA,INC,ITR)
1140 CONTINUE
IHH=0
DETR=SYSK(1,1)
DO 1145 I=2,L1
DETR=DETR*SYSK(I,1)
IF(DETR.GT.1000)IHH=IHH+1
IF(DETR.GT.1000)DETR=DETR/1000000
IF(DETR.LT.-1000)IHH=IHH-1
1145 IF(DETR.LT.-1000)DETR=DETR*1000000
WRITE(4,1146)INC,ITR,DETR,IHH*6
1146 FORMAT(INC,ITR,'215,' DETERMINANT=',F8.2,'*10^',I5)
RETURN
END
CCCCC EFFECTIVE STREES AND 3D FLOW VECTOR
CCCCC CALCULATION OF STRESS INVARIANTS AND THE CURRENT VALUE OF THE YIELD
FUNC.
SUBROUTINE INVARc(BEE,CEE,CES,AV,ST,YIELD)
IMPLICIT REAL*8 (A-H,O-Z)
DIMENSION DEV(6),AV(6),ST(6)
VARI1=ST(1)+ST(2)+ST(3)
DO 1200 I=1,6
IF(I.LE.3)DEV(I)=ST(I)-(ST(1)+ST(2)+ST(3))/3.0
1200 IF(I.GT.3)DEV(I)=ST(I)
A=DEV(1)*DEV(1)+DEV(2)*DEV(2)+DEV(3)*DEV(3)
B=DEV(4)*DEV(4)+DEV(5)*DEV(5)+DEV(6)*DEV(6)
VARJ2=0.5*A+B
YIELD=CEE*VARI1+SQRT(CES*VARI1*VARI1+3.0*BEE*VARJ2)
DT1=ST(1)*ST(1)+ST(2)*ST(2)+ST(3)*ST(3)
DT2=ST(1)*ST(2)+ST(2)*ST(3)+ST(3)*ST(1)

```

```

DT3=ST(4)*ST(4)+ST(5)*ST(5)+ST(6)*ST(6)
DL=2.0*SQRT((CES+BEE)*DT1+(2.0*CES-BEE)*DT2+3.0*BEE*DT3)
IF(DL.EQ.0.0)DL=0.1D-39
EMAN=2.0*CES-BEE
AV(1)=CEE+(2.0*(CES+BEE)*ST(1)+EMAN*(ST(2)+ST(3)))/DL
AV(2)=CEE+(2.0*(CES+BEE)*ST(2)+EMAN*(ST(1)+ST(3)))/DL
AV(3)=CEE+(2.0*(CES+BEE)*ST(3)+EMAN*(ST(2)+ST(1)))/DL
AV(4)=6.0*BEE*ST(4)/DL
AV(5)=6.0*BEE*ST(5)/DL
AV(6)=6.0*BEE*ST(6)/DL
RETURN
END
CCCCC      EFFECTIVE STRESS AND 2D FLOW VECTOR ,CALCULATION
CCCCC OF STRESS INVARIANTS AND THE CURRENT VALUE OF THE YIELD FUNCTION
SUBROUTINE INVAN(BEE,CEE,CES,AVECTA,STEMP,YIELD)
IMPLICIT REAL*8 (A-H,O-Z)
DIMENSION DEVIAA(4),AVECTA(3),STEMP(3)
VARI1=STEMP(1)+STEMP(2)+0.0
DEVIAA(1)=STEMP(1)-(STEMP(1)+STEMP(2)+0.0)/3.0
DEVIAA(2)=STEMP(2)-(STEMP(1)+STEMP(2)+0.0)/3.0
DEVIAA(3)=STEMP(3)
DEVIAA(4)=0.0-(STEMP(1)+STEMP(2)+0.0)/3.0
VARJ2=0.5*(DEVIAA(1)**2+DEVIAA(2)**2+DEVIAA(4)**2)+DEVIAA(3)**2
YIELD=CEE*VARI1+SQRT(CES*VARI1*VARI1+3.0*BEE*VARJ2)
DELT1=STEMP(1)*STEMP(1)+STEMP(2)*STEMP(2)
DELT2=STEMP(1)*STEMP(2)
DELT3=STEMP(3)*STEMP(3)
DELT=2.0*SQRT((CES+BEE)*DELT1+(2.0*CES-BEE)*DELT2+3.0*BEE*DELT3)
AVECTA(1)=CEE+(2.0*(CES+BEE)*STEMP(1)+(2.0*CES-BEE)*STEMP(2))/DELT
AVECTA(2)=CEE+(2.0*(CES+BEE)*STEMP(2)+(2.0*CES-BEE)*STEMP(1))/DELT
AVECTA(3)=6.0*BEE*STEMP(3)/DELT
RETURN
END
CCCCC
SUBROUTINE FLOWPLc(AVECT,DVECT,D,ABETA,EPSTN,KGT,E,FC,L5)
IMPLICIT REAL*8 (A-H,O-Z)
DIMENSION AVECT(6),DVECT(6),D(6,6),EPSTN(L5)
CALL MATVEC(D,6,6,AVECT,6,6,6,DVECT,6)
IF(EPSTN(KGT).EQ.0.0)ABETA=0.1D-39
IF(EPSTN(KGT).EQ.0.0)GOTO 88
DENOM=(SQRT(0.7*FC/(E*EPSTN(KGT)))-1.0)*E
IF(DENOM.LT.0.0)DENOM=0.0
DO 1230 I=1,6
1230 DENOM=DENOM+AVECT(I)*DVECT(I)
IF(DENOM.EQ.0)DENOM=0.1D-39
ABETA=1.0/DENOM
88 RETURN
END
CCCCC
SUBROUTINE FLOWPN(AV,DV,DE,DAM,DENOM,ABETA,KGS,E,FC,EPSTN,L5)
IMPLICIT REAL*8 (A-H,O-Z)
DIMENSION AV(3),DV(3),DE(3,3),EPSTN(L5)
CALL MATVEC(DE,3,3,AV,3,3,3,DV,3)
IF(EPSTN(KGS).EQ.0.0)ABETA=0.1D-39
IF(EPSTN(KGS).EQ.0.0)GOTO 888
DENOM=(SQRT(0.7*FC*DAM/(E*EPSTN(KGS)))-1.0)*E
IF(DENOM.LT.0.0)DENOM=0.0
DO 2100 I=1,3
2100 DENOM=DENOM+AV(I)*DV(I)
ABETA=1.0/DENOM
888 RETURN
END

```

```

C *****
C ***** RESIDUAL FORCES *****
C *****
SUBROUTINE RESIDU(BEE,CEE,CES,NTEMP,DE,INC,ITR,A1,A2,GA1,GA2,GA3,
*Ecrsh,ZFC,KGC)
  IMPLICIT REAL*8 (A-H,O-Z)
  INTEGER STEER,ELTOP,ELTOPB
  PARAMETER(L1=3207,L4=1101,L5=4640,L6=3888,L7=144,L8=376,L9=123)
  REAL *8 LOADS, NU ,INLOAD ,MEAN
  DIMENSION B(6,60),BT(60,6),DPTARR(3),DE(3,3),ECR(3),TSTR(6),BR(60)
  *,STEER(60),STRN(6),SGTOT(6),DC(6,6),CRSTRS(6),COSS(6,6),DCRSTRN(3)
  *,SIGMA(6),DN1(3,3),SSSTRN(3),STRSGA(3),STRSA(3),COSA(6,6),COST(3,3)
  *,AVECT(6),DVECT(6),RNOL(60),COSN(3,3),PSTRN(6),PSTRS(6),COSST(6,6)
  *,PSARR(3),PTARR(3),DC1(6,6),TARR(3),DN(3,3),SARR(3),STRS(6),FAC(4)
  *,BETA(3),AMA(3),CRSTRN(6),ELDIS(60)
  COMMON SYSK(L1,L9),TDISP(L1),INLOAD(L1),COORD(L4,3),Dco(6,6),AA(7)
  *,Dst(6,6),LOADS(L1),FTFT(7),FCFC(7),DDC(L6,6,6),SSLN(7),CLOS(3,L6)
  *,DCOSN(L6,3,3),HH(7),ABC(3,L6),RLNTH(L8,3),STRNG(6,L5),DDN(L6,3,3)
  *,FYFY(7),H1H1(L8,2),STRSG(6,L5),PLOAD(L1),EFFST(L5),WGHT(27),EE(7)
  *,ECRK(3,L6),CURY(L6),EPSTN(L5),TRSTRN(6,L6),DCOSS(L6,6,6),ABSSR(2)
  *,TPSTRN(3,L6),SCR(3,L6),UX(L7),UY(L7),UZ(L7),TRSTRS(6,L6),NF(L4,3)
  *,TPSTRS(3,L6),IND(3,L5),ELTOP(L7,22),ABSS(3,27),DDET(L7,27),POS(7)
  *,MPROP(L7+L8),WGHTR(2),ELTOPB(L8,2),DM(L6),DCOSA(L6,6,6)
  KGT=0
  KGC=0
  AAA=A1-1.0
  CALL VECNUL(PLOAD,L1)
CCCC  LOOP OVER EACH ELEMENT          CCCCC
  DO 1260 NEL=1,L7
  CALL VECNUL(RNOL,60)
  IMAT=MPROP(NEL)
  FY=FYFY(IMAT)
  H=HH(IMAT)
  NU=POS(IMAT)
  E=EE(IMAT)
  FT=FTFT(IMAT)
  FC=FCFC(IMAT)
  SLN=SSLN(IMAT)
  A=AA(IMAT)
  G=E/(2.0+2.0*NU)
CCCC  COMPUTE INCREMENTAL DISPLACEMENTS OF THE ELEMENT NODES  CCCCC
  IF(MPROP(NEL).LE.2.OR.MPROP(NEL).GE.6)THEN
  CALL DIRECT(NEL,ELTOP,L7,22, NF,L4,3,3,STEER,60)
  CALL VECNUL(ELDIS,60)
  DO 1270 I=1,60
  JSTEER = STEER(I)
  IF (JSTEER.NE.0) ELDIS(I) = LOADS(JSTEER)
1270  CONTINUE
  ENDIF

  If(mprop(NEL).eq.1.or.mprop(NEL).eq.6)then
C ***** RESUDUAL FOR CONCRETE ELEMENTS *****
C -----
C  LOOP OVER EACH SAMPLING POINT
  DO 1290 IGP=1,27
  CALL VECNUL(FAC,4)
  CALL VECNUL(AMA,3)
  KGT=KGT+1
  KGC=KGC+1
  READ (NTEMP) ((B(I,J),I=1,6),J=1,60)
CCCC  CHECK FOR PREVIOUSLY CRUSHED SAMPLING POINT  CCCCC

```

```

IF(IND(1,KGT).EQ.7.OR.IND(2,KGT).EQ.7.OR.IND(3,KGT).EQ.7)GOTO 7580

CALL MATVEC(B,6,60,ELDIS,60,6,60,STRN,6)
CALL MATVEC(Dco,6,6,STRN,6,6,6,STRS,6)
DO 1300 I=1,6
STRNG(I,KGT)=STRNG(I,KGT)+STRN(I)
TSTR(I)=STRNG(I,KGT)
1300 SIGMA(I)=STRSG(I,KGT)+STRS(I)

CCCCC      CHECK FOR PREVIOUS CRACKS OR CLOSED      CCCCC
IF(IND(1,KGT).EQ.2.OR.CLOS(1,KGC).EQ.1)GOTO 7590
C      ----- elastic or plastic -----
      CALL CALPRS(TSTR,SIGMA,PSTRN,PSTRS,COSS,COSA)
      IF(PSTRS(1).GT.0.0.AND.PSTRS(2).GE.0.0.AND.PSTRS(3).GE.0.0)THEN
        CRCK=FT
      ELSEIF(PSTRS(1).GT.0.AND.PSTRS(2).GE.0.0.AND.PSTRS(3).LT.0.0)THEN
        CRCK=FT*(1.0+0.75*PSTRS(3)/FC)
      ELSEIF(PSTRS(1).GT.0.AND.PSTRS(2).LT.0.0.AND.PSTRS(3).LT.0.0)THEN
        CRCK=FT*(1.0+0.75*PSTRS(2)/FC)*(1.0+0.75*PSTRS(3)/FC)
      ENDIF
      IF(CRCK.LT.0.00*FT)CRCK=0.00*FT
      IF(PSTRS(1)-CRCK.GT.0.00001)GOTO 7590
      CALL CRUSHS(INC,ITR,NEL,IGP,SIGMA,TSTR,CRUSH,Ecrsh)
      IF(CRUSH.EQ.1)GOTO 7580
      CALL TRI(EPSTN,L5,FC,E,BEE,CEE,CES,SIGMA,IND,KGT,EFFST,STRSG,STRS
*,Dco,INC,ITR,NEL,Ecrsh,ZFC,KGC)
      GOTO 7565
C*****C
C*****      CRACKED SAMPLING POINT      *****C
C*****C
7590 IF(A2.EQ.0.0)A2=0.0001
      IF(IND(1,KGT).NE.2.AND.CLOS(1,KGC).EQ.0)THEN
        WRITE(6,197)INC,ITR,NEL,IGP,PSTRS(1),CRCK
197  FORMAT('CRCK( 1 )INC,ITR,NE,GP',4I4,' PSTRS(1),CRCK',2F8.4)
      SCR(1,KGC)=CRCK
      ABC(1,KGC)=SCR(1,KGC)/E
      PSTRN(1)=PSTRS(1)/E
      IND(1,KGT)=2
      ECR(1)=(A2*SCR(1,KGC)/PSTRN(1))*(A1-PSTRN(1)/ABC(1,KGC))/(A1-1)
      IF(ECR(1).LT.0.0)ECR(1)=0.0
      IF(ECR(1).GT.(A2*E))ECR(1)=(A2*E)
      PSTRS(1)=ECR(1)*PSTRN(1)
      BETA(1)=(GA2-GA3)*(GA1-PSTRN(1)/ABC(1,KGC))/(GA1-1)+GA3
      IF(BETA(1).GT.1.0)BETA(1)=1.0
      IF(BETA(1).LT.GA3)BETA(1)=GA3
      ECRK(1,KGC)=ECR(1)
      SARR(1)=PSTRS(2)
      SARR(2)=PSTRS(3)
      SARR(3)=PSTRS(5)
      TARR(1)=PSTRN(2)
      TARR(2)=PSTRN(3)
      TARR(3)=PSTRN(5)
      CALL CALPRN(TARR,SARR,PTARR,PSARR,COSN)
      DO 1520 I=2,3
      IF(PSARR(I-1)-CRCK.GT.0.00001)THEN
        WRITE(6,199)I,INC,ITR,NEL,IGP,PSARR(I-1),CRCK
199  FORMAT('CRCK(',I3,' )INC,ITR,NE,GP',4I4,' PSARR(X),CRCK',2F8.4)
      SCR(I,KGC)=CRCK
      ABC(I,KGC)=SCR(I,KGC)/E
      PTARR(I-1)=PSARR(I-1)/E
      IND(I,KGT)=2
      ECR(I)=(A2*SCR(I,KGC)/PTARR(I-1))*(A1-PTARR(I-1)/ABC(I,KGC))/AAA
      IF(ECR(I).LT.0.0)ECR(I)=0.0
      IF(ECR(I).GT.(A2*E))ECR(I)=A2*E

```



```

IF(AMA(1).EQ.0.AND.AMA(2).EQ.1.AND.AMA(3).EQ.0)NSTP=2
IF(AMA(1).EQ.0.AND.AMA(2).EQ.0.AND.AMA(3).EQ.1)NSTP=2
IF(AMA(1).EQ.1.AND.AMA(2).EQ.1.AND.AMA(3).EQ.0)NSTP=3
IF(AMA(1).EQ.1.AND.AMA(2).EQ.0.AND.AMA(3).EQ.1)NSTP=3
IF(AMA(1).EQ.0.AND.AMA(2).EQ.1.AND.AMA(3).EQ.1)NSTP=3
IF(AMA(1).EQ.1.AND.AMA(2).EQ.1.AND.AMA(3).EQ.1)NSTP=4
C#####      COMPUTE THE FACTORS      #####C
  IF(NSTP.EQ.2)THEN
    IF(AMA(1).EQ.1)FAC(1)=ABS(TRSTRN(1,KGC)/CRSTRN(1))
    IF(AMA(2).EQ.1)FAC(1)=ABS(TPSTRN(1,KGC)/TARR(1))
    IF(AMA(3).EQ.1)FAC(1)=ABS(TPSTRN(2,KGC)/TARR(2))
    FAC(2)=1-FAC(1)
    ELSEIF(NSTP.EQ.3.OR.NSTP.EQ.4)THEN
      FAC(1)=ABS(TRSTRN(1,KGC)/CRSTRN(1))
      DO 6010 I=1,3
6010  PTARR(I)=TPSTRN(I,KGC)+TARR(I)*FAC(1)
      IF(NSTP.EQ.3)THEN
        IF(AMA(2).EQ.0.OR.AMA(3).EQ.0)THEN
          KK=1
        IF(AMA(2).EQ.0)KK=2
          IF(PTARR(KK).LT.0)THEN
            FAC(1)=ABS(TPSTRN(KK,KGC)/TARR(KK))
            FAC(2)=ABS((TRSTRN(1,KGC)+CRSTRN(1)*FAC(1))/CRSTRN(1))
          ELSE
            FAC(2)=ABS(PTARR(KK)/TARR(KK))
          ENDIF
        ELSEIF(AMA(1).EQ.0)THEN
          FAC(1)=ABS(TPSTRN(1,KGC)/TARR(1))
          IF((TPSTRN(2,KGC)+TARR(2)*FAC(1)).LT.0)THEN
            FAC(1)=ABS(TPSTRN(2,KGC)/TARR(2))
          FAC(2)=ABS((TPSTRN(1,KGC)+TARR(1)*FAC(1))/TARR(1))
          ELSE
            FAC(2)=ABS((TPSTRN(2,KGC)+TARR(2)*FAC(1))/TARR(2))
          ENDIF
        ENDIF
        FAC(3)=1-FAC(1)-FAC(2)
        ELSEIF(NSTP.EQ.4)THEN
          IF(PTARR(1).LT.0.AND.PTARR(2).LT.0)THEN
            FAC(1)=ABS(TPSTRN(1,KGC)/TARR(1))
            IF((TPSTRN(2,KGC)+TARR(2)*FAC(1)).LT.0)THEN
              FAC(1)=ABS(TPSTRN(2,KGC)/TARR(2))
            FAC(2)=ABS((TPSTRN(1,KGC)+TARR(1)*FAC(1))/TARR(1))
            ELSE
              FAC(2)=ABS((TPSTRN(2,KGC)+TARR(2)*FAC(1))/TARR(2))
            ENDIF
            FAC(3)=ABS((TRSTRN(1,KGC)+CRSTRN(1)*(FAC(1)+FAC(2)))/CRSTRN(1))
          ELSEIF(PTARR(1).LT.0.AND.PTARR(2).GE.0)THEN
            FAC(1)=ABS(TPSTRN(1,KGC)/TARR(1))
            FAC(2)=ABS((TRSTRN(1,KGC)+CRSTRN(1)*FAC(1))/CRSTRN(1))
            FAC(3)=ABS((TPSTRN(2,KGC)+TARR(2)*(FAC(1)+FAC(2)))/TARR(2))
          ELSEIF(PTARR(1).GE.0.AND.PTARR(2).LT.0)THEN
            FAC(1)=ABS(TPSTRN(2,KGC)/TARR(2))
            FAC(2)=ABS((TRSTRN(1,KGC)+CRSTRN(1)*FAC(1))/CRSTRN(1))
            FAC(3)=ABS((TPSTRN(1,KGC)+TARR(1)*(FAC(1)+FAC(2)))/TARR(1))
          ENDIF
          FAC(4)=1-FAC(1)-FAC(2)-FAC(3)
        ENDIF
      ENDIF
C#####      END OF FACTORS      #####C
    DO 6100 ISP=1,NSTP
    DO 6020 II=1,6
    IF(II.LE.3)DPTARR(II)=TARR(II)*FAC(ISP)
6020  DCRSTRN(II)=CRSTRN(II)*FAC(ISP)
    CALL DN1DC1(IND,KGT,Dco,L5,DC,DC1,DN,DN1,DE,COSN,E)

```



```

83 FORMAT('PRE CLOS P1,TR1,CR1',3F10.6,'INS,ITR,NE,GP',4I4,'NSTP,IS'
*,2I4,'CLOS',3F5.2)
GOTO 7570
ENDIF
C=====C
C====          END OF PREVIOUSLY CLOSED          =====C
C=====C
IF(IND(2,KGT).LT.2.AND.IND(3,KGT).LT.2)THEN
CALL CRUSHN(INC,ITR,NEL,IGP,PSARR,PTARR,CRUSH,NU,Ecrsh)
IF(CRUSH.EQ.1)GOTO 7580
CALL TWO(PSTRN,DM,EPSTN,L5,L6,FC,E,BEE,CEE,CES,IND,KGT,KGC,ZFC,
* PSARR,EFFST,STRSGA,STRSA,DE,CURY,INC,ITR,NEL,223,PTARR,Ecrsh)
ELSEIF(IND(2,KGT).LT.2.OR.IND(3,KGT).LT.2)THEN
CALL ONE(K,PSTRN,PTARR,DM,EPSTN,L5,L6,FC,E,IND,KGT,KGC,PSARR,ZFC,
* EFFST,STRSGA,STRSA,DVEC,ABETA,CURY,BEE,CEE,CES,INC,ITR,NEL,PSTRS,
* CRSTRS,CRUSH,IGP,Ecrsh)
IF(CRUSH.EQ.1)GOTO 7580
ENDIF
C*****C
C****  END OF PREVIOUSLY CRACKED (CLOSED OR OPEN) SAMPLING POINT  ****C
C*****C
ENDIF
CALL FIDCDN(DN,DC,DN1,IND,DE,BEE,CEE,CES,PTARR,PSARR,DM,EPSTN,E,
*FC,G,ECR,COSN,COSS,L5,L6,KGT,KGC,BETA,DVEC,ABETA,PSTRN,IS,PSTRS
*,STRSG)
DO 1611 I=1,6
IF(I.LE.3)TPSTRN(I,KGC)=PTARR(I)
IF(I.LE.3)TPSTRS(I,KGC)=PSARR(I)
TRSTRN(I,KGC)=PSTRN(I)
1611 TRSTRS(I,KGC)=PSTRS(I)
GOTO 7570
7580 CONTINUE
DO 1630 I=1,6
IF(I.LE.3)IND(I,KGT)=7
GOTO 7565
1630 STRSG(I,KGT)=0.1D-50
7570 CONTINUE
DO 1541 I=1,6
DO 1541 J=1,6
DDC(KGC,I,J)=DC(I,J)
IF(I.LE.3.AND.J.LE.3)DCOSN(KGC,I,J)=COSN(I,J)
IF(I.LE.3.AND.J.LE.3)DDN(KGC,I,J)=DN(I,J)
DCOSA(KGC,I,J)=COSA(I,J)
1541 DCOSS(KGC,I,J)=COSS(I,J)
C      CALCULATION OF THE EQUIVALENT NODAL FORCES
7565 READ(NTEMP)((BT(I,J),I=1,60),J=1,6)
QUOT=ABS(DDET(NEL,IGP))*WGHT(IGP)
DO 1370 I = 1, 60
DO 1370 J = 1, 6
1370 RNOL(I) = RNOL(I) + QUOT * BT(I,J) * STRSG(J,KGT)
1290 CONTINUE
C      EMBEDDED REINFORCEMENT
DO 1960 IBAR=1,L8
IF(ELTOPB(IBAR,1).EQ.NEL)THEN
IMAT=MPROP(IBAR+L7)
E=EE(IMAT)
H=HH(IMAT)
A=AA(IMAT)
FY=FYFY(IMAT)
DO 1970 IGP=1,2
KGT=KGT+1
READ(NTEMP)(BR(J),J=1,60)
RSTRN=0.0
DO 2000 K=1,60

```

```

2000 RSTRN=RSTRN+BR(K)*ELDIS(K)
      IF(IND(1,KGT).EQ.7)GOTO 7550
      STRNG(1,KGT)=STRNG(1,KGT)+RSTRN
      ABSLUT=ABS(STRNG(1,KGT))
      IF(IMAT.EQ.4.AND.ABSLUT.GE.0.200)WRITE(5,19)INC,ITR,IBAR,IGP
      IF(IMAT.EQ.4.AND.ABSLUT.GE.0.200)GOTO 7550
19  FORMAT('RUPTURE IN STIRRUP REINF.INS,ITR,IB,IG',4I3)
      IF(IMAT.EQ.5.AND.ABSLUT.GE.0.120)WRITE(5,29)INC,ITR,IBAR,IGP
      IF(IMAT.EQ.5.AND.ABSLUT.GE.0.120)GOTO 7550
29  FORMAT('RUPTURE IN LONGITUDENAL REINF.INS,ITR,IB,IG',4I3)
      STLIN=E*RSTRN
      STCUR=STRSG(1,KGT)+STLIN
      PREYS=FY+H*ABS(EPSTN(KGT))
      IF(ABS(STRSG(1,KGT)).LT.PREYS)THEN
          ESCUR=ABS(STCUR)-PREYS
          IF(ESCUR.LE.0.0)GOTO 7950
          RFACT=ESCUR/ABS(STLIN)
      ELSE
          IF(STRSG(1,KGT).GT.0.0.AND.STLIN.LT.0.0)IND(1,KGT)=5
          IF(STRSG(1,KGT).GT.0.0.AND.STLIN.LT.0.0)GOTO 7950
          IF(STRSG(1,KGT).LT.0.0.AND.STLIN.GT.0.0)IND(1,KGT)=5
          IF(STRSG(1,KGT).LT.0.0.AND.STLIN.GT.0.0)GOTO 7950
          RFACT=1.0
      ENDIF
      REDUC=1.0-RFACT
      IND(1,KGT)=4
      STRSG(1,KGT)=STRSG(1,KGT)+REDUC*STLIN+RFACT*E*(1.0-E/(E+H))*RSTRN
      EPSTN(KGT)=EPSTN(KGT)+RFACT*RSTRN*E/(E+H)
      GOTO 7940
7950 STRSG(1,KGT)=STRSG(1,KGT)+STLIN
      GOTO 7940
7550 STRSG(1,KGT)=0.1D-50
      IND(1,KGT)=7
7940 CONTINUE
      QUOT=WGHTR(IGP)*H1H1(IBAR,IGP)*A
      DO 1980 I=1,60
1980 RNOL(I)=RNOL(I)+QUOT*BR(I)*STRSG(1,KGT)
1970 CONTINUE
      ENDIF
1960 CONTINUE

```

```

      elseif(mprop(NEL).eq.2.or.mprop(NEL).eq.7)then
CC ***** RESIDUAL OF STEEL ELEMENTS *****

```

```

C-----
      DO 1291 IGP=1,27
      KGT=KGT+1
      READ (NTEMP) ((B(I,J),I=1,6),J=1,60)
      CALL MATVEC(B,6,60, ELDIS,60,6,60,STRN,6)
      CALL MATVEC(Dst,6,6,STRN,6,6,6, STRS,6)
      PREYS=FY+EPSTN(KGT)*H
      DO 1309 I=1,6
      STRNG(I,KGT)=STRNG(I,KGT)+STRN(I)
1309 SIGMA(I)=STRSG(I,KGT)+STRS(I)
      CALL INVAR3(SIGMA,MEAN,YIELD,THETA)
      ESPRE=EFFST(KGT)-PREYS
      IF(ESPRE.LT.0.0)THEN

          ESCUR=YIELD-PREYS
          IF(ESCUR.LE.0.0)GOTO 7971
          RFACT=ESCUR/(YIELD-EFFST(KGT))
      ELSE
          ESCUR=YIELD-EFFST(KGT)
          IF(ESCUR.LE.0.0)GOTO 7971
          RFACT=1.0

```

```

ENDIF
MSTEP=ESCUR*8/FY+1.0
ASTEP=MSTEP
REDUC=1.0-RFACT
DO 1311 I=1,6
  SGTOT(I)=STRSG(I,KGT)+REDUC*STRS(I)
1311 STRS(I)=RFACT*STRS(I)/ASTEP
  DO 1321 ISTEP=1,MSTEP
    CALL INVAR3(SGTOT,MEAN,YIELD,THETA)
    CALL YIELDIF(AVECT,DVECT,Dst,H,SGTOT,YIELD,ABETA)
    AGASH=0.0
    DO 1331 I=1,6
1331 AGASH=AGASH+AVECT(I)*STRS(I)
    DLAMD=AGASH*ABETA
    IF(DLAMD.LT.0.0)DLAMD=0.0
    BGASH=0.0
    DO 1341 I=1,6
    BGASH=BGASH+AVECT(I)*SGTOT(I)
1341 SGTOT(I)=SGTOT(I)+STRS(I)-DLAMD*DVECT(I)
    EPSTN(KGT)=EPSTN(KGT)+DLAMD*BGASH/YIELD
1321 CONTINUE
    CALL INVAR3(SGTOT,MEAN,YIELD,THETA)
    CURYS=FY+EPSTN(KGT)*H
    BRING=1.0
    IF(YIELD.GT.CURYS)BRING=CURYS/YIELD
    DO 1351 I=1,6
1351 STRSG(I,KGT)=BRING*SGTOT(I)
    EFFST(KGT)=BRING*YIELD
    GOTO 7961
7971 DO 1361 I=1,6
1361 STRSG(I,KGT)=STRSG(I,KGT)+STRS(I)
    EFFST(KGT)=YIELD
7961 CONTINUE
C      CALCULATION OF THE EQUIVALENT NODAL FORCES
  READ(NTEMP)((BT(I,J),I=1,60),J=1,6)
  QUOT=ABS(DDET(NEL,IGP))*WGHT(IGP)
  DO 1371 I = 1,60
  DO 1371 J = 1,6
1371 RNOL(I) = RNOL(I) + QUOT * BT(I,J) * STRSG(J,KGT)
1291 CONTINUE

  endif
  IF(MPROP(NEL).EQ.3)GOTO 1260
  DO 1391 I=1,20
  NODNUM = ELTOP(NEL, I+2)
  DO 1391 J = 1,3
  K2 = NF(NODNUM,J)
  IF(K2.NE.0)L=3*(I-1)+J
  IF(K2.NE.0)PLOAD(K2) = PLOAD(K2) + RNOL(L)
1391 CONTINUE
1260 CONTINUE
  RETURN
  END
CCCCC          COMPUTE INITIAL DC1(6,6) & DN1(6,6)          CCCCC
C=====C
  SUBROUTINE DN1DC1(IND,KT,Dco,L5,DC,DC1,DN,DN1,DE,COSN,E)
  IMPLICIT REAL*8 (A-H,O-Z)
  DIMENSION IND(3,L5),Dco(6,6),DC(6,6),DC1(6,6),DN(3,3),DN1(3,3),
  *DE(3,3),COSN(3,3),TT(3,3),COST(3,3),DL(3,3)
  CALL MATNUL(DC1,6,6)
  DO 4000 I=1,3
  DO 4000 J=1,3
4000 DN1(I,J)=DE(I,J)
  IF(IND(1,KT).NE.2.AND.IND(2,KT).NE.2.AND.IND(3,KT).NE.2)THEN

```

```

DO 4100 I=1,6
DO 4100 J=1,6
4100 DC1(I,J)=Dco(I,J)
      ELSE
      CALL MATNUL (DN1,3,3)
      IF(IND(2,KT).NE.2.AND.IND(3,KT).NE.2)THEN
      DO 4150 I=1,3
      DO 4150 J=1,3
4150 DN1(I,J)=DE(I,J)
      ELSEIF(IND(2,KT).EQ.2.AND.IND(3,KT).NE.2)THEN
      DN1(1,1)=DN(1,1)
      DN1(2,2)=E
      DN1(3,3)=DN(3,3)
      ELSEIF(IND(2,KT).NE.2.AND.IND(3,KT).EQ.2)THEN
      DN1(1,1)=E
      DN1(2,2)=DN(2,2)
      DN1(3,3)=DN(3,3)
      ELSEIF(IND(2,KT).EQ.2.AND.IND(3,KT).EQ.2)THEN
      DN1(1,1)=DN(1,1)
      DN1(2,2)=DN(2,2)
      DN1(3,3)=DN(3,3)
      ENDIF
      CALL MATMUL(COSN,3,3,DN1,3,3,TT,3,3,3,3,3)
      CALL MATRAN(COSN,3,3,COST,3,3,3,3)
      CALL MATMUL(TT,3,3,COST,3,3,DL,3,3,3,3,3)
      DC1(2,2)=DL(1,1)
      DC1(2,3)=DL(1,2)
      DC1(3,2)=DC1(2,3)
      DC1(2,5)=DL(1,3)
      DC1(5,2)=DC1(2,5)
      DC1(3,3)=DL(2,2)
      DC1(3,5)=DL(2,3)
      DC1(5,3)=DC1(3,5)
      DC1(5,5)=DL(3,3)
      IF(IND(1,KT).EQ.2)THEN
      DC1(1,1)=DC(1,1)
      DC1(4,4)=DC(4,4)
      DC1(6,6)=DC(6,6)
      ELSEIF(IND(2,KT).EQ.2.AND.IND(3,KT).NE.2)THEN
      DC1(1,1)=DE(1,1)
      DC1(1,3)=DE(1,2)
      DC1(3,1)=DE(2,1)
      DC1(6,6)=DE(3,3)
      DC1(4,4)=DC(4,4)
      ELSEIF(IND(2,KT).EQ.2.AND.IND(3,KT).EQ.2)THEN
      DC1(1,1)=DC(1,1)
      DC1(4,4)=DC(4,4)
      DC1(6,6)=DC(6,6)
      ELSEIF(IND(2,KT).NE.2.AND.IND(3,KT).EQ.2)THEN
      DC1(1,1)=DE(1,1)
      DC1(1,2)=DE(1,2)
      DC1(2,1)=DE(2,1)
      DC1(4,4)=DE(3,3)
      DC1(6,6)=DC(6,6)
      ENDIF
      ENDIF
      RETURN
      END
CCCCC   CRACKED OR RECRACKED CLOSED OR RECLOSED GAUSS POINT   CCCCC
C=====C
      SUBROUTINE CRKCLO(PSTRN,A1,A2,SCR,KGC,ABC,ECRK,PSTRS,BETA,GA1,GA2,
      *GA3,IND,KGT,L5,PTARR,PSARR,FT,DM,FC,COSN,STRSA,STRSGA,E,CLOS,L6,
      *AMA,AAA,INC,ITR,NEL,IGP,IMK)
      IMPLICIT REAL*8 (A-H,O-Z)

```

```

DIMENSION PSTRN(6),SCR(3,L6),AMA(3),DM(L6),ECLK(3,L6),PSTRS(6)
*,BETA(3),IND(3,L5),PTARR(3),PSARR(3),PPTARR(3),PPSARR(3),COSM(3,3)
*,ECLK(3),COSN(3,3),COSNN(3,3),STRSA(3),STRSGA(3),STRSB(3),STRSGB(3)
*,ABC(3,L6),CLOS(3,L6)
    IF(PSTRN(1).GT.0.0)THEN
        IF(IMK.EQ.0)GOTO 1527
        ECLK(1)=(A2*SCR(1,KGC)/PSTRN(1))*(A1-PSTRN(1)/ABC(1,KGC))/AAA
        IF(ECLK(1).LT.0.0)ECLK(1)=0.0
        IF(ECLK(1).GT.ECLK(1,KGC))ECLK(1)=ECLK(1,KGC)
        PSTRS(1)=ECLK(1)*PSTRN(1)
        BETA(1)=(GA2-GA3)*(GA1-PSTRN(1)/ABC(1,KGC))/(GA1-1)+GA3
        IF(BETA(1).GT.1.0)BETA(1)=1.0
        IF(BETA(1).LT.GA3)BETA(1)=GA3
        ECLK(1,KGC)=ECLK(1)
        IF(IMK.EQ.2)IND(1,KGT)=2
1527    CLOS(1,KGC)=0
        ELSE
        IF(IMK.EQ.2)IND(1,KGT)=0
        IF(CLOS(1,KGC).EQ.0.0.AND.IMK.EQ.0)AMA(1)=1
        ECLK(1)=E
        CLOS(1,KGC)=1
        BETA(1)=1.0
    ENDIF
C    ***** 1 CLOSSED *****
    IF(CLOS(2,KGC).EQ.1.OR.CLOS(3,KGC).EQ.1)GOTO 1568
    IF(IND(2,KGT).LT.2.AND.IND(3,KGT).LT.2)THEN
        CALL CALPRN(PTARR,PSARR,PPTARR,PPSARR,COSM)
        IF(IND(1,KGT).EQ.2)THEN
            IF( PPSARR(1).GE.0.0.AND.PPSARR(2).GE.0.0)THEN
                CRCK=FT
            ELSEIF(PPSARR(1).GT.0.AND.PPSARR(2).LT.0)THEN
                CRCK=FT*(1.0+0.75*PPSARR(2)/(DM(KGC)*FC))
            ELSEIF(PPSARR(2).GT.0.0.AND.PPSARR(1).LT.0.0)THEN
                CRCK=FT*(1.0+0.75*PPSARR(1)/(DM(KGC)*FC))
            ENDIF
        ELSE
            IF(PPSARR(1).GE.0.AND.PPSARR(2).GE.0)THEN
                CRCK=FT*(1.0+0.75*PSTRS(1)/FC)
            ELSEIF(PPSARR(1).GE.0.AND.PPSARR(2).LT.0)THEN
                CRCK=FT*(1.0+0.75*PSTRS(1)/FC)*(1.0+0.75*PPSARR(2)/FC)
            ELSEIF(PPSARR(1).LT.0.AND.PPSARR(2).GE.0)THEN
                CRCK=FT*(1.0+0.75*PSTRS(1)/FC)*(1.0+0.75*PPSARR(1)/FC)
            ENDIF
        ENDIF
        IF(CRCK.LT.0.0)CRCK=0.00
        IF(PPSARR(1)-CRCK.GT.0.00001.OR.PPSARR(2)-CRCK.GT.0.00001)THEN
            DO 1530 I=1,3
                PSARR(I)=PPSARR(I)
                PTARR(I)=PPTARR(I)
                STRSB(I)=STRSA(I)
                STRSGB(I)=STRSGA(I)
            DO 1530 J=1,3
1530    COSN(I,J)=COSM(I,J)
                CALL MATINV(COSN,3,3,COSNN,3,3,3,DOT)
                CALL MATVEC(COSNN,3,3,STRSGB,3,3,3,STRSGA,3)
                CALL MATVEC(COSNN,3,3,STRSB,3,3,3,STRSA,3)
            ENDIF
        ENDIF
1568    CONTINUE
        DO 1570 I=2,3
            IF(IND(I,KGT).EQ.2.OR.CLOS(I,KGC).EQ.1)THEN
                IF(PTARR(I-1).GT.0.0)THEN
                    IF(IMK.EQ.0)GOTO 1528
                    ECLK(I)=(A2*SCR(I,KGC)/PTARR(I-1))*(A1-PTARR(I-1)/ABC(I,KGC))/AAA

```

```

IF(ECR(I).LT.0.0)ECR(I)=0.0
IF(ECR(I).GT.ECRK(I,KGC))ECR(I)=ECRK(I,KGC)
PSARR(I-1)=ECR(I)*PTARR(I-1)
BETA(I)=(GA2-GA3)*(GA1-PTARR(I-1)/ABC(I,KGC))/(GA1-1)+GA3
IF(BETA(I).GT.1.0)BETA(I)=1.0
IF(BETA(I).LT.GA3)BETA(I)=GA3
ECRK(I,KGC)=ECR(I)
    IF(IMK.EQ.2)IND(I,KGT)=2
1528 CLOS(I,KGC)=0
ELSE
    IF(IMK.EQ.2)IND(I,KGT)=0
        IF(CLOS(I,KGC).EQ.0.0.AND.IMK.EQ.0)AMA(I)=1
    ECR(I)=E
    CLOS(I,KGC)=1
    BETA(I)=1.0
ENDIF
C    ***** 2 or 3 CLOSSED *****
ELSE
    IF(IMK.EQ.0.OR.IMK.EQ.2)GOTO 1570
    IF(IND(2,KGT).EQ.2.OR.IND(3,KGT).EQ.2)THEN
    IF(IND(1,KGT).EQ.2)CRCK=FT
    IF(IND(1,KGT).NE.2)CRCK=FT*(1.0+0.75*PSTRS(1)/(FC*DM(KGC)))
    IF(CRCK.LT.0.00*FT)CRCK=0.00*FT
    ENDIF
    IF(PSARR(I-1)-CRCK.GT.0.00001)THEN
        WRITE(6,192)I,INC,ITR,NEL,IGP,PSARR(I-1),CRCK
192    FORMAT('CRCK('I3,' )INC,ITR,NE,GP,4I4,' PSARR(X),CRCK',2F8.4)
        SCR(I,KGC)=CRCK
        ABC(I,KGC)=SCR(I,KGC)/E
        PTARR(I-1)=PSARR(I-1)/E
        IF(IMK.EQ.2)IND(I,KGT)=2
        ECR(I)=(A2*SCR(I,KGC)/PTARR(I-1))*(A1-PTARR(I-1)/ABC(I,KGC))/AAA
        IF(ECR(I).LT.0.0)ECR(I)=0.0
        IF(ECR(I).GT.A2*E)ECR(I)=A2*E
        PSARR(I-1)=ECR(I)*PTARR(I-1)
        BETA(I)=(GA2-GA3)*(GA1-PTARR(I-1)/ABC(I,KGC))/(GA1-1)+GA3
        IF(BETA(I).GT.1.0)BETA(I)=1.0
        IF(BETA(I).LT.GA3)BETA(I)=GA3
        ECRK(I,KGC)=ECR(I)
    ENDIF
ENDIF
1570 CONTINUE
RETURN
END
CCCCC                                FINAL DC(6,6) & DN(3,3) & STRSG                                CCCCC
C=====C
SUBROUTINE FIDCDN(DN,DC,DN1,IND,DE,BEE,CEE,CES,PTARR,PSARR,DM
*,EPSTN,E,FC,G,ECR,COSN,COSS,L5,L6,KGT,KGC,BETA,DVECTA,ABETA,PSTRN,IS
*,PSTRS,STRSG)
IMPLICIT REAL*8 (A-H,O-Z)
DIMENSION DN(3,3),IND(3,L5),DE(3,3),PSARR(3),STRSG(6,L5),DVECTA(3)
*,PLASR(6),EPSTN(L5),COST(3,3),BETA(3),PTARR(3),COSN(3,3),AVECTA(3)
*,TT(3,3),DN1(3,3),DL(3,3),DC(6,6),PLAS(3),PSTRN(6),PSTRS(6),ECR(3)
*,COSS(6,6),DM(L6)
CALL MATNUL(DN,3,3)
IF(IND(2,KGT).LT.2.AND.IND(3,KGT).LT.2)THEN
IF(IND(2,KGT).EQ.-4.AND.IND(3,KGT).EQ.-4)THEN
CALL INVAN(BEE,CEE,CES,AVECTA,PSARR,YIELD)
DAM=DM(KGC)
CALL FLOWPN(AVECTA,DVECTA,DE,DAM,DENOM,ABETA,KGT,E,FC,EPSTN,L5)
DO 3540 I=1,3
DO 3540 J=1,3
3540 DN(I,J)=DE(I,J)-ABETA*DVECTA(I)*DVECTA(J)
ELSE

```

```

DO 3520 I=1,3
DO 3520 J=1,3
3520 DN(I,J)=DE(I,J)
ENDIF
ENDIF
IF(IND(2,KGT).EQ.2.AND.IND(3,KGT).NE.2)THEN
DN(1,1)=ECR(2)
DN(2,2)=E
IF(IND(3,KGT).EQ.-4)DN(2,2)=E-ABETA*DVEC*DVEC
IF(IS.EQ.213)DN(2,2)=DN1(2,2)
DN(3,3)=BETA(2)*G
PSARR(3)=DN(3,3)*PTARR(3)
ELSEIF(IND(2,KGT).NE.2.AND.IND(3,KGT).EQ.2)THEN
DN(1,1)=E
IF(IND(2,KGT).EQ.-4)DN(1,1)=E-ABETA*DVEC*DVEC
IF(IS.EQ.212)DN(1,1)=DN1(2,2)
DN(2,2)=ECR(3)
DN(3,3)=BETA(3)*G
PSARR(3)=DN(3,3)*PTARR(3)
ELSEIF(IND(2,KGT).EQ.2.AND.IND(3,KGT).EQ.2)THEN
DN(1,1)=ECR(2)
DN(2,2)=ECR(3)
DN(3,3)=BETA(2)*G
IF(BETA(2).GE.BETA(3))DN(3,3)=BETA(3)*G
PSARR(3)=DN(3,3)*PTARR(3)
ENDIF
CALL MATVEC(COSN,3,3,PSARR,3,3,PLAS,3)
PSTRS(2)=PLAS(1)
PSTRS(3)=PLAS(2)
PSTRS(5)=PLAS(3)
CALL MATMUL(COSN,3,3,DN,3,3,TT,3,3,3,3,3)
CALL MATRAN(COSN,3,3,COST,3,3,3,3,3)
CALL MATMUL(TT,3,3,COST,3,3,DL,3,3,3,3,3)
CALL MATNUL(DC,6,6)
DC(1,1)=ECR(1)
IF(IND(1,KGT).EQ.00.AND.IS.EQ.11)DC(1,1)=E
IF(IND(1,KGT).EQ.-4.AND.IS.EQ.11)DC(1,1)=E-ABETA*DVEC*DVEC
IF(IS.EQ.212.OR.IS.EQ.213)DC(1,1)=DN1(1,1)
IF(IS.EQ.212)DC(1,2)=DN1(1,2)
IF(IS.EQ.212)DC(2,1)=DN1(2,1)
IF(IS.EQ.213)DC(1,3)=DN1(1,2)
IF(IS.EQ.213)DC(3,2)=DN1(1,2)
DC(2,2)=DL(1,1)
DC(2,3)=DL(1,2)
DC(3,2)=DC(2,3)
DC(2,5)=DL(1,3)
DC(5,2)=DC(2,5)
DC(3,3)=DL(2,2)
DC(3,5)=DL(2,3)
DC(5,3)=DC(3,5)
DC(5,5)=DL(3,3)
DC(4,4)=BETA(1)*G
DC(6,6)=BETA(1)*G
PSTRS(4)=DC(4,4)*PSTRN(4)
PSTRS(6)=DC(6,6)*PSTRN(6)
CALL MATVEC(COSS,6,6,PSTRS,6,6,PLASR,6)
DO 1620 I=1,6
1620 STRSG(I,KGT)=PLASR(I)
RETURN
END
CCCCC STATE OF STRESSES ( 1 or 2 or 3 ) DIMENSIONS CCCCC
C=====C
SUBROUTINE STATE(PSTRN,PSTRS,CRSTRS,PTARR,PSARR,STRSGA,STRSA,DM,
*IS,COSN,TRSTRS,NU,CRUSH,DE,COSS,STRSG,Dco,COSA,EFFST,EPSTN,IND,

```

```

*L5,L6,FC,KGT,KGC,DVEC,ABETA,CURY,BEE,CEE,CES,INC,ITR,NEL,IGP,
*E,SARR,TPSTRS,Ecrsh)
IMPLICIT REAL*8 (A-H,O-Z)
REAL *8 NU
DIMENSION PSTRN(6),PSTRS(6),CRSTRS(6),PTARR(3),PSARR(3),STRSGA(3),
*STRSA(3),DM(L6),COSN(3,3),TRSTRS(6,L6),DE(3,3),CURY(L6),DN(3,3),
*TMTARR(3),TMSARR(3),AVECTA(3),DVECTA(3),SGTOT(6),SIGMA(6),STRS(6),
*SARR(3),Dco(6,6),COSA(6,6),EFFST(L5),EPSTN(L5),IND(3,L5),COSS(6,6)
*,COST(3,3),STRSG(6,L5),TPSTRS(3,L6)
  IF(IND(1,KGT).EQ.2.AND.IND(2,KGT).EQ.2.AND.IND(3,KGT).EQ.2)IS=0
  IF(IND(1,KGT).NE.2.AND.IND(2,KGT).EQ.2.AND.IND(3,KGT).EQ.2)IS=11
  IF(IND(1,KGT).EQ.2.AND.IND(2,KGT).NE.2.AND.IND(3,KGT).EQ.2)IS=12
  IF(IND(1,KGT).EQ.2.AND.IND(2,KGT).EQ.2.AND.IND(3,KGT).NE.2)IS=13
  IF(IND(1,KGT).NE.2.AND.IND(2,KGT).NE.2.AND.IND(3,KGT).EQ.2)IS=212
  IF(IND(1,KGT).NE.2.AND.IND(2,KGT).EQ.2.AND.IND(3,KGT).NE.2)IS=213
  IF(IND(1,KGT).EQ.2.AND.IND(2,KGT).NE.2.AND.IND(3,KGT).NE.2)IS=223
  IF(IND(1,KGT).NE.2.AND.IND(2,KGT).NE.2.AND.IND(3,KGT).NE.2)IS=3
  IF(IS.GT.10.AND.IS.LT.14)THEN
    IF(IS.EQ.11)K=3
  CALL ONE(K,PSTRN,PTARR,DM,EPSTN,L5,L6,FC,E,IND,KGT,KGC,PSARR,ZFC,
* EFFST,STRSGA,STRSA,DVEC,ABETA,CURY,BEE,CEE,CES,INC,ITR,NEL,PSTRS,
* CRSTRS,CRUSH,IGP,Ecrsh)
    IF(CRUSH.EQ.1)GOTO 3533
    ELSEIF(IS.GT.210.AND.IS.LT.224)THEN
      IF(IS.EQ.212.OR.IS.EQ.213)THEN
        THE=ASIN(SQRT(COSN(1,2)))
        WRITE(2,*)'THE=',THE,' IS=',IS
        DO 6040 I=1,3
          TMTARR(I)=PTARR(I)
6040 TMSARR(I)=PSARR(I)
          PTARR(1)=PSTRN(1)
          PSARR(1)=PSTRS(1)
          STRSGA(1)=TRSTRS(1,KGC)
          STRSA(1)=CRSTRS(1)
          IF(IS.EQ.212)THEN
            PTARR(2)=TMTARR(1)
            PTARR(3)=PSTRN(4)*COS(THE)+PSTRN(6)*SIN(THE)
            PSARR(2)=TMSARR(1)
            PSARR(3)=PSTRS(4)*COS(THE)+PSTRS(6)*SIN(THE)
            STRSGA(2)=TPSTRS(1,KGC)
            STRSGA(3)=TRSTRS(4,KGC)*COS(THE)+TRSTRS(6,KGC)*SIN(THE)
            STRSA(2)=SARR(1)
            STRSA(3)=CRSTRS(4)*COS(THE)+CRSTRS(6)*SIN(THE)
          ELSEIF(IS.EQ.213)THEN
            PTARR(2)=TMTARR(2)
            PTARR(3)=PSTRN(6)*COS(THE)-PSTRN(4)*SIN(THE)
            PSARR(2)=TMSARR(2)
            PSARR(3)=PSTRS(6)*COS(THE)-PSTRS(4)*SIN(THE)
            STRSGA(2)=TPSTRS(2,KGC)
            STRSGA(3)=TRSTRS(6,KGC)*COS(THE)-TRSTRS(4,KGC)*SIN(THE)
            STRSA(2)=SARR(2)
            STRSA(3)=CRSTRS(6)*COS(THE)-CRSTRS(4)*SIN(THE)
          ENDIF
        ENDIF
      CALL CRUSHN(INC,ITR,NEL,IGP,PSARR,PTARR,CRUSH,NU,Ecrsh)
      IF(CRUSH.EQ.1)GOTO 3533
      CALL TWO(PSTRN,DM,EPSTN,L5,L6,FC,E,BEE,CEE,CES,IND,KGT,KGC,ZFC
* ,PSARR,EFFST,STRSGA,STRSA,DE,CURY,INC,ITR,NEL,IS,PTARR,Ecrsh)
      IF(IS.EQ.212.OR.IS.EQ.213)THEN
        PSTRS(1)=PSARR(1)
        IF(IS.EQ.212)TMSARR(1)=PSARR(2)
        IF(IS.EQ.213)TMSARR(2)=PSARR(2)
        DO 6090 I=1,3
          PTARR(I)=TMTARR(I)

```

```

6090 PSARR(I)=TMSARR(I)
      IF(IND(1,KGT).EQ.-4)THEN
        CALL INVAN(BEE,CEE,CES,AVECTA,PSARR,YIELD)
          DAM=DM(KGC)
        CALL FLOWPN(AVECTA,DVECTA,DE,DAM,DENOM,ABETA,KGT,E,FC,EPSTN,L5)
        DO 3540 I=1,3
        DO 3540 J=1,3
3540  DN(I,J)=DE(I,J)-ABETA*DVECTA(I)*DVECTA(J)
      ELSE
        DO 3520 I=1,3
        DO 3520 J=1,3
3520  DN(I,J)=DE(I,J)
      ENDIF
      ENDIF
      ELSEIF(IS.EQ.3)THEN
        CALL CRUSHS(INC,ITR,NEL,IGP,PSTRS,PSTRN,CRUSH,Ecrsh)
        IF(CRUSH.EQ.1)GOTO 3533
        DO 3526 I=1,6
3526  SGTOT(I)=TRSTRS(I,KGC)
        CALL MATVEC(COSS,6,6,SGTOT,6,6,6,SIGMA,6)
        CALL MATVEC(COSS,6,6,CRSTRS,6,6,6,STRS,6)
        CALL TRI(EPSTN,L5,FC,E,BEE,CEE,CES,SIGMA,IND,KGT,EFFST,STRSG,STRS
* ,Dco,INC,ITR,NEL,Ecrsh,ZFC,KGC)
        CALL MATVEC(COSA,6,6,STRSG,6,6,6,PSTRS,6)
        SARR(1)=PSTRS(2)
        SARR(2)=PSTRS(3)
        SARR(3)=PSTRS(5)
        CALL MATINV(COSN,3,3,COST,3,3,3,DOT)
        CALL MATVEC(COST,3,3,SARR,3,3,3,PSARR,3)
      ENDIF
3533 RETURN
      END
CCCCC          3D CRUSH STRAINS          CCCCC
      SUBROUTINE CRUSHS(INC,ITR,NEL,IGP,ST,STRN,CRUSH,Ecrsh)
      IMPLICIT REAL*8 (A-H,O-Z)
      DIMENSION STRN(6),ST(6),DEV(6)
      VAR1=STRN(1)-STRN(2)
      VAR2=STRN(2)-STRN(3)
      VAR3=STRN(3)-STRN(1)
      VAR4=VAR1*VAR1+VAR2*VAR2+VAR3*VAR3
      VAR5=STRN(4)**2+STRN(5)**2+STRN(6)**2
      VARRNJ2=VAR4/6.0+VAR5/4.0
      VARSTI1=ST(1)+ST(2)+ST(3)
      DO 1212 I=1,6
        IF(I.LE.3)DEV(I)=ST(I)-(ST(1)+ST(2)+ST(3))/3.0
1212  IF(I.GT.3)DEV(I)=ST(I)
        A=DEV(1)*DEV(1)+DEV(2)*DEV(2)+DEV(3)*DEV(3)
        B=DEV(4)*DEV(4)+DEV(5)*DEV(5)+DEV(6)*DEV(6)
        VARSTJ2=0.5*A+B
        IF(VARSTI1.LE.0.AND.SQRT(VARSTJ2).LE.(-VARSTI1/SQRT(3.0)))THEN
          IF(VARRNJ2.GE.(0.333333*(Ecrsh)**2)) CRUSH = 1.0
        ELSE
          CRUSH=0.0
        ENDIF
        IF(CRUSH.EQ.1.0)WRITE(11,7)INC,ITR,NEL,IGP
        IF(CRUSH.EQ.1.0)WRITE(*,7)INC,ITR,NEL,IGP
7    FORMAT('SPACE.CR.INS,ITR,NE,IGP',4I3)
      RETURN
      END
CCCCC          2D CRUSH STRAINS          CCCCC
      SUBROUTINE CRUSHN(INC,ITR,NEL,IGP,STA,STRNA,CRUSH,NU,Ecrsh)
      IMPLICIT REAL*8 (A-H,O-Z)
      REAL *8 NU
      DIMENSION STRNA(3),STA(3),DEVA(4)

```

```

ABSLN3=-NU*(STRNA(1)+STRNA(2))
A=(STRNA(1)+STRNA(2)+ABSLN3)/3.0
A1=STRNA(1)-A
A2=STRNA(2)-A
A3=ABSLN3-A
VARRNJ2=0.5*(A1*A1+A2*A2+A3*A3)+STRNA(3)*STRNA(3)/4.0
VARSTI1=STA(1)+STA(2)+0.0
DEVA(1)=STA(1)-(STA(1)+STA(2)+0.0)/3.0
DEVA(2)=STA(2)-(STA(1)+STA(2)+0.0)/3.0
DEVA(3)=STA(3)
DEVA(4)=0.0-(STA(1)+STA(2)+0.0)/3.0
VARSTJ2=0.5*(DEVA(1)**2+DEVA(2)**2+DEVA(4)**2)+DEVA(3)**2
      IF(VARSTI1.LE.0.AND.SQRT(VARSTJ2).LE.(-VARSTI1/SQRT(3.0)))THEN
      IF(VARRNJ2.GE.(0.333333*(Ecrsh)**2))CRUSH=1.0
      ELSE
      CRUSH=0.0
      ENDF
      IF(CRUSH.EQ.1.0)WRITE(11,1)INC,ITR,NEL,IGP
      IF(CRUSH.EQ.1.0)WRITE(*,1)INC,ITR,NEL,IGP
1  FORMAT(' PNAN CR.INS,ITR,NE,GP',4I3)
      RETURN
      END
CCCCC          3D PRINCIPAL STRESSES          CCCCC
SUBROUTINE CALPRS(STRN,STRS,PSTRN,PSTRS,COSS,COSA)
IMPLICIT REAL*8 (A-H,O-Z)
DIMENSION STRS(6),PSTRS(6),COO(3,3),COSA(6,6),COSS(6,6),REZ(3),
*STRN(6),PSTRN(6),T(6,6)
CALL VECNUL(PSTRS,6)
      CALL INVAR3(STRS,SIGM,DSBAR,THETA)
PI=4.0*ATAN(1.0)
REZ(1)=SIGM+2.0*DSBAR/3.0*SIN(THETA-2.0*PI/3.0)
REZ(2)=SIGM+2.0*DSBAR/3.0*SIN(THETA)
REZ(3)=3.0*SIGM-REZ(1)-REZ(2)
      DO 99 I=1,3
      PSTRS(I)=REZ(I)
99  CONTINUE
      DO 11 I=1,2
      IMAX=I
      AMAX=PSTRS(IMAX)
      DO 12 J=I+1,3
      IF(PSTRS(J).GT.AMAX)IMAX=J
12  IF(PSTRS(J).GT.AMAX)AMAX=PSTRS(J)
      PSTRS(IMAX)=PSTRS(I)
11  PSTRS(I)=AMAX
      DO 101 I=1,3
      C1=(STRS(2)-PSTRS(I))*(STRS(3)-PSTRS(I))-STRS(5)*STRS(5)
      C2=STRS(5)*STRS(6)-STRS(4)*(STRS(3)-PSTRS(I))
      C3=STRS(4)*STRS(5)-STRS(6)*(STRS(2)-PSTRS(I))
      C4=SQRT(C1**2+C2**2+C3**2)
      COO(I,1)=C1/C4
      COO(I,2)=C2/C4
101  COO(I,3)=C3/C4
      DO 103 I=1,3
      DO 103 J=1,3
103  COSS(I,J)=COO(J,I)*COO(J,I)
      DO 104 J=1,3
      COSS(4,J)=COO(J,1)*COO(J,2)
      COSS(5,J)=COO(J,2)*COO(J,3)
104  COSS(6,J)=COO(J,3)*COO(J,1)
      DO 105 I=1,3
      COSS(I,4)=2.0*COO(1,I)*COO(2,I)
      COSS(I,5)=2.0*COO(2,I)*COO(3,I)
105  COSS(I,6)=2.0*COO(3,I)*COO(1,I)
      COSS(4,4)=COO(1,1)*COO(2,2)+COO(2,1)*COO(1,2)

```

```

COSS(4,5)=COO(2,1)*COO(3,2)+COO(3,1)*COO(2,2)
COSS(4,6)=COO(3,1)*COO(1,2)+COO(1,1)*COO(3,2)
COSS(5,4)=COO(1,2)*COO(2,3)+COO(2,2)*COO(1,3)
COSS(5,5)=COO(2,2)*COO(3,3)+COO(3,2)*COO(2,3)
COSS(5,6)=COO(3,2)*COO(1,3)+COO(1,2)*COO(3,3)
COSS(6,4)=COO(1,3)*COO(2,1)+COO(2,3)*COO(1,1)
COSS(6,5)=COO(2,3)*COO(3,1)+COO(3,3)*COO(2,1)
COSS(6,6)=COO(3,3)*COO(1,1)+COO(1,3)*COO(3,1)
    CALL MATRAN(COSS,6,6,T,6,6,6,6)
CALL MATVEC(T,6,6,STRN,6,6,6,PSTRN,6)
DO 80 I=1,6
DO 80 J=1,6
    COSA(I,J)=T(I,J)
    IF(I.GT.3.AND.J.LE.3)COSA(I,J)=T(I,J)/2.0
    IF(I.LE.3.AND.J.GT.3)COSA(I,J)=T(I,J)*2.0
80 CONTINUE
RETURN
END
CCCC
SUBROUTINE INVAR3(STRESS,SMEAN,DSBAR,THETA)
IMPLICIT REAL *8 (A-H,O-Z)
DIMENSION STRESS(6)
S1=STRESS(1)
S2=STRESS(2)
S3=STRESS(3)
S4=STRESS(4)
S5=STRESS(5)
S6=STRESS(6)
SMEAN=(S1+S2+S3)/3.0
D2=((S1-S2)**2+(S2-S3)**2+(S3-S1)**2)/6.0+S4**2+S5**2+S6**2
DS1=S1-SMEAN
DS2=S2-SMEAN
DS3=S3-SMEAN
D3=DS1*DS2*DS3-DS1*S5*S5-DS2*S6*S6-DS3*S4*S4+2.0*S4*S5*S6
DSBAR=SQRT(3.0*D2)
SINE=-3.0*SQRT(3.0)*D3/(2.0*SQRT(1.0*D2)**3)
IF(SINE.GT.1.0)SINE=1.0
IF(SINE.LT.-1.0)SINE=-1.0
THETA=ASIN(SINE)/3.0
IF(DSBAR.EQ.0.0)THETA=0.0
RETURN
END
CCCC      2D PRINCIPAL STRESSES      CCCCC
SUBROUTINE CALPRN(STRN,STRS,PSTRN,PSTRS,COSS)
IMPLICIT REAL*8 (A-H,O-Z)
DIMENSION STRS(3),PSTRS(3),COSS(3,3),STRN(3),PSTRN(3),T(3,3)
CALL VECNUL(PSTRS,3)
B1=STRS(1)-STRS(2)
B2=SQRT(B1*B1/4.0+STRS(3)*STRS(3))
B3=0.5*(STRS(1)+STRS(2))
PSTRS(1)=B3+B2
PSTRS(2)=B3-B2
IF(B1.EQ.0.0)B1=0.000000001
ANG=180.0*(ATAN(2.0*STRS(3)/B1))/3.141593
IF(STRS(1).LT.STRS(2))THETA=0.5*ANG+90.0
IF(STRS(1).GE.STRS(2))THETA=0.5*ANG
AT=THETA*3.141593/180.0
T(1,1)=COS(AT)*COS(AT)
T(1,2)=SIN(AT)*SIN(AT)
T(1,3)=SIN(AT)*COS(AT)
T(2,1)=SIN(AT)*SIN(AT)
T(2,2)=COS(AT)*COS(AT)
T(2,3)=-SIN(AT)*COS(AT)
T(3,1)=-2.0*COS(AT)*SIN(AT)

```

```

T(3,2)=2.0*SIN(AT)*COS(AT)
T(3,3)=COS(AT)*COS(AT)-SIN(AT)*SIN(AT)
CALL MATRAN(T,3,3,COSS,3,3,3,3)
CALL MATVEC(T,3,3,STRN,3,3,3,PSTRN,3)
RETURN
END
CCCC
SUBROUTINE MATNUL(ARR,IR,JR)
IMPLICIT REAL*8 (A-H,O-Z)
DIMENSION ARR(IR,JR)
DO 10 I=1,IR
DO 10 J=1,JR
10 ARR(I,J)=0.0
RETURN
END
CCCC
SUBROUTINE VECNUL(AR,IR)
IMPLICIT REAL*8 (A-H,O-Z)
DIMENSION AR(IR)
DO 20 I=1,IR
20 AR(I)=0.0
RETURN
END
CCCC
SUBROUTINE DISO(D,ID,JD,E,NU,IUMSS)
IMPLICIT REAL*8 (A-H,O-Z)
REAL*8 NU
DIMENSION D(ID,JD)
CALL MATNUL(D,IUMSS,IUMSS)
DO 30 I=1,3
DO 30 J=1,3
IF(I.EQ.J)D(I,J)=E*(1.0-NU)/((1.0+NU)*(1.0-2.0*NU))
IF(I.NE.J)D(I,J)=NU*E/((1.0+NU)*(1.0-2.0*NU))
30 CONTINUE
D(4,4)=E/(2.0+2.0*NU)
D(5,5)=E/(2.0+2.0*NU)
D(6,6)=E/(2.0+2.0*NU)
RETURN
END
CCCC
SUBROUTINE BRK20(FUN,IFUN,DER,IDER,JDER,X,Y,Z)
IMPLICIT REAL*8 (A-H,O-Z)
DIMENSION FUN(IFUN),DER(IDER,JDER)
FUN(1)=0.125*(1.0-X)*(1.0-Y)*(1.0-Z)*(-X-Y-Z-2.0)
DER(1,1)=-0.125*(1.0-Y)*(1.0-Z)*(-2.0*X-Y-Z-1.0)
DER(2,1)=-0.125*(1.0-X)*(1.0-Z)*(-X-2.0*Y-Z-1.0)
DER(3,1)=-0.125*(1.0-X)*(1.0-Y)*(-X-Y-2.0*Z-1.0)
FUN(2)=0.25*(1.0-X)*(1.0-Z)*(1.0-Y)*(1.0+Y)
DER(1,2)=-0.25*(1.0-Z)*(1.0-Y)*(1.0+Y)
DER(2,2)=-0.5*(1.0-X)*(1.0-Z)*Y
DER(3,2)=-0.25*(1.0-X)*(1.0-Y)*(1.0+Y)
FUN(3)=0.125*(1.0-X)*(1.0+Y)*(1.0-Z)*(-X+Y-Z-2.0)
DER(1,3)=-0.125*(1.0+Y)*(1.0-Z)*(-2.0*X+Y-Z-1.0)
DER(2,3)=0.125*(1.0-X)*(1.0-Z)*(-X+2.0*Y-Z-1.0)
DER(3,3)=-0.125*(1.0-X)*(1.0+Y)*(-X+Y-2.0*Z-1.0)
FUN(4)=0.25*(1.0+Y)*(1.0-Z)*(1.0-X)*(1.0+X)
DER(1,4)=-0.5*(1.0+Y)*(1.0-Z)*X
DER(2,4)=0.25*(1.0-Z)*(1.0-X)*(1.0+X)
DER(3,4)=-0.25*(1.0+Y)*(1.0-X)*(1.0+X)
FUN(5)=0.125*(1.0+X)*(1.0+Y)*(1.0-Z)*(X+Y-Z-2.0)
DER(1,5)=0.125*(1.0+Y)*(1.0-Z)*(2.0*X+Y-Z-1.0)
DER(2,5)=0.125*(1.0+X)*(1.0-Z)*(X+2.0*Y-Z-1.0)
DER(3,5)=-0.125*(1.0+X)*(1.0+Y)*(X+Y-2.0*Z-1.0)
FUN(6)=0.25*(1.0+X)*(1.0-Z)*(1.0-Y)*(1.0+Y)

```

```

DER(1,6)=0.25*(1.0-Z)*(1.0-Y)*(1.0+Y)
DER(2,6)=-0.5*(1.0+X)*(1.0-Z)*Y
DER(3,6)=-0.25*(1.0+X)*(1.0-Y)*(1.0+Y)
FUN(7)=0.125*(1.0+X)*(1.0-Y)*(1.0-Z)*(X-Y-Z-2.0)
DER(1,7)=0.125*(1.0-Y)*(1.0-Z)*(2.0*X-Y-Z-1.0)
DER(2,7)=-0.125*(1.0+X)*(1.0-Z)*(X-2.0*Y-Z-1.0)
DER(3,7)=-0.125*(1.0+X)*(1.0-Y)*(X-Y-2.0*Z-1.0)
FUN(8)=0.25*(1.0-Y)*(1.0-Z)*(1.0-X)*(1.0+X)
DER(1,8)=-0.5*(1.0-Y)*(1.0-Z)*X
DER(2,8)=-0.25*(1.0-Z)*(1.0-X)*(1.0+X)
DER(3,8)=-0.25*(1.0-Y)*(1.0-X)*(1.0+X)
FUN(9)=0.25*(1.0-X)*(1.0-Y)*(1.0-Z)*(1.0+Z)
DER(1,9)=-0.25*(1.0-Y)*(1.0-Z)*(1.0+Z)
DER(2,9)=-0.25*(1.0-X)*(1.0-Z)*(1.0+Z)
DER(3,9)=-0.5*(1.0-X)*(1.0-Y)*Z
FUN(10)=0.25*(1.0-X)*(1.0+Y)*(1.0-Z)*(1.0+Z)
DER(1,10)=-0.25*(1.0+Y)*(1.0-Z)*(1.0+Z)
DER(2,10)=0.25*(1.0-X)*(1.0-Z)*(1.0+Z)
DER(3,10)=-0.5*(1.0-X)*(1.0+Y)*Z
FUN(11)=0.25*(1.0+X)*(1.0+Y)*(1.0-Z)*(1.0+Z)
DER(1,11)=0.25*(1.0+Y)*(1.0-Z)*(1.0+Z)
DER(2,11)=0.25*(1.0+X)*(1.0-Z)*(1.0+Z)
DER(3,11)=-0.5*(1.0+X)*(1.0+Y)*Z
FUN(12)=0.25*(1.0+X)*(1.0-Y)*(1.0-Z)*(1.0+Z)
DER(1,12)=0.25*(1.0-Y)*(1.0-Z)*(1.0+Z)
DER(2,12)=-0.25*(1.0+X)*(1.0-Z)*(1.0+Z)
DER(3,12)=-0.5*(1.0+X)*(1.0-Y)*Z
FUN(13)=0.125*(1.0-X)*(1.0-Y)*(1.0+Z)*(-X-Y+Z-2.0)
DER(1,13)=-0.125*(1.0-Y)*(1.0+Z)*(-2.0*X-Y+Z-1.0)
DER(2,13)=-0.125*(1.0-X)*(1.0+Z)*(-X-2.0*Y+Z-1.0)
DER(3,13)=0.125*(1.0-X)*(1.0-Y)*(-X-Y+2.0*Z-1.0)
FUN(14)=0.25*(1.0-X)*(1.0+Z)*(1.0-Y)*(1.0+Y)
DER(1,14)=-0.25*(1.0+Z)*(1.0-Y)*(1.0+Y)
DER(2,14)=-0.5*(1.0+Z)*(1.0-X)*Y
DER(3,14)=0.25*(1.0-X)*(1.0-Y)*(1.0+Y)
FUN(15)=0.125*(1.0-X)*(1.0+Y)*(1.0+Z)*(-X+Y+Z-2.0)
DER(1,15)=-0.125*(1.0+Y)*(1.0+Z)*(-2.0*X+Y+Z-1.0)
DER(2,15)=0.125*(1.0-X)*(1.0+Z)*(-X+2.0*Y+Z-1.0)
DER(3,15)=0.125*(1.0-X)*(1.0+Y)*(-X+Y+2.0*Z-1.0)
FUN(16)=0.25*(1.0+Y)*(1.0+Z)*(1.0-X)*(1.0+X)
DER(1,16)=-0.5*(1.0+Y)*(1.0+Z)*X
DER(2,16)=0.25*(1.0+Z)*(1.0-X)*(1.0+X)
DER(3,16)=0.25*(1.0+Y)*(1.0-X)*(1.0+X)
FUN(17)=0.125*(1.0+X)*(1.0+Y)*(1.0+Z)*(X+Y+Z-2.0)
DER(1,17)=0.125*(1.0+Y)*(1.0+Z)*(2.0*X+Y+Z-1.0)
DER(2,17)=0.125*(1.0+X)*(1.0+Z)*(X+2.0*Y+Z-1.0)
DER(3,17)=0.125*(1.0+X)*(1.0+Y)*(X+Y+2.0*Z-1.0)
FUN(18)=0.25*(1.0+X)*(1.0+Z)*(1.0-Y)*(1.0+Y)
DER(1,18)=0.25*(1.0+Z)*(1.0-Y)*(1.0+Y)
DER(2,18)=-0.5*(1.0+X)*(1.0+Z)*Y
DER(3,18)=0.25*(1.0+X)*(1.0-Y)*(1.0+Y)
FUN(19)=0.125*(1.0+X)*(1.0-Y)*(1.0+Z)*(X-Y+Z-2.0)
DER(1,19)=0.125*(1.0-Y)*(1.0+Z)*(2.0*X-Y+Z-1.0)
DER(2,19)=-0.125*(1.0+X)*(1.0+Z)*(X-2.0*Y+Z-1.0)
DER(3,19)=0.125*(1.0+X)*(1.0-Y)*(X-Y+2.0*Z-1.0)
FUN(20)=0.25*(1.0-Y)*(1.0+Z)*(1.0-X)*(1.0+X)
DER(1,20)=-0.5*(1.0-Y)*(1.0+Z)*X
DER(2,20)=-0.25*(1.0+Z)*(1.0-X)*(1.0+X)
DER(3,20)=0.25*(1.0-Y)*(1.0-X)*(1.0+X)
RETURN
END
CCCC
SUBROUTINE MATMUL(A,IA,JA,B,IB,JB,C,IC,JC,K,L,M)
IMPLICIT REAL *8 (A-H,O-Z)

```

```

    DIMENSION A(IA,JA),B(IB,JB),C(IC,JC)
    DO 10 I=1,K
    DO 10 J=1,M
    D=0.0
    DO 20 II=1,L
20  D=D+A(I,II)*B(II,J)
10  C(I,J)=D
    RETURN
    END
CCCCC
    SUBROUTINE MATRAN(A,IA,JA,B,IB,JB,K,L)
    IMPLICIT REAL*8 (A-H,O-Z)
    DIMENSION A(IA,JA),B(IB,JB)
    DO 10 I=1,K
    DO 10 J=1,L
10  B(J,I)=A(I,J)
    RETURN
    END
CCCCC
    SUBROUTINE MATINV(JA,IJAC,JJAC,JACIN,IJACIN,JJACIN,IMEN,DET)
    IMPLICIT REAL *8 (A-H,O-Z)
    REAL *8 JA,JACIN
    DIMENSION JA(IJAC,JJAC),JACIN(IJACIN,JJACIN),COF(3,3)
    DET=JA(1,1)*JA(2,2)*JA(3,3)-JA(2,3)*JA(3,2)-JA(1,2)*(JA(2,1)*
*JA(3,3)-JA(2,3)*JA(3,1))+JA(1,3)*(JA(2,1)*JA(3,2)-JA(2,2)*JA(3,1))
    COF(1,1)=(JA(2,2)*JA(3,3)-JA(2,3)*JA(3,2))
    COF(1,2)=-JA(2,1)*JA(3,3)-JA(2,3)*JA(3,1)
    COF(1,3)=JA(2,1)*JA(3,2)-JA(2,2)*JA(3,1)
    COF(2,1)=-JA(1,2)*JA(3,3)-JA(1,3)*JA(3,2)
    COF(2,2)=(JA(1,1)*JA(3,3)-JA(1,3)*JA(3,1))
    COF(2,3)=-JA(1,1)*JA(3,2)-JA(1,2)*JA(3,1)
    COF(3,1)=(JA(1,2)*JA(2,3)-JA(1,3)*JA(2,2))
    COF(3,2)=-JA(1,1)*JA(2,3)-JA(1,3)*JA(2,1)
    COF(3,3)=(JA(1,1)*JA(2,2)-JA(1,2)*JA(2,1))
    IF (DET.EQ.0.0)WRITE(2,*)'DET IS ZERO LINE 2228'
    IF (DET.EQ.0.0)PAUSE
    IF (DET.EQ.0.0)DET=0.1D-39
    DO 10 I=1,IMEN
    DO 10 J=1,IMEN
10  JACIN(I,J)=COF(J,I)/DET
    RETURN
    END
CCCCC
    SUBROUTINE B3C3(B,IB,JB,DERIV,IDERIV,JDERIV,NODEL)
    IMPLICIT REAL*8 (A-H,O-Z)
    DIMENSION B(IB,JB),DERIV(IDERIV,JDERIV)
    N=0
    DO 30 I=1,NODEL
    L=N+1
    M=L+1
    N=M+1
    B(1,L)=DERIV(1,I)
    B(1,M)=0.0
    B(1,N)=0.0
    B(2,L)=0.0
    B(2,M)=DERIV(2,I)
    B(2,N)=0.0
    B(3,L)=0.0
    B(3,M)=0.0
    B(3,N)=DERIV(3,I)
    B(4,L)=DERIV(2,I)
    B(4,M)=DERIV(1,I)
    B(4,N)=0.0
    B(5,L)=0.0

```

```

      B(5,M)=DERIV(3,I)
      B(5,N)=DERIV(2,I)
      B(6,L)=DERIV(3,I)
      B(6,M)=0.0
      B(6,N)=DERIV(1,I)
30  CONTINUE
      RETURN
      END
CCCCC
      SUBROUTINE MATADD(AA,IA,JA,BB,IB,JB,M,N)
      IMPLICIT REAL*8 (A-H,O-Z)
      DIMENSION AA(IA,JA),BB(IB,JB)
      DO 10 I=1,M
      DO 10 J=1,N
10  AA(I,J)=AA(I,J)+BB(I,J)
      RETURN
      END
CCCCC
      SUBROUTINE DIRECT(NEL,ELTOP,IELTOP,JH,NF,INF,JNF,DOFNOD,STEER,IH)
      IMPLICIT REAL*8 (A-H,O-Z)
      INTEGER ELTOP,DOFNOD,STEER
      DIMENSION ELTOP(IELTOP,JH),NF(INF,JNF),STEER(IH)
      L=ELTOP(NEL,2)
      JJ=0
      DO 100 I=1,L
      K=I+2
      KK=ELTOP(NEL,K)
      DO 100 J=1,DOFNOD
      JJ=JJ+1
100 STEER(JJ)=NF(KK,J)
      RETURN
      END
CCCCC
      SUBROUTINE MATVEC(B,IB,JB,V,IV,NN,MM,S,IS)
      IMPLICIT REAL*8 (A-H,O-Z)
      DIMENSION B(IB,JB),V(IV),S(IS)
      DO 10 I=1,NN
      T=0.0
      DO 20 J=1,MM
20  T=T+B(I,J)*V(J)
10  S(I)=T
      RETURN
      END
CCCCC
      SUBROUTINE ELGEOM(NEL,ELTOP,IN,JN,COORD,IH,JH,GEOM,IM,JM,DIMEN)
      IMPLICIT REAL*8 (A-H,O-Z)
      INTEGER ELTOP,DIMEN
      DIMENSION ELTOP(IN,JN),COORD(IH,JH),GEOM(IM,JM)
      L=ELTOP(NEL,2)
      DO 50 I=1,L
      K=I+2
      KK=ELTOP(NEL,K)
      DO 60 J=1,DIMEN
60  GEOM(I,J)=COORD(KK,J)
50  CONTINUE
      RETURN
      END
CCCCC
      SUBROUTINE ASSYM(SYSK,I,J,ELK,IL,JL,STEER,IR,DOFEL,MBA,INC,ITR)
      IMPLICIT REAL*8 (A-H,O-Z)
      INTEGER STEER,DOFEL
      DIMENSION SYSK(I,J),ELK(IL,JL),STEER(IR)
      DO 90 I=1,DOFEL
      KK=STEER(I)

```

```

DO 90 J=1,DOFEL
LL=STEER(J)
IF(KK.NE.0.and.LL.NE.0)THEN
IF(KK.LE.LL)THEN
M=LL-KK+1
IF(MH.LT.M)MH=M
SYSK(KK,M)=SYSK(KK,M)+ELK(I,J)
ENDIF
ENDIF
90 CONTINUE
C      CALCULATION OF SEMI-BANDWIDTH      C
IF(MBA.EQ.1.AND.INC.EQ.2.AND.ITR.EQ.1)WRITE(*,*)'MH=HBAND=',MH
IF(MBA.EQ.1.AND.INC.EQ.2.AND.ITR.EQ.1)PAUSE
RETURN
END
CCCCC
SUBROUTINE SOLVE(NRM,NCM,NEQNS,NBW,BAND,RHS,IRES)
IMPLICIT REAL *8 (A-H,O-Z)
DIMENSION BAND(NRM,NCM),RHS(NRM)
MEQNS=NEQNS-1
DO 500 NPIV=1,MEQNS
NPIVOT=NPIV+1
LSTSUB=NPIV+NBW-1
IF(LSTSUB.GT.NEQNS) LSTSUB=NEQNS
DO 400 NROW=NPIVOT,LSTSUB
C      INVERT ROWS AND COLUMNS FOR ROW FACTOR
NCOL=NROW-NPIV+1
FACTOR=BAND(NPIV,NCOL)/BAND(NPIV,1)
IF(IRES.GT.0)GOTO 400
DO 200 NCOL=NROW,LSTSUB
ICOL=NCOL-NROW+1
JCOL=NCOL-NPIV+1
200  BAND(NROW,ICOL)=BAND(NROW,ICOL)-FACTOR*BAND(NPIV,JCOL)
400  RHS(NROW)=RHS(NROW)-FACTOR*RHS(NPIV)
500 CONTINUE
C      BACK SUBSTITUTION
DO 800 IJK=2,NEQNS
NPIV=NEQNS-IJK+2
RHS(NPIV)=RHS(NPIV)/BAND(NPIV,1)
LSTSUB=NPIV-NBW+1
IF (LSTSUB .LT. 1) LSTSUB=1
NPIVOT=NPIV-1
DO 700 JKI=LSTSUB,NPIVOT
NROW=NPIVOT-JKI+LSTSUB
NCOL=NPIV-NROW+1
FACTOR=BAND(NROW,NCOL)
700  RHS(NROW)=RHS(NROW)-FACTOR*RHS(NPIV)
800 CONTINUE
RHS(1)=RHS(1)/BAND(1,1)
RETURN
END
CCCCC  CALCULATION OF THE FLOW VECTOR BY VON MISES  CCCCC
SUBROUTINE YIELDIF(AVECT,DVECT,D,H,STEMP,YIELD,ABETA)
IMPLICIT REAL *8 (A-H,O-Z)
DIMENSION AVECT(6),STEMP(6),D(6,6),DEVIA(6),DVECT(6)
IF(YIELD.EQ.0.0)WRITE(2,*)'ERROR YIELD=0.0 LINE 2444'
SMEAN=(STEMP(1)+STEMP(2)+STEMP(3))/3.0
DO 1200 I=1,6
IF(I.LE.3)DEVIA(I)=STEMP(I)-SMEAN
1200 IF(I.GT.3)DEVIA(I)=STEMP(I)
IF(YIELD.EQ.0.0)RETURN
DO 1220 I=1,6
IF(I.LE.3)AVECT(I)=3.0*DEVIA(I)/(2.0*YIELD)
1220 IF(I.GT.3)AVECT(I)=3.0*DEVIA(I)/YIELD

```

```

CALL MATVEC(D,6,6,AVECT,6,6,DVECT,6)
DENOM=H
DO 1230 I=1,6
1230 DENOM=DENOM+AVECT(I)*DVECT(I)
ABETA=1.0/DENOM
RETURN
END
CCCC
SUBROUTINE TRI(EPSTN,L5,FC,E,BEE,CEE,CES,SIGMA,IND,KGT,EFFST,STRSG
*,STRS,Dco,INC,ITR,NEL,Ecrsh,ZFC,KGC)
IMPLICIT REAL*8 (A-H,O-Z)
DIMENSION EPSTN(L5),SIGMA(6),EFFST(L5),SGTOT(6),STRSG(6,L5)
*,STRS(6),AVECT(6),DVECT(6),Dco(6,6),IND(3,L5)
PREYS=-E*EPSTN(KGT)+SQRT(2.8*E*FC*EPSTN(KGT))+0.3*FC
IF(EPSTN(KGT).GE.0.7*FC/E)THEN
DFC=(EPSTN(KGT)-(0.7*FC/E))*(ZFC*FC)/(Ecrsh-(1.7*FC/E))
PREYS=FC-DFC
ENDIF
CALL INVARc(BEE,CEE,CES,AVECT,SIGMA,YIELD)
IF(EPSTN(KGT).EQ.0.0.OR.PREYS.GE.EFFST(KGT))ESCUR=YIELD-PREYS
IF(PREYS.LT.EFFST(KGT))ESCUR=YIELD-EFFST(KGT)
IF(IND(1,KGT).EQ.0.0.OR.IND(1,KGT).EQ.-5)THEN
IF(ESCUR.LE.0.0)GOTO 7970
RFACT=ESCUR/(YIELD-EFFST(KGT))
IND(1,KGT)=-4
IND(2,KGT)=-4
IND(3,KGT)=-4
ELSE
IF(ESCUR.LE.0.0)IND(1,KGT)=-5
IF(ESCUR.LE.0.0)IND(2,KGT)=-5
IF(ESCUR.LE.0.0)IND(3,KGT)=-5
IF(ESCUR.LE.0.0)GOTO 7970
RFACT=ESCUR/(YIELD-EFFST(KGT))
ENDIF
IF(ITR.EQ.1)WRITE(10,44)INC,ITR,NEL,KGC,DFC,EPSTN(KGT)
44 FORMAT('TRI.DIR.PLAS.GP AT INC,ITR,NE,KGC',4I4,'DFC,EPSTN',2F9.6)
MSTEP=ESCUR*40.0/(0.3*FC)+1.0
ASTEP=MSTEP
REDUC=1.0-RFACT
DO 1310 I=1,6
SGTOT(I)=STRSG(I,KGT)+REDUC*STRS(I)
1310 STRS(I)=RFACT*STRS(I)/ASTEP
DO 1320 ISTEP=1,MSTEP
CALL INVARc(BEE,CEE,CES,AVECT,SGTOT,YIELD)
CALL FLOWPLc(AVECT,DVECT,Dco,ABETA,EPSTN,KGT,E,FC,L5)
AGASH=0.0
DO 1330 I=1,6
1330 AGASH=AGASH+AVECT(I)*STRS(I)
DLAMD=AGASH*ABETA
IF(DLAMD.LT.0.0)DLAMD=0.0
BGASH=0.0
DO 1340 I=1,6
BGASH=BGASH+AVECT(I)*SGTOT(I)
1340 SGTOT(I)=SGTOT(I)+STRS(I)-DLAMD*DVECT(I)
EPSTN(KGT)=EPSTN(KGT)+DLAMD*BGASH/YIELD
1320 CONTINUE
CALL INVARc(BEE,CEE,CES,AVECT,SGTOT,YIELD)
CURYS=-E*EPSTN(KGT)+SQRT(2.8*E*FC*EPSTN(KGT))+0.3*FC
IF(EPSTN(KGT).GE.0.7*FC/E)THEN
DFC=(EPSTN(KGT)-(0.7*FC/E))*(ZFC*FC)/(Ecrsh-(1.7*FC/E))
IF(DFC.GT.ZFC*FC)DFC=ZFC*FC
CURYS=FC-DFC
ENDIF
BRING=1.0

```

```

      IF(YIELD.GT.CURYS)BRING=CURYS/YIELD
      DO 1350 I=1,6
1350 STRSG(I,KGT)=BRING*SGTOT(I)
      EFFST(KGT)=BRING*YIELD
      GOTO 7777
7970 DO 1360 I=1,6
1360 STRSG(I,KGT)=STRSG(I,KGT)+STRS(I)
      EFFST(KGT)=YIELD
7777 RETURN
      END
CCCCC
      SUBROUTINE TWO(PSTRN,DM,EPSTN,L5,L6,FC,E,BEE,CEE,CES,IND,KGT,KGC
*,ZFC,PSARR,EFFST,SGA,SA,DE,CURY,INC,ITR,NEL,IS,PTARR,Ecrsh)
      IMPLICIT REAL*8 (A-H,O-Z)
      DIMENSION PSTRN(6),DM(L6),EPSTN(L5),EFFST(L5),SGT(3),SGA(3),SA(3),
*AVCA(3),DV(3),DE(3,3),IND(3,L5),PSARR(3),CURY(L6),PTARR(3)
      IF(IS.EQ.212)DAM=1.00-0.50*ABS(PTARR(2)/0.005)
      IF(IS.EQ.213)DAM=1.00-0.50*ABS(PTARR(1)/0.005)
      IF(IS.EQ.223)DAM=1.00-0.50*ABS(PSTRN(1)/0.005)
      IF(DAM.GT.1)DAM=1.0
      IF(DAM.LT.0.50)DAM=0.50
      DM(KGC)=DAM
      PREYS=-E*EPSTN(KGT)+SQRT(2.8*E*FC*EPSTN(KGT)*DAM)+0.3*FC*DAM
      IF(EPSTN(KGT).GE.0.7*FC*DAM/E)THEN
      DFC=(EPSTN(KGT)-0.7*FC*DAM/E)*(ZFC*FC*DAM)/(Ecrsh-1.7*FC*DAM/E)
      IF(DFC.GT.ZFC*FC*DAM)DFC=ZFC*FC*DAM
      PREYS=FC*DAM-DFC
      ENDIF
      IF(IS.EQ.212.OR.IS.EQ.213)LM1=1
      IF(IS.EQ.212)LM2=2
      IF(IS.EQ.213)LM2=3
      IF(IS.EQ.223)LM1=2
      IF(IS.EQ.223)LM2=3
      CALL INVAN(BEE,CEE,CES,AVCA,PSARR,YIELD)
      IF(EPSTN(KGT).EQ.0.0.OR.PREYS.GE.EFFST(KGT))ESCUR=YIELD-PREYS
      IF(PREYS.LT.EFFST(KGT))ESCUR=YIELD-EFFST(KGT)
      IF(IND(LM1,KGT).EQ.0.OR.IND(LM1,KGT).EQ.-5)THEN
      IF(ESCUR.LE.0.0)GOTO 7170
      RFACT=ESCUR/(YIELD-EFFST(KGT))
      IND(LM1,KGT)=-4
      IND(LM2,KGT)=-4
      ELSE
      IF(ESCUR.LE.0.0)IND(LM1,KGT)=-5
      IF(ESCUR.LE.0.0)IND(LM2,KGT)=-5
      IF(ESCUR.LE.0.0)GOTO 7170
      RFACT=ESCUR/(YIELD-EFFST(KGT))
      ENDIF
      IF(ITR.EQ.1)WRITE(9,55)INC,ITR,NEL,KGC,DFC,EPSTN(KGT)
55 FORMAT('TWO.DIR.PLAS.GP AT INC,ITR,NE,KGC',4I4,'DFC,EPSTN',2F9.6)
      MSTEP=ESCUR*40.0/(0.3*FC)+1.0
      ASTEP=MSTEP
      REDUC=1.0-RFACT
      DO 3310 I=1,3
      SGT(I)=SGA(I)+REDUC*SA(I)
3310 SA(I)=RFACT*SA(I)/ASTEP
      DO 3320 ISTEP=1,MSTEP
      CALL INVAN(BEE,CEE,CES,AVCA,SGT,YIELD)
      CALL FLOWPN(AVCA,DV,DE,DAM,DENOM,ABETA,KGT,E,FC,EPSTN,L5)
      AGASH=0.0
      DO 3330 I=1,3
3330 AGASH=AGASH+AVCA(I)*SA(I)
      DLAMD=AGASH*ABETA
      IF(DLAMD.LT.0.0)DLAMD=0.0
      BGASH=0.0

```

```

DO 3340 I=1,3
  BGASH=BGASH+AVCA(I)*SGT(I)
3340 SGT(I)=SGT(I)+SA(I)-DLAMD*DV(I)
  EPSTN(KGT)=EPSTN(KGT)+DLAMD*BGASH/YIELD
3320 CONTINUE
  CALL INVAN(BEE,CEE,CES,AVCA,SGT,YIELD)
  CURYS=-E*EPSTN(KGT)+SQRT(2.8*E*FC*EPSTN(KGT)*DAM)+0.3*FC*DAM
  IF(EPSTN(KGT).GE.0.7*FC*DAM/E)THEN
    DFC=(EPSTN(KGT)-0.7*FC*DAM/E)*(ZFC*FC*DAM)/(Ecrsh-1.7*FC*DAM/E)
    IF(DFC.GT.ZFC*FC*DAM)DFC=ZFC*FC*DAM
    CURYS=FC*DAM-DFC
  ENDIF
  CURY(KGC)=CURYS
  BRING=1.0
  IF(YIELD.GT.CURYS)BRING=CURYS/YIELD
  DO 3350 I=1,3
3350 SGA(I)=BRING*SGT(I)
  EFFST(KGT)=BRING*YIELD
  GOTO 7160
7170 DO 3360 I=1,3
3360 SGA(I)=SGA(I)+SA(I)
  EFFST(KGT)=YIELD
7160 CONTINUE
  DO 3370 I=1,3
3370 PSARR(I)=SGA(I)
  RETURN
  END
CCCC
SUBROUTINE ONE(K,PSTRN,PTARR,DM,EPSTN,L5,L6,FC,E,IND,KGT,KGC,
*PSARR,ZFC,EFFST,STRSGA,STRSA,DVEC,ABETA,CURY,BEE,CEE,CES,INC,
*ITR,NEL,PSTRS,CRSTRS,CRUSH,IGP,Ecrsh)
  IMPLICIT REAL*8 (A-H,O-Z)
  DIMENSION PSTRN(6),DM(L6),EPSTN(L5),EFFST(L5),SGTOTA(3),
* STRSGA(3),STRSA(3),IND(3,L5),PTARR(3),PSARR(3),CURY(L6),
* PSTRS(6),CRSTRS(6)
  IF(IND(2,KGT).EQ.2.AND.IND(3,KGT).NE.2)K=2
  IF(IND(3,KGT).EQ.2.AND.IND(2,KGT).NE.2)K=1
  IF(K.EQ.1.OR.K.EQ.2)HM=PTARR(K)
  IF(K.EQ.3)HM=PSTRN(1)
  IF(HM.LT.-Ecrsh)THEN
    CRUSH=1
  WRITE(11,12)INC,ITR,NEL,IGP
  WRITE(*,12)INC,ITR,NEL,IGP
12  FORMAT(' UN.CR.INS,ITR,NE,IGP,EQ.UN',4I3)
  GOTO 7265
  ENDIF
  IF(K.EQ.1)KKK=2
  IF(K.EQ.2)KKK=1
  IF(K.EQ.1.OR.K.EQ.2)PST=PSTRN(1)**2+PTARR(KKK)**2
  IF(K.EQ.3)PST=PTARR(1)**2+PTARR(2)**2
  DAM=1.00-0.50*SQRT(PST)/0.005
  IF(DAM.GT.1)DAM=1.0
  IF(DAM.LT.0.50)DAM=0.50
  DM(KGC)=DAM
  PREYS=-E*EPSTN(KGT)+SQRT(2.8*E*FC*EPSTN(KGT)*DAM)+0.3*FC*DAM
  IF(EPSTN(KGT).GE.0.7*FC*DAM/E)THEN
    DFC=(EPSTN(KGT)-0.7*FC*DAM/E)*(ZFC*FC*DAM)/(Ecrsh-1.7*FC*DAM/E)
    IF(DFC.GT.ZFC*FC*DAM)DFC=ZFC*FC*DAM
    PREYS=FC*DAM-DFC
  ENDIF
  IF(K.EQ.1.OR.K.EQ.2)YIELD=ABS(PSARR(K))
  IF(K.EQ.3)YIELD=ABS(PSTRS(1))
  IF(K.EQ.1.OR.K.EQ.2)JK=K+1
  IF(K.EQ.3)JK=1

```

```

IF(EPSTN(KGT).EQ.0.0.OR.PREYS.GE.EFFST(KGT))ESCUR=YIELD-PREYS
IF(PREYS.LT.EFFST(KGT))ESCUR=YIELD-EFFST(KGT)
IF(IND(JK,KGT).EQ.0.0.OR.IND(JK,KGT).EQ.-5)THEN
  IF(ESCUR.LE.0.0)GOTO 7270
  RFACT=ESCUR/(YIELD-EFFST(KGT))
  IND(JK,KGT)=-4
ELSE
  IF(ESCUR.LE.0.0)IND(JK,KGT)=-5
  IF(ESCUR.LE.0.0) GOTO 7270
  RFACT=ESCUR/(YIELD-EFFST(KGT))
ENDIF
  WRITE(8,66)INC,ITR,NEL,KGC,DFC,EPSTN(KGT)
66  FORMAT('ONE.DIR.PLAS.GP AT INC,ITR,NE,KGC',4I4,'DFC,EPSTN',2F9.6)
MSTEP=ESCUR*40.0/(0.3*FC)+1.0
ASTEP=MSTEP
REDUC=1.0-RFACT
IF(K.EQ.1.OR.K.EQ.2)SGTOTA(K)=STRSGA(K)+REDUC*STRSA(K)
IF(K.EQ.1.OR.K.EQ.2)STRSA(K)=RFACT*STRSA(K)/ASTEP
  IF(K.EQ.3)SGTOTA(K)=(PSTRS(1)-CRSTRS(1))+REDUC*CRSTRS(1)
IF(K.EQ.3)STRSA(K)=RFACT*CRSTRS(1)/ASTEP
  DO 3420 ISTEP=1,MSTEP
AVEC=CEE+SQRT(CES+BEE)*SGTOTA(K)/SQRT(SGTOTA(K)*SGTOTA(K))
DVEC=AVEC*E
  IF(EPSTN(KGT).EQ.0.0)THEN
  ABETA=0.1D-39
  ELSE
  DEN=(SQRT(0.7*FC*DAM/(E*EPSTN(KGT)))-1.0)*E
  IF(DEN.LT.0.0)DEN=0.0
  DEN1=DEN+AVEC*DVEC
  ABETA=1.0/DEN1
  ENDIF
AGASH=0.0
AGASH=AGASH+AVEC*STRSA(K)
DLAMD=AGASH*ABETA
IF(DLAMD.LT.0.0)DLAMD=0.0
BGASH=0.0
BGASH=BGASH+AVEC*SGTOTA(K)
SGTOTA(K)=SGTOTA(K)+STRSA(K)-DLAMD*DVEC
EPSTN(KGT)=EPSTN(KGT)+DLAMD*BGASH/YIELD
3420 CONTINUE
YIELD=ABS(SGTOTA(K))
CURYS=-E*EPSTN(KGT)+SQRT(2.8*E*FC*EPSTN(KGT)*DAM)+0.3*FC*DAM
IF(EPSTN(KGT).GE.0.7*FC*DAM/E)THEN
DFC=(EPSTN(KGT)-0.7*FC*DAM/E)*(ZFC*FC*DAM)/(Ecrsh-1.7*FC*DAM/E)
  IF(DFC.GT.ZFC*FC*DAM)DFC=ZFC*FC*DAM
  CURYS=FC*DAM-DFC
ENDIF
CURY(KGC)=CURYS
BRING=1.0
IF(YIELD.GT.CURYS)BRING=CURYS/YIELD
STRSGA(K)=BRING*SGTOTA(K)
EFFST(KGT)=BRING*YIELD
GOTO 7260
7270 STRSGA(K)=STRSGA(K)+STRSA(K)
EFFST(KGT)=YIELD
7260 CONTINUE
  IF(K.EQ.1.OR.K.EQ.2)PSARR(K)=STRSGA(K)
  IF(K.EQ.3)PSTRS(1)=STRSGA(K)
7265 RETURN
END

```

Appendix (E)

The Input Data for Jordaan Reinforced Concrete
Horizontally Curved Beam of 144 Brick Element

'JORDAAN REIN. CONCRETE CURVED BEAM 144 ELEMENTS','UNITS ARE kN,mm'

1	2134.00	.00	.00
2	2172.00	.00	.00
3	2210.00	.00	.00
4	2248.00	.00	.00
5	2286.00	.00	.00
6	2134.00	76.25	.00
7	2210.00	76.25	.00
8	2286.00	76.25	.00
9	2134.00	152.50	.00
10	2172.00	152.50	.00
11	2210.00	152.50	.00
12	2248.00	152.50	.00
13	2286.00	152.50	.00
14	2134.00	228.75	.00
15	2210.00	228.75	.00
16	2286.00	228.75	.00
17	2134.00	305.00	.00
18	2172.00	305.00	.00
19	2210.00	305.00	.00
20	2248.00	305.00	.00
21	2286.00	305.00	.00
22	2133.61	.00	40.63
23	2209.60	.00	42.08
24	2285.59	.00	43.52
25	2133.61	152.50	40.63
26	2209.60	152.50	42.08
27	2285.59	152.50	43.52
28	2133.61	305.00	40.63
29	2209.60	305.00	42.08
30	2285.59	305.00	43.52
31	2132.45	.00	81.24
32	2170.43	.00	82.69
33	2208.40	.00	84.14
34	2246.37	.00	85.58
35	2284.34	.00	87.03
36	2132.45	76.25	81.24
37	2208.40	76.25	84.14
38	2284.34	76.25	87.03
39	2132.45	152.50	81.24
40	2170.43	152.50	82.69
41	2208.40	152.50	84.14
42	2246.37	152.50	85.58
43	2284.34	152.50	87.03
44	2132.45	228.75	81.24
45	2208.40	228.75	84.14
46	2284.34	228.75	87.03
47	2132.45	305.00	81.24
48	2170.43	305.00	82.69
49	2208.40	305.00	84.14
50	2246.37	305.00	85.58
51	2284.34	305.00	87.03
52	2130.52	.00	121.83
53	2206.40	.00	126.17
54	2282.27	.00	130.51
55	2130.52	152.50	121.83
56	2206.40	152.50	126.17
57	2282.27	152.50	130.51
58	2130.52	305.00	121.83
59	2206.40	305.00	126.17

60	2282.27	305.00	130.51
61	2127.81	.00	162.37
62	2165.70	.00	165.26
63	2203.59	.00	168.15
64	2241.48	.00	171.04
65	2279.37	.00	173.93
66	2127.81	76.25	162.37
67	2203.59	76.25	168.15
68	2279.37	76.25	173.93
69	2127.81	152.50	162.37
70	2165.70	152.50	165.26
71	2203.59	152.50	168.15
72	2241.48	152.50	171.04
73	2279.37	152.50	173.93
74	2127.81	228.75	162.37
75	2203.59	228.75	168.15
76	2279.37	228.75	173.93
77	2127.81	305.00	162.37
78	2165.70	305.00	165.26
79	2203.59	305.00	168.15
80	2241.48	305.00	171.04
81	2279.37	305.00	173.93
82	2124.34	.00	202.85
83	2199.99	.00	210.07
84	2275.65	.00	217.30
85	2124.34	152.50	202.85
86	2199.99	152.50	210.07
87	2275.65	152.50	217.30
88	2124.34	305.00	202.85
89	2199.99	305.00	210.07
90	2275.65	305.00	217.30
91	2120.09	.00	243.26
92	2157.84	.00	247.59
93	2195.59	.00	251.92
94	2233.35	.00	256.25
95	2271.10	.00	260.58
96	2120.09	76.25	243.26
97	2195.59	76.25	251.92
98	2271.10	76.25	260.58
99	2120.09	152.50	243.26
100	2157.84	152.50	247.59
101	2195.59	152.50	251.92
102	2233.35	152.50	256.25
103	2271.10	152.50	260.58
104	2120.09	228.75	243.26
105	2195.59	228.75	251.92
106	2271.10	228.75	260.58
107	2120.09	305.00	243.26
108	2157.84	305.00	247.59
109	2195.59	305.00	251.92
110	2233.35	305.00	256.25
111	2271.10	305.00	260.58
112	2115.07	.00	283.58
113	2190.40	.00	293.68
114	2265.73	.00	303.78
115	2115.07	152.50	283.58
116	2190.40	152.50	293.68
117	2265.73	152.50	303.78
118	2115.07	305.00	283.58
119	2190.40	305.00	293.68
120	2265.73	305.00	303.78
121	2109.29	.00	323.79
122	2146.85	.00	329.56
123	2184.41	.00	335.33
124	2221.97	.00	341.09
125	2259.53	.00	346.86
126	2109.29	76.25	323.79
127	2184.41	76.25	335.33
128	2259.53	76.25	346.86
129	2109.29	152.50	323.79
130	2146.85	152.50	329.56
131	2184.41	152.50	335.33

132	2221.97	152.50	341.09
133	2259.53	152.50	346.86
134	2109.29	228.75	323.79
135	2184.41	228.75	335.33
136	2259.53	228.75	346.86
137	2109.29	305.00	323.79
138	2146.85	305.00	329.56
139	2184.41	305.00	335.33
140	2221.97	305.00	341.09
141	2259.53	305.00	346.86
142	2102.75	.00	363.89
143	2177.63	.00	376.85
144	2252.52	.00	389.81
145	2102.75	152.50	363.89
146	2177.63	152.50	376.85
147	2252.52	152.50	389.81
148	2102.75	305.00	363.89
149	2177.63	305.00	376.85
150	2252.52	305.00	389.81
151	2095.44	.00	403.86
152	2132.75	.00	411.05
153	2170.06	.00	418.25
154	2207.38	.00	425.44
155	2244.69	.00	432.63
156	2095.44	76.25	403.86
157	2170.06	76.25	418.25
158	2244.69	76.25	432.63
159	2095.44	152.50	403.86
160	2132.75	152.50	411.05
161	2170.06	152.50	418.25
162	2207.38	152.50	425.44
163	2244.69	152.50	432.63
164	2095.44	228.75	403.86
165	2170.06	228.75	418.25
166	2244.69	228.75	432.63
167	2095.44	305.00	403.86
168	2132.75	305.00	411.05
169	2170.06	305.00	418.25
170	2207.38	305.00	425.44
171	2244.69	305.00	432.63
172	2087.37	.00	443.68
173	2161.71	.00	459.48
174	2236.05	.00	475.29
175	2087.37	152.50	443.68
176	2161.71	152.50	459.48
177	2236.05	152.50	475.29
178	2087.37	305.00	443.68
179	2161.71	305.00	459.48
180	2236.05	305.00	475.29
181	2078.54	.00	483.34
182	2115.55	.00	491.95
183	2152.57	.00	500.56
184	2189.58	.00	509.16
185	2226.59	.00	517.77
186	2078.54	76.25	483.34
187	2152.57	76.25	500.56
188	2226.59	76.25	517.77
189	2078.54	152.50	483.34
190	2115.55	152.50	491.95
191	2152.57	152.50	500.56
192	2189.58	152.50	509.16
193	2226.59	152.50	517.77
194	2078.54	228.75	483.34
195	2152.57	228.75	500.56
196	2226.59	228.75	517.77
197	2078.54	305.00	483.34
198	2115.55	305.00	491.95
199	2152.57	305.00	500.56
200	2189.58	305.00	509.16
201	2226.59	305.00	517.77
202	2068.96	.00	522.83
203	2142.65	.00	541.45

204	2216.33	.00	560.07
205	2068.96	152.50	522.83
206	2142.65	152.50	541.45
207	2216.33	152.50	560.07
208	2068.96	305.00	522.83
209	2142.65	305.00	541.45
210	2216.33	305.00	560.07
211	2058.63	.00	562.13
212	2095.29	.00	572.13
213	2131.95	.00	582.14
214	2168.61	.00	592.15
215	2205.27	.00	602.16
216	2058.63	76.25	562.13
217	2131.95	76.25	582.14
218	2205.27	76.25	602.16
219	2058.63	152.50	562.13
220	2095.29	152.50	572.13
221	2131.95	152.50	582.14
222	2168.61	152.50	592.15
223	2205.27	152.50	602.16
224	2058.63	228.75	562.13
225	2131.95	228.75	582.14
226	2205.27	228.75	602.16
227	2058.63	305.00	562.13
228	2095.29	305.00	572.13
229	2131.95	305.00	582.14
230	2168.61	305.00	592.15
231	2205.27	305.00	602.16
232	2047.56	.00	601.22
233	2120.48	.00	622.63
234	2193.40	.00	644.04
235	2047.56	152.50	601.22
236	2120.48	152.50	622.63
237	2193.40	152.50	644.04
238	2047.56	305.00	601.22
239	2120.48	305.00	622.63
240	2193.40	305.00	644.04
241	2035.74	.00	640.09
242	2071.99	.00	651.49
243	2108.24	.00	662.89
244	2144.49	.00	674.29
245	2180.74	.00	685.68
246	2035.74	76.25	640.09
247	2108.24	76.25	662.89
248	2180.74	76.25	685.68
249	2035.74	152.50	640.09
250	2071.99	152.50	651.49
251	2108.24	152.50	662.89
252	2144.49	152.50	674.29
253	2180.74	152.50	685.68
254	2035.74	228.75	640.09
255	2108.24	228.75	662.89
256	2180.74	228.75	685.68
257	2035.74	305.00	640.09
258	2071.99	305.00	651.49
259	2108.24	305.00	662.89
260	2144.49	305.00	674.29
261	2180.74	305.00	685.68
262	2023.18	.00	678.73
263	2095.24	.00	702.91
264	2167.29	.00	727.08
265	2023.18	152.50	678.73
266	2095.24	152.50	702.91
267	2167.29	152.50	727.08
268	2023.18	305.00	678.73
269	2095.24	305.00	702.91
270	2167.29	305.00	727.08
271	2009.90	.00	717.13
272	2045.69	.00	729.90
273	2081.48	.00	742.67
274	2117.27	.00	755.44
275	2153.06	.00	768.21

276	2009.90	76.25	717.13
277	2081.48	76.25	742.67
278	2153.06	76.25	768.21
279	2009.90	152.50	717.13
280	2045.69	152.50	729.90
281	2081.48	152.50	742.67
282	2117.27	152.50	755.44
283	2153.06	152.50	768.21
284	2009.90	228.75	717.13
285	2081.48	228.75	742.67
286	2153.06	228.75	768.21
287	2009.90	305.00	717.13
288	2045.69	305.00	729.90
289	2081.48	305.00	742.67
290	2117.27	305.00	755.44
291	2153.06	305.00	768.21
292	1995.88	.00	755.27
293	2066.96	.00	782.16
294	2138.04	.00	809.06
295	1995.88	152.50	755.27
296	2066.96	152.50	782.16
297	2138.04	152.50	809.06
298	1995.88	305.00	755.27
299	2066.96	305.00	782.16
300	2138.04	305.00	809.06
301	1981.14	.00	793.13
302	2016.42	.00	807.25
303	2051.69	.00	821.37
304	2086.97	.00	835.50
305	2122.25	.00	849.62
306	1981.14	76.25	793.13
307	2051.69	76.25	821.37
308	2122.25	76.25	849.62
309	1981.14	152.50	793.13
310	2016.42	152.50	807.25
311	2051.69	152.50	821.37
312	2086.97	152.50	835.50
313	2122.25	152.50	849.62
314	1981.14	228.75	793.13
315	2051.69	228.75	821.37
316	2122.25	228.75	849.62
317	1981.14	305.00	793.13
318	2016.42	305.00	807.25
319	2051.69	305.00	821.37
320	2086.97	305.00	835.50
321	2122.25	305.00	849.62
322	1965.68	.00	830.70
323	2035.68	.00	860.29
324	2105.69	.00	889.87
325	1965.68	152.50	830.70
326	2035.68	152.50	860.29
327	2105.69	152.50	889.87
328	1965.68	305.00	830.70
329	2035.68	305.00	860.29
330	2105.69	305.00	889.87
331	1949.51	.00	867.98
332	1984.22	.00	883.43
333	2018.94	.00	898.89
334	2053.65	.00	914.34
335	2088.36	.00	929.80
336	1949.51	76.25	867.98
337	2018.94	76.25	898.89
338	2088.36	76.25	929.80
339	1949.51	152.50	867.98
340	1984.22	152.50	883.43
341	2018.94	152.50	898.89
342	2053.65	152.50	914.34
343	2088.36	152.50	929.80
344	1949.51	228.75	867.98
345	2018.94	228.75	898.89
346	2088.36	228.75	929.80
347	1949.51	305.00	867.98

348	1984.22	305.00	883.43
349	2018.94	305.00	898.89
350	2053.65	305.00	914.34
351	2088.36	305.00	929.80
352	1933.75	.00	902.54
353	2002.61	.00	934.69
354	2071.48	.00	966.83
355	1933.75	152.50	902.54
356	2002.61	152.50	934.69
357	2071.48	152.50	966.83
358	1933.75	305.00	902.54
359	2002.61	305.00	934.69
360	2071.48	305.00	966.83
361	1917.37	.00	936.82
362	1951.52	.00	953.50
363	1985.66	.00	970.19
364	2019.80	.00	986.87
365	2053.94	.00	1003.55
366	1917.37	76.25	936.82
367	1985.66	76.25	970.19
368	2053.94	76.25	1003.55
369	1917.37	152.50	936.82
370	1951.52	152.50	953.50
371	1985.66	152.50	970.19
372	2019.80	152.50	986.87
373	2053.94	152.50	1003.55
374	1917.37	228.75	936.82
375	1985.66	228.75	970.19
376	2053.94	228.75	1003.55
377	1917.37	305.00	936.82
378	1951.52	305.00	953.50
379	1985.66	305.00	970.19
380	2019.80	305.00	986.87
381	2053.94	305.00	1003.55
382	1900.39	.00	970.81
383	1968.07	.00	1005.38
384	2035.75	.00	1039.95
385	1900.39	152.50	970.81
386	1968.07	152.50	1005.38
387	2035.75	152.50	1039.95
388	1900.39	305.00	970.81
389	1968.07	305.00	1005.38
390	2035.75	305.00	1039.95
391	1882.81	.00	1004.48
392	1916.34	.00	1022.37
393	1949.86	.00	1040.26
394	1983.39	.00	1058.14
395	2016.92	.00	1076.03
396	1882.81	76.25	1004.48
397	1949.86	76.25	1040.26
398	2016.92	76.25	1076.03
399	1882.81	152.50	1004.48
400	1916.34	152.50	1022.37
401	1949.86	152.50	1040.26
402	1983.39	152.50	1058.14
403	2016.92	152.50	1076.03
404	1882.81	228.75	1004.48
405	1949.86	228.75	1040.26
406	2016.92	228.75	1076.03
407	1882.81	305.00	1004.48
408	1916.34	305.00	1022.37
409	1949.86	305.00	1040.26
410	1983.39	305.00	1058.14
411	2016.92	305.00	1076.03
412	1864.63	.00	1037.84
413	1931.04	.00	1074.80
414	1997.44	.00	1111.76
415	1864.63	152.50	1037.84
416	1931.04	152.50	1074.80
417	1997.44	152.50	1111.76
418	1864.63	305.00	1037.84
419	1931.04	305.00	1074.80

420	1997.44	305.00	1111.76
421	1845.86	.00	1070.87
422	1878.73	.00	1089.94
423	1911.60	.00	1109.01
424	1944.47	.00	1128.07
425	1977.34	.00	1147.14
426	1845.86	76.25	1070.87
427	1911.60	76.25	1109.01
428	1977.34	76.25	1147.14
429	1845.86	152.50	1070.87
430	1878.73	152.50	1089.94
431	1911.60	152.50	1109.01
432	1944.47	152.50	1128.07
433	1977.34	152.50	1147.14
434	1845.86	228.75	1070.87
435	1911.60	228.75	1109.01
436	1977.34	228.75	1147.14
437	1845.86	305.00	1070.87
438	1878.73	305.00	1089.94
439	1911.60	305.00	1109.01
440	1944.47	305.00	1128.07
441	1977.34	305.00	1147.14
442	1826.50	.00	1103.56
443	1891.55	.00	1142.86
444	1956.60	.00	1182.16
445	1826.50	152.50	1103.56
446	1891.55	152.50	1142.86
447	1956.60	152.50	1182.16
448	1826.50	305.00	1103.56
449	1891.55	305.00	1142.86
450	1956.60	305.00	1182.16
451	1806.57	.00	1135.90
452	1838.74	.00	1156.12
453	1870.91	.00	1176.35
454	1903.08	.00	1196.58
455	1935.25	.00	1216.80
456	1806.57	76.25	1135.90
457	1870.91	76.25	1176.35
458	1935.25	76.25	1216.80
459	1806.57	152.50	1135.90
460	1838.74	152.50	1156.12
461	1870.91	152.50	1176.35
462	1903.08	152.50	1196.58
463	1935.25	152.50	1216.80
464	1806.57	228.75	1135.90
465	1870.91	228.75	1176.35
466	1935.25	228.75	1216.80
467	1806.57	305.00	1135.90
468	1838.74	305.00	1156.12
469	1870.91	305.00	1176.35
470	1903.08	305.00	1196.58
471	1935.25	305.00	1216.80
472	1786.06	.00	1167.88
473	1849.67	.00	1209.47
474	1913.28	.00	1251.06
475	1786.06	152.50	1167.88
476	1849.67	152.50	1209.47
477	1913.28	152.50	1251.06
478	1786.06	305.00	1167.88
479	1849.67	305.00	1209.47
480	1913.28	305.00	1251.06
481	1764.99	.00	1199.49
482	1796.42	.00	1220.85
483	1827.85	.00	1242.20
484	1859.28	.00	1263.56
485	1890.71	.00	1284.92
486	1764.99	76.25	1199.49
487	1827.85	76.25	1242.20
488	1890.71	76.25	1284.92
489	1764.99	152.50	1199.49
490	1796.42	152.50	1220.85
491	1827.85	152.50	1242.20

492	1859.28	152.50	1263.56
493	1890.71	152.50	1284.92
494	1764.99	228.75	1199.49
495	1827.85	228.75	1242.20
496	1890.71	228.75	1284.92
497	1764.99	305.00	1199.49
498	1796.42	305.00	1220.85
499	1827.85	305.00	1242.20
500	1859.28	305.00	1263.56
501	1890.71	305.00	1284.92
502	1743.36	.00	1230.72
503	1805.45	.00	1274.55
504	1867.53	.00	1318.38
505	1743.36	152.50	1230.72
506	1805.45	152.50	1274.55
507	1867.53	152.50	1318.38
508	1743.36	305.00	1230.72
509	1805.45	305.00	1274.55
510	1867.53	305.00	1318.38
511	1721.17	.00	1261.55
512	1751.82	.00	1284.02
513	1782.47	.00	1306.48
514	1813.12	.00	1328.95
515	1843.77	.00	1351.41
516	1721.17	76.25	1261.55
517	1782.47	76.25	1306.48
518	1843.77	76.25	1351.41
519	1721.17	152.50	1261.55
520	1751.82	152.50	1284.02
521	1782.47	152.50	1306.48
522	1813.12	152.50	1328.95
523	1843.77	152.50	1351.41
524	1721.17	228.75	1261.55
525	1782.47	228.75	1306.48
526	1843.77	228.75	1351.41
527	1721.17	305.00	1261.55
528	1751.82	305.00	1284.02
529	1782.47	305.00	1306.48
530	1813.12	305.00	1328.95
531	1843.77	305.00	1351.41
532	1698.44	.00	1291.99
533	1758.93	.00	1338.01
534	1819.42	.00	1384.02
535	1698.44	152.50	1291.99
536	1758.93	152.50	1338.01
537	1819.42	152.50	1384.02
538	1698.44	305.00	1291.99
539	1758.93	305.00	1338.01
540	1819.42	305.00	1384.02
541	1675.17	.00	1322.02
542	1705.00	.00	1345.56
543	1734.83	.00	1369.11
544	1764.66	.00	1392.65
545	1794.49	.00	1416.19
546	1675.17	76.25	1322.02
547	1734.83	76.25	1369.11
548	1794.49	76.25	1416.19
549	1675.17	152.50	1322.02
550	1705.00	152.50	1345.56
551	1734.83	152.50	1369.11
552	1764.66	152.50	1392.65
553	1794.49	152.50	1416.19
554	1675.17	228.75	1322.02
555	1734.83	228.75	1369.11
556	1794.49	228.75	1416.19
557	1675.17	305.00	1322.02
558	1705.00	305.00	1345.56
559	1734.83	305.00	1369.11
560	1764.66	305.00	1392.65
561	1794.49	305.00	1416.19
562	1651.38	.00	1351.63
563	1710.19	.00	1399.77

564	1769.00	.00	1447.91
565	1651.38	152.50	1351.63
566	1710.19	152.50	1399.77
567	1769.00	152.50	1447.91
568	1651.38	305.00	1351.63
569	1710.19	305.00	1399.77
570	1769.00	305.00	1447.91
571	1627.05	.00	1380.82
572	1656.03	.00	1405.41
573	1685.00	.00	1429.99
574	1713.97	.00	1454.58
575	1742.94	.00	1479.17
576	1627.05	76.25	1380.82
577	1685.00	76.25	1429.99
578	1742.94	76.25	1479.17
579	1627.05	152.50	1380.82
580	1656.03	152.50	1405.41
581	1685.00	152.50	1429.99
582	1713.97	152.50	1454.58
583	1742.94	152.50	1479.17
584	1627.05	228.75	1380.82
585	1685.00	228.75	1429.99
586	1742.94	228.75	1479.17
587	1627.05	305.00	1380.82
588	1656.03	305.00	1405.41
589	1685.00	305.00	1429.99
590	1713.97	305.00	1454.58
591	1742.94	305.00	1479.17
592	1602.21	.00	1409.56
593	1659.28	.00	1459.76
594	1716.34	.00	1509.96
595	1602.21	152.50	1409.56
596	1659.28	152.50	1459.76
597	1716.34	152.50	1509.96
598	1602.21	305.00	1409.56
599	1659.28	305.00	1459.76
600	1716.34	305.00	1509.96
601	1576.87	.00	1437.86
602	1604.95	.00	1463.46
603	1633.03	.00	1489.07
604	1661.11	.00	1514.67
605	1689.18	.00	1540.28
606	1576.87	76.25	1437.86
607	1633.03	76.25	1489.07
608	1689.18	76.25	1540.28
609	1576.87	152.50	1437.86
610	1604.95	152.50	1463.46
611	1633.03	152.50	1489.07
612	1661.11	152.50	1514.67
613	1689.18	152.50	1540.28
614	1576.87	228.75	1437.86
615	1633.03	228.75	1489.07
616	1689.18	228.75	1540.28
617	1576.87	305.00	1437.86
618	1604.95	305.00	1463.46
619	1633.03	305.00	1489.07
620	1661.11	305.00	1514.67
621	1689.18	305.00	1540.28
622	1551.02	.00	1465.70
623	1606.26	.00	1517.90
624	1661.50	.00	1570.10
625	1551.02	152.50	1465.70
626	1606.26	152.50	1517.90
627	1661.50	152.50	1570.10
628	1551.02	305.00	1465.70
629	1606.26	305.00	1517.90
630	1661.50	305.00	1570.10
631	1524.68	.00	1493.08
632	1551.83	.00	1519.67
633	1578.98	.00	1546.26
634	1606.13	.00	1572.84
635	1633.28	.00	1599.43

636	1524.68	76.25	1493.08
637	1578.98	76.25	1546.26
638	1633.28	76.25	1599.43
639	1524.68	152.50	1493.08
640	1551.83	152.50	1519.67
641	1578.98	152.50	1546.26
642	1606.13	152.50	1572.84
643	1633.28	152.50	1599.43
644	1524.68	228.75	1493.08
645	1578.98	228.75	1546.26
646	1633.28	228.75	1599.43
647	1524.68	305.00	1493.08
648	1551.83	305.00	1519.67
649	1578.98	305.00	1546.26
650	1606.13	305.00	1572.84
651	1633.28	305.00	1599.43
652	1497.86	.00	1519.99
653	1551.21	.00	1574.12
654	1604.55	.00	1628.25
655	1497.86	152.50	1519.99
656	1551.21	152.50	1574.12
657	1604.55	152.50	1628.25
658	1497.86	305.00	1519.99
659	1551.21	305.00	1574.12
660	1604.55	305.00	1628.25
661	1470.57	.00	1546.41
662	1496.76	.00	1573.95
663	1522.94	.00	1601.48
664	1549.13	.00	1629.02
665	1575.31	.00	1656.56
666	1470.57	76.25	1546.41
667	1522.94	76.25	1601.48
668	1575.31	76.25	1656.56
669	1470.57	152.50	1546.41
670	1496.76	152.50	1573.95
671	1522.94	152.50	1601.48
672	1549.13	152.50	1629.02
673	1575.31	152.50	1656.56
674	1470.57	228.75	1546.41
675	1522.94	228.75	1601.48
676	1575.31	228.75	1656.56
677	1470.57	305.00	1546.41
678	1496.76	305.00	1573.95
679	1522.94	305.00	1601.48
680	1549.13	305.00	1629.02
681	1575.31	305.00	1656.56
682	1442.81	.00	1572.34
683	1494.19	.00	1628.34
684	1545.58	.00	1684.34
685	1442.81	152.50	1572.34
686	1494.19	152.50	1628.34
687	1545.58	152.50	1684.34
688	1442.81	305.00	1572.34
689	1494.19	305.00	1628.34
690	1545.58	305.00	1684.34
691	1414.59	.00	1597.78
692	1439.78	.00	1626.23
693	1464.97	.00	1654.68
694	1490.16	.00	1683.13
695	1515.35	.00	1711.58
696	1414.59	76.25	1597.78
697	1464.97	76.25	1654.68
698	1515.35	76.25	1711.58
699	1414.59	152.50	1597.78
700	1439.78	152.50	1626.23
701	1464.97	152.50	1654.68
702	1490.16	152.50	1683.13
703	1515.35	152.50	1711.58
704	1414.59	228.75	1597.78
705	1464.97	228.75	1654.68
706	1515.35	228.75	1711.58
707	1414.59	305.00	1597.78

708	1439.78	305.00	1626.23
709	1464.97	305.00	1654.68
710	1490.16	305.00	1683.13
711	1515.35	305.00	1711.58
712	1385.92	.00	1622.71
713	1435.28	.00	1680.50
714	1484.64	.00	1738.29
715	1385.92	152.50	1622.71
716	1435.28	152.50	1680.50
717	1484.64	152.50	1738.29
718	1385.92	305.00	1622.71
719	1435.28	305.00	1680.50
720	1484.64	305.00	1738.29
721	1356.82	.00	1647.12
722	1380.98	.00	1676.45
723	1405.14	.00	1705.78
724	1429.30	.00	1735.11
725	1453.46	.00	1764.44
726	1356.82	76.25	1647.12
727	1405.14	76.25	1705.78
728	1453.46	76.25	1764.44
729	1356.82	152.50	1647.12
730	1380.98	152.50	1676.45
731	1405.14	152.50	1705.78
732	1429.30	152.50	1735.11
733	1453.46	152.50	1764.44
734	1356.82	228.75	1647.12
735	1405.14	228.75	1705.78
736	1453.46	228.75	1764.44
737	1356.82	305.00	1647.12
738	1380.98	305.00	1676.45
739	1405.14	305.00	1705.78
740	1429.30	305.00	1735.11
741	1453.46	305.00	1764.44
742	1327.28	.00	1671.01
743	1374.55	.00	1730.52
744	1421.82	.00	1790.04
745	1327.28	152.50	1671.01
746	1374.55	152.50	1730.52
747	1421.82	152.50	1790.04
748	1327.28	305.00	1671.01
749	1374.55	305.00	1730.52
750	1421.82	305.00	1790.04
751	1297.32	.00	1694.38
752	1320.42	.00	1724.55
753	1343.53	.00	1754.72
754	1366.63	.00	1784.89
755	1389.73	.00	1815.06
756	1297.32	76.25	1694.38
757	1343.53	76.25	1754.72
758	1389.73	76.25	1815.06
759	1297.32	152.50	1694.38
760	1320.42	152.50	1724.55
761	1343.53	152.50	1754.72
762	1366.63	152.50	1784.89
763	1389.73	152.50	1815.06
764	1297.32	228.75	1694.38
765	1343.53	228.75	1754.72
766	1389.73	228.75	1815.06
767	1297.32	305.00	1694.38
768	1320.42	305.00	1724.55
769	1343.53	305.00	1754.72
770	1366.63	305.00	1784.89
771	1389.73	305.00	1815.06
772	1266.96	.00	1717.20
773	1312.08	.00	1778.36
774	1357.20	.00	1839.51
775	1266.96	152.50	1717.20
776	1312.08	152.50	1778.36
777	1357.20	152.50	1839.51
778	1266.96	305.00	1717.20
779	1312.08	305.00	1778.36

780	1357.20	305.00	1839.51
781	1236.19	.00	1739.48
782	1258.20	.00	1770.46
783	1280.21	.00	1801.43
784	1302.22	.00	1832.41
785	1324.24	.00	1863.38
786	1236.19	76.25	1739.48
787	1280.21	76.25	1801.43
788	1324.24	76.25	1863.38
789	1236.19	152.50	1739.48
790	1258.20	152.50	1770.46
791	1280.21	152.50	1801.43
792	1302.22	152.50	1832.41
793	1324.24	152.50	1863.38
794	1236.19	228.75	1739.48
795	1280.21	228.75	1801.43
796	1324.24	228.75	1863.38
797	1236.19	305.00	1739.48
798	1258.20	305.00	1770.46
799	1280.21	305.00	1801.43
800	1302.22	305.00	1832.41
801	1324.24	305.00	1863.38
802	1205.02	.00	1761.21
803	1247.94	.00	1823.94
804	1290.86	.00	1886.66
805	1205.02	152.50	1761.21
806	1247.94	152.50	1823.94
807	1290.86	152.50	1886.66
808	1205.02	305.00	1761.21
809	1247.94	305.00	1823.94
810	1290.86	305.00	1886.66
811	1173.48	.00	1782.39
812	1194.38	.00	1814.12
813	1215.27	.00	1845.86
814	1236.17	.00	1877.60
815	1257.07	.00	1909.34
816	1173.48	76.25	1782.39
817	1215.27	76.25	1845.86
818	1257.07	76.25	1909.34
819	1173.48	152.50	1782.39
820	1194.38	152.50	1814.12
821	1215.27	152.50	1845.86
822	1236.17	152.50	1877.60
823	1257.07	152.50	1909.34
824	1173.48	228.75	1782.39
825	1215.27	228.75	1845.86
826	1257.07	228.75	1909.34
827	1173.48	305.00	1782.39
828	1194.38	305.00	1814.12
829	1215.27	305.00	1845.86
830	1236.17	305.00	1877.60
831	1257.07	305.00	1909.34
832	1141.57	.00	1802.99
833	1182.22	.00	1867.20
834	1222.88	.00	1931.42
835	1141.57	152.50	1802.99
836	1182.22	152.50	1867.20
837	1222.88	152.50	1931.42
838	1141.57	305.00	1802.99
839	1182.22	305.00	1867.20
840	1222.88	305.00	1931.42
841	1109.29	.00	1823.03
842	1129.04	.00	1855.49
843	1148.80	.00	1887.95
844	1168.55	.00	1920.42
845	1188.30	.00	1952.88
846	1109.29	76.25	1823.03
847	1148.80	76.25	1887.95
848	1188.30	76.25	1952.88
849	1109.29	152.50	1823.03
850	1129.04	152.50	1855.49
851	1148.80	152.50	1887.95

852	1168.55	152.50	1920.42
853	1188.30	152.50	1952.88
854	1109.29	228.75	1823.03
855	1148.80	228.75	1887.95
856	1188.30	228.75	1952.88
857	1109.29	305.00	1823.03
858	1129.04	305.00	1855.49
859	1148.80	305.00	1887.95
860	1168.55	305.00	1920.42
861	1188.30	305.00	1952.88
862	1076.66	.00	1842.49
863	1115.01	.00	1908.10
864	1153.35	.00	1973.72
865	1076.66	152.50	1842.49
866	1115.01	152.50	1908.10
867	1153.35	152.50	1973.72
868	1076.66	305.00	1842.49
869	1115.01	305.00	1908.10
870	1153.35	305.00	1973.72
871	1043.69	.00	1861.36
872	1062.28	.00	1894.51
873	1080.86	.00	1927.65
874	1099.45	.00	1960.80
875	1118.03	.00	1993.94
876	1043.69	76.25	1861.36
877	1080.86	76.25	1927.65
878	1118.03	76.25	1993.94
879	1043.69	152.50	1861.36
880	1062.28	152.50	1894.51
881	1080.86	152.50	1927.65
882	1099.45	152.50	1960.80
883	1118.03	152.50	1993.94
884	1043.69	228.75	1861.36
885	1080.86	228.75	1927.65
886	1118.03	228.75	1993.94
887	1043.69	305.00	1861.36
888	1062.28	305.00	1894.51
889	1080.86	305.00	1927.65
890	1099.45	305.00	1960.80
891	1118.03	305.00	1993.94
892	1010.39	.00	1879.64
893	1046.38	.00	1946.59
894	1082.36	.00	2013.53
895	1010.39	152.50	1879.64
896	1046.38	152.50	1946.59
897	1082.36	152.50	2013.53
898	1010.39	305.00	1879.64
899	1046.38	305.00	1946.59
900	1082.36	305.00	2013.53
901	976.77	.00	1897.33
902	994.17	.00	1931.12
903	1011.56	.00	1964.90
904	1028.95	.00	1998.69
905	1046.35	.00	2032.48
906	976.77	76.25	1897.33
907	1011.56	76.25	1964.90
908	1046.35	76.25	2032.48
909	976.77	152.50	1897.33
910	994.17	152.50	1931.12
911	1011.56	152.50	1964.90
912	1028.95	152.50	1998.69
913	1046.35	152.50	2032.48
914	976.77	228.75	1897.33
915	1011.56	228.75	1964.90
916	1046.35	228.75	2032.48
917	976.77	305.00	1897.33
918	994.17	305.00	1931.12
919	1011.56	305.00	1964.90
920	1028.95	305.00	1998.69
921	1046.35	305.00	2032.48
922	942.84	.00	1914.42
923	976.42	.00	1982.60

924	1010.00	.00	2050.78
925	942.84	152.50	1914.42
926	976.42	152.50	1982.60
927	1010.00	152.50	2050.78
928	942.84	305.00	1914.42
929	976.42	305.00	1982.60
930	1010.00	305.00	2050.78
931	908.61	.00	1930.90
932	924.79	.00	1965.28
933	940.97	.00	1999.67
934	957.15	.00	2034.05
935	973.33	.00	2068.43
936	908.61	76.25	1930.90
937	940.97	76.25	1999.67
938	973.33	76.25	2068.43
939	908.61	152.50	1930.90
940	924.79	152.50	1965.28
941	940.97	152.50	1999.67
942	957.15	152.50	2034.05
943	973.33	152.50	2068.43
944	908.61	228.75	1930.90
945	940.97	228.75	1999.67
946	973.33	228.75	2068.43
947	908.61	305.00	1930.90
948	924.79	305.00	1965.28
949	940.97	305.00	1999.67
950	957.15	305.00	2034.05
951	973.33	305.00	2068.43
952	874.10	.00	1946.77
953	905.23	.00	2016.10
954	936.36	.00	2085.43
955	874.10	152.50	1946.77
956	905.23	152.50	2016.10
957	936.36	152.50	2085.43
958	874.10	305.00	1946.77
959	905.23	305.00	2016.10
960	936.36	305.00	2085.43
961	839.30	.00	1962.02
962	854.25	.00	1996.96
963	869.19	.00	2031.90
964	884.14	.00	2066.83
965	899.08	.00	2101.77
966	839.30	76.25	1962.02
967	869.19	76.25	2031.90
968	899.08	76.25	2101.77
969	839.30	152.50	1962.02
970	854.25	152.50	1996.96
971	869.19	152.50	2031.90
972	884.14	152.50	2066.83
973	899.08	152.50	2101.77
974	839.30	228.75	1962.02
975	869.19	228.75	2031.90
976	899.08	228.75	2101.77
977	839.30	305.00	1962.02
978	854.25	305.00	1996.96
979	869.19	305.00	2031.90
980	884.14	305.00	2066.83
981	899.08	305.00	2101.77
982	804.24	.00	1976.65
983	832.88	.00	2047.05
984	861.53	.00	2117.44
985	804.24	152.50	1976.65
986	832.88	152.50	2047.05
987	861.53	152.50	2117.44
988	804.24	305.00	1976.65
989	832.88	305.00	2047.05
990	861.53	305.00	2117.44
991	768.93	.00	1990.65
992	782.62	.00	2026.10
993	796.31	.00	2061.55
994	810.00	.00	2097.00
995	823.70	.00	2132.44

996	768.93	76.25	1990.65
997	796.31	76.25	2061.55
998	823.70	76.25	2132.44
999	768.93	152.50	1990.65
1000	782.62	152.50	2026.10
1001	796.31	152.50	2061.55
1002	810.00	152.50	2097.00
1003	823.70	152.50	2132.44
1004	768.93	228.75	1990.65
1005	796.31	228.75	2061.55
1006	823.70	228.75	2132.44
1007	768.93	305.00	1990.65
1008	782.62	305.00	2026.10
1009	796.31	305.00	2061.55
1010	810.00	305.00	2097.00
1011	823.70	305.00	2132.44
1012	733.37	.00	2004.03
1013	759.49	.00	2075.40
1014	785.61	.00	2146.77
1015	733.37	152.50	2004.03
1016	759.49	152.50	2075.40
1017	785.61	152.50	2146.77
1018	733.37	305.00	2004.03
1019	759.49	305.00	2075.40
1020	785.61	305.00	2146.77
1021	697.58	.00	2016.76
1022	710.00	.00	2052.68
1023	722.42	.00	2088.59
1024	734.84	.00	2124.50
1025	747.27	.00	2160.41
1026	697.58	76.25	2016.76
1027	722.42	76.25	2088.59
1028	747.27	76.25	2160.41
1029	697.58	152.50	2016.76
1030	710.00	152.50	2052.68
1031	722.42	152.50	2088.59
1032	734.84	152.50	2124.50
1033	747.27	152.50	2160.41
1034	697.58	228.75	2016.76
1035	722.42	228.75	2088.59
1036	747.27	228.75	2160.41
1037	697.58	305.00	2016.76
1038	710.00	305.00	2052.68
1039	722.42	305.00	2088.59
1040	734.84	305.00	2124.50
1041	747.27	305.00	2160.41
1042	661.57	.00	2028.86
1043	685.13	.00	2101.12
1044	708.69	.00	2173.37
1045	661.57	152.50	2028.86
1046	685.13	152.50	2101.12
1047	708.69	152.50	2173.37
1048	661.57	305.00	2028.86
1049	685.13	305.00	2101.12
1050	708.69	305.00	2173.37
1051	625.35	.00	2040.32
1052	636.48	.00	2076.65
1053	647.62	.00	2112.98
1054	658.75	.00	2149.31
1055	669.89	.00	2185.65
1056	625.35	76.25	2040.32
1057	647.62	76.25	2112.98
1058	669.89	76.25	2185.65
1059	625.35	152.50	2040.32
1060	636.48	152.50	2076.65
1061	647.62	152.50	2112.98
1062	658.75	152.50	2149.31
1063	669.89	152.50	2185.65
1064	625.35	228.75	2040.32
1065	647.62	228.75	2112.98
1066	669.89	228.75	2185.65
1067	625.35	305.00	2040.32

1068	636.48	305.00	2076.65
1069	647.62	305.00	2112.98
1070	658.75	305.00	2149.31
1071	669.89	305.00	2185.65
1072	588.93	.00	2051.13
1073	609.90	.00	2124.18
1074	630.87	.00	2197.22
1075	588.93	152.50	2051.13
1076	609.90	152.50	2124.18
1077	630.87	152.50	2197.22
1078	588.93	305.00	2051.13
1079	609.90	305.00	2124.18
1080	630.87	305.00	2197.22
1081	552.32	.00	2061.29
1082	562.15	.00	2097.99
1083	571.99	.00	2134.70
1084	581.83	.00	2171.40
1085	591.66	.00	2208.11
1086	552.32	76.25	2061.29
1087	571.99	76.25	2134.70
1088	591.66	76.25	2208.11
1089	552.32	152.50	2061.29
1090	562.15	152.50	2097.99
1091	571.99	152.50	2134.70
1092	581.83	152.50	2171.40
1093	591.66	152.50	2208.11
1094	552.32	228.75	2061.29
1095	571.99	228.75	2134.70
1096	591.66	228.75	2208.11
1097	552.32	305.00	2061.29
1098	562.15	305.00	2097.99
1099	571.99	305.00	2134.70
1100	581.83	305.00	2171.40
1101	591.66	305.00	2208.11

1,144,20

1 1 6 9 10 11 7 3 2 22 25 26 23 31 36 39 40 41 37 33 32 1
 2 3 7 11 12 13 8 5 4 23 26 27 24 33 37 41 42 43 38 35 34 1
 3 31 36 39 40 41 37 33 32 52 55 56 53 61 66 69 70 71 67 63 62 1
 4 33 37 41 42 43 38 35 34 53 56 57 54 63 67 71 72 73 68 65 64 1
 5 61 66 69 70 71 67 63 62 82 85 86 83 91 96 99 100 101 97 93 92 1
 6 63 67 71 72 73 68 65 64 83 86 87 84 93 97 101 102 103 98 95 94 1
 7 91 96 99 100 101 97 93 92 112 115 116 113 121 126 129 130 131 127 123 122 1
 8 93 97 101 102 103 98 95 94 113 116 117 114 123 127 131 132 133 128 125 124 1
 9 121 126 129 130 131 127 123 122 142 145 146 143 151 156 159 160 161 157 153 152 1
 10 123 127 131 132 133 128 125 124 143 146 147 144 153 157 161 162 163 158 155 154 1
 11 151 156 159 160 161 157 153 152 172 175 176 173 181 186 189 190 191 187 183 182 1
 12 153 157 161 162 163 158 155 154 173 176 177 174 183 187 191 192 193 188 185 184 1
 13 181 186 189 190 191 187 183 182 202 205 206 203 211 216 219 220 221 217 213 212 1
 14 183 187 191 192 193 188 185 184 203 206 207 204 213 217 221 222 223 218 215 214 1
 15 211 216 219 220 221 217 213 212 232 235 236 233 241 246 249 250 251 247 243 242 1
 16 213 217 221 222 223 218 215 214 233 236 237 234 243 247 251 252 253 248 245 244 1
 17 241 246 249 250 251 247 243 242 262 265 266 263 271 276 279 280 281 277 273 272 1
 18 243 247 251 252 253 248 245 244 263 266 267 264 273 277 281 282 283 278 275 274 1
 19 271 276 279 280 281 277 273 272 292 295 296 293 301 306 309 310 311 307 303 302 1
 20 273 277 281 282 283 278 275 274 293 296 297 294 303 307 311 312 313 308 305 304 1
 21 301 306 309 310 311 307 303 302 322 325 326 323 331 336 339 340 341 337 333 332 1
 22 303 307 311 312 313 308 305 304 323 326 327 324 333 337 341 342 343 338 335 334 1
 23 331 336 339 340 341 337 333 332 352 355 356 353 361 366 369 370 371 367 363 362 1
 24 333 337 341 342 343 338 335 334 353 356 357 354 363 367 371 372 373 368 365 364 1
 25 361 366 369 370 371 367 363 362 382 385 386 383 391 396 399 400 401 397 393 392 1
 26 363 367 371 372 373 368 365 364 383 386 387 384 393 397 401 402 403 398 395 394 1
 27 391 396 399 400 401 397 393 392 412 415 416 413 421 426 429 430 431 427 423 422 1
 28 393 397 401 402 403 398 395 394 413 416 417 414 423 427 431 432 433 428 425 424 1
 29 421 426 429 430 431 427 423 422 442 445 446 443 451 456 459 460 461 457 453 452 1
 30 423 427 431 432 433 428 425 424 443 446 447 444 453 457 461 462 463 458 455 454 1
 31 451 456 459 460 461 457 453 452 472 475 476 473 481 486 489 490 491 487 483 482 1
 32 453 457 461 462 463 458 455 454 473 476 477 474 483 487 491 492 493 488 485 484 1
 33 481 486 489 490 491 487 483 482 502 505 506 503 511 516 519 520 521 517 513 512 1
 34 483 487 491 492 493 488 485 484 503 506 507 504 513 517 521 522 523 518 515 514 1
 35 511 516 519 520 521 517 513 512 532 535 536 533 541 546 549 550 551 547 543 542 1

36	513	517	521	522	523	518	515	514	533	536	537	534	543	547	551	552	553	548	545	544	1
37	541	546	549	550	551	547	543	542	562	565	566	563	571	576	579	580	581	577	573	572	1
38	543	547	551	552	553	548	545	544	563	566	567	564	573	577	581	582	583	578	575	574	1
39	571	576	579	580	581	577	573	572	592	595	596	593	601	606	609	610	611	607	603	602	1
40	573	577	581	582	583	578	575	574	593	596	597	594	603	607	611	612	613	608	605	604	1
41	601	606	609	610	611	607	603	602	622	625	626	623	631	636	639	640	641	637	633	632	1
42	603	607	611	612	613	608	605	604	623	626	627	624	633	637	641	642	643	638	635	634	1
43	631	636	639	640	641	637	633	632	652	655	656	653	661	666	669	670	671	667	663	662	1
44	633	637	641	642	643	638	635	634	653	656	657	654	663	667	671	672	673	668	665	664	1
45	661	666	669	670	671	667	663	662	682	685	686	683	691	696	699	700	701	697	693	692	1
46	663	667	671	672	673	668	665	664	683	686	687	684	693	697	701	702	703	698	695	694	1
47	691	696	699	700	701	697	693	692	712	715	716	713	721	726	729	730	731	727	723	722	1
48	693	697	701	702	703	698	695	694	713	716	717	714	723	727	731	732	733	728	725	724	1
49	721	726	729	730	731	727	723	722	742	745	746	743	751	756	759	760	761	757	753	752	1
50	723	727	731	732	733	728	725	724	743	746	747	744	753	757	761	762	763	758	755	754	1
51	751	756	759	760	761	757	753	752	772	775	776	773	781	786	789	790	791	787	783	782	1
52	753	757	761	762	763	758	755	754	773	776	777	774	783	787	791	792	793	788	785	784	1
53	781	786	789	790	791	787	783	782	802	805	806	803	811	816	819	820	821	817	813	812	1
54	783	787	791	792	793	788	785	784	803	806	807	804	813	817	821	822	823	818	815	814	1
55	811	816	819	820	821	817	813	812	832	835	836	833	841	846	849	850	851	847	843	842	1
56	813	817	821	822	823	818	815	814	833	836	837	834	843	847	851	852	853	848	845	844	1
57	841	846	849	850	851	847	843	842	862	865	866	863	871	876	879	880	881	877	873	872	1
58	843	847	851	852	853	848	845	844	863	866	867	864	873	877	881	882	883	878	875	874	1
59	871	876	879	880	881	877	873	872	892	895	896	893	901	906	909	910	911	907	903	902	1
60	873	877	881	882	883	878	875	874	893	896	897	894	903	907	911	912	913	908	905	904	1
61	901	906	909	910	911	907	903	902	922	925	926	923	931	936	939	940	941	937	933	932	1
62	903	907	911	912	913	908	905	904	923	926	927	924	933	937	941	942	943	938	935	934	1
63	931	936	939	940	941	937	933	932	952	955	956	953	961	966	969	970	971	967	963	962	1
64	933	937	941	942	943	938	935	934	953	956	957	954	963	967	971	972	973	968	965	964	1
65	961	966	969	970	971	967	963	962	982	985	986	983	991	996	999	1000	1001	997	993	992	1
66	963	967	971	972	973	968	965	964	983	986	987	984	993	997	1001	1002	1003	998	995	994	1
67	991	996	999	1000	1001	997	993	992	1012	1015	1016	1013	1021	1026	1029	1030	1031	1027	1023	1022	1
68	993	997	1001	1002	1003	998	995	994	1013	1016	1017	1014	1023	1027	1031	1032	1033	1028	1025	1024	1
69	1021	1026	1029	1030	1031	1027	1023	1022	1042	1045	1046	1043	1051	1056	1059	1060	1061	1057	1053	1052	1
70	1023	1027	1031	1032	1033	1028	1025	1024	1043	1046	1047	1044	1053	1057	1061	1062	1063	1058	1055	1054	1
71	1051	1056	1059	1060	1061	1057	1053	1052	1072	1075	1076	1073	1081	1086	1089	1090	1091	1087	1083	1082	1
72	1053	1057	1061	1062	1063	1058	1055	1054	1073	1076	1077	1074	1083	1087	1091	1092	1093	1088	1085	1084	1
73	9	14	17	18	19	15	11	10	25	28	29	26	39	44	47	48	49	45	41	40	1
74	11	15	19	20	21	16	13	12	26	29	30	27	41	45	49	50	51	46	43	42	1
75	39	44	47	48	49	45	41	40	55	58	59	56	69	74	77	78	79	75	71	70	1
76	41	45	49	50	51	46	43	42	56	59	60	57	71	75	79	80	81	76	73	72	1
77	69	74	77	78	79	75	71	70	85	88	89	86	99	104	107	108	109	105	101	100	1
78	71	75	79	80	81	76	73	72	86	89	90	87	101	105	109	110	111	106	103	102	1
79	99	104	107	108	109	105	101	100	115	118	119	116	129	134	137	138	139	135	131	130	1
80	101	105	109	110	111	106	103	102	116	119	120	117	131	135	139	140	141	136	133	132	1
81	129	134	137	138	139	135	131	130	145	148	149	146	159	164	167	168	169	165	161	160	1
82	131	135	139	140	141	136	133	132	146	149	150	147	161	165	169	170	171	166	163	162	1
83	159	164	167	168	169	165	161	160	175	178	179	176	189	194	197	198	199	195	191	190	1
84	161	165	169	170	171	166	163	162	176	179	180	177	191	195	199	200	201	196	193	192	1
85	189	194	197	198	199	195	191	190	205	208	209	206	219	224	227	228	229	225	221	220	1
86	191	195	199	200	201	196	193	192	206	209	210	207	221	225	229	230	231	226	223	222	1
87	219	224	227	228	229	225	221	220	235	238	239	236	249	254	257	258	259	255	251	250	1
88	221	225	229	230	231	226	223	222	236	239	240	237	251	255	259	260	261	256	253	252	1
89	249	254	257	258	259	255	251	250	265	268	269	266	279	284	287	288	289	285	281	280	1
90	251	255	259	260	261	256	253	252	266	269	270	267	281	285	289	290	291	286	283	282	1
91	279	284	287	288	289	285	281	280	295	298	299	296	309	314	317	318	319	315	311	310	1
92	281	285	289	290	291	286	283	282	296	299	300	297	311	315	319	320	321	316	313	312	1
93	309	314	317	318	319	315	311	310	325	328	329	326	339	344	347	348	349	345	341	340	1
94	311	315	319	320	321	316	313	312	326	329	330	327	341	345	349	350	351	346	343	342	1
95	339	344	347	348	349	345	341	340	355	358	359	356	369	374	377	378	379	375	371	370	1
96	341	345	349	350	351	346	343	342	356	359	360	357	371	375	379	380	381	376	373	372	1
97	369	374	377	378	379	375	371	370	385	388	389	386	399	404	407	408	409	405	401	400	1
98	371	375	379	380	381	376	373	372	386	389	390	387	401	405	409	410	411	406	403	402	1
99	399	404	407	408	409	405	401	400	415	418	419	416	429	434	437	438	439	435	431	430	1
100	401	405	409	410	411	406	403	402	416	419	420	417	431	435	439	440	441	436	433	432	1
101	429	434	437	438	439	435	431	430	445	448	449	446	459	464	467	468	469	465	461	460	1
102	431	435	439	440	441	436	433	432	446	449	450	447	461	465	469	470	471	466	463	462	1
103	459	464	467	468	469	465	461	460	475	478	479	476	489	494	497	498	499	495	491	490	1
104	461	465	469	470	471	466	463	462	476	479	480	477	491	495	499	500	501	496			

108 521 525 529 530 531 526 523 522 536 539 540 537 551 555 559 560 561 556 553 552 1
 109 549 554 557 558 559 555 551 550 565 568 569 566 579 584 587 588 589 585 581 580 1
 110 551 555 559 560 561 556 553 552 566 569 570 567 581 585 589 590 591 586 583 582 1
 111 579 584 587 588 589 585 581 580 595 598 599 596 609 614 617 618 619 615 611 610 1
 112 581 585 589 590 591 586 583 582 596 599 600 597 611 615 619 620 621 616 613 612 1
 113 609 614 617 618 619 615 611 610 625 628 629 626 639 644 647 648 649 645 641 640 1
 114 611 615 619 620 621 616 613 612 626 629 630 627 641 645 649 650 651 646 643 642 1
 115 639 644 647 648 649 645 641 640 655 658 659 656 669 674 677 678 679 675 671 670 1
 116 641 645 649 650 651 646 643 642 656 659 660 657 671 675 679 680 681 676 673 672 1
 117 669 674 677 678 679 675 671 670 685 688 689 686 699 704 707 708 709 705 701 700 1
 118 671 675 679 680 681 676 673 672 686 689 690 687 701 705 709 710 711 706 703 702 1
 119 699 704 707 708 709 705 701 700 715 718 719 716 729 734 737 738 739 735 731 730 1
 120 701 705 709 710 711 706 703 702 716 719 720 717 731 735 739 740 741 736 733 732 1
 121 729 734 737 738 739 735 731 730 745 748 749 746 759 764 767 768 769 765 761 760 1
 122 731 735 739 740 741 736 733 732 746 749 750 747 761 765 769 770 771 766 763 762 1
 123 759 764 767 768 769 765 761 760 775 778 779 776 789 794 797 798 799 795 791 790 1
 124 761 765 769 770 771 766 763 762 776 779 780 777 791 795 799 800 801 796 793 792 1
 125 789 794 797 798 799 795 791 790 805 808 809 806 819 824 827 828 829 825 821 820 1
 126 791 795 799 800 801 796 793 792 806 809 810 807 821 825 829 830 831 826 823 822 1
 127 819 824 827 828 829 825 821 820 835 838 839 836 849 854 857 858 859 855 851 850 1
 128 821 825 829 830 831 826 823 822 836 839 840 837 851 855 859 860 861 856 853 852 1
 129 849 854 857 858 859 855 851 850 865 868 869 866 879 884 887 888 889 885 881 880 1
 130 851 855 859 860 861 856 853 852 866 869 870 867 881 885 889 890 891 886 883 882 1
 131 879 884 887 888 889 885 881 880 895 898 899 896 909 914 917 918 919 915 911 910 1
 132 881 885 889 890 891 886 883 882 896 899 900 897 911 915 919 920 921 916 913 912 1
 133 909 914 917 918 919 915 911 910 925 928 929 926 939 944 947 948 949 945 941 940 1
 134 911 915 919 920 921 916 913 912 926 929 930 927 941 945 949 950 951 946 943 942 1
 135 939 944 947 948 949 945 941 940 955 958 959 956 969 974 977 978 979 975 971 970 1
 136 941 945 949 950 951 946 943 942 956 959 960 957 971 975 979 980 981 976 973 972 1
 137 969 974 977 978 979 975 971 970 985 988 989 986 999 1004 1007 1008 1009 1005 1001 1000 1
 138 971 975 979 980 981 976 973 972 986 989 990 987 1001 1005 1009 1010 1011 1006 1003 1002 1
 139 999 1004 1007 1008 1009 1005 1001 1000 1015 1018 1019 1016 1029 1034 1037 1038 1039 1035 1031 1030 1
 140 1001 1005 1009 1010 1011 1006 1003 1002 1016 1019 1020 1017 1031 1035 1039 1040 1041 1036 1033 1032 1
 141 1029 1034 1037 1038 1039 1035 1031 1030 1045 1048 1049 1046 1059 1064 1067 1068 1069 1065 1061 1060 1
 142 1031 1035 1039 1040 1041 1036 1033 1032 1046 1049 1050 1047 1061 1065 1069 1070 1071 1066 1063 1062 1
 143 1059 1064 1067 1068 1069 1065 1061 1060 1075 1078 1079 1076 1089 1094 1097 1098 1099 1095 1091 1090 1
 144 1061 1065 1069 1070 1071 1066 1063 1062 1076 1079 1080 1077 1091 1095 1099 1100 1101 1096 1093 1092 1

376

1 1 3 5 .00 -.50 .00
 2 1 2 4 -.34 .00 -.89
 3 1 1 4 .00 -.67 -.89
 4 2 3 5 .00 -.50 .00
 5 2 2 4 .34 .00 -.89
 6 2 1 4 .00 -.67 -.89
 7 3 3 5 .00 -.50 .00
 8 3 2 4 -.34 .00 -.45
 9 3 1 4 .00 -.67 -.45
 10 4 3 5 .00 -.50 .00
 11 4 2 4 .34 .00 -.45
 12 4 1 4 .00 -.67 -.45
 13 5 3 5 .00 -.50 .00
 14 5 2 4 -.34 .00 .00
 15 5 1 4 .00 -.67 .00
 16 6 3 5 .00 -.50 .00
 17 6 2 4 .34 .00 .00
 18 6 1 4 .00 -.67 .00
 19 7 3 5 .00 -.50 .00
 20 7 2 4 -.34 .00 .45
 21 7 1 4 .00 -.67 .45
 22 8 3 5 .00 -.50 .00
 23 8 2 4 .34 .00 .45
 24 8 1 4 .00 -.67 .45
 25 9 3 5 .00 -.50 .00
 26 9 2 4 -.34 .00 .90
 27 9 1 4 .00 -.67 .90
 28 10 3 5 .00 -.50 .00
 29 10 2 4 .34 .00 .90
 30 10 1 4 .00 -.67 .90
 31 11 3 5 .00 -.50 .00
 32 12 3 5 .00 -.50 .00
 33 13 3 5 .00 -.50 .00

34	13	2	4	-.34	.00	-.66
35	13	1	4	.00	-.67	-.66
36	14	3	5	.00	-.50	.00
37	14	2	4	.34	.00	-.66
38	14	1	4	.00	-.67	-.66
39	15	3	5	.00	-.50	.00
40	15	2	4	-.34	.00	-.21
41	15	1	4	.00	-.67	-.21
42	16	3	5	.00	-.50	.00
43	16	2	4	.34	.00	-.21
44	16	1	4	.00	-.67	-.21
45	17	3	5	.00	-.50	.00
46	17	2	4	-.34	.00	.24
47	17	1	4	.00	-.67	.24
48	18	3	5	.00	-.50	.00
49	18	2	4	.34	.00	.24
50	18	1	4	.00	-.67	.24
51	19	3	5	.00	-.50	.00
52	19	2	4	-.34	.00	.69
53	19	1	4	.00	-.67	.69
54	20	3	5	.00	-.50	.00
55	20	2	4	.34	.00	.69
56	20	1	4	.00	-.67	.69
57	21	3	5	.00	-.50	.00
58	22	3	5	.00	-.50	.00
59	23	3	5	.00	-.50	.00
60	23	2	4	-.34	.00	-.85
61	23	1	4	.00	-.67	-.85
62	24	3	5	.00	-.50	.00
63	24	2	4	.34	.00	-.85
64	24	1	4	.00	-.67	-.85
65	25	3	5	.00	-.50	.00
66	25	2	4	-.34	.00	-.24
67	25	1	4	.00	-.67	-.24
68	26	3	5	.00	-.50	.00
69	26	2	4	.34	.00	-.24
70	26	1	4	.00	-.67	-.24
71	27	3	5	.00	-.50	.00
72	27	2	4	-.34	.00	.38
73	27	1	4	.00	-.67	.38
74	28	3	5	.00	-.50	.00
75	28	2	4	.34	.00	.38
76	28	1	4	.00	-.67	.38
77	29	3	5	.00	-.50	.00
78	29	2	4	-.34	.00	1.00
79	29	1	4	.00	-.67	1.00
80	30	3	5	.00	-.50	.00
81	30	2	4	.34	.00	1.00
82	30	1	4	.00	-.67	1.00
83	31	3	5	.00	-.50	.00
84	32	3	5	.00	-.50	.00
85	33	3	5	.00	-.50	.00
86	33	2	4	-.34	.00	-.38
87	33	1	4	.00	-.67	-.38
88	34	3	5	.00	-.50	.00
89	34	2	4	.34	.00	-.38
90	34	1	4	.00	-.67	-.38
91	35	3	5	.00	-.50	.00
92	35	2	4	-.34	.00	.24
93	35	1	4	.00	-.67	.24
94	36	3	5	.00	-.50	.00
95	36	2	4	.34	.00	.24
96	36	1	4	.00	-.67	.24
97	37	3	5	.00	-.50	.00
98	37	2	4	-.34	.00	.85
99	37	1	4	.00	-.67	.85
100	38	3	5	.00	-.50	.00
101	38	2	4	.34	.00	.85
102	38	1	4	.00	-.67	.85
103	39	3	5	.00	-.50	.00
104	40	3	5	.00	-.50	.00
105	41	3	5	.00	-.50	.00

106	41	2	4	-.34	.00	-.53
107	41	1	4	.00	-.67	-.53
108	42	3	5	.00	-.50	.00
109	42	2	4	.34	.00	-.53
110	42	1	4	.00	-.67	-.53
111	43	3	5	.00	-.50	.00
112	43	2	4	-.34	.00	.09
113	43	1	4	.00	-.67	.09
114	44	3	5	.00	-.50	.00
115	44	2	4	.34	.00	.09
116	44	1	4	.00	-.67	.09
117	45	3	5	.00	-.50	.00
118	45	2	4	-.34	.00	.71
119	45	1	4	.00	-.67	.71
120	46	3	5	.00	-.50	.00
121	46	2	4	.34	.00	.71
122	46	1	4	.00	-.67	.71
123	47	3	5	.00	-.50	.00
124	48	3	5	.00	-.50	.00
125	49	3	5	.00	-.50	.00
126	49	2	4	-.34	.00	-.67
127	49	1	4	.00	-.67	-.67
128	50	3	5	.00	-.50	.00
129	50	2	4	.34	.00	-.67
130	50	1	4	.00	-.67	-.67
131	51	3	5	.00	-.50	.00
132	51	2	4	-.34	.00	-.06
133	51	1	4	.00	-.67	-.06
134	52	3	5	.00	-.50	.00
135	52	2	4	.34	.00	-.06
136	52	1	4	.00	-.67	-.06
137	53	3	5	.00	-.50	.00
138	53	2	4	-.34	.00	.56
139	53	1	4	.00	-.67	.56
140	54	3	5	.00	-.50	.00
141	54	2	4	.34	.00	.56
142	54	1	4	.00	-.67	.56
143	55	3	5	.00	-.50	.00
144	56	3	5	.00	-.50	.00
145	57	3	5	.00	-.50	.00
146	57	2	4	-.34	.00	-.82
147	57	1	4	.00	-.67	-.82
148	58	3	5	.00	-.50	.00
149	58	2	4	.34	.00	-.82
150	58	1	4	.00	-.67	-.82
151	59	3	5	.00	-.50	.00
152	59	2	4	-.34	.00	-.20
153	59	1	4	.00	-.67	-.20
154	60	3	5	.00	-.50	.00
155	60	2	4	.34	.00	-.20
156	60	1	4	.00	-.67	-.20
157	61	3	5	.00	-.50	.00
158	61	2	4	-.34	.00	.42
159	61	1	4	.00	-.67	.42
160	62	3	5	.00	-.50	.00
161	62	2	4	.34	.00	.42
162	62	1	4	.00	-.67	.42
163	63	3	5	.00	-.50	.00
164	64	3	5	.00	-.50	.00
165	65	3	5	.00	-.50	.00
166	65	2	4	-.34	.00	-.97
167	65	1	4	.00	-.67	-.97
168	66	3	5	.00	-.50	.00
169	66	2	4	.34	.00	-.97
170	66	1	4	.00	-.67	-.97
171	67	3	5	.00	-.50	.00
172	67	2	4	-.34	.00	-.35
173	67	1	4	.00	-.67	-.35
174	68	3	5	.00	-.50	.00
175	68	2	4	.34	.00	-.35
176	68	1	4	.00	-.67	-.35
177	69	3	5	.00	-.50	.00

178	69	2	4	-.34	.00	.27
179	69	1	4	.00	-.67	.27
180	70	3	5	.00	-.50	.00
181	70	2	4	.34	.00	.27
182	70	1	4	.00	-.67	.27
183	71	3	5	.00	-.50	.00
184	71	2	4	-.34	.00	.89
185	71	1	4	.00	-.67	.89
186	72	3	5	.00	-.50	.00
187	72	2	4	.34	.00	.89
188	72	1	4	.00	-.67	.89
189	73	3	5	.00	.50	.00
190	73	2	4	-.34	.00	-.89
191	73	1	4	.00	.67	-.89
192	74	3	5	.00	.50	.00
193	74	2	4	.34	.00	-.89
194	74	1	4	.00	.67	-.89
195	75	3	5	.00	.50	.00
196	75	2	4	-.34	.00	-.45
197	75	1	4	.00	.67	-.45
198	76	3	5	.00	.50	.00
199	76	2	4	.34	.00	-.45
200	76	1	4	.00	.67	-.45
201	77	3	5	.00	.50	.00
202	77	2	4	-.34	.00	.00
203	77	1	4	.00	.67	.00
204	78	3	5	.00	.50	.00
205	78	2	4	.34	.00	.00
206	78	1	4	.00	.67	.00
207	79	3	5	.00	.50	.00
208	79	2	4	-.34	.00	.45
209	79	1	4	.00	.67	.45
210	80	3	5	.00	.50	.00
211	80	2	4	.34	.00	.45
212	80	1	4	.00	.67	.45
213	81	3	5	.00	.50	.00
214	81	2	4	-.34	.00	.90
215	81	1	4	.00	.67	.90
216	82	3	5	.00	.50	.00
217	82	2	4	.34	.00	.90
218	82	1	4	.00	.67	.90
219	83	3	5	.00	.50	.00
220	84	3	5	.00	.50	.00
221	85	3	5	.00	.50	.00
222	85	2	4	-.34	.00	-.66
223	85	1	4	.00	.67	-.66
224	86	3	5	.00	.50	.00
225	86	2	4	.34	.00	-.66
226	86	1	4	.00	.67	-.66
227	87	3	5	.00	.50	.00
228	87	2	4	-.34	.00	-.21
229	87	1	4	.00	.67	-.21
230	88	3	5	.00	.50	.00
231	88	2	4	.34	.00	-.21
232	88	1	4	.00	.67	-.21
233	89	3	5	.00	.50	.00
234	89	2	4	-.34	.00	.24
235	89	1	4	.00	.67	.24
236	90	3	5	.00	.50	.00
237	90	2	4	.34	.00	.24
238	90	1	4	.00	.67	.24
239	91	3	5	.00	.50	.00
240	91	2	4	-.34	.00	.69
241	91	1	4	.00	.67	.69
242	92	3	5	.00	.50	.00
243	92	2	4	.34	.00	.69
244	92	1	4	.00	.67	.69
245	93	3	5	.00	.50	.00
246	94	3	5	.00	.50	.00
247	95	3	5	.00	.50	.00
248	95	2	4	-.34	.00	-.85
249	95	1	4	.00	.67	-.85

250	96	3	5	.00	.50	.00
251	96	2	4	.34	.00	-.85
252	96	1	4	.00	.67	-.85
253	97	3	5	.00	.50	.00
254	97	2	4	-.34	.00	-.24
255	97	1	4	.00	.67	-.24
256	98	3	5	.00	.50	.00
257	98	2	4	.34	.00	-.24
258	98	1	4	.00	.67	-.24
259	99	3	5	.00	.50	.00
260	99	2	4	-.34	.00	.38
261	99	1	4	.00	.67	.38
262	100	3	5	.00	.50	.00
263	100	2	4	.34	.00	.38
264	100	1	4	.00	.67	.38
265	101	3	5	.00	.50	.00
266	101	2	4	-.34	.00	1.00
267	101	1	4	.00	.67	1.00
268	102	3	5	.00	.50	.00
269	102	2	4	.34	.00	1.00
270	102	1	4	.00	.67	1.00
271	103	3	5	.00	.50	.00
272	104	3	5	.00	.50	.00
273	105	3	5	.00	.50	.00
274	105	2	4	-.34	.00	-.38
275	105	1	4	.00	.67	-.38
276	106	3	5	.00	.50	.00
277	106	2	4	.34	.00	-.38
278	106	1	4	.00	.67	-.38
279	107	3	5	.00	.50	.00
280	107	2	4	-.34	.00	.24
281	107	1	4	.00	.67	.24
282	108	3	5	.00	.50	.00
283	108	2	4	.34	.00	.24
284	108	1	4	.00	.67	.24
285	109	3	5	.00	.50	.00
286	109	2	4	-.34	.00	.85
287	109	1	4	.00	.67	.85
288	110	3	5	.00	.50	.00
289	110	2	4	.34	.00	.85
290	110	1	4	.00	.67	.85
291	111	3	5	.00	.50	.00
292	112	3	5	.00	.50	.00
293	113	3	5	.00	.50	.00
294	113	2	4	-.34	.00	-.53
295	113	1	4	.00	.67	-.53
296	114	3	5	.00	.50	.00
297	114	2	4	.34	.00	-.53
298	114	1	4	.00	.67	-.53
299	115	3	5	.00	.50	.00
300	115	2	4	-.34	.00	.09
301	115	1	4	.00	.67	.09
302	116	3	5	.00	.50	.00
303	116	2	4	.34	.00	.09
304	116	1	4	.00	.67	.09
305	117	3	5	.00	.50	.00
306	117	2	4	-.34	.00	.71
307	117	1	4	.00	.67	.71
308	118	3	5	.00	.50	.00
309	118	2	4	.34	.00	.71
310	118	1	4	.00	.67	.71
311	119	3	5	.00	.50	.00
312	120	3	5	.00	.50	.00
313	121	3	5	.00	.50	.00
314	121	2	4	-.34	.00	-.67
315	121	1	4	.00	.67	-.67
316	122	3	5	.00	.50	.00
317	122	2	4	.34	.00	-.67
318	122	1	4	.00	.67	-.67
319	123	3	5	.00	.50	.00
320	123	2	4	-.34	.00	-.06
321	123	1	4	.00	.67	-.06

322	124	3	5	.00	.50	.00
323	124	2	4	.34	.00	-.06
324	124	1	4	.00	.67	-.06
325	125	3	5	.00	.50	.00
326	125	2	4	-.34	.00	.56
327	125	1	4	.00	.67	.56
328	126	3	5	.00	.50	.00
329	126	2	4	.34	.00	.56
330	126	1	4	.00	.67	.56
331	127	3	5	.00	.50	.00
332	128	3	5	.00	.50	.00
333	129	3	5	.00	.50	.00
334	129	2	4	-.34	.00	-.82
335	129	1	4	.00	.67	-.82
336	130	3	5	.00	.50	.00
337	130	2	4	.34	.00	-.82
338	130	1	4	.00	.67	-.82
339	131	3	5	.00	.50	.00
340	131	2	4	-.34	.00	-.20
341	131	1	4	.00	.67	-.20
342	132	3	5	.00	.50	.00
343	132	2	4	.34	.00	-.20
344	132	1	4	.00	.67	-.20
345	133	3	5	.00	.50	.00
346	133	2	4	-.34	.00	.42
347	133	1	4	.00	.67	.42
348	134	3	5	.00	.50	.00
349	134	2	4	.34	.00	.42
350	134	1	4	.00	.67	.42
351	135	3	5	.00	.50	.00
352	136	3	5	.00	.50	.00
353	137	3	5	.00	.50	.00
354	137	2	4	-.34	.00	-.97
355	137	1	4	.00	.67	-.97
356	138	3	5	.00	.50	.00
357	138	2	4	.34	.00	-.97
358	138	1	4	.00	.67	-.97
359	139	3	5	.00	.50	.00
360	139	2	4	-.34	.00	-.35
361	139	1	4	.00	.67	-.35
362	140	3	5	.00	.50	.00
363	140	2	4	.34	.00	-.35
364	140	1	4	.00	.67	-.35
365	141	3	5	.00	.50	.00
366	141	2	4	-.34	.00	.27
367	141	1	4	.00	.67	.27
368	142	3	5	.00	.50	.00
369	142	2	4	.34	.00	.27
370	142	1	4	.00	.67	.27
371	143	3	5	.00	.50	.00
372	143	2	4	-.34	.00	.89
373	143	1	4	.00	.67	.89
374	144	3	5	.00	.50	.00
375	144	2	4	.34	.00	.89
376	144	1	4	.00	.67	.89

40,0.4,10,.5,0.10

5

1,0.2,25.76,0,0,0,0.001606,0.03004,0

2,0,0,0,0,0,0,0

3,0,0,0,0,0,0,0

4,0,200,0.300,39.59,0,0,0,0

5,0,200,0.475,283.53,0,0,0,0

32

1,1,2,3

2,1,2,3

3,1,2,3

4,1,2,3

5,1,2,3

6,1,2,3

8,1,2,3
9,1,2,3
13,1,2,3
14,1,2,3
16,1,2,3
17,1,2,3
18,1,2,3
19,1,2,3
20,1,2,3
21,1,2,3

1081,1,2,3
1082,1,2,3
1083,1,2,3
1084,1,2,3
1085,1,2,3
1086,1,2,3
1088,1,2,3
1089,1,2,3
1093,1,2,3
1094,1,2,3
1096,1,2,3
1097,1,2,3
1098,1,2,3
1099,1,2,3
1100,1,2,3
1101,1,2,3

3
348,0,-0.66,0
349,0,-0.66,0
350,0,-0.66,0


```

888 FORMAT(5X,'ISTEP =',I5,5X,'RATIO =',E20.5,'IITER =',I5)
      IF(NCHEK.EQ.1)GOTO 520
500 CONTINUE
520 CALL OUTDYN(DISPT,NGRQS,NPRQD,DISPQ,ISTAT,IFPRE,STRES,EFFST,WORKP,
      .
      WORKF,GPCOD,STRVP,STRAF,ALPHI,EFFSS)
510 CONTINUE
      STOP
      END
C *****
C ***          THIS SUBROUTINE ACCEPTS THE CONTROL INPUT DATA          ***
C *****
      SUBROUTINE INPUT0
      COMMON/CTRL/NECHO,NELEM,NGAUS,NMATS,NPOIN,NREIN,NSIZE,NTOTG,NTOTV,
      &
      &          NVFIX,NWKTL
      CHARACTER*40 TITLE
      READ(1,*) TITLE
      WRITE(2,910)TITLE
C ***          READ THE FIRST DATA CARD, AND ECHO IT IMMEDIATELY.          ***
      READ(1,*) NPOIN,NELEM,NVFIX,NMATS,NECHO,NREIN
      IF(NECHO.GE.1) WRITE(2,930)
      IF(NECHO.GE.2) WRITE(2,940)
      NTOTV=NPOIN*3
      NGAUS=2
      NTOTG=NELEM*27
      IF(NECHO.LT.2)WRITE(2,950)NPOIN,NELEM,NVFIX,NMATS,NREIN
      RETURN
910 FORMAT(10X,'TITLE OF RUN. ',A40/10X,12('=')//10X,
      .
      'ECHO OF INPUT DATA./10X,19('-'))
930 FORMAT(1H0,10X,'TOTAL LOAD MATRIX OUTPUT SUPPRESSED.')
940 FORMAT(1H0,10X,'ECHO OF DATA ALSO SUPPRESSED.')
950 FORMAT(/10X,'TOTAL NUMBER OF NODAL POINTS.....',I5/
      .
      ,10X,'TOTAL NUMBER OF ELEMENTS.....',I5/
      .
      ,10X,'TOTAL NUM. OF RESTRAINED BOUNDARY NDS.....',I5/
      .
      10X,'NUMBER OF DIFFERENT MATERIALS.....',I5/
      .
      10X,'NUM OF DIFFERENT REINFORCEMENT PATTERNS....',I5/
      .
      10X,'NUMBER OF STUDS.....',I5)
      END
C *****
C ***          THIS SUBROUTINE ACCEPTS MOST OF THE INPUT DATA          ***
C *****
      SUBROUTINE INPUT(COORD,LNODS,MATNO,IFPRE,PROPS,ELAST,MLAYR,NOCAP,
      .
      MBARS,VBARS,MPATT)
      COMMON/CTRL/NECHO,NELEM,NGAUS,NMATS,NPOIN,NREIN,NSIZE,NTOTG,NTOTV,
      &
      &          NVFIX,NWKTL
      DIMENSION COORD(3,1),LNODS(20,1),MATNO(1),IFPRE(3,1),ELAST(3,1),
      &          &PROPS(20,1),NOCAP(1),MPATT(1),VBARS(3,MLAYR,1),MBARS(2,MLAYR,1)
C ***          READ THE ELEMENT NODAL CONNECTIONS, AND THE PROPERTY NUMBERS          ***
      IF (NECHO.LT.2) WRITE(2,901)
      DO 2 IELEM = 1,NELEM
      READ(1,*)NE,MATNO(NE),MPATT(NE),(LNODS(I,NE),I=1,20)
      2  IF(NECHO.LT.2)WRITE(2,902)NE,MATNO(NE),MPATT(NE),
      .
      (LNODS(INODE,NE),INODE=1,20)
C ***          READ SOME NODAL COORDI.,FINISHING WITH THE LAST NODE OF ALL          ***
      IF(NECHO.LT.2) WRITE(2,903)
      6  READ(1,*) IPOIN,(COORD(ID,IPOIN),ID=1,3)
      IF(IPOIN.NE.NPOIN)GOTO 6
      DO 10 IPOIN=1,NPOIN
      10 IF(NECHO.LT.2) WRITE(2,905)IPOIN,(COORD(I,IPOIN),I=1,3)
C ***          READ THE FIXED VALUES          ***
      PI = 4.*ATAN(1.)
      IF (NECHO.LT.2) WRITE(2,906)
      DO 31 IVFIX = 1,NVFIX
      READ(1,*) IPOIN,(IFPRE(IDOFN,IPOIN),IDOFN=1,3)
      IF(NECHO.LT.2) WRITE(2,908)IPOIN,(IFPRE(I,IPOIN),I=1,3)
      31 CONTINUE
C ***          READ THE AVAILABLE SELECTION OF ELEMENT PROPERTIES          ***
      IF(NECHO.LT.2) WRITE(2,909)
      DO 18 IMATS=1,NMATS
      READ(1,*) NUMAT
      READ(1,*) (PROPS(IPROP,NUMAT),IPROP=1,20)
C ***          COMPUTE ELASTIC CONSTANTS          ***
      YOUNG = PROPS(1,IMATS)
      POISS = PROPS(2,IMATS)
      CONST = YOUNG*(1.-POISS)/((1.+POISS)*(1.-2.*POISS))
      ELAST(1,IMATS) = CONST
      ELAST(2,IMATS) = CONST*POISS/(1.-POISS)
      18 ELAST(3,IMATS) = CONST*(1.-2.*POISS)/(2.*(1.-POISS))
      IF (NECHO.GE.2)GOTO 19
      WRITE(2,911)(I,I=1,NMATS)
      WRITE(2,912)(PROPS(1,IMATS),IMATS=1,NMATS)
      WRITE(2,913)(PROPS(2,IMATS),IMATS=1,NMATS)

```

```

WRITE(2,914)(PROPS(3,IMATS),IMATS=1,NMATS)
WRITE(2,915)(PROPS(4,IMATS),IMATS=1,NMATS)
WRITE(2,916)(PROPS(5,IMATS),IMATS=1,NMATS)
WRITE(2,917)(PROPS(6,IMATS),IMATS=1,NMATS)
WRITE(2,918)(PROPS(7,IMATS),IMATS=1,NMATS)
WRITE(2,919)(PROPS(8,IMATS),IMATS=1,NMATS)
WRITE(2,920)(PROPS(9,IMATS),IMATS=1,NMATS)
WRITE(2,921)(PROPS(10,IMATS),IMATS=1,NMATS)
WRITE(2,922)(PROPS(11,IMATS),IMATS=1,NMATS)
WRITE(2,923)(PROPS(12,IMATS),IMATS=1,NMATS)
WRITE(2,924)(PROPS(13,IMATS),IMATS=1,NMATS)
WRITE(2,925)(PROPS(14,IMATS),IMATS=1,NMATS)
WRITE(2,926)(PROPS(15,IMATS),IMATS=1,NMATS)
19 CONTINUE
C *** READ THE AVAILABLE SELECTION OF REINFORCEMENT PATTERNS ***
IF(NREIN.EQ.0)GOTO 334
IF(NECHO.LT.2)WRITE(2,927)
DO 21 IREIN = 1,NREIN
READ (1,*) KREIN,NOCAP(KREIN)
NLAYR=NOCAP(KREIN)
DO 21 ILAYR=1,NLAYR
READ(1,*)(MBARS(1,ILAYR,KREIN),I=1,2),(VBARS(1,ILAYR,KREIN),I=1,3)
VBARS(3,ILAYR,KREIN)=VBARS(3,ILAYR,KREIN)*ATAN(1.0)/45.
21 CONTINUE
IF(NECHO.GE.2)GOTO 334
DO 333 IREIN = 1,NREIN
NLAYR=NOCAP(IREIN)
WRITE(2,929)IREIN
WRITE(2,930)(I,I=1,NLAYR)
WRITE(2,931)(MBARS(1,ILAYR,IREIN),ILAYR=1,NLAYR)
WRITE(2,932)(MBARS(2,ILAYR,IREIN),ILAYR=1,NLAYR)
WRITE(2,933)(VBARS(1,ILAYR,IREIN),ILAYR=1,NLAYR)
WRITE(2,934)(VBARS(2,ILAYR,IREIN),ILAYR=1,NLAYR)
WRITE(2,935)(VBARS(3,ILAYR,IREIN),ILAYR=1,NLAYR)
333 CONTINUE
334 CONTINUE
RETURN
901 FORMAT(//1X,' NODAL CONNECTION CLOCKWISE AROUND',
. ' ELEMENT. LEFT HAND SCREW RULE.'/2X,16('*')/3X,
. ' ELEMENT PROPERTY REINFORC. NODE NUMBERS.'/3X,
. ' NUMBER SET. PATTERN N1 N2 N3 N4 N5 N6',
. ' N7 N8 N9 N10')
902 FORMAT(1X,I5,3X,I9,6X,I5,3X,10I5/32X,10I5)
903 FORMAT(//10X,' NODAL CO-ORDINATES DATA.'/10X,24('*')/2X,
. ' NODE NUMBER X CO-ORDINATE. Y CO-ORDINATE.',
. ' Z CO-ORDINATE.')
905 FORMAT( 5X,I8,6X,3(6X,F10.3))
906 FORMAT(//1X,' RESTRAINED NODES RELATIVE TO THE',
. ' X-Y-Z CO-ORDINATE SYSTEM, AND THEIR ORIGINAL POSITION.'/1X,
. 90('*')/8X,' NODE X RESTRAINT ',
. ' Y RESTRAINT Z-RESTRAINT ')
908 FORMAT(8X,I5,3(6X,I5,7X),F10.5)
909 FORMAT(// 2X,' MATERIAL PROPERTY SETS.'/2X,23('*')/)
911 FORMAT(1H,42X,5(' SET',I2,' '))
912 FORMAT(1H ,1X,' YOUNG MODULUS.....',5(2X,E10.4))
913 FORMAT(1H ,1X,' POISSON RATIO.....',5(2X,E10.4))
914 FORMAT(1H ,1X,' COMPRESSION FLOW STRESS.....',5(2X,E10.4))
915 FORMAT(1H ,1X,' CRACKING STRESS(YOUNG*CRAC.STRAIN)...',5(2X,E10.4))
916 FORMAT(1H ,1X,' CRUSHING STRAIN.....',5(2X,E10.4))
917 FORMAT(1H ,1X,' FRACTURE ENERGY.....',5(2X,E10.4))
918 FORMAT(1H ,1X,' FACTOR FOR SHEAR REDUCTION.....',5(2X,E10.4))
919 FORMAT(1H ,1X,' YIELD CRITERION.....',5(2X,E10.4))
920 FORMAT(1H ,1X,' MATERIAL DENSITY.....',5(2X,E10.4))
921 FORMAT(1H ,1X,' FACTOR FOR END OF ELASTICITY.....',5(2X,E10.4))
922 FORMAT(1H ,1X,' A0 FOR FLUIDITY PARAMETER.....',5(2X,E10.4))
923 FORMAT(1H ,1X,' A1 FOR FLUIDITY PARAMETER.....',5(2X,E10.4))
924 FORMAT(1H ,1X,' ALFA-C FOR STRAIN-SOFTENING.....',5(2X,E10.4))
925 FORMAT(1H ,1X,' BETA0 FOR MONITORING SURFACE.....',5(2X,E10.4))
926 FORMAT(1H ,1X,' BETA1 FOR MONITORING SURFACE.....',5(2X,E10.4))
927 FORMAT(//2X,' REINFORCEMENT SETS.'/2X,23('*'))
929 FORMAT(//2X,' REINFORCEMENT SET NO.',I3)
930 FORMAT(44X,5(' LAYER',I2,' '))
931 FORMAT(1H ,1X,' MATERIAL NUMBER.....',5(4X,I5))
932 FORMAT(1H ,1X,' COORDINATE NUMBER.....',5(4X,I5))
933 FORMAT(1H ,1X,' COORDINATE POSITION.....',5(2X,F10.5))
934 FORMAT(1H ,1X,' THICKNESS.....',5(2X,F10.5))
935 FORMAT(1H ,1X,' ANGLE FROM EXI-AXIS.....',5(2X,F10.5))
END
C *****
C *** INPUT INITIAL VALUES AND TIME INTEGRATION DATA ***
C *****

```

```

SUBROUTINE INTIME(ACCEH,ACCEV,NGRQS,NPRQD,TDISP,VELOC,IFPRE)
COMMON/CTRL/NECHO,NELEM,NGAUS,NMATS,NPOIN,NREIN,NSIZE,NTOTG,NTOTV,
&
      NVFIX,NWKTL
COMMON/RUN/IFUNC,IPRED,KSTEP,MITER,NACCE,NOUTD,NOUTP,NREQD,NREQS,
&
      NSTEP
COMMON/CONST/AALFA,BEETA,GAAMA,DELTA,AZERO,BZERO,OMEGA,TMAXR,DTEND
&
      ,DTIME,AFACT,TOLER,ADISP,AVELO,CONSD,CONSF
DIMENSION TDISP(*),ACCEH(*),VELOC(*),ACCEV(*),IFPRE(3,*),NPRQD(1),
&
      NGRQS(1)
C *** READ TIME STEPPING AND SELECTIVE OUTPUT PARAMETERS ***
READ (1,*) NSTEP,NOUTD,NOUTP,NREQD,NREQS,NACCE,IFUNC,MITER,KSTEP
1
      ,IPRED,INDIP,INVEL
READ (1,*) DTIME,DTEND,DTREC,AALFA,BEETA,DELTA,GAAMA,AZERO,BZERO
1
      ,OMEGA,TOLER,TMAXR
WRITE(2,902)NSTEP,NOUTD,NOUTP,NREQD,NREQS,NACCE,IFUNC,MITER,KSTEP
1
      ,IPRED,INDIP,INVEL
WRITE(2,903)DTIME,DTEND,DTREC,AALFA,BEETA,DELTA,GAAMA,AZERO,BZERO
1
      ,OMEGA,TOLER,TMAXR
C *** SELECTED NODES AND GAUSS POINTS FOR OUTPUT ***
IF(NREQD.NE.0) READ(1,*) (NPRQD(IREQD),IREQD=1,NREQD)
IF(NREQS.NE.0) READ(1,*) (NGRQS(IREQS),IREQS=1,NREQS)
WRITE (2,904)
IF(NREQD.NE.0)WRITE(2,905)(NPRQD(IREQD),IREQD=1,NREQD)
IF(NREQS.NE.0)WRITE(2,906)(NGRQS(IREQS),IREQS=1,NREQS)
C *** INITIAL DISPLACEMENTS ***
IF(INDIP.EQ.0)GOTO 205
WRITE(2,908)
200 READ(1,*) NGASH,XGASH,YGASH,ZGASH
PAUSE
NPOSN = (NGASH-1)*3+1
TDISP(NPOSN) = XGASH
NPOSN = NPOSN + 1
TDISP(NPOSN) = YGASH
NPOSN = NPOSN + 1
TDISP(NPOSN)=ZGASH
WRITE(2,909) NGASH,XGASH,YGASH,ZGASH
IF(NGASH.NE.NPOIN)GOTO 200
C *** INITIAL VELOCITIES ***
205 IF(INVEL.EQ.0)GOTO 215
WRITE(2,910)
210 READ(1,*) NGASH,XGASH,YGASH,ZGASH
NPOSN =(NGASH-1)*3+1
VELOC(NPOSN)=XGASH
NPOSN = NPOSN + 1
VELOC(NPOSN) = YGASH
NPOSN = NPOSN + 1
VELOC(NPOSN)=ZGASH
WRITE(2,909) NGASH,XGASH,YGASH,ZGASH
IF (NGASH.NE.NPOIN)GOTO 210
C *** REAARANGE INITIAL DISPLACEMENTS AND VELOCITY VECTORS ***
215 KOUNT = 0
KOUND = 0
ADISP = 0
AVELO = 0
DO 510 IPOIN=1,NPOIN
DO 510 IDOFN=1,3
KOUNT=KOUNT+1
IF(IFPRE(IDOFN,IPOIN).NE.0)GOTO 510
KOUND=KOUND+1
TDISP(KOUND)=TDISP(KOUNT)
ADISP=ADISP+TDISP(KOUND)**2
VELOC(KOUND)=VELOC(KOUNT)
AVELO=AVELO+VELOC(KOUND)**2
510 CONTINUE
C *** READ ACCELEROGRAM DATA , FROM TAPE 1 ***
IF(IFUNC.NE.0)GOTO 250
AFACT = DTREC/DTIME
READ(1,*) (ACCEV(I),I=1,NACCE)
WRITE(2,913)DTREC
WRITE(2,912)(ACCEV(I),I=1,NACCE)
250 CONTINUE
C *** READ LOAD TIME HISTORY, FROM TAPE 1 ***
IF(IFUNC.NE.4)GOTO 260
READ(1,*) (ACCEH(I),ACCEV(I),I=1,NACCE)
WRITE(2,915)
WRITE(2,916) (ACCEH(I),ACCEV(I),I=1,NACCE)
260 CONTINUE
RETURN
902 FORMAT(/2X,'TIME STEPPING PARAMETERS',/2X,27(*)/
1/2X,'NSTEP=',I7,10X,'NOUTD=',I7,10X,'NOUTP=',I7,10X,'NREQD=',I7,
2/2X,'NREQS=',I7,10X,'NACCE=',I7,10X,'IFUNC=',I7,10X,'MITER=',I7,

```

```

3/2X,'KSTEP=',I7,10X,'IPRED=',I7,10X,'INDIP=',I7,10X,'INVEL=',I7)
903 FORMAT(/2X,'DTIME=',G10.4,5X,'DTEND=',G10.4,5X,'DTREC=',G10.4,
1 5X,'AALFA=',G10.4,2X,'BEETA=',G10.4,5X,'DELTA=',G10.4,
2 5X,'GAAMA=',G10.4,5X,'AZERO=',G10.4,2X,'BZERO=',G10.4,
3 5X,'OMEGA=',G10.4,5X,'TOLER=',G10.4,5X,'TMAXR=',G10.4)
904 FORMAT(/5X,41H SELECTIVE OUTPUT REQUESTED FOR FOLLOWING )
905 FORMAT(/,5X,6H NODES,12I5)
906 FORMAT(5X,' GAUSS POINTS' ,12I5)
908 FORMAT(/5X,5H NODE,2X,16H INITIAL X-DISP.,2X,
.16H INITIAL Y-DISP,2X,16H INITIAL Z-DISP./)
909 FORMAT (I10,3E18.5)
910 FORMAT (/5X,5H NODE,2X,16H INITIAL X-VELO.,2X,
1 16H INITIAL Y-VELO.,2X,16H INITIAL Z-VELO./)
912 FORMAT(7F10.3)
913 FORMAT(/5X,' ACCELERATION ORDINATES AT',F9.4,2X,'SEC'/)
915 FORMAT(5X,' TIME DEFINITION OF LOAD',
. /,11X,' TIME',4X,' LOAD FACTOR')
916 FORMAT(5X,F10.5,5X,F10.5)
END
C *****
C *** LINKS WITH PROFILE SOLVER ***
C *****
SUBROUTINE LINKIN(LNODS,IFPRE,LEQNS,MAXAI,MHIGH,MLARG,MATNO)
COMMON/CTRL/NECHO,NELEM,NGAUS,NMATS,NPOIN,NREIN,NEQNS,NTOTG,NTOTV,
&
NVFIX,NWKTL
DIMENSION LNODS(20,*),IFPRE(3,*),LEQNS(60,*),MHIGH(*),MAXAI(*),
MATNO(1)
C *** NUMBER OF UNKNOWNNS ***
NEQNS = 0
DO 100 IPOIN=1,NPOIN
DO 100 IDOFN=1,3
IF(IFPRE(IDOFN,IPOIN))110,120,110
120 NEQNS = NEQNS + 1
IFPRE(IDOFN,IPOIN)=NEQNS
GOTO 100
110 IFPRE(IDOFN,IPOIN) = 0
100 CONTINUE
C *** CONNECTIVITY ARRAY LEQNS ***
DO 50 IELEM = 1,NELEM
IEVAB = 1
NNODE=20
NEVAB=60
IF(MATNO(IELEM).EQ.3)NNODE=2
IF(MATNO(IELEM).EQ.3)NEVAB=6
DO 80 INODE = 1,NNODE
IDENT = LNODS(INODE,IELEM)
DO 80 IDOFN=1,3
LEQNS(IEVAB,IELEM)=IFPRE(IDOFN,IDENT)
80 IEVAB = IEVAB + 1
MAXAM = 2000000
DO 200 IEVAB = 1,NEVAB
IF (LEQNS(IEVAB,IELEM)) 210,200,210
210 IF (LEQNS(IEVAB,IELEM)-MAXAM) 220,200,200
220 MAXAM = LEQNS(IEVAB,IELEM)
200 CONTINUE
DO 250 IEVAB = 1,NEVAB
IEQNS = LEQNS(IEVAB,IELEM)
IF (IEQNS.EQ.0)GOTO 250
JHIGH = IEQNS - MAXAM
IF (JHIGH.GT.MHIGH(IEQNS)) MHIGH (IEQNS) = JHIGH
250 CONTINUE
50 CONTINUE
C *** ADDRESSES OF DIAGONAL ELEMENTS - MAXA ARRAY ***
MAXAI(1) = 1
MAXAI(2) = 2
DO 310 IEQNS = 2,NEQNS
310 MAXAI(IEQNS+1) = MAXAI(IEQNS) + MHIGH(IEQNS)+1
330 NWKTL = MAXAI(NEQNS+1) - MAXAI(1)
WRITE(2,920) NEQNS,NWKTL
IF(NWKTL.GT.MLARG)WRITE(2,910)
IF(NWKTL.GT.MLARG)STOP
RETURN
910 FORMAT('/ SET DIMENSION EXCEEDED - CHECK LINKIN '/')
920 FORMAT(5X,' NEQNS=',I5,5X,' NWKTL=',I7)
END
C *****
C *** CALCULATES THE LUMPED MASS MATRIX ***
C *****
SUBROUTINE LUMASS(COORD,LNODS,MATNO,PROPS,DVOLU,IFPRE,CARTD,GPCOD,
. WEIGN,DERIV,SHAPE,POSGN,YMASS)
COMMON/CTRL/NECHO,NELEM,NGAUS,NMATS,NPOIN,NREIN,NEQNS,NTOTG,NTOTV,

```

```

& NVFIX,NWKTL
DIMENSION COORD(3,1),ELCOD(3,20),LNODS(20,1),WEIG3(3),CARLC(3,20),
. CARTD(3,20,1),PROPS(20,1),GPCOD(3,1),DERIV(3,20,1),DVOLU(1),
. MATNO(1),DIAGM(20),XJACM(3,3),YMASS(1),DERLC(3,20),POSG3(3),
. POSGN(3,1),WEIGN(1),SHALC(20),GPCLC(3),SHAPE(20,1),IFPRE(3,1)
C *** SET UP SHAPE FUNC.,SHAPE FUNCTION DERIVATIVES AND DIFFERENTIAL ***
C *** VOLUME FOR INTEGRATION POINTS NEEDED FOR STIFF.COMPUTATION ***
CALL GAUSSN(POSGN,WEIGN)
DO 2 IGAUN = 1,27
  EXISP=POSGN(1,IGAUN)
  ETASP=POSGN(2,IGAUN)
  ZETSP=POSGN(3,IGAUN)
2 CALL SHAPE3(DERIV(1,1,IGAUN),ETASP,EXISP,ZETSP,SHAPE(1,IGAUN))
KGASP=0
DO 3 IELEM = 1,NELEM
  DO 5 INODE = 1,20
    LNODE=LNODS(INODE,IELEM)
    DO 5 IDIME=1,3
5 ELCOD(IDIME,INODE)=COORD(IDIME,LNODE)
  DO 3 IGAUN = 1,27
    KGASP=KGASP+1
    CALL JACO3(CARTD(1,1,KGASP),DERIV(1,1,IGAUN),DVOLU(KGASP),
      & ELCOD,IELEM,SHAPE(1,IGAUN),GPCOD(1,KGASP),XJACM)
3 DVOLU(KGASP)=DVOLU(KGASP)*WEIGN(IGAUN)
C *** COMPUTE ELEMENTAL LUMPED MASS MATRIX USING GAUSSIAN INTEGRATION***
NGASS=3
CALL GAUSSQ(NGASS,POSG3,WEIG3)
DO 100 IELEM=1,NELEM
  LPROP = MATNO(IELEM)
  RHOEL=PROPS(9,LPROP)
  DO 10 INODE = 1,20
    DIAGM(INODE)=0.0
    LNODE=LNODS(INODE,IELEM)
    DO 10 IDIME = 1,3
10 ELCOD(IDIME,INODE)=COORD(IDIME,LNODE)
  TMASS = 0.0
  DO 11 IGAUS = 1,NGASS
    EXISP=POSG3(IGAUS)
  DO 11 JGAUS = 1,NGASS
    ETASP=POSG3(JGAUS)
  DO 11 KGAUS = 1,NGASS
    ZETSP=POSG3(KGAUS)
    CALL SHAPE3(DERLC,ETASP,EXISP,ZETSP,SHALC)
    CALL JACO3(CARLC,DERLC,DVOLC,ELCOD,IELEM,SHALC,GPCLC,XJACM)
    DVOLC=DVOLC*WEIG3(IGAUS)*WEIG3(JGAUS)*WEIG3(KGAUS)
    DMASS=DVOLC*RHOEL
    TMASS=TMASS+DMASS
  DO 11 INODE = 1,20
    SHAPI=SHALC(INODE)
11 DIAGM(INODE)=DIAGM(INODE)+SHAPI*SHAPI*DMASS
C *** GENERATE LUMPED MASS MATRIX PROPORTIONAL TO DIAGONAL ***
SUMAS=0.0
DO 40 INODE = 1,20
40 SUMAS=SUMAS+DIAGM(INODE)
SUMAS=TMASS/SUMAS
DO 100 INODE = 1,20
  LNODE=LNODS(INODE,IELEM)
  IPOSN=(LNODE-1)*3
  DO 100 IDOFN=1,3
    IPOSN=IPOSN+1
100 YMASS(IPOSN)=YMASS(IPOSN)+DIAGM(INODE)*SUMAS
C *** GLOBAL MASS VECTOR ***
NPOSM=0
DO 200 IPOIN=1,NPOIN
  DO 200 IDOFN = 1,3
    NPOSM=NPOSM+1
    NPOSN=IFPRE(IDOFN,IPOIN)
200 IF(NPOSN.NE.0) YMASS(NPOSN)=YMASS(NPOSM)
RETURN
END
C *****
C *** GAUSS-LEGENDRE NUMERICAL INTEGRATION CONSTANTS ***
C *****
SUBROUTINE GAUSSQ(NGAUS,POSGP,WEIGP)
DIMENSION POSGP(1),WEIGP(1)
POSGP(1) = 0.0D0
WEIGP(1) = 2.0D0
IF(NGAUS.EQ.1)RETURN
IF(NGAUS.GT.2)GOTO 4
2 POSGP(1) = -1.0D0/ DSQRT(3.0D0)
WEIGP(1) = 1.0D0

```

```

    POSGP(2) = -POSGP(1)
    WEIGP(2) = 1.0D0
    RETURN
4  POSGP(1) = -DSQRT(3.0D0/5.0D0)
    POSGP(2) = 0.0D0
    POSGP(3) = -POSGP(1)
    WEIGP(1) = 5.0D0/9.0D0
    WEIGP(2) = 8.0D0/9.0D0
    WEIGP(3) = 5.0D0/9.0D0
    RETURN
    END
C *****
C ***      GAUSS-LEGENDRE NUMER.INTEGT.CONSTANTS FOR ELEMENTS      ***
C *****
    SUBROUTINE GAUSSN(POSGN,WEIGP)
    DIMENSION POSGN(3,27),WEIGP(27)
    A=0.774596669
        DO 210 I=1,3
            DO 210 J=1,27
210  POSGN(I,J)=0.0
    POSGN(1,1)=A
    POSGN(1,3)=-A
    POSGN(1,4)=-A
    POSGN(1,5)=-A
    POSGN(1,7)=A
    POSGN(1,8)=A
    POSGN(1,10)=A
    POSGN(1,12)=-A
    POSGN(1,13)=-A
    POSGN(1,14)=-A
    POSGN(1,16)=A
    POSGN(1,17)=A
    POSGN(1,19)=A
    POSGN(1,21)=-A
    POSGN(1,22)=-A
    POSGN(1,23)=-A
    POSGN(1,25)=A
    POSGN(1,26)=A
    POSGN(2,1)=-A
    POSGN(2,2)=-A
    POSGN(2,3)=-A
    POSGN(2,5)=A
    POSGN(2,6)=A
    POSGN(2,7)=A
    POSGN(2,10)=-A
    POSGN(2,11)=-A
    POSGN(2,12)=-A
    POSGN(2,14)=A
    POSGN(2,15)=A
    POSGN(2,16)=A
    POSGN(2,19)=-A
    POSGN(2,20)=-A
    POSGN(2,21)=-A
    POSGN(2,23)=A
    POSGN(2,24)=A
    POSGN(2,25)=A
    DO 162 L=1,9
162  POSGN(3,L)=-A
    DO 164 L1=19,27
164  POSGN(3,L1)=A
    H1=125.0/729.0
    H2=200.0/729.0
    H3=320.0/729.0
    H4=512.0/729.0
    WEIGP(1)=H1
    WEIGP(2)=H2
    WEIGP(3)=H1
    WEIGP(4)=H2
    WEIGP(5)=H1
    WEIGP(6)=H2
    WEIGP(7)=H1
    WEIGP(8)=H2
    WEIGP(9)=H3
    WEIGP(10)=H2
    WEIGP(11)=H3
    WEIGP(12)=H2
    WEIGP(13)=H3
    WEIGP(14)=H2
    WEIGP(15)=H3
    WEIGP(16)=H2
    WEIGP(17)=H3

```

```

WEIGP(18)=H4
WEIGP(19)=H1
WEIGP(20)=H2
WEIGP(21)=H1
WEIGP(22)=H2
WEIGP(23)=H1
WEIGP(24)=H2
WEIGP(25)=H1
WEIGP(26)=H2
WEIGP(27)=H3
RETURN
END
C *****
C *** THIS SUBROUTINE EVALUATES SHAPE FUNCTIONS AND THEIR ***
C *** DERIVATIVES FOR LINEAR AND QUADRATIC SERENDIPITY 3D ELEMENTS ***
C *** BY LEFT HAND SCROW ***
C *****
SUBROUTINE SHAPE3(DERIV,Y,X,Z,SHAPE)
DIMENSION DERIV(3,*,SHAPE*)
SHAPE(1)=0.125*(1.0-X)*(1.0-Y)*(1.0-Z)*(-X-Y-Z-2.0)
DERIV(1,1)=-0.125*(1.0-Y)*(1.0-Z)*(-2.0*X-Y-Z-1.0)
DERIV(2,1)=-0.125*(1.0-X)*(1.0-Z)*(-X-2.0*Y-Z-1.0)
DERIV(3,1)=-0.125*(1.0-X)*(1.0-Y)*(-X-Y-2.0*Z-1.0)
SHAPE(2)=0.25*(1.0-X)*(1.0-Z)*(1.0-Y)*(1.0+Y)
DERIV(1,2)=-0.25*(1.0-Z)*(1.0-Y)*(1.0+Y)
DERIV(2,2)=-0.5*(1.0-X)*(1.0-Z)*Y
DERIV(3,2)=-0.25*(1.0-X)*(1.0-Y)*(1.0+Y)
SHAPE(3)=0.125*(1.0-X)*(1.0+Y)*(1.0-Z)*(-X+Y-Z-2.0)
DERIV(1,3)=-0.125*(1.0+Y)*(1.0-Z)*(-2.0*X+Y-Z-1.0)
DERIV(2,3)=0.125*(1.0-X)*(1.0-Z)*(-X+2.0*Y-Z-1.0)
DERIV(3,3)=-0.125*(1.0-X)*(1.0+Y)*(-X+Y-2.0*Z-1.0)
SHAPE(4)=0.25*(1.0+Y)*(1.0-Z)*(1.0-X)*(1.0+X)
DERIV(1,4)=-0.5*(1.0+Y)*(1.0-Z)*X
DERIV(2,4)=0.25*(1.0-Z)*(1.0-X)*(1.0+X)
DERIV(3,4)=-0.25*(1.0+Y)*(1.0-X)*(1.0+X)
SHAPE(5)=0.125*(1.0+X)*(1.0+Y)*(1.0-Z)*(X+Y-Z-2.0)
DERIV(1,5)=0.125*(1.0+Y)*(1.0-Z)*(2.0*X+Y-Z-1.0)
DERIV(2,5)=0.125*(1.0+X)*(1.0-Z)*(X+2.0*Y-Z-1.0)
DERIV(3,5)=-0.125*(1.0+X)*(1.0+Y)*(X+Y-2.0*Z-1.0)
SHAPE(6)=0.25*(1.0+X)*(1.0-Z)*(1.0-Y)*(1.0+Y)
DERIV(1,6)=0.25*(1.0-Z)*(1.0-Y)*(1.0+Y)
DERIV(2,6)=-0.5*(1.0+X)*(1.0-Z)*Y
DERIV(3,6)=-0.25*(1.0+X)*(1.0-Y)*(1.0+Y)
SHAPE(7)=0.125*(1.0+X)*(1.0-Y)*(1.0-Z)*(X-Y-Z-2.0)
DERIV(1,7)=0.125*(1.0-Y)*(1.0-Z)*(2.0*X-Y-Z-1.0)
DERIV(2,7)=-0.125*(1.0+X)*(1.0-Z)*(X-2.0*Y-Z-1.0)
DERIV(3,7)=-0.125*(1.0+X)*(1.0-Y)*(X-Y-2.0*Z-1.0)
SHAPE(8)=0.25*(1.0-Y)*(1.0-Z)*(1.0-X)*(1.0+X)
DERIV(1,8)=-0.5*(1.0-Y)*(1.0-Z)*X
DERIV(2,8)=-0.25*(1.0-Z)*(1.0-X)*(1.0+X)
DERIV(3,8)=-0.25*(1.0-Y)*(1.0-X)*(1.0+X)
SHAPE(9)=0.25*(1.0-X)*(1.0-Y)*(1.0-Z)*(1.0+Z)
DERIV(1,9)=-0.25*(1.0-Y)*(1.0-Z)*(1.0+Z)
DERIV(2,9)=-0.25*(1.0-X)*(1.0-Z)*(1.0+Z)
DERIV(3,9)=-0.5*(1.0-X)*(1.0-Y)*Z
SHAPE(10)=0.25*(1.0-X)*(1.0+Y)*(1.0-Z)*(1.0+Z)
DERIV(1,10)=-0.25*(1.0+Y)*(1.0-Z)*(1.0+Z)
DERIV(2,10)=0.25*(1.0-X)*(1.0-Z)*(1.0+Z)
DERIV(3,10)=-0.5*(1.0-X)*(1.0+Y)*Z
SHAPE(11)=0.25*(1.0+X)*(1.0+Y)*(1.0-Z)*(1.0+Z)
DERIV(1,11)=0.25*(1.0+Y)*(1.0-Z)*(1.0+Z)
DERIV(2,11)=0.25*(1.0+X)*(1.0-Z)*(1.0+Z)
DERIV(3,11)=-0.5*(1.0+X)*(1.0+Y)*Z
SHAPE(12)=0.25*(1.0+X)*(1.0-Y)*(1.0-Z)*(1.0+Z)
DERIV(1,12)=0.25*(1.0-Y)*(1.0-Z)*(1.0+Z)
DERIV(2,12)=-0.25*(1.0+X)*(1.0-Z)*(1.0+Z)
DERIV(3,12)=-0.5*(1.0+X)*(1.0-Y)*Z
SHAPE(13)=0.125*(1.0-X)*(1.0-Y)*(1.0+Z)*(-X-Y+Z-2.0)
DERIV(1,13)=-0.125*(1.0-Y)*(1.0+Z)*(-2.0*X-Y+Z-1.0)
DERIV(2,13)=-0.125*(1.0-X)*(1.0+Z)*(-X-2.0*Y+Z-1.0)
DERIV(3,13)=0.125*(1.0-X)*(1.0-Y)*(-X-Y+2.0*Z-1.0)
SHAPE(14)=0.25*(1.0-X)*(1.0+Z)*(1.0-Y)*(1.0+Y)
DERIV(1,14)=-0.25*(1.0+Z)*(1.0-Y)*(1.0+Y)
DERIV(2,14)=-0.5*(1.0+Z)*(1.0-X)*Y
DERIV(3,14)=0.25*(1.0-X)*(1.0-Y)*(1.0+Y)
SHAPE(15)=0.125*(1.0-X)*(1.0+Y)*(1.0+Z)*(-X+Y+Z-2.0)
DERIV(1,15)=-0.125*(1.0+Y)*(1.0+Z)*(-2.0*X+Y+Z-1.0)
DERIV(2,15)=0.125*(1.0-X)*(1.0+Z)*(-X+2.0*Y+Z-1.0)
DERIV(3,15)=0.125*(1.0-X)*(1.0+Y)*(-X+Y+2.0*Z-1.0)
SHAPE(16)=0.25*(1.0+Y)*(1.0+Z)*(1.0-X)*(1.0+X)
DERIV(1,16)=-0.5*(1.0+Y)*(1.0+Z)*X

```

```

DERIV(2,16)=0.25*(1.0+Z)*(1.0-X)*(1.0+X)
DERIV(3,16)=0.25*(1.0+Y)*(1.0-X)*(1.0+X)
SHAPE(17)=0.125*(1.0+X)*(1.0+Y)*(1.0+Z)*(X+Y+Z-2.0)
DERIV(1,17)=0.125*(1.0+Y)*(1.0+Z)*(2.0*X+Y+Z-1.0)
DERIV(2,17)=0.125*(1.0+X)*(1.0+Z)*(X+2.0*Y+Z-1.0)
DERIV(3,17)=0.125*(1.0+X)*(1.0+Y)*(X+Y+2.0*Z-1.0)
SHAPE(18)=0.25*(1.0+X)*(1.0+Z)*(1.0-Y)*(1.0+Y)
DERIV(1,18)=0.25*(1.0+Z)*(1.0-Y)*(1.0+Y)
DERIV(2,18)=-0.5*(1.0+X)*(1.0+Z)*Y
DERIV(3,18)=0.25*(1.0+X)*(1.0-Y)*(1.0+Y)
SHAPE(19)=0.125*(1.0+X)*(1.0-Y)*(1.0+Z)*(X-Y+Z-2.0)
DERIV(1,19)=0.125*(1.0-Y)*(1.0+Z)*(2.0*X-Y+Z-1.0)
DERIV(2,19)=-0.125*(1.0+X)*(1.0+Z)*(X-2.0*Y+Z-1.0)
DERIV(3,19)=0.125*(1.0+X)*(1.0-Y)*(X-Y+2.0*Z-1.0)
SHAPE(20)=0.25*(1.0-Y)*(1.0+Z)*(1.0-X)*(1.0+X)
DERIV(1,20)=-0.5*(1.0-Y)*(1.0+Z)*X
DERIV(2,20)=-0.25*(1.0+Z)*(1.0-X)*(1.0+X)
DERIV(3,20)=0.25*(1.0-Y)*(1.0-X)*(1.0+X)
RETURN
END
C *****
C *** THIS SUB.EVALUATES THE JACO.MAT.& THE CARTESIAN SHAPE FUN.DERIV. *
C *****
SUBROUTINE JACOB3(CARTD,DERIV,DJACB,ELCOD,KELEM,SHAPE,GPCOD,XJACM)
DIMENSION CARTD(3,20),DERIV(3,1),ELCOD(3,20),GPCOD(3),SHAPE(20)
,XJACI(3,3),XJACM(3,3)
C*** CALCULATE COORDINATES OF SAMPLING POINT ***
DO 10 II=1,3
GPCOD(II)=0.0
DO 10 INODE=1,20
10 GPCOD(II)=GPCOD(II)+ELCOD(II,INODE)*SHAPE(INODE)
C*** CREATE JACOBIAN MATRIX XJACM ***
DO 30 II=1,3
DO 30 JJ=1,3
XJACM(II,JJ)=0.0
DO 30 INODE=1,20
30 XJACM(II,JJ)=XJACM(II,JJ)+DERIV(II,INODE)*ELCOD(JJ,INODE)
C*** CALCULATE DETERMINANT AND INVERSE OF JACOBIAN MATRIX ***
CALL DETINV3(XJACM,XJACI,DJACB)
IF(DJACB.LE.0.0)WRITE(2,600) KELEM
IF(DJACB.LE.0.0)STOP
C*** CALCULATE CARTESIAN DERIVATIVES ***
DO 60 II=1,3
DO 60 INODE=1,20
CARTD(II,INODE)=0.0
DO 60 JJ=1,3
60 CARTD(II,INODE)=CARTD(II,INODE)+XJACI(II,JJ)*DERIV(JJ,INODE)
600 FORMAT(/,36H PROGRAM HALTED IN SUBROUTINE JACOB3/,11X,
,22H ZERO OR NEGATIVE AREA./,10X,16H ELEMENT NUMBER ,I5)
RETURN
END
C *****
C *** A SUBROUTINE TO FIND THE DET. & INVERSE OF 3*3 MATRIX ***
C *****
SUBROUTINE DETINV3(X,XI,DET)
DIMENSION X(3,3),XI(3,3)
DET=X(1,1)*X(2,2)*X(3,3)-X(2,3)*X(3,2)- X(1,2)*X(2,1)*
.X(3,3)-X(2,3)*X(3,1)) + X(1,3)*X(2,1)*X(3,2)-X(2,2)*X(3,1))
DO 100 I=1,3
IP1 = I + 1 - I/3*3
IP2 = IP1 + 1 - IP1/3*3
DO 100 J=1,3
JP1 = J + 1 - J/3*3
JP2 = JP1 + 1 - JP1/3*3
100 XI(J,I)=(X(IP1,JP1)*X(IP2,JP2)-X(IP2,JP1)*X(IP1,JP2))/DET
RETURN
END
C *****
C *** THIS SUBROU.EVALUATES THE CONSISTENT NODAL FORCES FOR EACH ELE. ***
C *****
SUBROUTINE LOADPL(COORD,LNODS,MATNO,PROPS,RLOAD,SHAPE,IFPRE,MTOTG,
1 FORCE,DVOLUME)
CHARACTER*40 TITLE
COMMON/CTRL/NECHO,NELEM,NGAUS,NMATS,NPOIN,NREIN,NSIZE,NTOTG,NTOTV,
& NVFIX,NWKTL
DIMENSION CARTD(3,20),PVECT(3),COORD(3,1),PROPS(20,1),DVOLUME(MTOTG)
1,VAREA(3),GPCOD(3),DERIV(3,20),NOPRS(8),FORCE(1),WEIGP(3),POSGP(3)
2,ELCOD(3,20),GVECT(3),RLOAD(60,1),SHAPL(20),IFPRE(3,1),LNODS(20,1)
3 ,SHAPE(20,1),XJACM(3,3),PRESS(8,3),MATNO(1)
C*** INITIALIZE THE TOTAL LOAD ARRAY ***
CALL GAUSSQ(2,POSGP,WEIGP)

```

```

DO 9 ITOTV = 1,NTOTV
9  FORCE(ITOTV)=0.
DO 10 IELEM = 1,NELEM
DO 10 IEVAB = 1,60
10  RLOAD(IEVAB,IELEM) = 0.0D0
      READ(1,*)TITLE
      IF(NECHO.LT.1)WRITE(2,902) TITLE
902  FORMAT(/1X,' TITLE ',A40)
C ***  READ DATA CONTROLLING LOADING TYPES TO BE INPUT  ***
      READ(1,*)IPLD,IGRAV,IFACE
      IF(NECHO.LT.2) WRITE(2,904)IPLD,IGRAV,IFACE
904  FORMAT(/1X,' APPLIED LOADING TO STRUCTURE./1X,31(*)//1X,
. ' POINT LOAD PARAMETERS.....=',I5//1X,
. ' GRAVITY LOAD PARAMETER.....=',I5//1X,
. ' FACE LOADS PARAMETER.....=',I5//1X)
C ***  DATA CONTROLLING LOADING TYPES TO BE INPUT  ***
      IF(IPLD.EQ.0)GOTO 500
      IF(NECHO.LT.1)WRITE(2,905)
905  FORMAT(/10X,' POINT LOADING./10X,14('-)/10X,' NODE.',
. 15X,' PX',16X,' PY',18X,' PZ')
20  READ(1,*)LODPT,(PVECT(IDIME),IDIME=1,3)
      IF(NECHO.LT.1)WRITE(2,907) LODPT,(PVECT(IDIME),IDIME=1,3)
907  FORMAT(10X,I5,3(5X,F15.3))
C ***  ASSOCIATE THE NODAL POINT LOADS WITH AN ELEMENT  ***
DO 30 IELEM = 1,NELEM
DO 30 INODE = 1,20
LNODE = LNODS(INODE,IELEM)
IF(LODPT.EQ.LNODE)GOTO 40
30  CONTINUE
40  IEVAB = (INODE-1)*3
DO 50 IDIME = 1,3
IEVAB = IEVAB + 1
50  RLOAD(IEVAB,IELEM) = PVECT(IDIME)
      IF(LODPT.LT.NPOIN)GOTO 20
500  CONTINUE
C ***  GRAVITY LOADING SECTION AND ASSOCIATED VECTORS  ***
      IF(IGRAV.EQ.0)GOTO 600
C ***  READ GRAVITY DATA  ***
      READ(1,*)(GVECT(IDIME),IDIME=1,3),GCONS
      GSIZE =SQRT(GVECT(1)*GVECT(1)+GVECT(2)*GVECT(2)+GVECT(3)*GVECT(3))
      DO 55 IDIME = 1,3
55  GVECT(IDIME)=GVECT(IDIME)/GSIZE
      IF(NECHO.LT.1) WRITE(2,909)(GVECT(IDIME),IDIME=1,3),GCONS
909  FORMAT(/' GRAVITY UNIT VECTOR = ('3F10.5,') G.CONSTANT =',F10.5)
C ***  LOOP OVER EACH ELEMENT  ***
      KGAST = 0
      DO 90 IELEM = 1,NELEM
C ***  SET PRELIMINARY CONSTANTS  ***
      LPROP = MATNO(IELEM)
      DENSE = PROPS(9,LPROP)
      IF(DENSE.EQ.0.0D0)GOTO 90
      DO 75 IDIME = 1,3
75  PVECT(IDIME) = DENSE*GVECT(IDIME)*GCONS
C ***  STORE THE COORDINATES OF THE ELEMENT NODAL POINTS  ***
DO 60 INODE = 1,20
LNODE = LNODS(INODE,IELEM)
DO 60 IDIME = 1,3
60  ELCOD(IDIME,INODE) = COORD(IDIME,LNODE)
C ***  ENTER LOOPS FOR VOLUME NUMERICAL INTEGRATION  ***
DO 70 IGAUS = 1,27
KGAST = KGAST + 1
C ***  CALCULATE LOADS AND ASSOCIATE WITH ELEMENT NODAL POINTS  ***
IEVAB = 0
DO 70 INODE = 1,20
SHVOL = SHAPE(INODE,IGAUS)*DVOLU(KGAST)
DO 70 IDIME = 1,3
IEVAB = IEVAB + 1
70  RLOAD(IEVAB,IELEM)=RLOAD(IEVAB,IELEM)+PVECT(IDIME)*SHVOL
90  CONTINUE
600  CONTINUE
      IF(IFACE.EQ.0)GOTO 700
C ***  DISTRIBUTED FACE LOADS SECTION  ***
      READ(1,*)NFCES
      IF(NECHO.LT.1)WRITE(2,911) NFCES
911  FORMAT(1H,5X,21HNO. OF LOADED FACES =,I5)
      IF(NECHO.LT.1)WRITE(2,912)
912  FORMAT(1H,5X,38HLIST OF LOADED FACES AND APPLIED LOADS)
C ***  LOOP OVER EACH LOADED FACE  ***
      NODFC = 8
      DO 140 KFACE = 1,NFCES
C ***  READ DATA DEFINING THE LOADED FACE AND APPLIED LOAD  ***

```

```

READ(1,*) NEASS,(NOPRS(JODFC),JODFC=1,NODFC)
IF(NECHO.LT.1)WRITE(2,914)NEASS,(NOPRS(JODFC),JODFC=1,NODFC)
914 FORMAT(110,5X,815)
READ(1,*)((PRESS(JODFC,IDIME),IDIME=1,3),JODFC=1,NODFC)
IF(NECHO.LT.1)WRITE(2,915)((PRESS(JO,ID),ID=1,3),JO=1,NODFC)
915 FORMAT (6F10.3)
C *** STORE THE COORDINATES OF THE NODES OF THE ELEMENT FACE ***
DO 100 JODFC = 1,NODFC
LNODE = NOPRS(JODFC)
DO 100 IDIME = 1,3
100 ELCOD(IDIME,JODFC) = COORD(IDIME,LNODE)
C *** ENTER LOOP FOR AREA NUMERICAL INTEGRATION ***
KGASP = 0
ZETSP = -1.0
DO 140 IGAUS = 1,NGAUS
EXISP = POSGP(IGAUS)
DO 140 JGAUS = 1,NGAUS
ETASP = POSGP(JGAUS)
KGASP = KGASP + 1
C *** COMPUTE THE SHAPE FUNCTIONS AT THE SAMPLING POINT, THE "AREA" ***
C *** VECTOR AND SOME VECTOR NORMS ***
CALL SHAPE3(DERIV,ETASP,EXISP,ZETSP,SHAPL)
CALL JACOB3(CARTD,DERIV,DJACB,ELCOD,0,SHAPL,GPCOD,XJACM)
DAREA = 0.0
SNORM = 0.0
TNORM = 0.0
DO 105 IDOFA=1,3
IDOFB=IDOFA+1-IDOFA/3*3
IDOFC=IDOFB+1-IDOFB/3*3
VAREA(IDOFA)=XJACM(1,IDOFB)*XJACM(2,IDOFC)-
XJACM(2,IDOFB)*XJACM(1,IDOFC)
DAREA = DAREA + VAREA(IDOFA)*VAREA(IDOFA)
SNORM = SNORM+ XJACM(1,IDOFA)*XJACM(1,IDOFA)
105 TNORM = TNORM+ XJACM(2,IDOFA)*XJACM(2,IDOFA)
DAREA = SQRT(DAREA)
SNORM = SQRT(SNORM)
TNORM = SQRT(TNORM)
C *** COMPUTE THE LOCAL LOAD COMPONENTS AT THE CURRENT GAUSS POINT ***
DO 110 IDIME = 1,3
GVECT(IDIME) = 0.0D0
DO 110 JODFC = 1,NODFC
110 GVECT(IDIME) = GVECT(IDIME)+PRESS(JODFC,IDIME)*SHAPL(JODFC)
C *** COMPUTE THE CARTESIAN LOAD COMPONENTS AT THE CURRENT GAUSS POINT
DO 120 ID = 1,3
120 PVECT(ID)=GVECT(1)*XJACM(1,ID)/SNORM+GVECT(2)*XJACM(2,ID)/TNORM+
GVECT(3)*VAREA(ID)/DAREA
C *** COMPUTE THE ELEMENTAL AREA ***
DAREA = DAREA*WEIGP(IGAUS)*WEIGP(JGAUS)
C *** ASSOCIATE THE EQUIVALENT NODAL FACE LOADS WITH AN ELEMENT ***
DO 140 JODFC = 1,NODFC
LNODE = NOPRS(JODFC)
DO 130 INODE = 1,20
IF(LNODS(INODE,NEASS).EQ.LNODE)GOTO 135
130 CONTINUE
135 IEVAB = (INODE-1)*3
SAREA = SHAPL(JODFC)*DAREA
DO 140 IDIME = 1,3
IEVAB = IEVAB + 1
140 RLOAD(IEVAB,NEASS) = RLOAD(IEVAB,NEASS)+PVECT(IDIME)*SAREA
700 CONTINUE
IF(NECHO.GE.1)GOTO 999
C *** WRITE THE TOTAL NODAL FORCES FOR EACH ELEMENT ***
WRITE(2,916)
916 FORMAT(/6X,36H TOTAL NODAL FORCES FOR EACH ELEMENT,/6X,35('-'))
DO 290 IELEM = 1,NELEM
290 WRITE(2,917) IELEM,(RLOAD(IEVAB,IELEM),IEVAB=1,60)
917 FORMAT(15,/(4X,10F8.3))
999 CONTINUE
C *** ASSEMBLE INTO GLOBAL LOAD VECTOR ***
DO 5 IELEM = 1,NELEM
KEVAB = 0
DO 5 INODE = 1,20
LNODE = LNODS(INODE,IELEM)
NPOSN = (LNODE-1)*3
DO 5 IDOFN = 1,3
KEVAB = KEVAB + 1
NPOSN = NPOSN + 1
5 FORCE(NPOSN) = FORCE(NPOSN)+RLOAD(KEVAB,IELEM)
C *** GLOBAL FORCE VECTOR ***
NPOSM = 0
DO 7 IPOIN = 1,NPOIN

```

```

DO 7 IDOFN = 1,3
  NPOSM = NPOSM + 1
  NPOSN = IFPRE(IDOFN,IPOIN)
7   IF(NPOSN.NE.0) FORCE(NPOSN)=FORCE(NPOSM)
  RETURN
END
C *****
C ***   THIS SUB.EVAL.THE STIFFNESS MATRIX FOR EACH ELEMENT IN TURN   ***
C *****
SUBROUTINE GSTIFF(COORD,LNODS,MATNO,DMATX,PROPS,CARTD,MPATT,MLAYR,
INOCAP,MBARS,VBARS,ISTAT,DVOLS,TMATX,CRVAL,LEQNS,MAXAI,DVOLU,STIFF,
2     CARDS,GPCOS)
COMMON/CTRL/NECHO,NELEM,NGAUS,NMATS,NPOIN,NREIN,NSIZE,NTOTG,NTOTV,
&     NVFIX,NWKTL
COMMON/RUN/IFUNC,IPRED,KSTEP,MITER,NACCE,NOUTD,NOUTP,NREQD,NREQS,
&     NSTEP
COMMON/STAT/IITER,ISTEP,KTOLE
DIMENSION CARTD(3,20,*),ELCOD(3,20),LEQNS(60,*),DVOLS(*),DVOLU(*),
.TMATX(3,3,*),ESTIF(3,3,210),LNODS(20,*),PROPS(20,*),CARDS(3,20,*),
.MATNO(*),MPATT(*),NOCAP(*),ISTAT(*),MAXAI(*),STIFF(*),GPCOS(3,*),
.MBARS(2,MLAYR,*),VBARS(3,MLAYR,*),COORD(3,*),DMATX(6,*),CRVAL(4,*)
C ***   CHECK IF IT IS NECESSARY TO EVALUATE THE STIFFNESS MATRIX   ***
IF(ISTEP.EQ.1)GOTO 200
KOUNT=(ISTEP/KSTEP)*KSTEP
IF (KOUNT.NE.ISTEP) RETURN
IF(KTOLE.EQ.0) RETURN
200 CONTINUE
IF(IITER.GT.1) RETURN
KGAST=0
KREF=0
DO 81 I =1,NWKTL
81  STIFF(I)=0.0
C ***   LOOP OVER EACH ELEMENT   ***
DO 70 IELEM = 1,NELEM
C ***   EVALUATE THE COORDINATES OF THE ELEMENT NODAL POINTS   ***
  KMH=210
  IF(IELEM.GT.NELEM)KMH=3
  DO 20 INODE = 1,KMH
  DO 20 IDOFN = 1,3
  DO 20 JDOFN = 1,3
20  ESTIF(IDOFN,JDOFN,INODE)=0.0D0

  DO 10 INODE = 1,20
  LNODE = LNODS(INODE,IELEM)
  DO 10 IDIME = 1,3
10  ELCOD(IDIME,INODE) = COORD(IDIME,LNODE)
C ***   INITIALIZE THE ELEMENT STIFFNESS MATRIX.   ***
  DO 100 IGAUN = 1,27
  KGAST= KGAST + 1
C ***   EVALUATE THE D MATRIX   ***
  CALL MOD3(DMATX,IELEM,PROPS,MATNO,ISTAT,KGAST,CRVAL)
C ***   FORM THE ELEMENT STIFFNESS MATRIX   ***
  INDIC = 1
  IF(ISTAT(KGAST).GE.10) INDIC=2
  KNODE = 0
  DO 100 JNODE = 1,20
  DO 100 INODE = 1,JNODE
  KNODE = KNODE + 1
  CALL FORMK(INODE,JNODE,ESTIF(1,1,KNODE),CARTD(1,1,KGAST),DMATX,
.DVOLU(KGAST),INDIC)
100 CONTINUE
C ***   ADD REINFORCEMENT CONTRIBUTION TO ELEMENT STIFFNESS   ***
  CALL REINF3(IELEM,DMATX,ELCOD,PROPS,CARDS,GPCOS,ESTIF,MPATT,MLAYR,
.NOCAP,MBARS,VBARS,KREF,DVOLS,TMATX)
C ***   GENERATES GLOBAL STIFFNESS MATRIX IN COMPACTED COLUMN FORM   ***
  CALL ADDBAN(STIFF,MAXAI,ESTIF,LEQNS(1,IELEM),20)
70 CONTINUE
  RETURN
  END
C *****
C ***   THIS SUBROUTINE EVALUATES THE DMATX-MATRIX   ***
C *****
SUBROUTINE MOD3(DMATX,IELEM,PROPS,MATNO,ISTAT,KGAST,CRVAL)
DIMENSION DMATX(6,1),MATNO(1),PROPS(20,1),ISTAT(1),DLOCA(6,6)
.BETAM(3,3),T(6,6),CRVAL(4,1)
DO 10 ISTR=1,6
DO 10 JSTR=1,6
10 DMATX(ISTR,JSTR)=0.0D0
C ***   D MATRIX FOR ELASTIC CASE   ***
LPROP=MATNO(IELEM)
YOUNG=PROPS(1,LPROP)

```

```

POISS=PROPS(2,LPROP)
ALFA1=YOUNG*(1.-POISS)/((1.+POISS)*(1.-2*POISS))
ALFA2=ALFA1*POISS/(1.-POISS)
ALFA3=ALFA1*(1.-2.*POISS)/(2.*(1.-POISS))
DMATX(1,1)=ALFA1
DMATX(2,2)=ALFA1
DMATX(3,3)=ALFA1
DMATX(1,2)=ALFA2
DMATX(1,3)=ALFA2
DMATX(2,3)=ALFA2
DMATX(4,4)=ALFA3
DMATX(5,5)=ALFA3
DMATX(6,6)=ALFA3
C ***      CHECK IF THE CONCRETE IS ELASTIC      ***
  IT = ISTAT(KGAST)
  IF(IT.EQ.0.OR.IT.EQ.2)GOTO 60
C ***      IF THE CONCRETE IS CRACKED, CALCULATE THE D MATRIX      ***
  DO 21 ISTRE = 1,6
  DO 21 JSTRE = ISTRE,6
21  DMATX(ISTRE,JSTRE)=0.0
  IF (IT.EQ.13)GOTO 60
C ***      BUILD UP THE SYSTEM CHANGE MATRICES      ***
  CALL DTMAT(BETAM,T)
  ALPHA=0.5
  DO 34 I =1,6
  DO 34 J =1,6
34  DLOCA(I,J) = 0.0
     STIFF = YOUNG
     IF(CRVAL(1,KGAST).NE.0.0)
     .   STIFF=CRVAL(2,KGAST)/CRVAL(1,KGAST)
     .   IF(STIFF.GT.0.0.AND.STIFF.LT.YOUNG) THEN
     .     DLOCA(1,1)=STIFF
     .   ELSE
     .     DLOCA(1,1)=YOUNG
     .   ENDIF
     STIFF=YOUNG
     IF(CRVAL(3,KGAST).NE.0.0)
     .   STIFF=CRVAL(4,KGAST)/CRVAL(3,KGAST)
     .   IF(STIFF.GT.0.0.AND.STIFF.LT.YOUNG) THEN
     .     DLOCA(2,2)=STIFF
     .   ELSE
     .     DLOCA(2,2)=YOUNG
     .   ENDIF
     DLOCA(3,3)=YOUNG
     DLOCA(4,4)=ALPHA*YOUNG/2.
     DLOCA(5,5)=ALPHA*YOUNG/2.
     DLOCA(6,6)=ALPHA*YOUNG/2.
     IF(IT.NE.10.AND.IT.NE.110)GOTO 35
     DLOCA(2,2) = YOUNG
     DLOCA(5,5) = YOUNG/2.
35  CONTINUE
     DO 12 I =1,6
     DO 12 J =1,6
     DO 12 K =1,6
12  DMATX(I,J)=DMATX(I,J)+T(K,I)*DLOCA(K,K)*T(K,J)
60  DO 100 ISTRE = 1,6
     DO 100 JSTRE = ISTRE,6
100 DMATX(JSTRE,ISTRE) = DMATX(ISTRE,JSTRE)
     RETURN
     END
C *****
C ***      ROUTINE TO PERFORM THE PRODUCT BT * D * B * dV      ***
C *****
SUBROUTINE FORMK(I,J,A,S,D,V,IF)
DIMENSION E(3,3),S(3,1),D(6,6),A(3,3)
IF(IF.EQ.0) THEN
E(1,1)=S(1,I)*(D(1,1)*S(1,J)+D(1,4)*S(2,J)+D(1,6)*S(3,J))+
.   S(2,I)*(D(4,1)*S(1,J)+D(4,4)*S(2,J)+D(4,6)*S(3,J))+
.   S(3,I)*(D(6,1)*S(1,J)+D(6,4)*S(2,J)+D(6,6)*S(3,J))
E(2,1)=S(2,I)*(D(2,1)*S(1,J)+D(2,4)*S(2,J)+D(2,6)*S(3,J))+
.   S(1,I)*(D(4,1)*S(1,J)+D(4,4)*S(2,J)+D(4,6)*S(3,J))+
.   S(3,I)*(D(5,1)*S(1,J)+D(5,4)*S(2,J)+D(5,6)*S(3,J))
E(3,1)=S(3,I)*(D(3,1)*S(1,J)+D(3,4)*S(2,J)+D(3,6)*S(3,J))+
.   S(2,I)*(D(5,1)*S(1,J)+D(5,4)*S(2,J)+D(5,6)*S(3,J))+
.   S(1,I)*(D(6,1)*S(1,J)+D(6,4)*S(2,J)+D(6,6)*S(3,J))
E(1,2)=S(1,I)*(D(1,2)*S(2,J)+D(1,4)*S(1,J)+D(1,5)*S(3,J))+
.   S(2,I)*(D(4,2)*S(2,J)+D(4,4)*S(1,J)+D(4,5)*S(3,J))+
.   S(3,I)*(D(6,2)*S(2,J)+D(6,4)*S(1,J)+D(6,5)*S(3,J))
E(2,2)=S(2,I)*(D(2,2)*S(2,J)+D(2,4)*S(1,J)+D(2,5)*S(3,J))+
.   S(1,I)*(D(4,2)*S(2,J)+D(4,4)*S(1,J)+D(4,5)*S(3,J))+
.   S(3,I)*(D(5,2)*S(2,J)+D(5,4)*S(1,J)+D(5,5)*S(3,J))

```

```

E(3,2)=S(3,I)*(D(3,2)*S(2,J)+D(3,4)*S(1,J)+D(3,5)*S(3,J))+
. S(2,I)*(D(5,2)*S(2,J)+D(5,4)*S(1,J)+D(5,5)*S(3,J))+
. S(1,I)*(D(6,2)*S(2,J)+D(6,4)*S(1,J)+D(6,5)*S(3,J))
E(1,3)=S(1,I)*(D(1,3)*S(3,J)+D(1,5)*S(2,J)+D(1,6)*S(1,J))+
. S(2,I)*(D(4,3)*S(3,J)+D(4,5)*S(2,J)+D(4,6)*S(1,J))+
. S(3,I)*(D(6,3)*S(3,J)+D(6,5)*S(2,J)+D(6,6)*S(1,J))
E(2,3)=S(2,I)*(D(2,3)*S(3,J)+D(2,5)*S(2,J)+D(2,6)*S(1,J))+
. S(1,I)*(D(4,3)*S(3,J)+D(4,5)*S(2,J)+D(4,6)*S(1,J))+
. S(3,I)*(D(5,3)*S(3,J)+D(5,5)*S(2,J)+D(5,6)*S(1,J))
E(3,3)=S(3,I)*(D(3,3)*S(3,J)+D(3,5)*S(2,J)+D(3,6)*S(1,J))+
. S(2,I)*(D(5,3)*S(3,J)+D(5,5)*S(2,J)+D(5,6)*S(1,J))+
. S(1,I)*(D(6,3)*S(3,J)+D(6,5)*S(2,J)+D(6,6)*S(1,J))
ENDIF
IF(IF.EQ.1) THEN
E(1,1)=S(1,I)*D(1,1)*S(1,J)+S(2,I)*D(4,4)*S(2,J)+
. S(3,I)*D(6,6)*S(3,J)
E(2,1)=S(2,I)*D(2,1)*S(1,J)+S(1,I)*D(4,4)*S(2,J)
E(3,1)=S(3,I)*D(3,1)*S(1,J)+S(1,I)*D(6,6)*S(3,J)
E(1,2)=S(1,I)*D(1,2)*S(2,J)+S(2,I)*D(4,4)*S(1,J)
E(2,2)=S(2,I)*D(2,2)*S(2,J)+S(1,I)*D(4,4)*S(1,J)+
. S(3,I)*D(5,5)*S(3,J)
E(3,2)=S(3,I)*D(3,2)*S(2,J)+S(2,I)*D(5,5)*S(3,J)
E(1,3)=S(1,I)*D(1,3)*S(3,J)+S(3,I)*D(6,6)*S(1,J)
E(2,3)=S(2,I)*D(2,3)*S(3,J)+S(3,I)*D(5,5)*S(2,J)
E(3,3)=S(3,I)*D(3,3)*S(3,J)+S(2,I)*D(5,5)*S(2,J)+
. S(1,I)*D(6,6)*S(1,J)
ENDIF
IF(IF.EQ.2) THEN
E(1,1)=S(1,I)*D(1,1)*S(1,J)+S(2,I)*D(4,4)*S(2,J)+
. S(3,I)*D(6,6)*S(3,J)
E(2,1)=S(1,I)*D(4,4)*S(2,J)
E(3,1)=S(1,I)*D(6,6)*S(3,J)
E(1,2)=S(2,I)*D(4,4)*S(1,J)
E(2,2)=S(2,I)*D(2,2)*S(2,J)+S(1,I)*D(4,4)*S(1,J)+
. S(3,I)*D(5,5)*S(3,J)
E(3,2)=S(2,I)*D(5,5)*S(3,J)
E(1,3)=S(3,I)*D(6,6)*S(1,J)
E(2,3)=S(3,I)*D(5,5)*S(2,J)
E(3,3)=S(3,I)*D(3,3)*S(3,J)+S(2,I)*D(5,5)*S(2,J)+
. S(1,I)*D(6,6)*S(1,J)
ENDIF
DO 20 M = 1,3
DO 20 K =1,3
20 A(M,K)=A(M,K)+E(M,K)*V
RETURN
END
C *****
C *** SUB.EVALU.THE CONTRIBUTION OF THE REINF.TO THE ELE.STIF.MATRIX ***
C *****
SUBROUTINE REINF3(IELEM,DMATX,ELCOD,PROPS,CARDS,GPCOS,ESTIF,MPATT,
. MLAYR,NOCAP,MBARS,VBARS,KGREF,DVOLS,TMATX)
COMMON/CTRL/NECHO,NELEM,NGAUS,NMATS,NPOIN,NREIN,NSIZE,NTOTG,NTOTV,
. NVMAT,NWKTL
DIMENSION CARDS(3,20,1),ELCOD(3,20),DERIV(3,20),VECT1(3),DVOLS(1)
.,SHAPE(20),XIACM(3,3),POSGP(3),PROPS(20,1),ESTIF(3,3,1),DMATX(6,1)
.,WEIGP(3),MPATT(1),NOCAP(1),MBARS(2,MLAYR,1),TMATX(3,3,1),VECT2(3)
. ,VBARS(3,MLAYR,1),VNORM(3),GPCOS(3,1)
CALL GAUSSQ(2,POSGP,WEIGP)
KPATT=MPATT(IELEM)
IF(KPATT.EQ.0) RETURN
NLAYR=NOCAP(KPATT)
IF(NLAYR.EQ.0) RETURN
NGASS=NGAUS
C *** LOOP OVER THE REINFORCEMENT LAYERS ***
DO 10 ILAYR=1,NLAYR
IMATN=MBARS(1,ILAYR,KPATT)
ICOOR=MBARS(2,ILAYR,KPATT)
SPOS3=VBARS(1,ILAYR,KPATT)
ESPES=VBARS(2,ILAYR,KPATT)
ANGLE=VBARS(3,ILAYR,KPATT)
C *** ENTER LOOPS FOR AREA NUMERICAL INTEGRATION ***
DO 50 IGAUS=1,NGASS
SPOS1=POSGP(IGAUS)
DO 50 JGAUS=1,NGASS
SPOS2=POSGP(JGAUS)
IF(ICOOR.NE.1)GOTO 20
EXISP = SPOS3
ETASP = SPOS1
ZETSP = SPOS2
GOTO 25
20 IF(ICOOR.NE.2)GOTO 21

```

```

ETASP=SPOS3
ZETSP=SPOS1
EXISP=SPOS2
GOTO 25
21 ZETSP=SPOS3
EXISP=SPOS1
ETASP=SPOS2
25 CONTINUE
KGRF=KGRF+1
C *** EVALUATE THE SHAPE FUNCTIONS, ELEMENTAL VOLUME, ETC. ***
CALL SHAPE3(DERIV,ETASP,EXISP,ZETSP,SHAPE)
CALL JACOB3(CARDS(1,1,KGRF),DERIV,DJACB,ELCOD,
& IELEM,SHAPE,GPCOS(1,KGRF),XJACM)
C *** FIND THE LOCAL SYSTEM ***
ICOOA = ICOOR+1-ICOOR/3*3
ICOOB = ICOOA+1-ICOOA/3*3
DO 60 IDIME=1,3
VECT1(IDIME)=XJACM(ICOOA,IDIME)
60 VECT2(IDIME)=XJACM(ICOOB,IDIME)
VNORM(1)=VECT1(2)*VECT2(3)-VECT1(3)*VECT2(2)
VNORM(2)=VECT1(3)*VECT2(1)-VECT1(1)*VECT2(3)
VNORM(3)=VECT1(1)*VECT2(2)-VECT1(2)*VECT2(1)
DVEC1=0.
DJAC2=0.
DO 70 IDIME=1,3
DVEC1=DVEC1+VECT1(IDIME)*VECT1(IDIME)
70 DJAC2=DJAC2+VNORM(IDIME)*VNORM(IDIME)
DVEC1=SQRT(DVEC1)
DJAC2=SQRT(DJAC2)
VECT2(1)=VNORM(2)*VECT1(3)-VNORM(3)*VECT1(2)
VECT2(2)=VNORM(3)*VECT1(1)-VNORM(1)*VECT1(3)
VECT2(3)=VNORM(1)*VECT1(2)-VNORM(2)*VECT1(1)
DVEC2=SQRT(VECT2(1)**2+VECT2(2)**2+VECT2(3)**2)
DO 80 IDIME = 1,3
TMATX(1,IDIME,KGRF)=VECT1(IDIME)/DVEC1
TMATX(2,IDIME,KGRF)=VECT2(IDIME)/DVEC2
80 TMATX(3,IDIME,KGRF)=VNORM(IDIME)/DJAC2
C *** EVALUATE THE D-MATRIX ***
CALL DREIN(DMATX,PROPS,ANGLE,IMATN,TMATX(1,1,KGRF))
C *** CALCULATE THE DIFFERENTIAL VOLUME ***
DVOLS(KGRF)=DJAC2*ESPES*WEIGP(IGAUS)*WEIGP(JGAUS)
C *** FORM THE ELEMENT STIFFNESS MATRIX ***
INDIC=0
KNODE=0
DO 100 JNODE=1,20
DO 100 INODE=1,JNODE
KNODE=KNODE+1
CALL FORMK(INODE,JNODE,ESTIF(1,1,KNODE),CARDS(1,1,KGRF),DMATX,
DVOLS(KGRF),INDIC)
100 CONTINUE
50 CONTINUE
10 CONTINUE
RETURN
END
C *****
C *** ASSEMBLY OF TOTAL STIFFNESS VECTOR ***
C *****
SUBROUTINE ADDBAN(STIFF,MAXAI,ESTIF,LEQNS,NNODE)
DIMENSION ESTIF(3,3,1),LEQNS(3,1),STIFF(1),MAXAI(1)
DO 30 JNODE=1,NNODE
DO 30 JDOFN=1,3
JEQNS=LEQNS(JDOFN,JNODE)
IF(JEQNS.NE.0) THEN
DO 10 INODE=1,JNODE
MDOFN=3
IF(INODE.EQ.JNODE) MDOFN=JDOFN
KNODE=(JNODE*(JNODE-1))/2+INODE
DO 10 IDOFN=1,MDOFN
IEQNS=LEQNS(IDOFN,INODE)
IF(IEQNS.NE.0) THEN
MEQNS=MIN(IEQNS,JEQNS)
NEQNS=MAX(IEQNS,JEQNS)
NDIAG=MAXAI(NEQNS)
NPOS=NDIAG+NEQNS-MEQNS
STIFF(NPOS)=STIFF(NPOS)+ESTIF(IDOFN,JDOFN,KNODE)
ENDIF
10 CONTINUE
ENDIF
30 CONTINUE
RETURN
END

```

```

C *****
C ***          SUBROUTINE DTMAT          ***
C *****
SUBROUTINE DTMAT(B,T)
DIMENSION B(3,3),T(6,6)
DO 1 I =1,3
DO 1 J =1,3
1  T(I,J)=B(I,J)**2
T(1,4)=B(1,1)*B(1,2)
T(1,5)=B(1,2)*B(1,3)
T(1,6)=B(1,3)*B(1,1)
T(2,4)=B(2,1)*B(2,2)
T(2,5)=B(2,2)*B(2,3)
T(2,6)=B(2,3)*B(2,1)
T(3,4)=B(3,1)*B(3,2)
T(3,5)=B(3,2)*B(3,3)
T(3,6)=B(3,3)*B(3,1)
T(4,1)=B(1,1)*B(2,1)*2.
T(4,2)=B(1,2)*B(2,2)*2.
T(4,3)=B(1,3)*B(2,3)*2.
T(5,1)=B(2,1)*B(3,1)*2.
T(5,2)=B(2,2)*B(3,2)*2.
T(5,3)=B(2,3)*B(3,3)*2.
T(6,1)=B(3,1)*B(1,1)*2.
T(6,2)=B(3,2)*B(1,2)*2.
T(6,3)=B(3,3)*B(1,3)*2.
T(4,4)=B(1,1)*B(2,2)+B(1,2)*B(2,1)
T(4,5)=B(1,2)*B(2,3)+B(1,3)*B(2,2)
T(4,6)=B(1,3)*B(2,1)+B(1,1)*B(2,3)
T(5,4)=B(2,1)*B(3,2)+B(2,2)*B(3,1)
T(5,5)=B(2,2)*B(3,3)+B(2,3)*B(3,2)
T(5,6)=B(2,3)*B(3,1)+B(2,1)*B(3,3)
T(6,4)=B(3,1)*B(1,2)+B(3,2)*B(1,1)
T(6,5)=B(3,2)*B(1,3)+B(3,3)*B(1,2)
T(6,6)=B(3,3)*B(1,1)+B(3,1)*B(1,3)
RETURN
END
C *****
C ***          ROUTINE TO CALCULATE THE D-MATRIX FOR REINFORCEMENT          ***
C *****
SUBROUTINE DREIN(DMATX,PROPS,ANGLE,IMATN,TMATX)
DIMENSION DMATX(6,1),PROPS(20,1),TMATX(3,3),T(6,6),DLOCA(6,6)
DO 20 ISTRE=1,6
DO 20 JSTRE=1,6
DLOCA(ISTRE,JSTRE)=0.0
20  DMATX(ISTRE,JSTRE)=0.0
YOUNG=PROPS(1,IMATN)
COEFI=YOUNG
C=COS(ANGLE)
S=SIN(ANGLE)
C ***          COMPUTE THE ELASTIC D-MATRIX          ***
DLOCA(1,1)=COEFI*C*C*C*C
DLOCA(1,2)=COEFI*S*S*C*C
DLOCA(2,1)=COEFI*S*S*C*C
DLOCA(2,2)=COEFI*S*S*S*S
DLOCA(1,4)=COEFI*S*C*C*C
DLOCA(4,1)=COEFI*S*C*C*C
DLOCA(2,4)=COEFI*S*S*S*C
DLOCA(4,2)=COEFI*S*S*S*C
DLOCA(4,4)=COEFI*S*S*C*C
C ***          BUILD UP THE SYSTEM CHANGE MATRICES          ***
CALL DTMAT(TMATX,T)
DO 12 I = 1,6
DO 12 J = 1,6
DO 12 K = 1,6
DO 12 L = 1,6
12  DMATX(I,J)=DMATX(I,J)+T(K,I)*DLOCA(K,L)*T(L,J)
RETURN
END
C *****
C ***          GENERATES PARTIAL EFFECTIVE LOAD VECTOR          ***
C ***          AND THE EFFECTIVE STIFFNESS MATRIX K*          ***
C *****
SUBROUTINE NEWIMP(ACCEH,ACCEI,ACCEK,ACCEL,ACCEV,DISPI,DISPL,
.DISPT,IFPRE,MAXAI,RLOAD,STIFF,VELOI,VELOL,STIFS,VELOT,YMASS)
COMMON/CTRL/ NECHO,NELEM,NGAUS,NMATS,NPOIN,NREIN,NSIZE,NTOTG,NTOTV
&
,NVFIX,NWKTL
COMMON/RUN/ IFUNC,IPRED,KSTEP,MITER,NACCE,NOUTD,NOUTP,NREQD,NREQS
&
,NSTEP
COMMON/CONST/AALFA,BEETA,GAAMA,DELTA,AZERO,BZERO,OMEGA,TMAXR,DTEND
&
,DTIME,AFAC,TOLER,ADISP,AVELO,CONSD,CONSF

```

```

COMMON/STAT/ IITER,ISTEP,KTOLE
DIMENSION STIFF(1),DISPI(1),ACCEH(1),DISPL(1),IFPRE(3,1),YMASS(1),
. VELOI(1),ACCEV(1),VELOL(1),ACCEK(1),RLOAD(1),ACCEI(1),MAXAI(1),
. ACCEL(1),STIFS(1),DISPT(1),VELOT(1)
C *** COMPUTES THE SCALAR PARAMETERS ***
CONSA=DTIME*DTIME*(0.5-DELTA)
CONSB=DTIME*(1.0-GAAMA)
CONSC=DTIME*DTIME*DELTA
CONSD=DTIME*GAAMA
CONSF=1./CONSC
CONSG=BEETA*GAAMA*DTIME*CONSF+1.
CONSH=AALFA*GAAMA*DTIME*CONSF
CONSE=CONSF+CONSH
IF(ISTEP.EQ.1.AND.IITER.EQ.1) THEN
C *** COMPUTES THE IDENTITY VECTOR FOR SEISMIC EXCITATION ***
C *** AND MULTIPLIES IT BY THE MASS MATRIX ***
ISHOT = 0
IF(IFUNC.EQ.0) THEN
DO 10 IPOIN=1,NPOIN
DO 10 IDOFN=1,3
ISIZE=IFPRE(IDOFN,IPOIN)
IF(ISIZE.NE.0) THEN
ACCEL(ISIZE)=0.
IF(IDOFN.EQ.1) ACCEL(ISIZE)=YMASS(ISIZE)
ENDIF
10 CONTINUE
ENDIF
C *** COMPUTES THE INITIAL ELASTIC RESISTING FORCES ***
IF(ADISP.GT.0.1E-10) THEN
CALL MULTPY (DISPL,STIFF,DISPI,MAXAI,NSIZE,NWKTL)
ELSE
DO 30 ISIZE = 1,NSIZE
30 DISPL(ISIZE)=0.
ENDIF
C *** COMPU.THE INITIAL DAMPING FORCES(RAYLEIGH DAMPING IS ASSUMED) ***
IF(AVELO.GT.0.1E-10) THEN
C *** MULTIPLIES BY THE FIRST PART OF THE DAMPING MATRIX ***
IF(ABS(AALFA).GT.0.1E-10) THEN
DO 40 ISIZE=1,NSIZE
40 VELOL(ISIZE)=YMASS(ISIZE)*VELOI(ISIZE)
ELSE
DO 50 ISIZE = 1,NSIZE
50 VELOL(ISIZE)=0.0
ENDIF
C *** MULTIPLIES BY THE SECOND PART OF THE DAMPING MATRIX ***
IF(ABS(BEETA).GT.0.1E-10) THEN
CALL MULTPY (ACCEL,STIFF,VELOI,MAXAI,NSIZE,NWKTL)
ELSE
DO 60 ISIZE=1,NSIZE
60 ACCEL(ISIZE)=0.0
ENDIF
C *** ADDS THE TWO CONTRIBUTIONS ***
IF(ABS(AALFA)+ABS(BEETA).GT.0.1E-10) THEN
DO 70 ISIZE = 1,NSIZE
70 VELOL(ISIZE)=AALFA*VELOL(ISIZE)+BEETA*ACCEL(ISIZE)
ENDIF
ELSE
DO 80 ISIZE=1,NSIZE
80 VELOL(ISIZE)=0.0
ENDIF
C *** COMPUTES THE INITIAL INERTIAL FORCE VECTOR ***
FACTS=FUNCTS(AZERO,BZERO,DTEND,DTIME,IFUNC,0,OMEGA,TMAXR,ACCEH,
. ACCEV,NACCE)
XMODU=0.0
DO 90 ISIZE=1,NSIZE
ACCEI(ISIZE)=FACTS*RLOAD(ISIZE)-DISPL(ISIZE)-VELOL(ISIZE)
90 XMODU=XMODU+ACCEI(ISIZE)**2
C *** CALCULATES THE INITIAL ACCELERATION VECTOR ***
IF(XMODU.GE.1.E-11) THEN
DO 100 ISIZE=1,NSIZE
100 ACCEI(ISIZE)=ACCEI(ISIZE)/YMASS(ISIZE)
ENDIF
WRITE(2,900)
WRITE(2,910) (ACCEI(ISIZE),ISIZE=1,NSIZE)
ENDIF
C *** CALCULATES PREDICTED DISPLACEMENT AND VELOCITY VECTOR ***
IF(IITER.EQ.1) THEN
DO 110 ISIZE=1,NSIZE
IF(IPRED.NE.1) THEN
DISPT(ISIZE)=DISPI(ISIZE)
VELOT(ISIZE)=VELOI(ISIZE)

```

```

ENDIF
DISPI(ISIZE)=DISPI(ISIZE)+DTIME*VELOI(ISIZE)+CONSA*ACCEI(ISIZE)
VELOI(ISIZE)=VELOI(ISIZE)+CONSB*ACCEI(ISIZE)
IF(IPRED.NE.2) THEN
  DISPT(ISIZE)=DISPI(ISIZE)
  VELOT(ISIZE)=VELOI(ISIZE)
ENDIF
110 ACCEI(ISIZE)=CONSF*(DISPT(ISIZE)-DISPI(ISIZE))
C *** CALCULATE LOAD FACTORS ***
FACTS=FUNCTS (AZERO,BZERO,DTEND,DTIME,IFUNC,ISTEP,OMEGA,
. TMAXR,ACCEH,ACCEV,NACCE)
. FACTH=FUNCTA (ACCEV,AFAC,DTEND,DTIME,IFUNC,ISTEP)
ENDIF
C *** CALCULATES DAMPING FORCES (RAYLEIGH DAMPING IS ASSUMED) ***
IF(ISTEP.NE.1) THEN
C *** MULTIPLIES BY THE FIRST PART OF THE DAMPING MATRIX ***
IF (ABS(AALFA).GT.0.1E-10) THEN
  DO 120 ISIZE=1,NSIZE
120 VELOL(ISIZE)=YMASS(ISIZE)*VELOT(ISIZE)
  ELSE
  DO 130 ISIZE =1,NSIZE
130 VELOL(ISIZE)=0.0
  ENDIF
C *** MULTIPLIES BY THE SECOND PART OF THE DAMPING MATRIX ***
IF(ABS(BEETA).GT.0.1E-10) THEN
  CALL MULTPY (ACCEL,STIFF,VELOT,MAXAI,NSIZE,NWKTL)
  ELSE
  DO 140 ISIZE=1,NSIZE
140 ACCEL(ISIZE)=0.0
  ENDIF
C *** ADDS THE TWO CONTRIBUTIONS ***
IF(ABS(AALFA)+ABS(BEETA).GT.0.1E-10) THEN
  DO 150 ISIZE = 1,NSIZE
150 VELOL(ISIZE)=AALFA*VELOL(ISIZE)+BEETA*ACCEL(ISIZE)
  ENDIF
ENDIF
C *** COMPUTES THE K-STAR MATRIX ***
KOUNT=(ISTEP/KSTEP)*KSTEP
IF(KTOLE.EQ.0) KOUNT=0
IF(ISTEP.EQ.1) KOUNT=ISTEP
IF(KOUNT.EQ.ISTEP) THEN
  DO 160 ISIZE = 1,NSIZE
  NDIAG=MAXAI(ISIZE)
  NLAST=MAXAI(ISIZE+1)-1
  DO 170 IK=NDIAG,NLAST
  STIFS(IK)=CONSG*STIFF(IK)
170 CONTINUE
  STIFS(NDIAG)=STIFS(NDIAG)+CONSE*YMASS(ISIZE)
160 CONTINUE
  CALL DECOMP(STIFS,MAXAI,NSIZE)
ENDIF
C *** CALCULATES PARTIAL EFFECTIVE LOAD VECTOR ***
TOTAL = 0.0
DO 190 ISIZE=1,NSIZE
  IF(IFUNC.EQ.0) THEN
    TOTAL=TOTAL+RLOAD(ISIZE)*RLOAD(ISIZE)
    DISPL(ISIZE)=-VELOL(ISIZE)-FACTH*ACCEK(ISIZE)+RLOAD(ISIZE)
  ELSE
    TOTAL=TOTAL+RLOAD(ISIZE)*RLOAD(ISIZE)*FACTS*FACTS
    DISPL(ISIZE)=-VELOL(ISIZE)+RLOAD(ISIZE)*FACTS
  ENDIF
190 CONTINUE
RETURN
900 FORMAT(/ ' INITIAL ACCELERATION '/')
910 FORMAT(1X,9E12.5)
END
C *****
C *** HEAVISIDE AND HARMONIC TIME FUNCTION ***
C *****
FUNCTION FUNCTS (AZERO,BZERO,DTEND,DTIME,IFUNC,ISTEP,OMEGA,TMAXR
. ,ACCEH,ACCEV,NACCE)
.
DIMENSION ACCEH(1),ACCEV(1)
IF (IFUNC.EQ.0) RETURN
FUNCTS = 0.0
IF (FLOAT(ISTEP)*DTIME.GT.DTEND) RETURN
IF (IFUNC.EQ.4)GOTO 10
IF (IFUNC.EQ.5)GOTO 30
IF (IFUNC.EQ.1) FUNCTS = 1.0D0
IF (IFUNC.EQ.2) ARGUM=OMEGA*ISTEP*DTIME
IF (IFUNC.EQ.2) FUNCTS=AZERO+BZERO*SIN(ARGUM)
IF (IFUNC.EQ.3) FUNCTS=DTIME*FLOAT(ISTEP)/TMAXR

```

```

IF (IFUNC.EQ.3.AND.FUNCTS.GT.1.0) FUNCTS=1.0D0
RETURN
10 PTIME = FLOAT(ISTEP)*DTIME
DO 15 IACCE = 1,NACCE
TIME2=ACCEH(IACCE)
IF(TIME2.GT.PTIME)GOTO 20
15 CONTINUE
RETURN
20 TIME1=ACCEH(IACCE-1)
FACT1=ACCEV(IACCE-1)
FACT2=ACCEV(IACCE)
FUNCTS=FACT1+(PTIME-TIME1)*(FACT2-FACT1)/(TIME2-TIME1)
RETURN
30 PTIME=FLOAT(ISTEP)*DTIME
ARGUM = OMEGA*(PTIME-TMAXR)
IF(PTIME.LE.TMAXR) FUNCTS=AZERO*PTIME/TMAXR
IF(PTIME.GT.TMAXR) FUNCTS=AZERO+BZERO*SIN(ARGUM)
RETURN
END
FUNCTION FUNCTA (ACCER,AFACT,DTEND,DTIME,IFUNC,ISTEP)
C *****
C *** ACCELERATION INTERPOLATION ***
C *****
DIMENSION ACCER(1)
IF (IFUNC.NE.0) RETURN
FUNCTA = 0.0
IF (ISTEP.EQ.0.OR.FLOAT(ISTEP)*DTIME.GT.DTEND) RETURN
XGASH = (FLOAT(ISTEP)-1.0D0)/AFACT+1.0D0
MGASH = XGASH
NGASH = MGASH + 1
XGASH = XGASH - FLOAT(MGASH)
FUNCTA = ACCER(MGASH)*(1.0D0-XGASH)+XGASH*ACCER(NGASH)
RETURN
END
C *****
C *** FACTORISES [L]*[D]*[L] TRANSPOSE OF STIFFNESS MATRIX ***
C *****
SUBROUTINE DECOMP(STIFF,MAXAI,NEQNS)
DIMENSION STIFF(1),MAXAI(1)
DO 200 IEQNS = 1,NEQNS
IMAXA = MAXAI(IEQNS)
LOWER = IMAXA + 1
KUPER = MAXAI(IEQNS+1)-1
KHIGH = KUPER - LOWER
IF (KHIGH) 304,240,210
210 KSIZE = IEQNS - KHIGH
ICOUN = 0
JUPER = KUPER
DO 260 JHIGH = 1,KHIGH
ICOUN = ICOUN + 1
JUPER = JUPER - 1
KMAXA = MAXAI(KSIZE)
NDIAG = MAXAI(KSIZE+1)-KMAXA-1
IF (NDIAG)260,260,270
270 NCOLM = MIN0(ICOUN,NDIAG)
COUNT = 0.0D0
DO 280 ICOLM = 1,NCOLM
280 COUNT = COUNT + STIFF(KMAXA+ICOLM)*STIFF(JUPER+ICOLM)
STIFF(JUPER) = STIFF(JUPER)-COUNT
260 KSIZE = KSIZE + 1
240 KSIZE = IEQNS
BSUMM = 0.0D0
DO 300 ICOLM = LOWER,KUPER
KSIZE = KSIZE - 1
JMAXA = MAXAI(KSIZE)
RATIO = STIFF(ICOLM)/STIFF(JMAXA)
BSUMM=BSUMM+ RATIO*STIFF(ICOLM)
300 STIFF(ICOLM) = RATIO
STIFF(IMAXA) = STIFF(IMAXA)-BSUMM
304 IF(STIFF(IMAXA).GT.0.0)GOTO 200
WRITE(2,2000) IEQNS,STIFF(IMAXA)
STOP
200 CONTINUE
2000 FORMAT(/48H STOP - STIFFNESS MATRIX NOT POSITIVE DEFINITE ,//
132H NONPOSITIVE PIVOT FOR EQUATION ,I4,//10H PIVOT = ,E20.12)
RETURN
END
C *****
C *** SUBROUTINE MULTPY ***
C *****
SUBROUTINE MULTPY (DISPL,STIFF,DISPI,MAXAI,NSIZE,NWKTL)

```

```

DIMENSION STIFF(1),MAXAI(1),DISPI(1),DISPL(1)
IF(NWKTL.GT.NSIZE)GOTO 20
DO 10 I = 1,NSIZE
10 DISPL(I) = STIFF(1)*DISPI(I)
RETURN
20 CONTINUE
DO 1 J = 1,NSIZE
NDIAG=MAXAI(J)-1
NLAST=MAXAI(J+1)-1
NALTO=NLAST-NDIAG
SUMA=0.
NBACK=J
DO 2 L =1,NALTO
SUMA=SUMA+DISPI(NBACK)*STIFF(NDIAG+L)
2 NBACK=NBACK-1
DISPL(J)=SUMA
NDIAG=NDIAG+1
NALTO=NALTO-1
IF(NALTO)1,1,4
4 DO 3 K=1,NALTO
3 DISPL(J-K)=DISPL(J-K)+DISPI(J)*STIFF(NDIAG+K)
1 CONTINUE
RETURN
END
C *****
C *** ROUTINE TO EVALUATE STRESSES AND EQUIVALENT RESISTING FORCES ***
C *****
SUBROUTINE RESEVP(CRVAL,ELAST,MATNO,DVOLUME,DVOLS,CARDS,PROPS,ELDIS,
1TMATX,TMATC,CARTD,STRES,MLAYR,VBARS,STREF,ISTAT,ALPHI,EFFST,DISPL,
2 LEQNS,MPATT,NOCAP,MBARS,RESID,STRVP,STRAF,WORKP,WORKF,MREIN)
COMMON/CTRL/NECHO,NELEM,NGAUS,NMATS,NPOIN,NREIN,NSIZE,NTOTG,NTOTV,
& NVFIX,NWKTL
COMMON/RUN/IFUNC,IPRED,KSTEP,MITER,NACCE,NOUTD,NOUTP,NREQD,NREQS,
& NSTEP
COMMON/CONST/AALFA,BEETA,GAAMA,DELTA,AZERO,BZERO,OMEGA,TMAXR,DTEND
& DTIME,AFACT,TOLER,ADISP,AVELO,CONSD,CONSF
COMMON/STAT/IITER,ISTEP,KTOLE
DIMENSION TMATX(3,3,1),ELDIS(3,1),MATNO(1),RESID(1),TMATC(3,3,1),
. STRAT(6),STRES(6,1),CARTD(3,20,1),STRAF(2,6,1),DVOLUME(1),STRAN(6),
. EFFST(2,1),DISPL(1),PROPS(20,1),WORKP(2,1),WORKF(2,1),ELAST(3,1),
. VBARS(3,MLAYR,1),STREF(6,1),ELOAD(3,20),ALPHI(4,1),CARDS(3,20,1),
. LEQNS(60,1),CRVAL(4,1),STRVP(2,6,1),ISTAT(1),DVOLS(1),
. MPATT(1),NOCAP(MREIN),MBARS(2,MLAYR,1)
DO 10 ITOTV=1,NTOTV
10 RESID(ITOTV)=0.0
C *** LOOP OVER THE ELEMENTS ***
KGAST=0
KGRF=0
DO 20 IELEM=1,NELEM
C *** INITIALIZE ELEMENT RESISTING FORCES ***
DO 25 IDOFN=1,3
DO 25 INODE=1,20
25 ELOAD(IDOFN,INODE)=0.0
C *** SCALAR GATHER OPERATION ***
NPOSN=0
NNODE=20
IF(IELEM.GT.NELEM)NNODE=2
DO 30 INODE=1,NNODE
DO 30 IDOFN=1,3
NPOSN=NPOSN+1
IEQNS=LEQNS(NPOSN,IELEM)
30 ELDIS(IDOFN,INODE)=DISPL(IEQNS)
C *** ENTER LOOPS FOR AREA NUMERICAL INTEGRATION ***
DO 50 IGAUN=1,27
KGAST=KGAST+1
DLENG=DVOLUME(KGAST)**(1./3.)
C *** EVALUATE THE STRAINS ***
DO 40 ISTRE=1,6
40 STRAT(ISTRE)=0.0
CALL STRAIN(ELDIS,CARTD(1,1,KGAST),STRAT)
DO 41 ISTRE=1,6
41 STRAN(ISTRE)=STRAT(ISTRE)-STRVP(1,ISTRE,KGAST)
C *** EVALUATE STRESSES ***
CALL STREC(IELEM,KGAST,MATNO,PROPS,ELAST,ISTAT,ALPHI,STRAT,DLENG,
. STRAN,STRES,EFFST,WORKP,WORKF,CRVAL,DTIME,STRVP,KTOLE,
. TMATC(1,1,KGAST))
C *** CALCULATE THE EQUIVALENT NODAL FORCES AND ASSOCIATE WITH THE ***
C *** ELEMENT NODES ***
DO 42 INODE = 1,20
42 CALL FORMP(CARTD(1,INODE,KGAST),STRES(1,KGAST),
& ELOAD(1,INODE),DVOLUME(KGAST))

```

```

50 CONTINUE
C *** EVALUATE NODAL FORCES DUE TO REINFORCEMENT ***
CALL RESREF(IELEM,ELOAD,KGREF,DVOLS,CARDS,TMATX,PROPS,ELDIS,STREF,
.
MPATT,MLAYR,NOCAP,MBARS,VBARS,STRAF)
C *** SCALAR SCATTER OPERATION ***
55 IEVAB=0
DO 60 INODE=1,NNODE
DO 60 IDOFN=1,3
IEVAB=IEVAB+1
LMVEB=LEQNS(IEVAB,IELEM)
IF(LMVEB.EQ.0)GOTO 60
RESID(LMVEB)=RESID(LMVEB)+ELOAD(IDOFN,INODE)
60 CONTINUE
20 CONTINUE
RETURN
END
C *****
C *** ROUTINE TO EVALUATE STRAINS ***
C *****
SUBROUTINE STRAIN(E,C,S)
DIMENSION E(3,1),C(3,1),S(1)
DO 10 I=1,20
S(1)=S(1)+C(1,I)*E(1,I)
S(2)=S(2)+C(2,I)*E(2,I)
S(3)=S(3)+C(3,I)*E(3,I)
S(4)=S(4)+C(2,I)*E(1,I)+C(1,I)*E(2,I)
S(5)=S(5)+C(3,I)*E(2,I)+C(2,I)*E(3,I)
10 S(6)=S(6)+C(3,I)*E(1,I)+C(1,I)*E(3,I)
RETURN
END
C *****
C *** ROUTINE TO PERFORM THE PRODUCT B * SIGMA * dV ***
C *****
SUBROUTINE FORMP(S,D,P,V)
DIMENSION S(1),D(1),P(1)
P(1)=P(1)+(S(1)*D(1)+S(2)*D(4)+S(3)*D(6))*V
P(2)=P(2)+(S(2)*D(2)+S(1)*D(4)+S(3)*D(5))*V
P(3)=P(3)+(S(3)*D(3)+S(2)*D(5)+S(1)*D(6))*V
RETURN
END
C *****
C *** ROUTINE TO EVALUATE THE STRESSES IN CONCRETE ***
C *****
SUBROUTINE STREC(IELEM,KGAST,MATNO,PROPS,ELAST,ISTAT,ALPHI,STRAT,
DLENG,STRAN,STRES,EFFST,WORKP,WORKF,CRVAL,DTIME,STRVP,KTOLE,TMATC)
DIMENSION MATNO(1),ELAST(3,1),PROPS(20,1),STRVP(2,6,1),WORKP(2,1),
.
ISTAT(1),D(3),TMATC(3,3),ALPHI(4,1),STRAT(6),STRAN(6),WORKF(2,1),
.
CRVAL(4,1),EFFST(2,1),STRES(6,1),STLIN(6)
LPROP=MATNO(IELEM)
YOUNG=PROPS(1,LPROP)
FCULT=PROPS(3,LPROP)
FTULT=PROPS(4,LPROP)
GFVAL=PROPS(6,LPROP)
FACK1=PROPS(7,LPROP)
NYIEL=PROPS(8,LPROP)
C *** CALCULATE THE ELASTIC STRESS ***
CRACK=FTULT/YOUNG
CONSS=(GFVAL-0.5*FTULT*CRACK*DLENG)/(FTULT*DLENG)
IF(CONSS.LT.0.0) CONSS=.1E-06
CALL ELSTR(STLIN,STRAN,ELAST(1,LPROP))
C *** CHECK IF THE POINT WAS CRACKED PREVIOUSLY ***
IT = ISTAT(KGAST)
IF(IT.NE.10.AND.IT.NE.11.AND.IT.NE.12.AND.IT.NE.13)GOTO 15
CALL FISUR2(KGAST,LPROP,PROPS,TMATC,ISTAT,STRAN,KTOLE,STRAT,STLIN,
.
ALPHI,STRES,EFFST,WORKP,WORKF,CRVAL,YOUNG,CRACK,CONSS,FTULT,FACK1,
DTIME,STRVP)
RETURN
C *** CHECK IF THE POINT CRACKS NOW ***
15 CALL PRINCI(STRAT,D)
IF(D(1).GE.CRACK) KTOLE=1
100 FORMAT(5X,'KGAST=',I5,1X,'CRACK stri=',F10.5,' *** D = ',3E20.5)
IF(D(1).GE.CRACK)GOTO 20
GOTO 15
20 CALL FISUR1(IELEM,KGAST,YOUNG,FACK1,LPROP,TMATC,ISTAT,STRAN,CONSS,
.
FTULT,STRAT,STLIN,ALPHI,CRACK,EFFST,WORKP,WORKF,STRES,
.
CRVAL,DTIME,STRVP,KTOLE,D,PROPS)
RETURN
25 CONTINUE
C *** NON CRACKED CONCRETE ***
CALL INVA2(STRAT,CRUSH)
IF(CRUSH.LT.PROPS(5,LPROP))GOTO 50

```

```

16 ISTAT(KGAST)=13
   DO 51 ISTRE = 1,6
51 STRES(ISTRE,KGAST)=0.0
   EFFST(2,KGAST)=0.0
   RETURN
C ***      NON-CRUSHED CONCRETE CHECK FOR YIELDING      ***
50 CONTINUE
   DO 60 ISTRE = 1,6
60 STRES(ISTRE,KGAST)=STLIN(ISTRE)
   CALL VISCOP(STRAN,DTIME,EFFST,KGAST,WORKP,WORKF,STLIN,PROPS,LPROP,
     .
     STRVP,KTOLE)
   RETURN
   END
C *****
C ***      ROUTINE TO EVALUATE ELASTIC STRESSES      ***
C *****
SUBROUTINE ELSTR(SG,ST,E)
DIMENSION SG(6),ST(6),E(3)
SG(1)=E(1)*ST(1)+E(2)*(ST(2)+ST(3))
SG(2)=E(1)*ST(2)+E(2)*(ST(1)+ST(3))
SG(3)=E(1)*ST(3)+E(2)*(ST(2)+ST(1))
SG(4)=E(3)*ST(4)
SG(5)=E(3)*ST(5)
SG(6)=E(3)*ST(6)
RETURN
END
C *****
C ***      SUBROUTINE PRINCIPAL      ***
C *****
SUBROUTINE PRINCI(S,D)
DIMENSION S(6),D(3),X(6)
S3=SQRT(3.0)
PI=ATAN(1.0)*4.0
XJ1=S(1)+S(2)+S(3)
SM=XJ1/3.0
X(1)=S(1)-SM
X(2)=S(2)-SM
X(3)=S(3)-SM
X(4)=S(4)/2.0
X(5)=S(5)/2.0
X(6)=S(6)/2.0
XJ2=(X(1)**2+X(2)**2+X(3)**2)/2.0+X(4)**2+X(5)**2+X(6)**2
XJ3=X(1)*(X(2)*X(3)-X(5)*X(5))-X(4)*(X(4)*X(3)-X(5)*X(6))+
& X(6)*(X(4)*X(5)-X(2)*X(6))
IF(XJ2.NE.0.) THEN
ARG= -.3*S3*XJ3/(2.*XJ2**1.5)
IF(ARG.LT.-1.) ARG=-1.
IF(ARG.GT.+1.) ARG=+1.
T=ASIN(ARG)/3.
ELSE
T=0.
ENDIF
CO=2.*SQRT(XJ2)/S3
D(1)=CO*SIN(T+2.*PI/3.)+SM
D(2)=CO*SIN(T) +SM
D(3)=CO*SIN(T+4.*PI/3.)+SM
RETURN
END
C *****
C ***      ROUTINE TO EVA. STRESSES IN REINF. & EQUIVALENT NODAL FORCES      ***
C *****
SUBROUTINE RESREF(IELEM,ELOAD,KGREF,DVOLS,CARDS,TMATX,PROPS,ELDIS,
  .
  STREF,MPATT,MLAYR,NOCAP,MBARS,VBARS,STRAF)
COMMON/CTRL/NECHO,NELEM,NGAUS,NMATS,NPOIN,NREIN,NSIZE,NTOTG,NTOTV,
  &
  NVFIX,NWKTL
COMMON/STAT/IITER,ISTEP,KTOLE
COMMON/CONST/AALFA,BEETA,GAAMA,DELTA,AZERO,BZERO,OMEGA,TMAXR,DTEND
&
  ,DTIME,AFACT,TOLER,ADISP,AVELO,CONSD,CONSF
DIMENSION ELDIS(3,1),ELOAD(3,1),PROPS(20,1),NOCAP(1),
.MPATT(1),MBARS(2,MLAYR,1),VBARS(3,MLAYR,1),STREF(6,1),STRAT(6)
.
,STRAN(6),STRAF(2,6,1),DVOLS(1),CARDS(3,20,1),TMATX(3,3,1)
KPATT = MPATT(IELEM)
IF (KPATT.EQ.0) RETURN
NLAYR = NOCAP(KPATT)
IF(NLAYR.EQ.0) RETURN
C ***      LOOP OVER THE REINFORCEMENT LAYERS      ***
DO 10 ILAYR = 1,NLAYR
IMATN = MBARS(1,ILAYR,KPATT)
ICOOR = MBARS(2,ILAYR,KPATT)
SPOS3 = VBARS(1,ILAYR,KPATT)
ESPES = VBARS(2,ILAYR,KPATT)

```

```

ANGLE = VBARS(3,ILAYR,KPATT)
C ***      ENTER LOOPS FOR AREA NUMERICAL INTEGRATION      ***
DO 50 IGAUS = 1,NGAUS
DO 50 JGAUS = 1,NGAUS
KGRES = KGRES + 1
C ***      EVALUATE THE STRAINS      ***
DO 40 ISTRE = 1,6
40 STRAT(ISTRE) = 0.0
CALL STRAIN(ELDIS,CARDS(1,1,KGRES),STRAT)
DO 41 ISTRE = 1,6
41 STRAN(ISTRE) = STRAT(ISTRE)-STRAF(1,ISTRE,KGRES)
C ***      EVALUATE STRESSES      ***
CALL STRST(STRAN,TMATX(1,1,KGRES),STREF,PROPS,IMATN,KGRES,ANGLE,
.          STRAF,DTIME,KTOLE)
C *** CALCU.THE EQUIV.NODAL FORCES AND ASSOCIATE WITH THE ELE.NODES ***
DO 45 INODE = 1,20
45 CALL FORMP(CARDS(1,INODE,KGRES),STREF(1,KGRES),
&          ELOAD(1,INODE),DVOLS(KGRES))
50 CONTINUE
10 CONTINUE
RETURN
END
C *****
C ***      ROUTINE TO EVALUATE THE STRESSES IN REINFORCEMENT      ***
C *****
SUBROUTINE STRST(STRAN,TMATX,STREF,PROPS,IMATN,KGRES,ANGLE,STRAF,
.          DTIME,KTOLE)
DIMENSION PROPS(20,1),STREF(6,1),STRAN(6),STRIN(6),TMATX(3,3)
.          ..STANO(6),STALO(6),STOLD(6),C1(3,3),T(3,3),STRAF(2,6,1),STRAS(6)
YOUNG=PROPS(1,IMATN)
YIELD=PROPS(3,IMATN)
AZERO=PROPS(11,IMATN)
C ***      SET UP THE TRANSFORMATION MATRIX      ***
DO 10 I = 1,3
DO 10 J = 1,3
C1(I,J)=0.0
10 T(I,J)=0.0
C = COS(ANGLE)
S = SIN(ANGLE)
C1(1,1)=C
C1(2,2)=C
C1(1,2)=-S
C1(2,1)= S
C1(3,3)=1.
DO 12 I = 1,3
DO 12 J = 1,3
DO 12 K = 1,3
12 T(I,J)=T(I,J)+TMATX(K,I)*C1(K,J)
C ***      TRANSFORM ELASTIC STRAIN TO LOCAL SYSTEM      ***
CALL TSTRN(STRAN,STANO,T,0)
STRAI=STANO(1)
STLIN=YOUNG*STRAI
FLUID = AZERO
DO 20 ISTRE = 1,6
STOLD(ISTRE)=0.0
STALO(ISTRE)=0.0
20 CONTINUE
C ***      CHECK IF THE POINT IS FLOWING      ***
IF(ABS(STLIN).GT.YIELD) THEN
KTOLE=1
ESCUR=(ABS(STLIN)-YIELD)/YIELD
CMULT=FLUID*ESCUR
STALO(1)=CMULT*(STLIN/ABS(STLIN))
ENDIF
STOLD(1)=STLIN
C ***      TRANSFORM TO GLOBAL SYSTEM      ***
CALL TSTRN(STALO,STRIN,T,1)
CALL TSTRS(STOLD,STRAS,T,1)
C ***      UPDATE VISCOPLASTIC STRAIN      ***
DO 60 ISTRE = 1,6
STRAF(2,ISTRE,KGRES)=STRAF(1,ISTRE,KGRES)+DTIME*STRIN(ISTRE)
60 STREF(ISTRE,KGRES)=STRAS(ISTRE)
RETURN
END
C *****
C ***      TRANSFORMATION MATRICES      ***
C *****
SUBROUTINE TSTRS(ST,SR,B,IN)
DIMENSION ST(6),SR(6),B(3,3),S(3,3)
IF(IN.EQ.0)THEN
C ***      TRANSFORMS FROM GLOBAL TO LOCAL      ***

```

```

S(1,1)=B(1,1)*ST(1)+B(2,1)*ST(4)+B(3,1)*ST(6)
S(1,2)=B(1,1)*ST(4)+B(2,1)*ST(2)+B(3,1)*ST(5)
S(1,3)=B(1,1)*ST(6)+B(2,1)*ST(5)+B(3,1)*ST(3)
S(2,1)=B(1,2)*ST(1)+B(2,2)*ST(4)+B(3,2)*ST(6)
S(2,2)=B(1,2)*ST(4)+B(2,2)*ST(2)+B(3,2)*ST(5)
S(2,3)=B(1,2)*ST(6)+B(2,2)*ST(5)+B(3,2)*ST(3)
S(3,1)=B(1,3)*ST(1)+B(2,3)*ST(4)+B(3,3)*ST(6)
S(3,2)=B(1,3)*ST(4)+B(2,3)*ST(2)+B(3,3)*ST(5)
S(3,3)=B(1,3)*ST(6)+B(2,3)*ST(5)+B(3,3)*ST(3)
SR(1)=S(1,1)*B(1,1)+S(1,2)*B(2,1)+S(1,3)*B(3,1)
SR(4)=S(1,1)*B(1,2)+S(1,2)*B(2,2)+S(1,3)*B(3,2)
SR(6)=S(1,1)*B(1,3)+S(1,2)*B(2,3)+S(1,3)*B(3,3)
SR(2)=S(2,1)*B(1,2)+S(2,2)*B(2,2)+S(2,3)*B(3,2)
SR(5)=S(2,1)*B(1,3)+S(2,2)*B(2,3)+S(2,3)*B(3,3)
SR(3)=S(3,1)*B(1,3)+S(3,2)*B(2,3)+S(3,3)*B(3,3)
ELSE
C ***      TRANSFORM FROM LOCAL TO GLOBAL      ***
S(1,1)=B(1,1)*ST(1)+B(1,2)*ST(4)+B(1,3)*ST(6)
S(1,2)=B(1,1)*ST(4)+B(1,2)*ST(2)+B(1,3)*ST(5)
S(1,3)=B(1,1)*ST(6)+B(1,2)*ST(5)+B(1,3)*ST(3)
S(2,1)=B(2,1)*ST(1)+B(2,2)*ST(4)+B(2,3)*ST(6)
S(2,2)=B(2,1)*ST(4)+B(2,2)*ST(2)+B(2,3)*ST(5)
S(2,3)=B(2,1)*ST(6)+B(2,2)*ST(5)+B(2,3)*ST(3)
S(3,1)=B(3,1)*ST(1)+B(3,2)*ST(4)+B(3,3)*ST(6)
S(3,2)=B(3,1)*ST(4)+B(3,2)*ST(2)+B(3,3)*ST(5)
S(3,3)=B(3,1)*ST(6)+B(3,2)*ST(5)+B(3,3)*ST(3)
SR(1)=S(1,1)*B(1,1)+S(1,2)*B(1,2)+S(1,3)*B(1,3)
SR(4)=S(1,1)*B(2,1)+S(1,2)*B(2,2)+S(1,3)*B(2,3)
SR(6)=S(1,1)*B(3,1)+S(1,2)*B(3,2)+S(1,3)*B(3,3)
SR(2)=S(2,1)*B(2,1)+S(2,2)*B(2,2)+S(2,3)*B(2,3)
SR(5)=S(2,1)*B(3,1)+S(2,2)*B(3,2)+S(2,3)*B(3,3)
SR(3)=S(3,1)*B(3,1)+S(3,2)*B(3,2)+S(3,3)*B(3,3)
ENDIF
RETURN
END
C *****
C ***      SUBROUTINE TSTRN      ***
C *****
SUBROUTINE TSTRN(ST,SR,B,IN)
DIMENSION ST(6),SR(6),B(3,3)
C *** TRANSFORM GLOBAL STRAINS INTO LOCAL STRAINS OR VICE VERSA
ST(4)=ST(4)*0.5
ST(5)=ST(5)*0.5
ST(6)=ST(6)*0.5
CALL TSTRS(ST,SR,B,IN)
SR(4)=SR(4)*2
SR(5)=SR(5)*2
SR(6)=SR(6)*2
ST(4)=ST(4)*2
ST(5)=ST(5)*2
ST(6)=ST(6)*2
RETURN
END
C *****
C ***      ROUTINE TO EVALUATE THE STRESSES IN CONCRETE      ***
C ***      THAT WAS PREVIOUSLY NON-CRACKED      ***
C *****
SUBROUTINE FISUR1(IELEM,KGAST,YOUNG,FAK1,LPROP,BETAM,ISTAT,STRAN,
.      CONSS,FTULT,STRAT,STLIN,ALPHI,CRACK,EFFST,WORKP,WORKF,
.      STRES,CRVAL,DTIME,STRVP,KTOLE,D,PROPS)
DIMENSION ALPHI(4,1),PROPS(20,1),ISTAT(1),STRVP(2,6,1),STRAN(6),
.      STRAT(6),STALO(6),STALO(6),STRAL(6),CRVAL(4,1),WORKF(2,1),
.      STLIN(6),BETAM(3,3),STRES(6,1),EFFST(2,1),WORKP(2,1),D(3)
PI=4.0*ATAN(1.0)
TENST=1.0E-10
IELEM=IELEM
C ***      FIND OUT THE STRAIN PRINCIPAL DIRECTIONS      ***
CALL PDIREC(STRAT,D,BETAM)
DO 90 I=1,3
STALO(I)=D(I)
90 STALO(3+I)=0.0
DO 91 I=1,6
91 STRAL(I)=STALO(I)
ALPHI(2,KGAST)=ASIN(BETAM(3,1))
IF(ABS(BETAM(2,1))+ABS(BETAM(1,1)).EQ.0.0) THEN
ALPHI(1,KGAST)=PI/2.
ELSE
ALPHI(1,KGAST)=ATAN2(BETAM(2,1),BETAM(1,1))
ENDIF
ALPHI(4,KGAST)=ASIN(BETAM(3,2))
IF(ABS(BETAM(2,2))+ABS(BETAM(1,2)).EQ.0.0) THEN

```

```

ALPHI(3,KGAST)=PI/2.
ELSE
  ALPHI(3,KGAST)=ATAN2(BETAM(2,2),BETAM(1,2))
ENDIF
C ***      FIND OUT THE LOCAL STRESSES          ***
CALL TSTRS(STLIN,STRLO,BETAM,0)
C *** -----LAYER IS CRACKED IN ONE DIRECTION AT LEAST----- ***
  ISTAT(KGAST)=10
  STRAV=STALO(1)
  STREV=FTULT
  STRIV=STRAV
  CALL TSEFF(FTULT,CRACK,CONSS,STRIV,STRAV,STREV)
  STRLO(1)=STREV
  CRVAL(1,KGAST)=STRAV
  CRVAL(2,KGAST)=STREV
  IF(STRAV.GT.TENST)TENST=STRAV
  STRAL(1)=0.0
C *** -----CHECK IF A SECOND CRACK IS FORMED----- ***
  IF(STALO(2)-CRACK) 125,125,93
C *** -----LAYER IS CRACKED IN TWO DIRECTIONS----- ***
93  ISTAT(KGAST)=12
  STRAV=STALO(2)
  STREV=FTULT
  STRIV=STRAV
  CALL TSEFF(FTULT,CRACK,CONSS,STRIV,STRAV,STREV)
  STRAL(2)=0.0
  STRLO(2)=STREV
  CRVAL(3,KGAST)=STRAV
  CRVAL(4,KGAST)=STREV
  IF(STRAV.GT.TENST)TENST=STRAV
125 CONTINUE
C ***      ADJUST SHEAR STRESSES          ***
  COECQ=(1.0-(TENST/0.005)**FACK1)
  IF(COECQ.LT.0.1)COECQ=0.1
  STRLO(4)=COECQ*STALO(4)*YOUNG/2.
  STRLO(6)=COECQ*STALO(6)*YOUNG/2.
  IF(ISTAT(KGAST).EQ.12) STRLO(5)=COECQ*STALO(5)*YOUNG/2.
C ***      CHECK AGAINST CRUSHING          ***
  CALL INVA2(STRAL,CRUSH)
  IF(CRUSH.GT.PROPS(5,LPROP))GOTO 203
C *** -----NON-CRUSHED CONCRETE----- ***
C ***      TRANSFORM STRESSES INTO GLOBAL COORDINATE SYSTEM      ***
  CALL TSTRS(STRLO,STRES(1,KGAST),BETAM,1)
  CALL VISCOP(STRAN,DTIME,EFFST,KGAST,WORKP,WORKF,STRES(1,KGAST),
    PROPS,LPROP,STRVP,KTOLE)
  RETURN
C *** -----CRUSHED CONCRETE----- ***
203 DO 204 ISTRE=1,6
204 STRES(ISTRE,KGAST)=0.0
  EFFST(2,KGAST)=0.0
  ISTAT(KGAST)=13
  RETURN
END
C *****
C ***      SUBROUTINE INVA2          ***
C *****
SUBROUTINE INVA2(SN,CRUSH)
  DIMENSION SN(6)
  BEETA=1.
  ALPHA=0.
  GASH1=BEETA*(SN(1)*SN(1)+SN(2)*SN(2)+SN(3)*SN(3)-SN(1)*SN(2)-SN(1)
    *SN(3)-SN(2)*SN(3)+0.75*(SN(6)*SN(6)+SN(4)*SN(4)+SN(5)*SN(5)))
  GESH1=ALPHA*(SN(1)+SN(2)+SN(3))*0.5
  GISH1=SQRT(GESH1*GESH1+GASH1)
  CRUSH=GESH1+GISH1
  RETURN
END
C *****
C ***      SUBROUTINE TSEFF          ***
C *****
SUBROUTINE TSEFF(SIGM1,DEFO1,CONSS,STRIV,STRAV,STREV)
  STREV=STREV*STRAV/STRIV
  EXPUP=-((STRAV-DEFO1)/CONSS)
  IF(EXPUP.GT.0.5E+02) EXPUP=50.
  VALUE=SIGM1*EXP(EXPUP)
  IF(VALUE.LT.STREV) STREV=VALUE
  IF(STREV.GT.SIGM1) STREV=SIGM1
  IF(STREV.LT.0.0) STREV=0.0
  RETURN
END
C *****

```

```

C ***          SUBROUTINE TO COMPUTE EIGENVECTORS          ***
C *****
SUBROUTINE PDIREC(S,XL,V)
DIMENSION S(6),XL(3),V(3,3)
COMP=XL(1)+XL(2)+XL(3)
COMP2=COMP*COMP
A3=ABS((XL(1)-XL(2))/COMP)
A2=ABS((XL(1)-XL(3))/COMP)
A1=ABS((XL(2)-XL(3))/COMP)
C ***          CASE-A: THREE EQUAL EIGENVALUES          ***
IF(A1.LT.1.E-10.AND.A2.LT.1.E-10) THEN
  V(1,1)=1.0
  V(2,2)=1.0
  V(3,3)=1.0
  V(1,2)=0.0
  V(1,3)=0.0
  V(2,1)=0.0
  V(2,3)=0.0
  V(3,1)=0.0
  V(3,2)=0.0
  RETURN
ENDIF
C ***          CASE-B: TWO EQUAL EIGENVALUES          ***
IF(A1.LT.1.E-10) THEN
  CALL EIGVC1(S,XL(1),V(1,1),COMP2)
  CALL VECPRO(V(1,1),V(1,2),V(1,3))
  RETURN
ENDIF
IF(A2.LT.1.E-10) THEN
  CALL EIGVC1(S,XL(2),V(1,2),COMP2)
  CALL VECPRO(V(1,2),V(1,3),V(1,1))
  RETURN
ENDIF
IF(A3.LT.1.E-10) THEN
  CALL EIGVC1(S,XL(3),V(1,3),COMP2)
  CALL VECPRO(V(1,3),V(1,1),V(1,2))
  RETURN
ENDIF
C ***          CASE-C: THREE DIFFERENT EIGENVALUES          ***
CALL EIGVC1(S,XL(1),V(1,1),COMP2)
CALL EIGVC1(S,XL(2),V(1,2),COMP2)
DOT = V(1,1)*V(1,2)+V(2,1)*V(2,2)+V(3,1)*V(3,2)
V(1,2)=V(1,2)-DOT*V(1,1)
V(2,2)=V(2,2)-DOT*V(2,1)
V(3,2)=V(3,2)-DOT*V(3,1)
XN=SQRT(V(1,2)*V(1,2)+V(2,2)*V(2,2)+V(3,2)*V(3,2))
XN=1./XN
V(1,2)=V(1,2)*XN
V(2,2)=V(2,2)*XN
V(3,2)=V(3,2)*XN
V(1,3)=V(2,1)*V(3,2)-V(3,1)*V(2,2)
V(2,3)=V(3,1)*V(1,2)-V(1,1)*V(3,2)
V(3,3)=V(1,1)*V(2,2)-V(2,1)*V(1,2)
RETURN
END
C *****
C ***          SUBROUTINE TO COMPUTE EIGVC1          ***
C *****
SUBROUTINE EIGVC1(S,XL,V,COM)
DIMENSION S(6),V(3)
C ***          EVALUATES ONE EIGENVECTOR          ***
X1 = S(1) - XL
X2 = S(2) - XL
X3 = S(3) - XL
X4 = S(4)*0.5
X5 = S(5)*0.5
X6 = S(6)*0.5
DET = X1*X2-X4*X4
IF (ABS(DET/COM).GT.1.E-10) THEN
  V1 = (X4*X5-X6*X2)/DET
  V2 = (X6*X4-X5*X1)/DET
  XN = SQRT(V1*V1+V2*V2+1.0)
  XN = 1. / XN
  V(1) = V1*XN
  V(2) = V2*XN
  V(3) = XN
  RETURN
ENDIF
DET = X4*X5 - X6*X2
IF (ABS(DET/COM).GT.1.E-10) THEN
  V1 = (X6*X4-X5*X1)/DET

```

```

      XN = SQRT(V1*V1+1.0)
      XN = 1./XN
      V(1) = XN
      V(2) = V1*XN
      V(3) = 0.0
      RETURN
ENDIF
DET = X1*X5-X4*X6
IF (ABS(DET/COM).GT.1.E-10) THEN
  V(1) = 0.0
  V(2) = 1.0
  V(3) = 0.0
  RETURN
ENDIF
DET = X4*X3-X5*X6
IF (ABS(DET/COM).GT.1.E-10) THEN
  V1 = (X5*X5-X2*X3)/DET
  XN = SQRT(V1*V1+1.0)
  XN = 1./XN
  V(1) = V1*XN
  V(2) = XN
  V(3) = 0.0
  RETURN
ENDIF
DET = X2*X3-X5*X5
IF (ABS(DET/COM).GT.1.E-10) THEN
  V(1) = 1.0
  V(2) = 0.0
  V(3) = 0.0
  RETURN
ENDIF
V(1) = 0.0
V(2) = 1.0
V(3) = 0.0
RETURN
END
C *****
C ***          COMPUTES AN ORTHONORMAL BASE FROM V1          ***
C *****
SUBROUTINE VECPRO(A,B,C)
DIMENSION A(3),B(3),C(3)
XN = A(2)*A(2)+A(3)*A(3)
IF (XN.GT.1.E-10) THEN
  B(1) = 0.0
  XN = SQRT(XN)
  B(2) = A(3)/XN
  B(3) = -A(2)/XN
  C(1) = A(2)*B(3)-A(3)*B(2)
  C(2) = -A(1)*B(3)
  C(3) = A(1)*B(2)
ELSE
  B(1) = 0.0
  B(2) = 1.0
  B(3) = 0.0
  C(1) = 0.0
  C(2) = 0.0
  C(3) = 1.0
ENDIF
RETURN
END
C *****
C ***          ROUTINE TO EVALUATE VISCOPLASTIC STRAINS          ***
C *****
SUBROUTINE VISCOP(STRAN,DTIME,EFFST,KGAST,WORKP,WORKF,STLIN,PROPS
, LPROP,STRVP,KTOLE)
DIMENSION EFFST(2,1),WORKP(2,1),WORKF(2,1),PROPS(20,1),
.STRVP(2,6,1),STRAN(6),STLIN(6),STRIN(6),AVECT(6)
C***          IDENTIFY MATERIAL PROPERTIES          ***
POISS=PROPS(2,LPROP)
FCULT=PROPS(3,LPROP)
NYIEL=PROPS(8,LPROP)
CONST=PROPS(10,LPROP)
AZERO=PROPS(11,LPROP)
AONEP=PROPS(12,LPROP)
ALFAC=PROPS(13,LPROP)
BETA0=PROPS(14,LPROP)
BETA1=PROPS(15,LPROP)
C ***          EVALUATE RATE OF ELASTIC STRAIN AND GAAMA          ***
PJ2IN=((((STRAN(1)-STRAN(2))**2+(STRAN(2)-STRAN(3))**2+(STRAN(1)
.STRAN(3))**2)/6.+(STRAN(4)**2+STRAN(5)**2+STRAN(6)**2)/4.)
EEFFV=SQRT(3.*PJ2IN/(1.+POISS)**2)

```

```

ERATE=ABS((EEFFV-EFFST(1,KGAST))/DTIME)
IF(ERATE.LT. 1.0E-07) ERATE = 1.0E-07
IF(ERATE.GT. 1.0E+03) ERATE = 1.0E+03
EFFST(2,KGAST)=EEFFV
FLUID = AZERO
IF(AONEP.NE.0.0) FLUID=FLUID*(ERATE**AONEP)
C ***   FIND VALUE OF DISCONTINUITY AND FAILURE SURFACES   ***
  TWORK=WORKP(1,KGAST)
  FWORK=WORKF(1,KGAST)
  CALL INVAR(NYIEL,STLIN,YIELD)
  PREYO=CONST*FCULT
  PREYS=PREYO
  EXPOC=-ALFAC*(TWORK-FWORK)
  IF(EXPOC.GT.0.) WRITE(2,*)EXPOC GT 0 LINE 2244',EXPOC,TWORK,FWORK
  IF(EXPOC.LT.-100.) EXPOC=-100.
  IF(FWORK.NE.0.) PREYS=PREYO*EXP(EXPOC)
  IF(PREYS.LT.PREYO/10.) PREYS=PREYO/10.
  FAILV=BETA0*FCULT*(1.-BETA1*TWORK)
C ***   CHECK IF THE POINT IS FAILING   ***
  IF(FWORK.EQ.0.0.AND.YIELD.GT.FAILV) WORKF(2,KGAST)=TWORK
C ***   CHECK IF THE POINT IS FLOWING   ***
  IF(PREYS.GT.YIELD) THEN
    DO 10 ISTRE = 1,6
10   STRIN(ISTRE)=0.
  ELSE
    KTOLE=1
    ESCUR=(YIELD-PREYS)/PREYO
    CMULT=FLUID*ESCUR
    CALL FLOWVP(AVECT,NYIEL,STLIN)
    DO 20 ISTRE=1,6
20   STRIN(ISTRE)=CMULT*AVECT(ISTRE)
  ENDIF
C ***   UPDATE VISCOPLASTIC WORK AND VP STRAINS   ***
  DWORK=0.
  DO 30 ISTRE=1,6
    DWORK=DWORK+DTIME*STRIN(ISTRE)*STLIN(ISTRE)
    STRVP(2,ISTRE,KGAST)=STRVP(1,ISTRE,KGAST)+DTIME*STRIN(ISTRE)
30  CONTINUE
  IF(DWORK.LT.0.0)WRITE(2,*)'LINE2269',KGAST,DWORK,TWORK,STRIN,STLIN
  WORKP(2,KGAST)=TWORK+DWORK
  RETURN
  END
C *****
C *** ROUTINE CALCULATE STRESS RESULTANT CONTRIBUTION TO YIELD FUNC. ***
C *****
  SUBROUTINE INVAR(NCRIT,ST,YIELD)
  DIMENSION ST(6)
C ***   SELECT YIELD CRITERIA   ***

C ***   VON MISES   ***
  IF(NCRIT.EQ.1)BEETA=1.0
  IF(NCRIT.EQ.1)ALPHA=0.0
C ***   3-D CONCRETE YIELD CRITERIA   ***
  IF(NCRIT.EQ.2)BEETA=1.355
  IF(NCRIT.EQ.2)ALPHA=0.355
  GJNV2=BEETA*(ST(1)**2+ST(2)**2+ST(3)**2-ST(1)*ST(2)-ST(2)*ST(3)-
    .      ST(3)*ST(1)+3.0*(ST(4)**2+ST(5)**2+ST(6)**2))
  GINV1=ALPHA*(ST(1)+ST(2)+ST(3))*0.5
  GASH1=SQRT(GINV1*GINV1+GJNV2)
  YIELD=GINV1+GASH1
  RETURN
  END
C *****
C ***   TO DETER. DERIVATIVE OF YIELD FUN.:1-VON MISES 3- 3D YIELD FUN.   ***
C *****
  SUBROUTINE FLOWVP (AVECT,NCRIT,SG)
  DIMENSION AVECT(6),SG(6)
C ***   SELECT YIELD CRITERIA   ***
  GOTO(1,3,3)NCRIT
C ***   VON MISES   ***
1  BEETA=1.0
  ALPHA=0.0
  GOTO 4
C ***   3-D YIELD FUNCTION FOR CONCRETE   ***
3  BEETA=1.355
  ALPHA=0.355
4  CONS1=ALPHA*0.5
  CONS2=CONS1*CONS1+BEETA
  CONS3=2.0*CONS1*CONS1-BEETA
  CONS4=BEETA*3.0
  AFUNC=(CONS2*(SG(1)**2+SG(2)**2+SG(3)**2)+CONS3*(SG(1)*SG(2)+SG(1)

```



```

C *** -----IF THE LAYER IS COMPLETELY DEGRADATED,DO NOTHING----- ***
  STRAL(5)=0.0
  IF(STALO(1).LT.0.0.AND.STALO(2).LT.0.0)GOTO 150
  IF(STALO(1).LT.0.0.AND.STALO(2).GE.0.0)GOTO 105
C *** ----- FIRST CRACK IS OPENED ----- ***
  STRAL(1)=0.0
  IF(STANO(1))62,62,69
62  DESIG=CRVAL(2,KGAST)*STALO(1)/CRVAL(1,KGAST)
  GOTO 65
69  STRAV=STALO(1)
  STREV=CRVAL(2,KGAST)
  STRIV=CRVAL(1,KGAST)
  CALL TSEFF(FTULT,CRACK,CONSS,STRIV,STRAV,STREV)
  DESIG=STREV
65  STRLO(1)=DESIG
  IF(STALO(1).GT.CRVAL(1,KGAST)) THEN
    CRVAL(1,KGAST)=STALO(1)
    CRVAL(2,KGAST)=STRLO(1)
  ENDIF
  IF(STALO(2).LT.0.0)GOTO 150
C *** -----SECOND CRACK IS OPENED----- ***
105 STRAL(2)=0.0
  IF(STANO(2))63,63,68
63  DESIG=CRVAL(4,KGAST)*STALO(2)/CRVAL(3,KGAST)
  GOTO 66
68  STRAV=STALO(2)
  STREV=CRVAL(4,KGAST)
  STRIV=CRVAL(3,KGAST)
  CALL TSEFF(FTULT,CRACK,CONSS,STRIV,STRAV,STREV)
  DESIG=STREV
66  STRLO(2)=DESIG
  IF(STALO(2).GT.CRVAL(3,KGAST)) THEN
    CRVAL(3,KGAST)=STALO(2)
    CRVAL(4,KGAST)=STRLO(2)
  ENDIF
150 CONTINUE
C *** ADJUST SHEAR STRESSES ***
  TENST=MAX(CRVAL(1,KGAST),CRVAL(3,KGAST))
  COECQ=(1.-(TENST/0.005)**FACK1)
  IF(COECQ.LT.0.1) COECQ=0.1
  STRLO(4)=COECQ*STALO(4)*YOUNG*0.5
  STRLO(6)=COECQ*STALO(6)*YOUNG*0.5
  IF(ISTAT(KGAST).EQ.12) STRLO(5)=COECQ*STALO(5)*YOUNG*0.5
C *** TRANSFORM STRESSES TO GLOBAL COORDINATE SYSTEM ***
  CALL TSTRS(STRLO,STRES(1,KGAST),BETAM,1)
C *** CHECK AGAINST CRUSHING ***
  CALL INVA2(STRAL,CRUSH)
  IF(CRUSH.GT.PROPS(5,LPROP))GOTO 203
C *** -----NON CRUSHED CONCRETE----- ***
  CALL VISCOP(STRAN,DTIME,EFFST,KGAST,WORKP,WORKF,STRES(1,KGAST),
  PROPS,LPROP,STRVP,KTOLE)
210 CONTINUE
  RETURN
C *** -----CRUSHED OR TOO CRACKED CONCRETE----- ***
203 ISTAT(KGAST)=13
200 EFFST(2,KGAST)=0.0
  DO 251 ISTR=1,6
251 STRES(ISTR,KGAST)=0.0
  RETURN
  END
C *****
C *** SUBROUTINE ROTATE ***
C *****
SUBROUTINE ROTATE(STRLO,BETAM,ALPHI,KGAST,STRAT,STALO,STRAN,STANO,
  .
  .
  .
  STLIN,STRAS,STOLD,STRAL)
  DIMENSION BETAM(3,3),STANO(6),ALPHI(4,1),STRAT(6),STRAN(6),
  .
  .
  .
  STLIN(6),STOLD(6),STALO(6),BETA2(3,3),BETA0(3,3),
  .
  .
  STRAS(6),STRLO(6),STRAL(6)
  PI=4.0*ATAN(1.0)
  ERROR=1.E-10
C *** FIND DIRECTION OF MAXIMUM STRAIN ***
  STR11=STALO(2)
  STR22=STALO(3)
  STR12=STALO(5)*0.5
  DENTA=STR11-STR22
  IF(ABS(STR12).GT.ERROR)GOTO 90
  ANGLE = 0.0
  IF(DENTA.LT.0.0)ANGLE=PI/2.
  GOTO 80
90 IF(ABS(DENTA).GT.ERROR)GOTO 70
  ANGLE = PI/4.

```

```

IF(STR12.LT.0.0)ANGLE=-PI/4.
GOTO 80
70 ANGLE=0.5*ATAN(2.*STR12/DENTA)
CA=COS(ANGLE)
SA=SIN(ANGLE)
PSTR1=CA*CA*STR11+SA*SA*STR22+2.*SA*CA*STR12
PSTR2=SA*SA*STR11+CA*CA*STR22-2.*SA*CA*STR12
IF(PSTR1.GE.PSTR2)GOTO 80
ANGLE=ANGLE+PI/2.
80 CONTINUE
C ***          FIND NEW TRANSFORMATION MATRIX          ***
DO 1 I =1,3
DO 1 J =1,3
BETA2(I,J)=0.0
BETA0(I,J)=BETAM(I,J)
1  BETAM(I,J)=0.0
BETA2(1,1)=1.
BETA2(2,2)= COS(ANGLE)
BETA2(3,3)= COS(ANGLE)
BETA2(2,3)=-SIN(ANGLE)
BETA2(3,2)= SIN(ANGLE)
DO 2 I=1,3
DO 2 J=1,3
DO 2 K=1,3
2  BETAM(I,J)=BETAM(I,J)+BETA0(I,K)*BETA2(K,J)
ALPHI(4,KGAST)=ASIN(BETAM(3,2))
IF(ABS(BETAM(2,2))+ABS(BETAM(1,2)).EQ.0.0)
.ALPHI(3,KGAST)=PI/2.
IF(ABS(BETAM(2,2))+ABS(BETAM(1,2)).NE.0.0)
.ALPHI(3,KGAST)=ATAN2(BETAM(2,2),BETAM(1,2))
CALL ODIREC(ALPHI,BETAM,KGAST,0)
C ***          TRANSFORM STRESS AND STRAIN TO NEW SYSTEM          ***
STREV=STRLO(1)
CALL TSTRN(STRAT,STALO,BETAM,0)
CALL TSTRN(STRAN,STANO,BETAM,0)
CALL TSTRS(STLIN,STRLO,BETAM,0)
CALL TSTRS(STRAS,STOLD,BETAM,0)
STRLO(1)=STREV
STRAL(1)=0.0
STRAL(2)=STALO(2)
STRAL(3)=STALO(3)
STRAL(4)=0.0
STRAL(5)=STALO(5)
STRAL(6)=0.0
RETURN
END
C *****
C ***          SUBROUTINE ODIREC          ***
C *****
SUBROUTINE ODIREC(ALPHI,BETAM,KGAST,INDEX)
DIMENSION ALPHI(4,1),BETAM(3,3),A(3,3)
SA1=SIN(ALPHI(1,KGAST))
CA1=COS(ALPHI(1,KGAST))
SB1=SIN(ALPHI(2,KGAST))
CB1=COS(ALPHI(2,KGAST))
SA2=SIN(ALPHI(3,KGAST))
CA2=COS(ALPHI(3,KGAST))
SB2=SIN(ALPHI(4,KGAST))
CB2=COS(ALPHI(4,KGAST))
BETAM(1,1)=CB1*CA1
BETAM(2,1)=CB1*SA1
BETAM(3,1)=SB1
BETAM(1,2)=CB2*CA2
BETAM(2,2)=CB2*SA2
BETAM(3,2)=SB2
BETAM(1,3)=BETAM(2,1)*BETAM(3,2)-BETAM(3,1)*BETAM(2,2)
BETAM(2,3)=BETAM(1,2)*BETAM(3,1)-BETAM(1,1)*BETAM(3,2)
BETAM(3,3)=BETAM(1,1)*BETAM(2,2)-BETAM(2,1)*BETAM(1,2)
IF(INDEX.EQ.0) RETURN
DO 1 I =1,3
DO 1 J =1,3
1  A(J,I)=BETAM(I,J)
DO 2 I =1,3
DO 2 J =1,3
2  BETAM(I,J)=A(I,J)
RETURN
END
C *****
C ***          CALCULATES CORRECTOR VALUES AND CHECKS CONVERGENCE          ***
C *****
SUBROUTINE ITRATE(ACCEI,ACCEL,YMASS,DISPI,DISPL,DISPT,MAXAI,NCHEK,

```

```

1          RESID,STIFS,VELOI,VELOT,RATIO)
COMMON/CTRL/ NECHO,NELEM,NGAUS,NMATS,NPOIN,NREIN,NSIZE,NTOTG,NTOTV
1          ,NVFIX,NWKTL
COMMON/RUN/ IFUNC,IPRED,KSTEP,MITER,NACCE,NOUTD,NOUTP,NREQD,NREQS
1          ,NSTEP
COMMON/CONST/AALFA,BEETA,GAAMA,DELTA,AZERO,BZERO,OMEGA,TMAXR,DTEND
1          ,DTIME,AFACT,TOLER,ADISP,AVELO,CONSD,CONSF
COMMON/STAT/ IITER,ISTEP,KTOLE
DIMENSION DISPI(1),VELOI(1),ACCEI(1),RESID(1),MAXAI(1),DISPL(1),
1          ACCEL(1),STIFS(1),DISPT(1),YMASS(1),VELOT(1)
NCHEK = 0
C ***      COMPUTE INERTIAL FORCES          ***
DO 10 ISIZE = 1,NSIZE
10 ACCEL(ISIZE) = YMASS(ISIZE)*ACCEI(ISIZE)
C ***      CALCULATES TOTAL EFFECTIVE LOAD VECTOR      ***

SUMRS=0.0
DO 660 ISIZE = 1,NSIZE
ACCEL(ISIZE)=DISPL(ISIZE)-ACCEL(ISIZE)-RESID(ISIZE)
660 SUMRS=SUMRS+ACCEL(ISIZE)*ACCEL(ISIZE)
SUMRS=SQRT(SUMRS)
IF(IITER.EQ.1)SUMP1=SUMRS
RATI1=RATIO
RATIO=0.0
IF(SUMP1.NE.0.0) RATIO=SUMRS/SUMP1
C ***      CALCULATES DELTA DISPLACEMENT          ***
210 CALL REDBAK(STIFS,ACCEL,MAXAI,NSIZE)
C ***      CORRECT DISPLACEMENTS, ACCELERATION AND VELOCITIES      ***
DO 670 ISIZE = 1,NSIZE
DISPT(ISIZE) = DISPT(ISIZE)+ACCEL(ISIZE)
ACCEI(ISIZE) = CONSF*(DISPT(ISIZE)-DISPI(ISIZE))
670 VELOT(ISIZE) = VELOI(ISIZE)+CONSD*ACCEI(ISIZE)
C ***      CHECK CONVERGENCE          ***
C   TOLE1=2
TOLE1=TOLER
IF(KTOLE.EQ.1) TOLE1=TOLER
IF(RATIO.GT.TOLE1)GOTO 550
NCHEK = 1
GOTO 240
550 IF(IITER.LT.MITER)GOTO 230
240 DO 540 ISIZE = 1,NSIZE
VELOI(ISIZE) = VELOT(ISIZE)
540 DISPI(ISIZE) = DISPT(ISIZE)
230 CONTINUE
RETURN
END
C *****
C ***      TO REDUCE AND BACKSUBSTITUTE ITERATION VECTORS      ***
C *****
SUBROUTINE REDBAK (STIFF,FORCE,MAXAI,NEQNS)
DIMENSION FORCE(1),STIFF(1),MAXAI(1)
DO 400 IEQNS = 1,NEQNS
LOWER = MAXAI(IEQNS)+1
KUPER = MAXAI(IEQNS+1)-1
IF (KUPER-LOWER) 400,410,410
410 JEQNS = IEQNS
SUMCC = 0.0
DO 420 ICOLM=LOWER,KUPER
JEQNS=JEQNS-1
420 SUMCC=SUMCC+STIFF(ICOLM)*FORCE(JEQNS)
FORCE(IEQNS)=FORCE(IEQNS)-SUMCC
400 CONTINUE
DO 480 IEQNS = 1,NEQNS
KMAXA = MAXAI(IEQNS)
480 FORCE(IEQNS)=FORCE(IEQNS)/STIFF(KMAXA)
IF (NEQNS.EQ.1) RETURN
JEQNS = NEQNS
DO 500 IEQNS = 2,NEQNS
LOWER = MAXAI(JEQNS)+1
KUPER = MAXAI(JEQNS+1)-1
IF(KUPER-LOWER) 500,510,510
510 KEQNS = JEQNS
DO 520 ICOLM = LOWER,KUPER
KEQNS = KEQNS - 1
520 FORCE(KEQNS)=FORCE(KEQNS)-STIFF(ICOLM)*FORCE(JEQNS)
500 JEQNS=JEQNS-1
RETURN
END
C *****
C ***      OUTPUT ROUTINE          ***
C *****

```

```

SUBROUTINE OUTDYN(DISPT,NGRQS,NPRQD,TDISP,ISTAT,IFPRE,STRES,EFFST,
1      WORKP,WORKF,GPCOD,STRVP,STRAF,ALPHI,EFFSS)
COMMON/CTRL/NECHO,NELEM,NGAUS,NMATS,NPOIN,NREIN,NSIZE,NTOTG,NTOTV,
&      NVFIX,NWKTL
COMMON/RUN/IFUNC,IPRED,KSTEP,MITER,NACCE,NOUTD,NOUTP,NREQD,NREQS,
&      NSTEP
COMMON/STAT/IITER,ISTEP,KTOLE
COMMON/CONST/AALFA,BEETA,GAAMA,DELTA,AZERO,BZERO,OMEGA,TMAXR,DTEND
&      ,DTIME,AFACT,TOLER,ADISP,AVELO,CONSD,CONSF
DIMENSION DISPT(1),NPRQD(1),TDISP(1),IFPRE(3,1),NGRQS(1),ISTAT(1),
. StrAIL(7,15),StrAIW(7,15),STRES(6,1),STRVP(2,6,1),STRAF(2,6,1),
.EFFSS(2,1),WORKP(2,1),WORKF(2,1),ALPHI(4,1),GPCOD(3,1),EFFST(2,1)

DO 5 ITOTG = 1,NTOTG
5  EFFST(1,ITOTG)=EFFST(2,ITOTG)
IF(KTOLE.NE.0) THEN
DO 10 ITOTG = 1,NTOTG
WORKP(1,ITOTG)=WORKP(2,ITOTG)
WORKF(1,ITOTG)=WORKF(2,ITOTG)
DO 10 ISTRE = 1,6
10  STRVP(1,ISTRE,ITOTG)=STRVP(2,ISTRE,ITOTG)
NTOTS = NELEM*27
DO 30 ITOTG = 1,NTOTS
EFFSS(1,ITOTG)=EFFSS(2,ITOTG)
DO 30 ISTRE=1,6
30  STRAF(1,ISTRE,ITOTG)=STRAF(2,ISTRE,ITOTG)
ENDIF
C *** REARRANGE DISPLACEMENT VECTOR ***
KOUNT = 0
DO 60 IPOIN=1,NPOIN
DO 60 IDOFN=1,3
IEQNS=IFPRE(IDOFN,IPOIN)
KOUNT = KOUNT + 1
IF(IEQNS.NE.0) TDISP(KOUNT)=DISPT(IEQNS)
60 CONTINUE
C *** OUTPUT REQUIRED DISPLACEMENTS ***
TTIME=DTIME*FLOAT(ISTEP)
KOUND=(ISTEP/NOUTP)*NOUTP
IF(KOUND.EQ.ISTEP) THEN
WRITE(2,900)TTIME,ISTEP
IF(NREQD.NE.0) THEN
WRITE(2,910)
DO 80 IPOIN=1,NPOIN
DO 80 IREQD=1,NREQD
IF(IPOIN.EQ.NPRQD(IREQD)) THEN
NPOSN=(IPOIN-1)*3+1
NPOSM=IPOIN*3
WRITE(3,920)ISTEP,(TDISP(IPOSN),IPOSN=NPOSN,NPOSM)
WRITE(*,920)ISTEP,(TDISP(IPOSN),IPOSN=NPOSN,NPOSM)
ENDIF
80 CONTINUE
ENDIF
C *** OUTPUT REQUIRED STRESSES ***
CCCCCCCCCCCCCCCCCCCCCCCCCCCCCCCCCCCCCCCCCCCCCCCCCCCCCCCC
CCCC stresses along the span CCCCCCCCCCCC
CCCCCCCCCCCCCCCCCCCCCCCCCCCCCCCCCCCCCCCCCCCCCCCCCCCCCCCC
IF(ISTEP.EQ.7700)THEN
DO 980 JL=1,15
DO 980 IS=1,7
IF(IS.EQ.1)KOKO=0
IF(IS.EQ.2)KOKO=2
IF(IS.EQ.3)KOKO=3
IF(IS.EQ.4)KOKO=4
IF(IS.EQ.5)KOKO=6
IF(IS.EQ.6)KOKO=11
IF(IS.EQ.7)KOKO=18
KMKM=KOKO*27+(JL-1)*23*27
980 StrAIL(IS,JL)=STRES(3,33+KMKM)

DO 981 JL=1,15
DO 981 IS=1,7
KMKM=(IS-1)*27+(JL-1)*23*27
981 StrAIW(IS,JL)=STRES(3,450+KMKM)

DO 982 I=1,7
WRITE(6,979)(StrAIL(I,J),J=1,15)
982 WRITE(7,979)(StrAIW(I,J),J=1,15)

ENDIF
CCCCCCCCCCCCCCCCCCCCCCCCCCCCCCCCCCCCCCCCCCCCCCCCCCCCCCCC

```

```

CCCCCCCCCCCCCCCCCCCCCCCCCCCCCCCCCCCCCCCCCCCCCCCC
IF(NREQS.NE.0) THEN
  IYY=IYY+1
  IF(IYY.EQ.1)WRITE(4,930)
  IF(IYY.EQ.1)WRITE(5,930)
  IF(IYY.EQ.1)WRITE(8,930)
  DO 100 ITOTG = 1,NTOTG
    IGP1=NGRQS(1)
    IGP2=NGRQS(2)
    IGP3=NGRQS(3)
    IF(ITOTG.EQ.IGP1)WRITE(4,940)ISTEP,(STRES(IS,ITOTG),IS=1,6)
    IF(ITOTG.EQ.IGP2)WRITE(5,940)ISTEP,(STRES(IS,ITOTG),IS=1,6)
    IF(ITOTG.EQ.IGP3)WRITE(8,940)ISTEP,(STRES(IS,ITOTG),IS=1,6)
100  CONTINUE
  ENDIF
ENDIF
C ***      OUTPUT TO TAPE FOR PLOTTING          ***
IF(NOUTD.EQ.0) RETURN
KOUND=IABS((ISTEP/NOUTD)*NOUTD)
IF(KOUND.NE.ISTEP) RETURN
IF(KTOLE.EQ.0.AND.NOUTD.GT.0) RETURN
IINCS=IINCS+1
WRITE(10,950) IINCS,TTIME
C ***      OUTPUT ALL DISPLACEMENTS          ***
IF(NOUTD.LT.0) THEN
  WRITE(10,955)
  DO 115 IPOIN=1,NPOIN
    NPOSN=(IPOIN-1)*3+1
    NPOSM=NPOSN+3-1
115  WRITE(10,956) IPOIN,(TDISP(IPOSN),IPOSN=NPOSN,NPOSM)
  ENDIF
C ***      WRITE OUT MATERIAL STATE          ***
DO 120 IELEM = 1,NELEM
  WRITE(10,960) IELEM
  PI=4.0*ATAN(1.0)
  DO 120 IGAUS = 1,27
    IGAUG=(IELEM-1)*27+IGAUS
    ALPH1=ALPHI(1,IGAUG)*180./PI
    ALPH2=ALPHI(2,IGAUG)*180./PI
    ALPH3=ALPHI(3,IGAUG)*180./PI
    ALPH4=ALPHI(4,IGAUG)*180./PI
120  WRITE(10,970) IGAUG,ISTAT(IGAUG),ALPH1,ALPH2,ALPH3,ALPH4,
    & (GPCOD(IDIME,IGAUG),IDIME=1,3)
C-----
900 FORMAT(5X, 'RESULTS AT TIME ',F14.7,5X,' ISTEP =',I8)
910 FORMAT(5X, 'DISPLACEMENTS',/1X,'NNODE',3X,
. 'X-DISP',6X,'Y-DISP',6X,'Z-DISP',/)
920 FORMAT(2(1X,I8,3E12.5))
930 FORMAT(5X,'STRESSES',/1X,' G.P.',3X,'X-STRE',6X,'Y-STRES',
. 6X,'Z-STRES',6X,'XZ-STR',6X,'YZ-STR',6X,'XY-STR',/)
940 FORMAT(1X,I8,6E12.5)
950 FORMAT(/5X,'INCREMENT NUMBER ',I5,5X,'AT TIME',F10.5)
955 FORMAT(/10X,'DISPLACEMENTS')
956 FORMAT(1H0,5X,I5,10X,3F12.5)
957  FORMAT(/10X,'RELATIVE DISPLACEMENTS OF STUDS')
958  FORMAT(1H0,5X,I5,10X,3F12.5)
960 FORMAT(1H0,10X,'ELEMENT NUMBER',I5/9X,19('*))' G.P.',
. ' ISTAT  ALPHI1  ALPHI2  ALPHI3 ',
. ' ALPHI4',4X,'G.P. X  G.P. Y  ',G.P. Z  ')
970 FORMAT(1H ,I3,1X,I12,4(1X,F12.5),1X,3F9.3)
977 FORMAT(1H ,I3,1X,I12,4(1X,F12.5),1X,3F9.3)
979  FORMAT(1H ,1X,30(1X,F12.5))
RETURN
END

```

Appendix (G)

The Input Data for Composite Horizontally Curved
Beam of 345 Brick Element

"Ex3-Dynamic-Composite Curved Beam"

2232,345,14,3,0,2

1,1,0,1,8,12,13,14,9,3,2,103,107,108,104,143,150,154,155,156,151,145,144
 2,1,0,3,9,14,15,16,10,5,4,104,108,109,105,145,151,156,157,158,152,147,146
 3,1,0,5,10,16,17,18,11,7,6,105,109,110,106,147,152,158,159,160,153,149,148
 4,1,0,14,19,21,22,23,20,16,15,108,111,112,109,156,161,163,164,165,162,158,157
 5,1,0,21,24,26,27,28,25,23,22,111,113,114,112,163,166,168,169,170,167,165,164
 6,1,0,26,29,33,34,35,30,28,27,113,116,117,114,168,171,175,176,177,172,170,169
 7,1,0,31,38,46,47,48,39,33,32,115,121,122,116,173,180,188,189,190,181,175,174
 8,1,0,33,39,48,49,50,40,35,34,116,122,123,117,175,181,190,191,192,182,177,176
 9,1,0,35,40,50,51,52,41,37,36,117,123,124,118,177,182,192,193,194,183,179,178
 10,2,2,42,57,65,66,67,58,44,43,119,127,128,120,184,199,207,208,209,200,186,185
 11,2,2,44,58,67,68,69,59,46,45,120,128,129,121,186,200,209,210,211,201,188,187
 12,2,2,46,59,69,70,71,60,48,47,121,129,130,122,188,201,211,212,213,202,190,189
 13,2,2,48,60,71,72,73,61,50,49,122,130,131,123,190,202,213,214,215,203,192,191
 14,2,2,50,61,73,74,75,62,52,51,123,131,132,124,192,203,215,216,217,204,194,193
 15,2,2,52,62,75,76,77,63,54,53,124,132,133,125,194,204,217,218,219,205,196,195
 16,2,2,54,63,77,78,79,64,56,55,125,133,134,126,196,205,219,220,221,206,198,197
 17,2,1,65,80,88,89,90,81,67,66,127,135,136,128,207,222,230,231,232,223,209,208
 18,2,1,67,81,90,91,92,82,69,68,128,136,137,129,209,223,232,233,234,224,211,210
 19,2,1,69,82,92,93,94,83,71,70,129,137,138,130,211,224,234,235,236,225,213,212
 20,2,1,71,83,94,95,96,84,73,72,130,138,139,131,213,225,236,237,238,226,215,214
 21,2,1,73,84,96,97,98,85,75,74,131,139,140,132,215,226,238,239,240,227,217,216
 22,2,1,75,85,98,99,100,86,77,76,132,140,141,133,217,227,240,241,242,228,219,218
 23,2,1,77,86,100,101,102,87,79,78,133,141,142,134,219,228,242,243,244,229,221,220
 24,1,0,143,150,154,155,156,151,145,144,245,249,250,246,285,292,296,297,298,293,287,286
 25,1,0,145,151,156,157,158,152,147,146,246,250,251,247,287,293,298,299,300,294,289,288
 26,1,0,147,152,158,159,160,153,149,148,247,251,252,248,289,294,300,301,302,295,291,290
 27,1,0,156,161,163,164,165,162,158,157,250,253,254,251,298,303,305,306,307,304,300,299
 28,1,0,163,166,168,169,170,167,165,164,253,255,256,254,305,308,310,311,312,309,307,306
 29,1,0,168,171,175,176,177,172,170,169,255,258,259,256,310,313,317,318,319,314,312,311
 30,1,0,173,180,188,189,190,181,175,174,257,263,264,258,315,322,330,331,332,323,317,316
 31,1,0,175,181,190,191,192,182,177,176,258,264,265,259,317,323,332,333,334,324,319,318
 32,1,0,177,182,192,193,194,183,179,178,259,265,266,260,319,324,334,335,336,325,321,320
 33,2,2,184,199,207,208,209,200,186,185,261,269,270,262,326,341,349,350,351,342,328,327
 34,2,2,186,200,209,210,211,201,188,187,262,270,271,263,328,342,351,352,353,343,330,329
 35,2,2,188,201,211,212,213,202,190,189,263,271,272,264,330,343,353,354,355,344,332,331
 36,2,2,190,202,213,214,215,203,192,191,264,272,273,265,332,344,355,356,357,345,334,333
 37,2,2,192,203,215,216,217,204,194,193,265,273,274,266,334,345,357,358,359,346,336,335
 38,2,2,194,204,217,218,219,205,196,195,266,274,275,267,336,346,359,360,361,347,338,337
 39,2,2,196,205,219,220,221,206,198,197,267,275,276,268,338,347,361,362,363,348,340,339
 40,2,1,207,222,230,231,232,223,209,208,269,277,278,270,349,364,372,373,374,365,351,350
 41,2,1,209,223,232,233,234,224,211,210,270,278,279,271,351,365,374,375,376,366,353,352
 42,2,1,211,224,234,235,236,225,213,212,271,279,280,272,353,366,376,377,378,367,355,354
 43,2,1,213,225,236,237,238,226,215,214,272,280,281,273,355,367,378,379,380,368,357,356
 44,2,1,215,226,238,239,240,227,217,216,273,281,282,274,357,368,380,381,382,369,359,358
 45,2,1,217,227,240,241,242,228,219,218,274,282,283,275,359,369,382,383,384,370,361,360
 46,2,1,219,228,242,243,244,229,221,220,275,283,284,276,361,370,384,385,386,371,363,362
 47,1,0,285,292,296,297,298,293,287,286,387,391,392,388,427,434,438,439,440,435,429,428
 48,1,0,287,293,298,299,300,294,289,288,388,392,393,389,429,435,440,441,442,436,431,430
 49,1,0,289,294,300,301,302,295,291,290,389,393,394,390,431,436,442,443,444,437,433,432
 50,1,0,298,303,305,306,307,304,300,299,392,395,396,393,440,445,447,448,449,446,442,441
 51,1,0,305,308,310,311,312,309,307,306,395,397,398,396,447,450,452,453,454,451,449,448
 52,1,0,310,313,317,318,319,314,312,311,397,400,401,398,452,455,459,460,461,456,454,453
 53,1,0,315,322,330,331,332,323,317,316,399,405,406,400,457,464,472,473,474,465,459,458
 54,1,0,317,323,332,333,334,324,319,318,400,406,407,401,459,465,474,475,476,466,461,460
 55,1,0,319,324,334,335,336,325,321,320,401,407,408,402,461,466,476,477,478,467,463,462
 56,2,2,326,341,349,350,351,342,328,327,403,411,412,404,468,483,491,492,493,484,470,469
 57,2,2,328,342,351,352,353,343,330,329,404,412,413,405,470,484,493,494,495,485,472,471
 58,2,2,330,343,353,354,355,344,332,331,405,413,414,406,472,485,495,496,497,486,474,473
 59,2,2,332,344,355,356,357,345,334,333,406,414,415,407,474,486,497,498,499,487,476,475
 60,2,2,334,345,357,358,359,346,336,335,407,415,416,408,476,487,499,500,501,488,478,477
 61,2,2,336,346,359,360,361,347,338,337,408,416,417,409,478,488,501,502,503,489,480,479

62,2,2,338,347,361,362,363,348,340,339,409,417,418,410,480,489,503,504,505,490,482,481
63,2,1,349,364,372,373,374,365,351,350,411,419,420,412,491,506,514,515,516,507,493,492
64,2,1,351,365,374,375,376,366,353,352,412,420,421,413,493,507,516,517,518,508,495,494
65,2,1,353,366,376,377,378,367,355,354,413,421,422,414,495,508,518,519,520,509,497,496
66,2,1,355,367,378,379,380,368,357,356,414,422,423,415,497,509,520,521,522,510,499,498
67,2,1,357,368,380,381,382,369,359,358,415,423,424,416,499,510,522,523,524,511,501,500
68,2,1,359,369,382,383,384,370,361,360,416,424,425,417,501,511,524,525,526,512,503,502
69,2,1,361,370,384,385,386,371,363,362,417,425,426,418,503,512,526,527,528,513,505,504
70,1,0,427,434,438,439,440,435,429,428,529,533,534,530,569,576,580,581,582,577,571,570
71,1,0,429,435,440,441,442,436,431,430,530,534,535,531,571,577,582,583,584,578,573,572
72,1,0,431,436,442,443,444,437,433,432,531,535,536,532,573,578,584,585,586,579,575,574
73,1,0,440,445,447,448,449,446,442,441,534,537,538,535,582,587,589,590,591,588,584,583
74,1,0,447,450,452,453,454,451,449,448,537,539,540,538,589,592,594,595,596,593,591,590
75,1,0,452,455,459,460,461,456,454,453,539,542,543,540,594,597,601,602,603,598,596,595
76,1,0,457,464,472,473,474,465,459,458,541,547,548,542,599,606,614,615,616,607,601,600
77,1,0,459,465,474,475,476,466,461,460,542,548,549,543,601,607,616,617,618,608,603,602
78,1,0,461,466,474,477,478,467,463,462,543,549,550,544,603,608,618,619,620,609,605,604
79,2,2,468,483,491,492,493,484,470,469,545,553,554,546,610,625,633,634,635,626,612,611
80,2,2,470,484,493,494,495,485,472,471,546,554,555,547,612,626,635,636,637,627,614,613
81,2,2,472,485,495,496,497,486,474,473,547,555,556,548,614,627,637,638,639,628,616,615
82,2,2,474,486,497,498,499,487,476,475,548,556,557,549,616,628,639,640,641,629,618,617
83,2,2,476,487,499,500,501,488,478,477,549,557,558,550,618,629,641,642,643,630,620,619
84,2,2,478,488,501,502,503,489,480,479,550,558,559,551,620,630,643,644,645,631,622,621
85,2,2,480,489,503,504,505,490,482,481,551,559,560,552,622,631,645,646,647,632,624,623
86,2,1,491,506,514,515,516,507,493,492,553,561,562,554,633,648,656,657,658,649,635,634
87,2,1,493,507,516,517,518,508,495,494,554,562,563,555,635,649,658,659,660,650,637,636
88,2,1,495,508,518,519,520,509,497,496,555,563,564,556,637,650,660,661,662,651,639,638
89,2,1,497,509,520,521,522,510,499,498,556,564,565,557,639,651,662,663,664,652,641,640
90,2,1,499,510,522,523,524,511,501,500,557,565,566,558,641,652,664,665,666,653,643,642
91,2,1,501,511,524,525,526,512,503,502,558,566,567,559,643,653,666,667,668,654,645,644
92,2,1,503,512,526,527,528,513,505,504,559,567,568,560,645,654,668,669,670,655,647,646
93,1,0,569,576,580,581,582,577,571,570,671,675,676,672,711,718,722,723,724,719,713,712
94,1,0,571,577,582,583,584,578,573,572,672,676,677,673,713,719,724,725,726,720,715,714
95,1,0,573,578,584,585,586,579,575,574,673,677,678,674,715,720,726,727,728,721,717,716
96,1,0,582,587,589,590,591,588,584,583,676,679,680,677,724,729,731,732,733,730,726,725
97,1,0,589,592,594,595,596,593,591,590,679,681,682,680,731,734,736,737,738,735,733,732
98,1,0,594,597,601,602,603,598,596,595,681,684,685,682,736,739,743,744,745,740,738,737
99,1,0,599,606,614,615,616,607,601,600,683,689,690,684,741,748,756,757,758,749,743,742
100,1,0,601,607,616,617,618,608,603,602,684,690,691,685,743,749,758,759,760,750,745,744
101,1,0,603,608,618,619,620,609,605,604,685,691,692,686,745,750,760,761,762,751,747,746
102,2,2,610,625,633,634,635,626,612,611,687,695,696,688,752,767,775,776,777,768,754,753
103,2,2,612,626,635,636,637,627,614,613,688,696,697,689,754,768,777,778,779,769,756,755
104,2,2,614,627,637,638,639,628,616,615,689,697,698,690,756,769,779,780,781,770,758,757
105,2,2,616,628,639,640,641,629,618,617,690,698,699,691,758,770,781,782,783,771,760,759
106,2,2,618,629,641,642,643,630,620,619,691,699,700,692,760,771,783,784,785,772,762,761
107,2,2,620,630,643,644,645,631,622,621,692,700,701,693,762,772,785,786,787,773,764,763
108,2,2,622,631,645,646,647,632,624,623,693,701,702,694,764,773,787,788,789,774,766,765
109,2,1,633,648,656,657,658,649,635,634,695,703,704,696,775,790,798,799,800,791,777,776
110,2,1,635,649,658,659,660,650,637,636,696,704,705,697,777,791,800,801,802,792,779,778
111,2,1,637,650,660,661,662,651,639,638,697,705,706,698,779,792,802,803,804,793,781,780
112,2,1,639,651,662,663,664,652,641,640,698,706,707,699,781,793,804,805,806,794,783,782
113,2,1,641,652,664,665,666,653,643,642,699,707,708,700,783,794,806,807,808,795,785,784
114,2,1,643,653,666,667,668,654,645,644,700,708,709,701,785,795,808,809,810,796,787,786
115,2,1,645,654,668,669,670,655,647,646,701,709,710,702,787,796,810,811,812,797,789,788
116,1,0,711,718,722,723,724,719,713,712,813,817,818,814,853,860,864,865,866,861,855,854
117,1,0,713,719,724,725,726,720,715,714,814,818,819,815,855,861,866,867,868,862,857,856
118,1,0,715,720,726,727,728,721,717,716,815,819,820,816,857,862,868,869,870,863,859,858
119,1,0,724,729,731,732,733,730,726,725,818,821,822,819,866,871,873,874,875,872,868,867
120,1,0,731,734,736,737,738,735,733,732,821,823,824,822,873,876,878,879,880,877,875,874
121,1,0,736,739,743,744,745,740,738,737,823,826,827,824,878,881,885,886,887,882,880,879
122,1,0,741,748,756,757,758,749,743,742,825,831,832,826,883,890,898,899,900,891,885,884
123,1,0,743,749,758,759,760,750,745,744,826,832,833,827,885,891,900,901,902,892,887,886
124,1,0,745,750,760,761,762,751,747,746,827,833,834,828,887,892,902,903,904,893,889,888
125,2,2,752,767,775,776,777,768,754,753,829,837,838,830,894,909,917,918,919,910,896,895
126,2,2,754,768,777,778,779,769,756,755,830,838,839,831,896,910,919,920,921,911,898,897
127,2,2,756,769,779,780,781,770,758,757,831,839,840,832,898,911,921,922,923,912,900,899
128,2,2,758,770,781,782,783,771,760,759,832,840,841,833,900,912,923,924,925,913,902,901
129,2,2,760,771,783,784,785,772,762,761,833,841,842,834,902,913,925,926,927,914,904,903
130,2,2,762,772,785,786,787,773,764,763,834,842,843,835,904,914,927,928,929,915,906,905
131,2,2,764,773,787,788,789,774,766,765,835,843,844,836,906,915,929,930,931,916,908,907
132,2,1,775,790,798,799,800,791,777,776,837,845,846,838,917,932,940,941,942,933,919,918
133,2,1,777,791,800,801,802,792,779,778,838,846,847,839,919,933,942,943,944,934,921,920

134,2,1,779,792,802,803,804,793,781,780,839,847,848,840,921,934,944,945,946,935,923,922
 135,2,1,781,793,804,805,806,794,783,782,840,848,849,841,923,935,946,947,948,936,925,924
 136,2,1,783,794,806,807,808,795,785,784,841,849,850,842,925,936,948,949,950,937,927,926
 137,2,1,785,795,808,809,810,796,787,786,842,850,851,843,927,937,950,951,952,938,929,928
 138,2,1,787,796,810,811,812,797,789,788,843,851,852,844,929,938,952,953,954,939,931,930
 139,1,0,853,860,864,865,866,861,855,854,955,959,960,956,995,1002,1006,1007,1008,1003,997,996
 140,1,0,855,861,866,867,868,862,857,856,956,960,961,957,997,1003,1008,1009,1010,1004,999,998
 141,1,0,857,862,868,869,870,863,859,858,957,961,962,958,999,1004,1010,1011,1012,1005,1001,1000
 142,1,0,866,871,873,874,875,872,868,867,960,963,964,961,1008,1013,1015,1016,1017,1014,1010,1009
 143,1,0,873,876,878,879,880,877,875,874,963,965,966,964,1015,1018,1020,1021,1022,1019,1017,1016
 144,1,0,878,881,885,886,887,882,880,879,965,968,969,966,1020,1023,1027,1028,1029,1024,1022,1021
 145,1,0,883,890,898,899,900,891,885,884,967,973,974,968,1025,1032,1040,1041,1042,1033,1027,1026
 146,1,0,885,891,900,901,902,892,887,886,968,974,975,969,1027,1033,1042,1043,1044,1034,1029,1028
 147,1,0,887,892,902,903,904,893,889,888,969,975,976,970,1029,1034,1044,1045,1046,1035,1031,1030
 148,2,2,894,909,917,918,919,910,896,895,971,979,980,972,1036,1051,1059,1060,1061,1052,1038,1037
 149,2,2,896,910,919,920,921,911,898,897,972,980,981,973,1038,1052,1061,1062,1063,1053,1040,1039
 150,2,2,898,911,921,922,923,912,900,899,973,981,982,974,1040,1053,1063,1064,1065,1054,1042,1041
 151,2,2,900,912,923,924,925,913,902,901,974,982,983,975,1042,1054,1065,1066,1067,1055,1044,1043
 152,2,2,902,913,925,926,927,914,904,903,975,983,984,976,1044,1055,1067,1068,1069,1056,1046,1045
 153,2,2,904,914,927,928,929,915,906,905,976,984,985,977,1046,1056,1069,1070,1071,1057,1048,1047
 154,2,2,906,915,929,930,931,916,908,907,977,985,986,978,1048,1057,1071,1072,1073,1058,1050,1049
 155,2,1,917,932,940,941,942,933,919,918,979,987,988,980,1059,1074,1082,1083,1084,1075,1061,1060
 156,2,1,919,933,942,943,944,934,921,920,980,988,989,981,1061,1075,1084,1085,1086,1076,1063,1062
 157,2,1,921,934,944,945,946,935,923,922,981,989,990,982,1063,1076,1086,1087,1088,1077,1065,1064
 158,2,1,923,935,946,947,948,936,925,924,982,990,991,983,1065,1077,1088,1089,1090,1078,1067,1066
 159,2,1,925,936,948,949,950,937,927,926,983,991,992,984,1067,1078,1090,1091,1092,1079,1069,1068
 160,2,1,927,937,950,951,952,938,929,928,984,992,993,985,1069,1079,1092,1093,1094,1080,1071,1070
 161,2,1,929,938,952,953,954,939,931,930,985,993,994,986,1071,1080,1094,1095,1096,1081,1073,1072
 162,1,0,995,1002,1006,1007,1008,1003,997,996,1097,1101,1102,1098,1137,1144,1148,1149,1150,1145,1139,1138
 163,1,0,997,1003,1008,1009,1010,1004,999,998,1098,1102,1103,1099,1139,1145,1150,1151,1152,1146,1141,1140
 164,1,0,999,1004,1010,1011,1012,1005,1001,1000,1099,1103,1104,1100,1141,1146,1152,1153,1154,1147,1143,1142
 165,1,0,1008,1013,1015,1016,1017,1014,1010,1009,1102,1105,1106,1103,1150,1155,1157,1158,1159,1156,1152,1151
 166,1,0,1015,1018,1020,1021,1022,1019,1017,1016,1105,1107,1108,1106,1157,1160,1162,1163,1164,1161,1159,1158
 167,1,0,1020,1023,1027,1028,1029,1024,1022,1021,1107,1110,1111,1108,1162,1165,1169,1170,1171,1166,1164,1163
 168,1,0,1025,1032,1040,1041,1042,1033,1027,1026,1109,1115,1116,1110,1167,1174,1182,1183,1184,1175,1169,1168
 169,1,0,1027,1033,1042,1043,1044,1034,1029,1028,1110,1116,1117,1111,1169,1175,1184,1185,1186,1176,1171,1170
 170,1,0,1029,1034,1044,1045,1046,1035,1031,1030,1111,1117,1118,1112,1171,1176,1186,1187,1188,1177,1173,1172
 171,2,2,1036,1051,1059,1060,1061,1052,1038,1037,1113,1121,1122,1114,1178,1193,1201,1202,1203,1194,1180,1179
 172,2,2,1038,1052,1061,1062,1063,1053,1040,1039,1114,1122,1123,1115,1180,1194,1203,1204,1205,1195,1182,1181
 173,2,2,1040,1053,1063,1064,1065,1054,1042,1041,1115,1123,1124,1116,1182,1195,1205,1206,1207,1196,1184,1183
 174,2,2,1042,1054,1065,1066,1067,1055,1044,1043,1116,1124,1125,1117,1184,1196,1207,1208,1209,1197,1186,1185
 175,2,2,1044,1055,1067,1068,1069,1056,1046,1045,1117,1125,1126,1118,1186,1197,1209,1210,1211,1198,1188,1187
 176,2,2,1046,1056,1069,1070,1071,1057,1048,1047,1118,1126,1127,1119,1188,1198,1211,1212,1213,1199,1190,1189
 177,2,2,1048,1057,1071,1072,1073,1058,1050,1049,1119,1127,1128,1120,1190,1199,1213,1214,1215,1200,1192,1191
 178,2,1,1059,1074,1082,1083,1084,1075,1061,1060,1121,1129,1130,1122,1201,1216,1224,1225,1226,1217,1203,1202
 179,2,1,1061,1075,1084,1085,1086,1076,1063,1062,1122,1130,1131,1123,1203,1217,1226,1227,1228,1218,1205,1204
 180,2,1,1063,1076,1086,1087,1088,1077,1065,1064,1123,1131,1132,1124,1205,1218,1228,1229,1230,1219,1207,1206
 181,2,1,1065,1077,1088,1089,1090,1078,1067,1066,1124,1132,1133,1125,1207,1219,1230,1231,1232,1220,1209,1208
 182,2,1,1067,1078,1090,1091,1092,1079,1069,1068,1125,1133,1134,1126,1209,1220,1232,1233,1234,1221,1211,1210
 183,2,1,1069,1079,1092,1093,1094,1080,1071,1070,1126,1134,1135,1127,1211,1221,1234,1235,1236,1222,1213,1212
 184,2,1,1071,1080,1094,1095,1096,1081,1073,1072,1127,1135,1136,1128,1213,1222,1236,1237,1238,1232,1215,1214
 185,1,0,1137,1144,1148,1149,1150,1145,1139,1138,1239,1243,1244,1240,1279,1286,1290,1291,1292,1287,1281,1280
 186,1,0,1139,1145,1150,1151,1152,1146,1141,1140,1240,1244,1245,1241,1281,1287,1292,1293,1294,1288,1283,1282
 187,1,0,1141,1146,1152,1153,1154,1147,1143,1142,1241,1245,1246,1242,1283,1288,1294,1295,1296,1289,1285,1284
 188,1,0,1150,1155,1157,1158,1159,1156,1152,1151,1244,1247,1248,1245,1292,1297,1299,1300,1301,1298,1294,1293
 189,1,0,1157,1160,1162,1163,1164,1161,1159,1158,1247,1249,1250,1248,1299,1302,1304,1305,1306,1303,1301,1300
 190,1,0,1162,1165,1169,1170,1171,1166,1164,1163,1249,1252,1253,1250,1304,1307,1311,1312,1313,1308,1306,1305
 191,1,0,1167,1174,1182,1183,1184,1175,1169,1168,1251,1257,1258,1252,1309,1316,1324,1325,1326,1317,1311,1310
 192,1,0,1169,1175,1184,1185,1186,1176,1171,1170,1252,1258,1259,1253,1311,1317,1326,1327,1328,1318,1313,1312
 193,1,0,1171,1176,1186,1187,1188,1177,1173,1172,1253,1259,1260,1254,1313,1318,1328,1329,1330,1319,1315,1314
 194,2,2,1178,1193,1201,1202,1203,1194,1180,1179,1255,1263,1264,1256,1320,1335,1343,1344,1345,1336,1322,1321
 195,2,2,1180,1194,1203,1204,1205,1195,1182,1181,1256,1264,1265,1257,1322,1336,1345,1346,1347,1337,1324,1323
 196,2,2,1182,1195,1205,1206,1207,1196,1184,1183,1257,1265,1266,1258,1324,1337,1347,1348,1349,1338,1326,1325
 197,2,2,1184,1196,1207,1208,1209,1197,1186,1185,1258,1266,1267,1259,1326,1338,1349,1350,1351,1339,1328,1327
 198,2,2,1186,1197,1209,1210,1211,1198,1188,1187,1259,1267,1268,1260,1328,1339,1351,1352,1353,1340,1330,1329
 199,2,2,1188,1198,1211,1212,1213,1199,1190,1189,1260,1268,1269,1261,1330,1340,1353,1354,1355,1341,1332,1331
 200,2,2,1190,1199,1213,1214,1215,1200,1192,1191,1261,1269,1270,1262,1332,1341,1355,1356,1357,1342,1334,1333
 201,2,1,1201,1216,1224,1225,1226,1217,1203,1202,1263,1271,1272,1264,1343,1358,1366,1367,1368,1359,1345,1344
 202,2,1,1203,1217,1226,1227,1228,1218,1205,1204,1264,1272,1273,1265,1345,1359,1368,1369,1370,1360,1347,1346
 203,2,1,1205,1218,1228,1229,1230,1219,1207,1206,1265,1273,1274,1266,1347,1360,1370,1371,1372,1361,1349,1348
 204,2,1,1207,1219,1230,1231,1232,1220,1209,1208,1266,1274,1275,1267,1349,1361,1372,1373,1374,1362,1351,1350
 205,2,1,1209,1220,1232,1233,1234,1221,1211,1210,1267,1275,1276,1268,1351,1362,1374,1375,1376,1363,1353,1352

206,2,1,1211,1221,1234,1235,1236,1222,1213,1212,1268,1276,1277,1269,1353,1363,1376,1377,1378,1364,1355,1354
207,2,1,1213,1222,1236,1237,1238,1223,1215,1214,1269,1277,1278,1270,1355,1364,1378,1379,1380,1365,1357,1356
208,1,0,1279,1286,1290,1291,1292,1287,1281,1280,1381,1385,1386,1382,1421,1428,1432,1433,1434,1429,1423,1422
209,1,0,1281,1287,1292,1293,1294,1288,1283,1282,1382,1386,1387,1383,1423,1429,1434,1435,1436,1430,1425,1424
210,1,0,1283,1288,1294,1295,1296,1289,1285,1284,1383,1387,1388,1384,1425,1430,1436,1437,1438,1431,1427,1426
211,1,0,1292,1297,1299,1300,1301,1298,1294,1293,1386,1389,1390,1387,1434,1439,1441,1442,1443,1440,1436,1435
212,1,0,1299,1302,1304,1305,1306,1303,1301,1300,1389,1391,1392,1390,1441,1444,1446,1447,1448,1445,1443,1442
213,1,0,1304,1307,1311,1312,1313,1308,1306,1305,1391,1394,1395,1392,1446,1449,1453,1454,1455,1450,1448,1447
214,1,0,1309,1316,1324,1325,1326,1317,1311,1310,1393,1399,1400,1394,1451,1458,1466,1467,1468,1459,1453,1452
215,1,0,1311,1317,1326,1327,1328,1318,1313,1312,1394,1400,1401,1395,1453,1459,1468,1469,1470,1463,1455,1454
216,1,0,1313,1318,1328,1329,1330,1319,1315,1314,1395,1401,1402,1396,1455,1460,1470,1471,1472,1461,1457,1456
217,2,2,1320,1335,1343,1344,1345,1336,1322,1321,1397,1405,1406,1398,1462,1477,1485,1486,1487,1478,1464,1463
218,2,2,1322,1336,1345,1346,1347,1337,1324,1323,1398,1406,1407,1399,1464,1478,1487,1488,1489,1479,1466,1465
219,2,2,1324,1337,1347,1348,1349,1338,1326,1325,1399,1407,1408,1400,1466,1479,1489,1490,1491,1480,1468,1467
220,2,2,1326,1338,1349,1350,1351,1339,1328,1327,1400,1408,1409,1401,1468,1480,1491,1492,1493,1481,1470,1469
221,2,2,1328,1339,1351,1352,1353,1340,1330,1329,1401,1409,1410,1402,1470,1481,1493,1494,1495,1482,1472,1471
222,2,2,1330,1340,1353,1354,1355,1341,1332,1331,1402,1410,1411,1403,1472,1482,1495,1496,1472,1483,1474,1473
223,2,2,1332,1341,1355,1356,1357,1342,1334,1333,1403,1411,1412,1404,1474,1483,1497,1498,1499,1484,1476,1475
224,2,1,1343,1358,1366,1367,1368,1359,1345,1344,1405,1413,1414,1406,1485,1500,1508,1509,1510,1501,1487,1486
225,2,1,1345,1359,1368,1369,1370,1360,1347,1346,1406,1414,1415,1407,1487,1501,1510,1511,1512,1502,1489,1488
226,2,1,1347,1360,1370,1371,1372,1361,1349,1348,1407,1415,1416,1408,1489,1502,1512,1513,1514,1503,1491,1490
227,2,1,1349,1361,1372,1373,1374,1362,1351,1350,1408,1416,1417,1409,1491,1503,1514,1515,1516,1504,1493,1492
228,2,1,1351,1362,1374,1375,1376,1363,1353,1352,1409,1417,1418,1418,1410,1493,1504,1516,1517,1518,1505,1495,1494
229,2,1,1353,1363,1376,1377,1378,1364,1355,1354,1410,1418,1419,1411,1495,1505,1518,1519,1520,1506,1497,1496
230,2,1,1355,1364,1378,1379,1380,1365,1357,1356,1411,1419,1420,1412,1497,1506,1520,1521,1522,1507,1499,1498
231,1,0,1421,1428,1432,1433,1434,1429,1423,1422,1523,1527,1528,1524,1563,1570,1574,1575,1576,1571,1565,1564
232,1,0,1423,1429,1434,1435,1436,1430,1425,1424,1524,1528,1529,1525,1565,1571,1576,1577,1578,1572,1567,1566
233,1,0,1425,1430,1436,1437,1438,1431,1427,1426,1525,1529,1530,1526,1567,1572,1578,1579,1580,1573,1569,1568
234,1,0,1434,1439,1441,1442,1443,1440,1436,1435,1528,1531,1532,1529,1576,1581,1583,1584,1585,1582,1578,1577
235,1,0,1441,1444,1446,1447,1448,1445,1443,1442,1531,1533,1534,1532,1583,1586,1588,1589,1590,1587,1585,1584
236,1,0,1446,1449,1453,1454,1455,1450,1448,1447,1533,1536,1537,1534,1588,1591,1595,1596,1597,1592,1590,1589
237,1,0,1451,1458,1466,1467,1468,1459,1453,1452,1535,1541,1542,1536,1593,1600,1608,1609,1610,1601,1595,1594
238,1,0,1453,1459,1468,1469,1470,1460,1455,1454,1536,1542,1543,1537,1595,1601,1610,1611,1612,1602,1597,1596
239,1,0,1455,1460,1470,1471,1472,1461,1457,1456,1537,1543,1544,1538,1597,1602,1612,1613,1614,1603,1599,1598
240,2,2,1462,1477,1485,1486,1487,1478,1464,1463,1539,1547,1548,1540,1604,1619,1627,1628,1629,1620,1606,1605
241,2,2,1464,1478,1487,1488,1489,1479,1466,1465,1540,1548,1549,1541,1606,1620,1629,1630,1631,1621,1608,1607
242,2,2,1466,1479,1489,1490,1491,1480,1468,1467,1541,1549,1550,1542,1608,1621,1631,1632,1633,1622,1610,1609
243,2,2,1468,1480,1491,1492,1493,1481,1470,1469,1542,1550,1551,1543,1610,1622,1633,1634,1635,1623,1612,1611
244,2,2,1470,1481,1493,1494,1495,1482,1472,1471,1543,1551,1552,1544,1612,1623,1635,1636,1637,1624,1614,1613
245,2,2,1472,1482,1495,1496,1497,1483,1474,1473,1544,1552,1553,1545,1614,1624,1637,1638,1639,1625,1616,1615
246,2,2,1474,1483,1497,1498,1499,1484,1476,1475,1545,1553,1554,1546,1616,1625,1639,1640,1641,1626,1618,1617
247,2,1,1485,1500,1508,1509,1510,1501,1487,1486,1547,1555,1556,1548,1627,1642,1650,1651,1652,1643,1629,1628
248,2,1,1487,1501,1510,1511,1512,1502,1489,1488,1548,1556,1557,1549,1629,1643,1652,1653,1654,1644,1631,1630
249,2,1,1489,1502,1512,1513,1514,1503,1491,1490,1549,1557,1558,1550,1631,1644,1654,1655,1656,1645,1633,1632
250,2,1,1491,1503,1514,1515,1516,1504,1493,1492,1550,1558,1559,1551,1633,1645,1656,1657,1658,1646,1635,1634
251,2,1,1493,1504,1516,1517,1518,1505,1495,1494,1551,1559,1560,1552,1635,1646,1658,1659,1660,1647,1637,1636
252,2,1,1495,1505,1518,1519,1520,1506,1497,1496,1552,1560,1561,1553,1637,1647,1660,1661,1662,1648,1639,1638
253,2,1,1497,1506,1520,1521,1522,1507,1499,1498,1553,1561,1562,1554,1639,1648,1662,1663,1664,1649,1641,1640
254,1,0,1563,1570,1574,1575,1576,1571,1565,1564,1665,1669,1670,1666,1705,1712,1716,1717,1718,1713,1707,1706
255,1,0,1565,1571,1576,1577,1578,1572,1567,1566,1666,1670,1671,1667,1707,1713,1718,1719,1720,1714,1709,1708
256,1,0,1567,1572,1578,1579,1580,1573,1569,1568,1667,1671,1672,1668,1709,1714,1720,1721,1722,1715,1711,1710
257,1,0,1576,1581,1583,1584,1585,1582,1578,1577,1670,1673,1674,1671,1718,1723,1725,1726,1727,1724,1720,1719
258,1,0,1583,1586,1588,1589,1590,1587,1585,1584,1673,1675,1676,1674,1725,1728,1730,1731,1732,1729,1727,1726
259,1,0,1588,1591,1595,1596,1597,1592,1590,1589,1675,1678,1679,1676,1730,1733,1737,1738,1739,1734,1732,1731
260,1,0,1593,1600,1608,1609,1610,1601,1595,1594,1677,1683,1684,1678,1735,1742,1750,1751,1752,1743,1737,1736
261,1,0,1595,1601,1610,1611,1612,1602,1597,1596,1678,1684,1685,1679,1737,1743,1752,1753,1754,1744,1739,1738
262,1,0,1597,1602,1612,1613,1614,1603,1599,1598,1679,1685,1686,1680,1739,1744,1754,1755,1756,1745,1741,1740
263,2,2,1604,1619,1627,1628,1629,1620,1606,1605,1681,1689,1690,1682,1746,1761,1769,1770,1771,1762,1748,1747
264,2,2,1606,1620,1629,1630,1631,1621,1608,1607,1682,1690,1691,1683,1748,1762,1771,1772,1773,1763,1750,1749
265,2,2,1608,1621,1631,1632,1633,1622,1610,1609,1683,1691,1692,1684,1750,1763,1773,1774,1775,1764,1752,1751
266,2,2,1610,1622,1633,1634,1635,1623,1612,1611,1684,1692,1693,1685,1752,1764,1775,1776,1777,1765,1754,1753
267,2,2,1612,1623,1635,1636,1637,1624,1614,1613,1685,1693,1694,1686,1754,1765,1777,1778,1779,1766,1756,1755
268,2,2,1614,1624,1637,1638,1639,1625,1616,1615,1686,1694,1695,1687,1756,1766,1779,1780,1781,1767,1758,1757
269,2,2,1616,1625,1639,1640,1641,1626,1618,1617,1687,1695,1696,1688,1758,1767,1781,1782,1783,1768,1760,1759
270,2,1,1627,1642,1650,1651,1652,1643,1629,1628,1689,1697,1698,1690,1769,1784,1792,1793,1794,1785,1771,1770
271,2,1,1629,1643,1652,1653,1654,1644,1631,1630,1690,1698,1699,1691,1771,1785,1794,1795,1796,1786,1773,1772
272,2,1,1631,1644,1654,1655,1656,1645,1633,1632,1691,1699,1700,1692,1773,1786,1796,1797,1798,1787,1775,1774
273,2,1,1633,1645,1656,1657,1658,1646,1635,1634,1692,1700,1701,1693,1775,1787,1798,1799,1800,1788,1777,1776
274,2,1,1635,1646,1658,1659,1660,1647,1637,1636,1693,1701,1702,1694,1777,1788,1800,1801,1802,1789,1779,1778
275,2,1,1637,1647,1660,1661,1662,1648,1639,1638,1694,1702,1703,1695,1779,1789,1802,1803,1804,1790,1781,1780
276,2,1,1639,1648,1662,1663,1664,1649,1641,1640,1695,1703,1704,1696,1781,1790,1804,1805,1806,1791,1783,1782
277,1,0,1705,1712,1716,1717,1718,1713,1707,1706,1807,1811,1812,1808,1847,1854,1858,1859,1860,1855,1849,1848

278,1,0,1707,1713,1718,1719,1720,1714,1709,1708,1808,1812,1813,1809,1849,1855,1860,1861,1862,1856,1851,1850
 279,1,0,1709,1714,1720,1721,1722,1715,1711,1710,1809,1813,1814,1810,1851,1856,1862,1863,1864,1857,1853,1852
 280,1,0,1718,1723,1725,1726,1727,1724,1720,1719,1812,1815,1816,1813,1860,1865,1867,1868,1869,1866,1862,1861
 281,1,0,1725,1728,1730,1731,1732,1729,1727,1726,1815,1817,1818,1816,1867,1870,1872,1873,1874,1871,1869,1868
 282,1,0,1730,1733,1737,1738,1739,1734,1732,1731,1817,1820,1821,1818,1872,1875,1879,1880,1881,1876,1874,1873
 283,1,0,1735,1742,1750,1751,1752,1743,1737,1736,1819,1825,1826,1820,1877,1884,1892,1893,1894,1885,1879,1878
 284,1,0,1737,1743,1752,1753,1754,1744,1739,1738,1820,1826,1827,1821,1879,1885,1894,1895,1896,1886,1881,1880
 285,1,0,1739,1744,1754,1755,1756,1745,1741,1740,1821,1827,1828,1822,1881,1886,1896,1897,1898,1887,1883,1882
 286,2,2,1746,1761,1769,1770,1771,1762,1748,1747,1823,1831,1832,1824,1888,1903,1911,1912,1913,1904,1890,1889
 287,2,2,1748,1762,1771,1772,1773,1763,1750,1749,1824,1832,1833,1825,1890,1904,1913,1914,1915,1905,1892,1891
 288,2,2,1750,1763,1773,1774,1775,1764,1752,1751,1825,1833,1834,1826,1892,1905,1915,1916,1917,1906,1894,1893
 289,2,2,1752,1764,1775,1776,1777,1765,1754,1753,1826,1834,1835,1827,1894,1906,1917,1918,1919,1907,1896,1895
 290,2,2,1754,1765,1777,1778,1779,1766,1756,1755,1827,1835,1836,1828,1896,1907,1919,1920,1921,1908,1898,1897
 291,2,2,1756,1766,1779,1780,1781,1767,1758,1757,1828,1836,1837,1829,1898,1908,1921,1922,1923,1909,1900,1899
 292,2,2,1758,1767,1781,1782,1783,1768,1760,1759,1829,1837,1838,1830,1900,1909,1923,1924,1925,1910,1902,1901
 293,2,1,1769,1784,1792,1793,1794,1785,1771,1770,1831,1839,1840,1832,1911,1926,1934,1935,1936,1927,1913,1912
 294,2,1,1771,1785,1794,1795,1796,1786,1773,1772,1824,1840,1841,1833,1913,1927,1936,1937,1938,1928,1915,1914
 295,2,1,1773,1786,1796,1797,1798,1787,1775,1774,1833,1841,1842,1834,1915,1928,1938,1939,1940,1929,1917,1916
 296,2,1,1775,1787,1798,1799,1800,1788,1777,1776,1834,1842,1843,1835,1917,1929,1940,1941,1942,1930,1919,1918
 297,2,1,1777,1788,1800,1801,1802,1789,1779,1778,1835,1843,1844,1836,1919,1930,1942,1943,1944,1931,1921,1920
 298,2,1,1779,1789,1802,1803,1804,1790,1781,1780,1836,1844,1845,1837,1921,1931,1944,1945,1946,1932,1923,1922
 299,2,1,1781,1790,1804,1805,1806,1791,1783,1782,1837,1845,1846,1838,1923,1932,1946,1947,1948,1933,1925,1924
 300,1,0,1847,1854,1858,1859,1860,1855,1849,1848,1949,1953,1954,1950,1989,1996,2000,2001,2002,1997,1991,1990
 301,1,0,1849,1855,1860,1861,1862,1856,1851,1850,1950,1954,1955,1951,1991,1997,2002,2003,2004,1998,1993,1992
 302,1,0,1851,1856,1862,1863,1864,1857,1853,1852,1951,1955,1956,1952,1993,1998,2004,2005,2006,1999,1995,1994
 303,1,0,1860,1865,1867,1868,1869,1866,1862,1861,1954,1957,1958,1955,2002,2007,2009,2010,2011,2008,2004,2003
 304,1,0,1867,1870,1872,1873,1874,1871,1869,1868,1957,1959,1960,1958,2009,2012,2014,2015,2016,2013,2011,2010
 305,1,0,1872,1875,1879,1880,1881,1876,1874,1873,1959,1962,1963,1960,2014,2017,2021,2022,2023,2018,2016,2015
 306,1,0,1877,1884,1892,1893,1894,1885,1879,1878,1961,1967,1968,1962,2019,2026,2034,2035,2036,2027,2021,2020
 307,1,0,1879,1885,1894,1895,1896,1886,1881,1880,1962,1968,1969,1963,2021,2027,2036,2037,2038,2028,2023,2022
 308,1,0,1881,1886,1896,1897,1898,1887,1883,1882,1963,1969,1970,1964,2023,2028,2038,2039,2040,2029,2025,2024
 309,2,2,1888,1903,1911,1912,1913,1904,1890,1889,1965,1973,1974,1966,2030,2045,2053,2054,2055,2046,2032,2031
 310,2,2,1890,1904,1913,1914,1915,1905,1892,1891,1966,1974,1975,1967,2032,2046,2055,2056,2057,2047,2034,2033
 311,2,2,1892,1905,1915,1916,1917,1906,1894,1893,1967,1975,1976,1968,2034,2047,2057,2058,2059,2048,2036,2035
 312,2,2,1894,1906,1917,1918,1919,1907,1896,1895,1968,1976,1977,1969,2036,2048,2059,2060,2061,2049,2038,2037
 313,2,2,1896,1907,1919,1920,1921,1908,1898,1897,1969,1977,1978,1970,2038,2049,2061,2062,2063,2050,2040,2039
 314,2,2,1898,1908,1921,1922,1923,1909,1900,1899,1970,1978,1979,1971,2040,2050,2063,2064,2065,2051,2042,2041
 315,2,2,1900,1909,1923,1924,1925,1910,1902,1901,1971,1979,1980,1972,2042,2051,2065,2066,2067,2052,2044,2043
 316,2,1,1911,1926,1934,1935,1936,1927,1913,1912,1973,1981,1982,1974,2053,2068,2076,2077,2078,2069,2055,2054
 317,2,1,1913,1927,1936,1937,1938,1928,1915,1914,1974,1982,1983,1975,2055,2069,2078,2079,2080,2070,2057,2056
 318,2,1,1915,1928,1938,1939,1940,1929,1917,1916,1975,1983,1984,1976,2057,2070,2080,2081,2082,2071,2059,2058
 319,2,1,1917,1929,1940,1941,1942,1930,1919,1918,1976,1984,1985,1977,2059,2071,2082,2083,2084,2072,2061,2060
 320,2,1,1919,1930,1942,1943,1944,1931,1921,1920,1977,1985,1986,1978,2061,2072,2084,2085,2086,2073,2063,2062
 321,2,1,1921,1931,1944,1945,1946,1932,1923,1922,1978,1986,1987,1979,2063,2073,2086,2087,2088,2074,2065,2064
 322,2,1,1923,1932,1946,1947,1948,1933,1925,1924,1979,1987,1988,1980,2065,2074,2088,2089,2090,2075,2067,2066
 323,1,0,1989,1996,2000,2001,2002,1997,1991,1990,2091,2095,2096,2092,2131,2138,2142,2143,2144,2139,2133,2132
 324,1,0,1991,1997,2002,2003,2004,1998,1993,1992,2092,2096,2097,2093,2133,2139,2144,2145,2146,2140,2135,2134
 325,1,0,1993,1998,2004,2005,2006,1999,1995,1994,2093,2097,2098,2094,2135,2140,2146,2147,2148,2141,2137,2136
 326,1,0,2002,2007,2009,2010,2011,2008,2004,2003,2096,2099,2100,2097,2144,2149,2151,2152,2153,2150,2146,2145
 327,1,0,2009,2012,2014,2015,2016,2013,2011,2010,2099,2101,2102,2100,2151,2154,2156,2157,2158,2155,2153,2152
 328,1,0,2014,2017,2021,2022,2023,2018,2016,2015,2101,2104,2105,2102,2156,2159,2163,2164,2165,2160,2158,2157
 329,1,0,2019,2026,2034,2035,2036,2027,2021,2020,2103,2109,2110,2104,2161,2168,2176,2177,2178,2169,2163,2162
 330,1,0,2021,2027,2036,2037,2038,2028,2023,2022,2104,2110,2111,2105,2163,2169,2178,2179,2180,2170,2165,2164
 331,1,0,2023,2028,2038,2039,2040,2029,2025,2024,2105,2111,2112,2106,2165,2170,2180,2181,2182,2171,2167,2166
 332,2,2,2030,2045,2053,2054,2055,2046,2032,2031,2107,2115,2116,2108,2172,2187,2195,2196,2197,2188,2174,2173
 333,2,2,2032,2046,2055,2056,2057,2047,2034,2033,2108,2116,2117,2109,2174,2188,2197,2198,2199,2189,2176,2175
 334,2,2,2034,2047,2057,2058,2059,2048,2036,2035,2109,2117,2118,2110,2176,2189,2199,2200,2201,2190,2178,2177
 335,2,2,2036,2048,2059,2060,2061,2049,2038,2037,2110,2118,2119,2111,2178,2190,2201,2202,2203,2191,2180,2179
 336,2,2,2038,2049,2061,2062,2063,2050,2040,2039,2111,2119,2120,2112,2180,2191,2203,2204,2205,2192,2182,2181
 337,2,2,2040,2050,2063,2064,2065,2051,2042,2041,2112,2120,2121,2113,2182,2192,2205,2206,2207,2193,2184,2183
 338,2,2,2042,2051,2065,2066,2067,2052,2044,2043,2113,2121,2122,2114,2184,2193,2207,2208,2209,2194,2186,2185
 339,2,1,2053,2068,2076,2077,2078,2069,2055,2054,2115,2123,2124,2116,2195,2210,2218,2219,2220,2211,2197,2196
 340,2,1,2055,2069,2078,2079,2080,2070,2057,2056,2116,2124,2125,2117,2197,2211,2220,2221,2222,2212,2199,2198
 341,2,1,2057,2070,2080,2081,2082,2071,2059,2058,2117,2125,2126,2118,2199,2212,2222,2223,2224,2213,2201,2200
 342,2,1,2059,2071,2082,2083,2084,2072,2061,2060,2118,2126,2127,2119,2201,2213,2224,2225,2226,2214,2203,2202
 343,2,1,2061,2072,2084,2085,2086,2073,2063,2062,2119,2127,2128,2120,2203,2214,2226,2227,2228,2215,2205,2204
 344,2,1,2063,2073,2086,2087,2088,2074,2065,2064,2120,2128,2129,2121,2205,2215,2228,2229,2230,2216,2207,2206
 345,2,1,2065,2074,2088,2089,2090,2075,2067,2066,2121,2129,2130,2122,2207,2216,2230,2231,2232,2217,2209,2208

1	9960.0000	.0000	.0000
2	9977.5000	.0000	.0000
3	9995.0000	.0000	.0000

4	1000.0000	.0000	.0000
5	10005.0000	.0000	.0000
6	10022.5000	.0000	.0000
7	10040.0000	.0000	.0000
8	9960.0000	6.5000	.0000
9	9995.0000	6.5000	.0000
10	10005.0000	6.5000	.0000
11	10040.0000	6.5000	.0000
12	9960.0000	13.0000	.0000
13	9977.5000	13.0000	.0000
14	9995.0000	13.0000	.0000
15	10000.0000	13.0000	.0000
16	10005.0000	13.0000	.0000
17	10022.5000	13.0000	.0000
18	10040.0000	13.0000	.0000
19	9995.0000	38.0000	.0000
20	10005.0000	38.0000	.0000
21	9995.0000	63.0000	.0000
22	10000.0000	63.0000	.0000
23	10005.0000	63.0000	.0000
24	9995.0000	88.0000	.0000
25	10005.0000	88.0000	.0000
26	9995.0000	113.0000	.0000
27	10000.0000	113.0000	.0000
28	10005.0000	113.0000	.0000
29	9995.0000	138.0000	.0000
30	10005.0000	138.0000	.0000
31	9960.0000	163.0000	.0000
32	9977.5000	163.0000	.0000
33	9995.0000	163.0000	.0000
34	10000.0000	163.0000	.0000
35	10005.0000	163.0000	.0000
36	10022.5000	163.0000	.0000
37	10040.0000	163.0000	.0000
38	9960.0000	169.5000	.0000
39	9995.0000	169.5000	.0000
40	10005.0000	169.5000	.0000
41	10040.0000	169.5000	.0000
42	9695.0000	176.0000	.0000
43	9761.2500	176.0000	.0000
44	9827.5000	176.0000	.0000
45	9893.7500	176.0000	.0000
46	9960.0000	176.0000	.0000
47	9977.5000	176.0000	.0000
48	9995.0000	176.0000	.0000
49	10000.0000	176.0000	.0000
50	10005.0000	176.0000	.0000
51	10022.5000	176.0000	.0000
52	10040.0000	176.0000	.0000
53	10106.2500	176.0000	.0000
54	10172.5000	176.0000	.0000
55	10238.7500	176.0000	.0000
56	10305.0000	176.0000	.0000
57	9695.0000	191.0000	.0000
58	9827.5000	191.0000	.0000
59	9960.0000	191.0000	.0000
60	9995.0000	191.0000	.0000
61	10005.0000	191.0000	.0000
62	10040.0000	191.0000	.0000
63	10172.5000	191.0000	.0000
64	10305.0000	191.0000	.0000
65	9695.0000	206.0000	.0000
66	9761.2500	206.0000	.0000
67	9827.5000	206.0000	.0000
68	9893.7500	206.0000	.0000
69	9960.0000	206.0000	.0000
70	9977.5000	206.0000	.0000
71	9995.0000	206.0000	.0000
72	10000.0000	206.0000	.0000
73	10005.0000	206.0000	.0000
74	10022.5000	206.0000	.0000
75	10040.0000	206.0000	.0000

76	10106.2500	206.0000	.0000
77	10172.5000	206.0000	.0000
78	10238.7500	206.0000	.0000
79	10305.0000	206.0000	.0000
80	9695.0000	221.0000	.0000
81	9827.5000	221.0000	.0000
82	9960.0000	221.0000	.0000
83	9995.0000	221.0000	.0000
84	10005.0000	221.0000	.0000
85	10040.0000	221.0000	.0000
86	10172.5000	221.0000	.0000
87	10305.0000	221.0000	.0000
88	9695.0000	236.0000	.0000
89	9761.2500	236.0000	.0000
90	9827.5000	236.0000	.0000
91	9893.7500	236.0000	.0000
92	9960.0000	236.0000	.0000
93	9977.5000	236.0000	.0000
94	9995.0000	236.0000	.0000
95	10000.0000	236.0000	.0000
96	10005.0000	236.0000	.0000
97	10022.5000	236.0000	.0000
98	10040.0000	236.0000	.0000
99	10106.2500	236.0000	.0000
100	10172.5000	236.0000	.0000
101	10238.7500	236.0000	.0000
102	10305.0000	236.0000	.0000
103	9959.7199	.0000	74.7019
104	9994.7189	.0000	74.9644
105	10004.7186	.0000	75.0394
106	10039.7176	.0000	75.3019
107	9959.7199	13.0000	74.7019
108	9994.7189	13.0000	74.9644
109	10004.7186	13.0000	75.0394
110	10039.7176	13.0000	75.3019
111	9994.7189	63.0000	74.9644
112	10004.7186	63.0000	75.0394
113	9994.7189	113.0000	74.9644
114	10004.7186	113.0000	75.0394
115	9959.7199	163.0000	74.7019
116	9994.7189	163.0000	74.9644
117	10004.7186	163.0000	75.0394
118	10039.7176	163.0000	75.3019
119	9694.7273	176.0000	72.7144
120	9827.2236	176.0000	73.7081
121	9959.7199	176.0000	74.7019
122	9994.7189	176.0000	74.9644
123	10004.7186	176.0000	75.0394
124	10039.7176	176.0000	75.3019
125	10172.2139	176.0000	76.2957
126	10304.7102	176.0000	77.2895
127	9694.7273	206.0000	72.7144
128	9827.2236	206.0000	73.7081
129	9959.7199	206.0000	74.7019
130	9994.7189	206.0000	74.9644
131	10004.7186	206.0000	75.0394
132	10039.7176	206.0000	75.3019
133	10172.2139	206.0000	76.2957
134	10304.7102	206.0000	77.2895
135	9694.7273	236.0000	72.7144
136	9827.2236	236.0000	73.7081
137	9959.7199	236.0000	74.7019
138	9994.7189	236.0000	74.9644
139	10004.7186	236.0000	75.0394
140	10039.7176	236.0000	75.3019
141	10172.2139	236.0000	76.2957
142	10304.7102	236.0000	77.2895
143	9958.8794	.0000	149.3996
144	9976.3775	.0000	149.6621
145	9993.8755	.0000	149.9246
146	9998.8749	.0000	149.9996
147	10003.8744	.0000	150.0746

148	10021.3724	.0000	150.3371
149	10038.8704	.0000	150.5996
150	9958.8794	6.5000	149.3996
151	9993.8755	6.5000	149.9246
152	10003.8744	6.5000	150.0746
153	10038.8704	6.5000	150.5996
154	9958.8794	13.0000	149.3996
155	9976.3775	13.0000	149.6621
156	9993.8755	13.0000	149.9246
157	9998.8749	13.0000	149.9996
158	10003.8744	13.0000	150.0746
159	10021.3724	13.0000	150.3371
160	10038.8704	13.0000	150.5996
161	9993.8755	38.0000	149.9246
162	10003.8744	38.0000	150.0746
163	9993.8755	63.0000	149.9246
164	9998.8749	63.0000	149.9996
165	10003.8744	63.0000	150.0746
166	9993.8755	88.0000	149.9246
167	10003.8744	88.0000	150.0746
168	9993.8755	113.0000	149.9246
169	9998.8749	113.0000	149.9996
170	10003.8744	113.0000	150.0746
171	9993.8755	138.0000	149.9246
172	10003.8744	138.0000	150.0746
173	9958.8794	163.0000	149.3996
174	9976.3775	163.0000	149.6621
175	9993.8755	163.0000	149.9246
176	9998.8749	163.0000	149.9996
177	10003.8744	163.0000	150.0746
178	10021.3724	163.0000	150.3371
179	10038.8704	163.0000	150.5996
180	9958.8794	169.5000	149.3996
181	9993.8755	169.5000	149.9246
182	10003.8744	169.5000	150.0746
183	10038.8704	169.5000	150.5996
184	9693.9093	176.0000	145.4246
185	9760.1518	176.0000	146.4184
186	9826.3943	176.0000	147.4121
187	9892.6369	176.0000	148.4059
188	9958.8794	176.0000	149.3996
189	9976.3775	176.0000	149.6621
190	9993.8755	176.0000	149.9246
191	9998.8749	176.0000	149.9996
192	10003.8744	176.0000	150.0746
193	10021.3724	176.0000	150.3371
194	10038.8704	176.0000	150.5996
195	10105.1130	176.0000	151.5934
196	10171.3555	176.0000	152.5871
197	10237.5981	176.0000	153.5808
198	10303.8406	176.0000	154.5746
199	9693.9093	191.0000	145.4246
200	9826.3943	191.0000	147.4121
201	9958.8794	191.0000	149.3996
202	9993.8755	191.0000	149.9246
203	10003.8744	191.0000	150.0746
204	10038.8704	191.0000	150.5996
205	10171.3555	191.0000	152.5871
206	10303.8406	191.0000	154.5746
207	9693.9093	206.0000	145.4246
208	9760.1518	206.0000	146.4184
209	9826.3943	206.0000	147.4121
210	9892.6369	206.0000	148.4059
211	9958.8794	206.0000	149.3996
212	9976.3775	206.0000	149.6621
213	9993.8755	206.0000	149.9246
214	9998.8749	206.0000	149.9996
215	10003.8744	206.0000	150.0746
216	10021.3724	206.0000	150.3371
217	10038.8704	206.0000	150.5996
218	10105.1130	206.0000	151.5934
219	10171.3555	206.0000	152.5871

220	10237.5981	206.0000	153.5808
221	10303.8406	206.0000	154.5746
222	9693.9093	221.0000	145.4246
223	9826.3943	221.0000	147.4121
224	9958.8794	221.0000	149.3996
225	9993.8755	221.0000	149.9246
226	10003.8744	221.0000	150.0746
227	10038.8704	221.0000	150.5996
228	10171.3555	221.0000	152.5871
229	10303.8406	221.0000	154.5746
230	9693.9093	236.0000	145.4246
231	9760.1518	236.0000	146.4184
232	9826.3943	236.0000	147.4121
233	9892.6369	236.0000	148.4059
234	9958.8794	236.0000	149.3996
235	9976.3775	236.0000	149.6621
236	9993.8755	236.0000	149.9246
237	9998.8749	236.0000	149.9996
238	10003.8744	236.0000	150.0746
239	10021.3724	236.0000	150.3371
240	10038.8704	236.0000	150.5996
241	10105.1130	236.0000	151.5934
242	10171.3555	236.0000	152.5871
243	10237.5981	236.0000	153.5808
244	10303.8406	236.0000	154.5746
245	9957.4788	.0000	224.0889
246	9992.4699	.0000	224.8764
247	10002.4674	.0000	225.1014
248	10037.4586	.0000	225.8888
249	9957.4788	13.0000	224.0889
250	9992.4699	13.0000	224.8764
251	10002.4674	13.0000	225.1014
252	10037.4586	13.0000	225.8888
253	9992.4699	63.0000	224.8764
254	10002.4674	63.0000	225.1014
255	9992.4699	113.0000	224.8764
256	10002.4674	113.0000	225.1014
257	9957.4788	163.0000	224.0889
258	9992.4699	163.0000	224.8764
259	10002.4674	163.0000	225.1014
260	10037.4586	163.0000	225.8888
261	9692.5459	176.0000	218.1267
262	9825.0123	176.0000	221.1078
263	9957.4788	176.0000	224.0889
264	9992.4699	176.0000	224.8764
265	10002.4674	176.0000	225.1014
266	10037.4586	176.0000	225.8888
267	10169.9250	176.0000	228.8699
268	10302.3915	176.0000	231.8510
269	9692.5459	206.0000	218.1267
270	9825.0123	206.0000	221.1078
271	9957.4788	206.0000	224.0889
272	9992.4699	206.0000	224.8764
273	10002.4674	206.0000	225.1014
274	10037.4586	206.0000	225.8888
275	10169.9250	206.0000	228.8699
276	10302.3915	206.0000	231.8510
277	9692.5459	236.0000	218.1267
278	9825.0123	236.0000	221.1078
279	9957.4788	236.0000	224.0889
280	9992.4699	236.0000	224.8764
281	10002.4674	236.0000	225.1014
282	10037.4586	236.0000	225.8888
283	10169.9250	236.0000	228.8699
284	10302.3915	236.0000	231.8510
285	9955.5180	.0000	298.7656
286	9973.0101	.0000	299.2905
287	9990.5023	.0000	299.8155
288	9995.5000	.0000	299.9655
289	10000.4978	.0000	300.1154
290	10017.9899	.0000	300.6404
291	10035.4820	.0000	301.1653

292	9955.5180	6.5000	298.7656
293	9990.5023	6.5000	299.8155
294	10000.4978	6.5000	300.1154
295	10035.4820	6.5000	301.1653
296	9955.5180	13.0000	298.7656
297	9973.0101	13.0000	299.2905
298	9990.5023	13.0000	299.8155
299	9995.5000	13.0000	299.9655
300	10000.4978	13.0000	300.1154
301	10017.9899	13.0000	300.6404
302	10035.4820	13.0000	301.1653
303	9990.5023	38.0000	299.8155
304	10000.4978	38.0000	300.1154
305	9990.5023	63.0000	299.8155
306	9995.5000	63.0000	299.9655
307	10000.4978	63.0000	300.1154
308	9990.5023	88.0000	299.8155
309	10000.4978	88.0000	300.1154
310	9990.5023	113.0000	299.8155
311	9995.5000	113.0000	299.9655
312	10000.4978	113.0000	300.1154
313	9990.5023	138.0000	299.8155
314	10000.4978	138.0000	300.1154
315	9955.5180	163.0000	298.7656
316	9973.0101	163.0000	299.2905
317	9990.5023	163.0000	299.8155
318	9995.5000	163.0000	299.9655
319	10000.4978	163.0000	300.1154
320	10017.9899	163.0000	300.6404
321	10035.4820	163.0000	301.1653
322	9955.5180	169.5000	298.7656
323	9990.5023	169.5000	299.8155
324	10000.4978	169.5000	300.1154
325	10035.4820	169.5000	301.1653
326	9690.6373	176.0000	290.8165
327	9756.8575	176.0000	292.8038
328	9823.0776	176.0000	294.7911
329	9889.2978	176.0000	296.7783
330	9955.5180	176.0000	298.7656
331	9973.0101	176.0000	299.2905
332	9990.5023	176.0000	299.8155
333	9995.5000	176.0000	299.9655
334	10000.4978	176.0000	300.1154
335	10017.9899	176.0000	300.6404
336	10035.4820	176.0000	301.1653
337	10101.7022	176.0000	303.1526
338	10167.9224	176.0000	305.1399
339	10234.1426	176.0000	307.1271
340	10300.3628	176.0000	309.1144
341	9690.6373	191.0000	290.8165
342	9823.0776	191.0000	294.7911
343	9955.5180	191.0000	298.7656
344	9990.5023	191.0000	299.8155
345	10000.4978	191.0000	300.1154
346	10035.4820	191.0000	301.1653
347	10167.9224	191.0000	305.1399
348	10300.3628	191.0000	309.1144
349	9690.6373	206.0000	290.8165
350	9756.8575	206.0000	292.8038
351	9823.0776	206.0000	294.7911
352	9889.2978	206.0000	296.7783
353	9955.5180	206.0000	298.7656
354	9973.0101	206.0000	299.2905
355	9990.5023	206.0000	299.8155
356	9995.5000	206.0000	299.9655
357	10000.4978	206.0000	300.1154
358	10017.9899	206.0000	300.6404
359	10035.4820	206.0000	301.1653
360	10101.7022	206.0000	303.1526
361	10167.9224	206.0000	305.1399
362	10234.1426	206.0000	307.1271
363	10300.3628	206.0000	309.1144

364	9690.6373	221.0000	290.8165
365	9823.0776	221.0000	294.7911
366	9955.5180	221.0000	298.7656
367	9990.5023	221.0000	299.8155
368	10000.4978	221.0000	300.1154
369	10035.4820	221.0000	301.1653
370	10167.9224	221.0000	305.1399
371	10300.3628	221.0000	309.1144
372	9690.6373	236.0000	290.8165
373	9756.8575	236.0000	292.8038
374	9823.0776	236.0000	294.7911
375	9889.2978	236.0000	296.7783
376	9955.5180	236.0000	298.7656
377	9973.0101	236.0000	299.2905
378	9990.5023	236.0000	299.8155
379	9995.5000	236.0000	299.9655
380	10000.4978	236.0000	300.1154
381	10017.9899	236.0000	300.6404
382	10035.4820	236.0000	301.1653
383	10101.7022	236.0000	303.1526
384	10167.9224	236.0000	305.1399
385	10234.1426	236.0000	307.1271
386	10300.3628	236.0000	309.1144
387	9952.9972	.0000	373.4255
388	9987.9726	.0000	374.7377
389	9997.9656	.0000	375.1126
390	10032.9410	.0000	376.4249
391	9952.9972	13.0000	373.4255
392	9987.9726	13.0000	374.7377
393	9997.9656	13.0000	375.1126
394	10032.9410	13.0000	376.4249
395	9987.9726	63.0000	374.7377
396	9997.9656	63.0000	375.1126
397	9987.9726	113.0000	374.7377
398	9997.9656	113.0000	375.1126
399	9952.9972	163.0000	373.4255
400	9987.9726	163.0000	374.7377
401	9997.9656	163.0000	375.1126
402	10032.9410	163.0000	376.4249
403	9688.1835	176.0000	363.4900
404	9820.5904	176.0000	368.4577
405	9952.9972	176.0000	373.4255
406	9987.9726	176.0000	374.7377
407	9997.9656	176.0000	375.1126
408	10032.9410	176.0000	376.4249
409	10165.3478	176.0000	381.3926
410	10297.7546	176.0000	386.3604
411	9688.1835	206.0000	363.4900
412	9820.5904	206.0000	368.4577
413	9952.9972	206.0000	373.4255
414	9987.9726	206.0000	374.7377
415	9997.9656	206.0000	375.1126
416	10032.9410	206.0000	376.4249
417	10165.3478	206.0000	381.3926
418	10297.7546	206.0000	386.3604
419	9688.1835	236.0000	363.4900
420	9820.5904	236.0000	368.4577
421	9952.9972	236.0000	373.4255
422	9987.9726	236.0000	374.7377
423	9997.9656	236.0000	375.1126
424	10032.9410	236.0000	376.4249
425	10165.3478	236.0000	381.3926
426	10297.7546	236.0000	386.3604
427	9949.9165	.0000	448.0644
428	9967.3988	.0000	448.8516
429	9984.8811	.0000	449.6389
430	9989.8760	.0000	449.8638
431	9994.8709	.0000	450.0888
432	10012.3532	.0000	450.8760
433	10029.8355	.0000	451.6633
434	9949.9165	6.5000	448.0644
435	9984.8811	6.5000	449.6389

436	9994.8709	6.5000	450.0888
437	10029.8355	6.5000	451.6633
438	9949.9165	13.0000	448.0644
439	9967.3988	13.0000	448.8516
440	9984.8811	13.0000	449.6389
441	9989.8760	13.0000	449.8638
442	9994.8709	13.0000	450.0888
443	10012.3532	13.0000	450.8760
444	10029.8355	13.0000	451.6633
445	9984.8811	38.0000	449.6389
446	9994.8709	38.0000	450.0888
447	9984.8811	63.0000	449.6389
448	9989.8760	63.0000	449.8638
449	9994.8709	63.0000	450.0888
450	9984.8811	88.0000	449.6389
451	9994.8709	88.0000	450.0888
452	9984.8811	113.0000	449.6389
453	9989.8760	113.0000	449.8638
454	9994.8709	113.0000	450.0888
455	9984.8811	138.0000	449.6389
456	9994.8709	138.0000	450.0888
457	9949.9165	163.0000	448.0644
458	9967.3988	163.0000	448.8516
459	9984.8811	163.0000	449.6389
460	9989.8760	163.0000	449.8638
461	9994.8709	163.0000	450.0888
462	10012.3532	163.0000	450.8760
463	10029.8355	163.0000	451.6633
464	9949.9165	169.5000	448.0644
465	9984.8811	169.5000	449.6389
466	9994.8709	169.5000	450.0888
467	10029.8355	169.5000	451.6633
468	9685.1848	176.0000	436.1430
469	9751.3677	176.0000	439.1233
470	9817.5506	176.0000	442.1037
471	9883.7336	176.0000	445.0840
472	9949.9165	176.0000	448.0644
473	9967.3988	176.0000	448.8516
474	9984.8811	176.0000	449.6389
475	9989.8760	176.0000	449.8638
476	9994.8709	176.0000	450.0888
477	10012.3532	176.0000	450.8760
478	10029.8355	176.0000	451.6633
479	10096.0184	176.0000	454.6436
480	10162.2014	176.0000	457.6240
481	10228.3843	176.0000	460.6043
482	10294.5672	176.0000	463.5847
483	9685.1848	191.0000	436.1430
484	9817.5506	191.0000	442.1037
485	9949.9165	191.0000	448.0644
486	9984.8811	191.0000	449.6389
487	9994.8709	191.0000	450.0888
488	10029.8355	191.0000	451.6633
489	10162.2014	191.0000	457.6240
490	10294.5672	191.0000	463.5847
491	9685.1848	206.0000	436.1430
492	9751.3677	206.0000	439.1233
493	9817.5506	206.0000	442.1037
494	9883.7336	206.0000	445.0840
495	9949.9165	206.0000	448.0644
496	9967.3988	206.0000	448.8516
497	9984.8811	206.0000	449.6389
498	9989.8760	206.0000	449.8638
499	9994.8709	206.0000	450.0888
500	10012.3532	206.0000	450.8760
501	10029.8355	206.0000	451.6633
502	10096.0184	206.0000	454.6436
503	10162.2014	206.0000	457.6240
504	10228.3843	206.0000	460.6043
505	10294.5672	206.0000	463.5847
506	9685.1848	221.0000	436.1430
507	9817.5506	221.0000	442.1037

508	9949.9165	221.0000	448.0644
509	9984.8811	221.0000	449.6389
510	9994.8709	221.0000	450.0888
511	10029.8355	221.0000	451.6633
512	10162.2014	221.0000	457.6240
513	10294.5672	221.0000	463.5847
514	9685.1848	236.0000	436.1430
515	9751.3677	236.0000	439.1233
516	9817.5506	236.0000	442.1037
517	9883.7336	236.0000	445.0840
518	9949.9165	236.0000	448.0644
519	9967.3988	236.0000	448.8516
520	9984.8811	236.0000	449.6389
521	9989.8760	236.0000	449.8638
522	9994.8709	236.0000	450.0888
523	10012.3532	236.0000	450.8760
524	10029.8355	236.0000	451.6633
525	10096.0184	236.0000	454.6436
526	10162.2014	236.0000	457.6240
527	10228.3843	236.0000	460.6043
528	10294.5672	236.0000	463.5847
529	9946.2761	.0000	522.6780
530	9981.2278	.0000	524.5148
531	9991.2141	.0000	525.0395
532	10026.1658	.0000	526.8763
533	9946.2761	13.0000	522.6780
534	9981.2278	13.0000	524.5148
535	9991.2141	13.0000	525.0395
536	10026.1658	13.0000	526.8763
537	9981.2278	63.0000	524.5148
538	9991.2141	63.0000	525.0395
539	9981.2278	113.0000	524.5148
540	9991.2141	113.0000	525.0395
541	9946.2761	163.0000	522.6780
542	9981.2278	163.0000	524.5148
543	9991.2141	163.0000	525.0395
544	10026.1658	163.0000	526.8763
545	9681.6412	176.0000	508.7714
546	9813.9586	176.0000	515.7247
547	9946.2761	176.0000	522.6780
548	9981.2278	176.0000	524.5148
549	9991.2141	176.0000	525.0395
550	10026.1658	176.0000	526.8763
551	10158.4833	176.0000	533.8296
552	10290.8007	176.0000	540.7829
553	9681.6412	206.0000	508.7714
554	9813.9586	206.0000	515.7247
555	9946.2761	206.0000	522.6780
556	9981.2278	206.0000	524.5148
557	9991.2141	206.0000	525.0395
558	10026.1658	206.0000	526.8763
559	10158.4833	206.0000	533.8296
560	10290.8007	206.0000	540.7829
561	9681.6412	236.0000	508.7714
562	9813.9586	236.0000	515.7247
563	9946.2761	236.0000	522.6780
564	9981.2278	236.0000	524.5148
565	9991.2141	236.0000	525.0395
566	10026.1658	236.0000	526.8763
567	10158.4833	236.0000	533.8296
568	10290.8007	236.0000	540.7829
569	9942.0761	.0000	597.2623
570	9959.5446	.0000	598.3117
571	9977.0131	.0000	599.3611
572	9982.0041	.0000	599.6610
573	9986.9951	.0000	599.9608
574	10004.4637	.0000	601.0102
575	10021.9322	.0000	602.0596
576	9942.0761	6.5000	597.2623
577	9977.0131	6.5000	599.3611
578	9986.9951	6.5000	599.9608
579	10021.9322	6.5000	602.0596

580	9942.0761	13.0000	597.2623
581	9959.5446	13.0000	598.3117
582	9977.0131	13.0000	599.3611
583	9982.0041	13.0000	599.6610
584	9986.9951	13.0000	599.9608
585	10004.4637	13.0000	601.0102
586	10021.9322	13.0000	602.0596
587	9977.0131	38.0000	599.3611
588	9986.9951	38.0000	599.9608
589	9977.0131	63.0000	599.3611
590	9982.0041	63.0000	599.6610
591	9986.9951	63.0000	599.9608
592	9977.0131	88.0000	599.3611
593	9986.9951	88.0000	599.9608
594	9977.0131	113.0000	599.3611
595	9982.0041	113.0000	599.6610
596	9986.9951	113.0000	599.9608
597	9977.0131	138.0000	599.3611
598	9986.9951	138.0000	599.9608
599	9942.0761	163.0000	597.2623
600	9959.5446	163.0000	598.3117
601	9977.0131	163.0000	599.3611
602	9982.0041	163.0000	599.6610
603	9986.9951	163.0000	599.9608
604	10004.4637	163.0000	601.0102
605	10021.9322	163.0000	602.0596
606	9942.0761	169.5000	597.2623
607	9977.0131	169.5000	599.3611
608	9986.9951	169.5000	599.9608
609	10021.9322	169.5000	602.0596
610	9677.5530	176.0000	581.3713
611	9743.6838	176.0000	585.3440
612	9809.8146	176.0000	589.3168
613	9875.9454	176.0000	593.2896
614	9942.0761	176.0000	597.2623
615	9959.5446	176.0000	598.3117
616	9977.0131	176.0000	599.3611
617	9982.0041	176.0000	599.6610
618	9986.9951	176.0000	599.9608
619	10004.4637	176.0000	601.0102
620	10021.9322	176.0000	602.0596
621	10088.0629	176.0000	606.0324
622	10154.1937	176.0000	610.0051
623	10220.3245	176.0000	613.9779
624	10286.4553	176.0000	617.9506
625	9677.5530	191.0000	581.3713
626	9809.8146	191.0000	589.3168
627	9942.0761	191.0000	597.2623
628	9977.0131	191.0000	599.3611
629	9986.9951	191.0000	599.9608
630	10021.9322	191.0000	602.0596
631	10154.1937	191.0000	610.0051
632	10286.4553	191.0000	617.9506
633	9677.5530	206.0000	581.3713
634	9743.6838	206.0000	585.3440
635	9809.8146	206.0000	589.3168
636	9875.9454	206.0000	593.2896
637	9942.0761	206.0000	597.2623
638	9959.5446	206.0000	598.3117
639	9977.0131	206.0000	599.3611
640	9982.0041	206.0000	599.6610
641	9986.9951	206.0000	599.9608
642	10004.4637	206.0000	601.0102
643	10021.9322	206.0000	602.0596
644	10088.0629	206.0000	606.0324
645	10154.1937	206.0000	610.0051
646	10220.3245	206.0000	613.9779
647	10286.4553	206.0000	617.9506
648	9677.5530	221.0000	581.3713
649	9809.8146	221.0000	589.3168
650	9942.0761	221.0000	597.2623
651	9977.0131	221.0000	599.3611

652	9986.9951	221.0000	599.9608
653	10021.9322	221.0000	602.0596
654	10154.1937	221.0000	610.0051
655	10286.4553	221.0000	617.9506
656	9677.5530	236.0000	581.3713
657	9743.6838	236.0000	585.3440
658	9809.8146	236.0000	589.3168
659	9875.9454	236.0000	593.2896
660	9942.0761	236.0000	597.2623
661	9959.5446	236.0000	598.3117
662	9977.0131	236.0000	599.3611
663	9982.0041	236.0000	599.6610
664	9986.9951	236.0000	599.9608
665	10004.4637	236.0000	601.0102
666	10021.9322	236.0000	602.0596
667	10088.0629	236.0000	606.0324
668	10154.1937	236.0000	610.0051
669	10220.3245	236.0000	613.9779
670	10286.4553	236.0000	617.9506
671	9937.3169	.0000	671.8130
672	9972.2372	.0000	674.1738
673	9982.2144	.0000	674.8483
674	10017.1347	.0000	677.2091
675	9937.3169	13.0000	671.8130
676	9972.2372	13.0000	674.1738
677	9982.2144	13.0000	674.8483
678	10017.1347	13.0000	677.2091
679	9972.2372	63.0000	674.1738
680	9982.2144	63.0000	674.8483
681	9972.2372	113.0000	674.1738
682	9982.2144	113.0000	674.8483
683	9937.3169	163.0000	671.8130
684	9972.2372	163.0000	674.1738
685	9982.2144	163.0000	674.8483
686	10017.1347	163.0000	677.2091
687	9672.9204	176.0000	653.9384
688	9805.1187	176.0000	662.8757
689	9937.3169	176.0000	671.8130
690	9972.2372	176.0000	674.1738
691	9982.2144	176.0000	674.8483
692	10017.1347	176.0000	677.2091
693	10149.3330	176.0000	686.1463
694	10281.5312	176.0000	695.0836
695	9672.9204	206.0000	653.9384
696	9805.1187	206.0000	662.8757
697	9937.3169	206.0000	671.8130
698	9972.2372	206.0000	674.1738
699	9982.2144	206.0000	674.8483
700	10017.1347	206.0000	677.2091
701	10149.3330	206.0000	686.1463
702	10281.5312	206.0000	695.0836
703	9672.9204	236.0000	653.9384
704	9805.1187	236.0000	662.8757
705	9937.3169	236.0000	671.8130
706	9972.2372	236.0000	674.1738
707	9982.2144	236.0000	674.8483
708	10017.1347	236.0000	677.2091
709	10149.3330	236.0000	686.1463
710	10281.5312	236.0000	695.0836
711	9931.9987	.0000	746.3259
712	9949.4495	.0000	747.6372
713	9966.9003	.0000	748.9485
714	9971.8862	.0000	749.3232
715	9976.8722	.0000	749.6978
716	9994.3230	.0000	751.0091
717	10011.7738	.0000	752.3205
718	9931.9987	6.5000	746.3259
719	9966.9003	6.5000	748.9485
720	9976.8722	6.5000	749.6978
721	10011.7738	6.5000	752.3205
722	9931.9987	13.0000	746.3259
723	9949.4495	13.0000	747.6372

724	9966.9003	13.0000	748.9485
725	9971.8862	13.0000	749.3232
726	9976.8722	13.0000	749.6978
727	9994.3230	13.0000	751.0091
728	10011.7738	13.0000	752.3205
729	9966.9003	38.0000	748.9485
730	9976.8722	38.0000	749.6978
731	9966.9003	63.0000	748.9485
732	9971.8862	63.0000	749.3232
733	9976.8722	63.0000	749.6978
734	9966.9003	88.0000	748.9485
735	9976.8722	88.0000	749.6978
736	9966.9003	113.0000	748.9485
737	9971.8862	113.0000	749.3232
738	9976.8722	113.0000	749.6978
739	9966.9003	138.0000	748.9485
740	9976.8722	138.0000	749.6978
741	9931.9987	163.0000	746.3259
742	9949.4495	163.0000	747.6372
743	9966.9003	163.0000	748.9485
744	9971.8862	163.0000	749.3232
745	9976.8722	163.0000	749.6978
746	9994.3230	163.0000	751.0091
747	10011.7738	163.0000	752.3205
748	9931.9987	169.5000	746.3259
749	9966.9003	169.5000	748.9485
750	9976.8722	169.5000	749.6978
751	10011.7738	169.5000	752.3205
752	9667.7437	176.0000	726.4688
753	9733.8074	176.0000	731.4331
754	9799.8712	176.0000	736.3973
755	9865.9349	176.0000	741.3616
756	9931.9987	176.0000	746.3259
757	9949.4495	176.0000	747.6372
758	9966.9003	176.0000	748.9485
759	9971.8862	176.0000	749.3232
760	9976.8722	176.0000	749.6978
761	9994.3230	176.0000	751.0091
762	10011.7738	176.0000	752.3205
763	10077.8375	176.0000	757.2847
764	10143.9013	176.0000	762.2490
765	10209.9650	176.0000	767.2132
766	10276.0288	176.0000	772.1775
767	9667.7437	191.0000	726.4688
768	9799.8712	191.0000	736.3973
769	9931.9987	191.0000	746.3259
770	9966.9003	191.0000	748.9485
771	9976.8722	191.0000	749.6978
772	10011.7738	191.0000	752.3205
773	10143.9013	191.0000	762.2490
774	10276.0288	191.0000	772.1775
775	9667.7437	206.0000	726.4688
776	9733.8074	206.0000	731.4331
777	9799.8712	206.0000	736.3973
778	9865.9349	206.0000	741.3616
779	9931.9987	206.0000	746.3259
780	9949.4495	206.0000	747.6372
781	9966.9003	206.0000	748.9485
782	9971.8862	206.0000	749.3232
783	9976.8722	206.0000	749.6978
784	9994.3230	206.0000	751.0091
785	10011.7738	206.0000	752.3205
786	10077.8375	206.0000	757.2847
787	10143.9013	206.0000	762.2490
788	10209.9650	206.0000	767.2132
789	10276.0288	206.0000	772.1775
790	9667.7437	221.0000	726.4688
791	9799.8712	221.0000	736.3973
792	9931.9987	221.0000	746.3259
793	9966.9003	221.0000	748.9485
794	9976.8722	221.0000	749.6978
795	10011.7738	221.0000	752.3205

796	10143.9013	221.0000	762.2490
797	10276.0288	221.0000	772.1775
798	9667.7437	236.0000	726.4688
799	9733.8074	236.0000	731.4331
800	9799.8712	236.0000	736.3973
801	9865.9349	236.0000	741.3616
802	9931.9987	236.0000	746.3259
803	9949.4495	236.0000	747.6372
804	9966.9003	236.0000	748.9485
805	9971.8862	236.0000	749.3232
806	9976.8722	236.0000	749.6978
807	9994.3230	236.0000	751.0091
808	10011.7738	236.0000	752.3205
809	10077.8375	236.0000	757.2847
810	10143.9013	236.0000	762.2490
811	10209.9650	236.0000	767.2132
812	10276.0288	236.0000	772.1775
813	9926.1217	.0000	820.7968
814	9961.0027	.0000	823.6811
815	9970.9687	.0000	824.5052
816	10005.8496	.0000	827.3895
817	9926.1217	13.0000	820.7968
818	9961.0027	13.0000	823.6811
819	9970.9687	13.0000	824.5052
820	10005.8496	13.0000	827.3895
821	9961.0027	63.0000	823.6811
822	9970.9687	63.0000	824.5052
823	9961.0027	113.0000	823.6811
824	9970.9687	113.0000	824.5052
825	9926.1217	163.0000	820.7968
826	9961.0027	163.0000	823.6811
827	9970.9687	163.0000	824.5052
828	10005.8496	163.0000	827.3895
829	9662.0231	176.0000	798.9583
830	9794.0724	176.0000	809.8775
831	9926.1217	176.0000	820.7968
832	9961.0027	176.0000	823.6811
833	9970.9687	176.0000	824.5052
834	10005.8496	176.0000	827.3895
835	10137.8989	176.0000	838.3087
836	10269.9482	176.0000	849.2280
837	9662.0231	206.0000	798.9583
838	9794.0724	206.0000	809.8775
839	9926.1217	206.0000	820.7968
840	9961.0027	206.0000	823.6811
841	9970.9687	206.0000	824.5052
842	10005.8496	206.0000	827.3895
843	10137.8989	206.0000	838.3087
844	10269.9482	206.0000	849.2280
845	9662.0231	236.0000	798.9583
846	9794.0724	236.0000	809.8775
847	9926.1217	236.0000	820.7968
848	9961.0027	236.0000	823.6811
849	9970.9687	236.0000	824.5052
850	10005.8496	236.0000	827.3895
851	10137.8989	236.0000	838.3087
852	10269.9482	236.0000	849.2280
853	9919.6864	.0000	895.2215
854	9937.1156	.0000	896.7944
855	9954.5447	.0000	898.3673
856	9959.5245	.0000	898.8168
857	9964.5043	.0000	899.2662
858	9981.9334	.0000	900.8391
859	9999.3626	.0000	902.4120
860	9919.6864	6.5000	895.2215
861	9954.5447	6.5000	898.3673
862	9964.5043	6.5000	899.2662
863	9999.3626	6.5000	902.4120
864	9919.6864	13.0000	895.2215
865	9937.1156	13.0000	896.7944
866	9954.5447	13.0000	898.3673
867	9959.5245	13.0000	898.8168

868	9964.5043	13.0000	899.2662
869	9981.9334	13.0000	900.8391
870	9999.3626	13.0000	902.4120
871	9954.5447	38.0000	898.3673
872	9964.5043	38.0000	899.2662
873	9954.5447	63.0000	898.3673
874	9959.5245	63.0000	898.8168
875	9964.5043	63.0000	899.2662
876	9954.5447	88.0000	898.3673
877	9964.5043	88.0000	899.2662
878	9954.5447	113.0000	898.3673
879	9959.5245	113.0000	898.8168
880	9964.5043	113.0000	899.2662
881	9954.5447	138.0000	898.3673
882	9964.5043	138.0000	899.2662
883	9919.6864	163.0000	895.2215
884	9937.1156	163.0000	896.7944
885	9954.5447	163.0000	898.3673
886	9959.5245	163.0000	898.8168
887	9964.5043	163.0000	899.2662
888	9981.9334	163.0000	900.8391
889	9999.3626	163.0000	902.4120
890	9919.6864	169.5000	895.2215
891	9954.5447	169.5000	898.3673
892	9964.5043	169.5000	899.2662
893	9999.3626	169.5000	902.4120
894	9655.7590	176.0000	871.4028
895	9721.7409	176.0000	877.3575
896	9787.7227	176.0000	883.3122
897	9853.7046	176.0000	889.2668
898	9919.6864	176.0000	895.2215
899	9937.1156	176.0000	896.7944
900	9954.5447	176.0000	898.3673
901	9959.5245	176.0000	898.8168
902	9964.5043	176.0000	899.2662
903	9981.9334	176.0000	900.8391
904	9999.3626	176.0000	902.4120
905	10065.3445	176.0000	908.3667
906	10131.3263	176.0000	914.3213
907	10197.3082	176.0000	920.2760
908	10263.2900	176.0000	926.2307
909	9655.7590	191.0000	871.4028
910	9787.7227	191.0000	883.3122
911	9919.6864	191.0000	895.2215
912	9954.5447	191.0000	898.3673
913	9964.5043	191.0000	899.2662
914	9999.3626	191.0000	902.4120
915	10131.3263	191.0000	914.3213
916	10263.2900	191.0000	926.2307
917	9655.7590	206.0000	871.4028
918	9721.7409	206.0000	877.3575
919	9787.7227	206.0000	883.3122
920	9853.7046	206.0000	889.2668
921	9919.6864	206.0000	895.2215
922	9937.1156	206.0000	896.7944
923	9954.5447	206.0000	898.3673
924	9959.5245	206.0000	898.8168
925	9964.5043	206.0000	899.2662
926	9981.9334	206.0000	900.8391
927	9999.3626	206.0000	902.4120
928	10065.3445	206.0000	908.3667
929	10131.3263	206.0000	914.3213
930	10197.3082	206.0000	920.2760
931	10263.2900	206.0000	926.2307
932	9655.7590	221.0000	871.4028
933	9787.7227	221.0000	883.3122
934	9919.6864	221.0000	895.2215
935	9954.5447	221.0000	898.3673
936	9964.5043	221.0000	899.2662
937	9999.3626	221.0000	902.4120
938	10131.3263	221.0000	914.3213
939	10263.2900	221.0000	926.2307

940	9655.7590	236.0000	871.4028
941	9721.7409	236.0000	877.3575
942	9787.7227	236.0000	883.3122
943	9853.7046	236.0000	889.2668
944	9919.6864	236.0000	895.2215
945	9937.1156	236.0000	896.7944
946	9954.5447	236.0000	898.3673
947	9959.5245	236.0000	898.8168
948	9964.5043	236.0000	899.2662
949	9981.9334	236.0000	900.8391
950	9999.3626	236.0000	902.4120
951	10065.3445	236.0000	908.3667
952	10131.3263	236.0000	914.3213
953	10197.3082	236.0000	920.2760
954	10263.2900	236.0000	926.2307
955	9912.6931	.0000	969.5959
956	9947.5268	.0000	973.0031
957	9957.4793	.0000	973.9766
958	9992.3131	.0000	977.3838
959	9912.6931	13.0000	969.5959
960	9947.5268	13.0000	973.0031
961	9957.4793	13.0000	973.9766
962	9992.3131	13.0000	977.3838
963	9947.5268	63.0000	973.0031
964	9957.4793	63.0000	973.9766
965	9947.5268	113.0000	973.0031
966	9957.4793	113.0000	973.9766
967	9912.6931	163.0000	969.5959
968	9947.5268	163.0000	973.0031
969	9957.4793	163.0000	973.9766
970	9992.3131	163.0000	977.3838
971	9648.9517	176.0000	943.7984
972	9780.8224	176.0000	956.6971
973	9912.6931	176.0000	969.5959
974	9947.5268	176.0000	973.0031
975	9957.4793	176.0000	973.9766
976	9992.3131	176.0000	977.3838
977	10124.1838	176.0000	990.2825
978	10256.0544	176.0000	1003.1813
979	9648.9517	206.0000	943.7984
980	9780.8224	206.0000	956.6971
981	9912.6931	206.0000	969.5959
982	9947.5268	206.0000	973.0031
983	9957.4793	206.0000	973.9766
984	9992.3131	206.0000	977.3838
985	10124.1838	206.0000	990.2825
986	10256.0544	206.0000	1003.1813
987	9648.9517	236.0000	943.7984
988	9780.8224	236.0000	956.6971
989	9912.6931	236.0000	969.5959
990	9947.5268	236.0000	973.0031
991	9957.4793	236.0000	973.9766
992	9992.3131	236.0000	977.3838
993	10124.1838	236.0000	990.2825
994	10256.0544	236.0000	1003.1813
995	9905.1421	.0000	1043.9157
996	9922.5457	.0000	1045.7499
997	9939.9493	.0000	1047.5841
998	9944.9218	.0000	1048.1081
999	9949.8942	.0000	1048.6322
1000	9967.2979	.0000	1050.4664
1001	9984.7015	.0000	1052.3005
1002	9905.1421	6.5000	1043.9157
1003	9939.9493	6.5000	1047.5841
1004	9949.8942	6.5000	1048.6322
1005	9984.7015	6.5000	1052.3005
1006	9905.1421	13.0000	1043.9157
1007	9922.5457	13.0000	1045.7499
1008	9939.9493	13.0000	1047.5841
1009	9944.9218	13.0000	1048.1081
1010	9949.8942	13.0000	1048.6322
1011	9967.2979	13.0000	1050.4664

1012	9984.7015	13.0000	1052.3005
1013	9939.9493	38.0000	1047.5841
1014	9949.8942	38.0000	1048.6322
1015	9939.9493	63.0000	1047.5841
1016	9944.9218	63.0000	1048.1081
1017	9949.8942	63.0000	1048.6322
1018	9939.9493	88.0000	1047.5841
1019	9949.8942	88.0000	1048.6322
1020	9939.9493	113.0000	1047.5841
1021	9944.9218	113.0000	1048.1081
1022	9949.8942	113.0000	1048.6322
1023	9939.9493	138.0000	1047.5841
1024	9949.8942	138.0000	1048.6322
1025	9905.1421	163.0000	1043.9157
1026	9922.5457	163.0000	1045.7499
1027	9939.9493	163.0000	1047.5841
1028	9944.9218	163.0000	1048.1081
1029	9949.8942	163.0000	1048.6322
1030	9967.2979	163.0000	1050.4664
1031	9984.7015	163.0000	1052.3005
1032	9905.1421	169.5000	1043.9157
1033	9939.9493	169.5000	1047.5841
1034	9949.8942	169.5000	1048.6322
1035	9984.7015	169.5000	1052.3005
1036	9641.6017	176.0000	1016.1408
1037	9707.4868	176.0000	1023.0845
1038	9773.3719	176.0000	1030.0282
1039	9839.2570	176.0000	1036.9720
1040	9905.1421	176.0000	1043.9157
1041	9922.5457	176.0000	1045.7499
1042	9939.9493	176.0000	1047.5841
1043	9944.9218	176.0000	1048.1081
1044	9949.8942	176.0000	1048.6322
1045	9967.2979	176.0000	1050.4664
1046	9984.7015	176.0000	1052.3005
1047	10050.5866	176.0000	1059.2443
1048	10116.4717	176.0000	1066.1880
1049	10182.3568	176.0000	1073.1317
1050	10248.2419	176.0000	1080.0754
1051	9641.6017	191.0000	1016.1408
1052	9773.3719	191.0000	1030.0282
1053	9905.1421	191.0000	1043.9157
1054	9939.9493	191.0000	1047.5841
1055	9949.8942	191.0000	1048.6322
1056	9984.7015	191.0000	1052.3005
1057	10116.4717	191.0000	1066.1880
1058	10248.2419	191.0000	1080.0754
1059	9641.6017	206.0000	1016.1408
1060	9707.4868	206.0000	1023.0845
1061	9773.3719	206.0000	1030.0282
1062	9839.2570	206.0000	1036.9720
1063	9905.1421	206.0000	1043.9157
1064	9922.5457	206.0000	1045.7499
1065	9939.9493	206.0000	1047.5841
1066	9944.9218	206.0000	1048.1081
1067	9949.8942	206.0000	1048.6322
1068	9967.2979	206.0000	1050.4664
1069	9984.7015	206.0000	1052.3005
1070	10050.5866	206.0000	1059.2443
1071	10116.4717	206.0000	1066.1880
1072	10182.3568	206.0000	1073.1317
1073	10248.2419	206.0000	1080.0754
1074	9641.6017	221.0000	1016.1408
1075	9773.3719	221.0000	1030.0282
1076	9905.1421	221.0000	1043.9157
1077	9939.9493	221.0000	1047.5841
1078	9949.8942	221.0000	1048.6322
1079	9984.7015	221.0000	1052.3005
1080	10116.4717	221.0000	1066.1880
1081	10248.2419	221.0000	1080.0754
1082	9641.6017	236.0000	1016.1408
1083	9707.4868	236.0000	1023.0845

1084	9773.3719	236.0000	1030.0282
1085	9839.2570	236.0000	1036.9720
1086	9905.1421	236.0000	1043.9157
1087	9922.5457	236.0000	1045.7499
1088	9939.9493	236.0000	1047.5841
1089	9944.9218	236.0000	1048.1081
1090	9949.8942	236.0000	1048.6322
1091	9967.2979	236.0000	1050.4664
1092	9984.7015	236.0000	1052.3005
1093	10050.5866	236.0000	1059.2443
1094	10116.4717	236.0000	1066.1880
1095	10182.3568	236.0000	1073.1317
1096	10248.2419	236.0000	1080.0754
1097	9897.0339	.0000	1118.1768
1098	9931.8127	.0000	1122.1061
1099	9941.7494	.0000	1123.2288
1100	9976.5282	.0000	1127.1581
1101	9897.0339	13.0000	1118.1768
1102	9931.8127	13.0000	1122.1061
1103	9941.7494	13.0000	1123.2288
1104	9976.5282	13.0000	1127.1581
1105	9931.8127	63.0000	1122.1061
1106	9941.7494	63.0000	1123.2288
1107	9931.8127	113.0000	1122.1061
1108	9941.7494	113.0000	1123.2288
1109	9897.0339	163.0000	1118.1768
1110	9931.8127	163.0000	1122.1061
1111	9941.7494	163.0000	1123.2288
1112	9976.5282	163.0000	1127.1581
1113	9633.7092	176.0000	1088.4261
1114	9765.3716	176.0000	1103.3014
1115	9897.0339	176.0000	1118.1768
1116	9931.8127	176.0000	1122.1061
1117	9941.7494	176.0000	1123.2288
1118	9976.5282	176.0000	1127.1581
1119	10108.1905	176.0000	1142.0335
1120	10239.8529	176.0000	1156.9088
1121	9633.7092	206.0000	1088.4261
1122	9765.3716	206.0000	1103.3014
1123	9897.0339	206.0000	1118.1768
1124	9931.8127	206.0000	1122.1061
1125	9941.7494	206.0000	1123.2288
1126	9976.5282	206.0000	1127.1581
1127	10108.1905	206.0000	1142.0335
1128	10239.8529	206.0000	1156.9088
1129	9633.7092	236.0000	1088.4261
1130	9765.3716	236.0000	1103.3014
1131	9897.0339	236.0000	1118.1768
1132	9931.8127	236.0000	1122.1061
1133	9941.7494	236.0000	1123.2288
1134	9976.5282	236.0000	1127.1581
1135	10108.1905	236.0000	1142.0335
1136	10239.8529	236.0000	1156.9088
1137	9888.3690	.0000	1192.3750
1138	9905.7432	.0000	1194.4700
1139	9923.1173	.0000	1196.5650
1140	9928.0813	.0000	1197.1636
1141	9933.0454	.0000	1197.7622
1142	9950.4195	.0000	1199.8572
1143	9967.7937	.0000	1201.9523
1144	9888.3690	6.5000	1192.3750
1145	9923.1173	6.5000	1196.5650
1146	9933.0454	6.5000	1197.7622
1147	9967.7937	6.5000	1201.9523
1148	9888.3690	13.0000	1192.3750
1149	9905.7432	13.0000	1194.4700
1150	9923.1173	13.0000	1196.5650
1151	9928.0813	13.0000	1197.1636
1152	9933.0454	13.0000	1197.7622
1153	9950.4195	13.0000	1199.8572
1154	9967.7937	13.0000	1201.9523
1155	9923.1173	38.0000	1196.5650

1156	9933.0454	38.0000	1197.7622
1157	9923.1173	63.0000	1196.5650
1158	9928.0813	63.0000	1197.1636
1159	9933.0454	63.0000	1197.7622
1160	9923.1173	88.0000	1196.5650
1161	9933.0454	88.0000	1197.7622
1162	9923.1173	113.0000	1196.5650
1163	9928.0813	113.0000	1197.1636
1164	9933.0454	113.0000	1197.7622
1165	9923.1173	138.0000	1196.5650
1166	9933.0454	138.0000	1197.7622
1167	9888.3690	163.0000	1192.3750
1168	9905.7432	163.0000	1194.4700
1169	9923.1173	163.0000	1196.5650
1170	9928.0813	163.0000	1197.1636
1171	9933.0454	163.0000	1197.7622
1172	9950.4195	163.0000	1199.8572
1173	9967.7937	163.0000	1201.9523
1174	9888.3690	169.5000	1192.3750
1175	9923.1173	169.5000	1196.5650
1176	9933.0454	169.5000	1197.7622
1177	9967.7937	169.5000	1201.9523
1178	9625.2749	176.0000	1160.6501
1179	9691.0484	176.0000	1168.5813
1180	9756.8219	176.0000	1176.5126
1181	9822.5955	176.0000	1184.4438
1182	9888.3690	176.0000	1192.3750
1183	9905.7432	176.0000	1194.4700
1184	9923.1173	176.0000	1196.5650
1185	9928.0813	176.0000	1197.1636
1186	9933.0454	176.0000	1197.7622
1187	9950.4195	176.0000	1199.8572
1188	9967.7937	176.0000	1201.9523
1189	10033.5672	176.0000	1209.8835
1190	10099.3408	176.0000	1217.8147
1191	10165.1143	176.0000	1225.7459
1192	10230.8878	176.0000	1233.6771
1193	9625.2749	191.0000	1160.6501
1194	9756.8219	191.0000	1176.5126
1195	9888.3690	191.0000	1192.3750
1196	9923.1173	191.0000	1196.5650
1197	9933.0454	191.0000	1197.7622
1198	9967.7937	191.0000	1201.9523
1199	10099.3408	191.0000	1217.8147
1200	10230.8878	191.0000	1233.6771
1201	9625.2749	206.0000	1160.6501
1202	9691.0484	206.0000	1168.5813
1203	9756.8219	206.0000	1176.5126
1204	9822.5955	206.0000	1184.4438
1205	9888.3690	206.0000	1192.3750
1206	9905.7432	206.0000	1194.4700
1207	9923.1173	206.0000	1196.5650
1208	9928.0813	206.0000	1197.1636
1209	9933.0454	206.0000	1197.7622
1210	9950.4195	206.0000	1199.8572
1211	9967.7937	206.0000	1201.9523
1212	10033.5672	206.0000	1209.8835
1213	10099.3408	206.0000	1217.8147
1214	10165.1143	206.0000	1225.7459
1215	10230.8878	206.0000	1233.6771
1216	9625.2749	221.0000	1160.6501
1217	9756.8219	221.0000	1176.5126
1218	9888.3690	221.0000	1192.3750
1219	9923.1173	221.0000	1196.5650
1220	9933.0454	221.0000	1197.7622
1221	9967.7937	221.0000	1201.9523
1222	10099.3408	221.0000	1217.8147
1223	10230.8878	221.0000	1233.6771
1224	9625.2749	236.0000	1160.6501
1225	9691.0484	236.0000	1168.5813
1226	9756.8219	236.0000	1176.5126
1227	9822.5955	236.0000	1184.4438

1228	9888.3690	236.0000	1192.3750
1229	9905.7432	236.0000	1194.4700
1230	9923.1173	236.0000	1196.5650
1231	9928.0813	236.0000	1197.1636
1232	9933.0454	236.0000	1197.7622
1233	9950.4195	236.0000	1199.8572
1234	9967.7937	236.0000	1201.9523
1235	10033.5672	236.0000	1209.8835
1236	10099.3408	236.0000	1217.8147
1237	10165.1143	236.0000	1225.7459
1238	10230.8878	236.0000	1233.6771
1239	9879.1479	.0000	1266.5061
1240	9913.8637	.0000	1270.9567
1241	9923.7826	.0000	1272.2283
1242	9958.4984	.0000	1276.6788
1243	9879.1479	13.0000	1266.5061
1244	9913.8637	13.0000	1270.9567
1245	9923.7826	13.0000	1272.2283
1246	9958.4984	13.0000	1276.6788
1247	9913.8637	63.0000	1270.9567
1248	9923.7826	63.0000	1272.2283
1249	9913.8637	113.0000	1270.9567
1250	9923.7826	113.0000	1272.2283
1251	9879.1479	163.0000	1266.5061
1252	9913.8637	163.0000	1270.9567
1253	9923.7826	163.0000	1272.2283
1254	9958.4984	163.0000	1276.6788
1255	9616.2990	176.0000	1232.8089
1256	9747.7234	176.0000	1249.6575
1257	9879.1479	176.0000	1266.5061
1258	9913.8637	176.0000	1270.9567
1259	9923.7826	176.0000	1272.2283
1260	9958.4984	176.0000	1276.6788
1261	10089.9228	176.0000	1293.5274
1262	10221.3473	176.0000	1310.3760
1263	9616.2990	206.0000	1232.8089
1264	9747.7234	206.0000	1249.6575
1265	9879.1479	206.0000	1266.5061
1266	9913.8637	206.0000	1270.9567
1267	9923.7826	206.0000	1272.2283
1268	9958.4984	206.0000	1276.6788
1269	10089.9228	206.0000	1293.5274
1270	10221.3473	206.0000	1310.3760
1271	9616.2990	236.0000	1232.8089
1272	9747.7234	236.0000	1249.6575
1273	9879.1479	236.0000	1266.5061
1274	9913.8637	236.0000	1270.9567
1275	9923.7826	236.0000	1272.2283
1276	9958.4984	236.0000	1276.6788
1277	10089.9228	236.0000	1293.5274
1278	10221.3473	236.0000	1310.3760
1279	9869.3709	.0000	1340.5660
1280	9886.7117	.0000	1342.9214
1281	9904.0525	.0000	1345.2768
1282	9909.0070	.0000	1345.9498
1283	9913.9615	.0000	1346.6227
1284	9931.3022	.0000	1348.9782
1285	9948.6430	.0000	1351.3336
1286	9869.3709	6.5000	1340.5660
1287	9904.0525	6.5000	1345.2768
1288	9913.9615	6.5000	1346.6227
1289	9948.6430	6.5000	1351.3336
1290	9869.3709	13.0000	1340.5660
1291	9886.7117	13.0000	1342.9214
1292	9904.0525	13.0000	1345.2768
1293	9909.0070	13.0000	1345.9498
1294	9913.9615	13.0000	1346.6227
1295	9931.3022	13.0000	1348.9782
1296	9948.6430	13.0000	1351.3336
1297	9904.0525	38.0000	1345.2768
1298	9913.9615	38.0000	1346.6227
1299	9904.0525	63.0000	1345.2768

1300	9909.0070	63.0000	1345.9498
1301	9913.9615	63.0000	1346.6227
1302	9904.0525	88.0000	1345.2768
1303	9913.9615	88.0000	1346.6227
1304	9904.0525	113.0000	1345.2768
1305	9909.0070	113.0000	1345.9498
1306	9913.9615	113.0000	1346.6227
1307	9904.0525	138.0000	1345.2768
1308	9913.9615	138.0000	1346.6227
1309	9869.3709	163.0000	1340.5660
1310	9886.7117	163.0000	1342.9214
1311	9904.0525	163.0000	1345.2768
1312	9909.0070	163.0000	1345.9498
1313	9913.9615	163.0000	1346.6227
1314	9931.3022	163.0000	1348.9782
1315	9948.6430	163.0000	1351.3336
1316	9869.3709	169.5000	1340.5660
1317	9904.0525	169.5000	1345.2768
1318	9913.9615	169.5000	1346.6227
1319	9948.6430	169.5000	1351.3336
1320	9606.7823	176.0000	1304.8983
1321	9672.4294	176.0000	1313.8152
1322	9738.0766	176.0000	1322.7321
1323	9803.7238	176.0000	1331.6491
1324	9869.3709	176.0000	1340.5660
1325	9886.7117	176.0000	1342.9214
1326	9904.0525	176.0000	1345.2768
1327	9909.0070	176.0000	1345.9498
1328	9913.9615	176.0000	1346.6227
1329	9931.3022	176.0000	1348.9782
1330	9948.6430	176.0000	1351.3336
1331	10014.2902	176.0000	1360.2505
1332	10079.9373	176.0000	1369.1674
1333	10145.5845	176.0000	1378.0843
1334	10211.2317	176.0000	1387.0012
1335	9606.7823	191.0000	1304.8983
1336	9738.0766	191.0000	1322.7321
1337	9869.3709	191.0000	1340.5660
1338	9904.0525	191.0000	1345.2768
1339	9913.9615	191.0000	1346.6227
1340	9948.6430	191.0000	1351.3336
1341	10079.9373	191.0000	1369.1674
1342	10211.2317	191.0000	1387.0012
1343	9606.7823	206.0000	1304.8983
1344	9672.4294	206.0000	1313.8152
1345	9738.0766	206.0000	1322.7321
1346	9803.7238	206.0000	1331.6491
1347	9869.3709	206.0000	1340.5660
1348	9886.7117	206.0000	1342.9214
1349	9904.0525	206.0000	1345.2768
1350	9909.0070	206.0000	1345.9498
1351	9913.9615	206.0000	1346.6227
1352	9931.3022	206.0000	1348.9782
1353	9948.6430	206.0000	1351.3336
1354	10014.2902	206.0000	1360.2505
1355	10079.9373	206.0000	1369.1674
1356	10145.5845	206.0000	1378.0843
1357	10211.2317	206.0000	1387.0012
1358	9606.7823	221.0000	1304.8983
1359	9738.0766	221.0000	1322.7321
1360	9869.3709	221.0000	1340.5660
1361	9904.0525	221.0000	1345.2768
1362	9913.9615	221.0000	1346.6227
1363	9948.6430	221.0000	1351.3336
1364	10079.9373	221.0000	1369.1674
1365	10211.2317	221.0000	1387.0012
1366	9606.7823	236.0000	1304.8983
1367	9672.4294	236.0000	1313.8152
1368	9738.0766	236.0000	1322.7321
1369	9803.7238	236.0000	1331.6491
1370	9869.3709	236.0000	1340.5660
1371	9886.7117	236.0000	1342.9214

1372	9904.0525	236.0000	1345.2768
1373	9909.0070	236.0000	1345.9498
1374	9913.9615	236.0000	1346.6227
1375	9931.3022	236.0000	1348.9782
1376	9948.6430	236.0000	1351.3336
1377	10014.2902	236.0000	1360.2505
1378	10079.9373	236.0000	1369.1674
1379	10145.5845	236.0000	1378.0843
1380	10211.2317	236.0000	1387.0012
1381	9859.0389	.0000	1414.5504
1382	9893.6841	.0000	1419.5212
1383	9903.5827	.0000	1420.9415
1384	9938.2279	.0000	1425.9123
1385	9859.0389	13.0000	1414.5504
1386	9893.6841	13.0000	1419.5212
1387	9903.5827	13.0000	1420.9415
1388	9938.2279	13.0000	1425.9123
1389	9893.6841	63.0000	1419.5212
1390	9903.5827	63.0000	1420.9415
1391	9893.6841	113.0000	1419.5212
1392	9903.5827	113.0000	1420.9415
1393	9859.0389	163.0000	1414.5504
1394	9893.6841	163.0000	1419.5212
1395	9903.5827	163.0000	1420.9415
1396	9938.2279	163.0000	1425.9123
1397	9596.7251	176.0000	1376.9143
1398	9727.8820	176.0000	1395.7324
1399	9859.0389	176.0000	1414.5504
1400	9893.6841	176.0000	1419.5212
1401	9903.5827	176.0000	1420.9415
1402	9938.2279	176.0000	1425.9123
1403	10069.3848	176.0000	1444.7304
1404	10200.5417	176.0000	1463.5484
1405	9596.7251	206.0000	1376.9143
1406	9727.8820	206.0000	1395.7324
1407	9859.0389	206.0000	1414.5504
1408	9893.6841	206.0000	1419.5212
1409	9903.5827	206.0000	1420.9415
1410	9938.2279	206.0000	1425.9123
1411	10069.3848	206.0000	1444.7304
1412	10200.5417	206.0000	1463.5484
1413	9596.7251	236.0000	1376.9143
1414	9727.8820	236.0000	1395.7324
1415	9859.0389	236.0000	1414.5504
1416	9893.6841	236.0000	1419.5212
1417	9903.5827	236.0000	1420.9415
1418	9938.2279	236.0000	1425.9123
1419	10069.3848	236.0000	1444.7304
1420	10200.5417	236.0000	1463.5484
1421	9848.1521	.0000	1488.4553
1422	9865.4556	.0000	1491.0706
1423	9882.7591	.0000	1493.6858
1424	9887.7030	.0000	1494.4331
1425	9892.6468	.0000	1495.1803
1426	9909.9503	.0000	1497.7955
1427	9927.2538	.0000	1500.4108
1428	9848.1521	6.5000	1488.4553
1429	9882.7591	6.5000	1493.6858
1430	9892.6468	6.5000	1495.1803
1431	9927.2538	6.5000	1500.4108
1432	9848.1521	13.0000	1488.4553
1433	9865.4556	13.0000	1491.0706
1434	9882.7591	13.0000	1493.6858
1435	9887.7030	13.0000	1494.4331
1436	9892.6468	13.0000	1495.1803
1437	9909.9503	13.0000	1497.7955
1438	9927.2538	13.0000	1500.4108
1439	9882.7591	38.0000	1493.6858
1440	9892.6468	38.0000	1495.1803
1441	9882.7591	63.0000	1493.6858
1442	9887.7030	63.0000	1494.4331
1443	9892.6468	63.0000	1495.1803

1444	9882.7591	88.0000	1493.6858
1445	9892.6468	88.0000	1495.1803
1446	9882.7591	113.0000	1493.6858
1447	9887.7030	113.0000	1494.4331
1448	9892.6468	113.0000	1495.1803
1449	9882.7591	138.0000	1493.6858
1450	9892.6468	138.0000	1495.1803
1451	9848.1521	163.0000	1488.4553
1452	9865.4556	163.0000	1491.0706
1453	9882.7591	163.0000	1493.6858
1454	9887.7030	163.0000	1494.4331
1455	9892.6468	163.0000	1495.1803
1456	9909.9503	163.0000	1497.7955
1457	9927.2538	163.0000	1500.4108
1458	9848.1521	169.5000	1488.4553
1459	9882.7591	169.5000	1493.6858
1460	9892.6468	169.5000	1495.1803
1461	9927.2538	169.5000	1500.4108
1462	9586.1280	176.0000	1448.8528
1463	9651.6341	176.0000	1458.7535
1464	9717.1401	176.0000	1468.6541
1465	9782.6461	176.0000	1478.5547
1466	9848.1521	176.0000	1488.4553
1467	9865.4556	176.0000	1491.0706
1468	9882.7591	176.0000	1493.6858
1469	9887.7030	176.0000	1494.4331
1470	9892.6468	176.0000	1495.1803
1471	9909.9503	176.0000	1497.7955
1472	9927.2538	176.0000	1500.4108
1473	9992.7598	176.0000	1510.3114
1474	10058.2658	176.0000	1520.2120
1475	10123.7719	176.0000	1530.1126
1476	10189.2779	176.0000	1540.0133
1477	9586.1280	191.0000	1448.8528
1478	9717.1401	191.0000	1468.6541
1479	9848.1521	191.0000	1488.4553
1480	9882.7591	191.0000	1493.6858
1481	9892.6468	191.0000	1495.1803
1482	9927.2538	191.0000	1500.4108
1483	10058.2658	191.0000	1520.2120
1484	10189.2779	191.0000	1540.0133
1485	9586.1280	206.0000	1448.8528
1486	9651.6341	206.0000	1458.7535
1487	9717.1401	206.0000	1468.6541
1488	9782.6461	206.0000	1478.5547
1489	9848.1521	206.0000	1488.4553
1490	9865.4556	206.0000	1491.0706
1491	9882.7591	206.0000	1493.6858
1492	9887.7030	206.0000	1494.4331
1493	9892.6468	206.0000	1495.1803
1494	9909.9503	206.0000	1497.7955
1495	9927.2538	206.0000	1500.4108
1496	9992.7598	206.0000	1510.3114
1497	10058.2658	206.0000	1520.2120
1498	10123.7719	206.0000	1530.1126
1499	10189.2779	206.0000	1540.0133
1500	9586.1280	221.0000	1448.8528
1501	9717.1401	221.0000	1468.6541
1502	9848.1521	221.0000	1488.4553
1503	9882.7591	221.0000	1493.6858
1504	9892.6468	221.0000	1495.1803
1505	9927.2538	221.0000	1500.4108
1506	10058.2658	221.0000	1520.2120
1507	10189.2779	221.0000	1540.0133
1508	9586.1280	236.0000	1448.8528
1509	9651.6341	236.0000	1458.7535
1510	9717.1401	236.0000	1468.6541
1511	9782.6461	236.0000	1478.5547
1512	9848.1521	236.0000	1488.4553
1513	9865.4556	236.0000	1491.0706
1514	9882.7591	236.0000	1493.6858
1515	9887.7030	236.0000	1494.4331

1516	9892.6468	236.0000	1495.1803
1517	9909.9503	236.0000	1497.7955
1518	9927.2538	236.0000	1500.4108
1519	9992.7598	236.0000	1510.3114
1520	10058.2658	236.0000	1520.2120
1521	10123.7719	236.0000	1530.1126
1522	10189.2779	236.0000	1540.0133
1523	9836.7115	.0000	1562.2765
1524	9871.2782	.0000	1567.7664
1525	9881.1544	.0000	1569.3350
1526	9915.7212	.0000	1574.8249
1527	9836.7115	13.0000	1562.2765
1528	9871.2782	13.0000	1567.7664
1529	9881.1544	13.0000	1569.3350
1530	9915.7212	13.0000	1574.8249
1531	9871.2782	63.0000	1567.7664
1532	9881.1544	63.0000	1569.3350
1533	9871.2782	113.0000	1567.7664
1534	9881.1544	113.0000	1569.3350
1535	9836.7115	163.0000	1562.2765
1536	9871.2782	163.0000	1567.7664
1537	9881.1544	163.0000	1569.3350
1538	9915.7212	163.0000	1574.8249
1539	9574.9917	176.0000	1520.7099
1540	9705.8516	176.0000	1541.4932
1541	9836.7115	176.0000	1562.2765
1542	9871.2782	176.0000	1567.7664
1543	9881.1544	176.0000	1569.3350
1544	9915.7212	176.0000	1574.8249
1545	10046.5810	176.0000	1595.6082
1546	10177.4409	176.0000	1616.3915
1547	9574.9917	206.0000	1520.7099
1548	9705.8516	206.0000	1541.4932
1549	9836.7115	206.0000	1562.2765
1550	9871.2782	206.0000	1567.7664
1551	9881.1544	206.0000	1569.3350
1552	9915.7212	206.0000	1574.8249
1553	10046.5810	206.0000	1595.6082
1554	10177.4409	206.0000	1616.3915
1555	9574.9917	236.0000	1520.7099
1556	9705.8516	236.0000	1541.4932
1557	9836.7115	236.0000	1562.2765
1558	9871.2782	236.0000	1567.7664
1559	9881.1544	236.0000	1569.3350
1560	9915.7212	236.0000	1574.8249
1561	10046.5810	236.0000	1595.6082
1562	10177.4409	236.0000	1616.3915
1563	9824.7174	.0000	1636.0098
1564	9841.9797	.0000	1638.8843
1565	9859.2420	.0000	1641.7588
1566	9864.1741	.0000	1642.5801
1567	9869.1062	.0000	1643.4014
1568	9886.3685	.0000	1646.2759
1569	9903.6308	.0000	1649.1504
1570	9824.7174	6.5000	1636.0098
1571	9859.2420	6.5000	1641.7588
1572	9869.1062	6.5000	1643.4014
1573	9903.6308	6.5000	1649.1504
1574	9824.7174	13.0000	1636.0098
1575	9841.9797	13.0000	1638.8843
1576	9859.2420	13.0000	1641.7588
1577	9864.1741	13.0000	1642.5801
1578	9869.1062	13.0000	1643.4014
1579	9886.3685	13.0000	1646.2759
1580	9903.6308	13.0000	1649.1504
1581	9859.2420	38.0000	1641.7588
1582	9869.1062	38.0000	1643.4014
1583	9859.2420	63.0000	1641.7588
1584	9864.1741	63.0000	1642.5801
1585	9869.1062	63.0000	1643.4014
1586	9859.2420	88.0000	1641.7588
1587	9869.1062	88.0000	1643.4014

1588	9859.2420	113.0000	1641.7588
1589	9864.1741	113.0000	1642.5801
1590	9869.1062	113.0000	1643.4014
1591	9859.2420	138.0000	1641.7588
1592	9869.1062	138.0000	1643.4014
1593	9824.7174	163.0000	1636.0098
1594	9841.9797	163.0000	1638.8843
1595	9859.2420	163.0000	1641.7588
1596	9864.1741	163.0000	1642.5801
1597	9869.1062	163.0000	1643.4014
1598	9886.3685	163.0000	1646.2759
1599	9903.6308	163.0000	1649.1504
1600	9824.7174	169.5000	1636.0098
1601	9859.2420	169.5000	1641.7588
1602	9869.1062	169.5000	1643.4014
1603	9903.6308	169.5000	1649.1504
1604	9563.3168	176.0000	1592.4814
1605	9628.6669	176.0000	1603.3635
1606	9694.0171	176.0000	1614.2456
1607	9759.3673	176.0000	1625.1277
1608	9824.7174	176.0000	1636.0098
1609	9841.9797	176.0000	1638.8843
1610	9859.2420	176.0000	1641.7588
1611	9864.1741	176.0000	1642.5801
1612	9869.1062	176.0000	1643.4014
1613	9886.3685	176.0000	1646.2759
1614	9903.6308	176.0000	1649.1504
1615	9968.9810	176.0000	1660.0325
1616	10034.3311	176.0000	1670.9146
1617	10099.6813	176.0000	1681.7967
1618	10165.0314	176.0000	1692.6788
1619	9563.3168	191.0000	1592.4814
1620	9694.0171	191.0000	1614.2456
1621	9824.7174	191.0000	1636.0098
1622	9859.2420	191.0000	1641.7588
1623	9869.1062	191.0000	1643.4014
1624	9903.6308	191.0000	1649.1504
1625	10034.3311	191.0000	1670.9146
1626	10165.0314	191.0000	1692.6788
1627	9563.3168	206.0000	1592.4814
1628	9628.6669	206.0000	1603.3635
1629	9694.0171	206.0000	1614.2456
1630	9759.3673	206.0000	1625.1277
1631	9824.7174	206.0000	1636.0098
1632	9841.9797	206.0000	1638.8843
1633	9859.2420	206.0000	1641.7588
1634	9864.1741	206.0000	1642.5801
1635	9869.1062	206.0000	1643.4014
1636	9886.3685	206.0000	1646.2759
1637	9903.6308	206.0000	1649.1504
1638	9968.9810	206.0000	1660.0325
1639	10034.3311	206.0000	1670.9146
1640	10099.6813	206.0000	1681.7967
1641	10165.0314	206.0000	1692.6788
1642	9563.3168	221.0000	1592.4814
1643	9694.0171	221.0000	1614.2456
1644	9824.7174	221.0000	1636.0098
1645	9859.2420	221.0000	1641.7588
1646	9869.1062	221.0000	1643.4014
1647	9903.6308	221.0000	1649.1504
1648	10034.3311	221.0000	1670.9146
1649	10165.0314	221.0000	1692.6788
1650	9563.3168	236.0000	1592.4814
1651	9628.6669	236.0000	1603.3635
1652	9694.0171	236.0000	1614.2456
1653	9759.3673	236.0000	1625.1277
1654	9824.7174	236.0000	1636.0098
1655	9841.9797	236.0000	1638.8843
1656	9859.2420	236.0000	1641.7588
1657	9864.1741	236.0000	1642.5801
1658	9869.1062	236.0000	1643.4014
1659	9886.3685	236.0000	1646.2759

1660	9903.6308	236.0000	1649.1504
1661	9968.9810	236.0000	1660.0325
1662	10034.3311	236.0000	1670.9146
1663	10099.6813	236.0000	1681.7967
1664	10165.0314	236.0000	1692.6788
1665	9812.1707	.0000	1709.6510
1666	9846.6512	.0000	1715.6588
1667	9856.5028	.0000	1717.3753
1668	9890.9833	.0000	1723.3831
1669	9812.1707	13.0000	1709.6510
1670	9846.6512	13.0000	1715.6588
1671	9856.5028	13.0000	1717.3753
1672	9890.9833	13.0000	1723.3831
1673	9846.6512	63.0000	1715.6588
1674	9856.5028	63.0000	1717.3753
1675	9846.6512	113.0000	1715.6588
1676	9856.5028	113.0000	1717.3753
1677	9812.1707	163.0000	1709.6510
1678	9846.6512	163.0000	1715.6588
1679	9856.5028	163.0000	1717.3753
1680	9890.9833	163.0000	1723.3831
1681	9551.1039	176.0000	1664.1633
1682	9681.6373	176.0000	1686.9072
1683	9812.1707	176.0000	1709.6510
1684	9846.6512	176.0000	1715.6588
1685	9856.5028	176.0000	1717.3753
1686	9890.9833	176.0000	1723.3831
1687	10021.5167	176.0000	1746.1270
1688	10152.0501	176.0000	1768.8708
1689	9551.1039	206.0000	1664.1633
1690	9681.6373	206.0000	1686.9072
1691	9812.1707	206.0000	1709.6510
1692	9846.6512	206.0000	1715.6588
1693	9856.5028	206.0000	1717.3753
1694	9890.9833	206.0000	1723.3831
1695	10021.5167	206.0000	1746.1270
1696	10152.0501	206.0000	1768.8708
1697	9551.1039	236.0000	1664.1633
1698	9681.6373	236.0000	1686.9072
1699	9812.1707	236.0000	1709.6510
1700	9846.6512	236.0000	1715.6588
1701	9856.5028	236.0000	1717.3753
1702	9890.9833	236.0000	1723.3831
1703	10021.5167	236.0000	1746.1270
1704	10152.0501	236.0000	1768.8708
1705	9799.0720	.0000	1783.1961
1706	9816.2892	.0000	1786.3292
1707	9833.5065	.0000	1789.4623
1708	9838.4257	.0000	1790.3575
1709	9843.3449	.0000	1791.2527
1710	9860.5621	.0000	1794.3858
1711	9877.7794	.0000	1797.5189
1712	9799.0720	6.5000	1783.1961
1713	9833.5065	6.5000	1789.4623
1714	9843.3449	6.5000	1791.2527
1715	9877.7794	6.5000	1797.5189
1716	9799.0720	13.0000	1783.1961
1717	9816.2892	13.0000	1786.3292
1718	9833.5065	13.0000	1789.4623
1719	9838.4257	13.0000	1790.3575
1720	9843.3449	13.0000	1791.2527
1721	9860.5621	13.0000	1794.3858
1722	9877.7794	13.0000	1797.5189
1723	9833.5065	38.0000	1789.4623
1724	9843.3449	38.0000	1791.2527
1725	9833.5065	63.0000	1789.4623
1726	9838.4257	63.0000	1790.3575
1727	9843.3449	63.0000	1791.2527
1728	9833.5065	88.0000	1789.4623
1729	9843.3449	88.0000	1791.2527
1730	9833.5065	113.0000	1789.4623
1731	9838.4257	113.0000	1790.3575

1732	9843.3449	113.0000	1791.2527
1733	9833.5065	138.0000	1789.4623
1734	9843.3449	138.0000	1791.2527
1735	9799.0720	163.0000	1783.1961
1736	9816.2892	163.0000	1786.3292
1737	9833.5065	163.0000	1789.4623
1738	9838.4257	163.0000	1790.3575
1739	9843.3449	163.0000	1791.2527
1740	9860.5621	163.0000	1794.3858
1741	9877.7794	163.0000	1797.5189
1742	9799.0720	169.5000	1783.1961
1743	9833.5065	169.5000	1789.4623
1744	9843.3449	169.5000	1791.2527
1745	9877.7794	169.5000	1797.5189
1746	9538.3537	176.0000	1735.7516
1747	9603.5333	176.0000	1747.6127
1748	9668.7128	176.0000	1759.4738
1749	9733.8924	176.0000	1771.3350
1750	9799.0720	176.0000	1783.1961
1751	9816.2892	176.0000	1786.3292
1752	9833.5065	176.0000	1789.4623
1753	9838.4257	176.0000	1790.3575
1754	9843.3449	176.0000	1791.2527
1755	9860.5621	176.0000	1794.3858
1756	9877.7794	176.0000	1797.5189
1757	9942.9590	176.0000	1809.3801
1758	10008.1385	176.0000	1821.2412
1759	10073.3181	176.0000	1833.1023
1760	10138.4977	176.0000	1844.9634
1761	9538.3537	191.0000	1735.7516
1762	9668.7128	191.0000	1759.4738
1763	9799.0720	191.0000	1783.1961
1764	9833.5065	191.0000	1789.4623
1765	9843.3449	191.0000	1791.2527
1766	9877.7794	191.0000	1797.5189
1767	10008.1385	191.0000	1821.2412
1768	10138.4977	191.0000	1844.9634
1769	9538.3537	206.0000	1735.7516
1770	9603.5333	206.0000	1747.6127
1771	9668.7128	206.0000	1759.4738
1772	9733.8924	206.0000	1771.3350
1773	9799.0720	206.0000	1783.1961
1774	9816.2892	206.0000	1786.3292
1775	9833.5065	206.0000	1789.4623
1776	9838.4257	206.0000	1790.3575
1777	9843.3449	206.0000	1791.2527
1778	9860.5621	206.0000	1794.3858
1779	9877.7794	206.0000	1797.5189
1780	9942.9590	206.0000	1809.3801
1781	10008.1385	206.0000	1821.2412
1782	10073.3181	206.0000	1833.1023
1783	10138.4977	206.0000	1844.9634
1784	9538.3537	221.0000	1735.7516
1785	9668.7128	221.0000	1759.4738
1786	9799.0720	221.0000	1783.1961
1787	9833.5065	221.0000	1789.4623
1788	9843.3449	221.0000	1791.2527
1789	9877.7794	221.0000	1797.5189
1790	10008.1385	221.0000	1821.2412
1791	10138.4977	221.0000	1844.9634
1792	9538.3537	236.0000	1735.7516
1793	9603.5333	236.0000	1747.6127
1794	9668.7128	236.0000	1759.4738
1795	9733.8924	236.0000	1771.3350
1796	9799.0720	236.0000	1783.1961
1797	9816.2892	236.0000	1786.3292
1798	9833.5065	236.0000	1789.4623
1799	9838.4257	236.0000	1790.3575
1800	9843.3449	236.0000	1791.2527
1801	9860.5621	236.0000	1794.3858
1802	9877.7794	236.0000	1797.5189
1803	9942.9590	236.0000	1809.3801

1804	10008.1385	236.0000	1821.2412
1805	10073.3181	236.0000	1833.1023
1806	10138.4977	236.0000	1844.9634
1807	9785.4221	.0000	1856.6408
1808	9819.8086	.0000	1863.1652
1809	9829.6333	.0000	1865.0293
1810	9864.0198	.0000	1871.5536
1811	9785.4221	13.0000	1856.6408
1812	9819.8086	13.0000	1863.1652
1813	9829.6333	13.0000	1865.0293
1814	9864.0198	13.0000	1871.5536
1815	9819.8086	63.0000	1863.1652
1816	9829.6333	63.0000	1865.0293
1817	9819.8086	113.0000	1863.1652
1818	9829.6333	113.0000	1865.0293
1819	9785.4221	163.0000	1856.6408
1820	9819.8086	163.0000	1863.1652
1821	9829.6333	163.0000	1865.0293
1822	9864.0198	163.0000	1871.5536
1823	9525.0670	176.0000	1807.2423
1824	9655.2445	176.0000	1831.9415
1825	9785.4221	176.0000	1856.6408
1826	9819.8086	176.0000	1863.1652
1827	9829.6333	176.0000	1865.0293
1828	9864.0198	176.0000	1871.5536
1829	9994.1974	176.0000	1896.2529
1830	10124.3749	176.0000	1920.9522
1831	9525.0670	206.0000	1807.2423
1832	9655.2445	206.0000	1831.9415
1833	9785.4221	206.0000	1856.6408
1834	9819.8086	206.0000	1863.1652
1835	9829.6333	206.0000	1865.0293
1836	9864.0198	206.0000	1871.5536
1837	9994.1974	206.0000	1896.2529
1838	10124.3749	206.0000	1920.9522
1839	9525.0670	236.0000	1807.2423
1840	9655.2445	236.0000	1831.9415
1841	9785.4221	236.0000	1856.6408
1842	9819.8086	236.0000	1863.1652
1843	9829.6333	236.0000	1865.0293
1844	9864.0198	236.0000	1871.5536
1845	9994.1974	236.0000	1896.2529
1846	10124.3749	236.0000	1920.9522
1847	9771.2217	.0000	1929.9811
1848	9788.3900	.0000	1933.3722
1849	9805.5583	.0000	1936.7632
1850	9810.4635	.0000	1937.7321
1851	9815.3687	.0000	1938.7009
1852	9832.5371	.0000	1942.0920
1853	9849.7054	.0000	1945.4830
1854	9771.2217	6.5000	1929.9811
1855	9805.5583	6.5000	1936.7632
1856	9815.3687	6.5000	1938.7009
1857	9849.7054	6.5000	1945.4830
1858	9771.2217	13.0000	1929.9811
1859	9788.3900	13.0000	1933.3722
1860	9805.5583	13.0000	1936.7632
1861	9810.4635	13.0000	1937.7321
1862	9815.3687	13.0000	1938.7009
1863	9832.5371	13.0000	1942.0920
1864	9849.7054	13.0000	1945.4830
1865	9805.5583	38.0000	1936.7632
1866	9815.3687	38.0000	1938.7009
1867	9805.5583	63.0000	1936.7632
1868	9810.4635	63.0000	1937.7321
1869	9815.3687	63.0000	1938.7009
1870	9805.5583	88.0000	1936.7632
1871	9815.3687	88.0000	1938.7009
1872	9805.5583	113.0000	1936.7632
1873	9810.4635	113.0000	1937.7321
1874	9815.3687	113.0000	1938.7009
1875	9805.5583	138.0000	1936.7632

1876	9815.3687	138.0000	1938.7009
1877	9771.2217	163.0000	1929.9811
1878	9788.3900	163.0000	1933.3722
1879	9805.5583	163.0000	1936.7632
1880	9810.4635	163.0000	1937.7321
1881	9815.3687	163.0000	1938.7009
1882	9832.5371	163.0000	1942.0920
1883	9849.7054	163.0000	1945.4830
1884	9771.2217	169.5000	1929.9811
1885	9805.5583	169.5000	1936.7632
1886	9815.3687	169.5000	1938.7009
1887	9849.7054	169.5000	1945.4830
1888	9511.2444	176.0000	1878.6312
1889	9576.2387	176.0000	1891.4687
1890	9641.2330	176.0000	1904.3062
1891	9706.2273	176.0000	1917.1437
1892	9771.2217	176.0000	1929.9811
1893	9788.3900	176.0000	1933.3722
1894	9805.5583	176.0000	1936.7632
1895	9810.4635	176.0000	1937.7321
1896	9815.3687	176.0000	1938.7009
1897	9832.5371	176.0000	1942.0920
1898	9849.7054	176.0000	1945.4830
1899	9914.6997	176.0000	1958.3205
1900	9979.6940	176.0000	1971.1580
1901	10044.6883	176.0000	1983.9954
1902	10109.6827	176.0000	1996.8329
1903	9511.2444	191.0000	1878.6312
1904	9641.2330	191.0000	1904.3062
1905	9771.2217	191.0000	1929.9811
1906	9805.5583	191.0000	1936.7632
1907	9815.3687	191.0000	1938.7009
1908	9849.7054	191.0000	1945.4830
1909	9979.6940	191.0000	1971.1580
1910	10109.6827	191.0000	1996.8329
1911	9511.2444	206.0000	1878.6312
1912	9576.2387	206.0000	1891.4687
1913	9641.2330	206.0000	1904.3062
1914	9706.2273	206.0000	1917.1437
1915	9771.2217	206.0000	1929.9811
1916	9788.3900	206.0000	1933.3722
1917	9805.5583	206.0000	1936.7632
1918	9810.4635	206.0000	1937.7321
1919	9815.3687	206.0000	1938.7009
1920	9832.5371	206.0000	1942.0920
1921	9849.7054	206.0000	1945.4830
1922	9914.6997	206.0000	1958.3205
1923	9979.6940	206.0000	1971.1580
1924	10044.6883	206.0000	1983.9954
1925	10109.6827	206.0000	1996.8329
1926	9511.2444	221.0000	1878.6312
1927	9641.2330	221.0000	1904.3062
1928	9771.2217	221.0000	1929.9811
1929	9805.5583	221.0000	1936.7632
1930	9815.3687	221.0000	1938.7009
1931	9849.7054	221.0000	1945.4830
1932	9979.6940	221.0000	1971.1580
1933	10109.6827	221.0000	1996.8329
1934	9511.2444	236.0000	1878.6312
1935	9576.2387	236.0000	1891.4687
1936	9641.2330	236.0000	1904.3062
1937	9706.2273	236.0000	1917.1437
1938	9771.2217	236.0000	1929.9811
1939	9788.3900	236.0000	1933.3722
1940	9805.5583	236.0000	1936.7632
1941	9810.4635	236.0000	1937.7321
1942	9815.3687	236.0000	1938.7009
1943	9832.5371	236.0000	1942.0920
1944	9849.7054	236.0000	1945.4830
1945	9914.6997	236.0000	1958.3205
1946	9979.6940	236.0000	1971.1580
1947	10044.6883	236.0000	1983.9954

1948	10109.6827	236.0000	1996.8329
1949	9756.4716	.0000	2003.2129
1950	9790.7564	.0000	2010.2523
1951	9800.5520	.0000	2012.2636
1952	9834.8368	.0000	2019.3030
1953	9756.4716	13.0000	2003.2129
1954	9790.7564	13.0000	2010.2523
1955	9800.5520	13.0000	2012.2636
1956	9834.8368	13.0000	2019.3030
1957	9790.7564	63.0000	2010.2523
1958	9800.5520	63.0000	2012.2636
1959	9790.7564	113.0000	2010.2523
1960	9800.5520	113.0000	2012.2636
1961	9756.4716	163.0000	2003.2129
1962	9790.7564	163.0000	2010.2523
1963	9800.5520	163.0000	2012.2636
1964	9834.8368	163.0000	2019.3030
1965	9496.8868	176.0000	1949.9146
1966	9626.6792	176.0000	1976.5637
1967	9756.4716	176.0000	2003.2129
1968	9790.7564	176.0000	2010.2523
1969	9800.5520	176.0000	2012.2636
1970	9834.8368	176.0000	2019.3030
1971	9964.6293	176.0000	2045.9521
1972	10094.4217	176.0000	2072.6013
1973	9496.8868	206.0000	1949.9146
1974	9626.6792	206.0000	1976.5637
1975	9756.4716	206.0000	2003.2129
1976	9790.7564	206.0000	2010.2523
1977	9800.5520	206.0000	2012.2636
1978	9834.8368	206.0000	2019.3030
1979	9964.6293	206.0000	2045.9521
1980	10094.4217	206.0000	2072.6013
1981	9496.8868	236.0000	1949.9146
1982	9626.6792	236.0000	1976.5637
1983	9756.4716	236.0000	2003.2129
1984	9790.7564	236.0000	2010.2523
1985	9800.5520	236.0000	2012.2636
1986	9834.8368	236.0000	2019.3030
1987	9964.6293	236.0000	2045.9521
1988	10094.4217	236.0000	2072.6013
1989	9741.1727	.0000	2076.3320
1990	9758.2882	.0000	2079.9801
1991	9775.4037	.0000	2083.6283
1992	9780.2939	.0000	2084.6706
1993	9785.1840	.0000	2085.7130
1994	9802.2995	.0000	2089.3611
1995	9819.4151	.0000	2093.0093
1996	9741.1727	6.5000	2076.3320
1997	9775.4037	6.5000	2083.6283
1998	9785.1840	6.5000	2085.7130
1999	9819.4151	6.5000	2093.0093
2000	9741.1727	13.0000	2076.3320
2001	9758.2882	13.0000	2079.9801
2002	9775.4037	13.0000	2083.6283
2003	9780.2939	13.0000	2084.6706
2004	9785.1840	13.0000	2085.7130
2005	9802.2995	13.0000	2089.3611
2006	9819.4151	13.0000	2093.0093
2007	9775.4037	38.0000	2083.6283
2008	9785.1840	38.0000	2085.7130
2009	9775.4037	63.0000	2083.6283
2010	9780.2939	63.0000	2084.6706
2011	9785.1840	63.0000	2085.7130
2012	9775.4037	88.0000	2083.6283
2013	9785.1840	88.0000	2085.7130
2014	9775.4037	113.0000	2083.6283
2015	9780.2939	113.0000	2084.6706
2016	9785.1840	113.0000	2085.7130
2017	9775.4037	138.0000	2083.6283
2018	9785.1840	138.0000	2085.7130
2019	9741.1727	163.0000	2076.3320

2020	9758.2882	163.0000	2079.9801
2021	9775.4037	163.0000	2083.6283
2022	9780.2939	163.0000	2084.6706
2023	9785.1840	163.0000	2085.7130
2024	9802.2995	163.0000	2089.3611
2025	9819.4151	163.0000	2093.0093
2026	9741.1727	169.5000	2076.3320
2027	9775.4037	169.5000	2083.6283
2028	9785.1840	169.5000	2085.7130
2029	9819.4151	169.5000	2093.0093
2030	9481.9949	176.0000	2021.0882
2031	9546.7894	176.0000	2034.8991
2032	9611.5838	176.0000	2048.7101
2033	9676.3783	176.0000	2062.5210
2034	9741.1727	176.0000	2076.3320
2035	9758.2882	176.0000	2079.9801
2036	9775.4037	176.0000	2083.6283
2037	9780.2939	176.0000	2084.6706
2038	9785.1840	176.0000	2085.7130
2039	9802.2995	176.0000	2089.3611
2040	9819.4151	176.0000	2093.0093
2041	9884.2095	176.0000	2106.8203
2042	9949.0039	176.0000	2120.6312
2043	10013.7984	176.0000	2134.4421
2044	10078.5928	176.0000	2148.2531
2045	9481.9949	191.0000	2021.0882
2046	9611.5838	191.0000	2048.7101
2047	9741.1727	191.0000	2076.3320
2048	9775.4037	191.0000	2083.6283
2049	9785.1840	191.0000	2085.7130
2050	9819.4151	191.0000	2093.0093
2051	9949.0039	191.0000	2120.6312
2052	10078.5928	191.0000	2148.2531
2053	9481.9949	206.0000	2021.0882
2054	9546.7894	206.0000	2034.8991
2055	9611.5838	206.0000	2048.7101
2056	9676.3783	206.0000	2062.5210
2057	9741.1727	206.0000	2076.3320
2058	9758.2882	206.0000	2079.9801
2059	9775.4037	206.0000	2083.6283
2060	9780.2939	206.0000	2084.6706
2061	9785.1840	206.0000	2085.7130
2062	9802.2995	206.0000	2089.3611
2063	9819.4151	206.0000	2093.0093
2064	9884.2095	206.0000	2106.8203
2065	9949.0039	206.0000	2120.6312
2066	10013.7984	206.0000	2134.4421
2067	10078.5928	206.0000	2148.2531
2068	9481.9949	221.0000	2021.0882
2069	9611.5838	221.0000	2048.7101
2070	9741.1727	221.0000	2076.3320
2071	9775.4037	221.0000	2083.6283
2072	9785.1840	221.0000	2085.7130
2073	9819.4151	221.0000	2093.0093
2074	9949.0039	221.0000	2120.6312
2075	10078.5928	221.0000	2148.2531
2076	9481.9949	236.0000	2021.0882
2077	9546.7894	236.0000	2034.8991
2078	9611.5838	236.0000	2048.7101
2079	9676.3783	236.0000	2062.5210
2080	9741.1727	236.0000	2076.3320
2081	9758.2882	236.0000	2079.9801
2082	9775.4037	236.0000	2083.6283
2083	9780.2939	236.0000	2084.6706
2084	9785.1840	236.0000	2085.7130
2085	9802.2995	236.0000	2089.3611
2086	9819.4151	236.0000	2093.0093
2087	9884.2095	236.0000	2106.8203
2088	9949.0039	236.0000	2120.6312
2089	10013.7984	236.0000	2134.4421
2090	10078.5928	236.0000	2148.2531
2091	9725.3258	.0000	2149.3342

2092	9759.5012	.0000	2156.8871
2093	9769.2656	.0000	2159.0451
2094	9803.4409	.0000	2166.5979
2095	9725.3258	13.0000	2149.3342
2096	9759.5012	13.0000	2156.8871
2097	9769.2656	13.0000	2159.0451
2098	9803.4409	13.0000	2166.5979
2099	9759.5012	63.0000	2156.8871
2100	9769.2656	63.0000	2159.0451
2101	9759.5012	113.0000	2156.8871
2102	9769.2656	113.0000	2159.0451
2103	9725.3258	163.0000	2149.3342
2104	9759.5012	163.0000	2156.8871
2105	9769.2656	163.0000	2159.0451
2106	9803.4409	163.0000	2166.5979
2107	9466.5697	176.0000	2092.1481
2108	9595.9477	176.0000	2120.7412
2109	9725.3258	176.0000	2149.3342
2110	9759.5012	176.0000	2156.8871
2111	9769.2656	176.0000	2159.0451
2112	9803.4409	176.0000	2166.5979
2113	9932.8190	176.0000	2195.1910
2114	10062.1971	176.0000	2223.7840
2115	9466.5697	206.0000	2092.1481
2116	9595.9477	206.0000	2120.7412
2117	9725.3258	206.0000	2149.3342
2118	9759.5012	206.0000	2156.8871
2119	9769.2656	206.0000	2159.0451
2120	9803.4409	206.0000	2166.5979
2121	9932.8190	206.0000	2195.1910
2122	10062.1971	206.0000	2223.7840
2123	9466.5697	236.0000	2092.1481
2124	9595.9477	236.0000	2120.7412
2125	9725.3258	236.0000	2149.3342
2126	9759.5012	236.0000	2156.8871
2127	9769.2656	236.0000	2159.0451
2128	9803.4409	236.0000	2166.5979
2129	9932.8190	236.0000	2195.1910
2130	10062.1971	236.0000	2223.7840
2131	9708.9319	.0000	2222.2156
2132	9725.9907	.0000	2226.1201
2133	9743.0496	.0000	2230.0246
2134	9747.9236	.0000	2231.1401
2135	9752.7975	.0000	2232.2557
2136	9769.8564	.0000	2236.1602
2137	9786.9153	.0000	2240.0647
2138	9708.9319	6.5000	2222.2156
2139	9743.0496	6.5000	2230.0246
2140	9752.7975	6.5000	2232.2557
2141	9786.9153	6.5000	2240.0647
2142	9708.9319	13.0000	2222.2156
2143	9725.9907	13.0000	2226.1201
2144	9743.0496	13.0000	2230.0246
2145	9747.9236	13.0000	2231.1401
2146	9752.7975	13.0000	2232.2557
2147	9769.8564	13.0000	2236.1602
2148	9786.9153	13.0000	2240.0647
2149	9743.0496	38.0000	2230.0246
2150	9752.7975	38.0000	2232.2557
2151	9743.0496	63.0000	2230.0246
2152	9747.9236	63.0000	2231.1401
2153	9752.7975	63.0000	2232.2557
2154	9743.0496	88.0000	2230.0246
2155	9752.7975	88.0000	2232.2557
2156	9743.0496	113.0000	2230.0246
2157	9747.9236	113.0000	2231.1401
2158	9752.7975	113.0000	2232.2557
2159	9743.0496	138.0000	2230.0246
2160	9752.7975	138.0000	2232.2557
2161	9708.9319	163.0000	2222.2156
2162	9725.9907	163.0000	2226.1201
2163	9743.0496	163.0000	2230.0246

2164	9747.9236	163.0000	2231.1401
2165	9752.7975	163.0000	2232.2557
2166	9769.8564	163.0000	2236.1602
2167	9786.9153	163.0000	2240.0647
2168	9708.9319	169.5000	2222.2156
2169	9743.0496	169.5000	2230.0246
2170	9752.7975	169.5000	2232.2557
2171	9786.9153	169.5000	2240.0647
2172	9450.6119	176.0000	2163.0903
2173	9515.1919	176.0000	2177.8717
2174	9579.7719	176.0000	2192.6530
2175	9644.3519	176.0000	2207.4343
2176	9708.9319	176.0000	2222.2156
2177	9725.9907	176.0000	2226.1201
2178	9743.0496	176.0000	2230.0246
2179	9747.9236	176.0000	2231.1401
2180	9752.7975	176.0000	2232.2557
2181	9769.8564	176.0000	2236.1602
2182	9786.9153	176.0000	2240.0647
2183	9851.4952	176.0000	2254.8460
2184	9916.0752	176.0000	2269.6273
2185	9980.6552	176.0000	2284.4086
2186	10045.2352	176.0000	2299.1899
2187	9450.6119	191.0000	2163.0903
2188	9579.7719	191.0000	2192.6530
2189	9708.9319	191.0000	2222.2156
2190	9743.0496	191.0000	2230.0246
2191	9752.7975	191.0000	2232.2557
2192	9786.9153	191.0000	2240.0647
2193	9916.0752	191.0000	2269.6273
2194	10045.2352	191.0000	2299.1899
2195	9450.6119	206.0000	2163.0903
2196	9515.1919	206.0000	2177.8717
2197	9579.7719	206.0000	2192.6530
2198	9644.3519	206.0000	2207.4343
2199	9708.9319	206.0000	2222.2156
2200	9725.9907	206.0000	2226.1201
2201	9743.0496	206.0000	2230.0246
2202	9747.9236	206.0000	2231.1401
2203	9752.7975	206.0000	2232.2557
2204	9769.8564	206.0000	2236.1602
2205	9786.9153	206.0000	2240.0647
2206	9851.4952	206.0000	2254.8460
2207	9916.0752	206.0000	2269.6273
2208	9980.6552	206.0000	2284.4086
2209	10045.2352	206.0000	2299.1899
2210	9450.6119	221.0000	2163.0903
2211	9579.7719	221.0000	2192.6530
2212	9708.9319	221.0000	2222.2156
2213	9743.0496	221.0000	2230.0246
2214	9752.7975	221.0000	2232.2557
2215	9786.9153	221.0000	2240.0647
2216	9916.0752	221.0000	2269.6273
2217	10045.2352	221.0000	2299.1899
2218	9450.6119	236.0000	2163.0903
2219	9515.1919	236.0000	2177.8717
2220	9579.7719	236.0000	2192.6530
2221	9644.3519	236.0000	2207.4343
2222	9708.9319	236.0000	2222.2156
2223	9725.9907	236.0000	2226.1201
2224	9743.0496	236.0000	2230.0246
2225	9747.9236	236.0000	2231.1401
2226	9752.7975	236.0000	2232.2557
2227	9769.8564	236.0000	2236.1602
2228	9786.9153	236.0000	2240.0647
2229	9851.4952	236.0000	2254.8460
2230	9916.0752	236.0000	2269.6273
2231	9980.6552	236.0000	2284.4086
2232	10045.2352	236.0000	2299.1899

1,1,1,1

2,1,1,1

3,1,1,1
4,1,1,1
5,1,1,1
6,1,1,1
7,1,1,1

2131,1,1,0
2132,1,1,0
2133,1,1,0
2134,1,1,0
2135,1,1,0
2136,1,1,0
2137,1,1,0

1
200000,0.3,285,1E+9,1E+9,1E+9,0,1,7.85E-9,1,1.539,0.971,1E+9,1E+9,0,0,0,0,0,0
2
32562,0.15,48,0,400,4.004,0.1,0,2,2.4E-9,1,0.405,0.831,10,1.967,0.792,0,0,0,0,0
3
200000,0.310,1E+9,1E+9,1E+9,0,1,7.85E-9,1,1.539,0.971,1E+9,1E+9,0,0,0,0,0,0
1,1
3,2,-1,1.03,0
2,1
3,2,+1,0.523,0

20000,0,100,1,3,0,1,25,20000,2,0,0
0.000001,100,0,0,0,0.25,0.5,0,0,0,0.05,1.0
1088
4866,4376,4551
"PAIR OF POINT LOAD"
1,0,0
1086,0,-25000,0
1088,0,-25000,0
1090,0,-25000,0
1092,0,-25000,0
2232,0,0,0

"END"



(Von-Mises)

(-)

.(-)

-(Smearred Crack Model)

()

.(-)

-(*ANSYS*)

)

(

40% 0.0%

23.4%

.14.9%

()

101.85% 25%

59.6% 16.0%

(fixed ended)

(simply supported)

(fixed ended)

91.3%

63.7% 19.8%

63° 43° 23°

(simply supported)

(fixed ended)



التأهيل الاستراتيجي و الديناميكي الإلكتروني للمتبات المنانية أفقياً

مختار مكي خانم حمير المطيري

(1997)

(2000 /)